

**THE DEVELOPMENT OF NEW ENGLERIN-INSPIRED
CHEMOTHERAPEUTIC DRUG CANDIDATES AND TOOL COMPOUNDS
&
THE SYNTHESIS OF AN ACYLDEPSIPEPTIDE FLOURESCENT PROBE**

by

Elijah J. Hudson

A dissertation submitted to the Faculty of the University of Delaware in partial fulfillment of the requirements for the degree of Doctor of Philosophy in Chemistry and Biochemistry

Winter 2024

© 2024 Elijah J. Hudson
All Rights Reserved

**THE DEVELOPMENT OF NEW ENGLERIN-INSPIRED
CHEMOTHERAPEUTIC DRUG CANDIDATES AND TOOL COMPOUNDS
&
THE SYNTHESIS OF AN ACYLDEPSIPEPTIDE FLOURESCENT PROBE**

by

Elijah J. Hudson

Approved: _____
Joel Rosenthal, Ph.D.
Chair of the Department of Chemistry and Biochemistry

Approved: _____
Debra Hess Norris
Interim Dean of the College of Arts and Sciences

Approved: _____
Louis F. Rossi, Ph.D.
Vice Provost for Graduate and Professional Education and
Dean of the Graduate College

I certify that I have read this dissertation and that in my opinion it meets the academic and professional standard required by the University as a dissertation for the degree of Doctor of Philosophy.

Signed:

William J. Chain, Ph.D.
Professor in charge of dissertation

I certify that I have read this dissertation and that in my opinion it meets the academic and professional standard required by the University as a dissertation for the degree of Doctor of Philosophy.

Signed:

Mary P. Watson, Ph.D.
Member of dissertation committee

I certify that I have read this dissertation and that in my opinion it meets the academic and professional standard required by the University as a dissertation for the degree of Doctor of Philosophy.

Signed:

Emil A. Hernandez-Pagan, Ph.D.
Member of dissertation committee

I certify that I have read this dissertation and that in my opinion it meets the academic and professional standard required by the University as a dissertation for the degree of Doctor of Philosophy.

Signed:

John A. Beutler, Ph.D.
Member of dissertation committee

ACKNOWLEDGMENTS

First, I would like to thank Prof. William J. Chain for giving me the opportunity to join his group and to further advance the englerin project to what may hopefully one day be a renal cancer therapeutic. BJ has given me the opportunity to learn and develop an immense amount throughout my time here and has continuously pushed me to strive for better. BJ has been an excellent advisor and has supported me in the exploration my own ideas towards the development of englerin. His belief in his students' abilities and his drive for excellence has been inspiring to me.

I would also like to thank my committee members Dr. John Beutler, Prof. Mary Watson, and Prof. Emil Hernandez-Pagan. They have always been there to support me when I needed help of any kind. I am also inspired by John's perseverance in the pursuit of an anti-renal cancer therapeutic based on englerin. The amount of research being conducted worldwide on (-)-englerin A has dropped significantly, but John never seemed to let up. He always holds an optimistic attitude and sees the potential of the project to have an immense positive impact on the greater good.

I would also like to thank the current and former members of the Chain group for always holding me accountable, keeping a positive attitude, and striving to think more deeply about not only my chemistry, but the chemistry of others as well. When I arrived in the lab, Dr. Chad Hatch and Dr. Marcel Achtenhagen were gracious enough to take me under their wings and guide me in the development of my skills as a synthetic chemist. Other group members that I would like to thank include Liam O'Grady, Alex Ziegelmeier, Leah White, Tyler Swanson, Nicole Kretekos, and Ali

Amiri-Naeni. Liam and Alex have been a great outlet for stress by allowing me to teach them a weekly lesson in a sport or game of their choice. My record in chess against Liam is 263-1-1 and against Alex is 139-0. Liam also has yet to beat me in racquetball with a record of 1-0 since the last time we played. I also made Liam throw up during a workout one time. I was fortunate enough to make lifelong friendships during my time here including other students in the program like Devonte Moore and Stephen Hyland.

I want to especially thank my family, including my parents Don and Beth Hudson; my siblings Ozzy, Tre', and Lola; and my grandparents Pat and Bob Davis, Bill and †Onita Altland, and †Donald Hudson I. The love, support, and encouragement from these people have been immeasurable and there is no way I could have done it without their help. They have always encouraged me to continue my education and to work hard for what I want in life. I am extremely grateful for the time and energy these people have spent to make me into the person I am today.

During my time here, I was fortunate enough to meet my future wife, Marisa Suhari. We lived in the same building across the hall from one another during my first year here and started dating during my second semester, the spring semester of her junior year. When she graduated the following year, we moved in together and adopted a dog together, Nova. Marisa is currently studying at Shenandoah to become a Physician Assistant. We are in the process of planning our wedding, which will be November 2, 2024. Throughout this process, Marisa has been my greatest supporter and I could not ask for a greater person to have by my side. Her incredible patience and understanding along with her willingness to push me outside of my comfort zone

were exceptionally helpful during this process. I also would like to thank my future in-laws, Cheryl and Ed Suhari, for their endless help and support during this process.

TABLE OF CONTENTS

LIST OF FIGURES	xi
LIST OF ABBREVIATIONS	xvi
ABSTRACT	xxiv

Chapter

1	ENGLERIN A: ISOLATION, BIOLOGICAL ACTIVITY, SYNTHESSES, AND DEVELOPMENT TOWARDS ANTI-RENAL CANCER THERAPAUTIC CANDIDACY	1
1.1	Introduction to (-)-Englerin A.....	1
1.2	Biological Mechanism of Action Investigations	3
1.2.1	Necrosis in RCC due to Ca ²⁺ uptake and Production of Reactive Oxygen Species	3
1.2.2	Stimulation of PKC θ in the A498 Renal Cancer Cell Line.....	4
1.2.3	Multiple Mechanisms of Cell Death and Autophagy	5
1.2.4	Modulation of L-Type Calcium Channels.....	6
1.2.5	Transient Receptor Potential Canonicals and their Role in RCC Cytotoxicity Mediated by EA.....	7
1.2.5.1	Further Investigation of TRPC Channels	10
1.2.6	Rewiring Phosphosignaling via Hsp27 Hyperphosphorylation ..	13
1.2.7	EA-Mediated Effects in Other Biological Systems.....	13
1.3	Total and Formal Syntheses of Englerin A	15
1.3.1	Christmann – Total Synthesis of (+)-Englerin A and Determination of Absolute Stereochemistry (October 2009).....	16
1.3.2	Echavarren – Total Synthesis of (-)-Englerin A (April 2010)....	17
1.3.3	Ma – Total Synthesis of (-)-Englerin A (April 2010).....	19
1.3.4	Nicolau and Chen – Total Synthesis of (\pm)-Englerin A & Formal Synthesis of (-)-Englerin A (May 2010)	20
1.3.5	Theodorakis – Formal Synthesis of (-)-Englerin A (August 2010).....	23

1.3.6	Chain – Total Synthesis of (–)-Englerin A (April 2011).....	25
1.3.7	Parker – Formal Synthesis of (–)-Englerin A (May 2012).....	26
1.3.8	Hatakeyama – Total Synthesis of (–)-Englerin A (August 2012).....	28
1.3.9	Shang, Sun, and Lin – Total Synthesis of (+)-Englerin A (January 2013).....	30
1.3.10	Metz – Total Synthesis of (–)-Englerin A (April 2013).....	32
1.3.11	Shen – Total Synthesis of (–)-Englerin A (January 2014).....	34
1.3.12	Hashimoto and Anada – Total Synthesis of (–)-Englerin A (July 2015).....	35
1.3.13	Iwasawa – Total Synthesis of (±)-Englerin A (January 2016)....	37
1.3.14	López and Masacareñas – Total Synthesis of (–)-Englerin A (October 2016).....	39
1.3.15	Iwabuchi – Formal Synthesis of (–)-Englerin A (September 2017).....	42
1.3.16	Shoji – Formal Synthesis of (±)-Englerin A (August 2017).....	44
1.3.17	Wang – Total Synthesis of (–)-Englerin A (April 2018).....	45
1.3.18	Tchabanenko – Total Synthesis of (±)-Englerin A (January 2019).....	47
1.3.19	Plietker – Total Synthesis of (–)-Englerin A (May 2019).....	50
1.3.20	Christmann and Liu – Total Synthesis of (–)-Englerin A (January 2020).....	51
1.3.21	Xiang – Total Synthesis of (–)-Englerin A (February 2020).....	53
1.3.22	Alternative Approaches to the Synthesis of Englerin A.....	55
1.4	Englerin Analogues and Structure–Function Studies.....	57
1.4.1	C1 – C5.....	58
1.4.2	C6.....	60
1.4.3	C7.....	62
1.4.4	C9.....	63
1.5	Proteomic Tool Compounds for Mechanistic Investigation.....	66
1.6	Conclusion.....	68
	REFERENCES.....	69
2	SYNTHESIS OF A NEXT-GENERATION SERIES OF ENGLERIN ANALOGUES CONTAINING A C7-CYCLOHEXYL GROUP, HYDROPHOBIC C6-ESTERS, AND C9-GLYOLATE ISOSTERES.....	79
2.1	Targeted series of analogues.....	79
2.2	Efforts Towards a Carbon–Carbon Homologation.....	81

2.2.1	Addition of Nitrile	92
2.2.2	Olefinations	97
2.2.3	Furan as a Masked Carboxylic Acid in Classic Total Syntheses and Methodologies	100
2.3	Application of Masked Carboxylic Acids to Englerin Analogue Synthesis.....	102
2.4	Oxy Analogues	111
2.5	Biological Data of Analogues Submitted to the NCI	118
	Experimental Procedures.....	120
	REFERENCES.....	197
3	EFFORTS TOWARD THE SYNTHESIS OF NOVEL TOOL COMPOUNDS FEATURING A C7-CYCLOHEXYL GROUP, MODIFIED C10-APPENDAGES, AND SUBSTITUTED C6- CINNAMATE MOIETIES	201
3.1	Targeted Series of Tool Compounds.....	201
3.2	Michael Addition and Samarium Diiodide Reductive Cyclization	208
3.3	Attempts to Fix Selectivity of Michael Addition	211
3.4	Attempt to Fix Diastereoselectivity with an Olefin.....	215
3.5	Future Work.....	217
	Experimental Procedures.....	220
	REFERENCES	271
4	SYNTHESIS OF AN ACYLDEPSIPEPTIDE FLUORESCENT MECHANISTIC PROBE.....	273
4.1	Introduction to Clp	273
4.1.1	Clp in Mycobacterium tuberculosis.....	274
4.1.2	Acyldepsipeptides (ADEPs) – Introduction and bioactivity	274
4.1.3	ADEP Fragments and Analogues.....	276
4.2	ADEP Fragment Tool Compound Exploration	278
4.2.1	Prior Synthesis of the ADEPs and their Fragments.....	279
4.2.2	Synthesis of ADEP Fluorescent Probe Compound	280
	REFERENCES	307

Appendix

A	CATALOG OF SPECTRA	310
B	CRYSTAL STRUCTURE DATA FOR PINACOL PRODUCT 3.24.....	446

LIST OF FIGURES

Figure 1.1 The structures of (-)-englerin A, englerin B, and englerin B acetate	3
Figure 1.2 The proposed biological mechanism of action of EA in the 786-0 cell line	5
Figure 1.3 The anti-cancer compound piperlongumine.....	6
Figure 1.4 Alternative TPRC channel activators and inhibitors used for biological investigations.....	12
Figure 1.5 Total synthesis of (+)-englerin A completed by Mathias Christmann et al.	17
Figure 1.6 Total synthesis of (-)-englerin A completed by Antonio Echavarren et al.	19
Figure 1.7 Total synthesis of (-)-englerin A completed by Dawei Ma et al.	20
Figure 1.8 Total synthesis of (±)-englerin A completed by the K. C. Nicolau and David Chen groups	22
Figure 1.9 Formal synthesis of (-)-englerin A completed by Emmanuel Theodorakis et al.	24
Figure 1.10 Total synthesis of (-)-englerin A completed by Chain and coworkers....	26
Figure 1.11 Formal synthesis of (-)-englerin A completed by Kathlyn Parker et al. .	28
Figure 1.12 Total synthesis of (-)-englerin A completed by Susumi Hatakeyama et al.	30
Figure 1.13 Total synthesis of (-)-englerin A completed by the groups of Bing-Feng Sun, Guo-Qiang Lin, and Yong-Jia Shang.....	32
Figure 1.14 Total synthesis of (-)-englerin A completed by Peter Metz et al.	33
Figure 1.15 Total synthesis of (-)-englerin A completed by Zhengwu Shen et al.....	34

Figure 1.16 Total synthesis of (–)-englerin A completed by the Masahiro Anada and Shunichi Hashimoto groups.....	36
Figure 1.17 Total synthesis of (–)-englerin A completed by Nobuharu Iwasawa et al.	38
Figure 1.18 Total synthesis of (–)-englerin A completed by the groups of Fernando López and José Mascareñas	41
Figure 1.19 Formal synthesis of (–)-englerin A completed by Yoshiharu Iwabuchi et al.	43
Figure 1.20 Formal synthesis of (±)-englerin A completed by Mitsuru Shoji et al. ...	45
Figure 1.21 Total synthesis of (–)-englerin A completed by Zhongwen Wang et al. .	46
Figure 1.22 Total synthesis of (±)-englerin A completed by Kirill Tchabanenko et al.	49
Figure 1.23 Total synthesis of (–)-englerin A completed by Bernd Plietker et al.....	51
Figure 1.24 Total synthesis of (–)-englerin A completed by the Mathias Christmann and Tiangang Liu groups	53
Figure 1.25 Total synthesis of (–)-englerin A completed by Zheng Xiang et al.	54
Figure 1.26 Method developed by Shao-Hua Wang et al. describing the synthesis of 8-oxabicyclo[3.2.1]octanes	57
Figure 1.27 (–)-Englerin A with its positions around the scaffold labeled	58
Figure 1.28 Englerin analogues featuring modifications from C1 through C5	59
Figure 1.29 Englerin analogues featuring modifications at C6	62
Figure 1.30 Englerin analogues featuring modifications at C7	63
Figure 1.31 Englerin analogues featuring modifications at C9	65
Figure 1.32 Proteomic tool compounds developed by Mathias Christmann et al. and William Chain et al.	67
Figure 2.1 Targeted novel englerin-based analogues	81
Figure 2.2 Retrosynthetic analysis of the core structure of the englerin analogues	82

Figure 2.3 Synthesis of furanone 2.1	83
Figure 2.4 Synthesis of cyclic unsaturated aldehyde 2.2	84
Figure 2.5 The Michael addition between furanone 2.1 and aldehyde 2.2	85
Figure 2.6 Samarium diiodide reductive coupling pathways and products.....	86
Figure 2.7 Proposed route to core compound 2.12 using electroauxiliaries.....	87
Figure 2.8 Electrochemical coupling to afford bicyclic ester 2.15 accomplished by R.D. Little.....	88
Figure 2.9 The electrochemical reductive cyclization of Michael adduct 2.7 to afford the core 2.12	88
Figure 2.10 Synthetic strategy to synthesize the core utilizing the acidic proton present in dithianes.....	90
Figure 2.11 Final conditions used after optimization of the SmI ₂ reductive coupling	91
Figure 2.12 Transformation of Michael adduct 2.7 to imidazole 2.20	92
Figure 2.13 Nitrile substitution attempt on imidazole 2.20 resulting in the 1,4- addition product 2.22	93
Figure 2.14 Cyanation conditions evaluated along with the observed products	94
Figure 2.15 Additional attempts at achieving nitrile 2.27	97
Figure 2.16 Olefination conditions attempted in the pursuit of vinyl ether 2.33 and aldehyde 2.34	99
Figure 2.17 Classic total syntheses featuring the masked carboxylic acid strategy through the incorporation of a furan.....	101
Figure 2.18 Methods developed to affect the oxidative cleavage of furans into carboxylic acids.....	101
Figure 2.19 Synthesis of furan 2.41 from the core 2.12	103
Figure 2.20 Attempted conditions to oxidatively cleave the furan 2.41 into the carboxylic acid 2.42	105
Figure 2.21 The Steglich esterification used to transform acid 2.42 into ester 2.44 .	106

Figure 2.22 nOe interactions to determine the stereochemistry of stereogenic center α to the ester	106
Figure 2.23 Attempted epimerization conditions	107
Figure 2.24 Completion of the reverse ester analogue 2.47	109
Figure 2.25 Other completed reverse ester analogues with variation at C6	111
Figure 2.26 An example of the reverse ester analogues with the C9-oxygen intact .	112
Figure 2.27 Conditions attempted in the protection of the alcohol resulting from the furan addition.....	115
Figure 2.28 Oxidative cleavage of the furan to reveal carboxylic acid 2.57	116
Figure 2.29 Conditions used in attempts to esterify 2.57 into reverse ester 2.58	117
Figure 2.30 The final 3 steps in the synthesis of the C6-methoxy analogue 2.61	118
Figure 3.1 Next-generation proteomic tool compounds incorporating covalent modifiers.....	202
Figure 3.2 Synthesis of the Furanone	203
Figure 3.2 Retrosynthetic analysis of the proteomic tool compounds	203
Figure 3.3 Synthetic routes to achieve α -chloroester 3.5	204
Figure 3.4 Attempts at affording ester 3.9	205
Figure 3.5 Synthesis of acid 3.14 and the undesired ester byproduct 3.15	206
Figure 3.6 Synthesis of furanone 3.21 from 1,5-pentanediol	207
Figure 3.7 The Michael addition and SmI ₂ cyclization using furanone 3.21	208
Figure 3.8 Structure of the pinacol product 3.24 resulting from the Michael addition and SmI ₂ cyclization of furanone 3.21	210
Figure 3.9 Transition state models of the Michael addition	210
Figure 3.10 Synthesis of TBDPS-protected furanone 3.30	212
Figure 3.11 Synthesis of PMB-protected furanone 3.37	213

Figure 3.12 Results of the Michael addition and SmI ₂ cyclization using furanones 3.30 and 3.37	214
Figure 3.13 Allylic furanone 3.39	215
Figure 3.14 An alternative route to allylic furanone 3.39 through an elimination	216
Figure 3.15 An alternative route to allylic furanone 3.39 through a Wittig olefination.....	217
Figure 3.16 Synthetic route towards the proteomic tool compounds using allylic furanone 3.39.....	219
Figure 4.1 Examples of acyldepsipeptide antibiotics	275
Figure 4.2 Selected acyldepsipeptide fragments and their minimum inhibitory concentrations.....	277
Figure 4.3 Acyldepsipeptide fragment fluorescent probe compound.....	279
Figure 4.4 Previous synthesis of the acyldepsipeptide fragment 4.5 by Jason Sello et al.	280
Figure 4.5 Synthesis of peptide 4.22 towards the synthesis of the probe compound 4.13	283
Figure 4.6 Proposed mechanism of the generation of HCl towards the deprotection of the Boc group	285
Figure 4.7 Final steps in the synthesis of fluorescent probe compound 4.13.....	285

LIST OF ABBREVIATIONS

Å	Ångström
Ac	acetyl
Ac ₂ O	acetic anhydride
Anis.	<i>p</i> -anisaldehyde
app	apparent
aq	aqueous
ATP	attached proton test
br	broadened
Bu	butyl
BHT	2,6-di- <i>tert</i> -butyl-4-methylphenol
°C	degrees Celsius
¹³ C	carbon-13 nuclear magnetic resonance
Calcd.	calculated
CAM	ceric ammonium molybdate
cat.	catalytic
CD	circular dichroism
CDCl ₃	deuterated chloroform

CH ₂ Cl ₂	dichloromethane
CI	chemical ionization
cm ⁻¹	reciprocal centimeters
COSY	homonuclear correlation spectroscopy
CPD	composite pulse decoupling
δ	chemical shift (parts per million)
2D	two dimensional
3D	three dimensional
d	doublet
dd	doublet of doublets
ddd	doublet of doublet of doublets
dppf	1,1'-bis(diphenylphosphino)ferrocene
dppp	1,3-bis(diphenylphosphino)propane
dt	doublet of triplets
DMA	<i>N,N</i> -dimethylacetamide
DMAP	4-(dimethylamino)pyridine
DME	1,2-dimethoxyethane
DMEDA	<i>N,N'</i> -dimethylethylenediamine
DMF	<i>N,N</i> -dimethylformamide
DMSO	Dimethyl sulfoxide
<i>E</i>	<i>Ger.</i> , entgegen
Ed.	editor

ed.	edition
EDCI	<i>N</i> -(3-dimethylaminopropyl)- <i>N'</i> -ethylcarbodiimide hydrochloride
EI	electron impact
equiv.	equivalent(s)
ES	electrospray ionization
Et	ethyl
Et ₂ O	diethyl ether
ether	diethyl ether
EtOAc	ethyl acetate
¹⁹ F	fluorine-19 nuclear magnetic resonance
FD	field desorption
g	gram(s)
¹ H	proton nuclear magnetic resonance
h	hour(s)
HFIP	hexafluoroisopropanol
HMBC	heteronuclear multiple-bond correlation spectroscopy
HOMO	highest occupied molecular orbital
HPLC	high performance liquid chromatography
HRMS	high resolution mass spectrum

HSQC	heteronuclear single-bond correlation spectroscopy
h ν	photoirradiation
Hz	hertz
IC ₅₀	half maximal inhibitory concentration
IR	infrared
<i>i</i> -Pr	isopropyl
J	coupling constant x
L	liter(s)
LAH	lithium aluminum hydride
LC	liquid chromatography
LDA	lithium diisopropylamide
LUMO	lowest unoccupied molecular orbital
<i>m</i>	<i>meta</i>
m	multiplet; or milli (10 ⁻³); or meter
M	molar (mol L ⁻¹); or metal
M ⁺	molecular ion (positive)
<i>m</i> -CPBA	<i>meta</i> -chloroperoxybenzoic acid
Me	methyl
MeOH	methanol
mg	milligram(s)
MHz	megahertz

min	minute(s)
mm	Hg millimeters of mercury
mL	milliliter(s)
mmol	millimole(s)
mol	mole
MOM	methoxymethyl
mp	melting point
μL	microliter(s)
MS	mass spectrometry; or molecular sieves
m/z	mass to charge ratio
N	normal (concentration)
N.A.	not available
NaOMe	sodium methoxide
<i>n</i> -BuLi	<i>n</i> -butyllithium
Et ₃ N	triethylamine
NHC	<i>N</i> -heterocyclic carbene
nm	nanometers
nM	nanomolar
NBS	<i>N</i> -bromosuccinimide
NMR	nuclear magnetic resonance
N. R.	no reaction
nOe	nuclear Overhauser effect

Nu	nucleophile
OAc	acetoxy
<i>o</i> -QM	<i>ortho</i> -quinone methide
ORTEP	Oak Ridge thermal ellipsoid plot
<i>p</i>	<i>para</i>
p	page
<i>p</i> -TSA	<i>para</i> -toluenesulfonic acid
Ph	phenyl
PMP	<i>para</i> -methoxy phenyl
ppm	parts per million
PPTS	pyridinium <i>para</i> -toluenesulfonate
Pr	propyl
pyr.	pyridine
q	quartet
quant.	quantitative
R	rectus
red.	reduction
R_f	retention factor
RT	room temperature
s	second(s); in NMR: singlet
S	sinister
satd.	saturated

Sc(OTf) ₃	scandium(III) trifluoromethanesulfonate
t	triplet
<i>t</i>	tertiary
<i>t</i> -Am	<i>tert</i> -amyl
TBAF	tetrabutylammonium fluoride
TBS	<i>tert</i> -butyldimethylsilyl
TBSCl	<i>tert</i> -butyldimethylsilyl chloride
TBSOTf	<i>tert</i> -butyldimethylsilyl trifluoromethanesulfonate
<i>t</i> -BuOH	<i>tert</i> -butyl alcohol
<i>t</i> -BuOOH	<i>tert</i> -butyl hydroperoxide
TCBC	2,4,6-trichlorobenzoyl chloride
td	triplet of doublets
TEA	triethylamine
Tf	triflate
TFA	trifluoroacetic acid
TFAA	trifluoroacetic anhydride
TFE	2,2,2-trifluoroethanol
THF	tetrahydrofuran
TiCl ₄	titanium(IV) chloride
TLC	thin layer chromatography
TMAF	tetramethylammonium fluoride

TMEDA	<i>N, N, N', N'</i> -tetramethylethylenediamine
TMS	trimethylsilyl
TMSCl	trimethylsilyl chloride
TMSOTf	trimethylsilyl trifluoromethanesulfonate
UPLC	ultra-performance liquid chromatography
wt. %	weight percent
Z	<i>Ger.</i> , zusammen

ABSTRACT

Chapter 1 outlines the discovery, biological mechanistic investigations, syntheses, and derivatization of (–)-englerin A, a guaiane sesquiterpene natural product exhibiting potent and selective renal cancer cell growth inhibition first described in 2009. The cellular mechanism by which the compound kills renal cancer cells is the subject of intense and ongoing study. The synthesis of new englerin tool compounds and analogues have been and continue to be used to investigate the mechanism(s) of action against renal cancer cells. The synthesis of analogues have also supported advancement of an englerin-derived compound to therapeutic candidacy.

Chapter 2, the first project herein, describes synthesis and development of a next generation series of analogues addressing the inherent therapeutic liabilities present within the natural product. This series of analogues is informed by a compendium of structure–function data and improved biological activities. The various substituents being incorporated into these analogues address the lethality observed in mice as well as the stability of the compound when administered orally. The goal of this project is to construct an analogue that may proceed through therapeutic candidacy ultimately leading to the development of an anti-cancer treatment.

Chapter 3 describes the efforts towards the synthesis and development of a new series of englerin-inspired proteomic tool compounds to aid in the elucidation of an unambiguous mechanism of action of (–)-englerin A against cancer cells. The tool

compounds will integrate covalent modifiers and clickable moieties for the purposes of cellular target identification and other mechanism studies in order to support the development of new drugs toward renal carcinoma based on englerins. Determining the mechanism of action is extremely important in the development of (–)-englerin A as a cancer therapeutic. Although there have been tool compounds developed in the past, the mechanism of action is still largely unknown. There is still a need for further development of tool compounds to probe this biological mechanism of action.

Chapter 4 describes the synthesis of an acyldepsipeptide fragment fluorescent tool compound used by the Karl Schmitz group to investigate the biological mechanism of action of acyldepsipeptide fragments towards tuberculosis. This tool compound was developed in a collaboration with Karl Schmitz and Joseph Fox of the University of Delaware.

Chapter 1

ENGLERIN A: ISOLATION, BIOLOGICAL ACTIVITY, SYNTHESSES, AND DEVELOPMENT TOWARDS ANTI-RENAL CANCER THERAPAUTIC CANDIDACY

1.1 Introduction to (-)-Englerin A

In 2018, 18.1 million new cases of cancer diagnosis and 9.6 million cancer-related deaths were reported by the World Health Organization. By 2040, it is estimated that there will be 29.5 million new cases of cancer per year and 9.5 million cancer-related deaths per year.¹ Renal cell carcinoma (RCC) is one type of cancer that affects the filtering of blood within the kidneys and is ranked as one of the top 10 most common malignancies in male and female subjects within the US.² Current strategies of treatment of RCC include surgery, immunotherapy, radiation therapy, molecular-targeted therapy, and chemotherapy. Within chemotherapy, the two drugs most commonly prescribed, bevacizumab and sorafenib, exhibit major side effects and require long-term administration. The treatment of renal cancer is a multi-billion dollar annual health burden in the United States alone. There is a need to further explore innovative treatment strategies for RCC.³

Small molecules are the most important approach to chemotherapy, representing more than 80% of the top 100 oncology drugs.⁴ In the context of renal cancer, three of the top four treatments are small molecules, one of which has its origin in a natural product. Biologically active natural products offer unique scaffolds that can be manipulated toward the development of novel drug leads.

The plant species *Phyllanthus engleri* is native to Tanzania and Zimbabwe and is known to traditional medicine systems of the indigenous cultures within these areas. The plant is most commonly used as a medicine for chest congestion by either smoking the stem bark or by consuming it as a gruel in water.⁵ The fruit and leaves are not considered to be toxic, however breathing the smoke from the burning root bark is reportedly lethal.⁶

In early 2009, the Molecular Targets Laboratory led by Dr. John Beutler at the National Cancer Institute discovered two new guaiane sesquiterpenes, englerins A (**1.1**) and B (**1.2**) (figure 1.1) in the 1:1 CH₂Cl₂ – MeOH extractives of the stem bark of *Phyllanthus engleri* in a bioassay-guided fractionation process specifically searching for renal cancer cell growth inhibitors; this study constituted the first interrogation of *Phyllanthus engleri* though the plant samples had been collected decades prior. (–)-Englerin A (EA) was shown to be responsible for the activity in the fractionation process – growth inhibition activity against the A498, 786–0, ACHN, RXF–393, SN12C, and UO–31 cell lines with GI₅₀ values under 11 nM except for SN12C (GI₅₀ = 87 nM).⁷ While EA was active in mouse xenografts, intravenous toxicity associated with the compound was observed and characterized by the Beutler group and independently as part of a Novartis study toward englerins as potential diabetes therapeutics.⁸ Englerin B has no significant activity.⁷

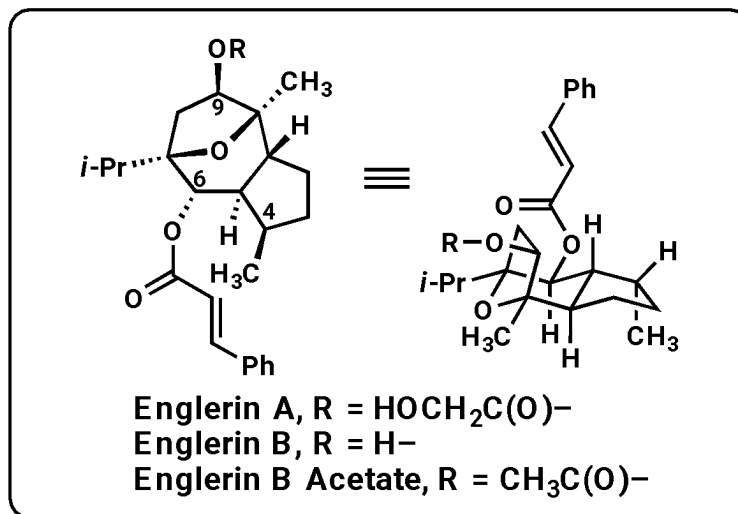


Figure 1.1 The structures of (-)-englerin A, englerin B, and englerin B acetate

1.2 Biological Mechanism of Action Investigations

Upon unveiling EA and its potent, selective anti-renal cancer activity, mechanism of action studies were conducted to elucidate the pathway by which EA causes death to cancer cells. Understanding the interactions between EA and the target site within these cancer cell lines is crucial to the development of EA as an anti-renal cancer drug candidate. An unambiguous determination of the structure and confirmation of the binding pocket along with the nature of the binding of EA to that pocket allows for greater predictions of relevant drug interactions and a more in depth understanding of structure–function relationships.

1.2.1 Necrosis in RCC due to Ca²⁺ uptake and Production of Reactive Oxygen Species

In 2012, the first study of the biological mechanism of action of EA was conducted by the Joe Ramos and William Chain groups.⁹ Within this study, there are a few key findings that are the basis for future biological research relevant to EA. They

used human RCC cell lines A-498 and UO-31 and the human glioblastoma cell line SF-295 as model cell lines for this experiment. First, it was reported that EA induces necrotic cell death of RCC cell lines but does not affect normal kidney cells. Next, they were able to identify evidence for two possible modes of action leading to the cell death. The first of which is the overproduction of reactive oxygen species (ROS) that are known to be typical inducers of necrotic signals. This study was also the first study to recognize an increase in cytoplasmic Ca^{2+} within the RCC cells, but they were not able to identify exact signaling pathways associated with these findings. These are extremely important findings, especially with the case of Ca^{2+} influx, that will end up being the subject of intense and ongoing studies related to the biological mechanism of action of EA.

1.2.2 Stimulation of PKC θ in the A498 Renal Cancer Cell Line

A 2013 study investigating the mechanism of action of EA within the 786-0, OK262, and UOK257 RCC cell lines implicated several isoforms of protein kinase C (PKC) as potential cellular molecular targets of the natural product.^{8b} The involvement of PKC and specifically PKC θ as the target isoform was strongly supported utilizing PKC knock-out studies within the 786-0 cell line.

A novel mechanism of action of EA in the context of cancer was proposed through further investigation into the involvement and role of PKC θ in the cytotoxicity of EA within this cell line (figure 1.2). The proposed mechanism of action is initiated by the binding and activation of PKC θ by EA within the cell; PKC θ then proceeds through two pathways simultaneously.

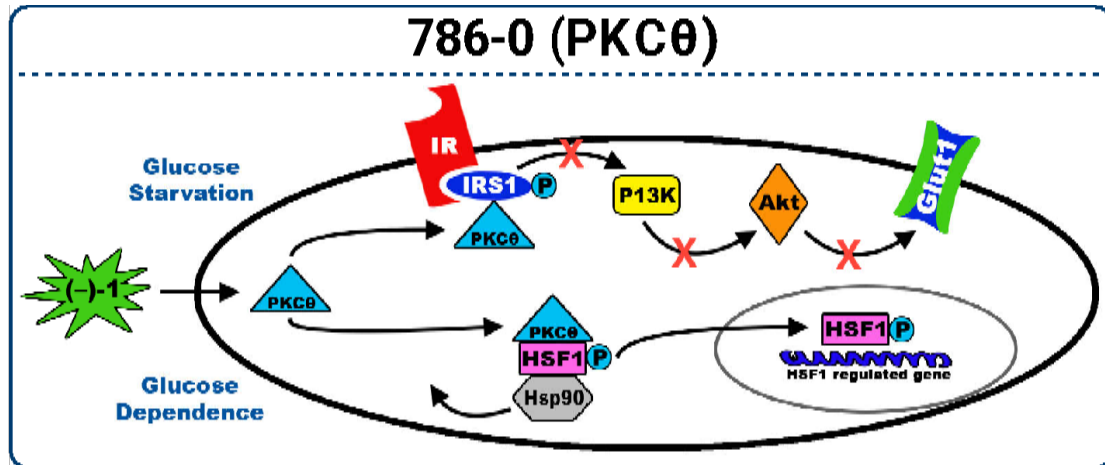


Figure 1.2 The proposed biological mechanism of action of EA in the 786-0 cell line

One of these pathways begins with the phosphorylation and inhibition of insulin receptor substrate 1 (IRS1), which reduces glucose intake through decreased signaling of Glut1 via the P13K/AKT pathway. This leads to glucose starvation within the cell. The second pathway involves the phosphorylation of the gene regulatory protein heat shock factor 1 (HSF1) by PKC θ and enhancement of the transcriptional activity of HSF1 through a dissociation from heat shock protein 90 (Hsp90). This results in a dependence of the cell on glucose, which when coupled with the absence of available glucose within the cell, leads to cell death.

1.2.3 Multiple Mechanisms of Cell Death and Autophagy

A 2013 study supported the conclusion that EA induces cellular death by multiple mechanisms and likely has multiple cellular targets.¹⁰ These results showed that EA induces caspase-independent apoptosis along with necrosis, as well as increasing the levels of autophagic vessels in A498 cells. It was suggested that autophagy is more likely a failed cell survival mechanism than a cell death mechanism

in the RCC cells. These results also demonstrated that EA may block the G2/M transition in the cell cycle and may inhibit the activation of AKT and ERK kinases, which are involved in cell proliferation and autophagy of cancer cells.

1.2.4 Modulation of L-Type Calcium Channels

In 2016, it was reported that voltage-dependent Ca^{2+} L-Type ($\text{Ca}_v1.2$) channels are a molecular target of EA.¹¹ Cross-natural product target-interference studies supported by molecular dynamics simulations supported this conclusion. Cross-natural product target-interference uses a small molecule with similar pharmacophore features to the molecule of interest as a tool compound to study the biological mechanism of action. In this study, the anti-cancer compound, piperlongumine (figure 1.3), was used to represent EA due to their similar shape, aromatic and hydrophobic features, and hydrogen bond character.

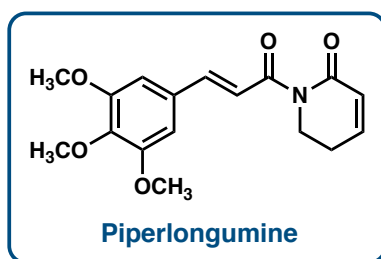


Figure 1.3 The anti-cancer compound piperlongumine

Using the rat cardiomyocytic cell line, H9C2, which does not express TRPC4/5, it was found that EA inhibits the influx of Ca^{2+} in a concentration-dependent manner. Molecular dynamics simulations using the open-state $\text{Ca}_v1.2$ homology model¹² were used to predict interactions of EA within the dihydropyridine

binding site. An important hydrogen-bonding interaction was identified between Leu121 and the glycolate hydroxyl present in EA, as well as hydrophobic CH- π interaction between the cinnamate phenyl in EA and the methylene of Phe202.

1.2.5 Transient Receptor Potential Canonicals and their Role in RCC Cytotoxicity Mediated by EA

Transient receptor potential (TRP) proteins are one class of nonselective cation channels used to control cellular function through the regulation of Na⁺, K⁺, and Ca²⁺ concentration within the cytosol. These channels can be activated through the voltage across the plasma membrane or through the binding of an external ligand or another protein.¹³ These proteins form homo- and heterotetramers to form the channels involved in the transportation of these cations. Within the mammalian TRP family, there exists a subfamily called the Transient Receptor Potential Canonicals (TRPC). There are 7 of these channels, all of which exist in humans except for TRPC2.¹⁴

The TRPCs can be found in a variety of cells and tissues including the brain, placenta, adrenal gland, retinal endothelia, testis, and kidneys.^{13, 15} The TRPCs can be divided into 3 structural subgroups, TRPC1/4/5, TRPC3/6/7, and TRPC2. TRPC1, TRPC4, and TRPC5 are reported to be involved in pathophysiological functions such as seizure, anxiety, fear, Huntington's disease, Parkinson's, intestinal motility, cardiac remodeling, visceral pain sensation, and neurite growth.¹⁶ TRPC1, TRPC4, and TRPC5 exist as both homomers and heteromers with one another, although it is suggested that homomeric TRPC1 channels do not serve any function.¹⁷ TRPC3/6/7 also tend to interact with one another forming heterotetramers, but the TRPC3/6/7 and TRPC1/4/5 subgroups do not normally interact with each other.¹⁸ It was also reported

that TRPC5 has a 65% and 45% sequence identity to TRPC4 and TRPC1, respectively.¹⁹

In 2015, the Christmann, Beech, and Waldmann groups identified TRPC1/4/5 ion channels as potential cellular targets of EA within the A498 RCC cell line.²⁰ Influenced by a study suggesting a link between TRPC4 and RCC²¹, they began their investigation by looking at the levels of expression of TRPC4 of the cell lines within the NCI60. They found that the A498 cell line exhibited the highest degree of expression of TRPC4 within the NCI60. Whole-cell voltage-clamp recordings revealed a large EA-induced current in cells expressing human TRPC1, TRPC4, and/or TRPC5. Their studies also suggested that EA does not proceed via G-protein signaling and appears to activate the ion channels through a direct external interaction at the leaflet of the bilayer. It was determined that the EA-induced activation of TRPC1, TRPC4, and/or TRPC5 causes an influx of Ca²⁺ into the cell, overloading the cell with these ions leading to cell death.

In 2016, David Beech published another article suggesting that the ion channels are not as selective as initially thought, and that Na⁺ and K⁺ are also included. Within this study, it was suggested that Na⁺/K⁺-ATPase counteracts the influx of cations through extrusion of these ions but is not able to keep up with the rate of influx. As a result, the cells are overloaded with Ca²⁺, Na⁺, and K⁺.²² It is suggested that this may be due to the presence of TRPC1.²²⁻²³

As mentioned previously, intravenous administration of EA to mice and rats is lethal.⁵⁻⁶ In 2018, David Beech et al. explored the nature of this lethality and the role that TRPC4/5 plays in mediating this adverse reaction.²⁴ Using TRPC4 and TRPC5 knockout studies, they were able to show that these ion channels appear to be directly

relevant to the adverse reactions. In TRPC4 and TRPC5 single knockout mice, partial protection of the mice against the adverse effects of EA is observed after intraperitoneal (i.p.) injection. In TRPC4/5 double knockout mice, mice show no adverse reaction to both intraperitoneal and intravenous (i.v.) administration. These results were further supported through the pre-administration of Pico145²⁵, a known selective inhibitor of TRPC4/5 channels with no known adverse effects, preventing the adverse effects of EA.

It has been suggested that investigation into the delivery of EA may allow for safe administration of the compound. It is shown that EA is lethal when administered via i.v. injection but explorations of other methods of delivery in a time-dependent manner may be beneficial for safe and efficient administration.¹⁷

In 2019, Insuk So et al. identified specific EA interaction sites within TRPC5 using a patch clamp technique.^{19b} They measured the EA-induced current increases of TRPC5 channels featuring various mutations within the pore region based on their propensity to sense H⁺ and HO⁻ ions. The TRPC currents were measured in human embryonic kidney cells (HEK293). Their results suggested that there are 3 residues that are involved in the EA interaction site; Lys554, His594, and Glu598; and several other residues that may be indirectly involved. They also mentioned that it is possible that the inactivity of EA on the channel because of these mutations may be a result of permeability changes or modulation of gating. They concluded that EA interacts with at least 3 amino acids causing activation and opening of the TRPC5 channel due to a conformational change in the selectivity filter gate and the inner gate at the bundle crossing.

1.2.5.1 Further Investigation of TRPC Channels

Due to the high abundance of TRPC1/4/5 in other parts of the body and its frequent involvement in other biological activities, research has been conducted to better understand these channels. This research can be applied to RCC cell lines featuring these channels to further develop our understanding of the interaction of EA with these ion channels to elucidate a biological mechanism of action. The research from a few of these articles is presented here.

Unambiguous determination of the structure of TRPC1, TRPC4, and TRPC5 have been under investigation as it would allow for an in-depth investigation of exactly how these channels interact with biologically active small molecules, such as EA. There have been a few reports regarding the structural determination of these ion channels.

The first of which was in May of 2018 by the Raunser group. Using cryo-electron microscopy (cryo-EM), they were able to isolate wild type TRPC4 in its unliganded (apo), closed state from zebrafish (76% sequence identity to human TRPC4).²⁶ They initially tried isolating human TRPC4 expressed in HEK293 cells but found it to be too unstable for structural investigations. The final structure that was elucidated using cryo-EM contained 70% of the entire structure, including residues 18–753 with some missing loops. Residues 754–915 could not be resolved suggesting a high flexibility in this region. This structure allows for the identification of the cation conducting pore, including the selectivity filter and lower gate. There were also 2 key sites identified as protein modulator interaction sites.

In June of 2018, the structure of mouse TRPC4 in its apo state was disclosed. The final structure featured residues 1–758 and excluded residues 759–974. Electrophysiological studies were performed to ensure the truncated structure featured

similar biophysical properties to full length TRPC4. With the structure in hand, they began exploration into its functional application by studying its interaction with EA. The results showed that mutation of Cys549A or Cys554A resulted in insensitivity to EA, suggesting that the structure's pore loop architecture is disrupted through disulfide bond formation, leading to an inaccessible channel.

In 2021, Chen et al. revealed the structure of human TRPC5 in its apo state as well as in complex with certain inhibitors.²⁷ There exist a few small molecule TRPC inhibitors that are used as tools in the investigation of these channels (figure 1.4). There are multiple classes of these inhibitors, one of which is the clemizole (CMZ) class featuring benzimidazole-derived compounds, including M084 and AC1903 that inhibit TRPC5.²⁸ Another class are methylxanthine derivatives such as HC-070, which is a TRPC4/5 inhibitor, Pico145, and the activator AM237.^{25, 29} Tonantzitolone is an activator of TRPC1/4/5 channels with nanomolar potency first reported in 2018.³⁰ EA is also used as a tool compound for TRPC channel investigation. The inhibitors used in Chen's investigation of TRPC5 were EA, CMZ, and HC-070.

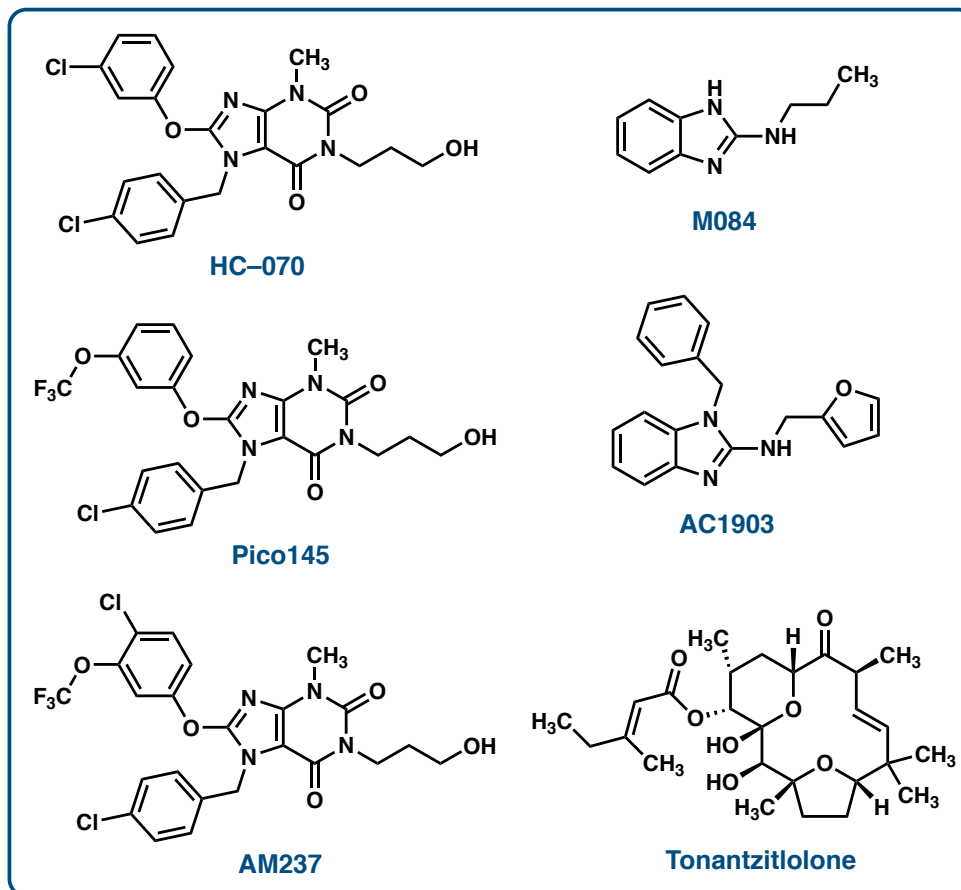


Figure 1.4 Alternative TRPC channel activators and inhibitors used for biological investigations

Unfortunately, they were not able to isolate the structure of the TRPC5 channel with EA bound, but they were able to prepare samples of the apo state of TRPC5, the CMZ-bound structure, and the HC-070-bound structure. Using these structures, they identified 3 possible inhibitor binding pockets (IBP-A-C). IBP-A is located inside the voltage sensor-like domain (VSLD). This binding site is accessible through the intracellular side via penetration of the plasma membrane. This aligns with the TRPC4 structure of the zebrafish showing inhibition inside the VSLD as well.²⁶ IBP-B is

located close to the extracellular side and is a common modulatory ligand binding site in the TRPC channels. IBP-C is the third binding site and is located between the VSLD and pore domain. It is suggested that this site is important for the gating of both TRPC and TRPV ion channels.²⁷

1.2.6 Rewiring Phosphosignaling via Hsp27 Hyperphosphorylation

In 2022, Gunaratne et al. explored other possible mechanisms of action of EA on RCC using proteomics mass spectrometry coupled with computational and biological techniques to develop an EA-responsive phosphorylation landscape of A498 cells.³¹ They compared the phosphoproteomic profile of EA-treated cells with that of the untreated cells followed by a phosphosignaling network analysis. They were able to identify key cellular stress signaling events induced by EA.

Their results show that EA activates p38 signaling leading to a downstream hyperphosphorylation of the mediator, heat shock protein 27 (Hsp27). One site of elevated phosphorylation on Hsp27 is Ser65, which reveals cytotoxic effects in the normally EA-unresponsive HEK293 cell line. This suggests that Hsp27 may play a key role in mediating the cytotoxic effects EA. It is also worth noting that kidney cancer cells feature the highest expression of Hsp27 when compared to 375 cancer cell lines, suggesting that this mechanism may persist in other RCC cell lines.³²

1.2.7 EA-Mediated Effects in Other Biological Systems

EA has not only been found to inhibit the growth of RCC cells but has shown to be active in other diseases as well. In 2017, David Beech et al. showed that EA mediates cytotoxicity in synovial sarcoma cells (SW982) ($IC_{50} = 30$ nM) through a similar manner to that of RCC cells. EA causes an influx of Na^+ into the cell through

an activation of heteromeric TRPC4/1 channels. This is coupled with insufficient counteractive expulsion of Na^+ and K^+ by Na^+/K^+ -ATPase ultimately leading to cell death.³³

In 2016, EA was found to be potently active in Ewing's sarcoma cells. The Woldemichael group studied the biological interactions between EA and Ewing's sarcoma cells causing the necrosis and apoptosis of these cells.³⁴ Through a high throughput screen, they were able to identify EA as inhibiting the activity of EWS-FLI1, an aberrant transcription factor seen as a key contributor in the tumorigenesis and progression of Ewing's sarcoma.³⁵ This transcription factor is only found in Ewing tumors leaving it as an attractive target for small molecule treatment of the disease. Through this study they were able to reveal a few things that may contribute to the mechanism of action of EA in these cells. EA was found to decrease the phosphorylation of EWS-FLI1 leading to a decreased ability to bind to DNA, which appears to be mediated by intracellular PKC β I as EA also leads to an increase in cytosolic calcium levels. It was also determined that EA correlated with decreased tumorigenicity in Ewing's cells and cell cycle arrest. This study was able to use EA to show possible targets for the treatment of Ewing's sarcoma and the biological mechanism of action of the treatment of these targets.

EA has also shown to be a potent inhibitor of triple-negative breast cancer cell lines, Hs578T and BT-549.³⁶ Triple-negative breast cancers (TNBCs) represent 15–20% of all breast cancers and are defined by a lack of estrogen receptor, progesterone receptor, and human epithelial growth factor receptor amplification. The current treatments for these cancers provide 23–55% relapse-free 10-year survival, emphasizing the demand for alternative treatment options.³⁷ The groups of John

Beutler and Susan Mooberry were able to identify 2 TNBC cell lines sensitive to cytotoxicity by EA, Hs578T ($IC_{50} = 16$ nM) and BT-549 ($IC_{50} = 5.4$ nM). The sensitivity of these cell lines is attributed to the higher levels of expression of TRPC4 in BT-549 and both TRPC4 and TRPC1 in Hs578T. Higher TRPC4 expression led to increased levels of Ca^{2+} , while when TRPC1 was present, it was mainly elevated levels of Na^{+} that were measured. It was also shown that increases in the Ca^{2+} concentration initiated mitochondrial depolarization which is likely contributing to the cytotoxicity observed in BT-549.³⁶

In 2021, EA was found to possess analgesic and anti-inflammatory properties unrelated to the TRPC4/5 channels.³⁸ Using a carrageenan model of inflammation in mice, treatment with EA showed a reduction in inflammation and an observed analgesic effect that was shown to be independent of TRPC4/5 channel activation. However, at the end of their study, they report that the lack of an identifiable target along with the reported cytotoxicity may render EA an invaluable drug discovery target for this application.

1.3 Total and Formal Syntheses of Englerin A

Since the first disclosure of EA in 2009, it has been a popular target for the synthetic community due its complex and intricate structure and promising biological activity. As of this writing, there are over twenty total and formal syntheses along with a few articles published featuring unique strategies of achieving adaptable core structures that could be applied to the synthesis of EA. This review features all of the published total and formal syntheses of EA in chronological order as well as the published alternative strategies that have not been used in the synthesis of EA.

1.3.1 Christmann – Total Synthesis of (+)-Englerin A and Determination of Absolute Stereochemistry (October 2009)

The first synthesis of englerin A was published in 2009 by Mathias Christmann et al. starting from *cis,trans*-nepetalactone, the psychoactive component of catnip.³⁹ The 5-membered ring of nepetalactone will be the 5-membered ring in englerin while the lactone will be transformed into the 7-membered ring through the following steps (figure 1.5). Using *m*-CPBA to afford epoxide **1.3**, they then performed a ring contraction using NaOMe to afford lactone **1.4**. A Barbier⁴⁰ coupling was used to afford homoallylic alcohol **1.6**. They perform a reductive ring opening of the lactone followed by the acetal protection of the resultant 1,2-diol. An oxidation of the primary alcohol using IBX, followed by an epimerization of the resultant aldehyde, and a Wittig⁴¹ olefination affords diene **1.7**. From here a ring closure, ether bridge formation, and installation of the cinnamate and glycolate esters is all that remains. This is accomplished through a Grubbs⁴² ring closing metathesis of **1.7**, acetal deprotection, and installation of the TBS-protected glycolate ester to afford **1.8**. An oxidation of the olefin to the epoxide and an epoxide ring opening cyclization under thermal conditions completes the core. A Yamaguchi⁴³ esterification to install the cinnamate ester followed by the removal of the TBS protecting group completes the synthesis of (+)-englerin A is 15 steps and a 10.9% yield overall. This allowed for the determination of the absolute configuration of englerin A, as (+)-englerin A is the inactive enantiomer of englerin A. In 2011, the Christmann group applied the same route in the synthesis of the biologically active enantiomer (–)-englerin A using a synthetic nepetalactone.⁴⁴

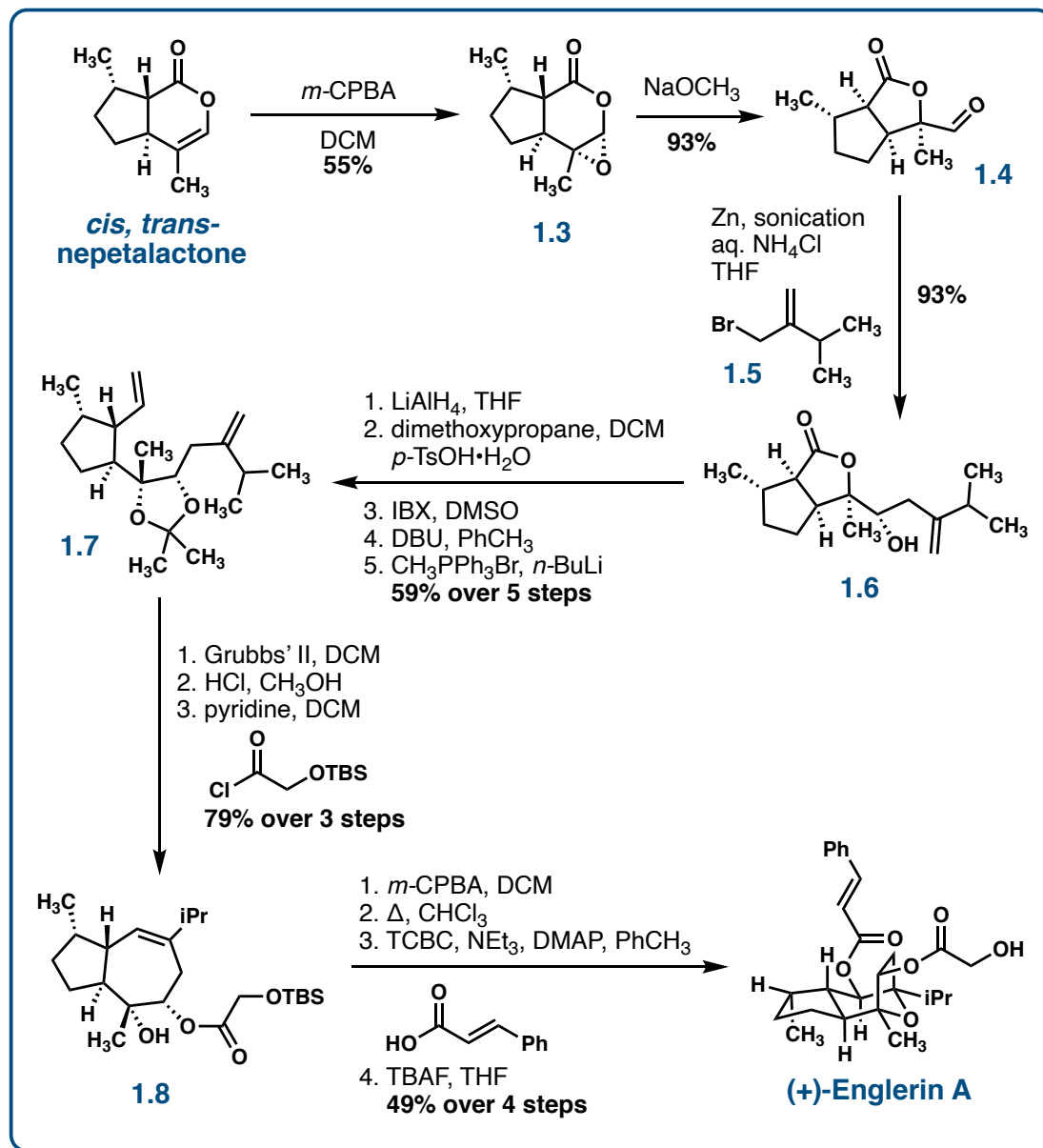


Figure 1.5 Total synthesis of (+)-englerin A completed by Mathias Christmann et al.

1.3.2 Echavarren – Total Synthesis of (–)-Englerin A (April 2010)

On April 6th of 2010, the Echavarren⁴⁵ and Ma⁴⁶ groups published concurrent total syntheses of EA using Au-catalyzed Prins⁴⁷ cyclizations of enynes developed by

Echavarren in 2006.⁴⁸ This methodology allowed for the completion of the 7,5-ring system featuring the ether bridge through a [2+2+2] cycloaddition of linear precursors.

In order to reach the linear precursor **1.14**, they started with commercially available and inexpensive geraniol (figure 1.6). A Sharpless⁴⁹ epoxidation of geraniol followed by an Appel⁵⁰ chlorination and reaction with *n*-BuLi afforded enyne **1.10**. A TES-protection, oxidative cleavage to afford the aldehyde, and Wittig⁴¹ olefination gave enal **1.11**. A stereoselective Denmark⁵¹ aldol reaction sets them up the Au-catalyzed Prins cyclization followed by a deprotection/protection sequence to afford the completed core **1.15**. A few oxidative manipulations along with installation of the acyl side chains will give them EA. Isomerization of **1.15** to **1.16** was accomplished through an epoxidation/reduction sequence. Diastereoselective, catalytic hydrogenation of the allylic alcohol **1.16** followed by an esterification of the alcohol installs the cinnamate ester. A deprotection of the TBS group gives (–)-englerin B. A Yamaguchi⁴³ esterification with the protected glycolate ester with a final deprotection of the TBDPS group completes the synthesis of EA in 18 steps at an overall yield of 7%.

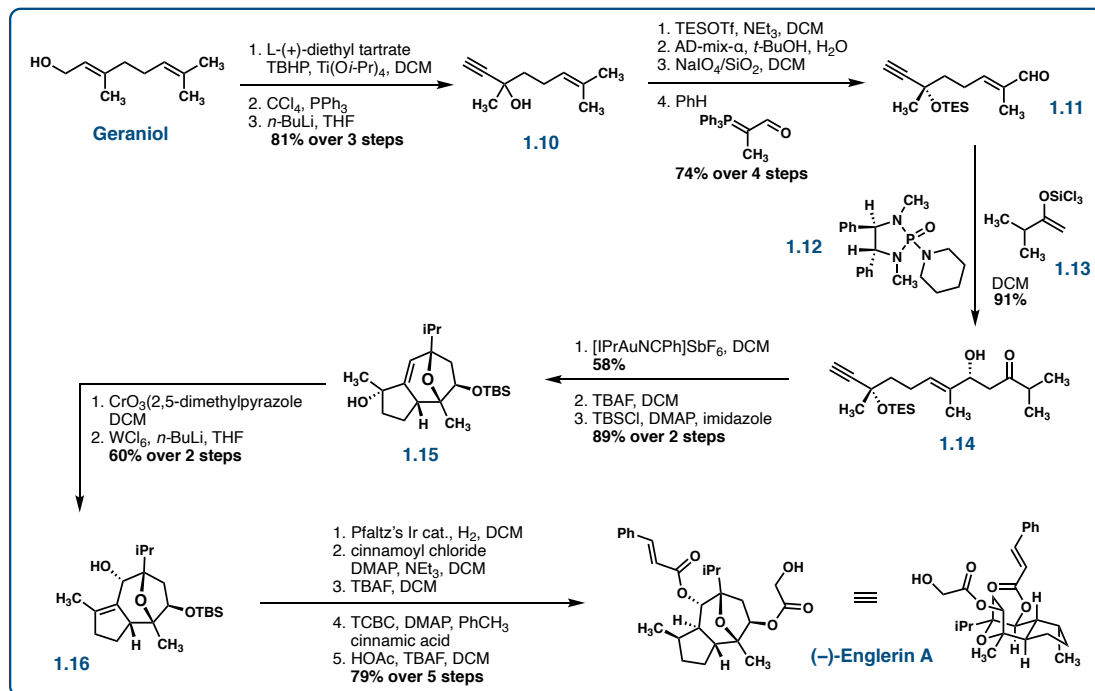


Figure 1.6 Total synthesis of (-)-englerin A completed by Antonio Echavarren et al.

1.3.3 Ma – Total Synthesis of (-)-Englerin A (April 2010)

Also on April 6th of 2010, the Ma group disclosed a synthesis of EA utilizing a similar strategy shown in figure 1.7.⁴⁶ Starting with (*R*)-(+)-citronellal, a geminal dibromination and elimination generates the terminal alkyne. Allylic oxidation with a boron-mediated enantioselective aldol addition of the resultant aldehyde affords enyne **1.17**. The Au-catalyzed [2+2+2] cycloaddition affords the core structure **1.18**. An epoxidation and subsequent epimerization give allylic alcohol **1.19**. Inversion of the stereochemistry of the two alcohols is informed through an oxidation and reduction of the resultant ketones. A directed hydrogenation of the alkene affords **1.20**. A selective Dess-Martin⁵² oxidation of one alcohol and Yamaguchi⁴³ esterification of the other affords ketone **1.21**. Installation of the glycolate was performed by reduction of the

ketone and activation of the alcohol with an imidazole sulfonate followed by substitution with cesium glycolate. This synthesis of EA was completed in 15 steps with an overall yield of 8.1%.

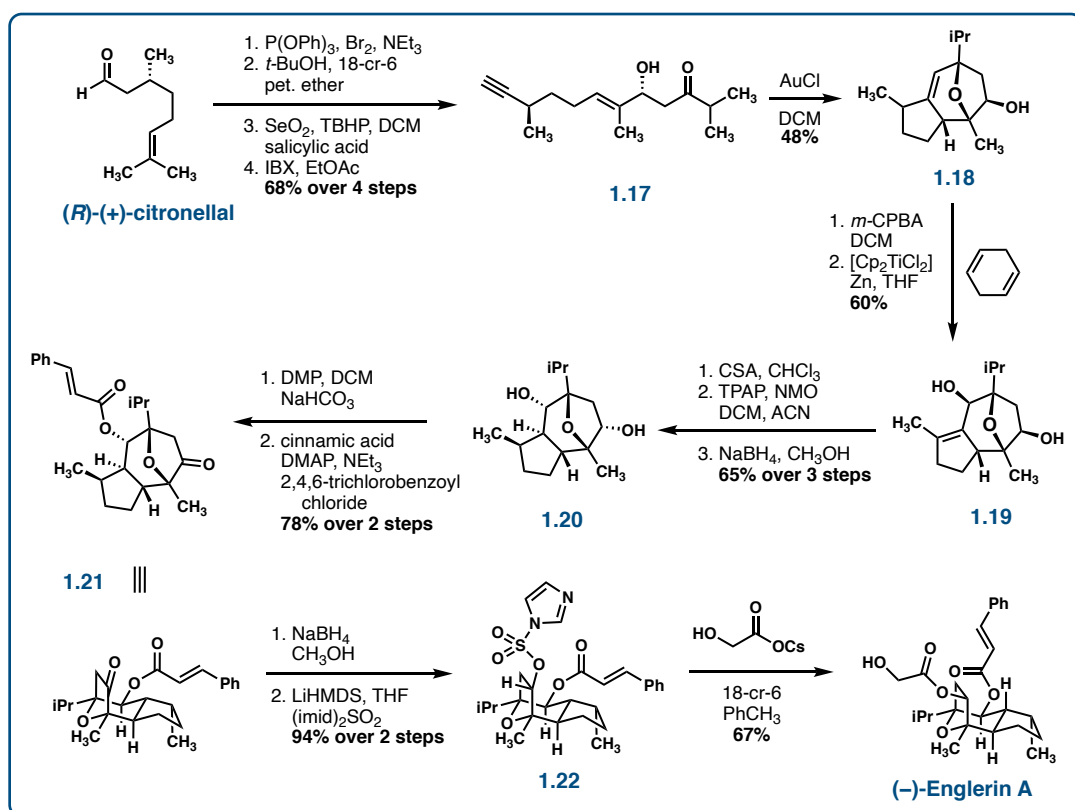


Figure 1.7 Total synthesis of (-)-englerin A completed by Dawei Ma et al.

1.3.4 Nicolau and Chen – Total Synthesis of (±)-Englerin A & Formal Synthesis of (-)-Englerin A (May 2010)

In 2010, the Nicolau and Chen groups described a synthesis of englerin A that featured a [5+2] cycloaddition reaction to form the 7-membered ring with the ether bridge.⁵³ The synthesis commenced with a regioselective iodination of propargylic

alcohol **1.23** setting them up for a Sonogashira⁵⁴ with TMS acetylene giving enyne **1.24** (figure 1.8). Removal of the TMS group followed by a gold-catalyzed ring closure forms furan **1.25**. A formylation and Grignard⁵⁵ addition into the newly formed aldehyde affords alcohol **1.26**. When treated with *m*-CPBA, **1.26** undergoes a Achmatowicz⁵⁶ rearrangement expanding the ring to lactol **1.27**. This sets them up for the [5+2] cycloaddition which is accomplished by activation of the alcohol with mesyl chloride and elimination of the mesylate to afford the oxopyrylium **1.28**. This oxopyrylium in the presence of ethyl acrylate completes the 7-membered ring featuring the ether bridge, **1.29**, through the [5+2] cycloaddition. The remainder of the synthesis involves formation of the 5-membered ring and installation of the ester side chains.

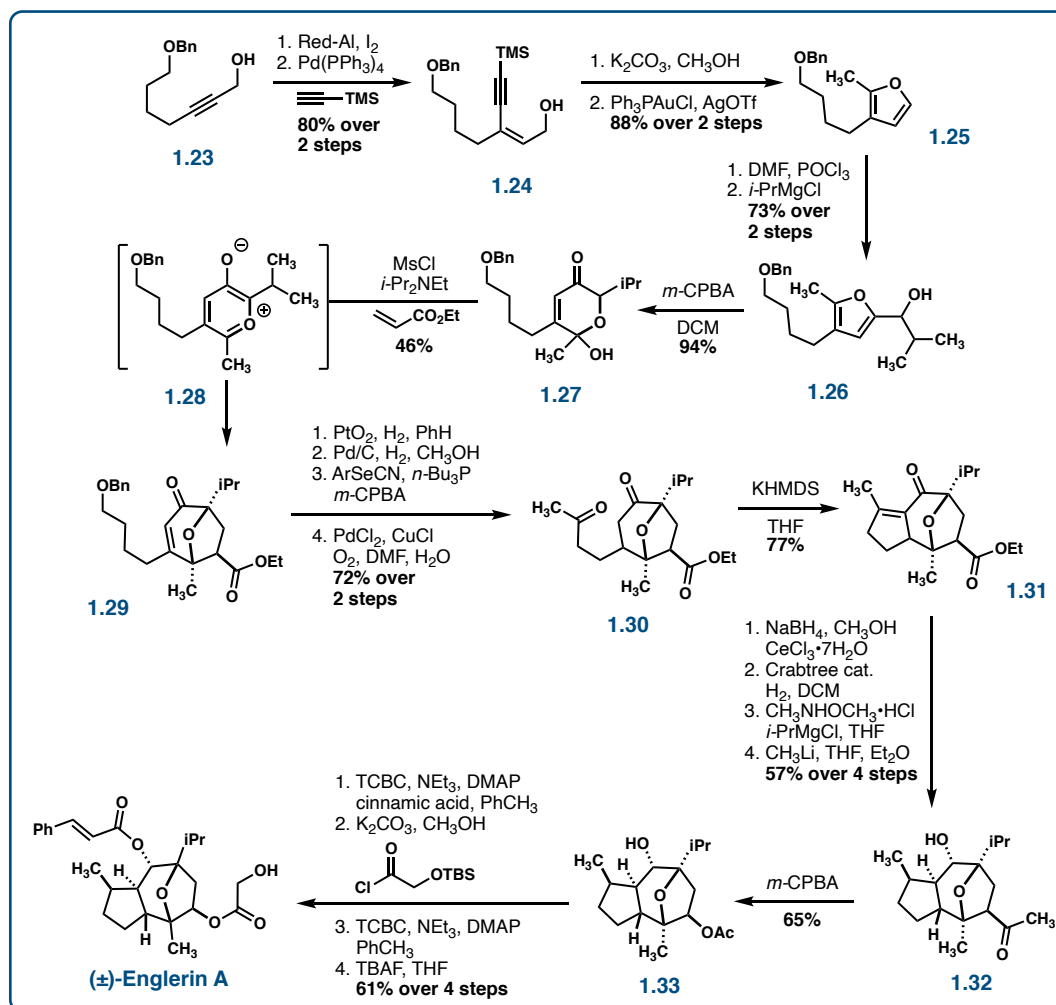


Figure 1.8 Total synthesis of (±)-englerin A completed by the K. C. Nicolau and David Chen groups

Removal of the benzyl protecting group and reduction of the alkene proceed under hydrogenation conditions. A selenide dehydration of the resultant free alcohol to afford a terminal alkene followed by the Wacker⁵⁷ oxidation of the alkene affords ketone **1.30**. Treatment with KHMDS completes formation of the 5-membered ring through an aldol condensation to give **1.31**. A Luche⁵⁸ reduction of the ketone to the

allylic alcohol is followed by a diastereoselective hydrogenation of the olefin. The ester is then transformed to the methyl ketone through the Weinreb⁵⁹ amide to afford **1.32**. Using a Baeyer-Villiger⁶⁰ oxidation, the ketone is taken to the acetate to install the oxygen at the correct position on the core, **1.33**. A Yamaguchi⁴³ esterification is used to install the cinnamate ester. Removal of the acetyl protecting group leaves the free alcohol where the glycolate is then installed through another Yamaguchi⁴³ esterification and a final deprotection of the TBS-protected glycolate. This completes their synthesis of (±)-englerin A in a total of 17 steps in a 2.9% yield overall.

They then proceeded to show the enantioselective formal synthesis of EA through a stereoselective [5+2] cycloaddition with the preceding steps leading to unsaturated ketoester **1.29**.

1.3.5 Theodorakis – Formal Synthesis of (–)-Englerin A (August 2010)

In August of 2010, the Theodorakis group published an enantioselective formal synthesis of EA that is initiated through a [4+3] cycloaddition between furan **1.35** and diazo compound **1.34** to afford the ether bridged 7-membered ring **1.36** (figure 1.9).⁶¹ Formation of the 5-membered ring ensues first through a removal of the auxiliary by treatment with DIBAL followed by Lewis acid to afford the rearrangement to the unsaturated ketone **1.37**. Next, a Rubottom⁶² oxidation oxidizes the α -position of the ketone to the alcohol retaining the undesired stereochemistry. Following a TBS protection of the alcohol, a thiazolium salt-catalyzed 1,4-addition with propanal afforded diketone **1.38**. An aldol condensation is accomplished using NaHMDS followed by heating in NaOMe/MeOH to complete the scaffold of EA **1.39**. Reduction and benzyl protection of the remaining ketone gives a benzyl protected allylic alcohol. A hydroboration/oxidation/TBS protection of the internal olefin within the 7-

membered ring with subsequent hydrogenation to remove the benzyl protecting group affords allylic alcohol **1.40**. Deoxygenation to remove the alcohol was achieved through dehydration with Burgess⁶³ reagent followed by hydrogenation. Global deprotection of the TBS alcohols achieves **1.41** completing their formal synthesis of EA in 15 steps at a 5% overall yield. They reference the work completed by Ma⁴⁶ to accomplish the rest of the synthesis from intermediate **1.41**.

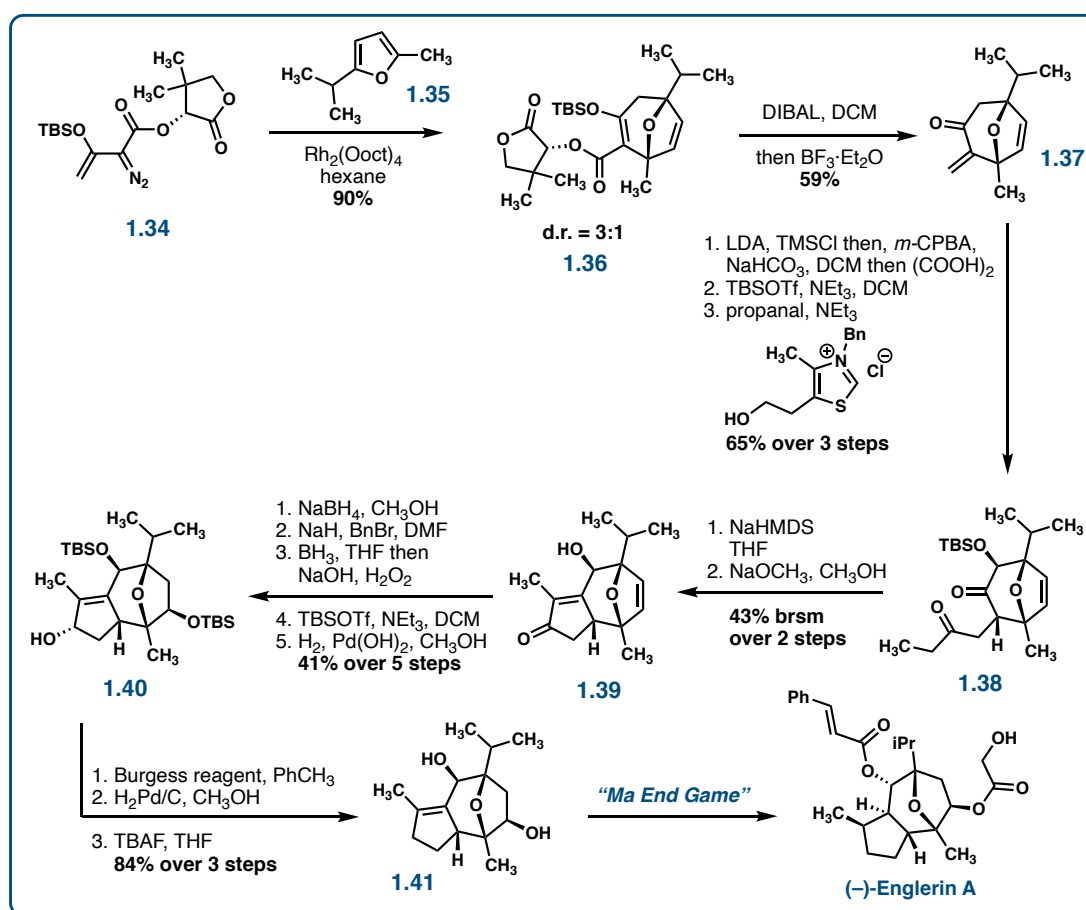


Figure 1.9 Formal synthesis of (-)-englerin A completed by Emmanuel Theodorakis et al.

1.3.6 Chain – Total Synthesis of (–)-Englerin A (April 2011)

In April of 2011, the Chain lab developed an innovative strategy towards the synthesis of EA by breaking the core into 2 key pieces, furanone **1.44** and enal **1.47**.⁶⁴ These pieces can be stitched together through a Michael addition⁶⁵ and SmI₂ reductive cyclization. The furanone and enal pieces can each be made in 2 steps from commercially available starting materials (figure 1.10). The synthesis of the furanone commences with a Claisen⁶⁶ condensation between isopropyl methyl ketone and α -chloroester **1.42**. The resultant diketone **1.43** is then cyclized under basic conditions to afford the furanone **1.44**. The second key piece, enal **1.47**, is obtained by starting with (*R*)-(+)-citronellal. Eschenmoser's⁶⁷ salt is used to complete an α -methenylation which can then be cyclized using Grubbs'⁴² olefin metathesis. This sets them up for the first key step, the Michael addition, connecting the α -position of the furanone to the β -position of the unsaturated aldehyde to afford **1.48** in a diastereomeric ratio of 2:1 of the desired diastereomer to the sum of the others. The aldehyde that is remaining is then coupled to the β -position of the unsaturated ketone to complete the core **1.49**. The resultant alcohol **1.49** is esterified with cinnamic acid under Yamaguchi⁴³ conditions. The remaining ketone is reduced to the alcohol and activated with a sulfonyl imidazole to give **1.51**. Substitution of the sulfonate with cesium hydroxyacetate affords EA in 8 steps in an overall yield of 20%; the Chain approach to EA remains the most efficient synthesis to date.

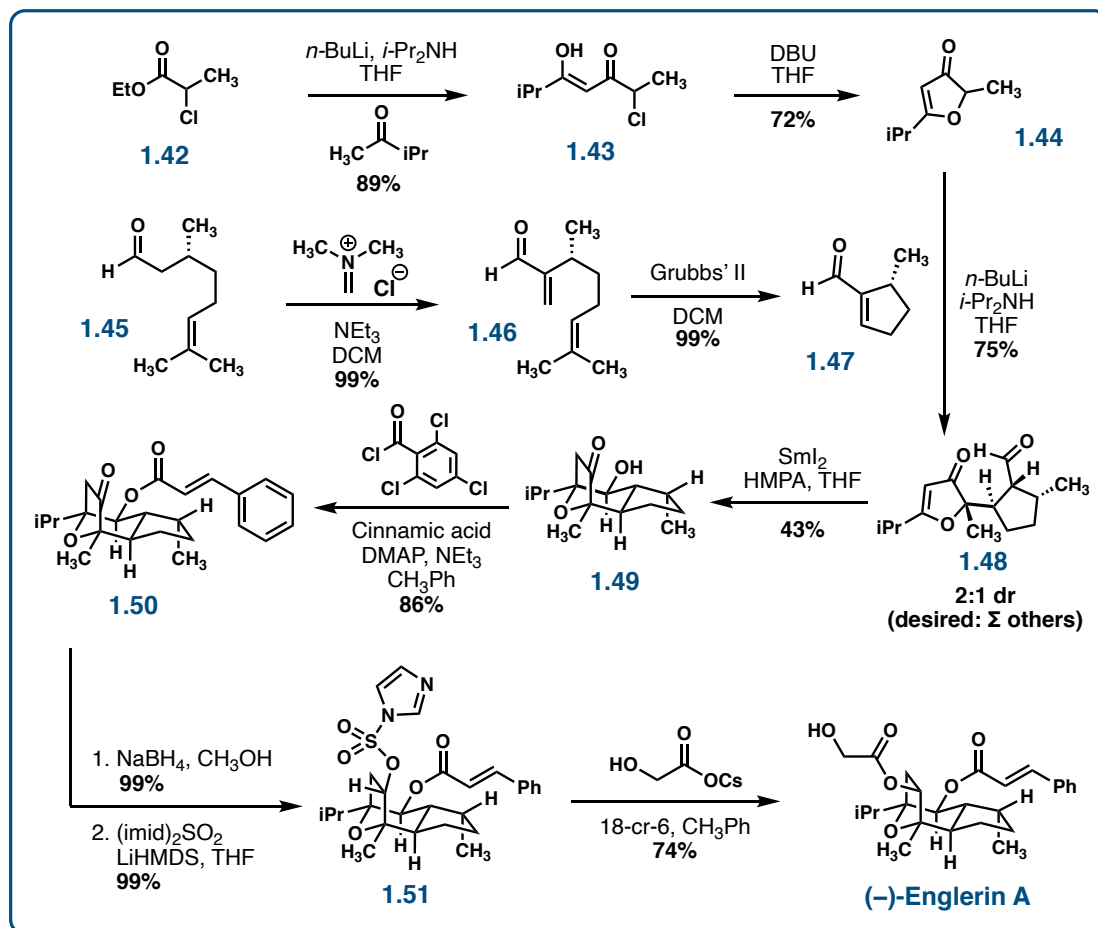


Figure 1.10 Total synthesis of (-)-englerin A completed by Chain and coworkers

1.3.7 Parker – Formal Synthesis of (-)-Englerin A (May 2012)

In May of 2012, Kathlyn Parker and her group described a formal synthesis of EA utilizing an olefin metathesis reaction to form the 7,5-ring system in one step from a linear precursor.⁶⁸ This synthesis begins with an allylation of geraniol followed by a Riley⁶⁹ oxidation of the tertiary olefin to generate an allylic alcohol (figure 1.11). An asymmetric epoxidation on the alkene of the allylic alcohol under Sharpless⁴⁹ conditions followed by the opening of the epoxide with lithium acetylide affords diol **1.52**. A Swern⁷⁰ oxidation brings the primary alcohol to the aldehyde allowing for a

Barbier⁴⁰ addition of allylic bromide **1.53** to install one final olefin. This produces a mixture of diastereomers at the newly formed alcohol, both of which are pushed forward. A protection of the 1,2-diol with a carbonate sets them up for the key relay ring closing metathesis reaction that completes the formation of the 7,5-ring system. This reaction allows for the coupling of both alkenes to the central alkyne using Stewart-Grubbs⁴² catalyst. Removal of the carbonate protecting group affords the diol **1.55**. The next thing that needs to be done is formation of the ether bridge. By first protecting the alcohol with a TBS group, they can use an oxymercuration reaction with $\text{Hg}(\text{O}_2\text{CCF}_3)_2$ to construct the alkyl mercury **1.56**. An oxidative demercuration removes the Hg leaving allylic alcohols **1.57** and **1.58**. EA can then be furnished from **1.58** through an interception of the synthesis described by Echavarren in 7 steps.⁴⁵ This completes the formal synthesis of EA by achieving intermediate **1.58** in 12 steps at a 6.8% yield overall.

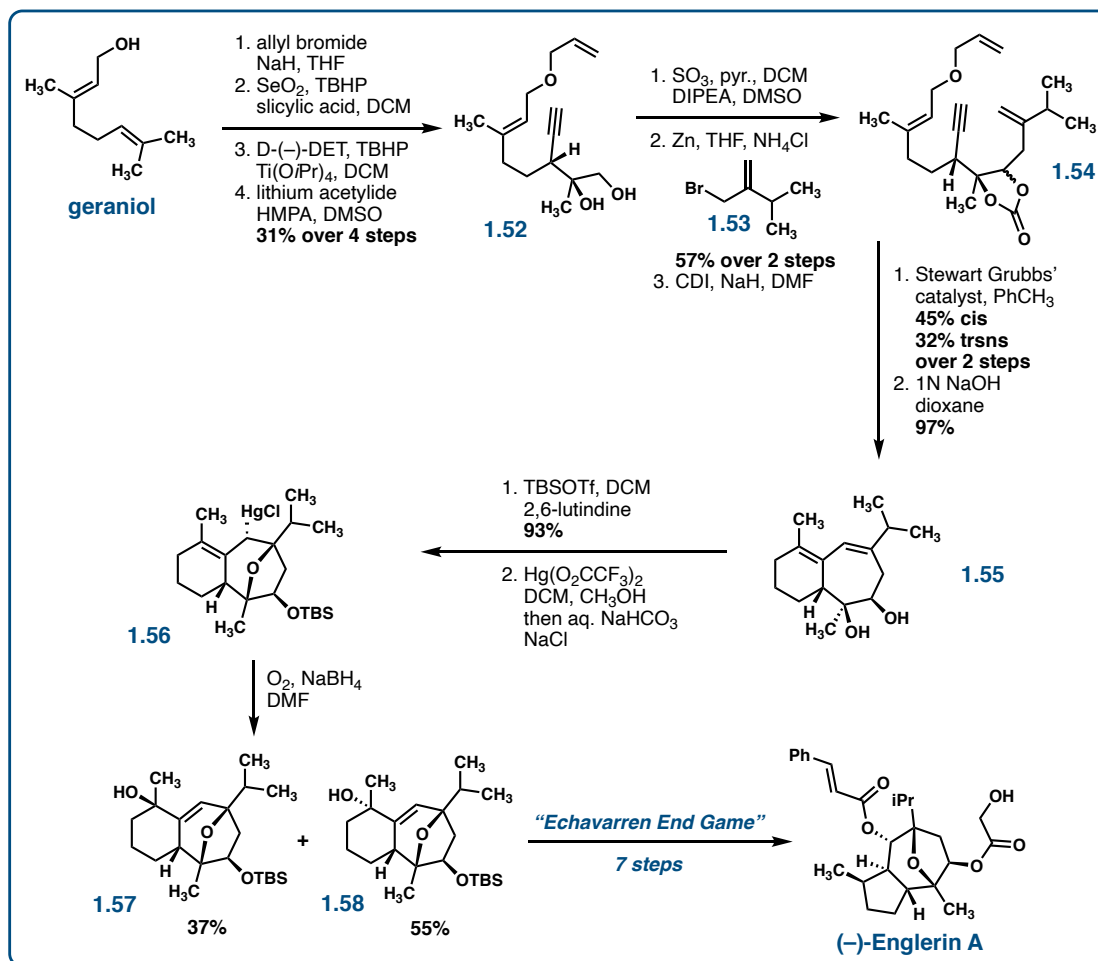


Figure 1.11 Formal synthesis of (-)-englerin A completed by Kathlyn Parker et al.

1.3.8 Hatakeyama – Total Synthesis of (-)-Englerin A (August 2012)

In August of 2012, Hatakeyama⁷¹ described a synthesis of EA using Stork's epoxynitrile cyclization⁷² to furnish the cyclopentyl ring system and a Grubbs⁴² metathesis to install the 7-membered ring. Their synthesis begins with a Baeyer-Villiger⁶⁰ oxidation of commercially available cyclopentanone **1.59** as shown in figure 1.12. A reductive ring opening of lactone **1.60** followed by a Wittig⁴¹ olefination of the resultant aldehyde affords unsaturated ester **1.61**. Installation of the nitrile is

achieved through a tosylation of the alcohol followed by reduction of the ester to the alcohol and finally substitution of the tosylate with NaCN. A Sharpless⁴⁹ asymmetric epoxidation is used followed by a TBS protection of the alcohol to transform allylic alcohol **1.62** into epoxynitrile **1.63**. Treatment of **1.63** under Stork's cyclization conditions completes the 5-membered ring in 9 steps. They then work to prepare for a Grubbs cyclization to construct the 7-membered ring.

The nitrile is transformed into an alkene first by protecting the alcohol with a MOM group. The nitrile is then reduced to the aldehyde with DIBAL and subjected to a Wittig⁴¹ olefination to afford terminal olefin **1.65**. On the other alkyl chain, the TBS on the primary alcohol is removed and the alcohol is oxidized to the aldehyde under Swern⁷⁰ conditions. Attempts at coupling the aldehyde with allylic bromide **1.66** under Barbier⁴⁰ conditions using Zn along with Nozaki-Hiyama⁷³ allylation conditions using CrCl₂ were unfruitful, resulting in either low yield or low diastereoselectivity. Treatment with indium afforded an 8:1 d.r. of the desired diastereomer **1.67** to its epimer in a 95% yield. The inseparable mixture of epimers is treated with concentrated HCl to remove the MOM protecting group and to allow for chromatographic separation of the epimers. Protection of the 1,2-diol sets them up for the Grubbs⁴² metathesis affording the internal olefin. Asymmetric epoxidation of the resulting olefin using monoperoxyphthalate (MMPP) gave epoxide **1.69**. A removal of the carbonate protecting group followed by selective esterification of the secondary alcohol using a Steglich⁷⁴ esterification affords the protected glycolate ester. The ether bridge can be formed through an epoxide ring opening cyclization under thermal conditions to afford free alcohol **1.70**. A Yamaguchi⁴³ esterification followed by a TBDPS deprotection affords EA in a total of 24 steps at an overall 14% yield.

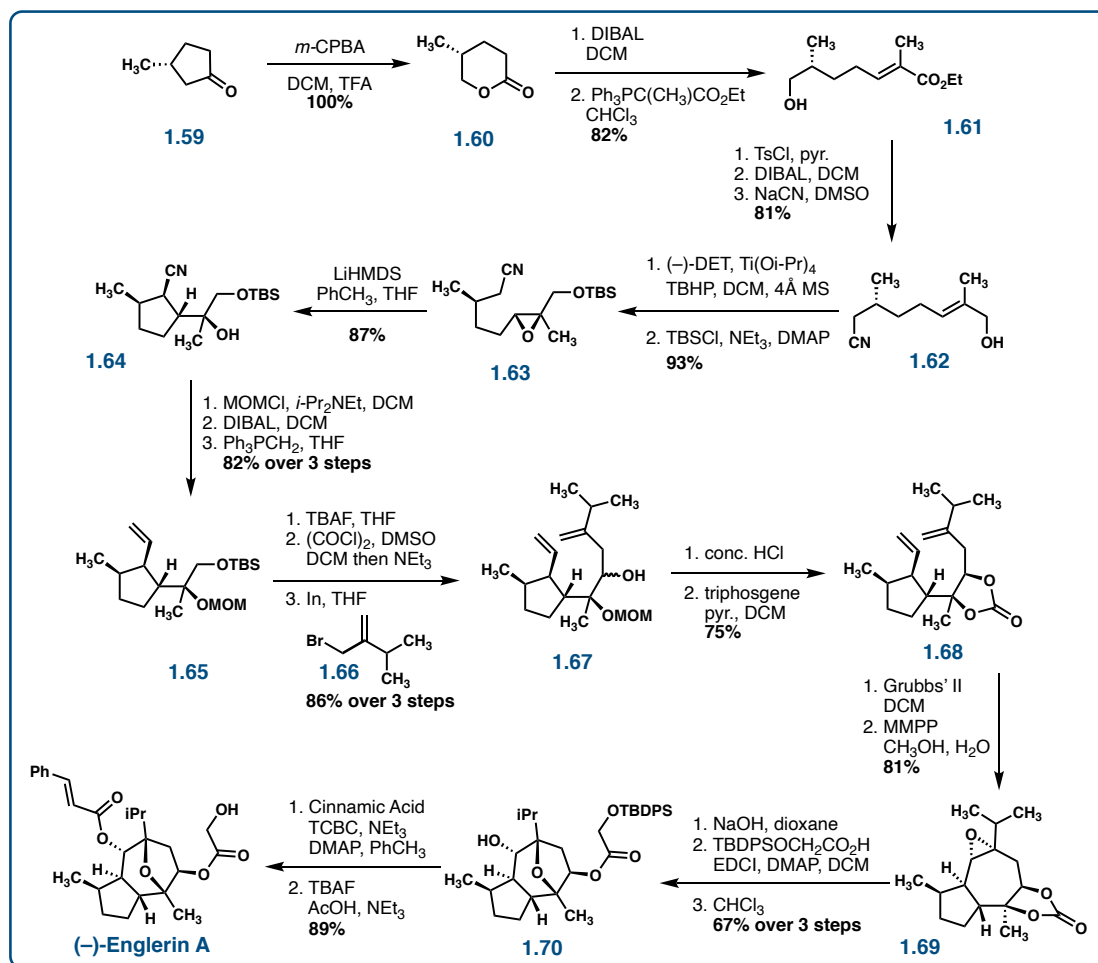


Figure 1.12 Total synthesis of (-)-englerin A completed by Susumi Hatakeyama et al.

1.3.9 Shang, Sun, and Lin – Total Synthesis of (+)-Englerin A (January 2013)

In January of 2013, the Shang, Sun, and Lin groups completed the synthesis of (+)-englerin A using a [4+3] cycloaddition between the known furan **1.71** and diene **1.72** to complete the ether bridged 7-membered ring (figure 1.13).⁷⁵ This [4+3] cycloaddition was achieved using catalyst **1.73** in TFA and nitromethane to afford compound **1.74** in 63% as a mixture of isomers. They then attempted multiple strategies to inform the construction of the 5-membered ring including an

intramolecular aldol condensation, SmI₂ cyclization, and a Shapiro⁷⁶ reaction using the hydrazone before realizing the transformation through an intramolecular Heck⁷⁷ reaction strategy. Vinyl Grignard⁵⁵ in the presence of cerium trichloride afforded allylic alcohol **1.75** through the addition into the aldehyde. An acylation of the resultant alcohol allowed for its removal using ammonium formate in the presence of palladium tetrakis affording olefin **1.76**. Enolization of the ketone followed by a Heck⁷⁷ coupling between the alkene and newly formed vinyl triflate completed the core structure of EA, **1.77**. A selective epoxidation of the more electron-rich olefin followed by reductive opening of the epoxide using DIBAL afforded alcohol **1.78**. Inversion of the alcohol was accomplished through an oxidation/reduction sequence and hydroboration–oxidation of the less substituted olefin affording diol **1.79**. Hydrogenation of the tetrasubstituted olefin using Pfaltz⁷⁸ catalyst followed by esterification with acyl protected glycolic acid chloride affords **1.80**. Yamaguchi⁴³ esterification and saponification of the acyl protecting group affords EA in a total of 15 steps in a 3.5% yield overall. In this publication, they were also able to complete the total syntheses of Englerin B, oxyphyllol, and orientalol E and F.

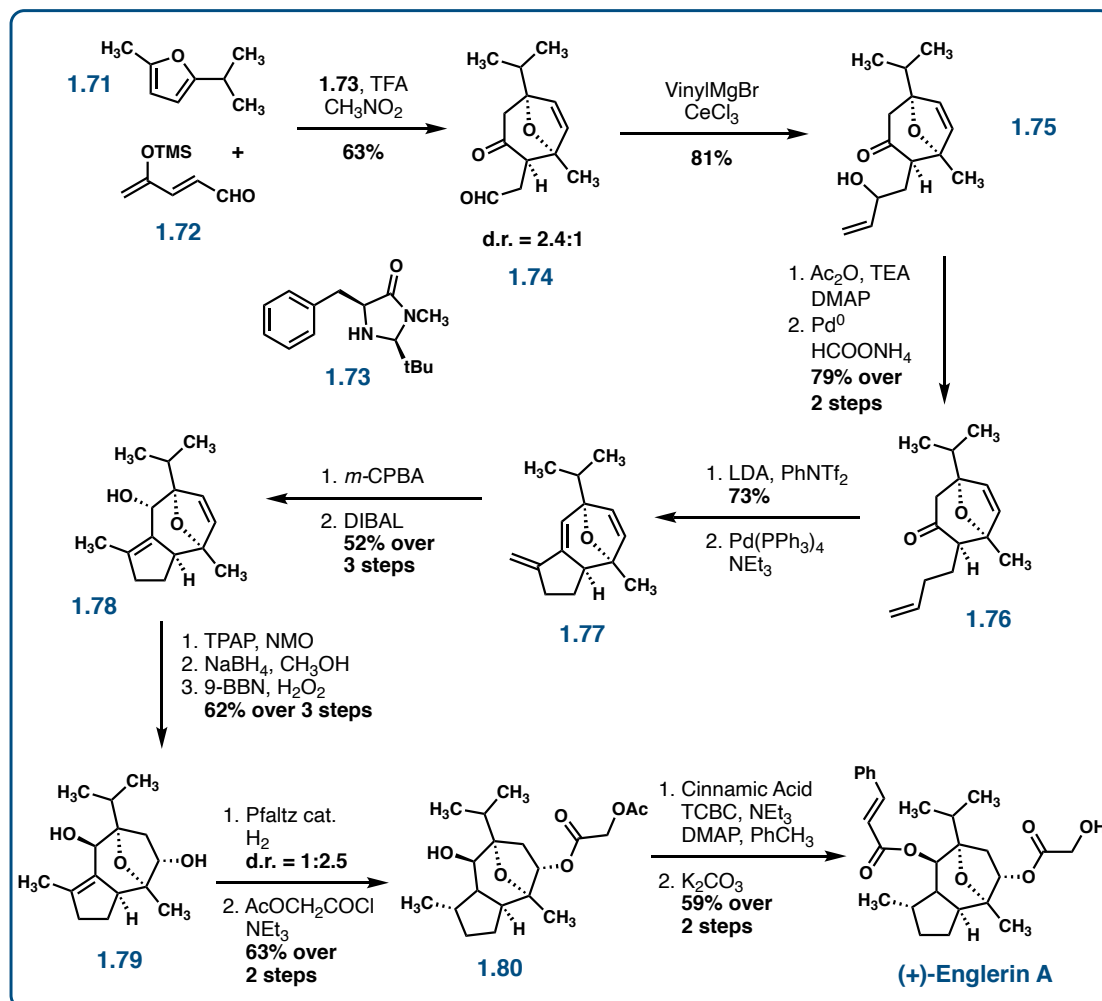


Figure 1.13 Total synthesis of (–)-englerin A completed by the groups of Bing-Feng Sun, Guo-Qiang Lin, and Yong-Jia Shang

1.3.10 Metz – Total Synthesis of (–)-Englerin A (April 2013)

In April of 2013, the Metz group completed the synthesis of EA by starting with the 5-membered ring in hand and forming the 7-membered ring through a Grubbs⁴² metathesis.⁷⁹ They wanted to begin their synthesis with (–)-photocitral A, which was obtained through a 2-step ring contraction of (–)-isopulegol. A Reformatsky⁸⁰ was used to add bromoester **1.81** into the aldehyde and a Grubbs' ring

closing metathesis was used to complete the core minus the ether bridge, **1.83** (figure 1.14). At this point, the ester was transformed into the methyl ketone through Weinreb⁵⁹ amide formation then treatment with MeLi. This also resulted in dehydration of the alcohol to give the unsaturated ketone **1.84**. An epoxidation of the unsaturated ketone followed by asymmetric dihydroxylation of the other olefin and selective esterification using the TBS-protected glycoloyl chloride affords epoxide **1.85**. A single pot Wittig⁴¹ olefination and ether bridge formation under acidic conditions affords enol **1.86**. A hydrogenation of the resultant olefin and esterification of the free alcohol using cinnamoyl chloride completes the synthesis of EA in 12 steps with an overall yield of 16%.

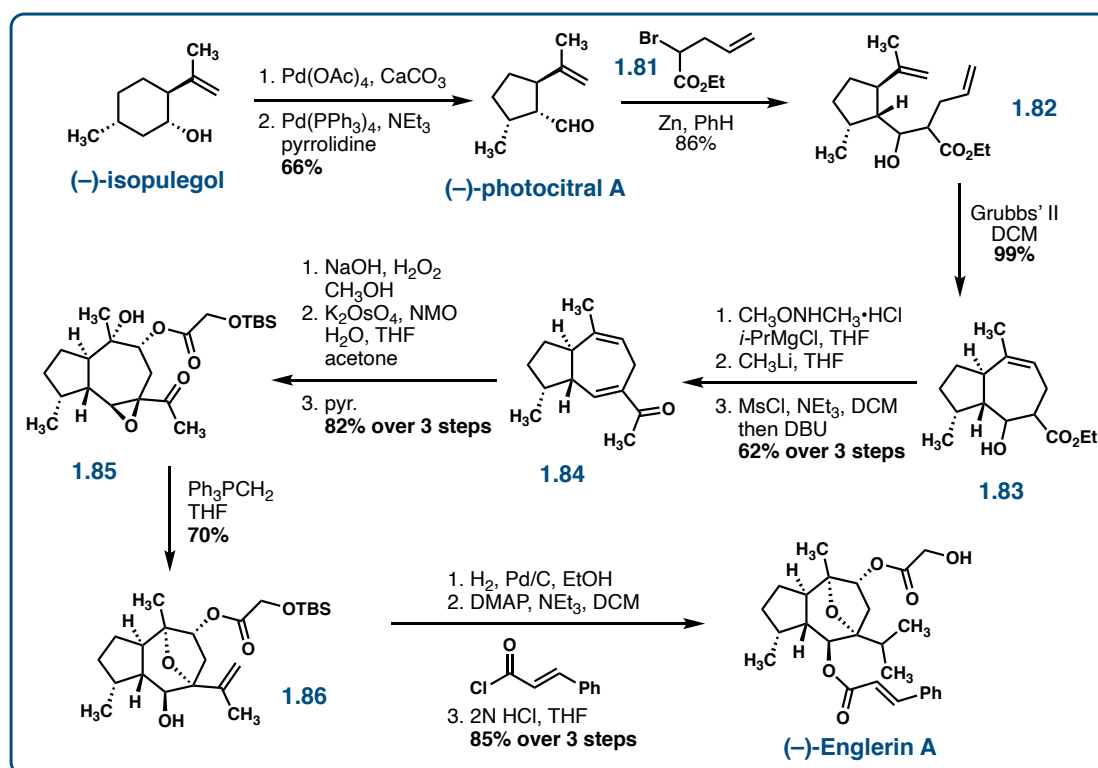


Figure 1.14 Total synthesis of (-)-englerin A completed by Peter Metz et al.

1.3.11 Shen – Total Synthesis of (–)-Englerin A (January 2014)

In 2014, the Shen group described a concise enantioselective total synthesis of EA featuring a pinacol coupling and Grubbs metathesis to complete the core (figure 1.15).⁸¹ Starting with the cyclopentyl enal **1.87**, a known compound prepared from (*R*)-(-)-carvone, they began exploring the pinacol coupling and Grubbs⁴² metathesis with a variety to ketones. Eventually, the pinacol product was obtained through the addition of dithiane **1.88** followed by deprotection and allyl Grignard⁵⁵ addition into the unmasked ketone to afford **1.89**. A Grubbs metathesis closes the 7-membered ring. The ether bridge was completed through an iodonium intermediate **1.90** using NaIO₄ and NaHSO₃ to afford iodo-compound **1.91**. Esterification of the alcohol using cinnamoyl chloride followed by substitution of the iodide with an acetate group affords (–)-englerin B acetate. Saponification, esterification with a protected glycolate, and deprotection affords EA in a total of 10 steps and an overall yield of 11%.

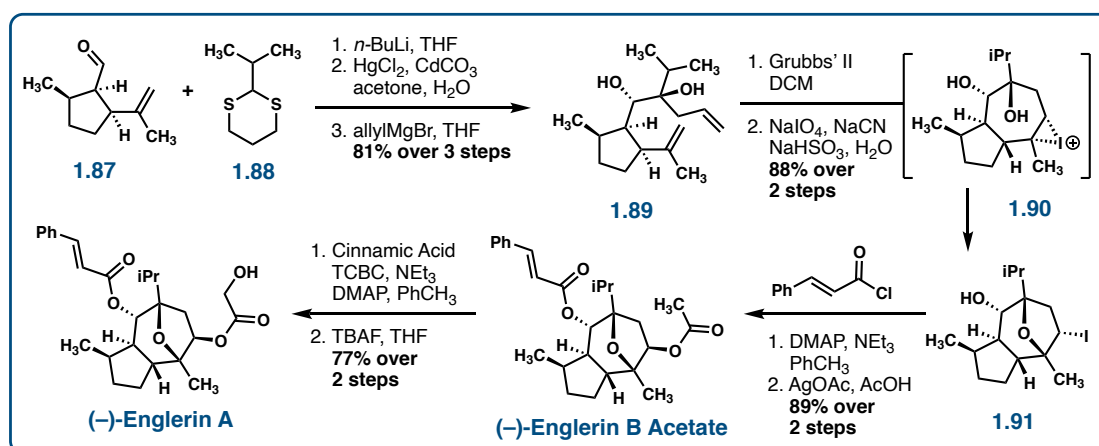


Figure 1.15 Total synthesis of (–)-englerin A completed by Zhengwu Shen et al.

1.3.12 Hashimoto and Anada – Total Synthesis of (–)-Englerin A (July 2015)

In 2015, Hashimoto and Anada collaborated on the asymmetric total synthesis of EA utilizing a carbonyl ylide cycloaddition along with an intramolecular aldol condensation to complete the core.⁸² Their synthesis commenced with the Reformatsky⁸⁰ reaction between succinic anhydride and 2-bromoisobutyrate with a subsequent decarboxylation under acidic conditions (figure 1.16). Treatment of the resultant keto acid with CDI followed by *t*-butyl malonic acid results in the diketoester **1.93**. This can then be treated with mesylazide to perform a diazo transfer producing the carbonyl ylide cycloaddition precursor **1.94**. A rhodium catalyst mediated the cycloaddition between **1.94** and ethyl vinyl ether to afford the oxa-bridged 7-membered ring, **1.95**. This method was originally developed by this group as a means of providing 8-oxabicyclo[3.2.1]octane derivatives with high enantioselectivity.⁸³ They recognized the utility of the reaction and saw its potential application to the synthesis of EA.

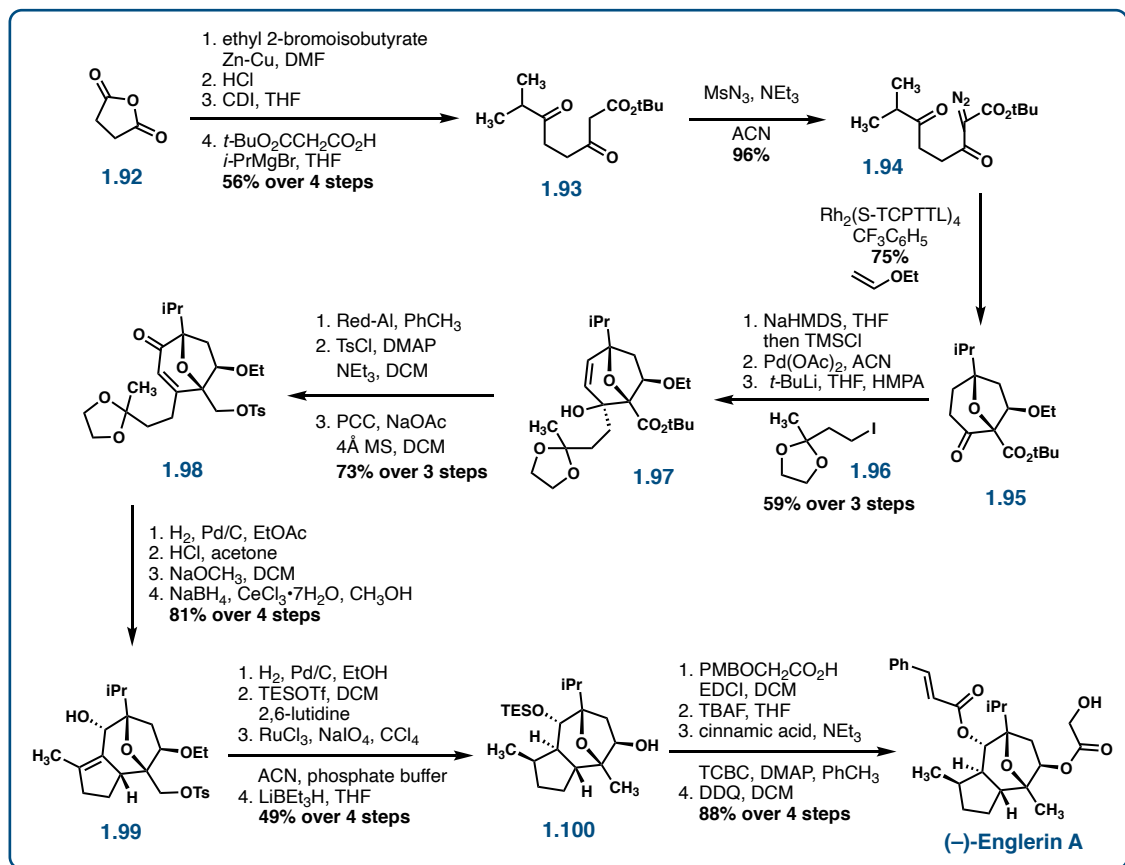


Figure 1.16 Total synthesis of (-)-englerin A completed by the Masahiro Anada and Shunichi Hashimoto groups

With the 7-membered ring in hand, they proceeded to install the 5-membered ring first by generating the unsaturation of the ketone by treatment with TMSCl and NaHMDS followed by the Saegusa-Ito⁸⁴ oxidation. Lithium-halogen exchange with alkyl iodide **1.96** allowed for addition into the ketone to afford **1.97**. Reduction of the ester with Red-Al is followed by tosylation of the resultant primary alcohol and an oxidative rearrangement to afford enone **1.98**. Diastereoselective hydrogenation of the olefin and removal of the ketal sets them up for completion of the core using an aldol condensation. A reduction of the ketone affords **1.99**, which is followed by a

diastereoselective hydrogenation of the endocyclic alkene. A TES protection of the alcohol and ruthenium tetroxide-mediated oxidation of the ethyl ether to the acetate is followed by a reductive excision of the tosylate group and removal of the acetate group to afford **1.100**. The PMB protected glycolate is installed followed by deprotection and cinnamate esterification of the other alcohol. A final deprotection of the PMB alcohol completes the synthesis of EA in 25 steps at an overall yield of 5.2%.

1.3.13 Iwasawa – Total Synthesis of (±)-Englerin A (January 2016)

In January of 2016, Iwasawa et al. described the racemic synthesis of englerin A using an intermolecular [3+2] cycloaddition strategy of a carbonyl ylide.⁸⁵ Similar cycloaddition strategies have been applied to the synthesis of englerin A, but these syntheses are limited by the fact that they require electron-deficient dipolarophiles. As a result, further functionalization is required for the transformation of these electron deficient groups, such as esters, into the oxygen featured at C9. The benefit of this method is that it is an inverse demand cycloaddition, so these oxidative transformations post-cycloaddition are not needed. They use a Pt catalyst to complete a cycloaddition between a carbonyl ylide **1.101**, made in 3 steps from hex-4-ynoic acid, and benzyl vinyl ether to furnish the ether-bridged 7-membered ring (figure 1.17).

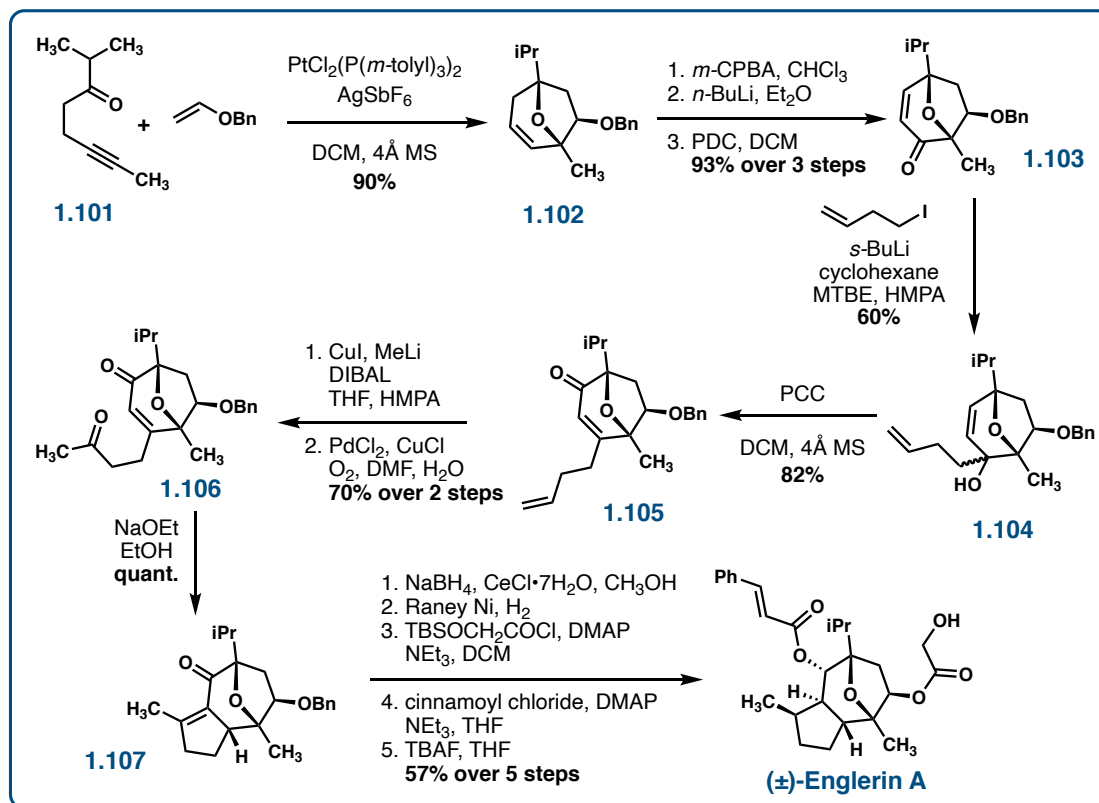


Figure 1.17 Total synthesis of (-)-englerin A completed by Nobuharu Iwasawa et al.

This synthesis is initiated by this cycloaddition reaction affording the 7-membered ring **1.102** as a single diastereomer featuring the benzyl protected C9-oxygen. The unsaturated ketone **1.103** is generated through an epoxidation, ring-opening elimination, and oxidation of the resultant allylic alcohol. A lithium-halogen exchange is then used to add a homoallyl group into the ketone resulting in alcohol **1.104**. A 1,3-allylic rearrangement mediated by PCC affords the unsaturated ketone **1.105**. A regio- and stereoselective hydrogenation of the electron-deficient olefin followed by a Wacker⁵⁷ oxidation affords ketone **1.106**, setting them up to form the 5-membered ring. Completion of the core was accomplished using an aldol condensation

to afford olefin **1.107**. From here, a series of oxidative manipulations and esterifications complete the synthesis of (±)-englerin A. A Luche⁵⁸ reduction of the ketone to the alcohol and a stereoselective hydrogenation of the tetrasubstituted olefin resulted in removal of the benzyl protecting affording the diol. A regioselective esterification to afford the protected glycolate followed by an esterification of the final alcohol and TBS deprotection of the glycolate complete the total synthesis of (±)-englerin A in 14 steps at an overall yield of 16% from the ynone **1.101**.

1.3.14 López and Masacareñas – Total Synthesis of (–)-Englerin A (October 2016)

In October of 2016, the López and Masacareñas groups collaborated on the synthesis of EA that also featured a cycloaddition strategy.⁸⁶ In this case the bicyclic core was synthesized through a [4+3] cycloaddition of an allenediene precursor catalyzed by Pt. This allenediene precursor is synthesized in 5 steps starting with the alkylation of diethyl malonate using bromodiene **1.108** shown in figure 1.18. A decarboxylation and Weinreb⁵⁹ amide formation affords **1.109**. Treatment with a lithium alkynylide results in the formation of the ynone **1.111**. Asymmetric hydrogenation using a Noyori⁸⁷ catalyst followed by reduction of the ketone and TBS protection of the resultant alcohol results in the formation of the allenediene **1.113**. Treatment with a Pt catalyst in *o*-xylene constructs the 7,5-ring system **1.114**. In order to install the ether bridge, a regioselective dihydroxylation of **1.114** followed by a selective pivaloyl monoprotection and deprotection of the TBS alcohol affords diol **1.115**. A tandem asymmetric epoxidation of the remaining olefin and ring opening cyclization afforded the completed core **1.116**. This was accomplished using the L-Shi⁸⁸ catalyst. A regioselective tosylation of the alcohol on the 5-membered ring

allowed for methyl substitution affording diol **1.117**. A Steglich⁷⁴ esterification was used to install the PMB-protected glycolate and a Yamaguchi⁴³ was used to install the cinnamate. A final removal of the PMB group with DDQ completes the total synthesis of EA in 17 steps at an 8.8% yield.

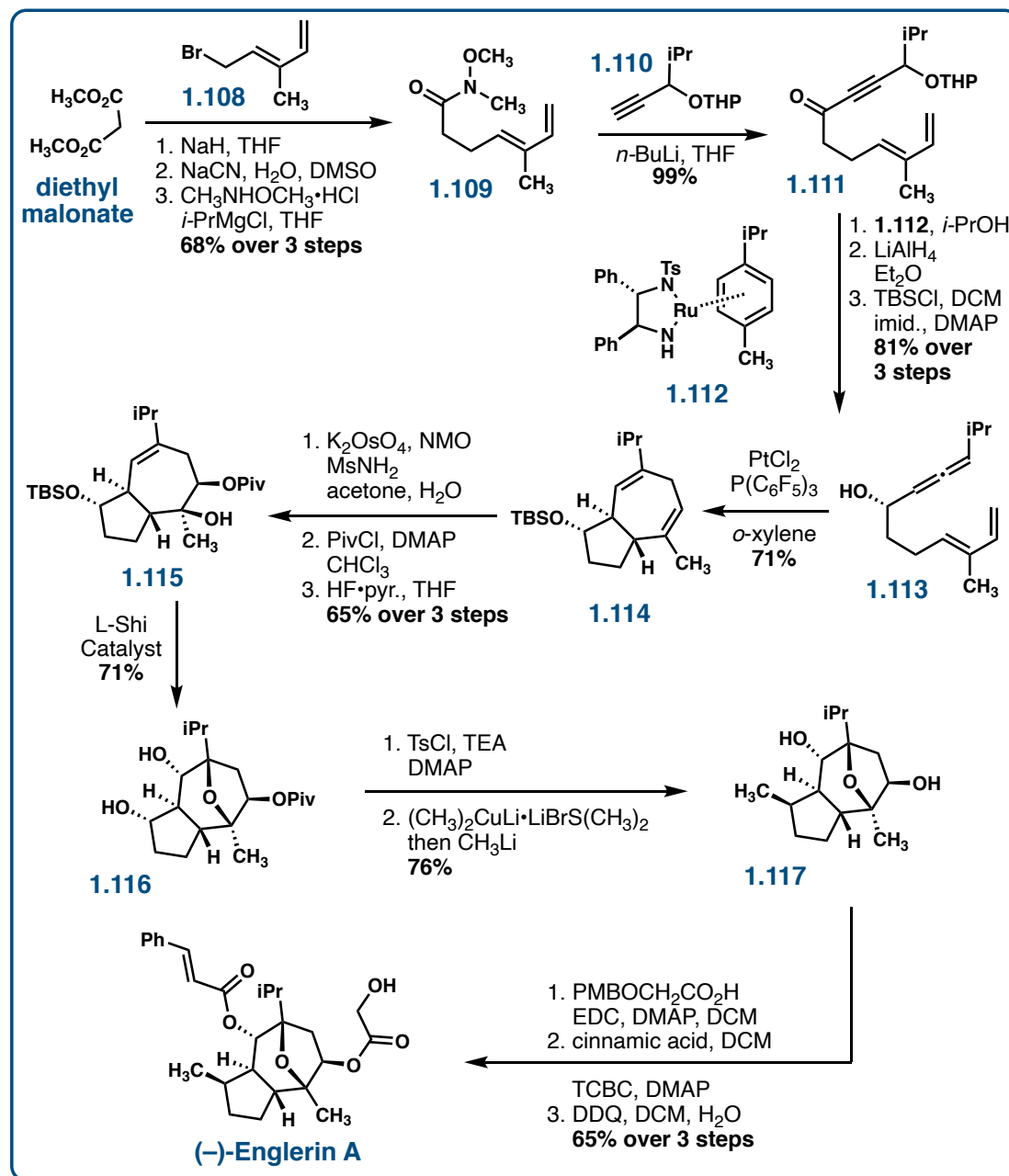


Figure 1.18 Total synthesis of (-)-englerin A completed by the groups of Fernando López and José Mascareñas

1.3.15 Iwabuchi – Formal Synthesis of (–)-Englerin A (September 2017)

In September of 2017, Iwabuchi described a formal synthesis of EA utilizing a strategy involving a Nazarov⁸⁹ cyclization in order to install the 5-membered ring onto the oxo-bridged 7-membered ring.⁹⁰ They can obtain the oxo-bridged 7-membered ring through a route previously developed by Iwabuchi by starting with 1,3-cycloheptadiene⁹¹ (figure 1.19). From **1.118**, they began with a 1,4-reduction of the enone followed by triflation of the resulting enolate. The vinyl triflate subjected to a Stille⁹² coupling to afford dienone **1.119**. The Nazarov cyclization is accomplished through treatment with triflic acid to complete the bicyclo[5.3.0]decane **1.120**. Hydrogenation using Pd/C followed by reduction and activation of the resulting alcohol affords sulfamate **1.121**. Under Du Bois's⁹³ conditions the sulfamate undergoes an oxidative annulation to afford the intermediate **1.122**. When treated with acid in THF an overall transposition of the initial ketone along with opening of the ether bridge affords **1.123**. The enone is subjected to a 1,4-reduction and the newly formed alcohol is MOM-protected. The remaining ketone was treated with LiHMDS and NTf₂Ph to give the enol triflate which was subjected to a Negishi⁹⁴ coupling to afford a trisubstituted olefin. A dihydroxylation of the olefin affords diol **1.124**. Their plan at this point was to intercept Hatakeyama's synthesis by reaching intermediate **1.125** which could be achieved in a few more steps. A one-pot procedure accomplishing protection of the diol along with removal of the MOM-group and oxidation of the resultant free alcohol gives the ketone. An isopropyl addition into the ketone using conditions developed by Ishihara⁹⁵ and dehydration using Burgess⁶³ reagent completed their formal synthesis of EA in 13 steps from ketone **1.118** in an overall yield of 58% to **1.125**.

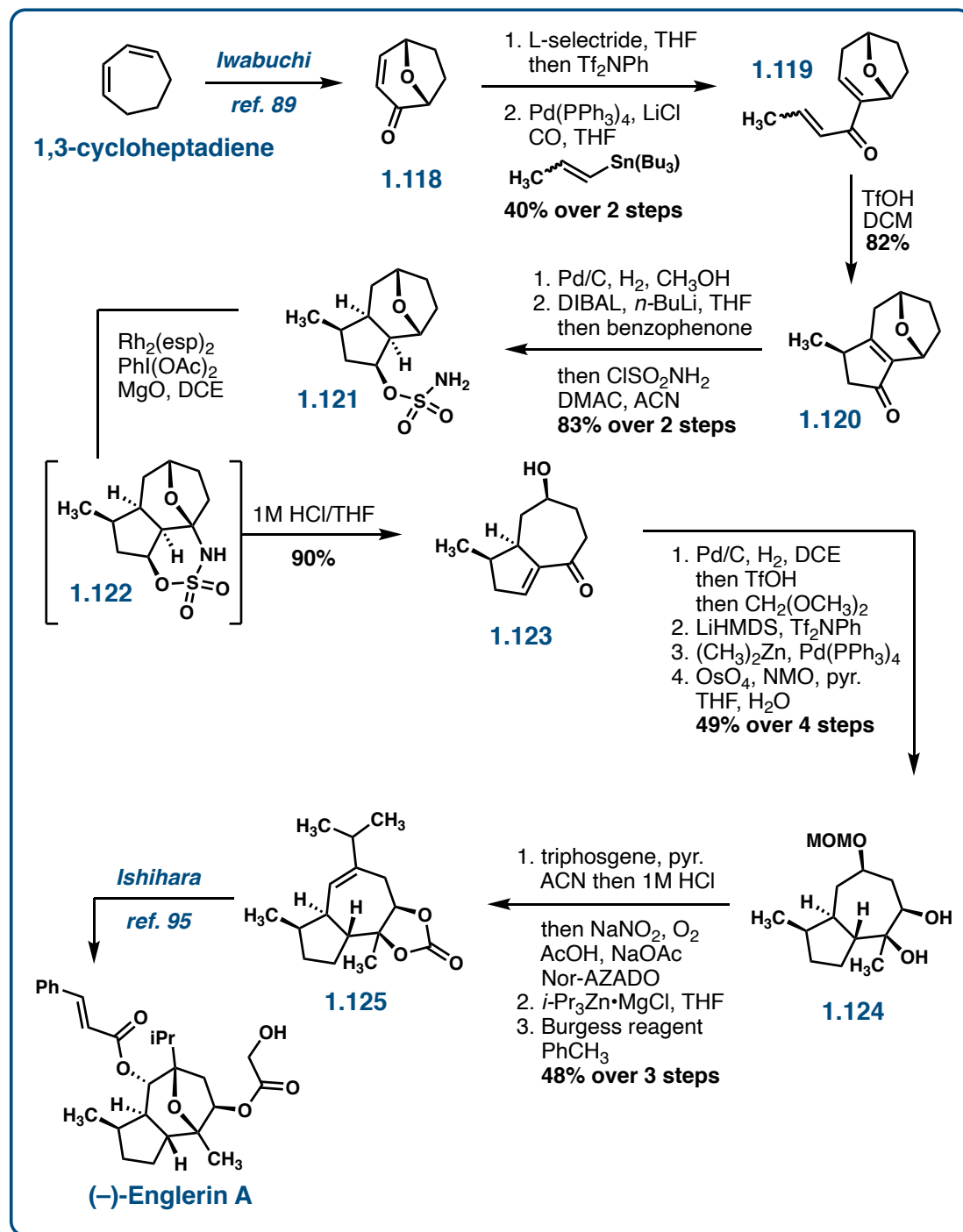


Figure 1.19 Formal synthesis of (-)-englerin A completed by Yoshiharu Iwabuchi et al.

1.3.16 Shoji – Formal Synthesis of (±)-Englerin A (August 2017)

In August of 2017, the Shoji group described a formal synthesis of racemic englerin A utilizing a regio- and diastereoselective [4+3] cycloaddition strategy to construct the oxo-bridged 7-membered ring.⁹⁶ This strategy achieves this cycloaddition using a furan **1.129** and an unsaturated aldehyde **1.128** as shown in figure 1.20. The aldehyde was synthesized in 4 steps starting with ketone **1.126**. Conversion of the ketone to the less electrophilic imine allowed for monoalkylation to afford ketone **1.127**. Treatment with NaHMDS and silyl chloride followed by heating in toluene afforded silyl enol ether **1.128**. This is the unsaturated aldehyde that is then subjected to the [4+3] cycloaddition with furan **1.129** to complete the bridged 7-membered ring **1.130**. From here, a benzylation of the free alcohol and Wacker⁵⁷ oxidation of the terminal olefin was followed by a McMurry⁹⁷ coupling to close the 5-membered ring **1.131**. A hydroboration–oxidation of the less substituted olefin followed by hydrogenation of the remaining alkene complete their formal synthesis of (±)-englerin A through intermediate **1.132**. They reference the synthesis completed by Shang et al. as a means of completing the total synthesis.⁷⁵ The complete formal synthesis from the starting ketone **1.126** to diol **1.132** was completed in a 4.8% yield over 10 steps.

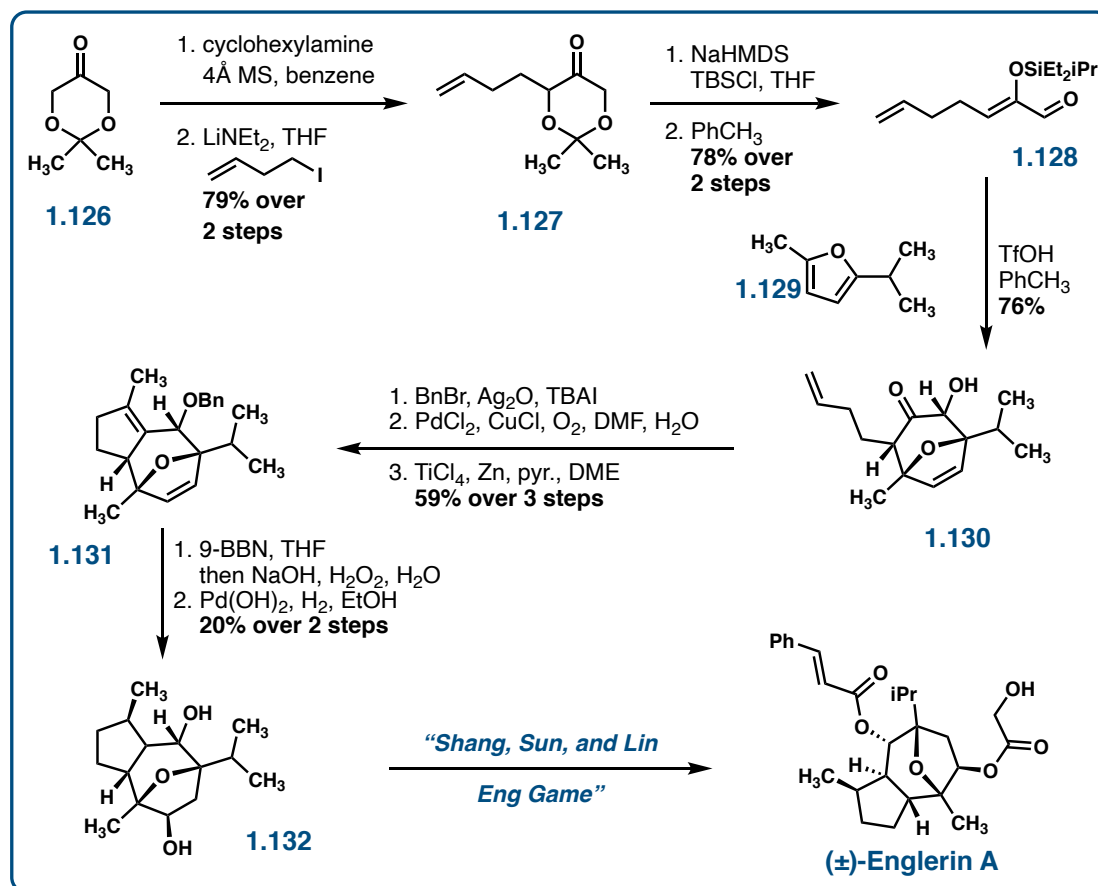


Figure 1.20 Formal synthesis of (±)-englerin A completed by Mitsuru Shoji et al.

1.3.17 Wang – Total Synthesis of (–)-Englerin A (April 2018)

In April of 2018, Wang et al. completed a total synthesis of (–)-englerin A using an intramolecular [3+2] cycloaddition reaction between a cyclopropyl ring and a ketone present on a 5-membered ring to complete the core.⁹⁸ The substituted 5-membered ring **1.135** is achieved starting with enal **1.133** which is derived in 2 steps from (*R*)-(+)-limonene (figure 1.21). A Shapiro⁷⁶ reaction of **1.133** affords alcohol **1.135** which is subjected to a 3-step sequence of a Mukaiyama⁹⁹ esterification of the free alcohol, a Regitz¹⁰⁰ diazotization, and a hydroxyl-directed intramolecular

cyclopropanation of an olefin to achieve lactone **1.136**. Opening the lactone and protecting the newly formed alcohol with a chloroacetyl group sets them up for an ozonolysis of the less substituted olefin to afford ketone **1.137**. This is then subjected to the intramolecular [3+2] cycloaddition mediated by scandium triflate to afford the completed core **1.138**.

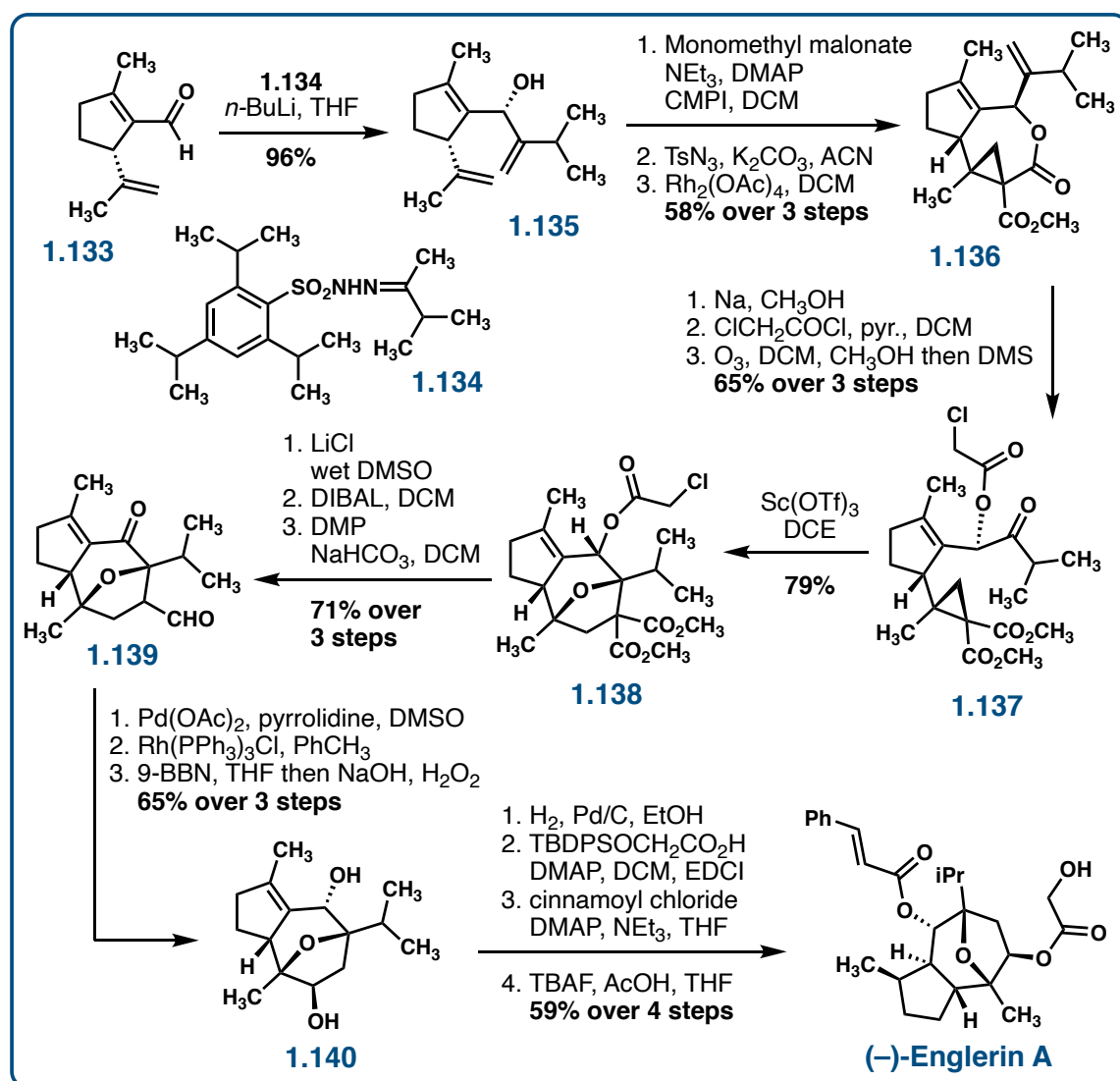


Figure 1.21 Total synthesis of (-)-englerin A completed by Zhongwen Wang et al.

Ketone **1.139** is achieved by decarboxylation to remove one ester followed reductive cleavage of the other ester using DIBAL and a Dess-Martin⁵² oxidation of the resultant alcohol. The unsaturated aldehyde is generated through a Saegusa⁸⁴ oxidation and the aldehyde is removed through a Tsuji-Wilkinson¹⁰¹ decarbonylation. Chemoselective hydroboration-oxidation of the resulting alkene affords diol **1.140**. Diastereoselective hydrogenation of the remaining olefin is followed by a Steglich⁷⁴ esterification to install the protected glycolate ester, incorporation of the cinnamate, and deprotection of the glycolate to complete the synthesis of (–)-englerin A. They achieved the synthesis of EA in 18 steps at a 7.8% yield. This synthesis was used as a way to showcase the intramolecular cross cycloaddition step used to construct the core of EA. They also completed the total syntheses of (–)-englerin B, (+)-orientalols E and F, and (–)-oxyphyllol using this strategy.

1.3.18 Tchabanenko – Total Synthesis of (±)-Englerin A (January 2019)

In January of 2019, Tchabanenko's group described a synthesis using a strategy similar to that of Nicolau and Chen⁵³ in 2010. Their strategy employed a [4+3] cycloaddition through a pyrylium ion generated in situ to construct the 7-membered ring with the ether bridge.¹⁰² This synthesis initiated with the transformation of furanal **1.141** into pyrone **1.142** through a Grignard⁵⁵ addition into the aldehyde, oxidative ring expansion using *m*-CPBA, and an acetate protection of the free alcohol (figure 1.22). When heated in a sealed tube with vinyl acetate, the [4+3] cycloaddition commences affording the 7-membered ring **1.143**. A vinyl 1,4 addition followed by an ozonolysis affords aldehyde **1.144**. An epimerization at the alpha position of the aldehyde followed by a Wittig⁴¹ olefination and hydrogenation of the resultant olefin affords ketone **1.145**. An aldol condensation is accomplished in 2

steps through the use of KHMDS followed by an elimination of the activated alcohol under basic conditions to afford the completed core **1.146**. A reduction of the ketone and olefin are followed by a Yamaguchi⁴³ esterification affording cinnamate **1.147**. The total synthesis is completed through removal of the acetate, activation of the alcohol with imidazolium sulfonate, and substitution with cesium glycolate. The synthesis of (±)-englerin A was accomplished in 17 steps at an overall yield of 5.7%.

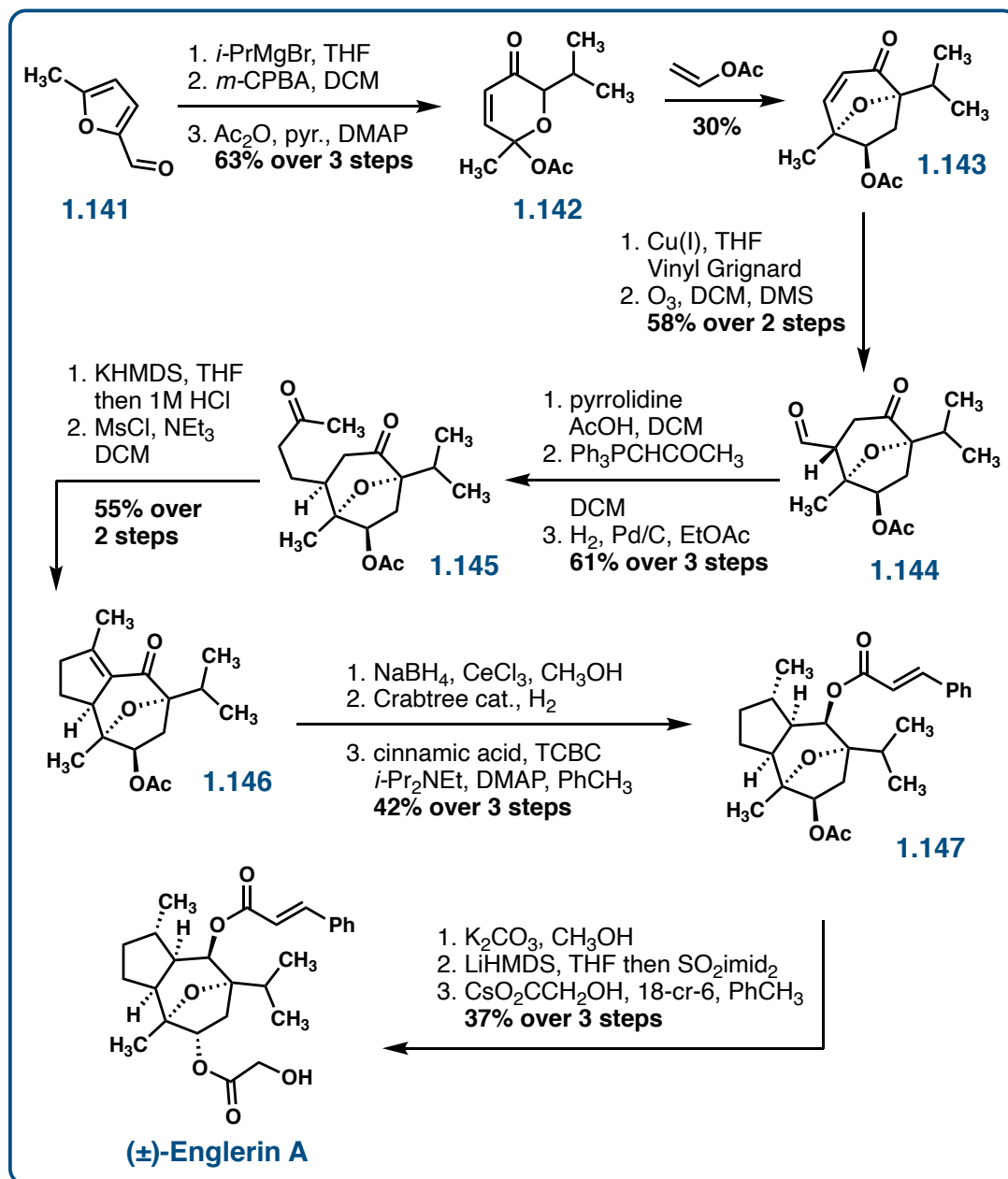


Figure 1.22 Total synthesis of (±)-englerin A completed by Kirill Tchabanenko et al.

1.3.19 Plietker – Total Synthesis of (–)-Englerin A (May 2019)

In May of 2019, the Plietker group used a TMSOTf-mediated [4+3] cycloaddition strategy between diketoester **1.150** and TMS enolate **1.152** (figure 1.23).¹⁰³ The diketoester **1.150** can be synthesized in 2 steps by an enantioselective, catalytic, decarbonylative aldol between ketodiol **1.148** and ketoester **1.149** along with a Yamaguchi⁴³ esterification to perform an early installation of the TBDPS-protected glycolate ester. The intramolecular [4+3] cycloaddition mediated by TMSOTf begins with nucleophilic attack between the ketones in **1.150** to afford oxonium **1.151**. A Mukaiyama⁹⁹ aldol with TMS enolate **1.152** affords intermediate **1.153**. Elimination of a TMS alcohol and a final Mukaiyama⁹⁹ aldol afford oxo-bridged 7-membered ring **1.155** diastereoselectively. Towards the construction of the 5-membered ring, alkylation and Krapcho¹⁰⁴ decarboxylation afford olefin **1.156**. A triflation of the ketone sets them up for a Heck⁷⁷ coupling to form the 5-membered ring **1.157**. When treated with MeSiCl₂H, a Pd-catalyzed regio- and diastereoselective 1,4-hydrosilation of diene **1.157** is accomplished. Upon oxidative work-up with hydrogen peroxide, core structure **1.159** is afforded. To invert the stereogenic center bearing the newly formed alcohol, oxidation to the ketone and a CBS¹⁰⁵-reduction is used. Hydrogenation of the remaining olefin, cinnamate esterification, and TBDPS deprotection afford the final product (–)-englerin A in a grand total of 12 steps with a 7.2% yield.

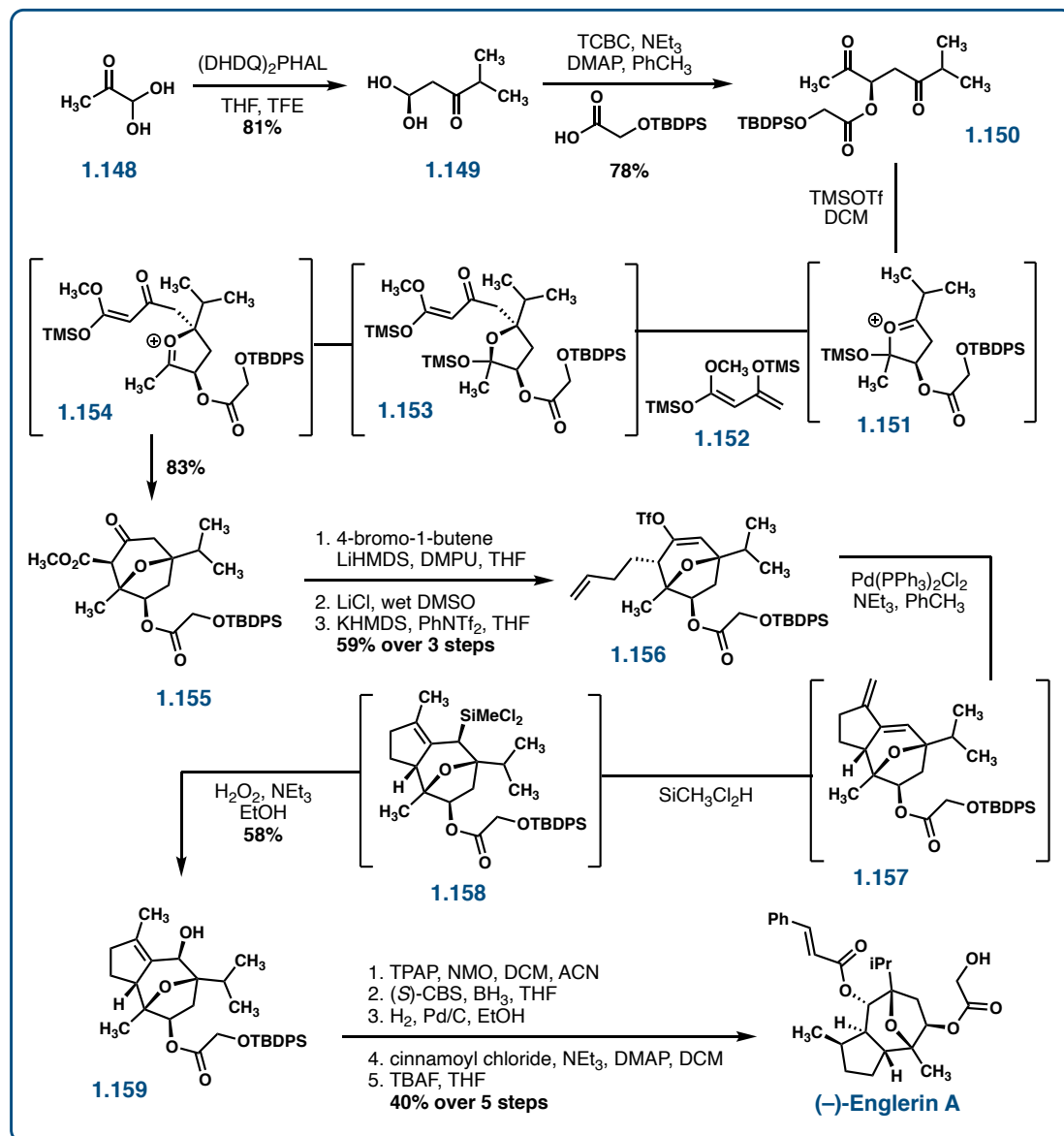


Figure 1.23 Total synthesis of (-)-englerin A completed by Bernd Plietker et al.

1.3.20 Christmann and Liu – Total Synthesis of (-)-Englerin A (January 2020)

In January of 2020, the Christmann and Liu groups collaborated on the synthesis of (-)-englerin A using an innovative biosynthetic approach with the help of enzymes.¹⁰⁶ After screening a variety of engineered bacterial cell lines, they were able

to produce guaia-6,10(14)-diene with a titer of 0.8 g/L through fed-batch fermentation of the engineered bacteria *S. cerevisiae* YL06. This cell line uses the mevalonate pathway to produce this scaffold. With guaia-6,10(14)-diene in hand, they can reach EA in just 6 steps as shown in figure 1.24. Using Shenvi's cobalt-catalyzed isomerization, they isomerized the exocyclic double bond into the 7-membered ring **1.160**.¹⁰⁷ A Sharpless⁴⁹ asymmetric dihydroxylation was achieved allowing for protected glycolate ester formation to give **1.161**. Asymmetric epoxide formation of the remaining olefin resulted in ether bridge formation when treated with acetic acid. Finally, a Yamaguchi⁴³ esterification and removal of the silyl protecting group affords (–)-englerin A in a total of 6 steps from the guaia-6,10(14)-diene with a yield of 38%.

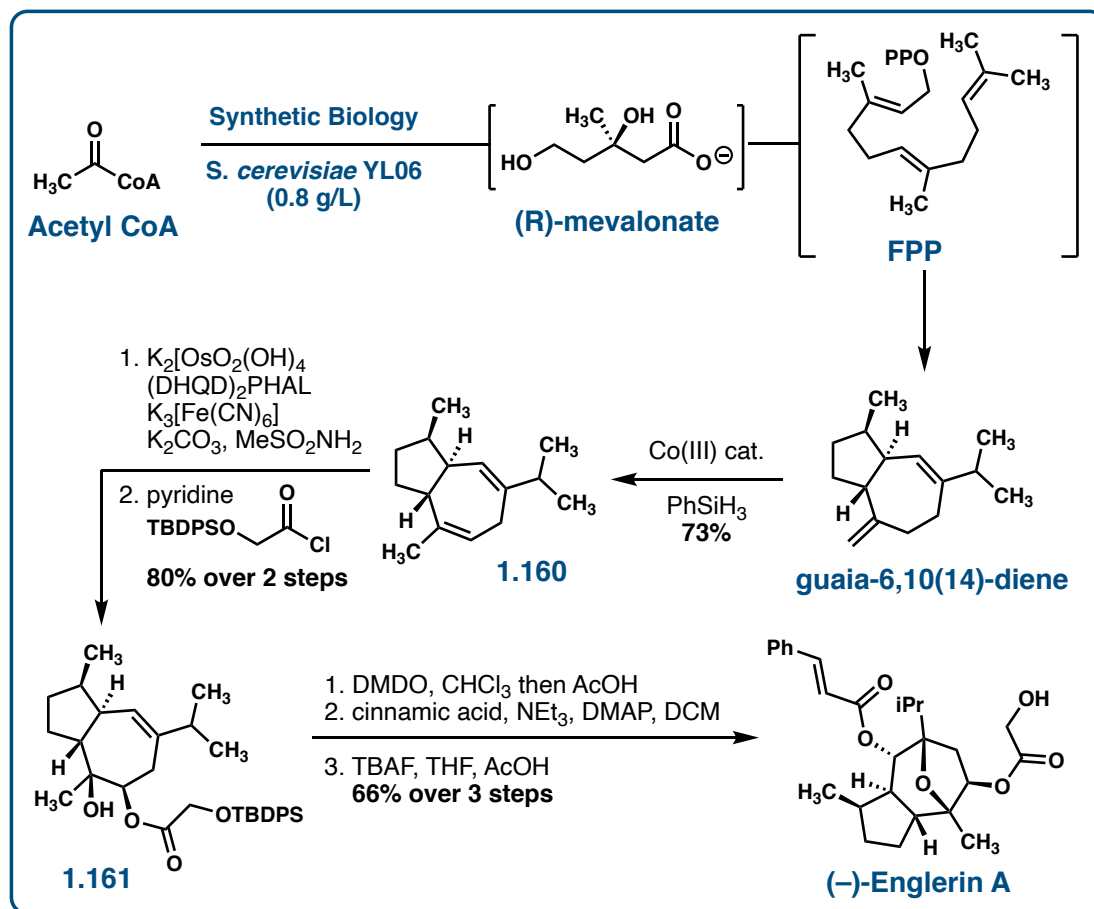


Figure 1.24 Total synthesis of (-)-englerin A completed by the Mathias Christmann and Tiangang Liu groups

1.3.21 Xiang – Total Synthesis of (-)-Englerin A (February 2020)

One month later in February of 2020, the Xiang group described a very similar synthesis of (-)-englerin A using bioengineered *E. Coli*.¹⁰⁸ With a guaiane sesquiterpene cyclase, guaia-6,10(14)-diene was produced through metabolic engineering of the isoprenoid pathway of microbes. They were able to accomplish this in a titer of 119.4 mg/L. From the guaia-6,10(14)-diene core scaffold, they followed a very similar series of steps as the Christmann group¹⁰⁶ as shown in figure 1.25. They

first epoxidized the internal olefin followed by a cobalt catalyzed epimerization of the external alkene to afford **1.162**. A dihydroxylation of the olefin results in ring closure and opening of the epoxide to the alcohol **1.163**. They then complete the synthesis by two esterification reactions and a PMB deprotection to afford (–)-englerin A in 6 steps and a 14.2% yield from guaia-6,10(14)-diene.

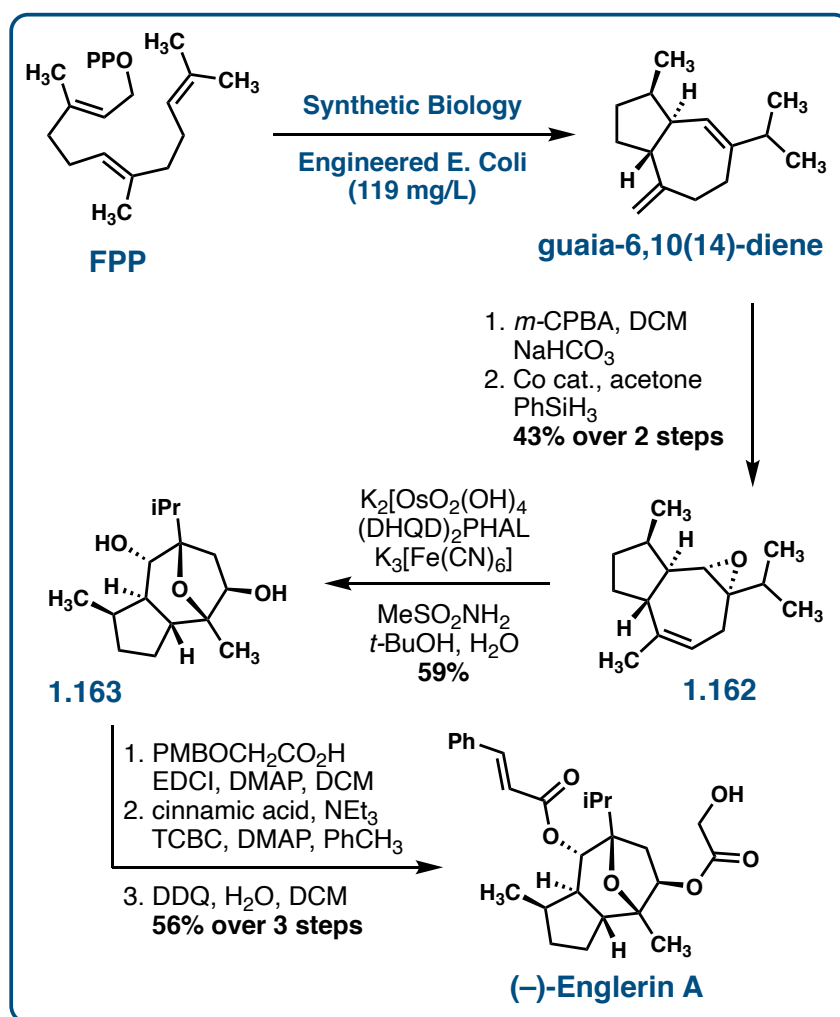
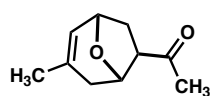
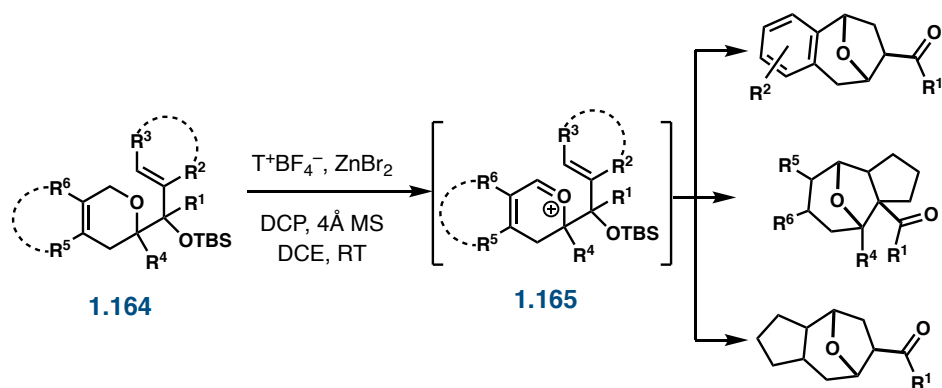


Figure 1.25 Total synthesis of (–)-englerin A completed by Zheng Xiang et al.

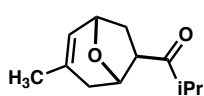
1.3.22 Alternative Approaches to the Synthesis of Englerin A

Several published works feature methodologies that could be used to form the guaiane scaffold, but that have not yet been applied toward the synthesis of EA or its associated analogues. A few of these publications are not directly applicable to the synthesis of englerin A but hold the potential of being applied to the synthesis of its analogues with some reaction modification.¹⁰⁹ One method that could be applied directly to the synthesis of englerin was completed by the Wang group in 2018.¹¹⁰

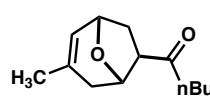
This methodology features a tandem C–H oxidation/oxa-[3,3] Cope¹¹¹ rearrangement/aldol cyclization as a means of constructing 8-oxabicyclo[3.2.1]octanes. Under their optimized conditions, they can perform this transformation under the promotion of the oxidant $T^+BF_4^-$ and $ZnBr_2$ with the additive 2,6-dichloropyridine (figure 1.26). This method is versatile as it is applied to a wide range of systems and can generate a few different mono- and bicyclic scaffolds featuring different substitution patterns and the ether bridge in moderate to high yields and diastereoselectivities. The 5,7-ring system **1.166o** shows that this method has the potential to be applied to the synthesis of EA.



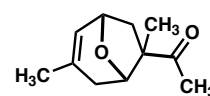
1.166a, 62%
d.r. = 12.5:1



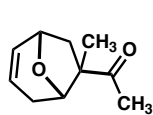
1.166b, 72%
d.r. = 11.1:1



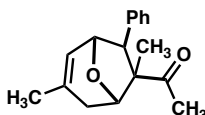
1.166c, 57%
d.r. = 7.7:1



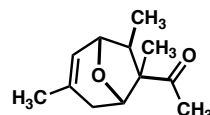
1.166d, 85%
d.r. = 12.5:1



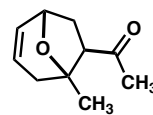
1.166e, 56%
d.r. > 20:1



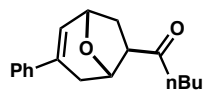
1.166f, 82%
d.r. = 12.5:1



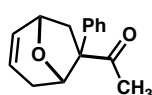
1.166g, 66%
d.r. > 20:1



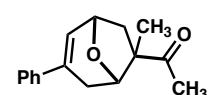
1.166h, 88%
d.r. > 20:1



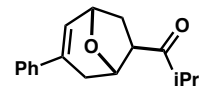
1.166i, 84%
d.r. > 20:1



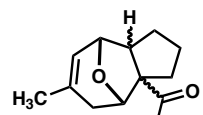
1.166j, 47%
d.r. > 20:1



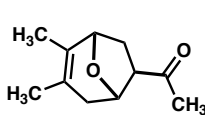
1.166k, 90%
d.r. > 20:1



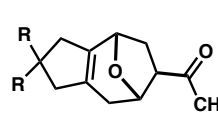
1.166l, 91%
d.r. > 20:1



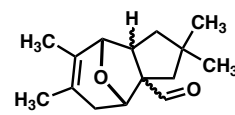
1.166m, 61%
d.r. = 16.5:1



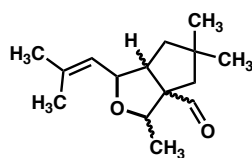
1.166n, 56%
d.r. > 20:1



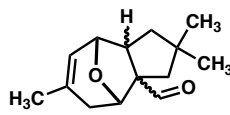
1.166o, 42%
R = CO₂Et
d.r. > 20:1



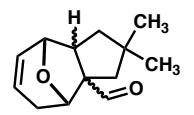
1.166p, 41%
d.r. = 3.5:1



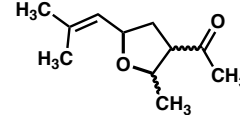
1.166q, 61%
d.r.(α:β) > 20:1



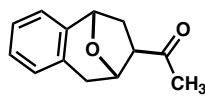
1.166r, 60%
d.r. = 2.2:1



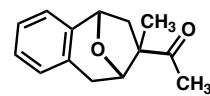
1.166s, 71%
d.r. = 4.0:1



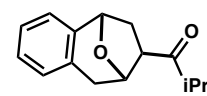
1.166t, 52%
d.r.(α:β) = 6.2:1



1.166u, 82%
d.r.(α:β) > 20:1



1.166v, 90%
d.r.(α:β) > 20:1



1.166w, 68%
d.r.(α:β) > 20:1

Figure 1.26 Method developed by Shao-Hua Wang et al. describing the synthesis of 8-oxabicyclo[3.2.1]octanes

1.4 Englerin Analogues and Structure–Function Studies

With over 20 different syntheses of englerin disclosed, many groups have contributed synthetic analogues of EA with the intent to develop a structure–function relationship study of englerins. This would allow for a greater understanding of the biological activity of englerin as well as increase the chances of developing englerin into a RCC therapeutic. To date, there are hundreds of analogues that have been evaluated giving the scientific community a growing data set and understanding of the importance of many of the positions on englerin along with respect to what can and cannot be altered in the pursuit of a therapeutic lead compound.

Ideally, when the analogues are prepared, these materials are screened via the NCI60¹¹², but at a minimum, most materials are evaluated in the A498 RCC cell line which is the most sensitive to EA. Unless otherwise noted, throughout this chapter the GI₅₀ and IC₅₀ values discussed are recorded with the A498 cell line. The overarching goal of the development of these analogues is to increase the pharmaceutical (or drug-like) properties of these materials while maintaining potency within the therapeutic window.¹¹³ This discussion is generally organized by the exploration of each position around the EA core structure rather than chronologically. The positions around EA are shown in figure 1.27.

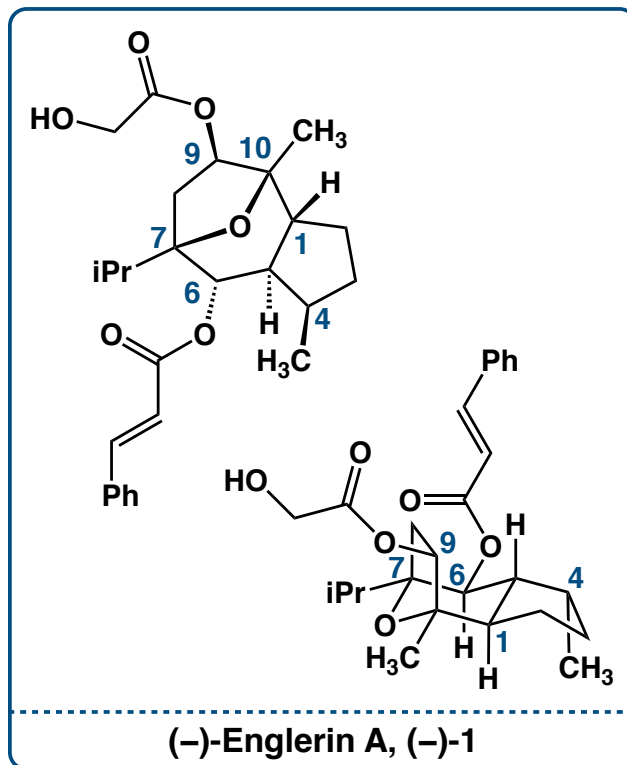


Figure 1.27 (-)-Englerin A with its positions around the scaffold labeled

1.4.1 C1 – C5

The cyclopentyl ring comprised of C1 through C5 has not been the subject of intensive investigation when compared to other positions on the molecule, however some modifications at these positions have been explored. The methyl-bearing stereogenic center at C4 of EA is tolerant of modification in active compounds. When the C4-methyl group is deleted, the GI_{50} increases from 10 nM to 123 nM, but when the C4-methyl is replaced with larger alkyl groups such as an ethyl or an isopropyl group, the potencies are 38 nM and 8.1 nM, respectively (figure 1.28).¹¹⁴

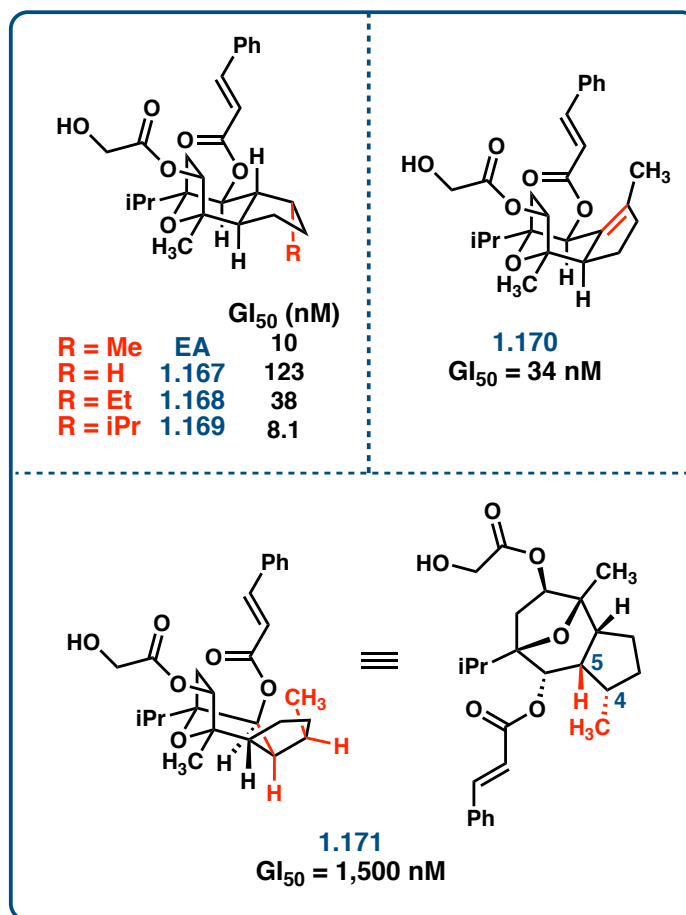


Figure 1.28 Englerin analogues featuring modifications from C1 through C5

Another impactful analogue series explored the oxidation level of the carbocyclic backbone and features a C4–C5 alkene, **1.170** (GI₅₀ = 34 nM).^{86, 115} This series has been widely explored through the synthesis of numerous analogues with this double bond incorporated. These analogues tend to be nearly as potent or more potent as their saturated counterparts despite the change in configuration and spatial orientation. However, when the geometry of this ring system is changed too drastically, such as **1.171**, the potency drops significantly to 1.50 μ M.

1.4.2 C6

The C6 position is one of the most widely explored positions on the molecule. EA features an *O*-linked cinnamate ester at C6 and this residue appears tolerant to the widest variety of manipulations. Several synthetic efforts have contributed to this growing dataset,^{44, 86, 116} and the most potent cinnamate modifications from these efforts are featured on the left side of figure 1.29 with GI₅₀ values less than 100 nM. A selected panel of other substitutions that were evaluated are shown to the right, all of which have GI₅₀ values greater than 1 μM. Included in these analogues are alterations in size, saturation levels, electronic nature, and hydrophilicity/phobicity, as well as incorporating a large number of different heterocycles. In general, what we have learned is that potency against RCC is maximized when this group is large and hydrophobic. A Michael acceptor moiety is not required for activity which is shown by the various naphthyl and fully saturated analogues which may alleviate some reservations for the pharmaceutical development of the englerins. Substitution on the phenyl ring seems to be tolerated though these modifications do not increase potency relative to EA. As of this writing, it would seem that the incorporation of heterocycles at this position is not tolerated.

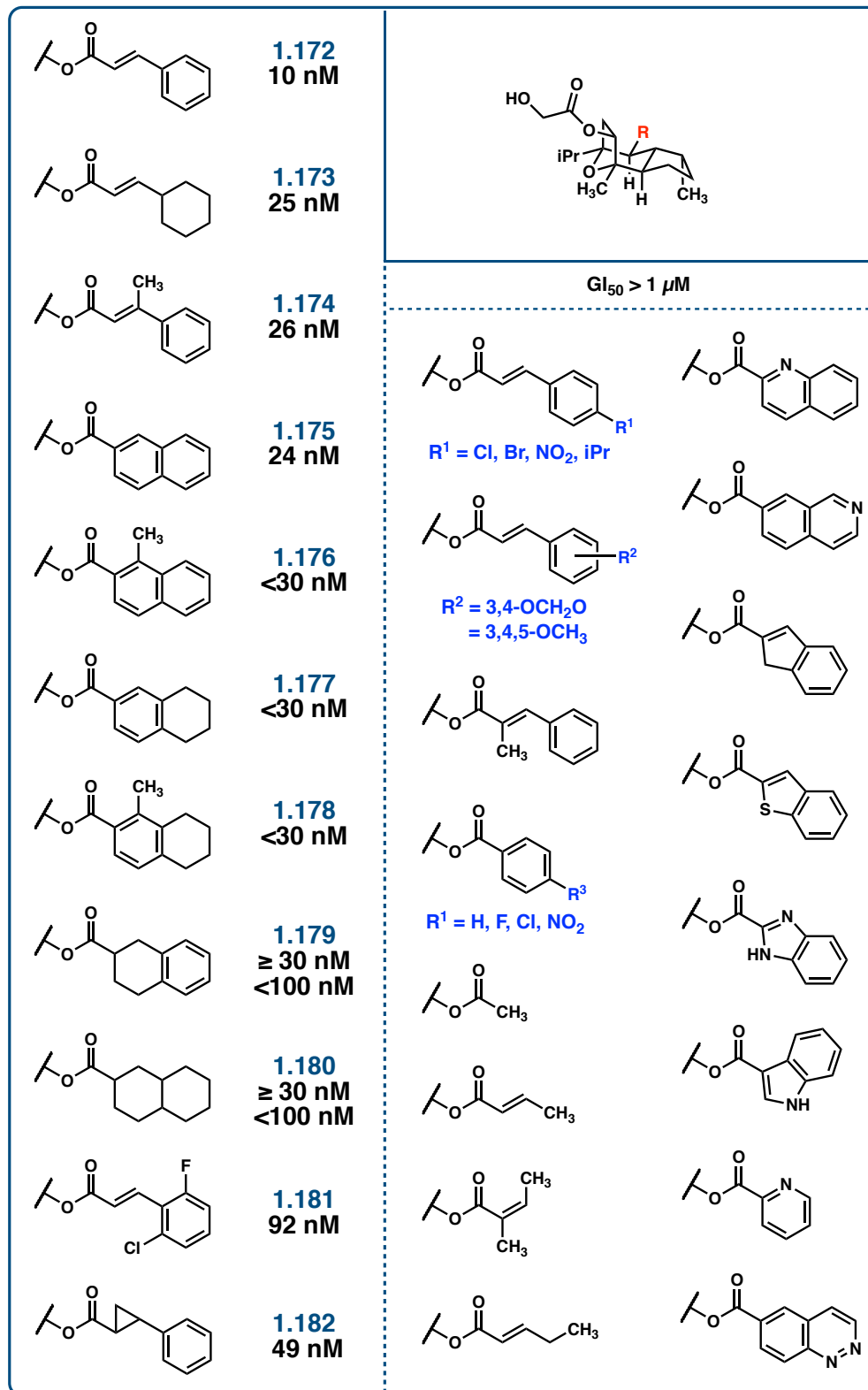


Figure 1.29 Englerin analogues featuring modifications at C6

The utility of changes to the C6 position include potency tuning and the opportunity for handles that support tool compound development. In ongoing studies of novel analogues, it is common to include a handful of the known potent cinnamate mimics along with the other modifications under investigation. It is important however to note that indeed there are cases where the identity of the C6 residue is critical. Such cases will be discussed further in Chapter 2.

1.4.3 C7

The C7 bridgehead is another position that has been examined less extensively, but indeed may be one of the most important positions on the molecule with respect to activity exploration. C7 features an isopropyl sidechain in EA, and known steric manipulations of the alkyl group at this position include decreasing its size to a methyl or an ethyl and increasing its size to a cyclohexyl (figure 1.30).^{44, 115-116} There are also substitutions of the isopropyl with cyclopropane, phenyl, and piperidine derivatives though these modifications were accompanied by unsaturation at C4–C5 elsewhere in the EA scaffold. Decreasing the size of the isopropyl unit (methyl **1.183**, ethyl **1.184**) resulted in significant loss of potency. The piperidine derivatives **1.188** and **1.189** were similarly inactive. The cyclohexyl analogue **1.186** retained potency beautifully ($GI_{50} = 19$ nM) while the phenyl **1.185** and cyclopropyl **1.187** analogues were less active at 191 nM and 100 nM, respectively. However, potency is not the most important consideration at C7; the mechanism of action of C7-modified EA analogues appears to be significantly different than EA itself.

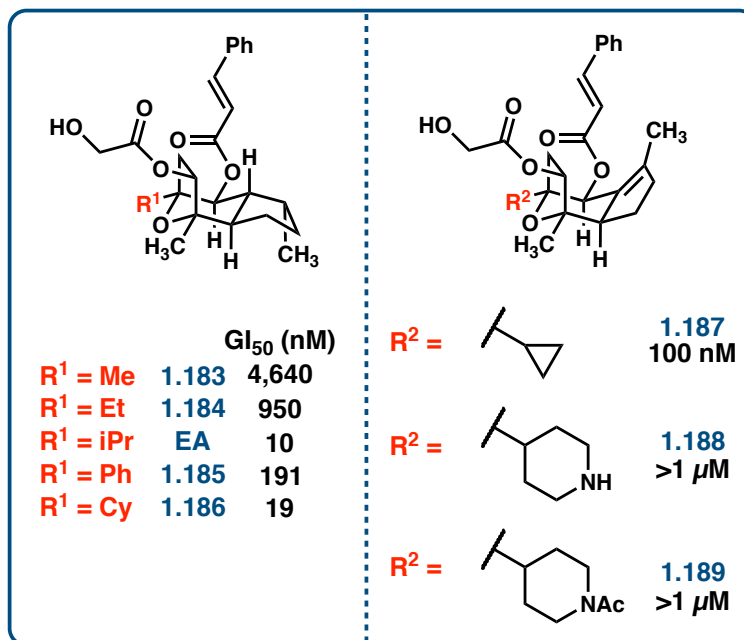


Figure 1.30 Englerin analogues featuring modifications at C7

In 2020, the Chain group along with John Beutler, David Beech, and Antonio Echavarren determined that the cyclohexyl compounds were not only extremely potent toward the A498 cell line but also showed a greatly diminished TRPC4 ion channel agonist activity;¹¹⁵ as a result, these compounds showed diminished adverse effects and lethality upon administration to mice relative to EA itself. This strongly suggests that there is an alternate target or multiple targets in sensitive cell lines.

1.4.4 C9

The C9 glycolate residue in EA is perhaps the most critical position to manipulate in structure–function studies. The first clue to the importance of the biological importance of the function at C9 was (–)-englerin B, which showed no significant cell growth inhibition activity at all.⁷ In their seminal isolation work, the

Beutler group prepared (–)-englerin B acetate which exhibited a GI₅₀ of 1,350 nM but importantly, retained selectivity towards the renal cancer cell lines. This suggests that the hydroxyl function or other heteroatoms at this position are extremely important, likely due to hydrogen bonding interactions present in the binding pocket of the biological target(s).

This position has been extensively investigated by several groups,^{44, 86, 116-117} but the therapeutic candidacy of EA-inspired materials requires more study of this position. Of the C9 analogues evaluated, the most potent are featured on the left side of figure 1.31. Some acceptable modifications include the α -methyl **1.190a**, reverse ester **1.190b**, and the esterified glycolate series **1.190g**. There was a slight increase in the value of the GI₅₀ within methyl glycolate **1.190c**, epoxide **1.190e**, and sulfonate **1.190f**. Other modifications that led to a more drastic decrease in potency include replacing the hydroxyl with an amine **1.191a**, incorporating an additional carbon between the core and the glycolate **1.190m**, and the furan series **1.190j** and **1.190k**.

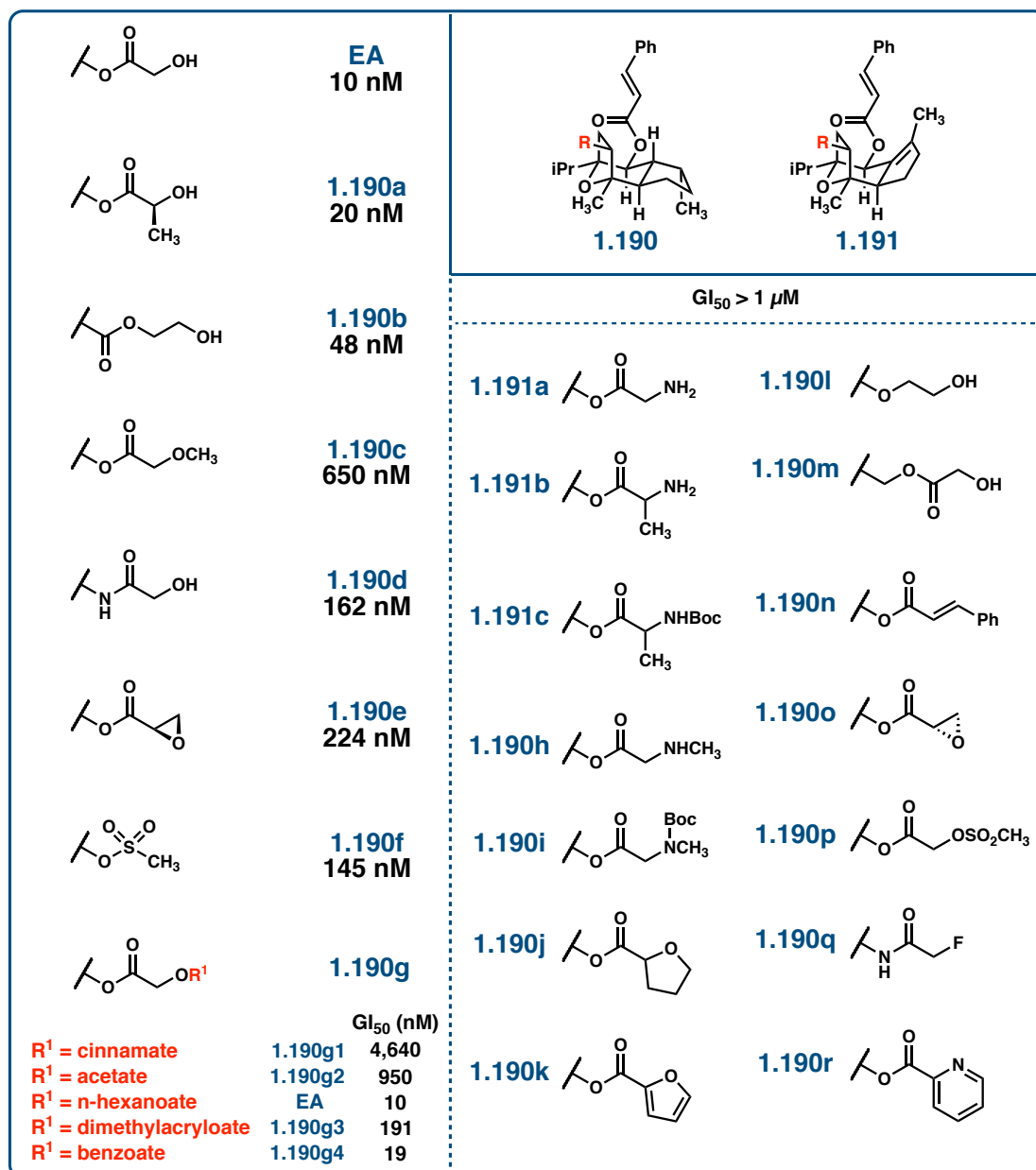


Figure 1.31 Englerin analogues featuring modifications at C9

The amide analogue series are a noteworthy series of analogues published by the Chain group in collaboration with John Beutler in 2016 as this modification

resulted in the development of orally bioavailable analogues.^{117a} With the glycolate ester at this position, there is an increased susceptibility to cleavage of this group by gastric acid. This is indicated by the detection of englerin B in the plasma of mice after treatment with EA. Modifications with C9-amino analogues were accomplished with the hopes of creating a more robust linkage to the scaffold while retaining the potency and selectivity of the natural product. While these analogues were more stable and retained good potency (GI_{50} (A498) = 162 nM for **1.190d**) the GI_{50} values of **1.190d** within the other RCC cell lines were greater than 1 μ M. In this case, variation of the other cinnamate moieties did not productively influence potency within all of the RCC cell lines.

Another interesting analogue is the ether analogue **1.190l**. While this compound is no longer lethal to RCC, it does still readily bind to the TRPC ion channels, acting as a competitive nonagonist binder and potent inhibitor of the effects of EA (IC_{50} = 62 nM). This could serve as a useful tool compound in the investigation of the mechanism of action of EA and its associated analogues.^{117c}

1.5 Proteomic Tool Compounds for Mechanistic Investigation

On top of the vast number of analogues synthesized in the context of structure–function studies, several tool compounds have been generated. Tool compounds include mechanistic probes that can enable the elucidation of molecular targets via binding of the tool compound to the target site and isolation of the compound–target complex using the tool compound as a functional handle. The Christmann group was the first to describe structural modifications for bioconjugation. The tool compounds developed by his group featured cinnamate and glycolate modifications at C6 and C9, respectively (figure 1.32).^{44, 116a}

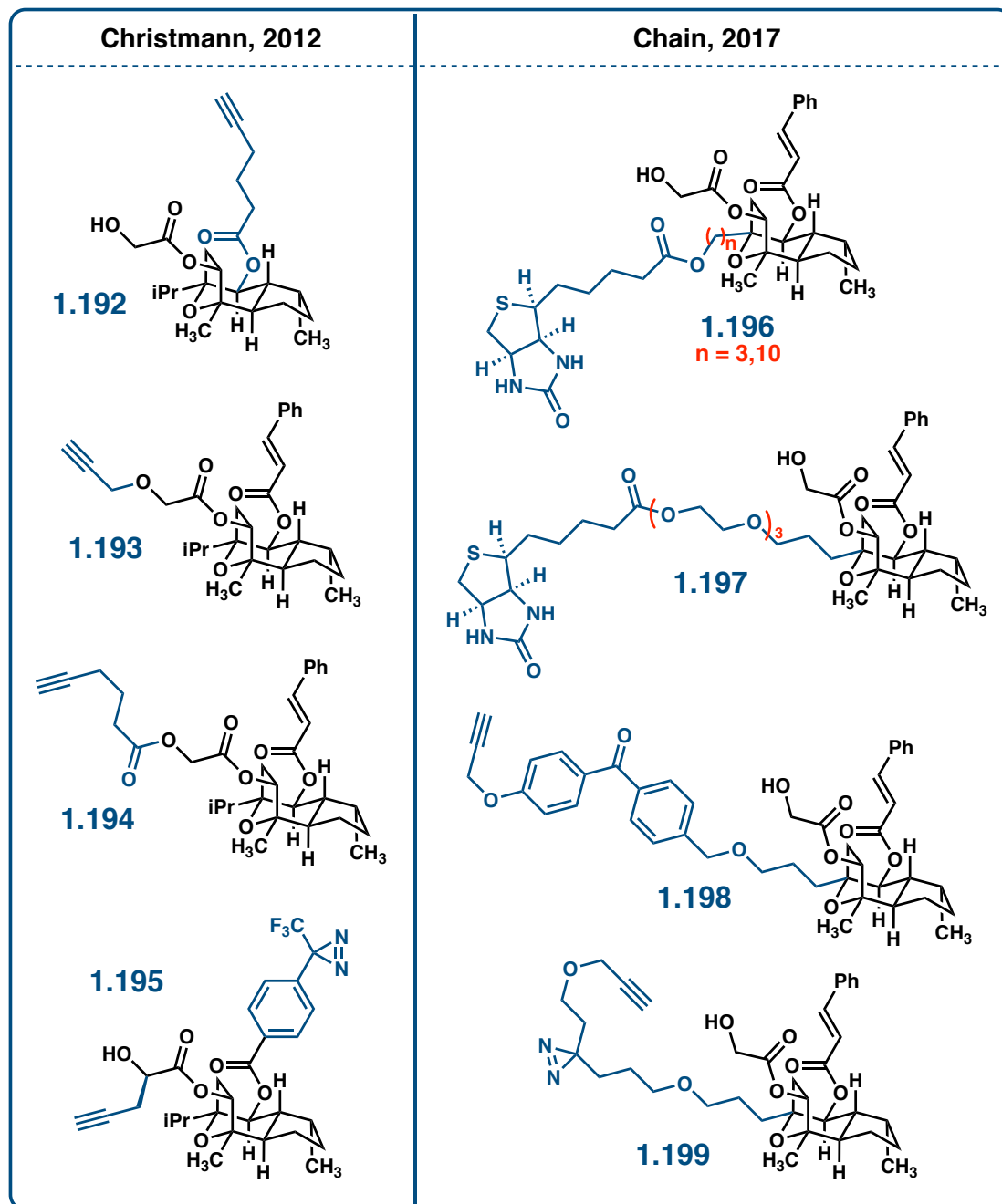


Figure 1.32 Proteomic tool compounds developed by Mathias Christmann et al. and William Chain et al.

The Chain group published a series of tool compounds in 2016 with modifications at C7, replacing the isopropyl sidechain with a label attachment point.¹¹⁸ These tool compounds featured long chains with a terminal alcohol which was subsequently labeled with biotin **1.196**, a diarylketone **1.198**, or a diazirine **1.199**. Due to the hydrophobic nature of the long chain alcohol, a second generation of compounds incorporated a polyethylene glycol chain (**1.197**) to increase its solubility in biological systems.

Unfortunately, no fruitful biological mechanistic information was acquired using these probes so there is still a need for functional proteomic tool compounds. The exact interactions that take place within these cells leading to their death is still a mystery and will require further investigation to elucidate.

1.6 Conclusion

Englerin A is a potent and selective anti-renal cancer compound discovered in 2009 by John Beutler in the Molecular Targets Laboratory (MTL) at the NCI from the extracts of the African plant *Phyllanthus engleri*. Although there is evidence to support specific biological mechanisms of action, the full mechanisms of action are still unclear and are the subject of intense and ongoing investigations. The development of englerin as an anti-renal cancer therapeutic through the synthesis and evaluation of analogues is ongoing. Piecing together the bits of information learned from each new series of analogues may allow for further progression of englerin. The community has arrived at an exciting point in the development of englerin-inspired materials for the treatment of human cancers.

REFERENCES

1. *Cancer Statistics*. National Cancer Institute, 2020.
<https://www.cancer.gov/about-cancer/understanding/statistics> (accessed 2023).
2. Saad, A. M.; Gad, M. M.; Al-Husseini, M. J.; Ruhban, I. A.; Sonbol, M. B.; Ho, T. H. *Clin Genitourin Cancer* **2019**, *17*, 46-57 e45.
3. Sewariya, S.; Singh, S.; Rana, N.; Kumar, Y.; Chandra, R.; Anderson, E. A. *European Journal of Medicinal Chemistry Reports* **2023**, *7*, 100101.
4. McGrath, N. A.; Brichacek, M.; Njardarson, J. T. *J. Chem. Educ.* **2010**, *87*, 1348-1349.
5. (a) Calixto, J. B.; Santos, A. R. S.; Filho, V. C.; Yunes, R. A. *Medicinal Research Reviews* **1998**, *18*, 225-258. (b) Bagalkotkar, G.; Sagineedu, S. R.; Saad, M. S.; Stanslas, J. *J. Pharm. Pharmacol.* **2010**, *58*, 1559-1570. (c) Unander, D. W.; Webster, G. L.; Blumberg, B. S. *J. Ethnopharmacol.* **1995**, *45*, 1-18.
6. Breyer-Brandwijk, M. G. *J. Pharm. Pharmacol.* **1934**, *7*, 167.
7. Ratnayake, R.; Covell, D.; Ransom, T. T.; Gustafson, K. R.; Beutler, J. A. *Org. Lett.* **2009**, *11*, 57-60.
8. (a) Carson, C.; Raman, P.; Tullai, J.; Xu, L.; Henault, M.; Thomas, E.; Yeola, S.; Lao, J.; McPate, M.; Verkuyl, J. M.; et al. *PLoS ONE* **2015**, *10*, e0127498. (b) Sourbier, C.; Bradley; Ratnayake, R.; Thomas; Lee, S.; Lee, M.-J.; Peter; Young; Jane; John; et al. *Cancer Cell* **2013**, *23*, 228-237.
9. Sulzmaier, F. J.; Li, Z.; Nakashige, M. L.; Fash, D. M.; Chain, W. J.; Ramos, J. W. *PLoS ONE* **2012**, *7*, e48032.
10. Williams, R. T.; Yu, A. L.; Diccianni, M. B.; Theodorakis, E. A.; Batova, A. *Journal of Experimental & Clinical Cancer Research* **2013**, *32*, 57.
11. Rodrigues, T.; Sieglitz, F.; Somovilla, V. J.; Cal, P. M. S. D.; Galione, A.; Corzana, F.; Bernardes, G. J. L. *Angew. Chem. Int. Ed.* **2016**, *55*, 11077-11081.

12. Tikhonov, D. B.; Zhorov, B. S. *J. Biol. Chem.* **2009**, *284*, 19006-19017.
13. Freichel, M.; Tsvilovskyy, V.; Camacho-Londoño, J. E. TRPC4- and TRPC4-Containing Channels. Springer Berlin Heidelberg, 2014; pp 85-128.
14. Damann, N.; Voets, T.; Nilius, B. *Curr Biol* **2008**, *18*, R880-889.
15. (a) Uhlen, M.; Fagerberg, L.; Hallstrom, B. M.; Lindskog, C.; Oksvold, P.; Mardinoglu, A.; Sivertsson, A.; Kampf, C.; Sjostedt, E.; Asplund, A.; et al. *Science* **2015**, *347*, 1260419. (b) Schaldecker, T.; Kim, S.; Tarabanis, C.; Tian, D.; Hakroush, S.; Castonguay, P.; Ahn, W.; Wallentin, H.; Heid, H.; Hopkins, C. R.; et al. *J Clin Invest* **2013**, *123*, 5298-5309.
16. (a) Montell, C.; Birnbaumer, L.; Flockerzi, V. *Cell* **2002**, *108*, 595-598. (b) Wu, L.-J.; Sweet, T.-B.; Clapham, D. E. *Pharmacological Reviews* **2010**, *62*, 381-404. (c) Riccio, A.; Li, Y.; Moon, J.; Kim, K. S.; Smith, K. S.; Rudolph, U.; Gapon, S.; Yao, G. L.; Tsvetkov, E.; Rodig, S. J.; et al. *Cell* **2009**, *137*, 761-772. (d) Riccio, A.; Li, Y.; Tsvetkov, E.; Gapon, S.; Yao, G. L.; Smith, K. S.; Engin, E.; Rudolph, U.; Bolshakov, V. Y.; Clapham, D. E. *J. Neurosci.* **2014**, *34*, 3653-3667.
17. Rubaiy, H. N.; Ludlow, M. J.; Henrot, M.; Gaunt, H. J.; Miteva, K.; Cheung, S. Y.; Tanahashi, Y.; Hamzah, N.; Musialowski, K. E.; Blythe, N. M.; et al. *J. Biol. Chem.* **2017**, *292*, 8158-8173.
18. Hofmann, T.; Schaefer, M.; Schultz, G.; Gudermann, T. *Proc Natl Acad Sci U S A* **2002**, *99*, 7461-7466.
19. (a) Gees, M.; Colsoul, B.; Nilius, B. *Cold Spring Harbor Perspectives in Biology* **2010**, *2*, a003962-a003962. (b) Jeong, S.; Ko, J.; Kim, M.; Park, K. C.; Park, E. Y. J.; Kim, J.; Baik, Y.; Wie, J.; Cho, A. E.; Jeon, J.-H.; et al. *The Korean Journal of Physiology & Pharmacology* **2019**, *23*, 191.
20. Akbulut, Y.; Gaunt, H. J.; Muraki, K.; Ludlow, M. J.; Amer, M. S.; Bruns, A.; Vasudev, N. S.; Radtke, L.; Willot, M.; Hahn, S.; et al. *Angew. Chem. Int. Ed.* **2015**, *54*, 3787-3791.
21. Veliceasa, D.; Ivanovic, M.; Hoepfner, F. T.; Thumbikat, P.; Volpert, O. V.; Smith, N. D. *FEBS J* **2007**, *274*, 6365-6377.
22. Ludlow, M. J.; Gaunt, H. J.; Rubaiy, H. N.; Musialowski, K. E.; Blythe, N. M.; Vasudev, N. S.; Muraki, K.; Beech, D. J. *J. Biol. Chem.* **2017**, *292*, 723-731.

23. Kim, J.; Ko, J.; Myeong, J.; Kwak, M.; Hong, C.; So, I. *Pflügers Archiv - European Journal of Physiology* **2019**, *471*, 1045-1053.
24. Cheung, S. Y.; Henrot, M.; Al-Saad, M.; Baumann, M.; Muller, H.; Unger, A.; Rubaiy, H. N.; Mathar, I.; Dinkel, K.; Nussbaumer, P.; et al. *Oncotarget* **2018**, *9*, 29634-29643.
25. Rubaiy, H. N.; Ludlow, M. J.; Bon, R. S.; Beech, D. J. *Channels* **2017**, *11*, 362-364.
26. Vinayagam, D.; Mager, T.; Apelbaum, A.; Bothe, A.; Merino, F.; Hofnagel, O.; Gatsogiannis, C.; Raunser, S. *Elife* **2018**, *7*.
27. Song, K.; Wei, M.; Guo, W.; Quan, L.; Kang, Y.; Wu, J. X.; Chen, L. *Elife* **2021**, *10*.
28. (a) Zhou, Y.; Castonguay, P.; Sidhom, E.-H.; Clark, A. R.; Dvela-Levitt, M.; Kim, S.; Sieber, J.; Wieder, N.; Jung, J. Y.; Andreeva, S.; et al. *Science* **2017**, *358*, 1332-1336. (b) Richter, J. M.; Schaefer, M.; Hill, K. *Mol. Pharmacol.* **2014**, *86*, 514-521.
29. (a) Just, S.; Chenard, B. L.; Ceci, A.; Strassmaier, T.; Chong, J. A.; Blair, N. T.; Gallaschun, R. J.; Del Camino, D.; Cantin, S.; D'Amours, M.; et al. *PLOS ONE* **2018**, *13*, e0191225. (b) Minard, A.; Bauer, C.; Wright, D.; Rubaiy, H.; Muraki, K.; Beech, D.; Bon, R. *Cells* **2018**, *7*, 52.
30. Rubaiy, H. N.; Ludlow, M. J.; Siems, K.; Norman, K.; Foster, R.; Wolf, D.; Beutler, J. A.; Beech, D. J. *British Journal of Pharmacology* **2018**, *175*, 3361-3368.
31. Neo, S. P.; Alli-Shaik, A.; Wee, S.; Lim, Z.; Gunaratne, J. *Journal of Proteome Research* **2022**, *21*, 1948-1960.
32. Nusinow, D. P.; Szpyt, J.; Ghandi, M.; Rose, C. M.; McDonald, E. R.; Kalocsay, M.; Jané-Valbuena, J.; Gelfand, E.; Schweppe, D. K.; Jedrychowski, M.; et al. *Cell* **2020**, *180*, 387-402.e316.
33. Muraki, K.; Ohnishi, K.; Takezawa, A.; Suzuki, H.; Hatano, N.; Muraki, Y.; Hamzah, N.; Foster, R.; Waldmann, H.; Nussbaumer, P.; et al. *Scientific Reports* **2017**, *7*.
34. Caropreso, V.; Darvishi, E.; Turbyville, T. J.; Ratnayake, R.; Grohar, P. J.; McMahon, J. B.; Woldemichael, G. M. *J. Biol. Chem.* **2016**, *291*, 10058-10066.

35. (a) Kovar, H. *Genome Medicine* **2010**, *2*, 8. (b) Leacock, S. W.; Basse, A. N.; Chandler, G. L.; Kirk, A. M.; Rakheja, D.; Amatruda, J. F. *Disease Models & Mechanisms* **2012**, *5*, 95-106.
36. Grant, C. V.; Carver, C. M.; Hastings, S. D.; Ramachandran, K.; Muniswamy, M.; Risinger, A. L.; Beutler, J. A.; Mooberry, S. L. *Breast Cancer Research and Treatment* **2019**, *177*, 345-355.
37. Hatzis, C.; Symmans, W. F.; Zhang, Y.; Gould, R. E.; Moulder, S. L.; Hunt, K. K.; Abu-Khalaf, M.; Hofstatter, E. W.; Lannin, D.; Chagpar, A. B.; et al. *Clin Cancer Res* **2016**, *22*, 26-33.
38. De Sousa Valente, J.; Alawi, K. M.; Bharde, S.; Zarban, A. A.; Kodji, X.; Thapa, D.; Argunhan, F.; Barrett, B.; Nagy, I.; Brain, S. D. *International Journal of Molecular Sciences* **2021**, *22*, 6380.
39. Willot, M.; Radtke, L.; Könning, D.; Fröhlich, R.; Gessner, V. H.; Strohmann, C.; Christmann, M. *Angew. Chem. Int. Ed.* **2009**, *48*, 9105-9108.
40. (a) Podlech, J.; Maier, T. C. *Synthesis* **2003**, 0633-0655. (b) Barbier, P. *C. R. Acad. Sci.* **1899**, 110.
41. (a) Heravi, M. M.; Zadsirjan, V.; Hamidi, H.; Daraie, M.; Momeni, T. Recent applications of the Wittig reaction in alkaloid synthesis. Elsevier, 2020; pp 201-334 (b) Wittig, G.; Fritze, P. *Angewandte Chemie International Edition in English* **2003**, *5*, 846-846. (c) Schlosser, M.; Christmann, K. F. *Angewandte Chemie International Edition in English* **2003**, *5*, 126-126.
42. (a) Ogba, O. M.; Warner, N. C.; O'Leary, D. J.; Grubbs, R. H. *Chem. Soc. Rev.* **2018**, *47*, 4510-4544. (b) Grubbs, R. H. *Angew. Chem. Int. Ed.* **2006**, *45*, 3760-3765. (c) Chatterjee, A. K.; Choi, T. L.; Sanders, D. P.; Grubbs, R. H. *J. Am. Chem. Soc.* **2003**, *125*, 11360-11370. (d) Trogler, W. C.; Stewart, R. C.; Marzilli, L. G. *J. Am. Chem. Soc.* **2002**, *96*, 3697-3699. (e) Nguyen, S. T.; Grubbs, R. H.; Ziller, J. W. *J. Am. Chem. Soc.* **2002**, *115*, 9858-9859. (f) Schwab, P.; Grubbs, R. H.; Ziller, J. W. *J. Am. Chem. Soc.* **1996**, *118*, 100-110.
43. (a) Majhi, S. *ChemistrySelect* **2021**, *6*, 4178-4206. (b) Inanaga, J.; Hirata, K.; Saeki, H.; Katsuki, T.; Yamaguchi, M. *Bull. Chem. Soc. Jpn.* **1979**, *52*, 1989-1993.
44. Radtke, L.; Willot, M.; Sun, H.; Ziegler, S.; Sauerland, S.; Strohmann, C.; Fröhlich, R.; Habenberger, P.; Waldmann, H.; Christmann, M. *Angew. Chem. Int. Ed.* **2011**, *50*, 3998-4002.

45. Molawi, K.; Delpont, N.; Echavarren, A. M. *Angew. Chem. Int. Ed.* **2010**, *49*, 3517-3519.
46. Zhou, Q.; Chen, X.; Ma, D. *Angew. Chem. Int. Ed.* **2010**, *49*, 3513-3516.
47. (a) Reyes, E.; Prieto, L.; Uria, U.; Carrillo, L.; Vicario, J. L. *ACS Omega* **2022**, *7*, 31621-31627. (b) Prins, H. J. *Chem. Weekblad* **1919**, *16*, 1510-1526.
48. Jimenez-Nunez, E.; Claverie, C. K.; Nieto-Oberhuber, C.; Echavarren, A. M. *Angew. Chem. Int. Ed. Engl.* **2006**, *45*, 5452-5455.
49. (a) Mushtaq, A.; Zahoor, A. F.; Bilal, M.; Hussain, S. M.; Irfan, M.; Akhtar, R.; Irfan, A.; Kotwica-Mojzych, K.; Mojzych, M. *Molecules* **2023**, *28*, 2722. (b) Katsuki, T.; Sharpless, K. B. *J. Am. Chem. Soc.* **2002**, *102*, 5974-5976.
50. (a) *Comprehensive Organic Name Reactions and Reagents* **2010**. (b) Appel, R. *Angewandte Chemie International Edition in English* **1975**, *14*, 801-811.
51. (a) Denmark, S. E.; Heemstra, J. R.; Beutner, G. L. *Angew. Chem. Int. Ed.* **2005**, *44*, 4682-4698. (b) Denmark, S. E.; Wong, K.-T.; Stavenger, R. A. *J. Am. Chem. Soc.* **1997**, *119*, 2333-2334.
52. (a) Heravi, M. M.; Momeni, T.; Zadsirjan, V.; Mohammadi, L. *Curr Org Synth* **2021**, *18*, 125-196. (b) Dess, D. B.; Martin, J. C. *The Journal of Organic Chemistry* **1983**, *48*, 4155-4156.
53. Nicolaou, K. C.; Kang, Q.; Ng, S. Y.; Chen, D. Y. K. *J. Am. Chem. Soc.* **2010**, *132*, 8219-8222.
54. (a) Choy, P. Y.; Gan, K. B.; Kwong, F. Y. *Chin. J. Chem.* **2023**, *41*, 1099-1118. (b) Mohajer, F.; Heravi, M. M.; Zadsirjan, V.; Poormohammad, N. *RSC Advances* **2021**, *11*, 6885-6925. (c) Sonogashira, K.; Tohda, Y.; Hagihara, N. *Tetrahedron Lett.* **1975**, *16*, 4467-4470.
55. (a) Peltzer, R. M.; Gauss, J.; Eisenstein, O.; Cascella, M. *J. Am. Chem. Soc.* **2020**, *142*, 2984-2994. (b) Grignard, V. *Compt. Rend.* **1900**, 1322-1325.
56. (a) Liang, L.; Guo, L. D.; Tong, R. *Acc. Chem. Res.* **2022**, *55*, 2326-2340. (b) Achmatowicz, O.; Bukowski, P.; Szechner, B.; Zwierzchowska, Z.; Zamojski, A. *Tetrahedron* **1971**, *27*, 1973-1996.
57. (a) Rajeshwaran, P.; Trouvé, J.; Youssef, K.; Gramage-Doria, R. *Angew. Chem. Int. Ed.* **2022**, *61*. (b) Phillips, F. C. *American Chemical Journal* **1894**, 255-277.

58. (a) Stastna, E.; Cerny, I.; Pouzar, V.; Chodounska, H. *Steroids* **2010**, *75*, 721-725. (b) Luche, J. L. *J. Am. Chem. Soc.* **2002**, *100*, 2226-2227.
59. (a) Khalid, M.; Mohammed, S.; Kalo, A. *Oriental Journal of Chemistry* **2020**, *36*, 206-219. (b) Nahm, S.; Weinreb, S. M. *Tetrahedron Lett.* **1981**, *22*, 3815-3818.
60. (a) Renz, M.; Meunier, B. *Eur. J. Org. Chem.* **1999**, 1999, 737-750. (b) Baeyer, A.; Villiger, V. *Berichte der deutschen chemischen Gesellschaft* **1899**, *32*, 3625-3633.
61. Xu, J.; Caro-Diaz, E. J. E.; Theodorakis, E. A. *Org. Lett.* **2010**, *12*, 3708-3711.
62. (a) Christoffers, J.; Baro, A.; Werner, T. *Advanced Synthesis & Catalysis* **2004**, *346*, 143-151. (b) Rubottom, G. M.; Vazquez, M. A.; Pelegrina, D. R. *Tetrahedron Lett.* **1974**, *15*, 4319-4322.
63. (a) Nicolaou, K. C.; Snyder, S. A.; Longbottom, D. A.; Nalbandian, A. Z.; Huang, X. *Chemistry – A European Journal* **2004**, *10*, 5581-5606. (b) Burgess, E. M.; Penton, H. R.; Taylor, E. A. *J. Am. Chem. Soc.* **2002**, *92*, 5224-5226.
64. Li, Z.; Nakashige, M.; Chain, W. J. *J. Am. Chem. Soc.* **2011**, *133*, 6553-6556.
65. (a) Hagiwara, H. *Natural Product Communications* **2021**, *16*. (b) Michael, A. *J. Prakt. Chem.* **1883**, *35*, 349.
66. (a) Khademi, Z.; Heravi, M. M. *Tetrahedron* **2022**, *103*. (b) Claisen, R. L.; Lowman, O. *Ber.* **1887**, *20*, 651-654.
67. (a) Antón-Cánovas, T.; Alonso, F. *Angew. Chem. Int. Ed.* **2023**, *62*. (b) Schreiber, J.; Maag, H.; Hashimoto, N.; Eschenmoser, A. *Angewandte Chemie International Edition in English* **1971**, *10*, 330-331.
68. Lee, J.; Parker, K. A. *Org. Lett.* **2012**, *14*, 2682-2685.
69. (a) Wang, P.; Lindsey, J. S. *Molecules* **2020**, *25*, 1858. (b) Riley, H. L.; Morley, J. F.; Friend, N. A. C. *Journal of the Chemical Society (Resumed)* **1932**, 1875.
70. (a) Arterburn, J. B. *Tetrahedron* **2001**, *57*, 9765-9788. (b) Sharma, A. K.; Swern, D. *Tetrahedron Lett.* **1974**, *15*, 1503-1506.
71. Takahashi, K.; Komine, K.; Yokoi, Y.; Ishihara, J.; Hatakeyama, S. *J. Org. Chem.* **2012**, *77*, 7364-7370.

72. (a) Levine, S. G.; Bonner, M. P. *Tetrahedron Lett.* **1989**, *30*, 4767-4770. (b) Stork, G.; Cama, L. D.; Coulson, D. R. *J. Am. Chem. Soc.* **1974**, *96*, 5268-5270. (c) Stork, G.; Cohen, J. F. *J. Am. Chem. Soc.* **1974**, *96*, 5270-5272.
73. (a) Gil, A.; Albericio, F.; Alvarez, M. *Chem Rev* **2017**, *117*, 8420-8446. (b) Okude, Y.; Hirano, S.; Hiyama, T.; Nozaki, H. *J. Am. Chem. Soc.* **2002**, *99*, 3179-3181. (c) Jin, H.; Uenishi, J.; Christ, W. J.; Kishi, Y. *J. Am. Chem. Soc.* **2002**, *108*, 5644-5646. (d) Takai, K.; Tagashira, M.; Kuroda, T.; Oshima, K.; Utimoto, K.; Nozaki, H. *J. Am. Chem. Soc.* **1986**, *108*, 6048-6050.
74. (a) Jordan, A.; Whymark, K. D.; Sydenham, J.; Sneddon, H. F. *Green Chemistry* **2021**, *23*, 6405-6413. (b) Neises, B.; Steglich, W. *Angewandte Chemie International Edition in English* **1978**, *17*, 522-524.
75. Wang, J.; Chen, S.-G.; Sun, B.-F.; Lin, G.-Q.; Shang, Y.-J. *Chemistry - A European Journal* **2013**, *19*, 2539-2547.
76. (a) Ghavre, M. *Asian Journal of Organic Chemistry* **2020**, *9*, 1901-1923. (b) Shapiro, R. H. *Organic Reactions* **2011**, 405-507.
77. (a) Xie, J. Q.; Liang, R. X.; Jia, Y. X. *Chin. J. Chem.* **2021**, *39*, 710-728. (b) Heck, R. F. *J. Am. Chem. Soc.* **2002**, *90*, 5518-5526.
78. (a) Helmchen, G. *Chemistry – A European Journal* **2023**, *29*. (b) Lightfoot, A.; Schnider, P.; Pfaltz, A. *Angew. Chem. Int. Ed.* **1998**, *37*, 2897-2899.
79. Zahel, M.; Keßberg, A.; Metz, P. *Angew. Chem. Int. Ed.* **2013**, *52*, 5390-5392.
80. (a) Saeed, S.; Zahoor, A. F.; Ahmad, S.; Akhtar, R.; Sikandar, S. *Synth. Commun.* **2022**, *52*, 317-345. (b) Reformatsky, S. *Berichte der deutschen chemischen Gesellschaft* **1887**, *20*, 1210-1211.
81. Zhang, J.; Zheng, S.; Peng, W.; Shen, Z. *Tetrahedron Lett.* **2014**, *55*, 1339-1341.
82. Hanari, T.; Shimada, N.; Kurosaki, Y.; Thrimurtulu, N.; Nambu, H.; Anada, M.; Hashimoto, S. *Chemistry - A European Journal* **2015**, *21*, 11671-11676.
83. (a) Lindsay, V. N. G.; Lin, W.; Charette, A. B. *J. Am. Chem. Soc.* **2009**, *131*, 16383-16385. (b) Yamawaki, M.; Tsutsui, H.; Kitagaki, S.; Anada, M.; Hashimoto, S. *Tetrahedron Lett.* **2002**, *43*, 9561-9564.

84. (a) Lu, Y.; Nguyen, P. L.; Levaray, N.; Lebel, H. *J. Org. Chem.* **2013**, *78*, 776-779. (b) Ito, Y.; Hirao, T.; Saegusa, T. *The Journal of Organic Chemistry* **1978**, *43*, 1011-1013.
85. Kusama, H.; Tazawa, A.; Ishida, K.; Iwasawa, N. *Chemistry - An Asian Journal* **2016**, *11*, 64-67.
86. López-Suárez, L.; Riesgo, L.; Bravo, F.; Ransom, T. T.; Beutler, J. A.; Echavarren, A. M. *ChemMedChem* **2016**, *11*, 1003-1007.
87. (a) Genet, J. P. *Acc. Chem. Res.* **2003**, *36*, 908-918. (b) Miyashita, A.; Yasuda, A.; Takaya, H.; Toriumi, K.; Ito, T.; Souchi, T.; Noyori, R. *J. Am. Chem. Soc.* **2002**, *102*, 7932-7934.
88. (a) Feng, X.; Du, H. *Chin. J. Chem.* **2021**, *39*, 2016-2026. (b) Tu, Y.; Wang, Z.-X.; Shi, Y. *J. Am. Chem. Soc.* **1996**, *118*, 9806-9807. (c) Curci, R.; Fiorentino, M.; Serio, M. R. *J. Chem. Soc., Chem. Commun.* **1984**, 155.
89. (a) Frontier, A. J.; Hernandez, J. J. *Acc. Chem. Res.* **2020**, *53*, 1822-1832. (b) Nazarov, I. N.; Zaretskaya, I. I. *Bulletin of the Academy of Sciences of the USSR* **1942**, 200-209.
90. Morisaki, K.; Sasano, Y.; Koseki, T.; Shibuta, T.; Kanoh, N.; Chiou, W.-H.; Iwabuchi, Y. *Org. Lett.* **2017**, *19*, 5142-5145.
91. Kawasumi, M.; Kanoh, N.; Iwabuchi, Y. *Org. Lett.* **2011**, *13*, 3620-3623.
92. (a) Aleena, M. B.; Philip, R. M.; Anilkumar, G. *Appl. Organomet. Chem.* **2021**, *35*. (b) Lautens, M.; Sanichar, R. *Synfacts* **2020**, *16*, 0314. (c) Heravi, M. M.; Mohammadkhani, L. *J. Organomet. Chem.* **2018**, *869*, 106-200. (d) De-Ping, W.; Xu-Dong, Z.; Yun, L.; Jin-Heng*, L. *Chinese Journal of Organic Chemistry* **2006**, *26*, 19-26. (e) Milstein, D.; Stille, J. K. *J. Am. Chem. Soc.* **2002**, *100*, 3636-3638. (f) Azarian, D.; Dua, S. S.; Eaborn, C.; Walton, D. R. M. *J. Organomet. Chem.* **1976**, *117*, C55-C57.
93. Fleming, J. J.; Du Bois, J. *J. Am. Chem. Soc.* **2006**, *128*, 3926-3927.
94. (a) Haas, D.; Hammann, J. M.; Greiner, R.; Knochel, P. *ACS Catalysis* **2016**, *6*, 1540-1552. (b) Baba, S.; Negishi, E. *J. Am. Chem. Soc.* **2002**, *98*, 6729-6731.
95. Hatano, M.; Suzuki, S.; Ishihara, K. *J. Am. Chem. Soc.* **2006**, *128*, 9998-9999.
96. Hagihara, S.; Hanaya, K.; Sugai, T.; Shoji, M. *The Journal of Antibiotics* **2018**, *71*, 257-262.

97. (a) Bongso, A.; Roswanda, R.; Syah, Y. M. *RSC Advances* **2022**, *12*, 15885-15909. (b) Mc Murry, J. E.; Fleming, M. P. *J. Am. Chem. Soc.* **1974**, *96*, 4708-4709.
98. Liu, P.; Cui, Y.; Chen, K.; Zhou, X.; Pan, W.; Ren, J.; Wang, Z. *Org. Lett.* **2018**, *20*, 2517-2521.
99. (a) Matsuo, J. I.; Murakami, M. *Angew. Chem. Int. Ed.* **2013**, *52*, 9109-9118. (b) Mukaiyama, T.; Narasaka, K.; Banno, K. *Chem. Lett.* **1973**, *2*, 1011-1014.
100. (a) Maas, G. *Angew. Chem. Int. Ed.* **2009**, *48*, 8186-8195. (b) Regitz, M. *Angewandte Chemie International Edition in English* **1967**, *6*, 733-749.
101. (a) Selaković, Ž.; Nikolić, A. M.; Ajdačić, V.; Opsenica, I. M. *Eur. J. Org. Chem.* **2022**, *2022*. (b) Tsuji, J.; Ohno, K. *Tetrahedron Lett.* **1965**, *6*, 3969-3971.
102. Reagan, C.; Trevitt, G.; Tchabanenko, K. *Eur. J. Org. Chem.* **2019**, *2019*, 1027-1037.
103. Guo, L.; Plietker, B. *Angew. Chem.* **2019**.
104. (a) *Comprehensive Organic Name Reactions and Reagents* **2010**. (b) Krapcho, A. P.; Glynn, G. A.; Grenon, B. J. *Tetrahedron Lett.* **1967**, *3*, 215-217.
105. (a) Kawanami, Y.; Yanagita, R. *Molecules* **2018**, *23*, 2408. (b) Corey, E. J.; Bakshi, R. K.; Shibata, S.; Chen, C. P.; Singh, V. K. *J. Am. Chem. Soc.* **2002**, *109*, 7925-7926. (c) Corey, E. J.; Bakshi, R. K.; Shibata, S. *J. Am. Chem. Soc.* **2002**, *109*, 5551-5553.
106. (106) Siemon, T.; Wang, Z.; Bian, G.; Seitz, T.; Ye, Z.; Lu, Y.; Cheng, S.; Ding, Y.; Huang, Y.; Deng, Z.; et al. *J. Am. Chem. Soc.* **2020**, *142*, 2760-2765.
107. Crossley, S. W. M.; Barabé, F.; Shenvi, R. A. *J. Am. Chem. Soc.* **2014**, *136*, 16788-16791.
108. Mou, S.-B.; Xiao, W.; Wang, H.-Q.; Wang, S.-J.; Xiang, Z. *Org. Lett.* **2020**, *22*, 1976-1979.
109. (a) Navickas, V.; Ushakov, D. B.; Maier, M. E.; Ströbele, M.; Meyer, H. J. *Org. Lett.* **2010**, *12*, 3418-3421. (b) Zhang, J.; Liao, Z.; Chen, L.; Zhu, S. *Chemistry – A European Journal* **2019**, *25*, 9405-9409. (c) Jin, M.; Tang, C.; Li, Y.; Yang, S.; Yang, Y.-T.; Peng, L.; Li, X.-N.; Zhang, W.; Zuo, Z.; Gagosz, F.; et al. *Nature Communications* **2021**, *12*.

110. Liu, L.; Cheng, H.-L.; Ma, W.-Q.; Hou, S.-H.; Tu, Y.-Q.; Zhang, F.-M.; Zhang, X.-M.; Wang, S.-H. *Chem. Commun.* **2018**, *54*, 196-199.
111. (a) Cope, A. C.; Hardy, E. M. *J. Am. Chem. Soc.* **2002**, *62*, 441-444. (b) Tomiczek, B. M.; Grenning, A. J. *Organic & Biomolecular Chemistry* **2021**, *19*, 2385-2398.
112. Shoemaker, R. H. *Nature Reviews Cancer* **2006**, *6*, 813-823.
113. (a) Wender, P. A.; Quiroz, R. V.; Stevens, M. C. *Acc. Chem. Res.* **2015**, *48*, 752-760. (b) Wender, P. A. *Nat. Prod. Rep.* **2014**, *31*, 433-440. (c) Wender, P. A.; Verma, V. A.; Paxton, T. J.; Pillow, T. H. *Acc. Chem. Res.* **2008**, *41*, 40-49.
114. Elliott, D. C.; Beutler, J. A.; Parker, K. A. *ACS Medicinal Chemistry Letters* **2017**, *8*, 746-750.
115. Wu, Z.; Suppo, J.-S.; Tumova, S.; Strobe, J.; Bravo, F.; Moy, M.; Weinstein, E. S.; Peer, C. J.; Figg, W. D.; Chain, W. J.; et al. *ACS Medicinal Chemistry Letters* **2020**, *11*, 1711-1716.
116. (a) Christmann, M.; Radtke, L.; Waldmann, H.; Willot, M.; Ziegler, S.; Sun, H. Derivatives of Englerin for the Treatment of Cancer. 2012(b) Chan, K. P.; Chen, D. Y. K. *ChemMedChem* **2011**, *6*, 420-423.
117. (a) Fash, D. M.; Peer, C. J.; Li, Z.; Talisman, I. J.; Hayavi, S.; Sulzmaier, F. J.; Ramos, J. W.; Sourbier, C.; Neckers, L.; Figg, W. D.; et al. *Bioorganic & Medicinal Chemistry Letters* **2016**, *26*, 2641-2644. (b) Seenadera, S. P. D.; Long, S. A.; Akee, R.; Bermudez, G.; Parsonage, G.; Strobe, J.; Peer, C.; Figg, W. D.; Parker, K. A.; Beech, D. J.; et al. *ACS Medicinal Chemistry Letters* **2022**, *13*, 1472-1476. (c) Rubaiy, H. N.; Seitz, T.; Hahn, S.; Choidas, A.; Habenberger, P.; Klebl, B.; Dinkel, K.; Nussbaumer, P.; Waldmann, H.; Christmann, M.; et al. *British Journal of Pharmacology* **2018**, *175*, 830-839.
118. Wu, Z.; Zhao, S.; Fash, D. M.; Li, Z.; Chain, W. J.; Beutler, J. A. *J. Nat. Prod.* **2017**, *80*, 771-781.

Chapter 2

SYNTHESIS OF A NEXT-GENERATION SERIES OF ENGLERIN ANALOGUES CONTAINING A C7-CYCLOHEXYL GROUP, HYDROPHOBIC C6-ESTERS, AND C9-GLYCOLATE ISOSTERES

2.1 Targeted series of analogues

With the combined knowledge gained through the synthesis and biological evaluation of the vast compendium of englerin analogues to date, front line efforts are directed toward the selection of bits and pieces of each generational advance to design new active, drug-like analogues.¹ In what is perhaps the most important advance to date, replacing the C7-isopropyl group with larger alkyl groups such as cyclohexyl is advantageous; large groups at C7 appear to directly ablate TRPC4 agonism and thus diminish or eliminate the non-specific lethality observed with the natural product associated with this activity *in vivo*.² Ablation of ion channel agonism activity while retaining potency toward RCC is of prime importance in the development of a safe therapeutic, and thus the focus of my work is the development of new analogues that feature a C7-cyclohexyl modification as the primary platform. It is also quite clear that the hydrogen bond donor/acceptor network presented by the C9-glycolate in the natural product is key to the activity in englerins, but such a function is also vulnerable to hydrolytic degradation. Hydrolysis of the glycolate leaves englerin B in its wake, which is inactive; thus, my research will also focus on finding a robust alternative to the glycolate function that retains the necessary hydrogen bonding capability. By incorporating a wide variety of isosteres and glycolate alternatives, we may be able to

determine a suitable group that is less sensitive to acid and base mediated hydrolysis, but that will retain potency within a desirable range and selectivity for RCC cell lines. The last major variable we will alter is the C6-ester function, which is a cinnamate in the natural product. As executed in the past, we will feature a variety of hydrophobic cinnamate moieties or mimics at C6 that have been shown to retain favorable activity. Indeed, relatively small changes at this position may allow us to greatly influence potency into desirable ranges.

The targeted analogues will feature the C9-isosteres and C6-cinnamate moieties shown in figure 2.1. Amongst these isosteres include more substituted glycolates, replacement of the carbonyl with groups such as fluorine and oxetane, amines and amides, ethers and esters, and heterocycles. One feature common to most of the isosteres is that they would be bound to the scaffold by a carbon-carbon bond linkage rather than by a carbon-heteroatom linkage such as the carbon-oxygen bond present in EA. The glycolate is particularly vulnerable to cleavage by gastric acid, which we attribute to the presence of the α -electron-withdrawing hydroxyl group, but importantly, the C6-cinnamate or cinnamate mimics are quite stable at a variety of pH ranges in vivo. Our “reverse ester” series of compounds (figure 2.1) should allow us to generate carbon-linked hydrogen bonding networks with favorable activity profiles. Amongst the C6 residues, our common pool includes cinnamate, 4-methylcinnamate, naphthoate, and the phenyl cyclopropyl ester, among other readily accessible hydrophobic mimics.

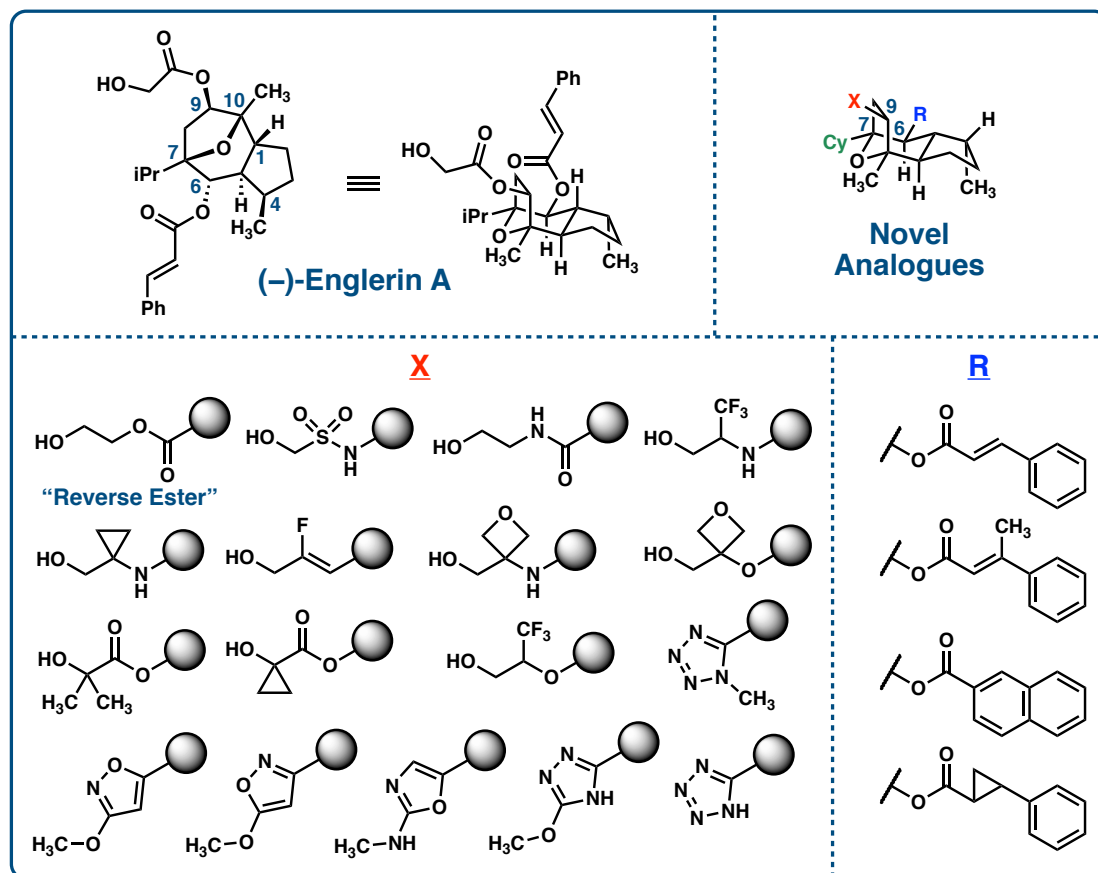


Figure 2.1 Targeted novel englerin-based analogues

2.2 Efforts Towards a Carbon–Carbon Homologation

Our long-standing priority has been the reverse ester series featuring carbon-linked glycolate isosteres and mimics. Based on a single reverse ester analogue featuring a C7-isopropyl and C6-cinnamate synthesized in the past by David Chen³ (A498 GI₅₀ = 48 nM), we approached this series of compounds with confidence. By merging this modification with the C7-cyclohexyl platform, our synthetic approach to the englerins presented our first challenge – identifying carbon–carbon bond-forming homologation strategies that might convert a C9-ketone to a suitable carbon-linked

function. The simplest means of incorporating carbon at C9 with the least changes to our synthetic route entailed installing a nitrile group via nucleophilic displacement of the known C9-sulfonylimidazole; with nitrile installed with the correct stereochemistry at C9, the desired analogue family could be accessed in just a few steps by transformation of the nitrile to the desired reverse esters or to a wide array of the other targeted isosteres.

Our approach to the next generation of analogues is based on the synthetic route developed by our group in 2020 in the development of the original series of C7-alkyl modified analogues,² which in turn was adapted from the 2011 total synthesis of (-)-englerin A developed by our group.⁴ The core scaffold of EA is constructed in two steps by joining two key intermediates together exploiting classical carbonyl chemistry.⁴ Thus, our approaches rely upon the furanone **2.1** and the aldehyde **2.2** (figure 2.2).

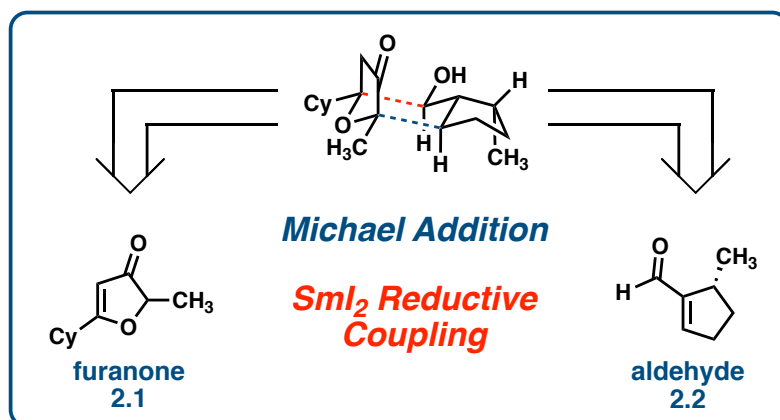


Figure 2.2 Retrosynthetic analysis of the core structure of the englerin analogues

The furanone **2.1** is synthesized in two steps starting with a Claisen⁵ condensation between cyclohexyl methyl ketone and α -chloroester **2.3** (figure 2.3), affording the chlorodiketone **2.4**. In solution, the chlorodiketone exists as a tautomeric mixture but is straightforward to characterize. Upon treatment of the chlorodiketone **2.4** with DBU, an intramolecular substitution reaction of the chlorine atom with the tautomeric alcohol is induced and cyclizes the system to afford the furanone **2.1**.

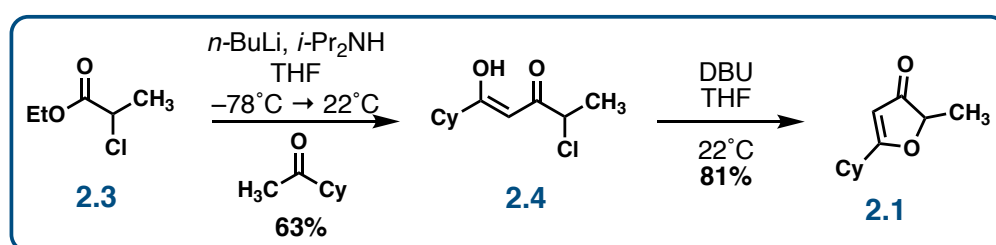


Figure 2.3 Synthesis of furanone **2.1**

The aldehyde is also synthesized in two steps starting from (*R*)-(+)-citronellal as shown in figure 2.4. Alternatively, enantiomerically pure citronellyl butyrate¹ can be reduced under the action of LiAlH_4 to give citronellol, and subsequent oxidation via the Swern⁶ protocol affords (*R*)-(+)-citronellal in higher enantiomeric purity than that which is received from typical suppliers. From here, treatment of citronellal with Eschenmoser's⁷ salt affords the unsaturated aldehyde **2.2**. A ring-closing metathesis under the action of the Grubbs'⁸ 2nd Generation catalyst results in the cyclopentenyl aldehyde **2.2**, setting the stage for the first key step, the Michael⁹ addition.

¹ We gratefully acknowledge Advanced Biotech for their gracious donation of 1 kg of enantiomerically pure citronellyl butyrate in support of our mission to develop anticancer natural product analogues.

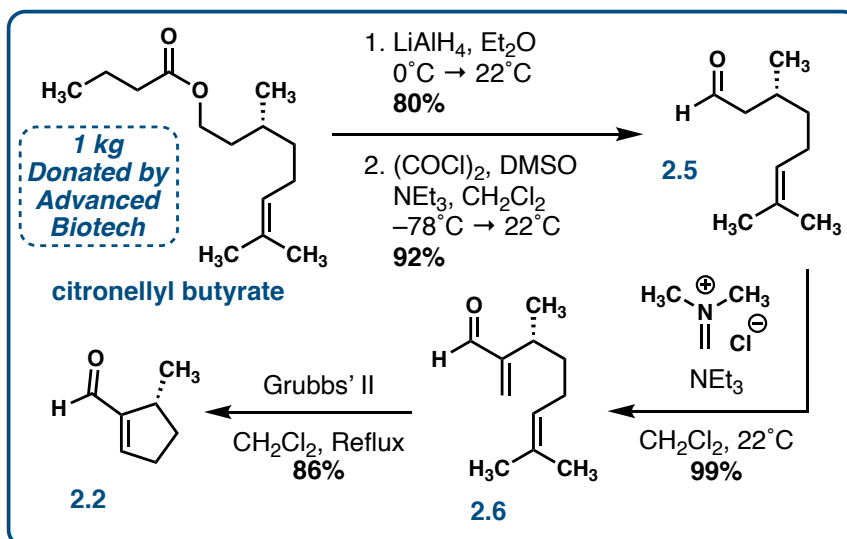


Figure 2.4 Synthesis of cyclic unsaturated aldehyde **2.2**

The Michael⁹ addition forms the first key carbon–carbon bond in the construction of the englerin core; the lithium enolate derived from the furanone **2.1** engages the unsaturated aldehyde **2.2** at the β -position (figure 2.5). Following quench with ammonium chloride, this reaction affords an inseparable mixture of diastereomers (ca. 2:1 desired: Σ others) which is inconsequential for subsequent steps. The mixture of diastereomers so obtained undergoes a carbonyl-alkene cyclization event to complete the englerin core; treatment of the diastereomeric mixture with a mixture of samarium(II) iodide (SmI_2) and hexamethylphosphoramide (HMPA) in THF reductively couples the aldehyde to the β -position of the unsaturated furanone.

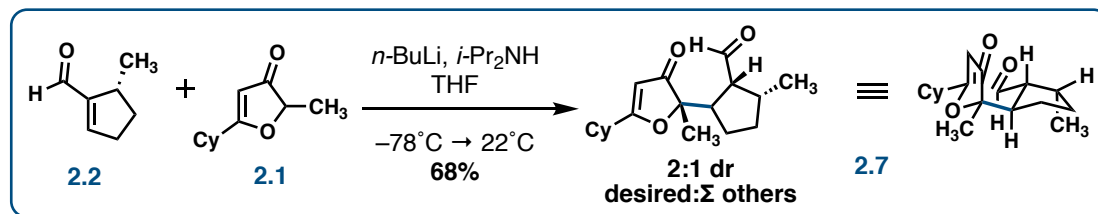


Figure 2.5 The Michael addition between furanone **2.1** and aldehyde **2.2**

This reaction proceeds through a radical mechanism featured in figure 2.6. Ketyl radical formation as a result of SmI_2 engaging a carbonyl results in the formation of a stable Sm(III) adduct. When generated at the aldehyde, the ketyl radical can either form a bond by engaging the neighboring carbonyl directly or the β -position of the unsaturated ketone. When coupling to the β -position of the unsaturated ketone, the desired englerin core scaffold is furnished, but when coupled to the ketone, the undesirable pinacol¹⁰ product is generated. Unfortunately, the vast majority of our material is funneled to the pinacol product, presumably due to some directing effect as a result of the samarium binding the carbonyl radical acceptor. It is also possible that the ketyl radical is generated at the furanone first, then attacking the aldehyde either directly or via through the β -position (one might consider the furanone ketyl radical as an extended system, expressed as resonance structures). The radical character at either the ketone carbonyl carbon or β -position can couple to the aldehyde resulting in the formation of pinacol and the desired products, respectively.

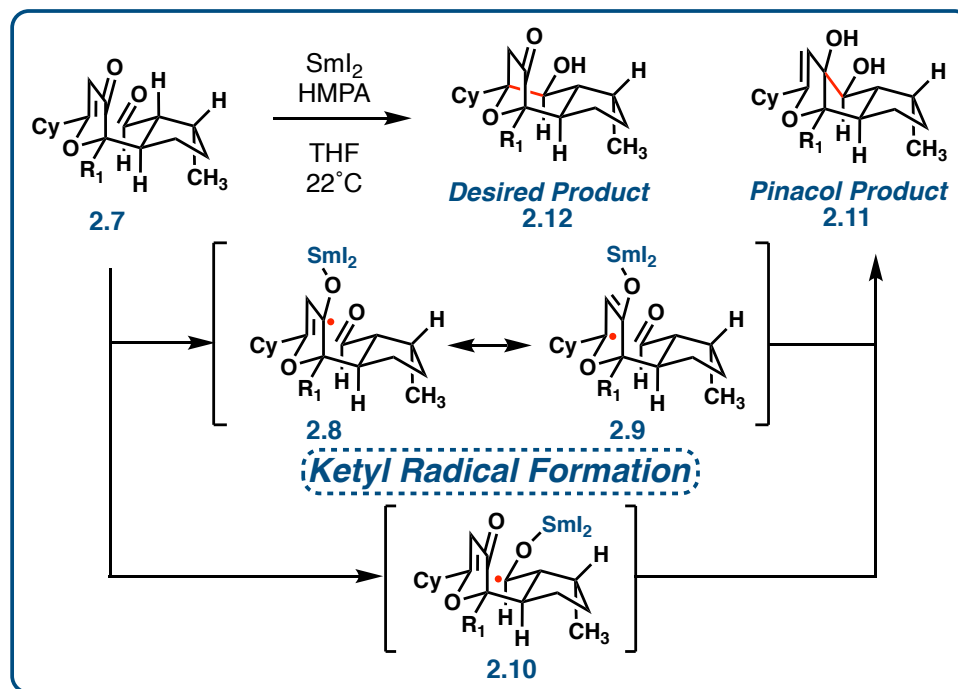


Figure 2.6 Samarium diiodide reductive coupling pathways and products

After extensive experimentation, when the mixture of diastereomers from the Michael addition are treated with SmI_2 (4.0 equiv) and HMPA (18.5 equiv) in THF (0.01 M) under scrupulously water- and air-free conditions, we observe an average yield of 5% at the low scale of 0.23 mmol or 69 mg. The radical cyclization has long stood as the bottleneck of our synthetic work and considerable effort has been directed toward reoptimizing these reaction conditions or finding a replacement for this reaction altogether.

One possible strategy toward the selective cyclization of the Michael adduct involves the installation of excisable groups that facilitate the desired radical formation. Considerable effort was directed toward the use of a silyl group as an electroauxiliary and a means of chemoselectively generating the radical at C7 as

shown in figure 2.7. This would remove the issues of selectivity observed within the SmI_2 coupling. One could generate the radical from this C–Si linkage electrochemically due to its low oxidation potential.¹¹ The silyl group could be added into the furan through a conjugate silyl addition.¹² Work toward the generation and use of these intermediates under electrooxidative conditions is ongoing, and a similar strategy wherein this silyl group is used to generate a radical via photochemical oxidation is also currently under investigation.¹³

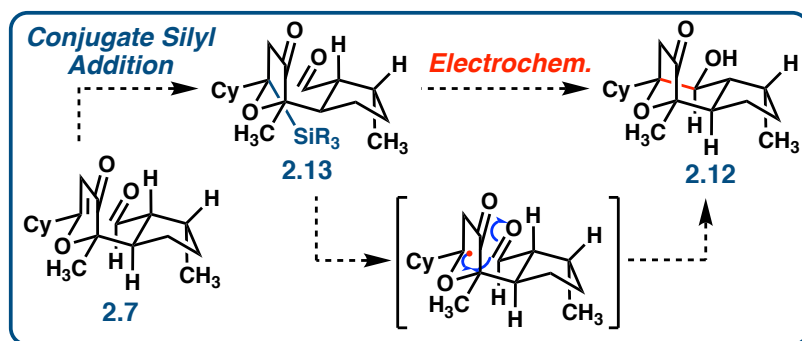


Figure 2.7 Proposed route to core compound 2.12 using electroauxiliaries

In ongoing collaborative electrochemical investigations with Professor Joel Rosenthal, we pursued the electrochemical reductive cyclization of the Michael product for a brief period. Methodology described by R.D. Little in 1985 demonstrated intramolecular reductive coupling of ketones and unsaturated esters (figure 2.8) which are electronically similar to our desired bond formation.¹⁴ We were able to observe a trace amount of desired product by ¹H-NMR upon our first attempt at an electrochemical cyclization using a modification of Little's conditions (figure 2.9). While we were not able to exactly replicate the mercury-based electrodes reported in

the original work, despite extensive efforts toward the optimization of this reaction by screening a variety of solvents, electrolytes, electrodes, and additives in divided and undivided cells under both constant current and constant potential, we were not able to obtain our product in any synthetically useful yield.

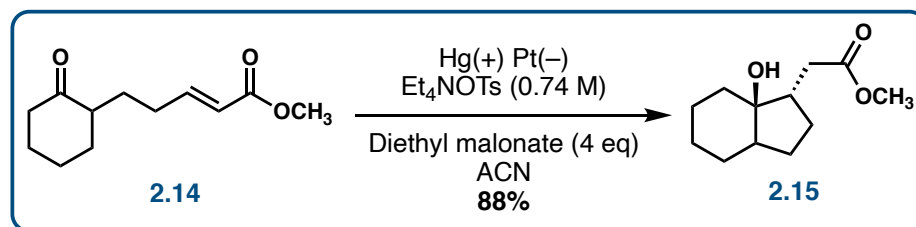


Figure 2.8 Electrochemical coupling to afford bicyclic ester **2.15** accomplished by R.D. Little

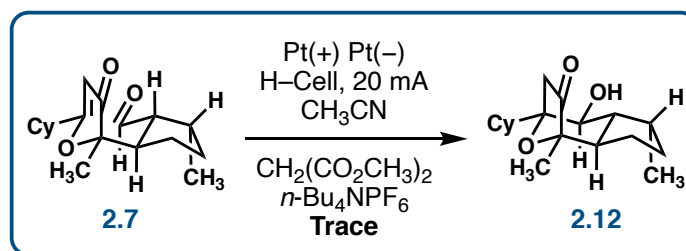


Figure 2.9 The electrochemical reductive cyclization of Michael adduct **2.7** to afford the core **2.12**

Extensive reports in the photochemical reductive intramolecular couplings of ketones and unsaturated esters under the action of ruthenium and iridium catalysts and a variety proton and electron transfer agents strongly suggested we might find conditions amenable to our desired cyclization – these constitute proton-coupled

electron transfer processes (PCET).^{2, 15} After trying a number of these conditions, we were not able to generate any synthetically useful amount of product.

In a final alternative strategy, we explored the use of dithianes as a possible entry point to alternative nucleophiles to forge the desired carbon–carbon bond. Following the condensation of a dithiol and an aldehyde, the resultant dithiane contains an acidic proton; treatment with *t*-BuLi in the presence of HMPA should afford a nucleophile that might undergo a 1,4-addition (figure 2.10). These reactions are well-known,¹⁶ although intramolecular examples are rare. The Michael adduct was readily converted into the dithiane **2.16** in 51% yield (78% brsm) by stirring with propanedithiol. However, extensive reaction screening with various butyllithiums in the presence of HMPA only afforded the desired cyclization product in low yields. Presumably, competitive extended deprotonation of the furanone precluded any productive cyclization sequences, however, lithiation experiments quenched with sources of deuterium did not provide any useful information to make any definitive conclusions.

² I gratefully acknowledge Profs. Tehshik Yoon and Uttam Tambar for detailed private communications and discussions of my work and the key suggestion to screen proton coupled electron transfer (PCET) processes toward the cyclized target.

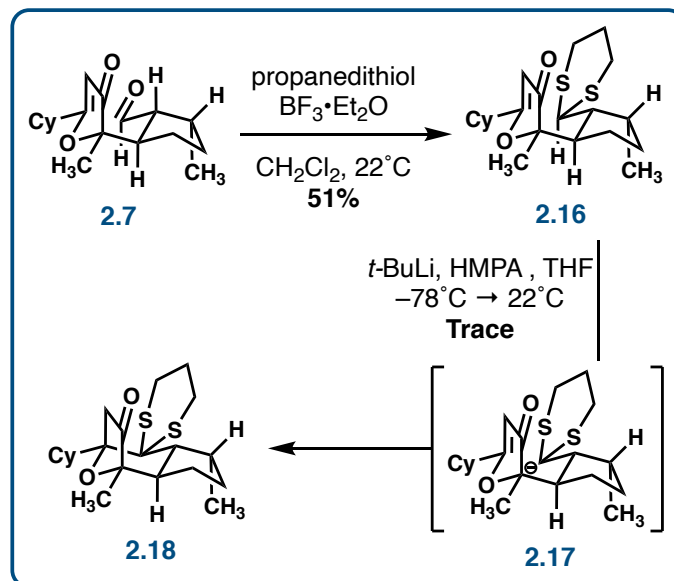


Figure 2.10 Synthetic strategy to synthesize the core utilizing the acidic proton present in dithianes

Returning reluctantly to the original samarium-mediated cyclization reaction, we decided to rescreen many conditions in order to optimize the cyclization for larger C7-alkyl groups. Previous conditions were developed via extensive exploration in the initial synthesis of EA by our group in 2011⁴, as well as during the development of the other C7 and C9-amide analogues. After extensively scouring the literature, we located a few more opportunities for further optimization that remained unexplored in the case of our cyclization. After rescreening ratios of reagents employed, sources and purification of the reagents (e.g. samarium dust, shavings, or ingot), alternative additives such as TPPA and 2,4,6-TTBP, reaction temperature profiles, and methods of quenching the reaction (e.g. water, saturated aqueous salt solutions, or organic solvents such as ethyl acetate or acetone), I was able to increase the average yield from 5% to 12% and increase the reaction scale from 69 mg to 150 mg. These changes

may appear trivial, and not much of an improvement, but we welcomed such a modest increase, and at greater scale.

The final conditions employed after optimization are as follows. The samarium powder used in the reaction must be freshly ground from the ingot and the diiodoethane must be washed and recrystallized by taking the powder up in diethyl ether, washing the organic solution with a saturated aqueous sodium thiosulfate solution (5x), and concentrating to afford a flakey, white crystal. 5.5 equivalents of samarium and 3.1 equivalents of diiodoethane are then charged into an oven-dried flask which is flushed with argon 3 times and backfilled with argon. Dry, degassed THF is then charged into the flask with stirring and stirred for at least 3 hours to afford SmI_2 as a deep purple solution. This solution is then transferred by cannula into an oven-dried flask containing 150 mg of the Michael adduct **2.7**, 12 equivalents of HMPA, and THF under argon over a 90-minute period. The resultant purple reaction mixture is then stirred for an additional 4 hours before quenching the remaining SmI_2 with saturated aqueous ammonium sulfate solution at 0°C . We employed these conditions for the remainder of our study toward next-generation analogues.

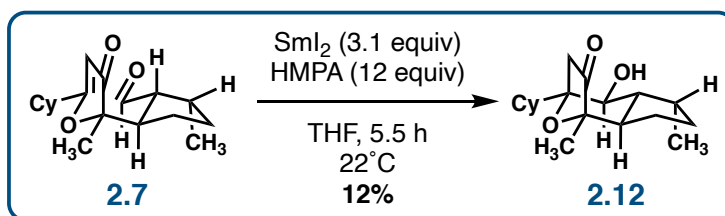


Figure 2.11 Final conditions used after optimization of the SmI_2 reductive coupling

With the core scaffold in hand in serviceable yield, the alcohol at C6 can be esterified using a Yamaguchi¹⁷ esterification to afford the cinnamate **2.19** as shown in figure 2.12. A stereoselective reduction of the ketone to the alcohol followed by activation of the alcohol with an imidazole sulfonate affords **2.20**. In the case of our syntheses of EA and its associated analogues, it is at this stage where cesium hydroxyacetate or an azide salt are employed in substitution reactions to displace the sulfonate to afford EA or an intermediate toward the synthesis of amide analogues, respectively. An analogous substitution reaction with a cyanide source should have provided access to the target carbon-linked analogue class.

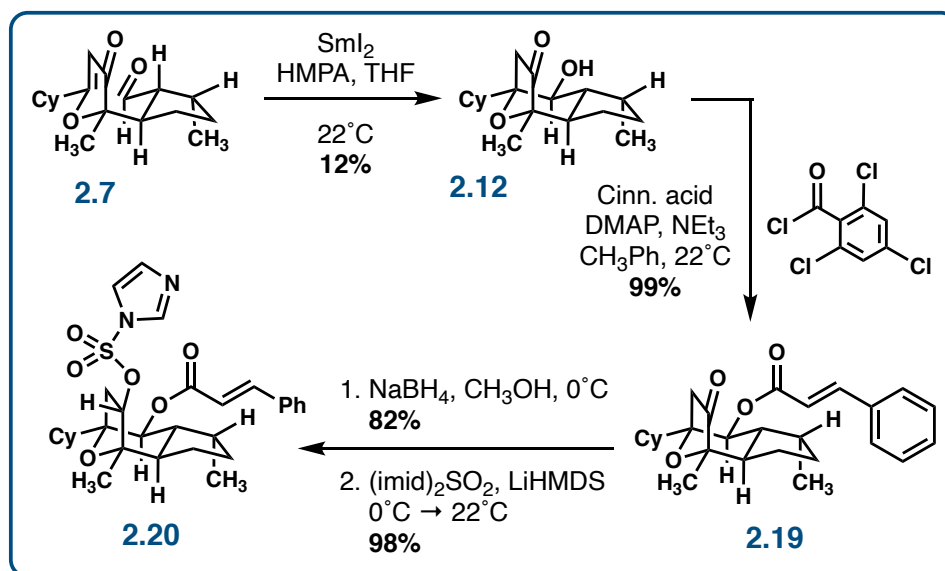


Figure 2.12 Transformation of Michael adduct **2.7** to imidazole **2.20**

2.2.1 Addition of Nitrile

Our first attempts to install a nitrile at C9 employed potassium cyanide as the nitrile source. Reactions employed 18-crown-6 in an attempt to sequester the

potassium ion and enhance the reactivity of the anion in THF, exploring temperature profiles from -10 to 60°C . After several attempts, we only recovered starting material under these conditions and so we moved to the use of sodium cyanide in DMSO. After prolonged heating at 80°C , starting material again remained unchanged. After switching the solvent to DMF and using NaCN, we were able to see some consumption of SM after heating the solution at 60°C for 20 hrs; however, the only product we could identify in this case was that resulting from conjugate addition of the cyanide into the cinnamate as shown in figure 2.13. On the basis of this result, we concluded that perhaps the nitrile installation should precede the C6-ester installation. We elected to protect the C6 hydroxyl group of the samarium cyclization product and reexplore the cyanation conditions.

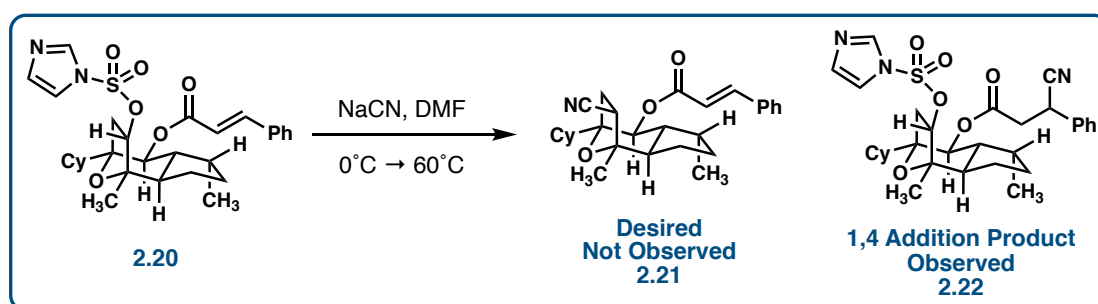


Figure 2.13 Nitrile substitution attempt on imidazole **2.20** resulting in the 1,4-addition product **2.22**

The protection of this alcohol with a PMB group was best accomplished using PMB acetimidate in the presence of the Lewis acid $\text{La}(\text{OTf})_3$, affording the desired ether in 49% isolated yield. Other Lewis and Brønsted acids as well as other protecting agents such as PMBCl were not as effective. With the alcohol protected, reduction of

the C9-ketone to the corresponding alcohol under the action of sodium borohydride proceeded in 55% yield; activation of the alcohol with sulfuryl imidazole proceeded smoothly in 66% isolated yield. Returning to screening conditions for the substitution of the sulfonate with a nitrile, multiple attempts only resulted in trace desired product (figure 2.14). The major isolated product in these screens was the alcohol **2.23**, presumably via cleavage of the sulfonate by the cyanate (figure 2.14).

Leaving Group (X)	Nitrile Source	Additives	Solvent	Temperature (°C)	Product Yield (%)	Side Products
-SO ₂ (imid)	KCN	18-cr-6	THF	0 – 60	–	RSM
-SO ₂ (imid)	KCN	18-cr-6	DMF	22 – 60	Trace	RSM/Alcohol
-SO ₂ (imid)	NaCN	–	DMF	22 – 60	–	RSM/Alcohol
-OTs	KCN	18-cr-6	DMF	22 – 110	–	RSM/Rev. Alcohol
-OTs	KCN	18-cr-6	DMSO	22 – 135	–	RSM/Rev. Alcohol
-OTs	NaCN	–	DMSO	22 – 135	Trace	RSM/Rev. Alcohol
-OTs	NaCN	–	DMPU	22 – 200	–	Rev. Alcohol/Elim.
-OTs	Cyanohydrin	LiOtBu	DMSO	22 – 120	–	RSM
-OMs	NaCN	–	DMPU	22 – 185	–	RSM/Elim.
-OTf	KCN	18-cr-6	THF	-10 – 22	–	RSM/Alcohol/PMB rem.
-OTf	NaCN	–	DMSO	-10 – 50	–	Alcohol/Elim.
-OTf	TBACN	–	THF	-10 – 22	–	–
-OTf	TBACN	–	THF	-10 – 60	Trace	–

Figure 2.14 Cyanation conditions evaluated along with the observed products

We decided to switch to alternative activating groups such as the p-toluenesulfonyl- or methanesulfonyl-groups, which could be readily installed on the

alcohol.¹⁸ We returned to the same series of conditions starting with KCN and 18-crown-6 in DMF, and brought the temperature up to reflux at 110°C. Along with recovered starting material, we obtained a new product – the alcohol **2.24** that resulted from the substitution of the tosylate with water (figure 2.14), which presumably occurred during the aqueous quench and workup. Most of the material was being recovered as starting material unchanged however, so we further explored traditional polar aprotic solvents such as DMSO which allowed more extensive temperature screening. Employing both NaCN and KCN with 18-crown-6 up to 135°C, we saw no difference in products other than a trace amount of the desired product. We again switched solvents to one with a higher boiling point which was DMPU and attempted the addition up to 200°C. With the use of NaCN, we observed full consumption of the starting material and isolated the same alcohol **2.24** as well as the olefin **2.25** that results from the elimination of the sulfonate. We also tried using a different cyanide source such as acetone cyanohydrin and saw only recovered starting material. We then decided to try the mesylate instead of the tosylate although in the research conducted by the Hamada group,¹⁸ they appeared to obtain better results with the tosyl group. When the mesylate was treated with NaCN in DMPU and was heated up to 185°C, we still were only able to obtain recovered starting material and the elimination product **2.25**.

We then decided to go to a much more reactive activating group and turned to the triflate. Repeating these same series of reaction conditions but with less heat, we again saw recovered starting material, the alcohol **2.24**, the elimination product **2.25**, and the product resulting from PMB removal. We also tried using

tetrabutylammonium cyanide due to its increased solubility in THF to avoid isolation of the triflate but were only able to see a trace amount of desired product by NMR.

We also explored more non-traditional means of achieving the desired cyanation outcome as shown in figure 2.15. One such approach is the Mitsunobu-type reaction developed by Shô Itô et al. using acetone cyanohydrin and phosphonium ylide **2.27** to replace an alcohol with a nitrile, but we only recovered starting material unchanged.¹⁹ The Van Leusen reaction employs TOSMIC in a single pot, multi-step transformation of ketones into alkyl nitriles.²⁰ This reagent is fairly versatile in that it can be used to achieve a number of different transformations, including formation of oxazoles and imidazoles. When ketone **2.26** was treated with TOSMIC, complete consumption of starting material was achieved relatively quickly and cleanly into one product. Upon intensive analysis using NMR, mass spectrometry, and IR spectroscopy, we were able to determine that it was not the desired nitrile product but unfortunately, we were never able to conclusively identify what this material was. We also attempted addition of the nitrile through a tosylhydrazone intermediate using the conditions shown in figure 2.15, but this failed to afford the desired product as well.

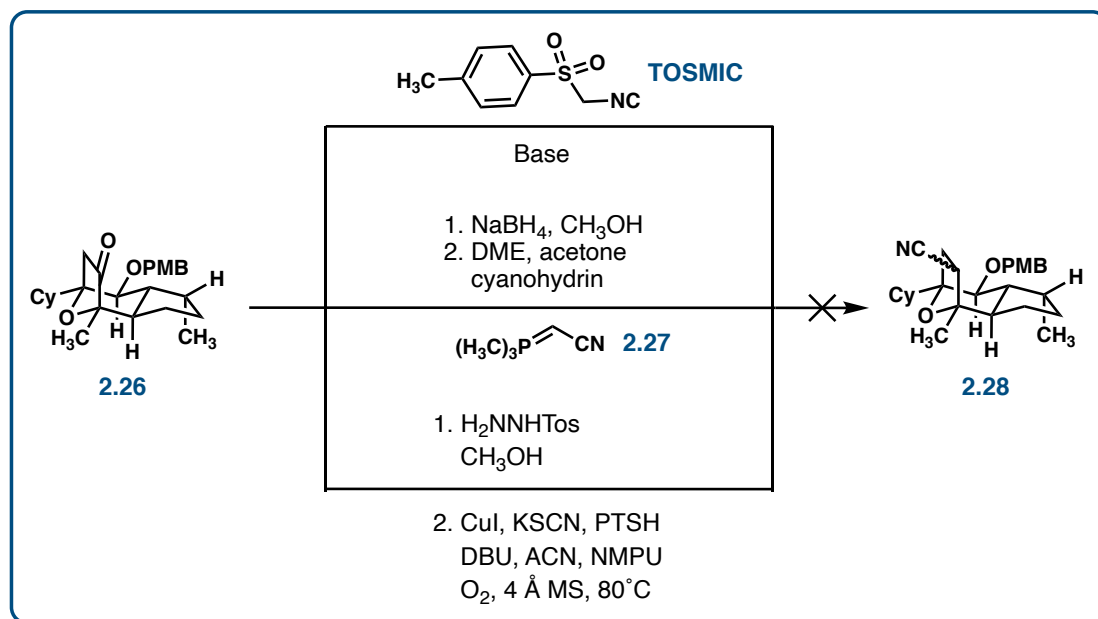


Figure 2.15 Additional attempts at achieving nitrile **2.27**

It was at this point that we decided it was time to readjust our strategy and attempt olefinations of the ketone **2.26** to afford the vinyl ether **2.33** as shown in figure 2.16.

2.2.2 Olefinations

A host of different methods have been described to transform ketones into alkenes via olefination reactions²¹ such as the venerable Wittig²² reaction. As shown in figure 2.16, the Wittig reagent that we explored was the phosphonium ylide generated in situ from phosphonium **2.27** and base. Through an investigation of different bases and temperatures, we were only able to recover starting material. Next, we found that the Bestmann-Ohira²³ reagent **2.28** has been used to achieve the same transformation.

²⁴ Unfortunately in our case, we again were only able to recover starting material when

using this reagent. We then began turning to less commonly used olefination reagents such as the phosphine oxide **2.29** shown in figure 2.16. Using a strong base such as *n*-BuLi to generate the anion, we still were only able to recover starting material out of this reaction. Because we did not observe any products resulting from addition of these reagents into the ketone, we moved to more reactive reagents.

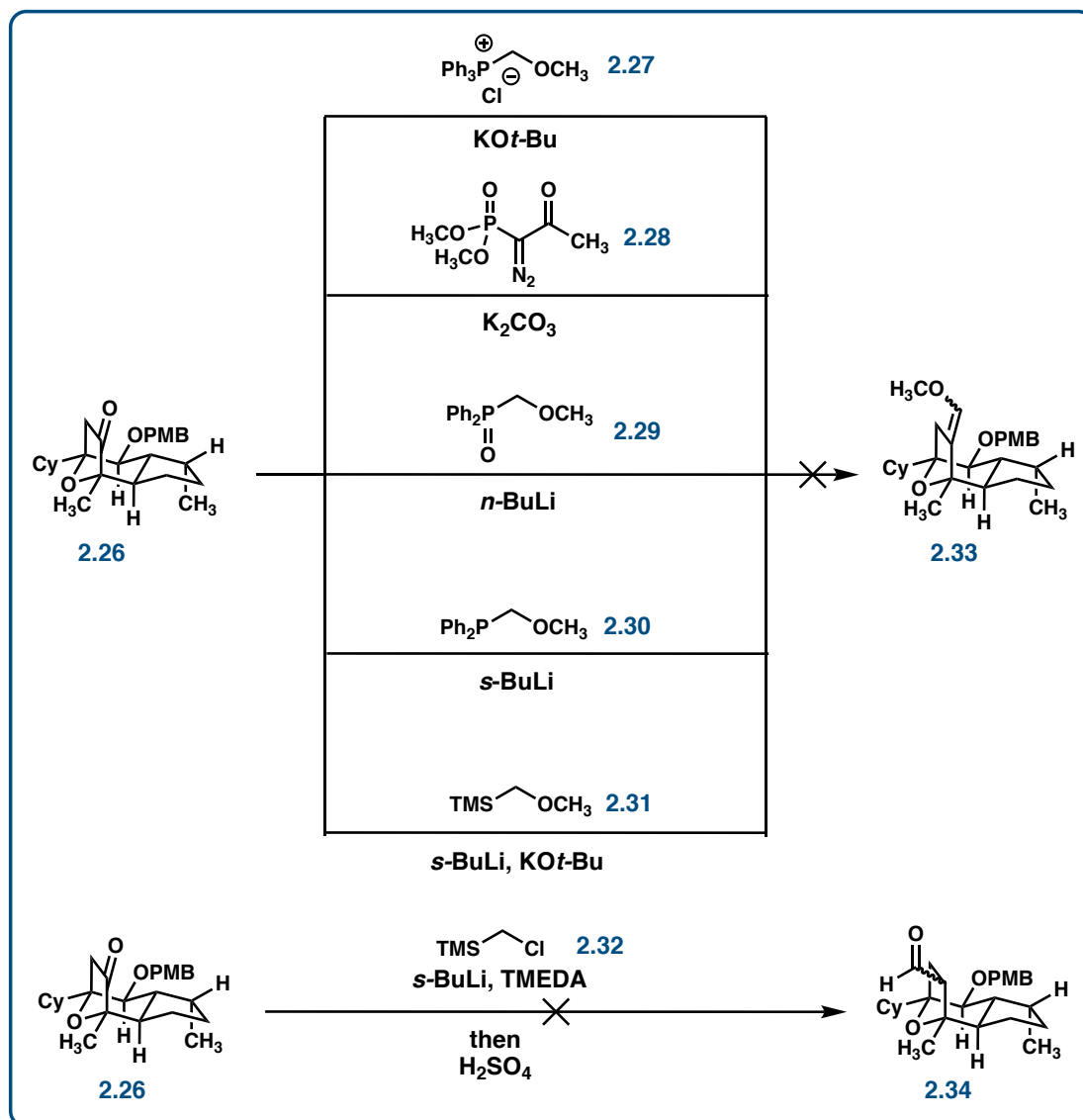


Figure 2.16 Olefination conditions attempted in the pursuit of vinyl ether **2.33** and aldehyde **2.34**

We then treated the ketone **2.26** with the phosphine **2.30** along with a strong base such as *s*-BuLi, but again we were only able to recover starting material unchanged. Moving to Peterson olefinations,^{21h, i, k} exposure of **2.26** to the silane **2.31**

and strong base, we again only recovered starting material. Interestingly, when we treated **2.26** with the chlorosilane **2.32** and base, starting material was consumed. This reagent is known to undergo a Peterson-type olefination that proceeds through an epoxide intermediate. In our hands, we believe starting material was transformed into the putative epoxide intermediate, but upon treatment with strong acid, we observed no hydrolysis to afford the desired product.

2.2.3 Furan as a Masked Carboxylic Acid in Classic Total Syntheses and Methodologies³

Furan has been employed as a masked carboxylic acid equivalent in a number of classic total syntheses of natural products and various methods have been developed to achieve oxidative cleavage of the furan to the carboxylic acid.²⁵ Landmark achievements in total synthesis exploiting this strategy include the completion of monensin in 1979 by Kishi^{25v} and the completion of *N*-acetylneuraminic acid in 1988 by Danishefsky,^{25e} both of which are shown in figure 2.17. In Kishi's synthesis of Monensin, this furan was unmasked to the acid using standard ozonolysis conditions and was achieved in a 55% yield. Danishefsky decided to use a modification of the oxidative cleavage conditions developed by Sharpless^{25d} in 1981 (figure 2.18) where RuO₄ is generated in situ to perform the transformation. Danishefsky was able to complete this transformation in a 90% yield. One significant drawback to the Sharpless conditions is CCl₄ as a required solvent. In an effort to replace this environmentally hazardous reagent, Prof. James Bull in 2020 optimized

³ I gratefully acknowledge Prof. Erik J. Sorensen for detailed private communications and discussions of my work and the key suggestion to screen furan nucleophiles as masked carboxylic acids.

these conditions using a greener solvent system of heptane, ethyl acetate, and water on azetidione, oxetane, and cyclobutene-containing substrates also shown in figure 2.18.^{25h}

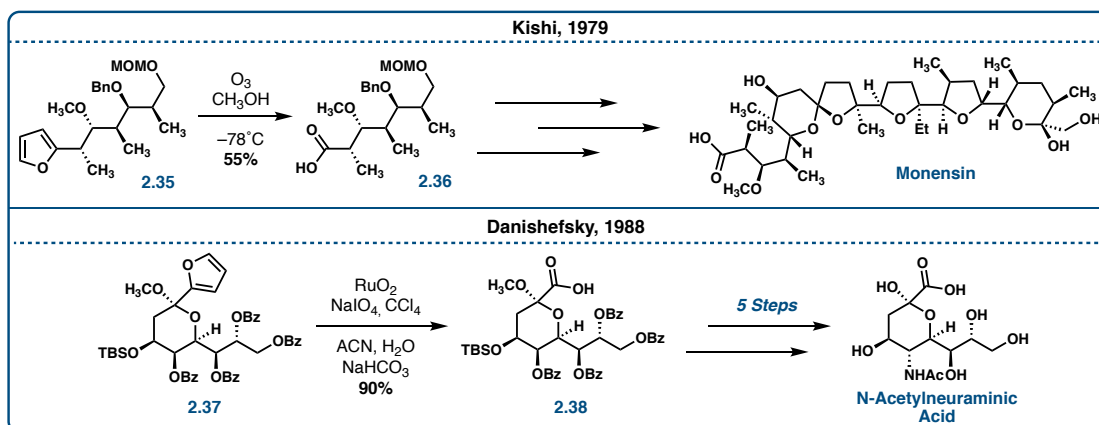


Figure 2.17 Classic total syntheses featuring the masked carboxylic acid strategy through the incorporation of a furan

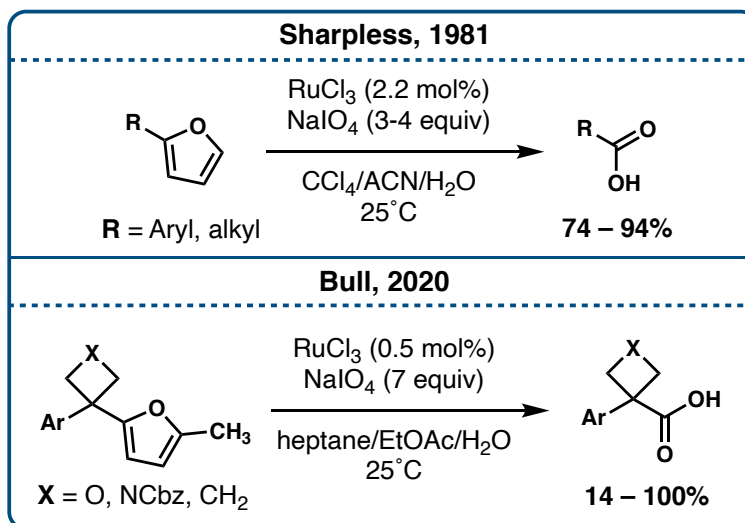


Figure 2.18 Methods developed to affect the oxidative cleavage of furans into carboxylic acids

2.3 Application of Masked Carboxylic Acids to Englerin Analogue Synthesis

We began our work with masked carboxylic acids by addressing a weakness identified in our prior work in cyanation chemistry. Due to the PMB ether being cleaved in previous reaction attempts when exploring addition of the nitrile, we switched to using a TBS group to protect the alcohol in core structure **2.12** (figure 2.19). Using TBSOTf and triethylamine in dichloromethane, the TBS protection can be accomplished in a 99% yield to afford ketone **2.39**. Furan was added to *n*-BuLi in the presence of TMEDA at -78°C and stirred at that temperature to afford the lithiated furan nucleophile. The ketone is then added to the resultant solution at -78°C , and upon warming, the furan addition product **2.40** was obtained in 59% yield as a single diastereomer. The exact configuration of the stereogenic center bearing the furan was unknown at this time, although we suspected it was the same configuration as that shown in figure 2.19 based on the outcomes of sodium borohydride-mediated reduction reactions with ketones like **2.39**.

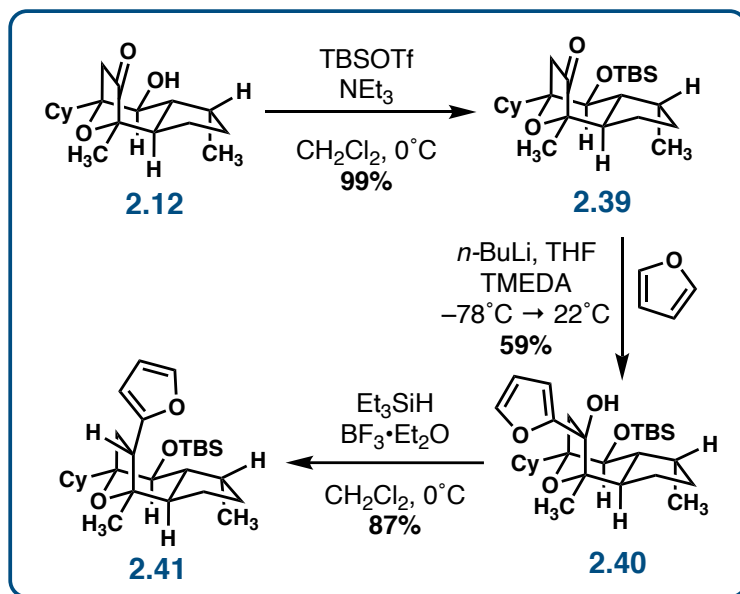


Figure 2.19 Synthesis of furan **2.41** from the core **2.12**

The next step of the reaction was a reductive excision of the alcohol. At this point, we were aware that there was the possibility of scrambled or otherwise undesired stereochemical outcomes at C9 after this series of reactions, but we were prepared to address that problem if it were to arise. Under Lewis acidic conditions, a hydride substitution reduces the alcohol to the alkyl furan **2.41** as a single diastereomer in an 87% yield as shown in 2.19. At this stage, detailed 2D-NMR analyses of **2.40** and **2.41** were not helpful in the determination of the configuration of these stereogenic centers.

The next step in the synthesis is the oxidative cleavage of the furan to reveal the carboxylic acid. The first set of conditions that we tried were the conditions developed by Bull using RuCl₃ and NaIO₄ in heptane, ethyl acetate, and water (figure 2.18).^{25h} After purification on SiO₂, the product was obtained in a 28% yield (figure

2.20). We decided to try the ozonolysis as featured in Kishi's synthesis of monensin in 1979.^{25v} The ozonolysis proceeded very quickly (ca. < 5 minutes) with clean conversion to the carboxylic acid product, but upon isolation, we obtained a yield of 13%. We then decided to employ the conditions developed by Sharpless in 1981.^{25d} Under these conditions, we were able to obtain product in a yield of 44% with 30% of the material being funneled into side product **2.43**. This is the result of incomplete oxidation due to the presence of acid in the solution.^{25t} The addition of sodium bicarbonate to the solution to act as a buffer has been successfully used to prevent the unproductive formation of these dicarbonyl compounds, such as in Danishefsky's synthesis of *N*-acetylneuraminic acid.^{25e, t, y} Upon trying these conditions used by Danishefsky, we observed full consumption of starting material completely void of dicarbonyl side product **2.43**, but upon isolation we realized the carboxylic acid product decomposes on silica gel. We also tried purification on deactivated silica gel and alumina and observed the same result. At this point we decided to push the crude material into the next step without further purification outside of routine workup and filtration over celite.

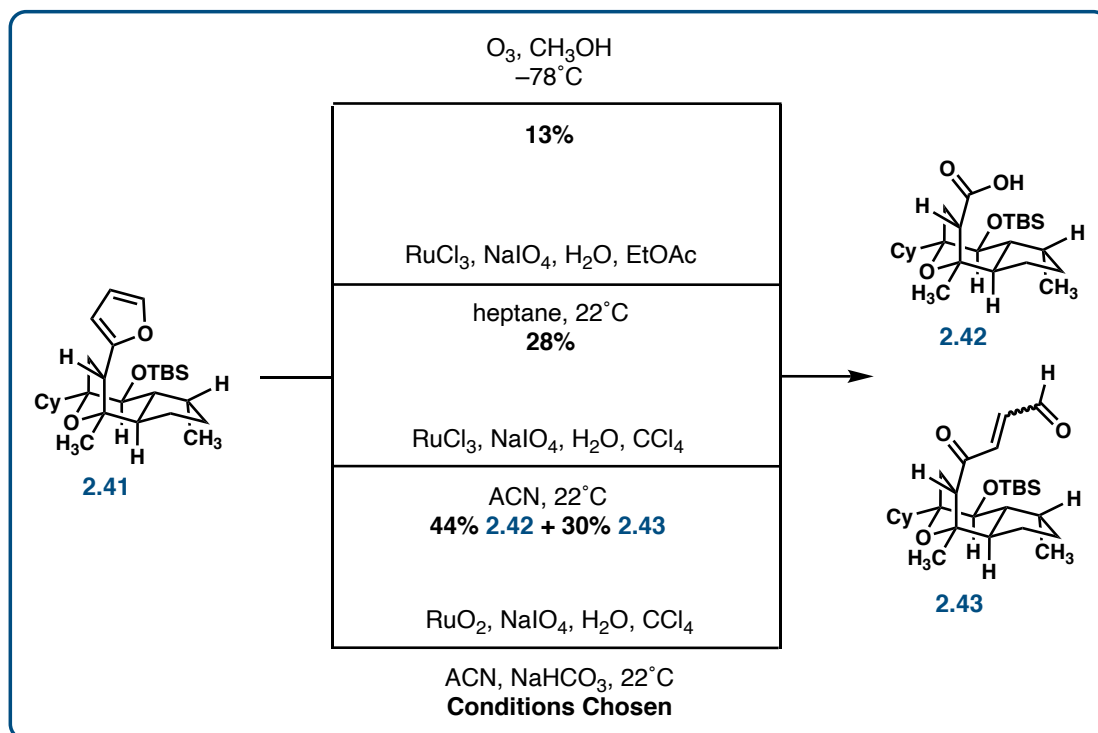


Figure 2.20 Attempted conditions to oxidatively cleave the furan **2.41** into the carboxylic acid **2.42**

The next step is the esterification of the acid through a Steglich²⁶ esterification using DCC, DMAP, and the PMB monoprotected ethylene glycol. This proceeded relatively smoothly to afford ester **2.44** in a 58% yield. After attempts at different purifications of this ester, we found it most productive to telescope the crude mixture directly into the next reaction (figure 2.21).

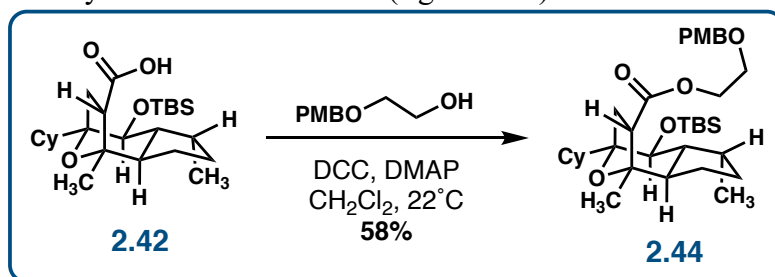


Figure 2.21 The Steglich esterification used to transform acid **2.42** into ester **2.44**

After esterification, our collection of thorough 2D-NMR data collected with all the products post furan addition up to this point still did not allow unambiguous assignment of the C9 stereochemistry. Experiments were focused upon any nOe data obtainable for the interaction of the C9 α -proton with the proton at the 6,5-ring juncture along with other protons on the 5-membered ring as shown in figure 2.22. Several proton signals in the carbon backbone overlap with the protons on the cyclohexyl substituent, leading to ambiguity in the nOe data. Observing these nOe interactions would be definitive evidence supporting the ester being in the correct position, but the absence of this interaction does not necessarily tell us anything.

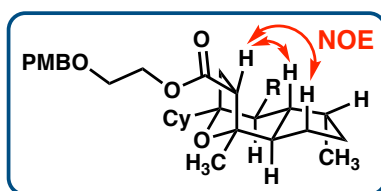


Figure 2.22 nOe interactions to determine the stereochemistry of stereogenic center α to the ester

We hypothesized that an epimerization of the C9 ester under basic conditions may provide a compound that would yield us sufficient data in order to decipher whether the stereochemistry at C9 was desirable or not. We began with more common epimerization conditions such as through the use of DBU, but all trials using DBU as the base returned starting material unchanged (figure 2.23). Other commonly used conditions for the epimerization of aldehydes, ketones, and esters involve the use of

alkoxide salts such as NaOCH₃ or NaOEt. We were more hesitant to treat this compound with these reagents due to a fear of transesterification. We instead decided to try NaOt-Bu but just as expected, we observed decomposition of the material as well as transesterification to the corresponding *tert*-butyl ester.

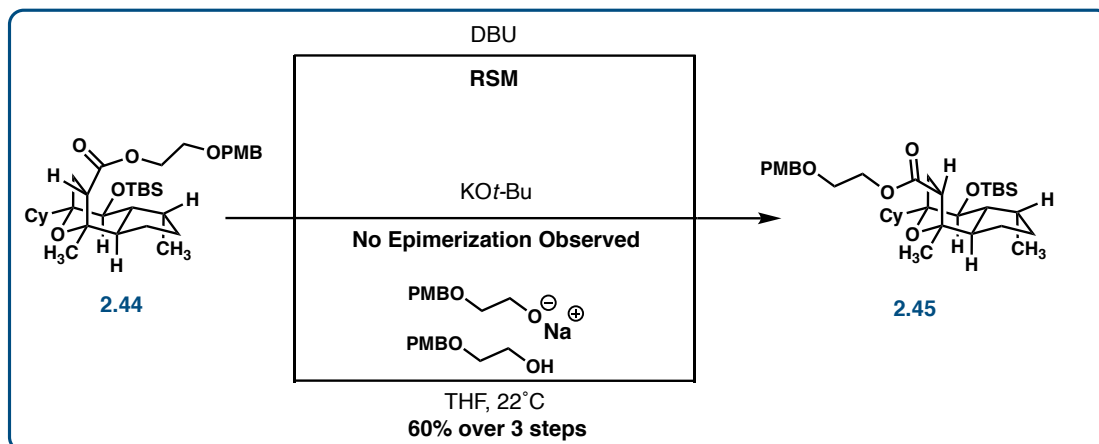


Figure 2.23 Attempted epimerization conditions

However, the use of the sodium salt of the PMB protected ethylene glycol presented an appropriate base for the desired epimerization and an inconsequential transesterification event. Treatment of the crude mixture of the ester **2.44** with the sodium salt of the PMB protected ethylene glycol (prepared from sodium hydride and the protected alcohol) in THF successfully epimerized the C9 stereogenic center α to the ester. Both diastereomeric esters are sensitive to purification through silica gel but can be cleanly separated on basic alumina. nOe analysis of the newly formed epimer shows a strong interaction between the α -proton and the proton at the 6,5-ring juncture, finally suggesting that the furan is inverted to the undesired stereochemistry

upon reductive excision of the alcohol. There may be a reaction that could replace the current method of reductive excision that is not guaranteed to invert this stereocenter. What we are battling is trying to attain the thermodynamic product while avoiding the kinetic protonation event leading to the undesired stereochemistry. As of this writing, we consider this as an acceptable route to the analogues especially with an optimized yield of 60% over those 3 steps (figure 2.23).

The next transformation to be completed is the installation of the cinnamate group. To accomplish this, the first step is a deprotection of the TBS group using TBAF in THF which proceeded smoothly to afford free alcohol **2.46** (figure 2.24). The product of this deprotection is also sensitive to silica gel and converts cleanly to an unusable compound during the column. After much trial and error, the best way to handle this compound is to subject the crude material to the next reaction after filtering through celite. If a higher purity of this material is necessary, it can be accomplished by quickly running the material through a short plug of deactivated silica gel.

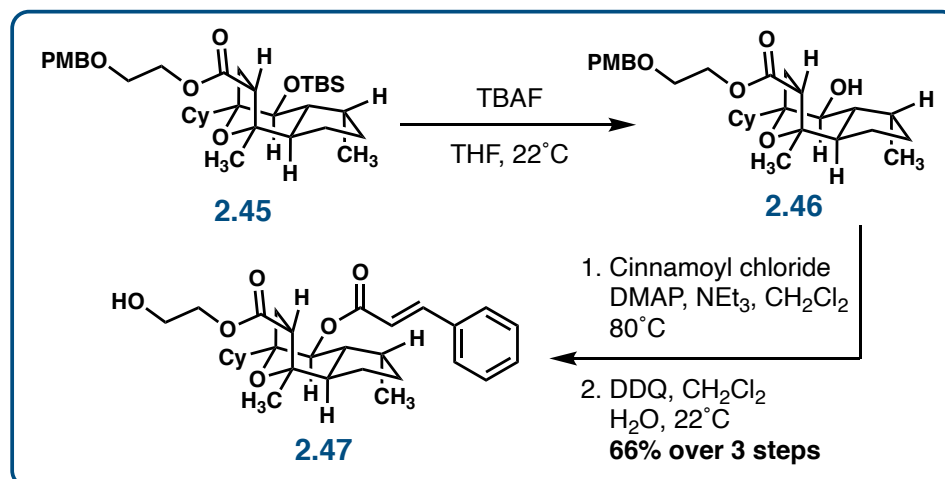


Figure 2.24 Completion of the reverse ester analogue **2.47**

Installation of the cinnamate group was accomplished through a Yamaguchi¹⁷ esterification with cinnamic acid. After work up and concentration, treatment with DDQ cleanly cleaves the PMB group off of the glycolate affording the final product, reverse ester analogue **2.47**. The yield over these final 2 steps was relatively low at 55%. We thought that it could have been due to incomplete removal of the PMB group, so we attempted cleaving this PMB with a dilute solution of TFA but saw decomposition of the material. We then realized we were losing material during the previous step, which was the Yamaguchi esterification. Altering the conditions of this reaction to the other conditions frequently used for this transformation in the synthesis of englerin A, we were able to cleanly convert the alcohol to the ester using cinnamoyl chloride and DMAP in triethylamine and dichloromethane when heated. After the PMB deprotection, we were able to accomplish these last 3 steps in an overall yield of 66%. This material was then sent to John Beutler at the NCI for biological evaluation

and the steps were repeated in the syntheses of the remaining analogues with variation of the cinnamate moiety.

The optimized route was applied to the synthesis of the naphthoate **2.48** and the cyclopropyl analogue **2.49** with overall yields of 18% and 44%, respectively, over the last 3 steps. These 2 compounds were also shipped to John Beutler at the NCI for biological evaluation. The 4th analogue that was made is the methyl cinnamate analogue **2.50**. This was made during the process of route optimization, so we were not able to acquire enough at the time to send to the NCI for biological testing. With the optimized route though, the synthesis of any of these reverse ester analogues with variation of the C6-cinnamate moiety can be readily accomplished.

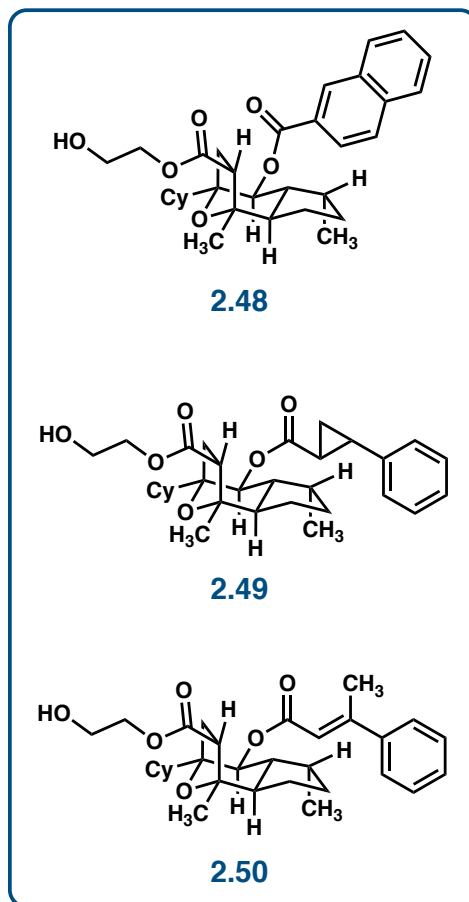


Figure 2.25 Other completed reverse ester analogues with variation at C6

2.4 Oxy Analogues

Our next idea avoided the epimerization step by leaving the alcohol in place resulting from the addition of the furan. By proceeding through the synthesis to the formation of the various isosteres with this alcohol intact, we were able to save 2 steps in the synthetic route, including the epimerization step. This would be extremely useful when it comes to the addition of the rest of the isosteres, as you may be able to lithiate and add a number of the different heterocycles into the ketone **2.39**. An alternative is to use the carboxylic acid after oxidative cleavage as a point of

divergence to the different isosteres if lithiation is an issue. The oxygen on the back side would also come with the added benefit of increased hydrophilicity.

For this to be a viable strategy, the analogues retaining this oxygenated group on the back side of the ester would have to show retained potency and selectivity against RCC cell lines. We decided to first target the reverse ester isostere with the free alcohol on the back side shown in figure 2.26. Oxidative cleavage of the furan was unsuccessful resulting in the spontaneous decomposition back to the ketone **2.39**, as expected, so we decided to protect this alcohol instead.

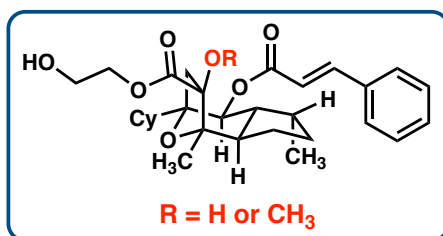


Figure 2.26 An example of the reverse ester analogues with the C9-oxygen intact

We initially began efforts to protect this alcohol with a PMB group, as the PMB groups on this alcohol and the reverse ester alcohol could be simultaneously deprotected on the last step of the synthesis. The first reaction conditions we tried were the same reaction conditions that were previously used in the protection of the SmI₂ adduct **2.12** which is PMB acetimidate and lanthanum triflate (figure 2.27). These conditions afforded the protected product **2.52** but in the low yield of 37%. We then proceeded to try the protection with PMBOH refluxed in the presence of Amberlyst-15 resin but were only able to recover starting material. The last set of conditions tried in the PMB protection of this alcohol were using NaH and PMBCl.

This one also formed a small amount of product, but the product was inseparable from the PMBCl under a variety of purification conditions. There is one other possible PMB protecting reagent **2.51** developed by Dudley²⁷ that reportedly works better for tertiary alcohols, but we have not had the opportunity to try this reagent on this substrate.

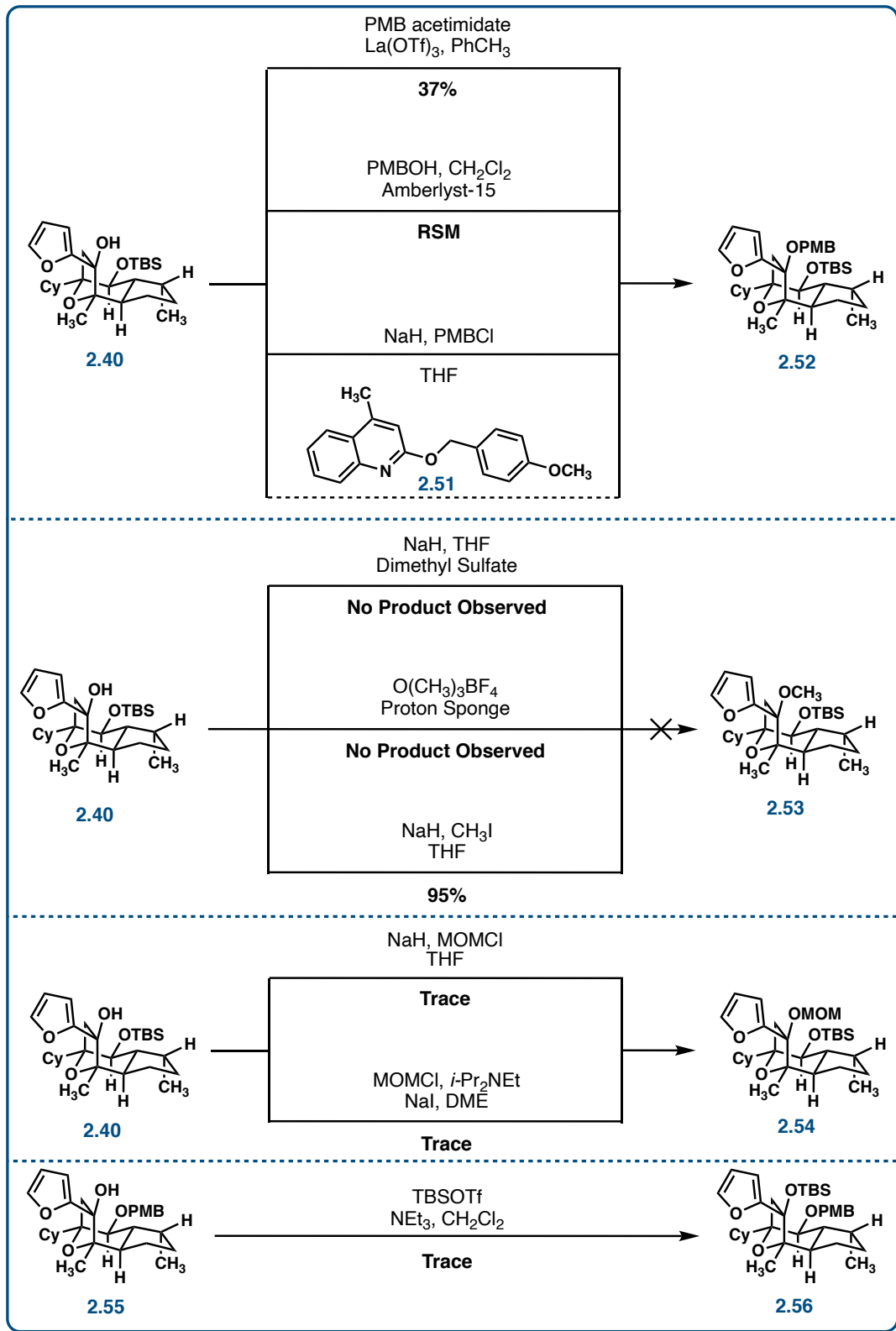


Figure 2.27 Conditions attempted in the protection of the alcohol resulting from the furan addition

We then moved to protecting this alcohol with a TBS group, but to avoid any overlapping protecting groups, we used the PMB protected C6-alcohol **2.55**. Employing the same conditions used to TBS protect the C6-alcohol, we treated alcohol **2.55** with TBSOTf and triethylamine in dichloromethane. After a few hours, only starting material was observed by TLC, so the solution was brought to 40°C. Although we were able to see a small amount of product, it was nothing worth further pursuit.

Another option would be the methyl group as a protecting group which is beneficial due to its ease of installation. The one drawback is that it is unlikely that this group could be easily removed after addition, which may not necessarily be a bad thing if the analogue is active with the methyl present. We initially tried the methylation using NaH and dimethylsulfate, which seemed to cause some decomposition of the starting material (figure 2.27). We tried 2 other sets of conditions including methyl iodide with NaH and trimethyloxonium tetrafluoroborate with Proton Sponge and were able to obtain a yield of 95% using the methyl iodide. Taking another attempt at including a removable protecting group, we attempted the protection of this alcohol with a MOM group but were unsuccessful. We decided to move forward with the methyl ether **2.53** into the next step.

Oxidative cleavage of the furan, featured in figure 2.28, seems to proceed relatively smoothly, although the sensitivity of the acid prevents further purification, so it is pushed to the next step as a crude mixture. The esterification of this acid does not proceed as readily as it has with the other reverse ester analogues and is possibly

the reason for the low yield in this synthesis. Attempting a few different sets of esterification conditions including the Yamaguchi¹⁷, a Steglich²⁶ esterification using EDC and DMAP, and a Steglich esterification using EDC and HOBT, we were really only able to see anything greater than a trace amount of product within the Yamaguchi esterification (figure 2.29). Purification of the product is no easy task either as it is inseparable from the 2,4,6-trichlorobenzoyl chloride. In an effort to reach the final analogue, we proceeded with this set of reaction conditions, although this step is definitely worth further investigation in the future.

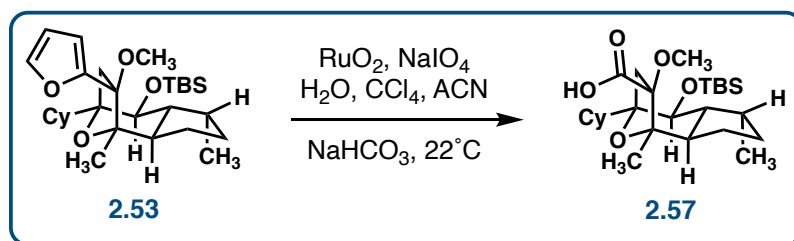


Figure 2.28 Oxidative cleavage of the furan to reveal carboxylic acid 2.57

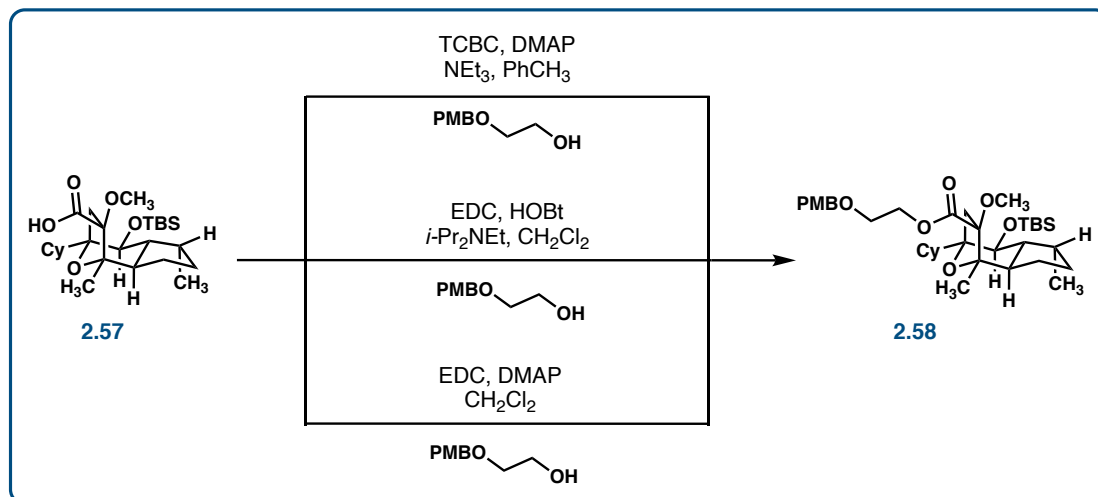


Figure 2.29 Conditions used in attempts to esterify **2.57** into reverse ester **2.58**

Treatment with TBAF appears to proceed cleanly to the alcohol, but upon purification through a short plug of deactivated silica gel, we isolate 8% of the material that we had going into the oxidative cleavage. This is an important issue that warrants further investigation to find out exactly at which step or steps we are losing the bulk of this material. It could be during any one of the three reactions or purification steps. The final two steps include the esterification of the free alcohol to install the cinnamate using cinnamoyl chloride and DMAP. The crude material from this reaction is then subjected to DDQ in dichloromethane and water to remove the PMB group revealing the final analogue **2.61** in a yield of 21% over the two steps. These last two steps will also need further investigation to ensure maximum efficiency in the production of these analogues.

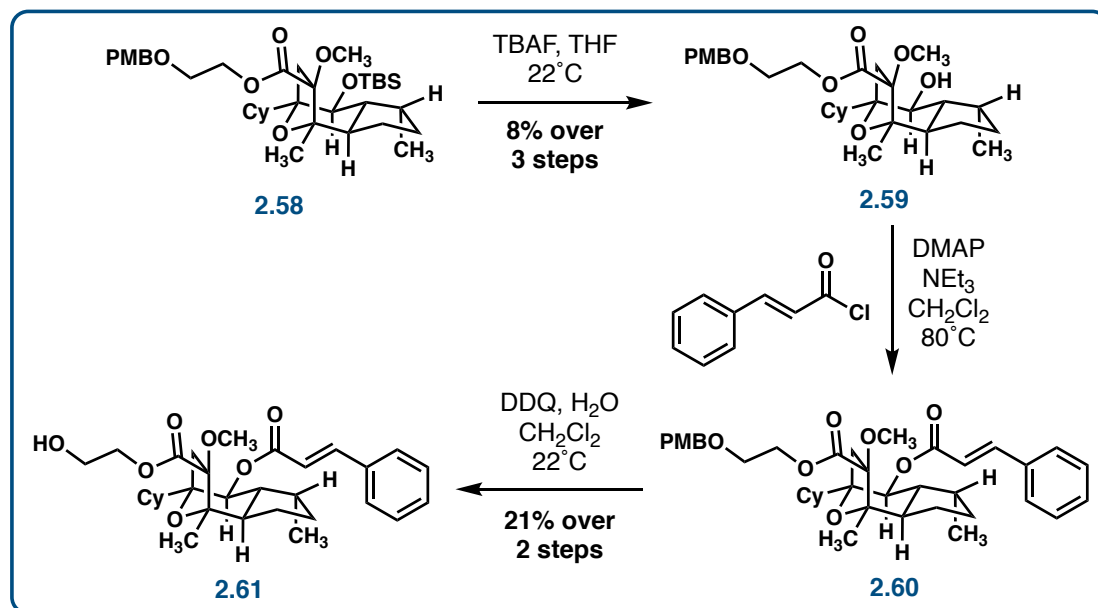


Figure 2.30 The final 3 steps in the synthesis of the C6-methoxy analogue **2.61**

2.5 Biological Data of Analogues Submitted to the NCI

At the time of this writing, there have been 5 analogues made, 3 of which have been sent to John Beutler at the NCI for biological evaluation. The 3 analogues that are currently being investigated at the NCI are the cinnamate analogue **2.47**, the naphthyl analogue **2.48**, and the cyclopropyl analogue **2.49**. We were not able to synthesize enough of the methylcinnamate analogue **2.50** and the C6-methoxy analogue **2.61** for proper biological testing, so we are waiting until we have more material to send these analogues off.

Of the 3 analogues that are being investigated at the NCI, we have NCI60 data for 2 of them, the cinnamate analogue **2.47** and the naphthyl analogue **2.48**. The desired biological properties that are being investigated are a selectivity towards cancer, high or maintained potency towards the death of those cancers, ablation of

nonspecific lethality, and increased stability to acidic and basic media. The data that we currently have on these 2 analogues is representative of 2 of those parameters.

The cinnamate analogue **2.47** and the naphthyl analogue **2.48** show a high selectivity for the renal cancer cell lines as well as for Triple Negative Breast Cancer (TNBC). Both of these analogues have an increase in the IC_{50} values when compared to the natural product, but the naphthyl analogue is promising as it still features potency in the nanomolar range. The IC_{50} values for these 2 analogues are shown for the RCC cell lines A498 and UO31 as well as the TNBC cell line HS578T and are as follows: cinnamate analogue **2.47** (A498 – $IC_{50} = 1.9 \mu\text{M}$; UO31 – $IC_{50} = 2.8 \mu\text{M}$; HS578T – $IC_{50} = 2.1 \mu\text{M}$) and naphthyl analogue **2.48** (A498 – $IC_{50} = 234 \text{ nM}$; UO31 – $IC_{50} = 355 \text{ nM}$; HS578T – $IC_{50} = 245 \text{ nM}$).

Further biological testing of these analogues is necessary to evaluate their safety and stability when administered to animals. As we await biological results, we continue to push through the synthesis of unique analogues based on the current structure–function data in the pursuit of developing a treatment for cancers.

Experimental Procedures

General Information: *These experimental procedures have been published previously in its current or a substantially similar form and I have obtained permission to republish it.*¹ All electrochemical reactions were performed in either an H-type divided cell separated by a sintered glass frit or a single compartment glassfalcon tube with electrodes separated by a glass microscope slide (Fisherbrand®, plain, precleaned, 2.5 cm x 7.5 cm x 0.1 cm). All non-electrochemical reactions were performed in single-neck oven- or flame-dried round bottom flasks fitted with rubber septa under a positive pressure of argon, unless otherwise noted. Air- and moisture-sensitive liquids were transferred via syringe or stainless-steel cannula. Organic solutions were concentrated by rotary evaporation at or below 35°C at 10 Torr (diaphragm vacuum pump) unless otherwise noted. Compounds were isolated using flash column chromatography² with silica gel (60-Å pore size, 40–63µm, standard grade, Silicycle). Analytical thin-layer chromatography (TLC) was performed using glass plates pre-coated with silica gel (0.25 mm, 60-Å pore size, 5–20 µm, Silicycle)

¹ (a) Wu, Z.; Suppo, J. S.; Tumova, S.; Strobe, J.; Bravo, F.; Moy, M.; Weinstein, E. S.; Peer, C. J.; Figg, W. D.; Chain, W. J.; Echavarren, A. M.; Beech, D. J.; Beutler, J. A., *ACS Med. Chem. Lett.* 2020, 11, 1711-1716. (b) Reed, H.; Paul, T. R.; Chain, W. J., *J. Org. Chem.* 2018, 83, 11359-11368. (c) Bush, T. S.; Yap, G. P. A.; Chain, W. J., *Org. Lett.* 2018, 20, 5406-5409. (d) Lewis, R. S.; Garza, C. J.; Dang, A. T.; Pedro, T. K.; Chain, W. J., *Org. Lett.* 2015, 17, 2278-2281. (e) Li, Z.; Nakashige, M.; Chain, W. J., *J. Am. Chem. Soc.* 2011, 133, 6553-6556.

² Still, W. C.; Kahn, M.; Mitra, A. *J. Org. Chem.* 1978, 43, 2923–2925.

impregnated with a fluorescent indicator (254 nm). TLC plates were visualized by exposure to ultraviolet light (UV), then were stained by submersion in aqueous ceric ammonium molybdate solution (CAM), acidic ethanolic p-anisaldehyde solution (anisaldehyde), or aqueous methanolic iron(III) chloride (FeCl₃), followed by brief heating on a hot plate (215°C, 10–15 s).

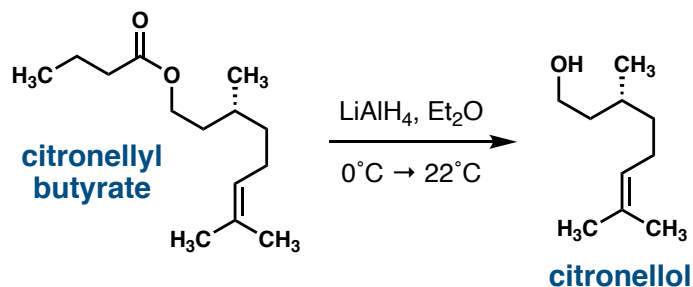
Materials: Commercial reagents and solvents were used as received with the following exceptions. Triethylamine, dichloromethane, diethyl ether, tetrahydrofuran, and 1,2-dimethoxyethane were purified by the method of Pangborn, et. al.³ Tetrabutylammonium hexafluorophosphate was recrystallized from ethanol (23 g /300 mL) at 65°C. Reticulated vitreous carbon (RVC) foam (carbon – vitreous – 3000C – foam; thickness: 10 mm; bulk density: 0.05 g/cm³; porosity: 96.5%; pores/cm: 40) was obtained from Goodfellow USA and cut to appropriate size for reaction scale. After 150 h of use, RVC electrodes were discarded and freshly cut electrodes were used.

Instrumentation: Proton (¹H), carbon (¹³C), fluorine (¹⁹F), and silicon (²⁹Si) nuclear magnetic resonance (NMR) spectra were recorded on Bruker AV400 CryoPlatform QNP or Bruker AVIII600 SMART NMR spectrometers at 23°C. Proton chemical shifts are expressed in parts per million (ppm, δ scale) downfield from tetramethylsilane and are referenced to residual protium in the NMR solvent (CHCl₃: δ 7.26, CD₃COCD₂H: δ 2.05). Carbon chemical shifts are expressed in parts per million

³ Pangborn, A. B.; Giardello, M. A.; Grubbs, R. H.; Rosen, R. K.; Timmers, F. J. *Organometallics* 1996, 15, 1518–1520.

(ppm, d scale) downfield from tetramethylsilane and are referenced to the carbon resonance of the NMR solvent (CDCl_3 : δ 77.16, $\text{CD}_3\text{COCD}_2\text{H}$: δ 29.84). Data are represented as follows: chemical shift, multiplicity (s = singlet, d = doublet, t = triplet, q = quartet, m = multiplet, br = broad, app = apparent), integration, and coupling constant (J) in Hertz (Hz). Accurate mass measurements were obtained using an Agilent 1100 quaternary LC system coupled to an Agilent 6210 LC/MSD-TOF fitted with an ESI or an APCI source, or Thermo Q-Exactive Orbitrap using electrospray ionization (ESI) or a Waters GCT Premier spectrometer using chemical ionization (CI).

Synthesis of Citronellol



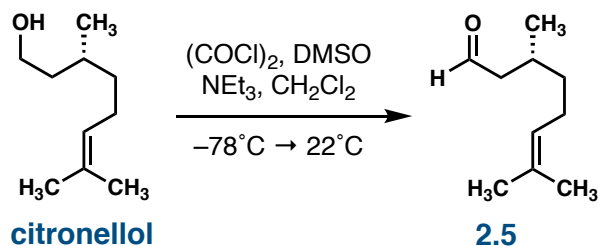
Citronellyl butyrate (51.5 mL, 200 mmol, 1 equiv) was added dropwise over 2 h to a stirred slurry of lithium aluminum hydride (8.3 g, 220 mmol, 1.1 equiv) in THF (1 L) at 0°C. The resultant solution was warmed to 22°C and stirred for 2 h. The solution was cooled to 0°C and the excess lithium aluminum hydride was carefully quenched through the sequential dropwise addition of water (25 mL), 3 N sodium hydroxide solution (25 mL), and water (40 mL) with 5 min in between additions. The organic layer was filtered over a pad of celite and dried over anhydrous sodium sulfate. The dried solution was concentrated, and the butanol byproduct was removed using vacuum distillation (70°C) to afford a clear, colorless oil (25.1 g, 161 mmol, 80%).

^1H NMR (400 MHz, CDCl_3) δ : 5.09 (tt, $J_1 = 7.1$, $J_2 = 1.5$ Hz, 1H), 3.76 – 3.60 (m, 2H), 1.98 (qq, $J = 14.4$, 6.9 Hz, 2H), 1.68 (s, 3H), 1.68 – 1.50 (m, 6H), 1.46 – 1.28 (m, 4H), 1.23 – 1.12 (m, 1H), 0.90 (d, $J = 6.5$ Hz, 3H).

^{13}C NMR (101 MHz, CDCl_3) δ : 131.4, 124.8, 61.3, 40.1, 37.4, 29.3, 25.9, 25.6,
19.7, 17.8.

TLC: 5% ethyl acetate–hexanes, $R_f = 0.06$ (CAM).

Synthesis of (R)-(+)-citronellal 2.5



DMSO (25.0 mL, 354 mmol, 2.20 equiv) was added dropwise to a solution of oxalyl chloride (15.0 mL, 177 mmol, 1.10 equiv) in dichloromethane (1 L) at -78°C . The resultant solution was stirred at that temperature until gas evolution ceased (ca. 35 min), then was stirred for an additional 5 min. A solution of citronellol (29.4 mL, 161 mmol, 1 equiv) in dichloromethane (50 mL) was added dropwise to the reaction mixture, and the resultant solution was stirred for 15 min, whereupon triethylamine (114 mL, 821 mmol, 5.10 equiv) is added. The resultant solution was warmed to 22°C over 30 min, then was stirred for an additional 45 min. The excess oxidant was quenched with 1N aqueous hydrochloric acid solution (100 mL) and the solution was extracted with dichloromethane (3 x 400 mL). The combined organic extracts were dried over anhydrous sodium sulfate and the dried solution was concentrated. The crude oil was taken up in diethyl ether (20 mL) and filtered through a plug of basic alumina to afford a clear, slightly yellow oil (22.9 g, 148 mmol, 92%) that was used without further purification.

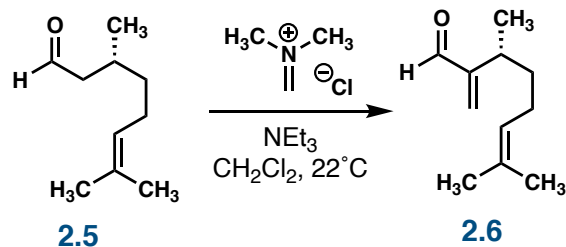
^1H NMR (400 MHz, CDCl_3) δ : 9.75 (t, $J = 2.4$ Hz, 1H), 5.11 – 5.05 (m, 1H), 2.40 (ddd, $J_1 = 16.0$ Hz, $J_2 = 5.6$ Hz, $J_3 = 2.1$ Hz, 1H), 2.22 (ddd, $J_1 = 16.0$ Hz, $J_2 = 8.0$ Hz,

$J_3 = 2.7$ Hz, 1H), 2.11 – 1.92 (m, 3H), 1.68 (s, 3H), 1.60 (s, 3H), 1.41 – 1.18 (m, 2H), 0.96 (d, $J = 6.7$ Hz, 3H).

^{13}C NMR (101 MHz, CDCl_3) δ : 203.2, 131.9, 124.2, 51.1, 37.1, 27.9, 25.8, 25.5, 20.0, 17.8.

TLC: 5% ethyl acetate–hexanes, $R_f = 0.42$ (CAM).

Synthesis of Unsaturated Aldehyde 2.6



A solution of triethylamine (54 mL, 390 mmol, 6.0 equiv) and (R)-(+)-citronellal (11.6 mL, 64.0 mmol, 1 equiv) in dichloromethane (50 mL) was added dropwise to a stirred suspension of Eschenmoser's salt (18 g, 190 mmol, 3.0 equiv) in dichloromethane (550 mL). The resultant clear, yellow solution was stirred for 48 h, whereupon excess Eschenmoser's salt was quenched by the addition of water (100 mL). The aqueous layer was extracted with dichloromethane (3 x 100 mL) and the combined organic extracts were washed with brine (200 mL) and dried over anhydrous sodium sulfate. The dried solution was partially concentrated, then silica gel (150 g) was added to the crude solution. The solution was stirred for 5.5 h, whereupon the solution was filtered using diethyl ether. The crude solution was concentrated and purified using flash column chromatography (silica gel, starting with 2% diethyl ether–hexanes, grading to 3% diethyl ether–hexanes) to afford a clear, yellow oil (10.5 g, 63.4 mmol, 99%).

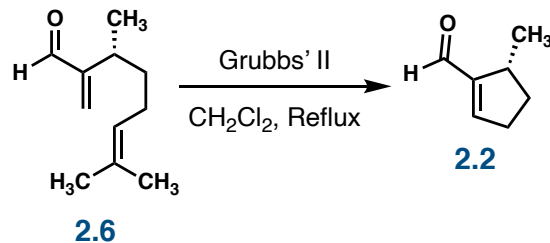
^1H NMR (400 MHz, CDCl_3) δ : 9.51 (s, 1H), 6.21 (s, 1H), 5.97 (s, 1H), 5.06 (t, J = 7.1, 1H), 2.75 – 2.62 (m, 1H), 1.93 – 1.81 (m, 2H), 1.65 (s, 3H), 1.55 (s, 3H), 1.53 – 1.46 (m,

1H), 1.42 – 1.30 (m, 1H), 1.05 (d, $J = 6.9$ Hz, 3H).

^{13}C NMR (100 MHz, CDCl_3) δ : 194.9, 155.6, 133.3, 131.8, 124.3, 35.7, 31.1, 25.9, 25.8, 19.7, 17.8.

TLC: 10% ethyl acetate–hexanes, $R_f = 0.59$ (UV, CAM).

Synthesis of Cyclic Enal 2.2



The second-generation Grubbs catalyst (933 mg, 1.10 mmol, 0.05 equiv) was added in portions to a solution of aldehyde **2.6** (3.60 g, 22.0 mmol) in dichloromethane (200 mL) heated at reflux. The resultant brown solution was heated at reflux for 48 h, then was cooled and concentrated. Purification of the residue by flash column chromatography (silica gel, 4% ethyl acetate–hexanes) afforded a pale yellow oil (2.40 g, 21.8 mmol, 99%).

^1H NMR (300 MHz, CDCl_3) δ : 9.76 (s, 1H), 6.80 (m, 1H), 3.06–2.98 (m, 1H), 2.68–2.55 (m, 1H), 2.27–2.14 (m, 1H), 1.63–1.53 (m, 2H), 1.13 (d, $J = 7.0$ Hz, 3H).

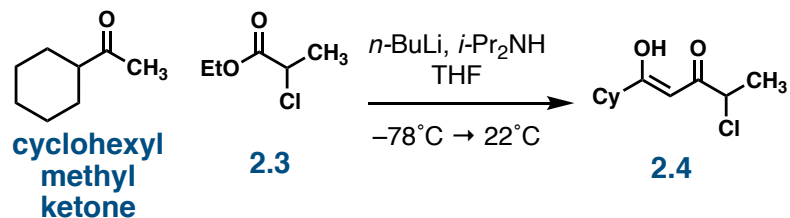
^{13}C NMR (75 MHz, CDCl_3) δ : 190.0, 153.2, 151.8, 36.8, 32.6, 32.1, 19.4.

FTIR (NaCl, thin film), cm^{-1} : 2957, 1716, 1683, 1458.

HRMS: ESI $[\text{M} - \text{H}]^-$ Calcd. for $\text{C}_7\text{H}_9\text{O}$: 111.0804.
Found: 111.0810.

TLC: 10% ethyl acetate–hexanes, $R_f = 0.47$ (UV,
KMnO₄)

Synthesis of Chlorodiketone 2.4



A solution of *n*-butyllithium (2.65 M, 4.90 mL, 13.0 mmol, 1.30 equiv) was added dropwise to a stirred solution of *N,N*-diisopropylamine (2.00 mL, 14.0 mmol, 1.40 equiv) in THF (20 mL) at -78°C . The resultant solution was warmed briefly to 0°C , then was cooled to -78°C whereupon a solution of cyclohexyl methyl ketone (1.27 g, 10.0 mmol, 1 equiv) in THF (4 mL) was added dropwise over 10 min. The resultant mixture was stirred at -78°C for 30 min, whereupon neat ethyl 2-chloropropanoate (1.50 mL, 12.0 mmol, 1.20 equiv) was added. The resultant mixture was allowed to warm to 23°C and stirred at that temperature for 16 h. The solution was cooled to 0°C and was quenched by the addition of saturated aqueous ammonium chloride solution (15 mL). The layers were separated and the aqueous layer was extracted with dichloromethane (3×10 mL). The combined organic layers were dried over anhydrous sodium sulfate and the dried solution was concentrated. Purification of the residue by flash column chromatography (silica gel, starting with 0% ethyl acetate–hexanes, grading to 4% ethyl acetate–hexanes) afforded the chlorodiketone 2.4 (1.42 g, 6.55 mmol, 65%) as a clear, yellow oil.

^1H NMR (400 MHz, CDCl_3) δ : 15.2 (s, 1H), 5.82 (s, 1H), 4.36 (q, $J = 6.9$ Hz, 1H), 2.22 (tt, $J_1 = 11.3$ Hz, $J_2 = 3.3$ Hz, 1H),

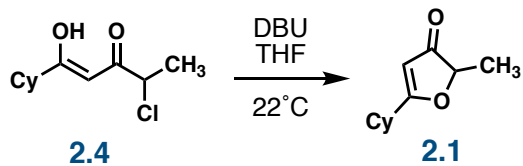
1.91-1.69 (m, 5H), 1.67 (d, $J = 6.9$ Hz, 3H),
1.45-1.18 (m, 5H).

^{13}C NMR (100 MHz, CDCl_3) δ : 197.2, 192.6, 94.9, 56.7, 46.3, 29.65, 29.63,
25.84, 25.81(2C), 21.9.

HRMS: ESI $[\text{M}+\text{H}]^+$ Calcd. for $\text{C}_{11}\text{H}_{18}\text{ClO}_2$: 217.0995.
Found: 217.0988.

TLC: 2% ethyl acetate–hexanes, $R_f = 0.37$ (UV).

Synthesis of Furanone 2.1



1,8-Diazabicyclo[5.4.0]undec-7-ene (5.50 mL, 36.7 mmol, 1.70 equiv) was added dropwise to a stirred solution of chlorodiketone **2.4** (4.68 g, 21.6 mmol, 1 equiv) in THF (100 mL) at 22°C. A pale, yellow precipitate formed immediately. The resultant suspension was stirred at 22°C for 12 h, whereupon the suspension was partitioned between water (60 mL) and ethyl acetate (60 mL). The layers were separated, and the aqueous phase was extracted with ethyl acetate (3 x 60 mL). The combined organic layers were dried over anhydrous sodium sulfate and the dried solution was concentrated. Purification of the residue using flash column chromatography (silica gel, starting with 5% ethyl acetate–hexanes, grading to 15% ethyl acetate–hexanes) afforded a pale, yellow oil (3.13 g, 17.4 mmol, 81%).

¹H NMR (400 MHz, CDCl₃) δ: 5.36 (s, 1H), 4.46 (q, *J* = 7.1 Hz, 1H), 2.47–2.38 (m, 1H), 2.01–1.93 (m, 2H), 1.84–1.77 (m, 2H), 1.75–1.68 (m, 1H), 1.42 (d, *J* = 7.1 Hz, 3H), 1.40–1.25 (m, 5H).

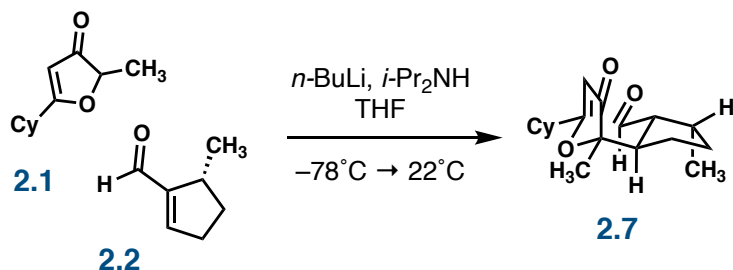
¹³C NMR (100 MHz, CDCl₃) δ: 206.1, 197.7, 100.8, 82.3, 39.8, 29.99, 29.94, 25.89, 25.72, 25.70, 16.6.

HRMS: ESI [M + H]⁺ Calcd. for C₁₁H₁₇O₂: 181.1229.

Found: 181.1222.

TLC: 20% ethyl acetate–hexanes, R_f = 0.30, (UV,
CAM).

Synthesis of Michael Adduct **2.7**



A solution of *n*-butyllithium (2.58 M, 8.20 mL, 21.1 mmol, 1.30 equiv) was added to a stirred solution of *N,N*-diisopropylamine (3.20 mL, 22.7 mmol, 1.40 equiv) in THF (170 mL) at -78°C . The resultant solution was warmed briefly to 0°C , then was cooled to -78°C whereupon a solution of the furanone **2.1** (2.92 g, 16.2 mmol, 1 equiv) in THF (15 mL) was added dropwise. The resultant mixture was stirred at -78°C for 30 min, whereupon a solution of the aldehyde **2.2** (1.87 g, 17.0 mmol, 1.16 equiv) in THF (8 mL) added dropwise. The reaction mixture was stirred at -78°C for 30 min, then was warmed to 22°C and stirred at that temperature for 2 h. The reaction mixture was then cooled to 0°C , whereupon saturated aqueous ammonium chloride solution (50 mL) was added carefully. The layers were separated and the aqueous layer was extracted with dichloromethane (3×60 mL). The combined organic layers were dried over anhydrous sodium sulfate and the dried solution was concentrated. Purification of the residue by flash column chromatography (silica gel, starting with 5% ethyl acetate–hexanes, grading to 18% ethyl acetate–hexanes) afforded the Michael adduct **2.7** (3.18 g, 11.0 mmol, 68%, 2:1 d.r. desired: Σ others) as a light yellow oil.

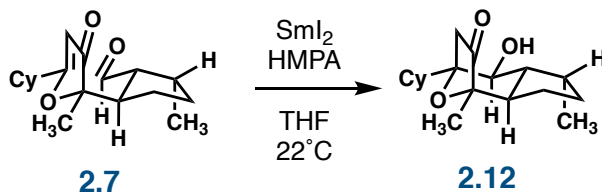
^1H NMR (400 MHz, CDCl_3) δ : 9.65 (d, $J = 3.3$ Hz, 1H), 5.34 (s, 1H), 2.93 (ddd, $J_1 = 15.6$ Hz, $J_2 = 8.6$ Hz, $J_3 = 7.2$ Hz, 1H), 2.70-2.64 (m, 1H), 2.46-2.32 (m, 2H), 2.01-1.67 (m, 7H), 1.41-1.21 (m, 7H), 1.32 (s, 3H), 1.02 (d, $J = 7.2$ Hz, 7 3H).

^{13}C NMR (100 MHz, CDCl_3) δ : 206.9, 204.6, 196.7, 101.4, 90.9, 54.4, 43.8, 39.8, 39.0, 34.6, 30.2, 29.7, 26.7, 25.9, 25.7, 25.6, 21.1, 16.1.

HRMS: ESI $[\text{M} + \text{H}]^+$ Calcd. for $\text{C}_{18}\text{H}_{27}\text{O}_3$: 291.1960.
Found: 291.1954.

TLC: 20% ethyl acetate–hexanes, $R_f = 0.41$ (UV, CAM).

Synthesis of Englerin Core 2.12



A solution of samarium(II) iodide in THF [0.1 M, 15.4 mL, 1.54 mmol, 3.09 equiv, freshly prepared from samarium powder ground from the ingot (427 mg, 2.84 mmol, 5.50 equiv) and 1,2-diiodoethane (435 mg, 1.54 mmol, 3.09 equiv) (washed with a saturated aqueous sodium thiosulfate solution (5x) and recrystallized from Et₂O)] was added dropwise to a solution of the Michael adduct **2.7** (150 mg, 0.50 mmol, 1 equiv) and HMPA (1.1 mL, 6.2 mmol, 12 equiv) in THF (15 mL) over 90 min. The resultant deep purple mixture was stirred at 22°C for 4 h, then was cooled to 0°C and excess samarium(II) iodide was quenched by the addition of saturated aqueous ammonium chloride solution (6 mL). The resultant mixture was diluted with diethyl ether (20 mL), the layers were separated and the aqueous layer was extracted with dichloromethane (3 × 10 mL). The combined organic layers were dried over anhydrous sodium sulfate, and the dried solution was concentrated. Purification of the residue by flash column chromatography (silica gel, starting with 5% ethyl acetate–hexanes, grading to 15% ethyl acetate–hexanes) afforded the ketoalcohol **2.12** (18 mg, 0.060 mmol, 12%) as a pale yellow oil.

¹H NMR (400 MHz, CDCl₃) δ: 3.92 (d, *J* = 10.5 Hz, 1H), 2.45 (d, *J* = 18.4 Hz, 1H), 2.33 (d, *J* = 18.4 Hz, 1H), 2.31-2.25 (m, 1H), 2.01-1.88 (m, 2H), 1.87-1.77 (m, 3H),

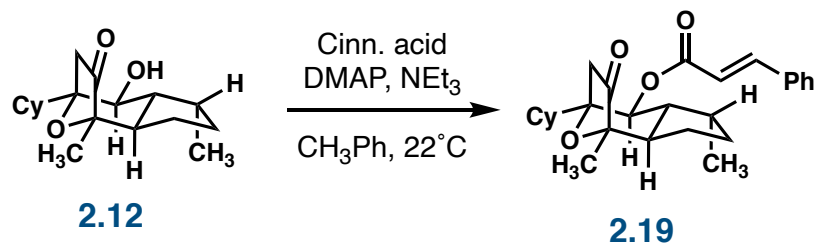
1.76-1.58 (m, 5H), 1.50 (br s, 1H), 1.41-1.23
(m, 6H), 1.21 (s, 3H), 1.17-1.14 (m, 1H), 0.89
(d, $J = 7.2$ Hz, 3H).

^{13}C NMR (100 MHz, CDCl_3) δ : 216.0, 83.5, 83.0, 70.2, 49.4, 46.5, 43.2, 41.7,
31.2, 30.6, 27.9, 27.20, 27.14, 26.8, 26.6, 24.4,
18.1, 16.9.

HRMS: ESI $[\text{M} + \text{H}]^+$ Calcd. for $\text{C}_{18}\text{H}_{29}\text{O}_3$: 293.2117.
Found: 293.2108.

TLC: 25% ethyl acetate–hexanes, $R_f = 0.44$ (CAM,
UV).

Synthesis of Cinnamate Ester 2.19



Cinnamic acid (10.5 mg, 0.071 mmol, 2.00 equiv), 2,4,6-trichlorobenzoyl chloride (22 mg, 0.089 mmol, 2.5 equiv), triethylamine (14 mg, 0.14 mmol, 4.0 equiv), and 4-dimethylaminopyridine (0.8 mg, 0.007 mmol, 0.2 equiv) were added sequentially to a solution of the ketoalcohol **2.12** (10.4 mg, 0.036 mmol, 1 equiv) in toluene (2 mL). The resultant mixture was stirred at 23°C for 41 h, then excess acid chloride was quenched by the addition of 1N aqueous hydrochloric acid solution (1 mL). The layers were separated and the aqueous layer was extracted with dichloromethane (3 × 2 mL). The combined organic layers were dried over anhydrous sodium sulfate and the dried solution was concentrated. Purification of the residue by flash column chromatography (silica gel, starting with 2% ethyl acetate–hexanes, grading to 3% ethyl acetate–hexanes) afforded the ketoester **2.19** (14.9 mg, 0.0353 mmol, 99%) as a colorless oil.

¹H NMR (400 MHz, CDCl₃) δ: 7.67 (d, *J* = 16.0 Hz, 1H), 7.56–7.52 (m, 2H), 7.42–7.38 (m, 3H), 6.40 (d, *J* = 16.0 Hz, 1H), 5.38 (d, *J* = 10.6 Hz, 1H), 2.61 (d, *J* = 18.4 Hz, 1H), 2.45 (d, *J* = 18.4 Hz, 1H), 2.14–2.05 (m, 1H), 1.90–1.71 (m, 6H), 1.69–1.59 (m, 3H),

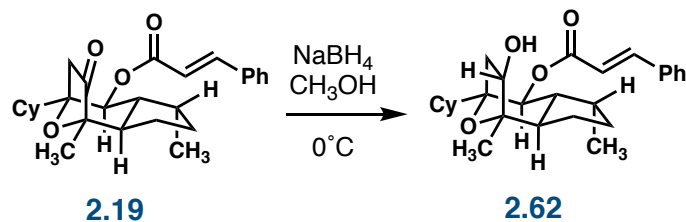
1.53 (ddd, $J_1 = 13.7$ Hz, $J_2 = 10.6$ Hz, $J_3 = 6.4$ Hz, 1H), 1.25 (s, 3H), 1.24–1.10 (m, 7H), 0.94 (d, $J = 7.1$ Hz, 3H).

^{13}C NMR (100 MHz, CDCl_3), δ : 215.6, 165.6, 145.6, 134.3, 130.7, 129.1 (2C), 128.4 (2C), 117.8, 83.5, 82.5, 70.7, 48.5, 46.1, 44.1, 42.9, 31.3, 30.8, 27.9, 27.2, 27.1, 26.7, 26.6, 23.4, 18.2, 17.0.

HRMS: ESI $[\text{M} + \text{H}]^+$ Calcd. for $\text{C}_{27}\text{H}_{35}\text{O}_4$: 423.2535.
Found: 423.2537.

TLC: 10% ethyl acetate–hexanes, $R_f = 0.53$ (UV, CAM).

Synthesis of Alcohol 2.62



Sodium borohydride (3.4 mg, 0.09 mmol, 2.0 equiv) was added to a solution of the ketoester **2.19** (19 mg, 0.045 mmol, 1 equiv) in methanol (2.5 mL) at 0°C. The resultant mixture was stirred at the temperature for 30 min, and excess borohydride was quenched by the addition of saturated aqueous ammonium chloride solution (2 mL). The resultant mixture was extracted with dichloromethane (3 × 10 mL), the combined organic layers were dried over anhydrous sodium sulfate, and the dried solution was concentrated. Purification of the residue by flash column chromatography (silica gel, 15% ethyl acetate–hexanes) afforded the alcohol **2.62** (15.7 mg, 0.0370 mmol, 82%) as a colorless oil.

¹H NMR (400 MHz, CDCl₃) δ: 7.66 (d, *J* = 16.0 Hz, 1H), 7.56–7.51 (m, 2H), 7.41–7.37 (m, 3H), 6.41 (d, *J* = 16.0 Hz, 1H), 5.21 (d, *J* = 10.2 Hz, 1H), 4.21–4.15 (m, 1H), 2.40–2.31 (m, 2H), 2.16–2.10 (m, 1H), 2.07 (dd, *J*₁ = 13.7 Hz, *J*₂ = 5.1 Hz, 1H), 1.99–1.88 (m, 1H), 1.87–1.77 (m, 4H), 1.77–1.62 (m, 4H), 1.59 (br d, *J* = 4.6 Hz, 1H), 1.45–1.36 (m, 1H),

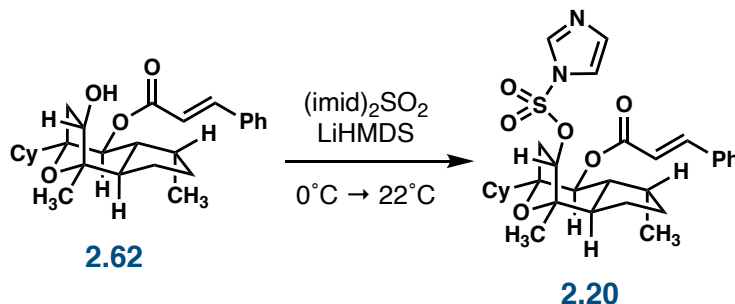
1.32 (s, 3H), 1.29-1.21 (m, 3H), 1.14-1.02 (m, 3H), 0.95 (d, $J = 7.1$ Hz, 3H).

^{13}C NMR (100 MHz, CDCl_3) δ : 165.9, 144.9, 134.6, 130.5, 129.0 (2C), 128.3 (2C), 118.5, 84.6, 81.5, 81.0, 72.3, 49.1, 46.4, 44.1, 39.6, 31.56, 31.41, 28.0, 27.4, 27.1, 26.9, 26.7, 24.4, 23.6, 17.0.

HRMS: ESI $[\text{M} + \text{H}]^+$ Calcd. for $\text{C}_{27}\text{H}_{37}\text{O}_4$: 425.2692.
Found: 425.2690.

TLC: 20% ethyl acetate–hexanes, $R_f = 0.42$ (UV, CAM).

Synthesis of Imidazole 2.20



A solution of *n*-butyllithium (2.60 M, 0.100 mL, 0.260 mmol, 7.00 equiv) was added to a stirred solution of hexamethyldisilazane (0.058 mL, 0.280 mmol, 7.70 equiv) in THF (1 mL) at 0°C . The resultant solution was warmed briefly to 23°C , then was cooled to 0°C whereupon a solution of alcohol **2.62** (15.7 mg, $37.0\ \mu\text{mol}$, 1 equiv) in THF (1 mL) was added. The resultant mixture was stirred at that temperature for 30 min, then was cooled to -10°C whereupon *N,N'*-sulfuryldiimidazole (55 mg, 0.28 mmol, 7.7 equiv) was added. The reaction mixture was warmed to 23°C and stirred at that temperature for 18 h. Excess *N,N'*-sulfuryldiimidazole was quenched by the addition of methanol (0.5 mL) and the resultant mixture was concentrated. The residue was partitioned between saturated aqueous sodium bicarbonate solution (2 mL) and dichloromethane (2 mL). The layers were separated and the aqueous layer was extracted with dichloromethane ($3 \times 2\ \text{mL}$). The combined organic layers were dried over anhydrous sodium sulfate and the dried solution was concentrated. Purification of the residue by flash column chromatography (silica gel, 33% ethyl acetate-hexanes) afforded the imidazole **2.20** (20.2 mg, $0.0364\ \text{mmol}$, 98%) as a colorless oil.

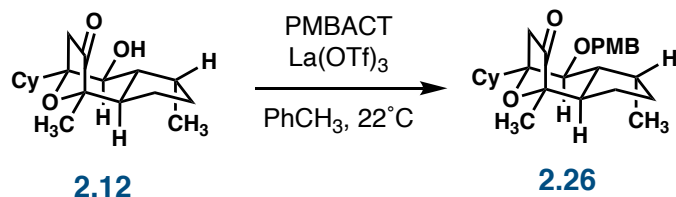
^1H NMR (400 MHz, CDCl_3) δ : 8.02 (s, 1H), 7.65 (d, $J = 16.0$ Hz, 1H), 7.58–7.52 (m, 2H), 7.42–7.39 (m, 3H), 7.37 (t, $J = 1.4$ Hz, 1H), 7.25–7.23 (m, 1H), 6.39 (d, $J = 16.0$ Hz, 1H), 5.19 (d, $J = 10.0$ Hz, 1H), 4.58 (dd, $J_1 = 10.9$ Hz, $J_2 = 4.7$ Hz, 1H), 2.29 (dd, $J_1 = 14.6$ Hz, $J_2 = 11.0$ Hz, 1H), 2.18–2.12 (m, 1H), 2.09 (dd, $J_1 = 14.5$ Hz, $J_2 = 4.8$ Hz, 1H), 2.04–1.90 (m, 2H), 1.85 (ddd, $J_1 = 12.3$ Hz, $J_2 = 12.3$ Hz, $J_3 = 7.8$ Hz, 1H), 1.79–1.53 (m, 8H), 1.41–1.20 (m, 3H), 1.18 (s, 3H), 1.12–1.00 (m, 3H), 0.93 (d, $J = 7.1$ Hz, 3H).

^{13}C NMR (100 MHz, CDCl_3), δ : 165.6, 145.6, 137.3, 134.3, 131.8, 130.7, 129.1 (2C), 128.4 (2C), 118.1, 117.8, 90.6, 85.2, 81.2, 70.9, 48.8, 46.5, 43.6, 35.7, 31.31, 31.28, 27.7, 27.1, 26.8, 26.7, 26.5, 23.9, 22.7, 16.8.

HRMS: ESI $[\text{M} + \text{H}]^+$ Calcd. for $\text{C}_{30}\text{H}_{39}\text{N}_2\text{O}_6\text{S}$: 555.2529. Found: 555.2526.

TLC: 20% ethyl acetate–hexanes, $R_f = 0.38$ (UV, CAM).

Synthesis of *p*-methoxybenzyl ether **2.26**



PMB acetimidate (230 mg, 0.81 mmol, 3.0 equiv) and lanthanum triflate (16 mg, 0.027 mmol, 0.10 equiv) are added to a stirred solution of ketoalcohol **2.12** (78.8 mg, 0.269 mmol, 1 equiv) in toluene (mL) at 22°C. The resultant solution is stirred for 24 h, whereupon the solution is concentrated and adhered to silica for purification using flash column chromatography (silica gel, starting with 1% ethyl acetate–hexanes, grading to 7% ethyl acetate–hexanes). PMB ether **2.26** (55.0 mg, 0.133 mmol, 49%) was isolated as a clear, yellow oil along with recovered starting material (38.9 mg, 0.133 mmol, 49%).

¹H NMR (600 MHz, CDCl₃) δ: 7.22 (d, *J* = 8.6 Hz, 2H), 6.87 (d, *J* = 8.6 Hz, 2H), 4.65 (d, *J* = 10.5 Hz, 1H), 4.53 (d, *J* = 10.5 Hz, 1H), 3.81 (s, 3H), 3.76 (d, *J* = 10.1 Hz, 1H), 2.48 (d, *J* = 18.6 Hz, 1H), 2.42 – 2.38 (m, 1H), 2.36 (d, *J* = 18.7 Hz, 1H), 1.95 – 1.90 (m, 1H), 1.90 – 1.85 (m, 1H), 1.85 – 1.75 (m, 4H), 1.75 – 1.63 (m, 2H), 1.63 – 1.57 (m, 1H), 1.45 (ddd, *J*₁ = 13.5, *J*₂ = 10.1, *J*₃ = 6.4 Hz,

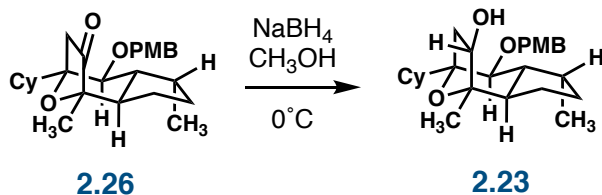
1H), 1.41 – 1.32 (m, 1H), 1.29 – 1.19 (m, 4H),
1.19 – 1.11 (m, 1H), 0.97 (d, $J = 7.1$ Hz, 3H).

^{13}C NMR (151 MHz, CDCl_3), δ : 216.3, 159.3, 131.0, 129.1 (2C), 113.9 (2C),
83.24, 83.17, 76.9, 72.5, 55.5, 49.5, 46.1, 42.5,
41.9, 32.6, 31.1, 29.9, 27.6, 27.3, 27.1, 26.9,
26.7, 22.8, 18.2, 17.3.

HRMS: ESI $[\text{M}+\text{H}]^+$ Calcd. for $\text{C}_{26}\text{H}_{37}\text{O}_4$: 412.2692.
Found: 413.2683.

TLC: 10% ethyl acetate–hexanes, $R_f = 0.43$ (UV,
CAM).

Synthesis of Alcohol 2.23



Sodium borohydride (10 mg, 0.27 mmol, 2.0 equiv) was added to a solution of the ketone **2.26** (55 mg, 0.13 mmol, 1 equiv) in methanol (8 mL) at 0°C. The resultant mixture was stirred at the temperature for 4.7 h, and excess borohydride was quenched by the addition of saturated aqueous ammonium chloride solution (2 mL). The resultant mixture was extracted with dichloromethane (3 × 15 mL), the combined organic layers were dried over anhydrous sodium sulfate, and the dried solution was concentrated. Purification of the residue by flash column chromatography (silica gel, starting with 3% ethyl acetate–hexanes, grading to 10% ethyl acetate–hexanes) afforded the alcohol **2.23** (26.5 mg, 0.064 mmol, 48%) as a colorless oil.

¹H NMR (600 MHz, CDCl₃) δ: 7.24 (d, *J* = 8.6 Hz, 2H), 6.87 (d, *J* = 8.6 Hz, 2H), 4.68 (d, *J* = 10.5 Hz, 1H), 4.51 (d, *J* = 10.5 Hz, 1H), 4.05 (dt, *J* = 10.1, 4.6 Hz, 1H), 3.80 (s, 3H), 3.62 (d, *J* = 9.6 Hz, 1H), 2.50 – 2.40 (m, 1H), 2.29 – 2.19 (m, 2H), 2.02 – 1.96 (m, 1H), 1.94 (dd, *J* = 13.8, 5.5 Hz, 1H), 1.84 – 1.71 (m, 5H), 1.68 – 1.59 (m, 2H), 1.47 (d, *J* =

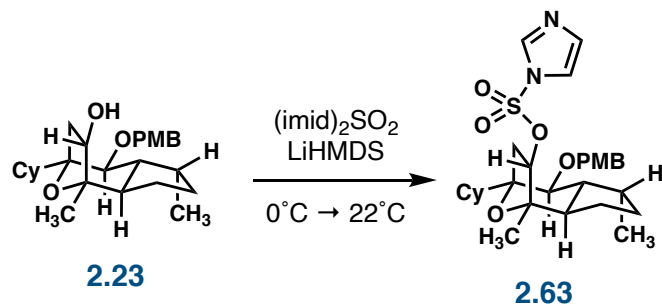
4.7 Hz, 1H), 1.28 (s, 3H), 1.27 – 1.24 (m, 2H),
1.24 – 1.15 (m, 3H), 0.97 (d, $J = 7.1$ Hz, 3H).

^{13}C NMR (151 MHz, CDCl_3) δ : 159.1, 131.6, 129.0 (2C), 113.9 (2C), 85.2,
81.2 (2C), 77.9, 72.1, 55.4, 49.3, 47.5, 42.3,
38.8, 32.9, 31.8, 29.9, 27.7, 27.2, 27.1, 27.0,
26.8, 23.8, 23.6, 17.4.

HRMS: ESI $[\text{M}+\text{H}]^+$ Calcd. for $\text{C}_{26}\text{H}_{39}\text{O}_4$: 415.2848.
Found: 415.2841.

TLC: 20% ethyl acetate–hexanes, $R_f = 0.28$ (UV,
CAM).

Synthesis of Imidazole 2.63



A solution of alcohol **2.23** (7.9 mg, 0.019 mmol, 1 equiv) in THF (1 mL) was added to a solution of potassium hexamethyldisilazane (27 mg, 0.13 mmol, 7.0 equiv) in THF (1 mL) at 0°C. The resultant solution was stirred for 30 min at that temperature, whereupon the solution is cooled to -10°C. Sulfuryl imidazole (29 mg, 0.15 mmol, 7.7 equiv) was added and the resultant solution was stirred for 22 h. Excess *N,N'*-sulfuryldiimidazole was quenched by the addition of methanol (0.5 mL) and the resultant mixture was concentrated. The residue was partitioned between saturated aqueous sodium bicarbonate solution (2 mL) and dichloromethane (2 mL). The layers were separated and the aqueous layer was extracted with dichloromethane (3 × 2 mL). The combined organic layers were dried over anhydrous sodium sulfate and the dried solution was concentrated. Purification of the residue by flash column chromatography (silica gel, starting with 5% diethyl ether–hexanes, grading to 12% diethyl ether–hexanes) afforded the imidazole **2.63** (6.8 mg, 0.012 mmol, 66%) as a clear, yellow oil.

^1H NMR (600 MHz, CDCl_3) δ : 7.97 (s, 1H), 7.32 (s, 1H), 7.20 (d, $J = 8.6$ Hz, 2H), 7.18 (s, 1H), 6.90 – 6.85 (m, 2H), 4.64 (d,

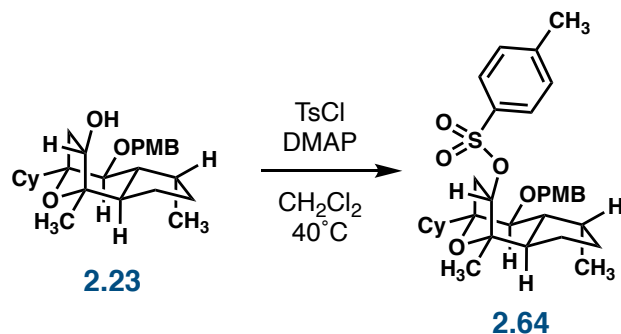
$J = 10.4$ Hz, 1H), 4.52 – 4.47 (m, 1H), 4.47 (d, $J = 10.2$ Hz, 1H), 3.81 (s, 3H), 3.60 (d, $J = 9.6$ Hz, 1H), 3.48 (q, $J = 7.0$ Hz, 2H), 2.50 – 2.41 (m, 1H), 2.19 – 2.11 (m, 1H), 2.06 – 1.99 (m, 2H), 1.95 (ddd, $J_1 = 13.4$, $J_2 = 9.6$, $J_3 = 6.4$ Hz, 1H), 1.80 – 1.67 (m, 2H), 1.67 – 1.59 (m, 1H), 1.59 – 1.50 (m, 1H), 1.43 (s, 2H), 1.28 – 1.22 (m, 3H), 1.20 (t, $J = 7.0$ Hz, 3H), 1.18 – 1.10 (m, 2H), 0.95 (d, $J = 7.1$ Hz, 3H), 0.90 – 0.86 (m, 2H), 0.86 – 0.82 (m, 1H).

^{13}C NMR (151 MHz, CDCl_3), δ : 159.3, 131.0, 129.1 (2C), 113.9 (2C), 90.9, 85.9, 80.8, 76.7, 72.3, 66.0, 55.5, 48.9, 47.4, 41.9, 34.8, 32.7, 31.5, 30.5, 29.85, 27.53, 27.0, 26.9, 26.8, 26.6, 23.4, 22.7, 17.3.

HRMS: ESI $[\text{M}+\text{H}]^+$ Calcd. for $\text{C}_{29}\text{H}_{41}\text{O}_6\text{N}_2\text{S}$: 545.2685. Found: 545.2673.

TLC: 20% ethyl acetate–hexanes, $R_f = 0.29$ (UV, CAM).

Synthesis of Tosylate 2.64



A solution of alcohol **2.23**, DMAP, and tosyl chloride in dichloromethane was heated at 40°C for 17 h, whereupon the solution was cooled to 22°C. The solution was adhered to silica gel and purified using flash column chromatography (silica gel, starting with 1% ethyl acetate–hexanes, grading to 12% ethyl acetate–hexanes) to afford tosylate **2.64** (9.7 mg, 0.017 mmol, 74%) as a clear yellow oil.

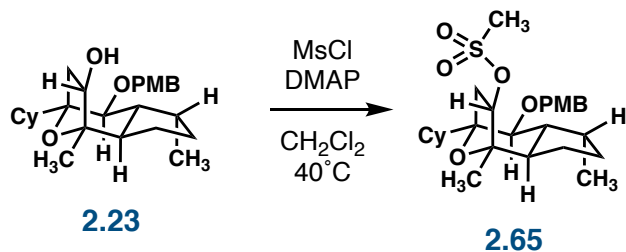
¹H NMR (600 MHz, CDCl₃) δ: 7.77 (d, *J* = 8.0 Hz, 2H), 7.33 (d, *J* = 8.0 Hz, 2H), 7.20 (d, *J* = 8.4 Hz, 2H), 6.87 (d, *J* = 8.5 Hz, 2H), 4.64 (d, *J* = 10.5 Hz, 1H), 4.48 – 4.43 (m, 2H), 3.81 (s, 3H), 3.58 (d, *J* = 9.7 Hz, 1H), 2.44 (s, 3H), 2.15 – 1.95 (m, 4H), 1.79 – 1.72 (m, 3H), 1.72 – 1.63 (m, 1H), 1.63 – 1.60 (m, 1H), 1.63 – 1.50 (m, 3H), 1.26 (s, 3H), 1.24 – 1.13 (m, 3H), 1.12 (s, 3H), 0.94 (d, *J* = 7.1 Hz, 3H).

^{13}C NMR (151 MHz, CDCl_3), δ : 159.2, 145.0, 131.3, 130.0, 129.0, 128.0, 113.9, 86.5, 85.7, 80.9, 77.2, 72.2, 55.4, 49.1, 47.2, 42.1, 35.7, 32.8, 31.7, 29.9, 27.6, 27.1, 27.0, 26.9, 26.7, 23.4, 22.8, 21.8, 17.3.

HRMS: ESI $[\text{M}+\text{H}]^+$ Calcd. for $\text{C}_{33}\text{H}_{44}\text{O}_6\text{S}$: 568.2859.
Found: 568.2860.

TLC: 20% ethyl acetate–hexanes, $R_f = 0.45$ (UV, CAM).

Synthesis of Mesylate **2.65**

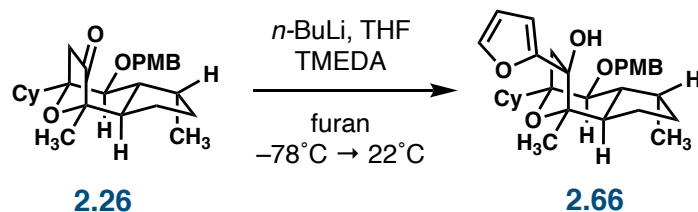


A solution of alcohol **2.23**, DMAP, and mesyl chloride in dichloromethane was heated at 40°C for 22 h, whereupon the solution was cooled to 22°C. The solution was adhered to silica gel and purified using flash column chromatography (silica gel, starting with 1% ethyl acetate–hexanes, grading to 12% ethyl acetate–hexanes) to afford mesylate **2.65** (4.4 mg, 0.0089 mmol, 52%) as a clear yellow oil.

¹H NMR (600 MHz, CDCl₃) δ: 7.27 – 7.20 (m, 4H), 6.89 – 6.84 (m, 4H), 4.72 – 4.64 (m, 3H), 4.51 (d, *J* = 10.5 Hz, 2H), 4.06 (dd, *J*₁ = 11.1, *J*₂ = 5.5 Hz, 1H), 3.80 (s, 6H), 3.63 (m, 2H), 2.99 (s, 3H), 2.51 – 2.42 (m, 2H), 2.40 – 2.33 (m, 1H), 2.29 – 2.17 (m, 3H), 2.10 – 2.03 (m, 1H), 2.04 – 1.91 (m, 2H), 1.83 – 1.70 (m, 12H), 1.68 – 1.55 (m, 9H), 1.35 (s, 4H), 1.30 – 1.12 (m, 12H), 0.97 (d, *J* = 7.1 Hz, 6H), 0.86 (m, 2H).

TLC: 20% ethyl acetate–hexanes, $R_f = 0.28$ (UV,
CAM).

Synthesis of Alcohol 2.66



Furan (42 mg, 0.62 mmol, 22 equiv) was added dropwise to a stirred solution of *N,N,N',N'*-tetramethylethylenediamine (42 μ L, 0.28 mmol, 10 equiv) and *n*-butyllithium (2.58 M in hexane, 0.11 mL, 0.28 mmol, 10 equiv) in THF (0.2 mL) at -78°C . The reaction was warmed to 0°C and stirred at that temperature for 65 min. The solution was cooled to -78°C , whereupon a solution of ketone **2.26** (11.6 mg, 0.028 mmol, 1 equiv) in THF (0.2 mL) was added via syringe. The resultant clear, yellow solution was warmed to 22°C and stirred at that temperature for 16 h and then was recooled to 0°C . Excess furanyllithium was quenched by the addition of saturated aqueous ammonium chloride solution (1 mL). The crude mixture was extracted with dichloromethane (3 x 3 mL), and the combined organic extracts were dried over anhydrous sodium sulfate. The dried solution was concentrated, then was adhered to silica and purified using flash column chromatography (silica gel, starting with 5% ethyl acetate–hexanes, grading to 10% ethyl acetate–hexanes) to afford a slightly yellow oil (6.7 mg, 0.014 mmol, 62%).

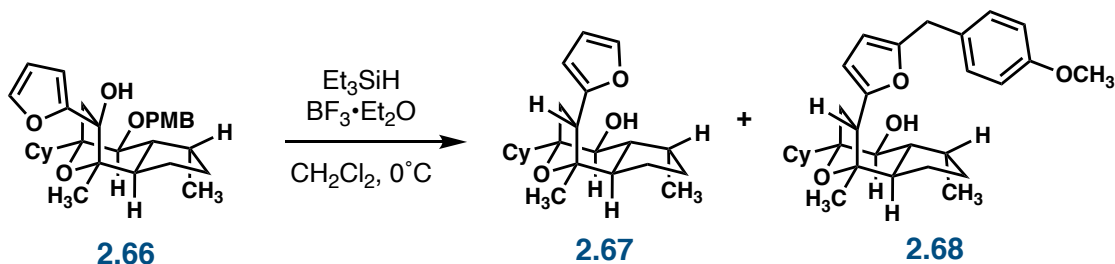
^1H NMR (600 MHz, CDCl_3) δ : 7.38 (d, $J = 1.8$ Hz, 1H), 7.27 (d, $J = 8.7$ Hz, 1H), 6.88 (d, $J = 8.5$ Hz, 2H), 6.34 (dd, $J_1 = 3.3$, $J_2 = 1.8$ Hz, 1H), 6.28 (d, $J = 3.3$ Hz, 1H),

4.71 (d, $J = 10.5$ Hz, 1H), 4.55 (d, $J = 10.5$ Hz, 1H), 3.81 (s, 3H), 3.68 (d, $J = 9.0$ Hz, 1H), 2.56 (d, $J = 14.4$ Hz, 1H), 2.51 – 2.44 (m, 2H), 2.41 (d, $J = 14.4$ Hz, 1H), 2.23 (s, 1H), 2.08 – 1.96 (m, 2H), 1.90 (qd, $J_1 = 11.5$, $J_2 = 6.0$ Hz, 1H), 1.86 – 1.81 (m, 2H), 1.80 – 1.70 (m, 2H), 1.70 – 1.60 (m, 1H), 1.44 – 1.14 (m, 4H), 1.12 – 1.03 (m, 1H), 0.99 (d, $J = 6.5$ Hz, 2H), 0.93 – 0.78 (m, 3H).

^{13}C NMR (151 MHz, CDCl_3) δ : 159.8, 159.2, 141.6, 131.6, 129.2, 113.9, 110.4, 106.2, 85.33, 84.9, 84.0, 78.1, 72.1, 55.4, 50.6, 46.9, 45.5, 43.9, 33.2, 31.8, 29.9, 28.5, 27.8, 27.5, 27.2, 26.8, 23.8, 22.8, 21.2, 17.3.

TLC: 10% ethyl acetate–hexanes, $R_f = 0.27$ (UV, CAM).

Synthesis of Furan 2.67 and Alcohol 2.68



Triethylsilane (4.5 μL , 0.028 mmol, 2.0 equiv) and trifluoroborane etherate (8.0 μL , 0.056 mmol, 4.0 equiv) were added to a solution of alcohol **2.66** (6.7 mg, 0.014 mmol, 1 equiv) in dichloromethane (0.3 mL) at 0°C . The resultant cloudy, brown solution was stirred for 20 min at that temperature, whereupon excess triethylsilane was quenched by the addition of saturated aqueous sodium bicarbonate solution (0.5 mL). The solution is warmed to 22°C and the biphasic mixture was extracted with dichloromethane (3 x 2 mL). The combined organic extracts were washed with saturated aqueous sodium bicarbonate solution (2 mL) and brine (2 mL) and then dried over anhydrous sodium sulfate. The dried solution was concentrated and adhered to silica for purification using flash column chromatography (silica gel, starting with 3% ethyl acetate–hexanes, grading to 10% ethyl acetate–hexanes) to afford the furan **2.67** (2.6 mg, 0.0075 mmol, 54%) as a yellow oil and *p*-methoxybenzyl furan **2.68** (2.0 mg, 0.043 mmol, 31%) as a yellow oil.

Furan 2.67:

^1H NMR (151 MHz, CDCl_3) δ : 7.31 (d, $J = 1.8$ Hz, 1H), 6.29 (dd, $J_1 = 3.2$, $J_2 = 1.8$ Hz, 1H), 6.14 (d, $J = 3.2$ Hz, 1H), 3.79 (d, J

= 11.1, 1H), 3.13 (dd, $J_1 = 11.8$, $J_2 = 8.2$ Hz, 1H), 2.34 (dd, $J_1 = 13.3$, $J_2 = 8.2$ Hz, 1H), 2.24 – 2.12 (m, 2H), 2.01 (ddd, $J_1 = 13.1$, $J_2 = 10.1$, $J_3 = 7.4$ Hz, 1H), 1.94 – 1.88 (m, 2H), 1.84 – 1.79 (m, 2H), 1.72 – 1.65 (m, 2H), 1.65 – 1.58 (m, 2H), 1.44 (s, 3H), 1.38 – 1.17 (m, 4H), 1.12 – 1.03 (m, 1H), 1.03 – 0.93 (m, 1H), 0.92 – 0.85 (m, 3H), 0.83 (d, $J = 7.1$ Hz, 3H).

^{13}C NMR (600 MHz, CDCl_3) δ : 153.8, 140.7, 110.4, 106.5, 85.5, 84.8, 71.5, 49.7, 47.3, 46.3, 42.6, 33.1, 31.8, 30.4, 28.2, 27.3, 27.10, 27.05, 26.8, 24.9, 24.4, 16.9, 14.3.

TLC: 20% ethyl acetate–hexanes, $R_f = 0.56$ (UV, CAM).

***p*-methoxybenzyl furan 2.68:**

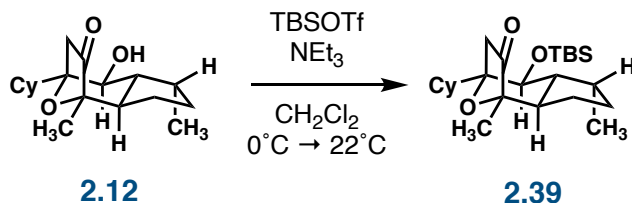
^1H NMR (151 MHz, CDCl_3) δ : 7.17 – 7.12 (m, 2H), 6.85 – 6.80 (m, 2H), 6.00 (dd, $J_1 = 3.1$, $J_2 = 1.1$ Hz, 1H), 5.89 (d, $J = 3.0$ Hz, 1H), 3.83 (s, 2H), 3.79 (s, 3H), 3.76 (d, $J = 10.2$ Hz, 1H), 3.07 (dd, $J_1 = 11.8$, $J_2 = 8.2$ Hz, 1H), 2.28 (dd, $J_1 = 13.3$, $J_2 = 8.2$ Hz, 1H), 2.19

- 2.07 (m, 2H), 1.95 (ddd, $J_1 = 13.1$, $J_2 = 10.2$,
 $J_3 = 7.4$ Hz, 1H), 1.91 – 1.86 (m, 2H), 1.85 –
1.78 (m, 3H), 1.69 – 1.57 (m, 2H), 1.37 (s, 3H),
1.33 – 1.18 (m, 4H), 1.18 – 1.02 (m, 3H), 0.90 –
0.82 (m, 3H), 0.81 (d, $J = 7.2$ Hz, 3H).

^{13}C NMR (600 MHz, CDCl_3) δ : 158.4, 153.5, 152.4, 130.7, 129.8 (2C), 114.0
(2C), 106.9, 106.4, 85.4, 84.6, 71.5, 55.5, 49.9,
47.3, 46.3, 42.7, 33.9, 32.9, 31.7, 30.3, 28.2,
27.27, 27.10, 27.05, 26.8, 24.9, 24.6, 22.9, 17.0,
14.3.

TLC: 20% ethyl acetate–hexanes, $R_f = 0.47$ (UV,
CAM).

Synthesis of Silyl Ether 2.39



TBSOTf (150 μ L, 0.70 mmol, 5.0 equiv) was added to a solution of alcohol **2.12** (42 mg, 0.14 mmol, 1 equiv) and triethylamine (195 μ L, 1.4 mmol, 10 equiv) in dichloromethane (2 mL) at -10°C . The resultant solution was stirred at that temperature for 30 min, then was warmed to 22°C and stirred at that temperature for 13 h. Silica was added to quench the excess TBSOTf and the solution was concentrated for purification using flash column chromatography (silica gel, starting with 1% ethyl acetate–hexanes, grading to 2% ethyl acetate–hexanes) to afford the ketone **2.39** (57.9 mg, 0.142 mmol, 99%) as a clear, yellow oil.

^1H NMR (151 MHz, CDCl_3) δ : 3.94 (d, $J = 9.8$ Hz, 1H), 2.42 (s, 2H), 2.29 – 2.20 (m, 1H), 1.92 – 1.75 (m, 4H), 1.74 – 1.56 (m, 4H), 1.37 – 1.09 (m, 12H), 0.87 – 0.85 (m, 10H), 0.17 – 0.05 (m, 9H).

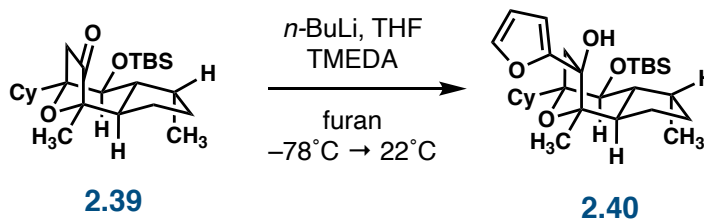
^{13}C NMR (600 MHz, CDCl_3) δ : 217.0, 83.6, 82.7, 68.9, 50.1, 45.5, 40.0, 37.9, 31.2, 30.4, 26.9, 26.7, 26.5, 26.3, 26.0 (3C), 26.0, 23.1, 18.4, 17.9, 16.7, -3.1, -4.3.

FTIR (KBr, pellet), cm^{-1} : 1755, 1113, 1094.

HRMS: ESI $[\text{M}+\text{H}]^+$ Calcd. for $\text{C}_{24}\text{H}_{43}\text{O}_3\text{Si}$: 407.2981.
Found: 407.2993.

TLC: 5% ethyl acetate–hexanes, $R_f = 0.60$ (CAM).

Synthesis of Alcohol 2.40



Furan (0.63 mL, 8.7 mmol, 22 equiv) was added dropwise to a stirred solution of *N,N,N',N'*-tetramethylethylenediamine (0.58 mL, 3.9 mmol, 10 equiv) and *n*-butyllithium (2.5 M in hexane, 1.6 mL, 3.9 mmol, 10 equiv) in THF (2 mL) at -78°C . The reaction was warmed to 0°C and stirred at that temperature for 65 min. The solution was cooled to -78°C , whereupon a solution of ketone **2.39** (160 mg, 0.393 mmol, 1.0 equiv) in THF (2 mL) was added via syringe. The resultant clear, yellow solution was warmed to 22°C and stirred at that temperature for 16 h and then was recooled to 0°C . Excess furanyllithium was quenched by the addition of saturated aqueous ammonium chloride solution (5 mL). The crude mixture was extracted with dichloromethane (3 x 15 mL), and the combined organic extracts were dried over anhydrous sodium sulfate. The dried solution was concentrated, then was adhered to silica and purified using flash column chromatography (silica gel, starting with 1% ethyl acetate–hexanes, grading to 2% ethyl acetate–hexanes) to afford a slightly yellow, puffy solid (110 mg, 0.232 mmol, 59%).

$^1\text{H NMR}$ (151 MHz, CDCl_3) δ : 7.37 (d, $J = 1.7$ Hz, 1H), 6.34 (dd, $J_1 = 3.3$, $J_2 = 1.6$ Hz, 1H), 6.31 (d, $J = 3.3$ Hz, 1H), 3.88 (d, $J = 8.7$ Hz, 1H), 2.60 (d, $J = 14.4$ Hz, 1H), 2.40 –

2.30 (m, 3H), 2.25 (s, 1H), 2.00 – 1.92 (m, 2H),
1.92 – 1.82 (m, 3H), 1.81 – 1.73 (m, 2H), 1.72 –
1.61 (m, 3H), 1.54 (s, 3H), 1.44 – 1.36 (m, 1H),
1.25 – 1.14 (m, 8H), 0.97 – 0.83 (m, 9H), 0.17 –
0.06 (m, 6H).

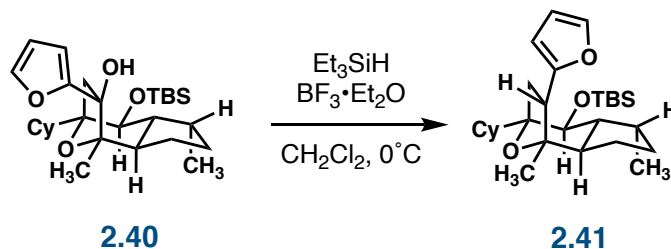
^{13}C NMR (600 MHz, CDCl_3) δ : 146.6, 141.4, 110.4, 106.2, 84.2, 70.3, 50.2,
47.4, 43.3, 39.2, 31.8, 31.3, 29.9, 27.4, 27.3,
27.1, 27.0, 26.5, 26.3 (3C), 24.5, 21.2, 18.6,
16.9, -2.8, -4.0.

FTIR (KBr, pellet), cm^{-1} : 3451 (br), 2928, 2854, 1462, 1106.

HRMS: ESI $[\text{M}+\text{H}]^+$ Calcd. for $\text{C}_{28}\text{H}_{47}\text{O}_4\text{Si}$: 475.3244.
Found: 475.3232.

TLC: 5% ethyl acetate–hexanes, $R_f = 0.36$ (CAM).

Synthesis of Furan 2.41



Triethylsilane (88 μL , 0.55 mmol, 2.0 equiv) and trifluoroborane etherate (140 μL , 1.1 mmol, 4.0 equiv) were added to a solution of alcohol **2.40** (131 mg, 0.277 mmol, 1 equiv) in dichloromethane (5.5 mL) at 0°C. The resultant solution was stirred for 20 min at that temperature, whereupon excess triethylsilane was quenched by the addition of saturated aqueous sodium bicarbonate solution (3 mL). The solution is warmed to 22°C and the biphasic mixture was extracted with dichloromethane (3 x 5 mL). The combined organic extracts were washed with saturated aqueous sodium bicarbonate solution (6 mL) and brine (6 mL) and then dried over anhydrous sodium sulfate. The dried solution was concentrated and adhered to silica for purification using flash column chromatography (silica gel, starting with 0% diethyl ether–hexanes, grading to 2% diethyl ether–hexanes) to afford the furan **2.41** (111 mg, 0.242 mmol, 87%) as a thick, clear, yellow oil.

¹H NMR (600 MHz, CDCl₃) δ : 7.31 (d, $J = 1.8$ Hz, 1H), 6.29 (dd, $J_1 = 3.2$, $J_2 = 1.9$ Hz, 1H), 6.10 (d, $J = 3.2$ Hz, 1H), 3.85 (d, $J = 9.4$ Hz, 1H), 3.05 (dd, $J_1 = 11.7$, $J_2 = 8.7$ Hz, 1H), 2.44 – 2.35 (m, 1H), 2.21 – 2.11 (m, 2H), 1.96 (ddd, $J_1 = 13.4$, $J_2 = 9.4$, $J_3 = 6.5$ Hz, 1H),

1.93 – 1.87 (m, 1H), 1.85 – 1.74 (m, $J_1 = 15.0$,
 $J_2 = 9.2$ Hz, 2H), 1.69 – 1.51 (m, 6H), 1.42 (s,
3H), 1.35 – 1.16 (m, 6H), 1.03 – 0.96 (m, 1H),
0.93 – 0.85 (m, 8H), 0.80 (d, $J = 7.1$ Hz, 3H),
0.16 – 0.04 (m, 6H).

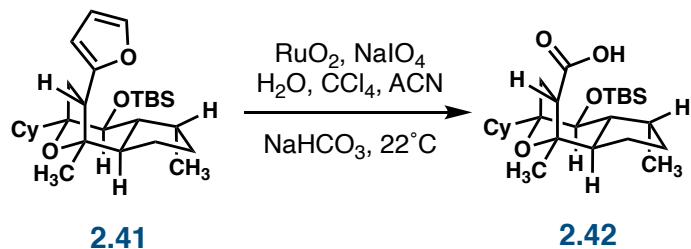
^{13}C NMR (151 MHz, CDCl_3) δ : 154.3, 140.7, 110.3, 106.3, 86.2, 84.1, 70.7,
48.9, 47.2, 47.1, 39.4, 32.2, 31.22, 31.18, 27.3,
27.1, 26.8, 26.7, 26.4, 26.3 (3C), 25.0, 23.1,
18.7, 16.7, -2.9, -3.9.

FTIR (KBr, pellet), cm^{-1} : 2922, 2851, 1463.

HRMS: ESI $[\text{M}+\text{H}]^+$ Calcd. for $\text{C}_{28}\text{H}_{47}\text{O}_3\text{Si}$: 459.3289.
Found: 459.3283.

TLC: 2.5% ethyl acetate–hexanes, $R_f = 0.73$ (CAM).

Synthesis of Carboxylic Acid 2.42



Ruthenium dioxide (39 mg, 0.29 mmol, 1.1 equiv) was added to a stirred solution of sodium periodate (342 mg, 1.60 mmol, 6.0 equiv) in carbon tetrachloride (4.0 mL), acetonitrile (6.0 mL), and water (4.0 mL) at 22°C. The resultant cloudy, black solution was stirred vigorously for 20 min, whereupon sodium bicarbonate (2.2 g, 26.1 mmol, 100 equiv) and water (2.6 mL) were added. The resultant solution was stirred for 5 min, whereupon a solution of furan **2.41** (120 mg, 0.261 mmol, 1 equiv) in acetonitrile (2.6 mL) and ethyl acetate (0.5 mL) was added. The solution is stirred for 1 h, whereupon sodium periodate is added until the solution becomes a dark green suspension. The suspension is diluted with water and brought to a pH less than 7 through the slow addition of 2 N hydrochloric acid solution. The resultant gray suspension was extracted with ethyl acetate (3 x 30 mL) and the combined organic layers were dried over anhydrous sodium sulfate. The dried solution was filtered through Celite® and concentrated to afford a sticky black oil that was used in the following step without further purification.

¹H NMR (600 MHz, CDCl₃) δ: 3.83 (d, *J* = 9.4 Hz, 1H), 2.77 – 2.70 (m, 1H), 2.51 (dd, *J*₁ = 13.7, *J*₂ = 7.9 Hz, 1H), 2.29 – 2.22 (m, 1H), 1.99 – 1.90 (m, 2H), 1.89 – 1.85

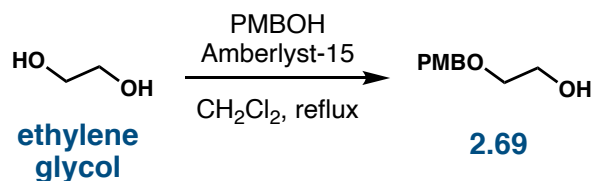
(m, 1H), 1.85 – 1.75 (m, 1H), 1.73 – 1.69 (m, 1H), 1.67 – 1.55 (m, 3H), 1.46 (s, 3H), 1.33 – 1.25 (m, 8H), 1.24 – 1.16 (m, 2H), 1.15 – 1.07 (m, 1H), 0.90 – 0.87 (m, 9H), 0.83 (d, $J = 7.1$ Hz, 3H), 0.14 – 0.05 (m, 6H).

^{13}C NMR (151 MHz, CDCl_3) δ : 175.8, 86.8, 84.0, 70.5, 52.0, 49.4, 47.6, 39.1, 31.2, 31.1, 30.7, 29.9, 27.2, 27.1, 26.7, 26.6, 26.3, 26.2 (3C), 25.0, 24.5, 16.8, -2.8, -4.0.

HRMS: ESI $[\text{M}-\text{H}]^-$ Calcd. for $\text{C}_{25}\text{H}_{43}\text{O}_4\text{Si}$: 435.2931.
Found: 435.2935.

TLC: 20% ethyl acetate–hexanes, $R_f = 0.28$ (CAM).

Synthesis of PMB-protected Ethylene Glycol 2.69

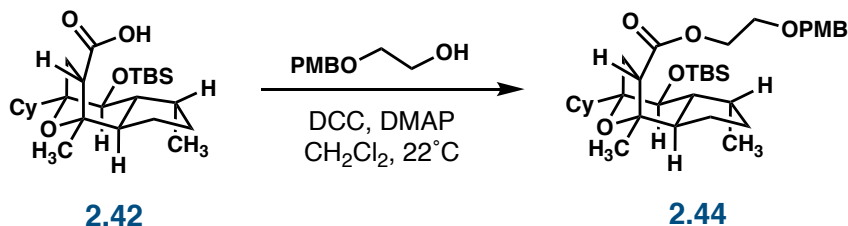


A stirred solution of ethylene glycol (6.90 mL, 124 mmol, 1 equiv), anisyl alcohol (17.0 mL, 137 mmol, 1.10 equiv), and Amberlyst-15 resin (730 mg) in dichloromethane (240 mL) was heated at reflux for 20 h, whereupon dichloromethane (50 mL) and water (100 mL) were added. The layers were separated and the aqueous layer was extracted with dichloromethane (3 x 100 mL). The combined organic extracts were dried over anhydrous sodium sulfate and the dried solution was concentrated. The crude yellow oil was purified using flash column chromatography (silica gel, starting with 15% ethyl acetate–hexanes, grading to 50% ethyl acetate–hexanes) to afford a clear, colorless oil.

^1H NMR (600 MHz, CDCl_3) δ : 7.27 (d, $J = 8.4$ Hz, 2H), 6.89 (d, $J = 7.8$ Hz, 2H), 4.49 (s, 2H), 3.80 (d, $J = 1.3$ Hz, 3H), 3.75 – 3.71 (m, 2H), 3.58 – 3.55 (m, 2H).

^{13}C NMR (151 MHz, CDCl_3) δ : 159.5, 130.2, 129.6 (2C), 114.0 (2C), 73.1, 71.2, 62.0, 55.4.

Synthesis of Ester 2.44



DCC (6.8 mg, 0.033 mmol, 1.3 equiv) was added to stirred solution of carboxylic acid **2.42**, DMAP (4.3 mg, 0.035 mmol, 1.4 equiv), and the PMB-protected ethylene glycol (27 mg, 0.15 mmol, 6.0 equiv) in dichloromethane (0.2 mL). The resultant solution was stirred for 44 h, whereupon the solution was diluted with dichloromethane (2 mL). The solution was then washed with water (2 x 1 mL) and saturated ammonium chloride solution (2 x 1 mL), then was dried over anhydrous sodium sulfate. The dried solution was filtered through Celite® and concentrated to afford a gray oil that was used without further purification.

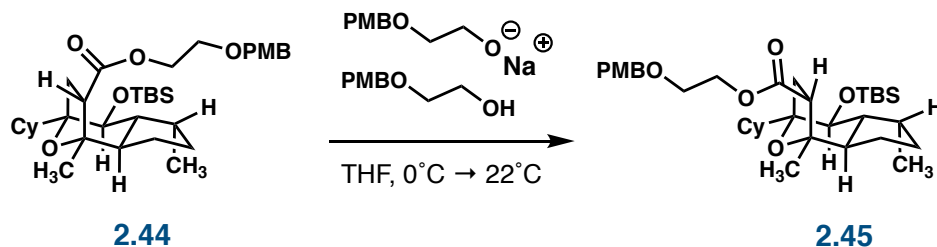
¹H NMR (600 MHz, CDCl₃) δ: 7.27 – 7.23 (m, 2H), 6.91 – 6.85 (m, 2H), 4.48 (s, 2H), 4.28 – 4.12 (m, 2H), 3.83 (d, *J* = 9.4 Hz, 1H), 3.81 (s, 3H), 3.64 (t, *J* = 4.8 Hz, 2H), 2.72 (dd, *J* = 11.6, 7.9 Hz, 1H), 2.55 (dd, *J* = 13.6, 8.0 Hz, 1H), 2.29 – 2.20 (m, 1H), 1.97 (ddd, *J* = 13.4, 9.4, 6.6 Hz, 1H), 1.94 – 1.85 (m, 1H), 1.85 – 1.66 (m, 2H), 1.66 – 1.59 (m, 5H), 1.53 – 1.46 (m, 1H), 1.43 (s, 4H), 1.39 –

1.20 (m, 9H), 1.19 – 1.13 (m, 4H), 1.12 – 1.04 (m, 2H), 0.92 – 0.84 (m, 3H), 0.83 (d, $J = 7.1$ Hz, 3H), 0.14 – 0.05 (m, 6H).

^{13}C NMR (151 MHz, CDCl_3) δ : 172.0, 159.5, 130.1, 129.5 (2C), 114.0 (2C), 86.7, 84.0, 73.0, 70.6, 67.6, 63.8, 55.4, 52.4, 49.3, 47.4, 39.3, 31.18, 31.16, 30.9, 27.2, 27.1, 26.8, 26.7, 26.3, 26.2 (3C), 25.1, 24.4, 16.9, 14.3, -2.8, -3.9.

TLC: 20% ethyl acetate–hexanes, $R_f = 0.63$ (CAM).

Synthesis of Reverse Ester 2.45



PMB-protected ethylene glycol (450 mg, 2.5 mmol, 100 equiv) was added dropwise to a stirred suspension of sodium hydride (60% in mineral oil, 19.1 mg, 0.478 mmol, 19.1 equiv, pre-washed with hexanes [3 x 1 mL]) in tetrahydrofuran (0.5 mL) at 0°C. The resultant clear, yellow solution was warmed to 22°C and stirred at that temperature until the bubbling ceased (ca. 5 min) whereupon a solution of the ester **2.44** in tetrahydrofuran (0.5 mL) was added dropwise. The resultant mixture was stirred for 48 h, then was cooled to -78°C and excess base was quenched by the addition of saturated aqueous ammonium chloride solution (2 mL). The resultant biphasic mixture was extracted with dichloromethane (3 x 10 mL) and the combined organic layers were dried over anhydrous sodium sulfate. The dried solution was concentrated to afford a gray oily residue. Purification by flash column chromatography (basic alumina, starting with 5% ethyl acetate–hexanes, grading to 25% ethyl acetate–hexanes) afforded the reverse ester **2.45** as a yellow oil (9.0 mg, 0.015 mmol, 60% over 3 steps).

¹H NMR (600 MHz, CDCl₃) δ: 7.25 (d, *J* = 5.7 Hz, 2H), 6.90 – 6.84 (m, 2H), 4.48 (d, *J* = 5.1 Hz, 2H), 4.24 (t, *J* = 4.8 Hz, 2H), 3.80 (s, 3H), 3.78 – 3.73 (m, 1H), 3.66 –

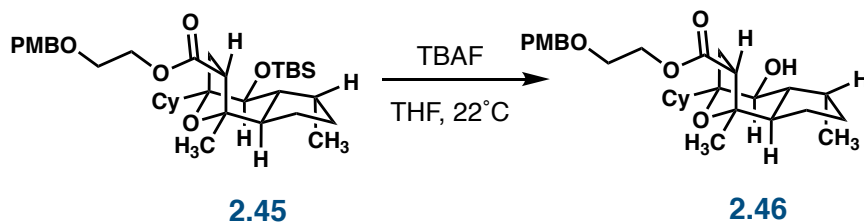
3.62 (m, 2H), 2.75 – 2.69 (m, 1H), 2.30 (td, J_1
= 13.9, J_2 = 6.0 Hz, 1H), 2.07 – 1.99 (m, 1H),
1.99 – 1.90 (m, 1H), 1.90 – 1.82 (m, 1H), 1.81
– 1.74 (m, 1H), 1.74 – 1.65 (m, 1H), 1.65 –
1.60 (m, 1H), 1.43 – 1.40 (m, 1H), 1.38 – 1.14
(m, 14H), 1.14 – 1.00 (m, 9H), 0.98 – 0.78 (m,
4H), 0.09 (s, 6H).

^{13}C NMR (151 MHz, CDCl_3) δ : 175.0, 143.5, 129.5 (2C), 126.7, 114.0 (2C),
84.8, 84.0, 72.9, 69.8, 67.8, 63.7, 55.4, 49.6,
49.1, 47.1, 38.8, 37.3, 32.9, 32.1, 31.4, 30.9,
30.2, 29.5, 27.3, 26.9, 26.2 (3C), 24.6, 22.9,
21.3, 17.2, 14.3.

FTIR (KBr, pellet), cm^{-1} : 2960, 2874, 1639, 1252, 1152.

TLC: 10% ethyl acetate–hexanes, R_f = 0.39 (CAM).

Synthesis of Alcohol 2.46



TBAF (1.0 M in THF, 0.24 mL, 0.24 mmol, 8.0 equiv) is added to a stirred solution of silyl ether **2.45** (18 mg, 0.029 mmol, 1 equiv) in THF (0.3 mL) at 22°C. The solution is stirred for 21 h, whereupon water (1 mL) is added. The resultant solution is extracted with diethyl ether (3 x 3 mL) and the combined organic extracts were washed with saturated aqueous ammonium chloride solution (4 mL). The solution was then filtered through a pad of celite and concentrated to afford the crude alcohol **2.46** as a clear, yellow oil that was used without further purification.

¹H NMR (600 MHz, CDCl₃) δ: 7.21 – 7.16 (m, 2H), 6.84 – 6.78 (m, 2H), 4.41 (s, 2H), 4.18 (dd, *J* = 5.7, 3.7 Hz, 2H), 3.74 (s, 3H), 3.65 (d, *J* = 10.2 Hz, 1H), 3.58 (dd, *J*₁ = 5.5, *J*₂ = 4.1 Hz, 2H), 3.47 (d, *J* = 5.5 Hz, 1H), 2.66 (dd, *J*₁ = 9.5, *J*₂ = 4.9 Hz, 1H), 2.46 – 2.37 (m, 2H), 2.30 – 2.24 (m, 2H), 2.20 (dd, *J*₁ = 13.5, *J*₂ = 4.9 Hz, 2H), 2.11 – 2.05 (m, 1H), 2.03 – 1.98 (m, 1H), 1.98 – 1.92 (m, 2H), 1.87 – 1.77 (m, 1H), 1.76 – 1.67 (m, 1H), 1.62 –

1.42 (m, 2H), 1.41 – 1.33 (m, 1H), 1.31 – 1.13 (m, 3H), 1.12 (s, 2H), 0.91 (t, $J = 7.3$ Hz, 1H), 0.88 – 0.76 (m, 5H).

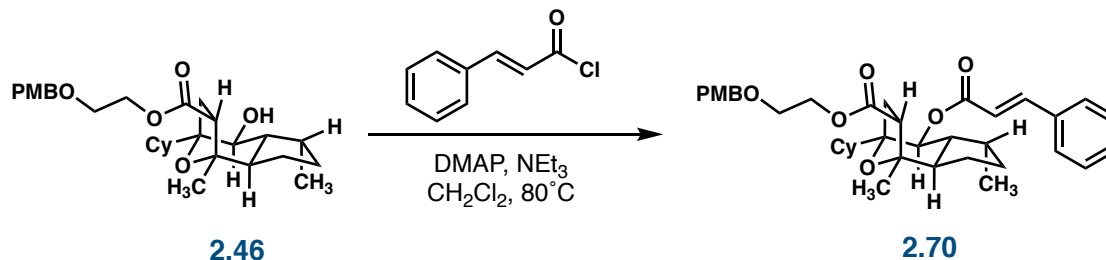
^{13}C NMR (151 MHz, CDCl_3) δ : 175.0, 159.4, 130.1, 129.5 (2C), 114.0 (2C), 86.5, 85.4, 72.9, 70.9, 67.8, 65.9, 63.8, 55.4, 50.3, 48.2, 47.2, 42.8, 40.7, 33.2, 32.0, 31.4, 31.1, 30.8, 30.6, 29.3, 28.7, 27.5, 27.4, 26.7, 25.6, 23.3, 22.8, 21.3, 17.2, 14.3.

FTIR (KBr, pellet), cm^{-1} : 3360 (br), 3182, 2924, 2853, 1729.

HRMS: ESI $[\text{M}-\text{H}]^-$ Calcd. for $\text{C}_{29}\text{H}_{42}\text{O}_6$: 485.2909.
Found: 485.2914.

TLC: 20% ethyl acetate–hexanes, $R_f = 0.16$ (CAM).

Synthesis of Cinnamate 2.70



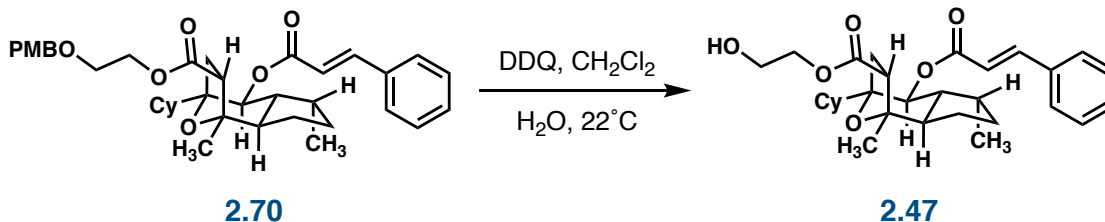
A solution of the alcohol **2.46**, cinnamoyl chloride (7.5 mg, 0.045 mmol, 3.0 equiv), DMAP (5.5 mg, 0.045 mmol, 3.0 equiv) in triethylamine (0.5 mL) and dichloromethane (1 mL) were stirred and heated to 80°C in a sealed flask for 18 h. The solution was then cooled to 22°C and concentrated. The crude residue was taken up in diethyl ether (10 mL) and filtered over celite. The crude solution was concentrated to a yellow oil and used without further purification.

HRMS: ESI $[\text{M}+\text{H}]^+$ Calcd. for $\text{C}_{38}\text{H}_{49}\text{O}_7$: 617.3478.

Found: 617.3455.

TLC: 10% ethyl acetate–hexanes, $R_f = 0.36$ (UV, CAM).

Synthesis of Reverse Ester Analogue 2.47



DDQ (36 mg, 0.15 mmol, 10 equiv) was added to a stirred solution of cinnamate **2.70** in dichloromethane (1 mL) and water (20 μ L). The resultant deep red solution was stirred for 18 h, whereupon saturated aqueous sodium bicarbonate solution (1 mL) is added. The biphasic solution was partitioned between ethyl acetate (5 mL) and water (2 mL) and the organic layer was dried over anhydrous sodium sulfate. The dried organic layer was concentrated and adhered to silica gel for purification using flash column chromatography (silica gel, starting with 15% diethyl ether–hexanes, grading to 50% diethyl ether–hexanes) to afford reverse ester analogue **2.47** (4.8 mg, 0.0097 mmol, 66% over 3 steps) as a clear, yellow oil.

^1H NMR (600 MHz, CDCl_3) δ : 7.67 (d, $J = 16.0$ Hz, 1H), 7.58 – 7.51 (m, 2H), 7.42 – 7.37 (m, 2H), 6.41 (d, $J = 16.0$ Hz, 1H), 5.15 (d, $J = 10.2$ Hz, 1H), 4.32 – 4.26 (m, 1H), 4.24 – 4.19 (m, 1H), 3.86 (t, $J = 4.7$ Hz, 2H), 2.85 (dd, $J_1 = 9.4$, $J_2 = 5.0$ Hz, 1H), 2.41 (dd, $J_1 = 13.5$, $J_2 = 5.0$ Hz, 1H), 2.22 (dd, $J_1 = 13.4$, $J_2 = 9.4$ Hz, 1H), 2.16 – 2.06 (m, 1H), 1.97 –

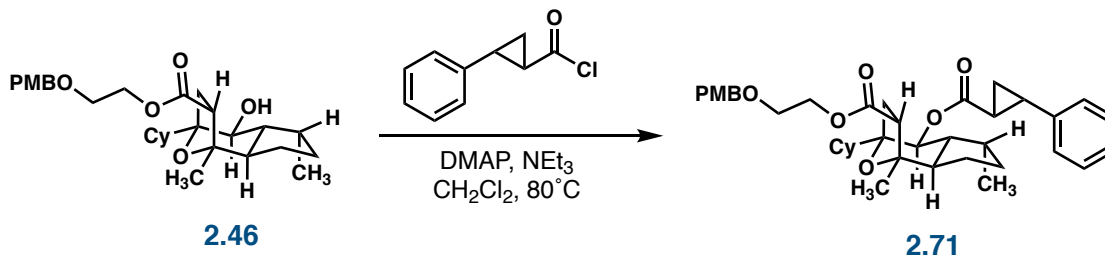
1.88 (m, 2H), 1.88 – 1.84 (m, 1H), 1.84 – 1.74 (m, 2H), 1.74 – 1.67 (m, 2H), 1.67 – 1.47 (m, 2H), 1.31 – 1.22 (m, 4H), 1.18 – 1.04 (m, 3H), 0.96 (d, $J = 7.1$ Hz, 3H), 0.91 – 0.86 (m, 3H), 0.86 – 0.80 (m, 3H).

^{13}C NMR (151 MHz, CDCl_3) δ : 175.3, 165.8, 145.2, 134.5, 130.5, 129.1 (2C), 128.3 (2C), 118.2, 86.1, 85.5, 71.7, 66.5, 61.5, 49.9, 47.4, 47.2, 43.9, 31.3, 31.1, 28.5, 27.7, 27.4, 26.9, 26.7, 24.6, 21.3, 17.2, 14.3.

HRMS: ESI $[\text{M}+\text{H}]^+$ Calcd. for $\text{C}_{30}\text{H}_{41}\text{O}_6$: 497.2903.
Found: 497.2896.

TLC: 50% ethyl acetate–hexanes, $R_f = 0.48$ (UV, CAM).

Synthesis of Diester 2.71



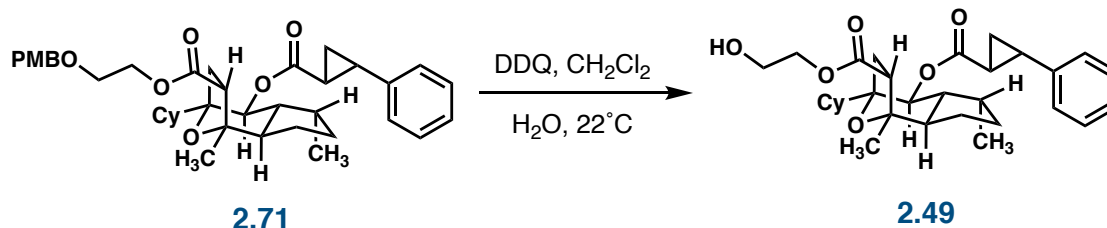
A solution of the alcohol **2.46**, the phenyl cyclopropyl acid chloride (8.1 mg, 0.045 mmol, 3.0 equiv), DMAP (6.9 mg, 0.056 mmol, 3.8 equiv) in triethylamine (0.5 mL) and dichloromethane (1 mL) were stirred and heated to 80°C in a sealed flask for 18 h. The solution was then cooled to 22°C and concentrated. The crude residue was taken up in diethyl ether (10 mL) and filtered over celite. The crude solution was concentrated to a yellow oil and used without further purification.

HRMS: ESI [M-H]⁻ Calcd. for C₃₉H₄₉O₇: 629.3478.

Found: 629.3488.

TLC: 20% ethyl acetate–hexanes, R_f = 0.64 (UV, CAM).

Synthesis of Reverse Ester Analogue 2.49



DDQ (39 mg, 0.15 mmol, 10 equiv) was added to a stirred solution of diester **2.71** in dichloromethane (1 mL) and water (20 μ L). The resultant deep red solution was stirred for 18 h, whereupon saturated aqueous sodium bicarbonate solution (1 mL) is added. The biphasic solution was partitioned between ethyl acetate (5 mL) and water (2 mL) and the organic layer was dried over anhydrous sodium sulfate. The dried organic layer was concentrated and adhered to silica gel for purification using flash column chromatography (silica gel, starting with 0% diethyl ether–dichloromethane, grading to 10% diethyl ether–dichloromethane) to afford reverse ester analogue **2.49** (3.3 mg, 0.0065 mmol, 44% over 3 steps) as a clear, yellow oil.

^1H NMR (600 MHz, CDCl_3) δ : 7.32 – 7.26 (m, 2H), 7.24 – 7.18 (m, 1H), 7.14 – 7.07 (m, 2H), 5.13 – 4.99 (m, 2H), 4.31 – 4.24 (m, 1H), 4.22 – 4.17 (m, 1H), 3.88 – 3.81 (m, 2H), 3.35 (s, 1H), 2.83 – 2.78 (m, 1H), 2.57 – 2.50 (m, 1H), 2.48 (ddd, $J_1 = 9.2$, $J_2 = 6.5$, $J_3 = 4.1$ Hz, 1H), 2.40 – 2.29 (m, 1H), 2.27 (s, 1H), 2.18 – 2.06 (m, 2H), 1.94 (m, 2H),

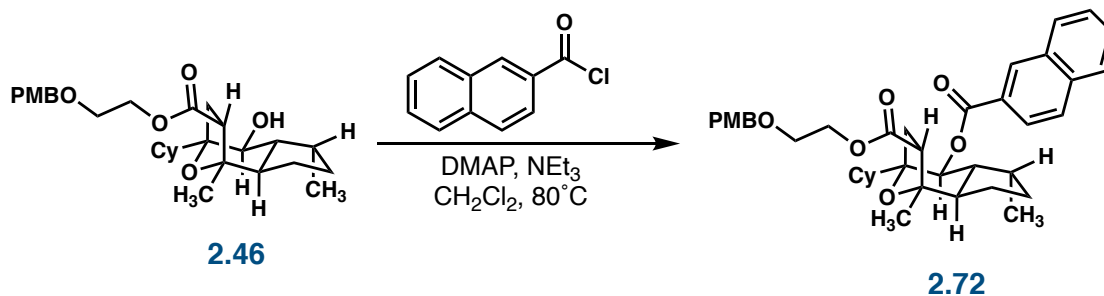
1.90 – 1.86 (m, 1H), 1.86 – 1.81 (m, 1H), 1.81 – 1.74 (m, 1 H), 1.74 – 1.67 (m, 1H), 1.67 – 1.58 (m, 2H), 1.52 – 1.45 (m, 1H), 1.43 (s, 3H), 1.31 – 1.18 (m, 4H), 1.18 – 1.08 (m, 3H), 0.93 – 0.90 (m, 3H), 0.90 – 0.86 (m, 2H), 0.86 – 0.80 (m, 2H).

¹³C NMR (151 MHz, CDCl₃) δ: 175.3, 172.2, 140.1, 128.7, 128.6, 126.7, 126.7, 126.4, 126.3, 126.3, 125.7, 86.0, 85.99, 85.5, 85.4, 72.2, 72.1, 66.5, 61.5, 49.9, 49.9, 47.2, 47.2, 47.1, 47.1, 44.3, 34.5, 31.2, 31.1, 30.5, 29.9, 29.8, 29.5, 28.5, 27.8, 27.4, 26.9, 26.83, 26.78, 24.70, 24.68, 22.8, 21.3, 17.2, 16.4, 14.3.

HRMS: ESI [M–H][–] Calcd. for C₃₁H₄₁O₆: 509.2903.
Found: 509.2909.

TLC: 20% ethyl acetate–hexanes, R_f = 0.16 (CAM).

Synthesis of Naphthoate 2.72



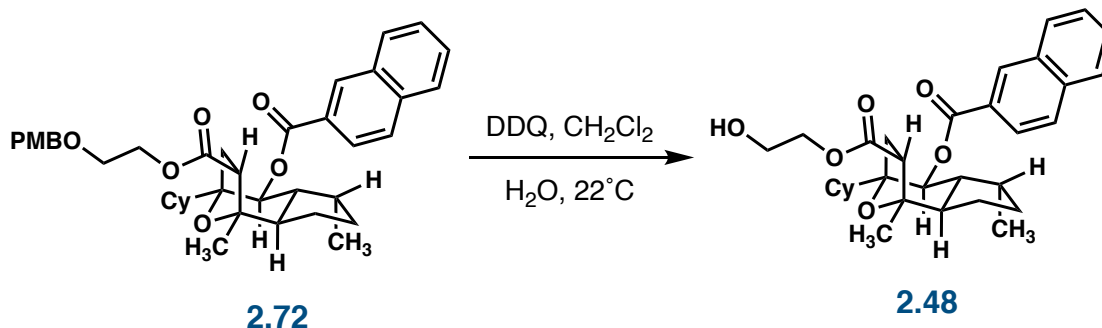
A solution of the alcohol **2.46**, 2-naphthoyl chloride (20 mg, 0.10 mmol, 3.0 equiv), DMAP (13 mg, 0.10 mmol, 3.0 equiv) in triethylamine (0.5 mL) and dichloromethane (1 mL) were stirred and heated to 80°C in a sealed flask for 18 h. The solution was then cooled to 22°C and concentrated. The crude residue was taken up in diethyl ether (10 mL) and filtered over celite. The crude solution was concentrated to a yellow oil and used without further purification.

HRMS: ESI [M+H]⁺ Calcd. for C₄₀H₄₉O₇: 641.3478.

Found: 641.3488.

TLC: 20% ethyl acetate–hexanes, R_f = 0.51 (UV, CAM).

Synthesis of Reverse Ester Analogue 2.48



DDQ (39 mg, 0.17 mmol, 5 equiv) was added to a stirred solution of diester **2.72** in dichloromethane (1 mL) and water (20 μL). The resultant deep red solution was stirred for 18 h, whereupon saturated aqueous sodium bicarbonate solution (1 mL) is added. The biphasic solution was partitioned between ethyl acetate (5 mL) and water (2 mL) and the organic layer was dried over anhydrous sodium sulfate. The dried organic layer was concentrated and adhered to silica gel for purification using flash column chromatography (silica gel, starting with 0% diethyl ether–dichloromethane, grading to 10% diethyl ether–dichloromethane) to afford reverse ester analogue **2.48** (3.1 mg, 0.0060 mmol, 18% over 3 steps) as a clear, yellow oil.

^1H NMR (600 MHz, CDCl_3) δ : 8.57 (s, 1H), 8.03 (dd, $J_1 = 8.6$, $J_2 = 1.7$ Hz, 1H), 7.96 (d, $J = 8.1$ Hz, 1H), 7.89 (d, $J = 8.7$ Hz, 2H), 7.63 – 7.53 (m, 2H), 5.35 (d, $J = 10.2$ Hz, 1H), 4.35 – 4.29 (m, 1H), 4.27 – 4.20 (m, 1H), 3.87 (t, $J = 4.8$ Hz, 2H), 3.51 – 3.45 (m, 1H), 2.93 (dd, $J_1 = 9.4$, $J_2 = 5.0$ Hz, 1H), 2.50

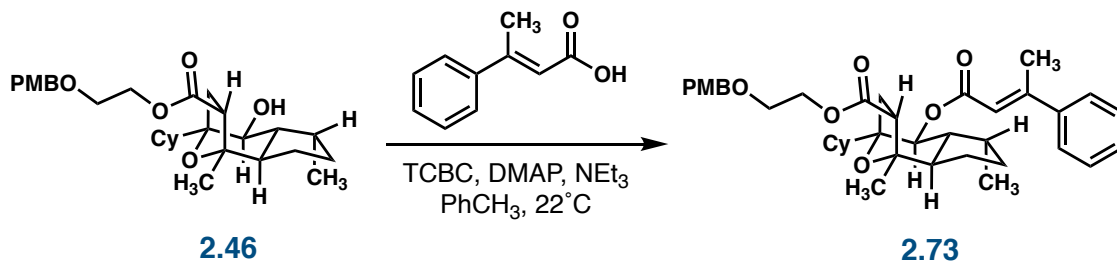
(dd, $J_1 = 13.4$, $J_2 = 5.0$ Hz, 1H), 2.40 (dd, $J_1 = 13.4$, $J_2 = 9.4$ Hz, 1H), 2.18 – 2.09 (m, 1H), 2.02 – 1.96 (m, 1H), 1.96 – 1.88 (m, 2H), 1.88 – 1.83 (m, 1H), 1.77 – 1.71 (m, 2H), 1.71 – 1.61 (m, 2H), 1.61 – 1.52 (m, 2H), 1.36 – 1.31 (m, 1H), 1.30 – 1.23 (m, 2H), 1.21 (t, $J = 7.1$ Hz, 2H), 1.17 – 1.04 (m, 2H), 1.01 (d, $J = 7.1$ Hz, 3H), 0.91 – 0.80 (m, 3H).

^{13}C NMR (151 MHz, CDCl_3) δ : 175.3, 165.4, 135.7, 132.6, 131.3, 129.5, 128.4, 127.9, 127.64, 126.9, 125.7, 125.4, 86.2, 85.6, 72.3, 66.5, 61.5, 50.0, 47.5, 47.2, 44.1, 34.8, 31.3, 31.1, 30.5, 28.6, 27.7, 27.3, 26.8, 26.6, 24.7, 21.3, 17.3.

HRMS: ESI $[\text{M}+\text{H}]^+$ Calcd. for $\text{C}_{32}\text{H}_{41}\text{O}_6$: 521.2903.
Found: 521.2891.

TLC: 50% ethyl acetate–hexanes, $R_f = 0.30$ (CAM).

Synthesis of Methyl Cinnamate 2.73



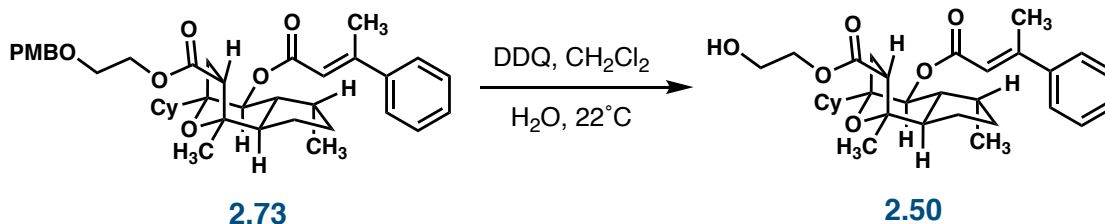
β -Methylcinnamic acid (6.6 mg, 0.041 mmol, 4.0 equiv), 2,4,6-trichlorobenzoyl chloride (12 mg, 0.050 mmol, 5.0 equiv), triethylamine (11 μ L, 0.080 mmol, 8.0 equiv), and DMAP (0.5 mg, 0.004 mmol, 0.4 equiv) were added sequentially to a stirred solution of alcohol **2.46** in toluene (0.5 mL) at 22°C. The solution was stirred at that temperature for 42 h, whereupon excess benzoyl chloride was quenched by the addition of 1N hydrochloric acid solution (0.3 mL). The resultant solution was extracted with dichloromethane (3 x 2 mL) and the combined organic extracts were washed with 0.1N sodium hydroxide solution (2 mL). The organic extracts were dried over anhydrous sodium sulfate and the dried solution was concentrated to afford the crude diester **2.73** as a greenish, yellow oil that was used without further purification.

HRMS: ESI [M+H]⁺ Calcd. for C₃₉H₅₁O₇: 631.3635.

Found: 631.3621.

TLC: 20% ethyl acetate–hexanes, R_f = 0.44 (UV, CAM).

Synthesis of Reverse Ester Analogue 2.50



DDQ (34 mg, 0.15 mmol, 15 equiv) was added to a stirred solution of diester **2.73** in dichloromethane (0.1 mL) and water (10 μ L). The resultant deep red solution was stirred for 96 h, whereupon saturated aqueous sodium bicarbonate solution (0.5 mL) is added. The biphasic solution was partitioned between ethyl acetate (5 mL) and water (2 mL) and the organic layer was dried over anhydrous sodium sulfate. The dried organic layer was concentrated and adhered to silica gel for purification using flash column chromatography (silica gel, starting with 15% diethyl ether–hexanes, grading to 50% diethyl ether–hexanes) to afford reverse ester analogue **2.50** (0.9 mg, 0.0018 mmol, 18% over 3 steps) as a clear, yellow oil.

^1H NMR (600 MHz, CDCl_3) δ : 7.49 (d, $J = 6.5$ Hz, 2H), 7.43 (d, $J = 7.6$ Hz, 1H), 7.41 – 7.35 (m, 2H), 6.09 (s, 1H), 5.12 (d, $J = 10.2$ Hz, 1H), 4.24 (ddt, $J_1 = 47.7$, $J_2 = 12.2$, $J_3 = 4.6$ Hz, 3H), 3.85 (s, 2H), 2.83 (dd, $J = 9.5$, 5.0 Hz, 1H), 2.57 (s, 3H), 2.40 – 2.27 (m, 2H), 2.21 – 2.10 (m, 2H), 2.06 – 1.83 (m, 3H), 1.83 – 1.68 (m, 3H), 1.65 – 1.47 (m, 2H),

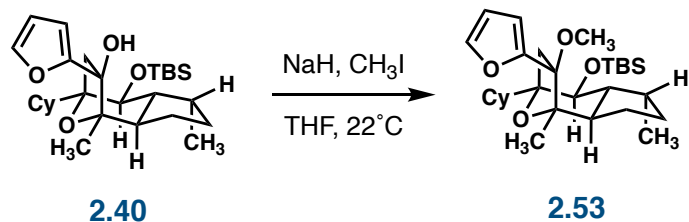
1.47 – 1.00 (m, 3H), 0.96 (d, $J = 7.0$ Hz, 3H),
0.92 – 0.80 (m, 5H), 0.78 – 0.68 (m, 1H).

^{13}C NMR (151 MHz, CDCl_3) δ : 175.3, 165.7, 156.0, 132.8, 129.2, 128.7 (2C),
126.5 (2C), 117.3, 86.2, 85.4, 71.1, 66.5, 61.5,
49.9, 47.4, 47.2, 43.9, 33.9, 32.1, 29.5, 28.5,
27.7, 27.4, 26.9, 22.9, 21.3, 18.20, 17.3, 14.3.

HRMS: ESI $[\text{M}+\text{H}]^+$ Calcd. for $\text{C}_{31}\text{H}_{43}\text{O}_6$: 511.3060.
Found: 511.3051.

TLC: 20% ethyl acetate–hexanes, $R_f = 0.13$ (CAM).

Synthesis of Methyl Ether 2.53



A solution of alcohol **2.40** (40 mg, 0.084 mmol, 1 equiv) in THF (0.4 mL) was added dropwise to a stirred suspension of sodium hydride (60% in mineral oil, 20 mg, 0.48 mmol, 5.0 equiv, pre-washed with hexanes [3 x 1 mL]) in tetrahydrofuran (0.4 mL) at 0°C. The resultant clear, yellow solution was warmed to 22°C and stirred at that temperature until the bubbling ceased (ca. 5 min). Methyl iodide (26 μ L, 0.42 mmol, 5.0 equiv) was added to the reaction mixture and the solution was stirred for 16 h. Saturated aqueous sodium bicarbonate solution (1 mL) was added to quench the excess sodium hydride and methyl iodide. The solution was extracted with dichloromethane (3 x 3 mL) and the combined organic extracts were dried over anhydrous sodium sulfate. The dried solution was concentrated, and the crude oil was adhered to silica gel for purification using flash column chromatography (silica gel, starting with 0% diethyl ether–hexanes, grading to 3% diethyl ether–hexanes) to afford methyl ether **2.53** (39.1 mg, 0.080 mmol, 95%) as a clear, yellow oil.

^1H NMR (600 MHz, CDCl_3) δ : 7.42 (dd, $J_1 = 1.9$, $J_2 = 0.8$ Hz, 1H), 6.38 – 6.31 (m, 2H), 3.85 (d, $J = 9.5$ Hz, 1H), 3.12 (s, 3H), 2.45 (d, $J = 14.4$, 1H), 2.34 – 2.26 (m, 2H), 2.10 (ddd, $J_1 = 12.8$, $J_2 = 9.4$, $J_3 = 6.5$ Hz, 1H), 1.98

(d, $J = 12.7$ Hz, 1H), 1.95 – 1.85 (m, 4H), 1.81 – 1.75 (m, 2H), 1.66 – 1.58 (m, 2H), 1.40 – 1.03 (m, 2H), 0.90 (s, 9H), 0.89 – 0.86 (m, 5H), 0.85 – 0.82 (m, 6H), 0.12 (d, $J = 7.6$ Hz, 6H).

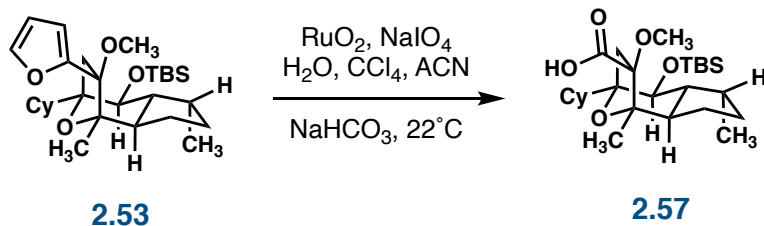
^{13}C NMR (151 MHz, CDCl_3) δ : 157.2, 142.0, 110.0, 109.8, 90.0, 85.7, 85.7, 70.2, 53.6, 50.4, 47.3, 39.3, 36.4, 31.8, 31.4, 27.4, 27.3, 27.2, 27.0, 26.5, 26.3 (3C), 24.4, 22.9, 21.9, 18.7, 17.0, 14.3, -2.8, -4.0.

FTIR (KBr, pellet), cm^{-1} : 2927, 2854, 1462, 1255, 1108.

HRMS: ESI $[\text{M}+\text{H}]^+$ Calcd. for $\text{C}_{29}\text{H}_{49}\text{O}_4\text{Si}$: 489.3400.
Found: 489.3396.

TLC: 5% ethyl acetate–hexanes, $R_f = 0.70$ (CAM).

Synthesis of Carboxylic Acid 2.57



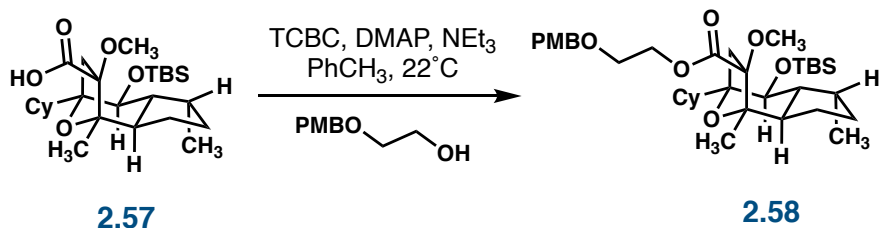
Ruthenium dioxide (12 mg, 0.088 mmol, 1.1 equiv) was added to a stirred solution of sodium periodate (100 mg, 0.48 mmol, 6.0 equiv) in carbon tetrachloride (1.4 mL), acetonitrile (2.1 mL), and water (1.4 mL) at 22°C. The resultant cloudy, black solution was stirred vigorously for 20 min, whereupon sodium bicarbonate (670 mg, 8.0 mmol, 100 equiv) and water (1.2 mL) were added. The resultant solution was stirred for 5 min, whereupon a solution of furan **2.53** (39 mg, 0.080 mmol, 1 equiv) in acetonitrile (1.2 mL) and ethyl acetate (0.3 mL) was added. The solution is stirred for 75 min, whereupon sodium periodate is added until the solution becomes a dark green suspension. The suspension is diluted with water and the resultant mixture was extracted with ethyl acetate (3 x 20 mL) and the combined organic layers were dried over anhydrous sodium sulfate. The dried solution was filtered through Celite® and concentrated to afford a sticky black oil that was used in the following step without further purification.

HRMS: ESI [M-H]⁻ Calcd. for C₂₆H₄₅O₅Si: 465.3036.

Found: 465.3036.

TLC: 20% ethyl acetate–hexanes, R_f = 0.25 (CAM).

Synthesis of Reverse Ester 2.58



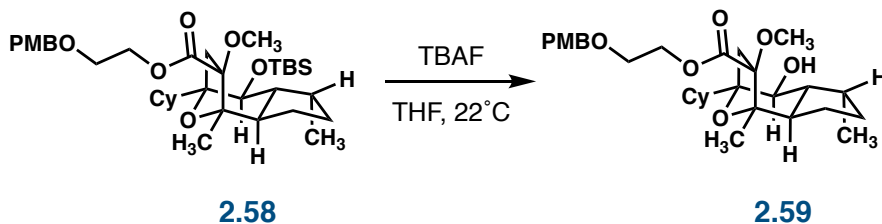
PMB-protected ethylene glycol (30 mg, 0.16 mmol, 2.0 equiv), 2,4,6-trichlorobenzoyl chloride (50 μ L, 0.32 mmol, 4.0 equiv), triethylamine (67 μ L, 0.48 mmol, 6.0 equiv), and DMAP (2.4 mg, 0.020 mmol, 0.25 equiv) were added sequentially to a stirred solution of acid **2.57** in toluene (4 mL) at 22°C. The solution was stirred at that temperature for 40 h, whereupon excess benzoyl chloride was quenched by the addition of saturated aqueous ammonium chloride solution (1 mL). The resultant solution was extracted with dichloromethane (3 x 2 mL) and the combined organic extracts were dried over anhydrous sodium sulfate. The dried solution was concentrated and filtered through a plug of basic alumina, starting with 3% ethyl acetate–hexanes, grading to 25% ethyl acetate–hexanes to afford a crude yellow oil containing ester **2.58** that was used without further purification.

HRMS: ESI [M+H]⁺ Calcd. for C₃₆H₅₉O₇Si: 631.4030.

Found: 631.4027.

TLC: 20% ethyl acetate–hexanes, R_f = 0.59 (CAM).

Synthesis of Alcohol 2.59



TBAF (1.0 M in THF, 0.64 mL, 0.64 mmol, 8.0 equiv) is added to a stirred solution of silyl ether **2.58** in THF (0.8 mL) at 22°C. The solution is stirred for 2 h, whereupon water (1 mL) is added. The resultant solution is extracted with diethyl ether (3 x 3 mL) and the combined organic extracts were washed with saturated aqueous ammonium chloride solution (4 mL). The solution was then filtered through a pad of celite and concentrated to afford the crude alcohol **2.59** as a clear, yellow oil that was purified using flash column chromatography (deactivated silica gel, starting with 5% ethyl acetate–hexanes, grading to 30% ethyl acetate–hexanes). Alcohol **2.59** (4.4 mg, 0.0085 mmol, 11% over 3 steps) was isolated as a clear, yellow oil.

^1H NMR (600 MHz, CDCl_3) δ : 7.19 – 7.14 (m, 2H), 6.81 – 6.78 (m, 2H), 5.23 (s, 2H), 4.47 – 4.43 (m, 1H), 4.43 (s, 1H), 4.41 (s, 2H), 4.40 – 4.30 (m, 2H), 3.91 – 3.86 (m, 1H), 3.75 – 3.72 (m, 3H), 3.68 (t, $J = 4.5$ Hz, 1H), 3.63 (t, $J = 4.8$ Hz, 2H), 3.51 (t, $J = 4.5$ Hz, 1H), 3.24 (s, 3H), 3.08 – 3.00 (m, 1H), 2.35 – 2.22 (m, 3H), 2.10 – 2.05 (m, 1H), 2.04

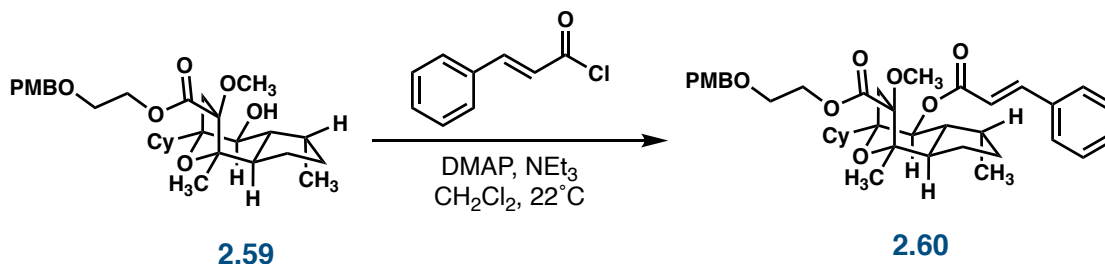
– 1.96 (m, 2H), 1.91 – 1.69 (m, 2H), 1.67 –
1.38 (m, 4H), 1.36 – 1.31 (m, 3H), 1.29 – 0.96
(m, 4H), 0.92 – 0.64 (m, 2H).

¹³C NMR (151 MHz, CDCl₃) δ: 165.2, 129.9, 129.5, 114.0, 97.0, 86.1, 85.7,
73.1, 73.0, 71.2, 70.9, 68.0, 67.3, 64.9, 62.1,
61.0, 56.3, 55.4, 52.4, 46.8, 46.0, 43.9, 37.3,
35.0, 32.1, 31.9, 30.8, 30.2, 29.5, 28.8, 27.5,
27.4, 27.2, 27.0, 26.9, 26.7, 25.4, 22.8, 21.6,
17.0, 14.3.

HRMS: ESI [M+H]⁺ Calcd. for C₃₀H₄₅O₇: 517.3165.
Found: 517.3168.

TLC: 20% ethyl acetate–hexanes, R_f = 0.18 (CAM).

Synthesis of Diester 2.60



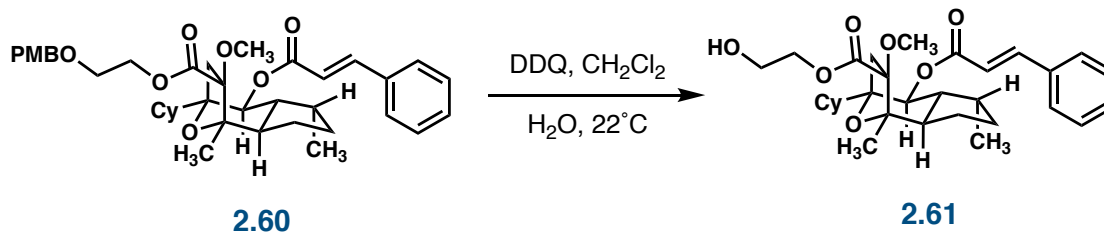
A solution of the alcohol **2.59** (4.4 mg, 0.0085 mmol, 1 equiv), cinnamoyl chloride (5.5 mg, 0.033 mmol, 3.9 equiv), DMAP (3.9 mg, 0.032 mmol, 3.8 equiv) in triethylamine (0.4 mL) and dichloromethane (0.8 mL) were stirred and heated to 80°C in a sealed flask for 18 h. The solution was then cooled to 22°C and concentrated. The crude residue was taken up in diethyl ether (10 mL) and filtered over celite. The crude solution was concentrated to a yellow oil and used without further purification.

^1H NMR (600 MHz, CDCl_3) δ : 8.02 – 7.99 (d, $J = 8.7$ Hz, 1H), 7.70 (d, $J = 16.1$ Hz, 2H), 7.58 – 7.50 (m, 3H), 7.43 – 7.33 (m, 5H), 7.31 – 7.26 (m, 2H), 6.94 – 6.90 (m, 4H), 6.90 – 6.85 (m, 4H), 6.48 (d, $J = 16.0$ Hz, 3H), 4.53 (s, 2H), 4.49 (s, 1H), 4.47 – 4.42 (m, 1H), 4.38 (t, $J = 4.8$ Hz, 2H), 3.87 – 3.85 (m, 1H), 3.81 – 3.79 (m, 4H), 3.72 (t, $J = 4.8$ Hz, 2H), 3.37 (s, 1H), 2.00 – 1.01 (m, 6H), 0.98 – 0.93 (m, 3H).

^{13}C NMR (151 MHz, CDCl_3) δ : 167.1, 159.5, 145.2, 130.5, 130.1, 129.6 (2C),
129.5, 129.1 (2C), 128.3, 128.3 (2C), 118.1,
114.0 (2C), 73.0, 67.8, 66.0, 63.9, 55.4, 53.6,
51.9, 37.3, 32.92, 32.1, 31.7, 30.2, 29.5, 28.1,
27.2, 22.9, 19.9, 15.4, 14.3, 11.6.

TLC: 20% ethyl acetate–hexanes, R_f = 0.40 (CAM).

Synthesis of Methyl Ether Analogue 2.61



DDQ (13 mg, 0.055 mmol, 6.5 equiv) was added to a stirred solution of diester **2.60** in dichloromethane (0.1 mL) and water (10 μ L). The resultant deep red solution was stirred for 25 h, whereupon saturated aqueous sodium bicarbonate solution (0.5 mL) is added. The biphasic solution was partitioned between ethyl acetate (5 mL) and water (2 mL) and the organic layer was dried over anhydrous sodium sulfate. The dried organic layer was concentrated and adhered to silica gel for purification using flash column chromatography (silica gel, starting with 20% diethyl ether–hexanes, grading to 50% diethyl ether–hexanes) to afford methyl ether analogue **2.61** (1.0 mg, 0.0019 mmol, 21% over 2 steps) as a clear, yellow oil.

^1H NMR (600 MHz, CDCl_3) δ : 7.70 (d, $J = 17.1$ Hz, 1H), 7.58 – 7.51 (m, 2H), 7.42 – 7.36 (m, 3H), 6.44 (d, $J = 16.0$ Hz, 1H), 5.22 (d, $J = 9.9$ Hz, 1H), 4.43 (tdd, $J_1 = 16.3$, $J_2 = 11.3$, $J_3 = 4.5$ Hz, 2H), 3.91 (t, $J = 5.0$, 2H), 3.42 (s, 3H), 2.56 (d, $J = 5.9$ Hz, 2H), 2.16 – 2.03 (m, 3H), 1.94 (d, $J = 13.2$ Hz, 1H), 1.90 – 1.85 (m, 2H), 1.83 – 1.74 (m, 1H), 1.74 – 1.62

(m, 2H), 1.38 (s, 3H), 1.31 – 1.18 (m, 6H),
1.03 – 1.16 (m, 2H), 0.95 (d, $J = 6.9$ Hz, 3H),
0.92 – 0.83 (m, 2H).

^{13}C NMR (151 MHz, CDCl_3) δ : 173.3, 165.1, 145.4, 133.7, 130.6, 129.1 (2C),
128.3 (2C), 118.2, 86.1, 85.4, 71.7, 67.4, 60.7,
56.4, 51.9, 46.3, 45.1, 36.2, 31.6, 31.4, 29.85,
28.7, 27.6, 27.4, 26.8, 26.6, 23.9, 21.5, 16.7.

HRMS: ESI $[\text{M}+\text{H}]^+$ Calcd. for $\text{C}_{31}\text{H}_{43}\text{O}_7$: 527.3009.
Found: 527.3009.

TLC: 50% ethyl acetate–hexanes, $R_f = 0.55$ (CAM).

REFERENCES

1. (a) Wender, P. A.; Quiroz, R. V.; Stevens, M. C. *Acc. Chem. Res.* **2015**, *48*, 752-760. (b) Wender, P. A.; Verma, V. A.; Paxton, T. J.; Pillow, T. H. *Acc. Chem. Res.* **2008**, *41*, 40-49. (c) Wender, P. A. *Nat. Prod. Rep.* **2014**, *31*, 433-440. (d) Lipinski, C. A.; Lombardo, F.; Dominy, B. W.; Feeney, P. J. *Advanced Drug Delivery Reviews* **1997**, *23*, 3-25. (e) Ghose, A. K.; Viswanadhan, V. N.; Wendoloski, J. J. *J. Comb. Chem.* **1999**, *1*, 55-68.
2. Wu, Z.; Suppo, J.-S.; Tumova, S.; Strope, J.; Bravo, F.; Moy, M.; Weinstein, E. S.; Peer, C. J.; Figg, W. D.; Chain, W. J.; et al. *ACS Medicinal Chemistry Letters* **2020**, *11*, 1711-1716.
3. Chan, K. P.; Chen, D. Y. K. *ChemMedChem* **2011**, *6*, 420-423.
4. Li, Z.; Nakashige, M.; Chain, W. J. *J. Am. Chem. Soc.* **2011**, *133*, 6553-6556.
5. (a) Khademi, Z.; Heravi, M. M. *Tetrahedron* **2022**, *103*. (b) Claisen, R. L.; Lowman, O. *Ber.* **1887**, *20*, 651-654.
6. (a) Arterburn, J. B. *Tetrahedron* **2001**, *57*, 9765-9788. (b) Sharma, A. K.; Swern, D. *Tetrahedron Lett.* **1974**, *15*, 1503-1506.
7. (a) Schreiber, J.; Maag, H.; Hashimoto, N.; Eschenmoser, A. *Angewandte Chemie International Edition in English* **1971**, *10*, 330-331. (b) Antón-Cánovas, T.; Alonso, F. *Angew. Chem. Int. Ed.* **2023**, *62*.
8. (a) Chatterjee, A. K.; Choi, T. L.; Sanders, D. P.; Grubbs, R. H. *J. Am. Chem. Soc.* **2003**, *125*, 11360-11370. (b) Grubbs, R. H. *Angew. Chem. Int. Ed.* **2006**, *45*, 3760-3765. (c) Ogba, O. M.; Warner, N. C.; O'Leary, D. J.; Grubbs, R. H. *Chem. Soc. Rev.* **2018**, *47*, 4510-4544. (d) Nguyen, S. T.; Grubbs, R. H.; Ziller, J. W. *J. Am. Chem. Soc.* **2002**, *115*, 9858-9859. (e) Schwab, P.; Grubbs, R. H.; Ziller, J. W. *J. Am. Chem. Soc.* **1996**, *118*, 100-110. (f) Trogler, W. C.; Stewart, R. C.; Marzilli, L. G. *J. Am. Chem. Soc.* **2002**, *96*, 3697-3699.
9. (a) Michael, A. *J. Prakt. Chem.* **1883**, *35*, 349. (b) Hagiwara, H. *Natural Product Communications* **2021**, *16*.

10. (a) Szostak, M.; Fazakerley, N. J.; Parmar, D.; Procter, D. J. *Chem Rev* **2014**, *114*, 5959-6039. (b) Fittig, R. W.; Demselben. *Justus Liebigs Annalen der Chemie* **1859**, *110*, 23-45.
11. (a) Yoshida, J.-i.; Murata, T.; Isoe, S. *Tetrahedron Lett.* **1986**, *27*, 3373-3376. (b) Yoshida, J.-i.; Watanabe, M.; Toshioka, H.; Imagawa, M.; Suga, S. *J. Electroanal. Chem.* **2001**, *507*, 55-65.
12. Lee, K.-S.; Hoveyda, A. H. *J. Am. Chem. Soc.* **2010**, *132*, 2898-2900.
13. (a) Milligan, J. A.; Phelan, J. P.; Badir, S. O.; Molander, G. A. *Angew. Chem. Int. Ed.* **2019**, *58*, 6152-6163. (b) Milligan, J. A.; Burns, K. L.; Le, A. V.; Polites, V. C.; Wang, Z. J.; Molander, G. A.; Kelly, C. B. *Adv Synth Catal* **2020**, *362*, 242-247. (c) Campbell, M. W.; Yuan, M.; Polites, V. C.; Gutierrez, O.; Molander, G. A. *J. Am. Chem. Soc.* **2021**, *143*, 3901-3910.
14. Fox, D. P.; Little, R. D.; Baizer, M. M. *The Journal of Organic Chemistry* **1985**, *50*, 2202-2204.
15. (a) Knowles, R.; Yayla, H. *Synlett* **2014**, *25*, 2819-2826. (b) Tarantino, K. T.; Liu, P.; Knowles, R. R. *J. Am. Chem. Soc.* **2013**, *135*, 10022-10025.
16. (a) Marc J. Chapdelaine, M. H. *Organic Reactions - Chapter 2*, 225-653. (b) Stetter, H. *Angewandte Chemie International Edition in English* **1976**, *15*, 639-647. (c) Tomioka, K.; Sudani, M.; Shinmi, Y.; Koga, K. *Chem. Lett.* **1985**, *14*, 329-332. (d) Sikorski, W. H.; Reich, H. J. *J. Am. Chem. Soc.* **2001**, *123*, 6527-6535.
17. (a) Majhi, S. *ChemistrySelect* **2021**, *6*, 4178-4206. (b) Inanaga, J.; Hirata, K.; Saeki, H.; Katsuki, T.; Yamaguchi, M. *Bull. Chem. Soc. Jpn.* **1979**, *52*, 1989-1993.
18. Hasegawa, T.; Kawanaka, Y.; Kasamatsu, E.; Ohta, C.; Nakabayashi, K.; Okamoto, M.; Hamano, M.; Takahashi, K.; Ohuchida, S.; Hamada, Y. *Organic Process Research & Development* **2005**, *9*, 774-781.
19. (a) Tsunoda, T.; Nagino, C.; Oguri, M.; Itô, S. *Tetrahedron Lett.* **1996**, *37*, 2459-2462. (b) Tsunoda, T.; Uemoto, K.; Nagino, C.; Kawamura, M.; Kaku, H.; Itô, S. *Tetrahedron Lett.* **1999**, *40*, 7355-7358.
20. (a) van Leusen, A. M.; Oomkes, P. G. *Synth. Commun.* **2006**, *10*, 399-403. (b) van Leusen, A. M. *Encyclopedia of Reagents for Organic Synthesis* **2001**. (c) van Leusen, A. M. *Organic Reactions - Chapter 3* **2004**. (d) Oldenziel, O. H.;

- Van Leusen, D.; Van Leusen, A. M. *The Journal of Organic Chemistry* **2002**, *42*, 3114-3118.
21. (a) Burke, S. D.; Murtiashaw, C. W.; Saunders, J. O.; Oplinger, J. A.; Dike, M. S. *J. Am. Chem. Soc.* **1984**, *106*, 4558-4566. (b) Corey, E. J.; Tius, M. A. *Tetrahedron Lett.* **1980**, *21*, 3535-3538. (c) Earnshaw, C.; Wallis, C. J.; Warren, S. *J. Chem. Soc., Perkin Trans. 1* **1979**, 3099-3106. (d) Gilbert, J. C.; Weerasooriya, U. *Tetrahedron Lett.* **1980**, *21*, 2041-2044. (e) Kende, A. S.; Blacklock, T. J. *Tetrahedron Lett.* **1980**, *21*, 3119-3122. (f) Li, W.-D. Z.; Gao, Z.-H. *Org. Lett.* **2005**, *7*, 2917-2920. (g) Li, Y.; Das, S.; Zhou, S.; Junge, K.; Beller, M. *J. Am. Chem. Soc.* **2012**, *134*, 9727-9732. (h) Magnus, P.; Roy, G. *J. Chem. Soc., Chem. Commun.* **1979**, 822. (i) Magnus, P.; Roy, G. *Organometallics* **1982**, *1*, 553-559. (j) Moskal, J.; Van Leusen, A. M. *Recl. Trav. Chim. Pays-Bas* **1987**, *106*, 137-141. (k) Speier, J. L. *J. Am. Chem. Soc.* **1948**, *70*, 4142-4143. (l) Surprenant, S.; Chan, W. Y.; Berthelette, C. *Org. Lett.* **2003**, *5*, 4851-4854. (m) Trost, B. M.; Caldwell, C. G.; Murayama, E.; Heissler, D. *The Journal of Organic Chemistry* **1983**, *48*, 3252-3265. (n) Tius, M. A. *Encyclopedia of Reagents for Organic Synthesis* **2001**.
22. (a) Wittig, G.; Fritze, P. *Angewandte Chemie International Edition in English* **2003**, *5*, 846-846. (b) Heravi, M. M.; Zadsirjan, V.; Hamidi, H.; Daraie, M.; Momeni, T. Recent applications of the Wittig reaction in alkaloid synthesis. Elsevier, 2020; pp 201-334. (c) Schlosser, M.; Christmann, K. F. *Angewandte Chemie International Edition in English* **2003**, *5*, 126-126.
23. (a) Bonnet, B.; Plé, G.; Duhamel, L. *Synlett* **1996**, *1996*, 221-224. (b) Ohira, S. *Synth. Commun.* **1989**, *19*, 561-564. (c) Brown, D. G.; Velthuisen, E. J.; Commerford, J. R.; Brisbois, R. G.; Thomas, R. H. *The Journal of Organic Chemistry* **1996**, *61*, 2540-2541.
24. Ohira, S. *Synth. Commun.* **1989**, *19*, 561-564.
25. (a) Alvaro, G.; Martelli, G.; Savoia, D.; Zoffoli, A. *Synthesis* **1998**, *1998*, 1773-1777. (b) Arai, Y.; Hayashi, Y.; Yamamoto, M.; Takayama, H.; Koizumi, T. *Chem. Lett.* **1987**, *16*, 185-186. (c) Bandyopadhyay, I.; Lee, H. M.; Tarakeshwar, P.; Cui, C.; Oh, K. S.; Chin, J.; Kim, K. S. *The Journal of Organic Chemistry* **2003**, *68*, 6571-6575. (d) Carlsen, P. H. J.; Katsuki, T.; Martin, V. S.; Sharpless, K. B. *The Journal of Organic Chemistry* **1981**, *46*, 3936-3938. (e) Danishefsky, S. J.; Deninno, M. P.; Chen, S. H. *J. Am. Chem. Soc.* **1988**, *110*, 3929-3940. (f) Danishefsky, S. J.; Pearson, W. H.; Segmuller, B. E. *J. Am. Chem. Soc.* **1985**, *107*, 1280-1285. (g) Demir, A. S.; Sesenoglu, Ö.; Ülkü, D.; Arıcı, C. *Helv. Chim. Acta* **2003**, *86*, 91-105. (h) Dubois, M. A. J.; Smith, M. A.; White, A. J. P.; Lee Wei Jie, A.; Mousseau, J. J.; Choi, C.; Bull, J. A. *Org. Lett.* **2020**, *22*, 5279-5283. (i) Gingerich, S. B.; Jennings, P. W.

- The Journal of Organic Chemistry* **1984**, *49*, 1284-1286. (j) Harada, T.; Adachi, S.; Tanaka, F.; Watanabe, K.; Watada, A. *Synthesis* **2010**, *2010*, 2652-2669. (k) Ishii, K.; Noji, M.; Sunahara, H.; Tsuchiya, K.-I.; Mukai, T.; Komasa, A. *Synthesis* **2008**, *2008*, 3835-3845. (l) Jiang, X.; Zhang, Y.; Chan, A. S. C.; Wang, R. *Org. Lett.* **2009**, *11*, 153-156. (m) Li-Xin Liao, W.-S. Z. **1996**, *37*, 6371-6374. (n) Lipshutz, B. H. *Chem. Rev.* **1986**, *86*, 795-819. (o) Marshall, J. A.; Luke, G. P. *The Journal of Organic Chemistry* **1993**, *58*, 6229-6234. (p) Meng, Z.; Fürstner, A. *J. Am. Chem. Soc.* **2022**, *144*, 1528-1533. (q) Nikolay E. Shevchenko, V. G. N., Gerd-Volker Roßschenthaler. *J. Fluorine Chem.* **2008**, *129*, 390-396. (r) Pearlman, B. A.; Padilla, A. G.; Hach, J. T.; Havens, J. L.; Pillai, M. D. *Org. Lett.* **2006**, *8*, 2111-2113. (s) Pedro Merino, S. F., Francisco Merchan, Tomás Tejero. *Recent Research Development in Synthetic Organic Chemistry* **2000**, *3*. (t) Piancatelli, G.; D'Auria, M.; D'Onofrio, F. *Synthesis* **1994**, *1994*, 867-889. (u) Plietker, B. *Synthesis* **2005**, *2005*, 2453-2472. (v) Schmid, G.; Fukuyama, T.; Akasaka, K.; Kishi, Y. *J. Am. Chem. Soc.* **1979**, *101*, 259-260. (w) Wei-Shan Zhou, Z.-R. L. a. Z.-W. W. *Tetrahedron: Asymmetry* **1993**, *49*, 2641-2654. (x) Yu, X.-Q.; Shirai, T.; Yamamoto, Y.; Miyaura, N. *Chemistry - An Asian Journal* **2011**, *6*, 932-937. (y) Yung-Son Hon, S.-W. L., Ling Lu, Yao-Jung Chen. *Tetrahedron* **1995**, *51*, 5019-5034.
26. (a) Neises, B.; Steglich, W. *Angewandte Chemie International Edition in English* **1978**, *17*, 522-524. (b) Jordan, A.; Whymark, K. D.; Sydenham, J.; Sneddon, H. F. *Green Chemistry* **2021**, *23*, 6405-6413.
27. Nwoye, E. O.; Dudley, G. B. *Chem. Commun.* **2007**, 1436.

Chapter 3

EFFORTS TOWARD THE SYNTHESIS OF NOVEL TOOL COMPOUNDS FEATURING A C7-CYCLOHEXYL GROUP, MODIFIED C10- APPENDAGES, AND SUBSTITUTED C6-CINNAMATE MOIETIES

3.1 Targeted Series of Tool Compounds

The development of proteomic tool compounds to aid in the elucidation of an unambiguous mechanism of action of EA against cancer cells is extremely important in the development of EA as a cancer therapeutic.¹ Although there have been tool compounds developed in the past², the mechanism of action is still ambiguous and an open question. There is still a need for further development of tool compounds to probe this biological mechanism.¹

The previous tool compounds that have been explored featured modifications at C6, C7, and C9 where the cinnamate, isopropyl, and glycolate reside in the natural product, respectively.² The probes that we are currently targeting will feature modifications at C6 and C10 in the form of covalent modifiers (figure 3.1). Because the analogue with the C7-cyclohexyl is not a TRPC4/5 agonist, new compounds will feature the C7-cyclohexyl to probe the underlying mechanism. These tool compounds will also feature the reverse ester appendage at C9 as this modification appears to be more likely to appear in a drug candidate than the glycolate. At C10 we will include a long alkyl chain with a terminal alcohol as an attachment point for the covalent linkers, such as radical generating diarylketones or carbene generators such as

diazirines. At C6 we will use coumaric acid instead of cinnamic acid to leave another attachment point for more functional handles.

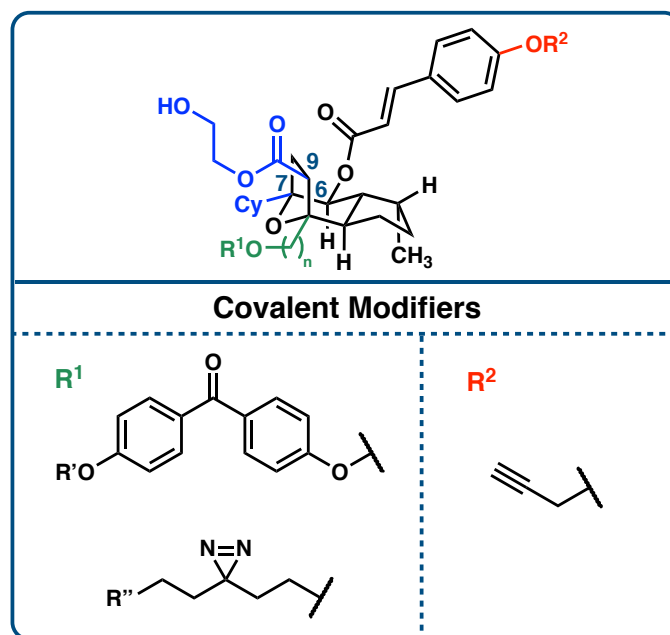


Figure 3.1 Next-generation proteomic tool compounds incorporating covalent modifiers

We imagine the tool compound being covalently bound to the target protein within the binding pocket using the covalent modifiers at C10 initiated by an external stimulus. When bound to the cellular target, we can use the functional handle on the coumarate group at C6 as means of isolating the protein. For example, if an alkyne were the functional handle at C6, one could use click chemistry to selectively couple to the tool compound using activated beads or a modified resin allowing for isolation of the protein.¹ The alcohol chain at C10 would be incorporated into the furanone from the beginning of the synthesis and carried through.

Figure 3.2 Synthesis of the Furanone

We will utilize the same strategy used in the synthesis of the analogues where the compound can be broken into a furanone intermediate **3.2** and an aldehyde intermediate **3.3** as shown in figure 3.2. The synthesis of these tool compounds would begin with the synthesis of the furanone **3.2**. As mentioned previously, the length of the alkyl chain at C9 is important in that it may have a negative effect on the solubility of the compound within a biological system if too long. For this reason, we will start with a 3-carbon linker to the attachment point. This means that the furanone will feature this alkyl chain, which can be followed back to the synthesis of the α -chloroester **3.4**.

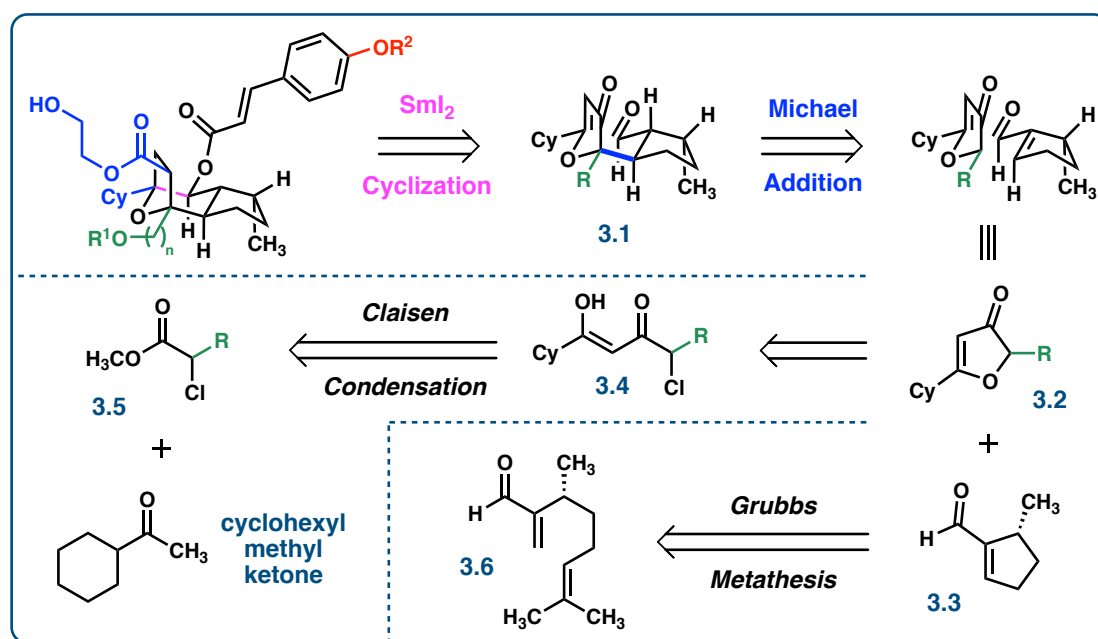


Figure 3.2 Retrosynthetic analysis of the proteomic tool compounds

There were two simple ways we could go about the synthesis of the α -chloroester **3.5**, both of which are shown in figure 3.3. The first option, and the one we tried first, was through a lactone ring opening of δ -valerolactone **3.7** to ester **3.8**. Protection of the resultant alcohol followed by an α -chlorination would yield α -chloroester **3.5**. When attempting this route, we found that the free alcohol was sensitive and would spontaneously lactonize back to lactone **3.7** during the process of attempting to protect the alcohol under both acidic and basic conditions (figure 3.4).

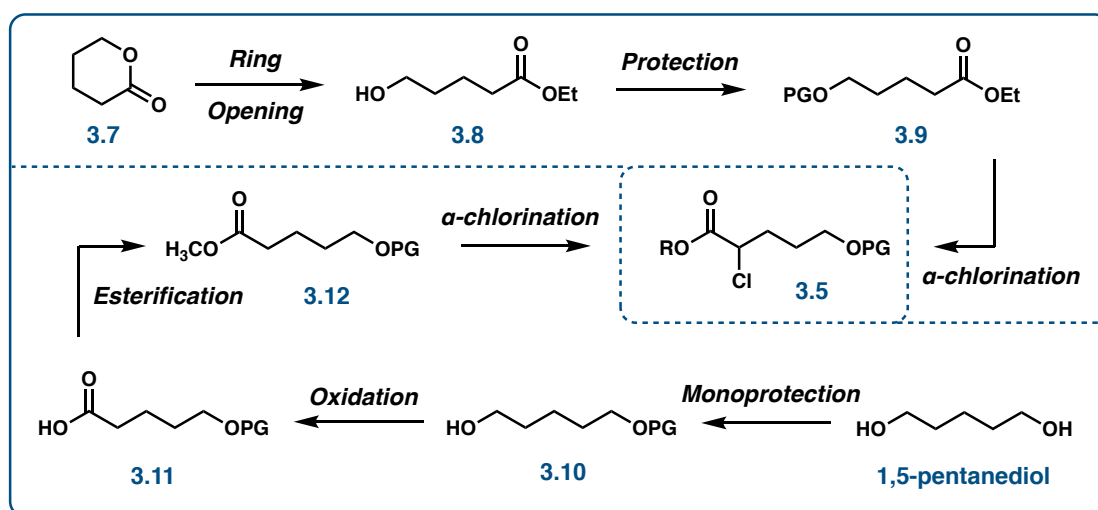


Figure 3.3 Synthetic routes to achieve α -chloroester **3.5**

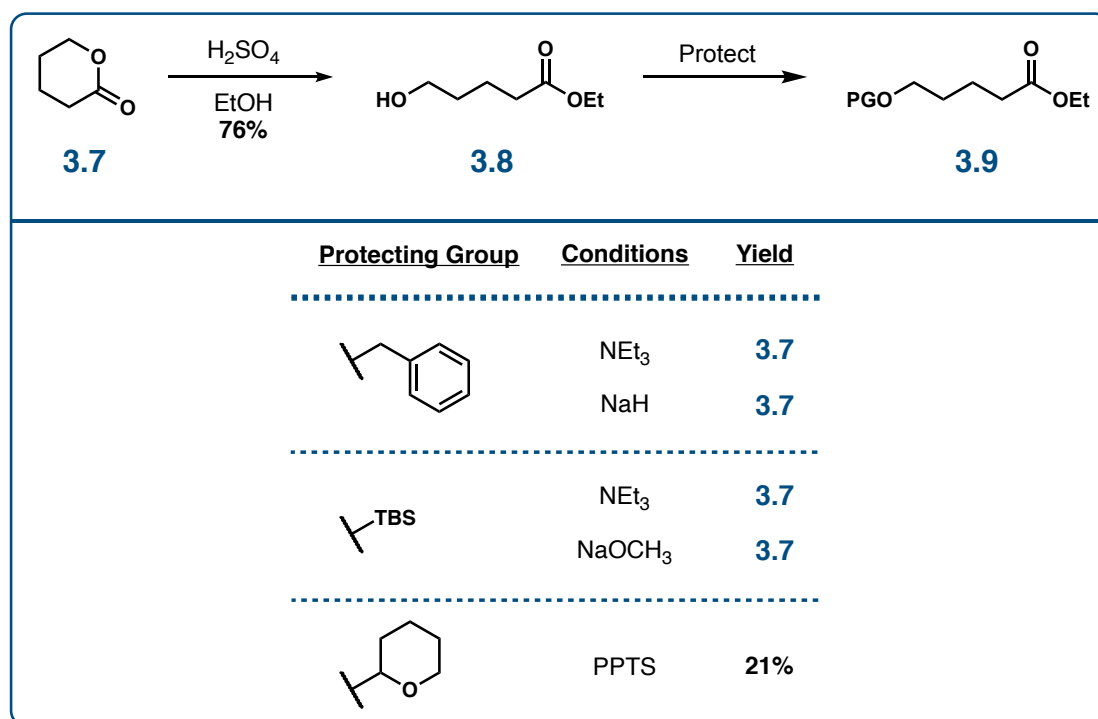


Figure 3.4 Attempts at affording ester **3.9**

We then decided to move to the second option of reaching α -chloroester **3.5**, which was by starting with 1,5-pentanediol. Starting with the diol, a monoprotection followed by an oxidation of the remaining alcohol affords the acid. From here the acid can be esterified and an α -chlorination would afford the α -chloroester **3.5** (figure 3.3). Upon execution, we performed a monoprotection of the diol using PMBOH and Amberlyst-15 resin to obtain the PMB protected alcohol **3.13** in a 69% yield (figure 3.5). Upon treatment of the alcohol **3.13** under Zhao's modified Anelli oxidation conditions³ to bring the alcohol to the acid, we were only able to obtain the product in a 20% yield with 50% of my material going towards the benzylic oxidation product **3.15**.

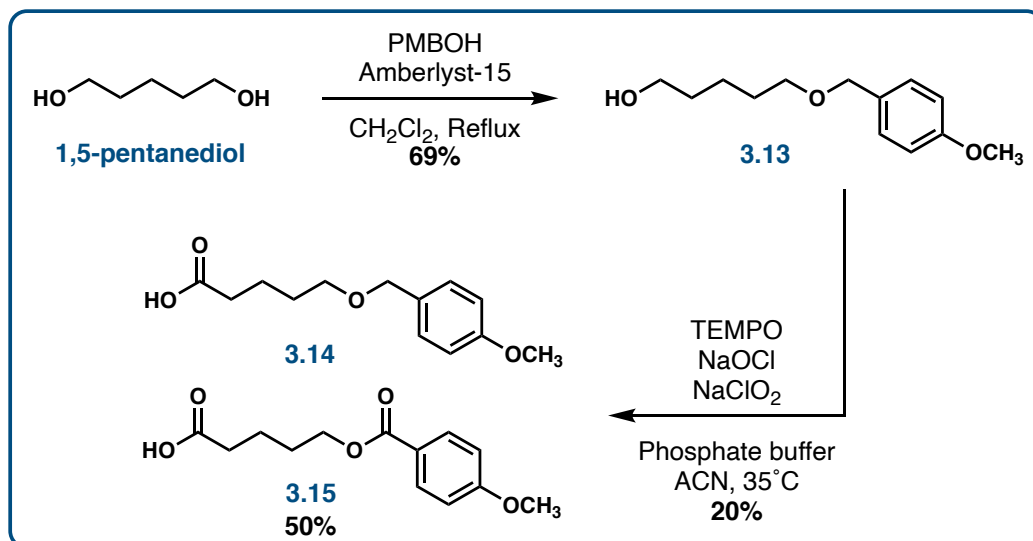


Figure 3.5 Synthesis of acid **3.14** and the undesired ester byproduct **3.15**

To avoid this undesired oxidation, we moved to protection using a TBS group and could accomplish this protection at a 75% yield (figure 3.6). When treated under the oxidation conditions, we could afford the acid **3.17** in 93% using an acid/base extraction to purify the acid which was used without further purification. The acid was then brought to the methyl ester **3.18** using dimethyl sulfate. A chlorination alpha to the ester was achieved through a trapping of the enolate as the silyl enol ether, then nucleophilic attack on the electrophilic chlorine source, NCS. This was achieved at 67% to afford α -chloroester **3.19**.

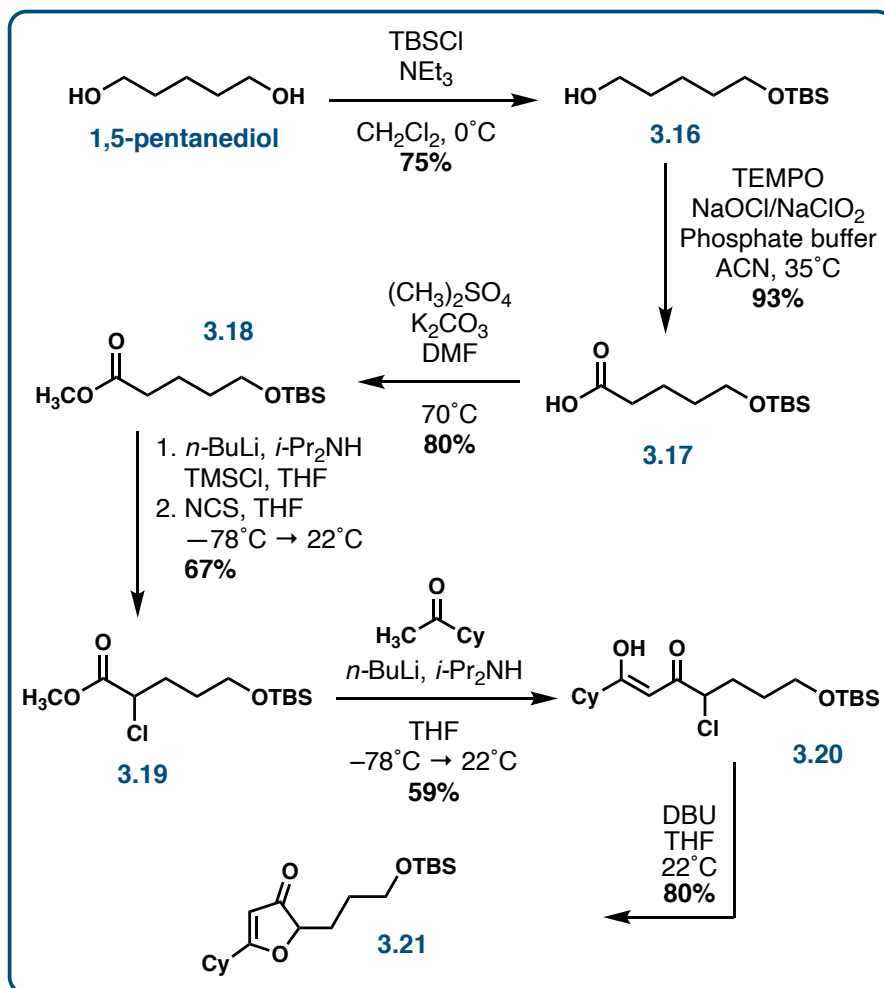


Figure 3.6 Synthesis of furanone **3.21** from 1,5-pentanediol

Subjecting this to the Claisen⁴ condensation with cyclohexyl methyl ketone affords diketone **3.20**, which can be cyclized to the furanone **3.21** under basic conditions by using DBU. With the furanone intermediate in hand, we were then set up to perform the Michael⁵ addition with the previously made aldehyde piece **3.3**.

3.2 Michael Addition and Samarium Diiodide Reductive Cyclization

Upon subsection of the furanone and aldehyde intermediates to the Michael addition, we obtained an inseparable mixture of diastereomers with a diastereomeric ratio of 3.6:1 of the major diastereomer to the sum of the other diastereomers (figure 3.7). It is difficult to tell exactly which diastereomer is which within this mixture, so the entire mixture is pushed into the next step. The conditions used for this transformation were the same conditions used in previous Michael additions towards our englerin analogues.

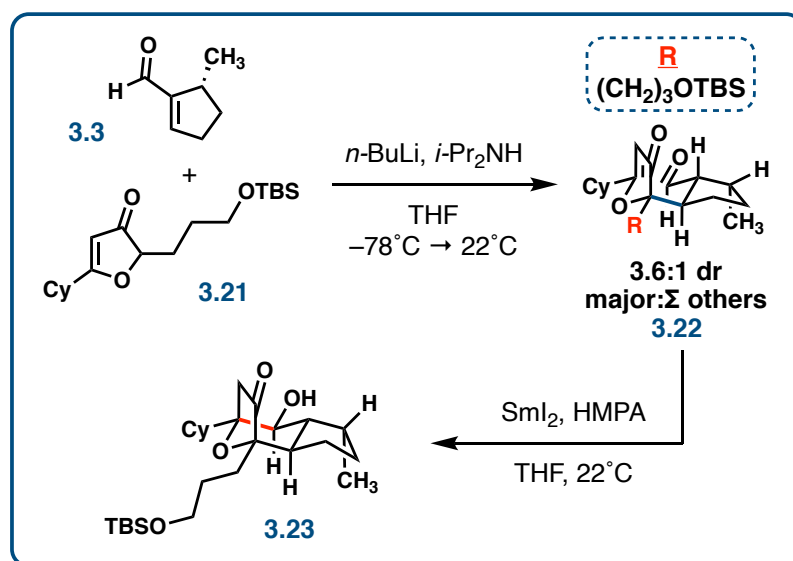


Figure 3.7 The Michael addition and SmI_2 cyclization using furanone **3.21**

When treated with samarium diiodide and HMPA, the reductive cyclization ensued. We purified the large number of fractions but were not able to see the presence of any product in the proton NMR signified by a doublet around 3.9 with a J-value of around 11 Hz. There was one product that was very clearly the major product,

which we presumed was the pinacol product, as observed in previous SmI_2 cyclizations. Upon attempts at elucidation of the exact structure using 1D and 2D NMR, it appeared to be the pinacol product with the TBS group removed. There were a few inconsistencies though that made for a tough elucidation, such as the absence of the olefin within the furanone portion that would be present in the pinacol product. Luckily, I was able to grow a crystal of the product that allowed for examination using X-Ray crystallography for its unambiguous structural determination.

The major product of the SmI_2 cyclization is shown in figure 3.8. The first thing that we noticed was that the TBS group was removed from the long chain alcohol and that the resultant free alcohol participated in a 1,4-addition into the furanone. Next, the product is the result of the pinacol coupling. Finally, the product is the result of the wrong diastereomer altogether, meaning that the Michael addition is no longer selective for the desired product when the long chain alcohol is present. Upon studying the transition state models of this Michael addition as shown in figure 3.9, it is apparent what happened.

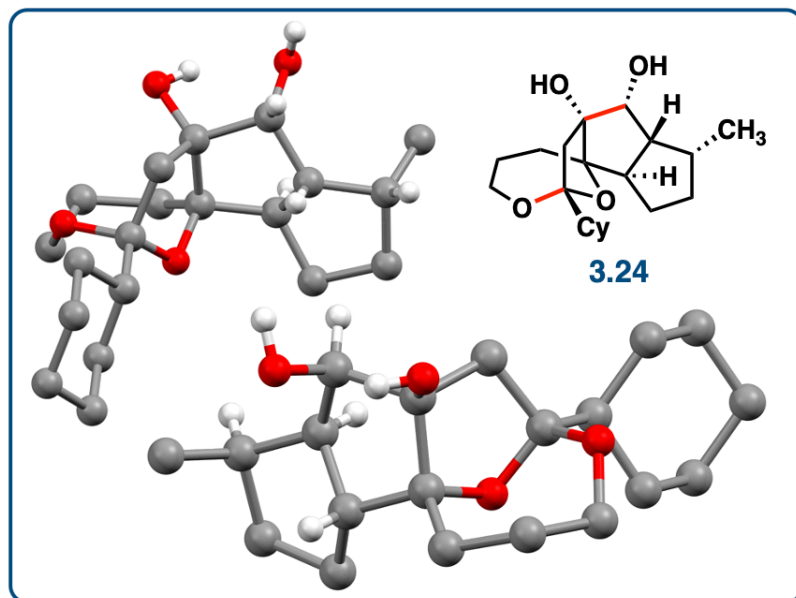


Figure 3.8 Structure of the pinacol product **3.24** resulting from the Michael addition and SmI_2 cyclization of furanone **3.21**

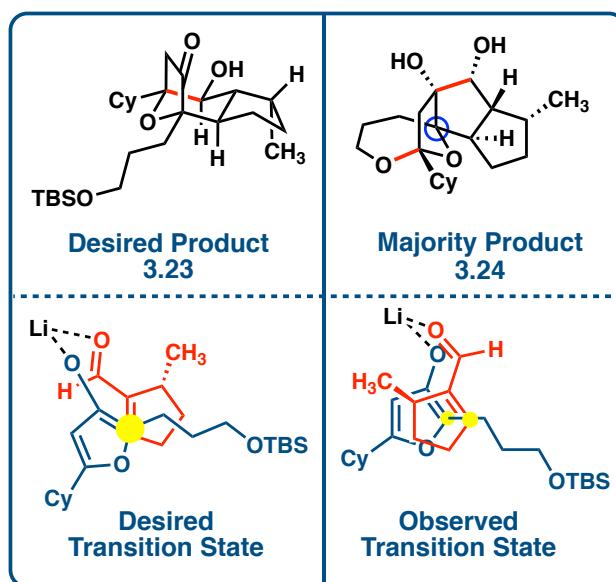


Figure 3.9 Transition state models of the Michael addition

The C4-methyl group of the aldehyde fragment effectively shields one face of the α,β -unsaturated system, encouraging approach of nucleophiles to the open surface. The face of the furanone that is approached by the aldehyde is then determined by the preference of either overlapping the ring systems or overlapping the aldehyde ring with the substituent alpha to the carbonyl in the furanone. In the case of the cyclohexyl analogues with a methyl at C10, the desired scenario is observed which involves the overlap of the aldehyde ring with the methyl group at C10. When this C10-methyl group is replaced with the alkyl chain with a terminal bulky TBS-protected alcohol, the system then shifts its preferred transition state to the overlapping rings. We had a couple ideas of how to overcome this transition state dilemma along with the issue of the protecting group cleavage.

3.3 Attempts to Fix Selectivity of Michael Addition

The first thing we would need to do is to replace the protecting group with a more robust protecting group. A TBDPS group is more robust, but is also larger and more sterically bulky, so we also decided to try a PMB group. The other modification we decided to make was to extend the alcohol out one more carbon. Again, we do not want to make this chain too long due to a fear of decreased solubility.

The application of these changes can be shown in figure 3.10. Instead of starting with 1,5-pentanediol, we started with 1,6-hexanediol. TBDPS monoprotection followed by oxidation affords acid **3.26**. An esterification using dimethyl sulfate followed by an α -chlorination leads to the α -chloroester **3.28**. This was then subjected to the Claisen⁴ condensation to afford diketone **3.29**, which can be cyclized under basic conditions to afford TBDPS-protected furanone **3.30**.

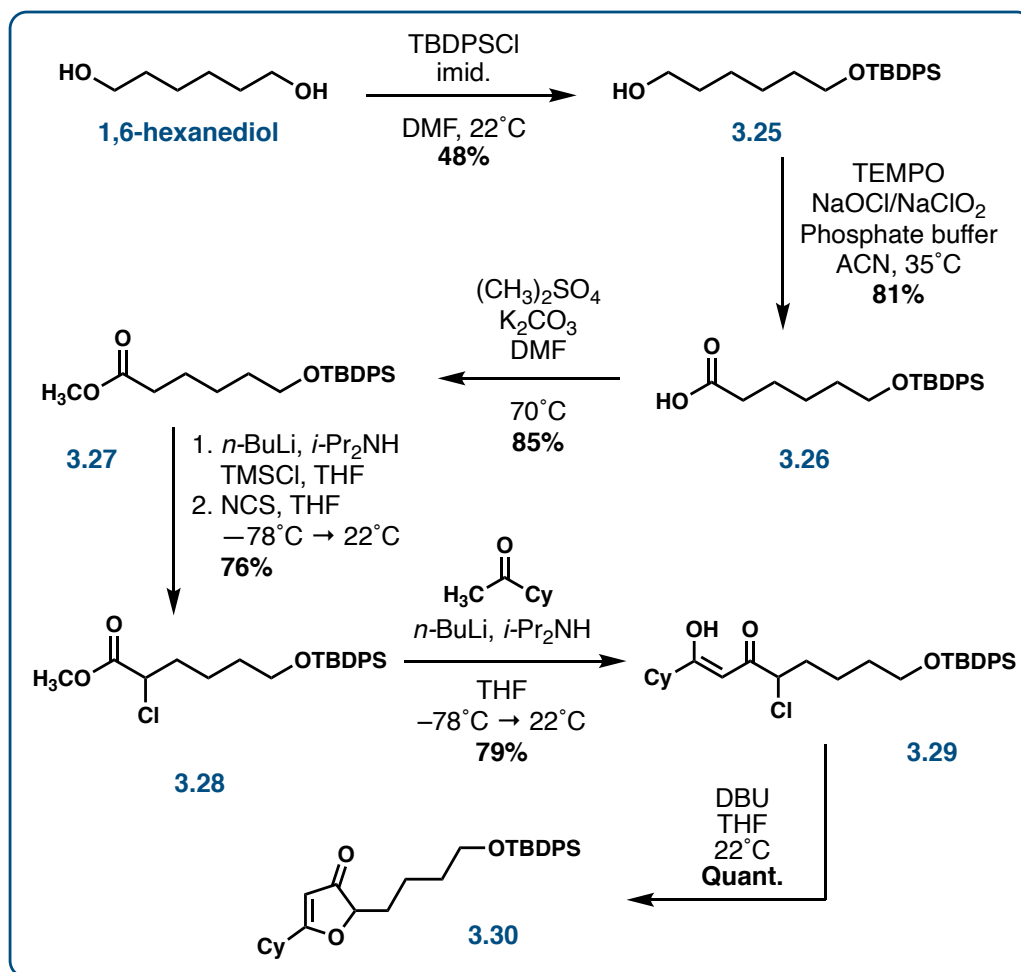


Figure 3.10 Synthesis of TBDPS-protected furanone **3.30**

Because the PMB cannot be subjected to the oxidation conditions due to the undesired benzylic oxidation, we used a TBS group instead to hold the place of the PMB, that would be installed after the oxidation. A TBS monoprotection of 1,6-hexanediol followed by oxidation of the free alcohol afforded the acid **3.32** (figure 3.11). Esterification of the acid using dimethyl sulfate followed by α-chlorination of the ester affords α-chloroester **3.34**. A Claisen⁴ condensation with cyclohexyl methyl ketone affords diketone **3.35**. When the TBS-protected diketone **3.35** is treated with

TBAF, the compound does a simultaneous TBS deprotection and cyclization to afford furanone **3.36** in a 31% yield along with 40% of the cyclized TBS-protected product. The TBS-protected product can be deprotected to afford the free alcohol **3.36** in a 47% yield. The free alcohol can then be protected as the PMB ether **3.37** using PMBOH and Amberlyst-15 resin.

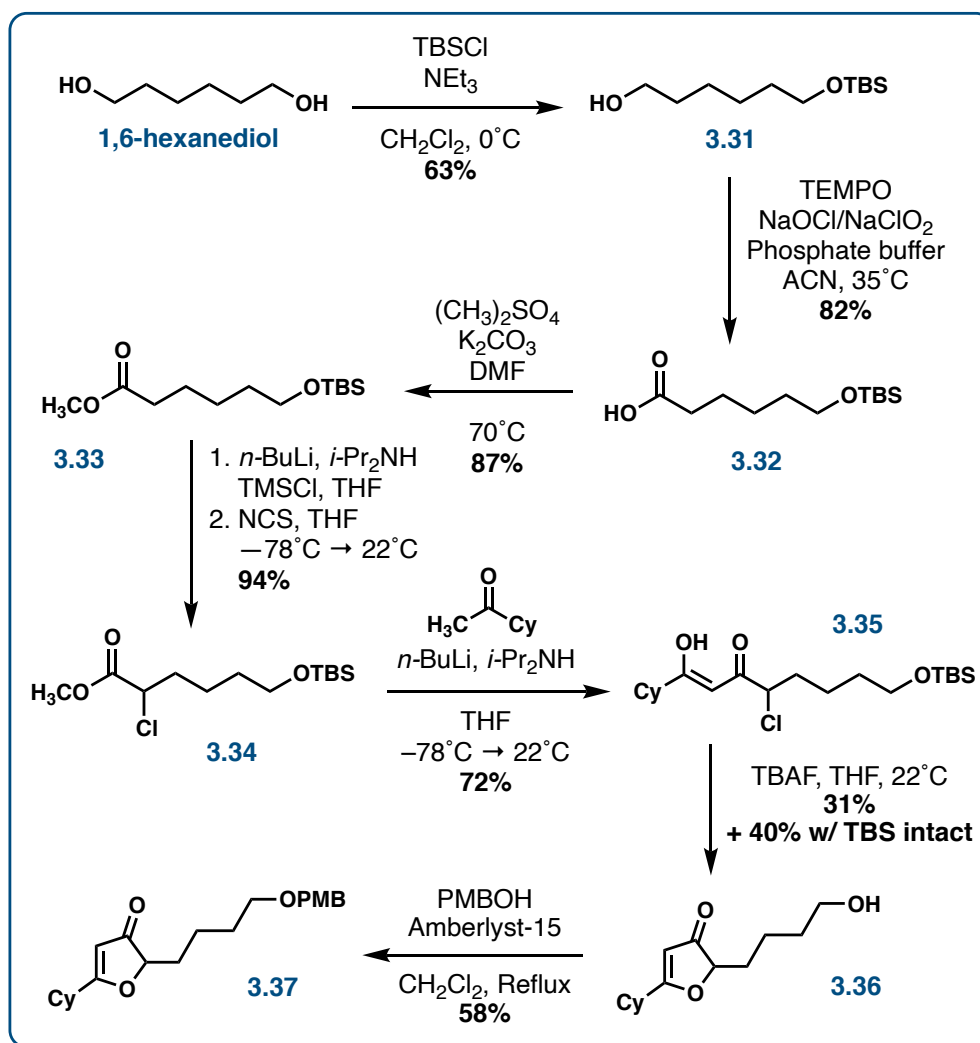


Figure 3.11 Synthesis of PMB-protected furanone **3.37**

When the TBDPS-protected furanone **3.30** was subjected to the Michael⁵ addition, we obtained a 1.2:1 diastereomeric mixture of the major diastereomer to the sum of the others (figure 3.12). When subjected to the SmI₂ cyclization, we were not able to observe any product by NMR. The 1.2:1 d.r. is suggestive of a decrease in the selectivity toward the undesired diastereomer observed previously.

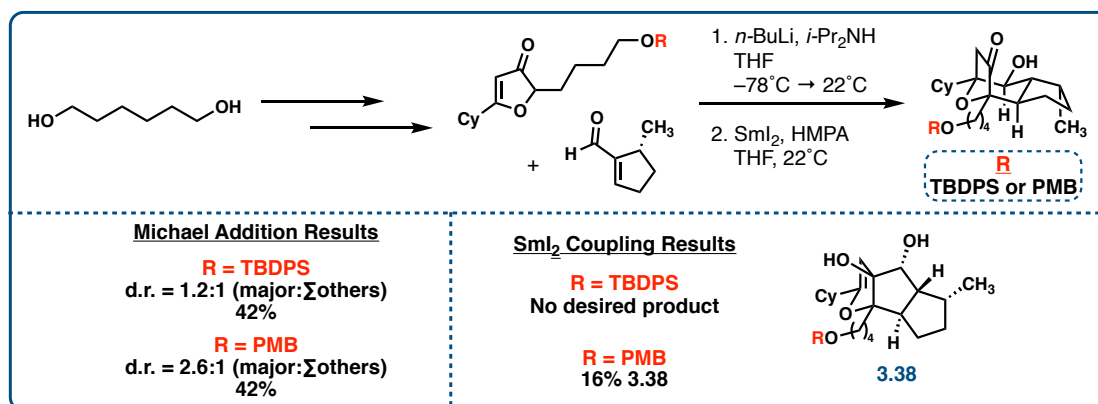


Figure 3.12 Results of the Michael addition and SmI₂ cyclization using furanones **3.30** and **3.37**

When the PMB-protected furanone **3.37** was subjected to the Michael⁵ addition, we observed a 2.6:1 diastereomeric ratio of the major diastereomer to the sum of the others (figure 3.12). When subjected to the SmI₂ cyclization, we were able to obtain a 16% yield of the pinacol product **3.38**, which was determined through 1D and 2D NMR analysis. We were not able to see any desired product however, but the presence of this pinacol product is a good sign as this product is a result of the correct diastereomer from the Michael addition. The low yield is suggestive that it is still not

the major diastereomer of the Michael addition though. We needed to come up with an alternate plan again.

3.4 Attempt to Fix Diastereoselectivity with an Olefin

Because it appeared that making the group on the alkyl chain smaller was pushing the selectivity of the Michael addition in our favor to some degree, we decided we needed to go even further. Our strategy was to get rid of the alcohol all together so that we would not have to worry about the steric bulk of a protecting group. We decided instead to use a terminal olefin at this position as shown in figure 3.13 with allylic furanone **3.39**. The synthesis of this furanone was attempted in a similar fashion but starting with 1-penten-5-ol.

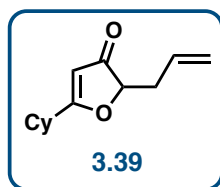


Figure 3.13 Allylic furanone **3.39**

Upon our first attempt at the oxidation of this alcohol to the acid, we were able to obtain the acid in a 63% yield under the previously used conditions. Upon a second and third attempt, we were only able to obtain the product in a 16% and 0% yield, respectively. It is possible that the olefin is interfering with the oxidation of the alcohol resulting in poor yields. It is also possible that the solutions of bleach and sodium chlorite were becoming less effective in the time left in between trials.

Regardless, methylation of the acid results in the volatile methyl ester, which we had trouble isolating as a pure sample.

The synthesis of this olefin may need to be approached from another angle. It should be possible to synthesize the allylic furanone **3.39** by using the same 1,5-diol route. Once the furanone is in hand as a protected alcohol, you can deprotect the alcohol and form the olefin through an elimination reaction (figure 3.14). The alcohol may have to be activated to encourage elimination.

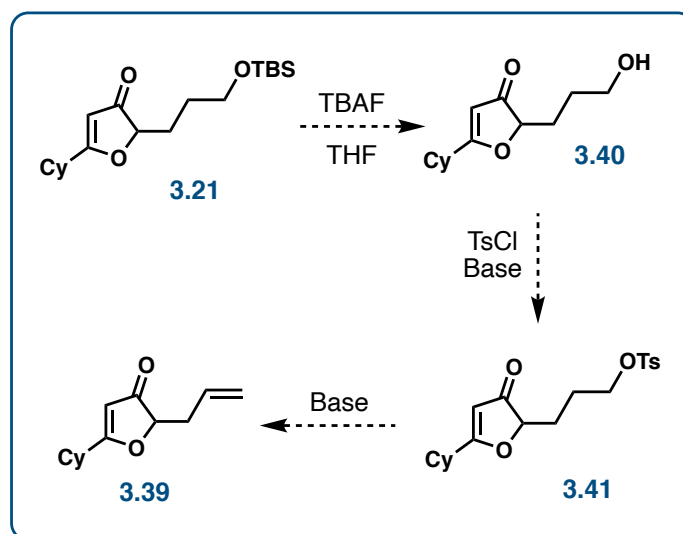


Figure 3.14 An alternative route to allylic furanone **3.39** through an elimination

An alternative route to the synthesis of the allylic furanone **3.39** is by starting with 1,4-butanediol, following the same series of steps, and using a Wittig⁶ olefination to install the alkene. In order to avoid dealing with selectivity issues that may arise from redundant functionality, it may be worth attempting to transform the alcohol to

the olefin on the α -chloroester **3.47** as shown in figure 3.15. With the allylic furanone **3.39** in hand, we can test it within the Michael⁵ addition and SmI₂ sequence.

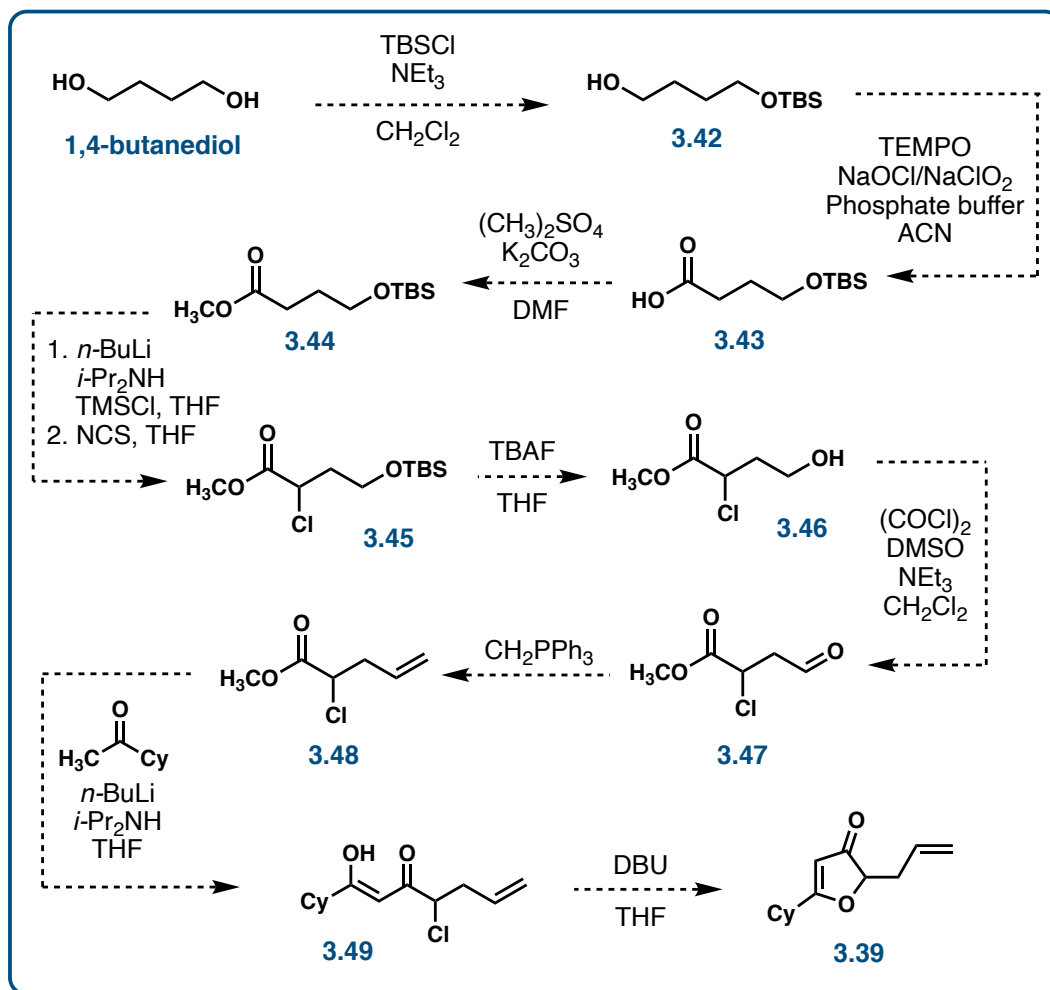


Figure 3.15 An alternative route to allylic furanone **3.39** through a Wittig olefination

3.5 Future Work

Assuming the allylic furanone makes it through the two-step sequence to afford the core structure **3.51** without any issues, we would then need to functionalize

the compound in a similar manner as done previously to afford the reverse ester tool compound. If there are issues with unwanted interactions of the olefin during the SmI_2 , it may be worth exploring the transformation of the olefin back into the protected alcohol after the Michael⁵ addition. But if this is not the case, we can take the olefin to the protected alcohol after a protection of the C6-alcohol **3.51**. If we were to leave the olefin as is throughout the synthesis, it would be cleaved to the aldehyde during the oxidative cleavage of the furan, which is one route that can be explored.

With the core in hand, one possible route to the tool compound scaffold **3.61** is shown in figure 3.16. A TBS protection of the alcohol can be followed by a hydroboration/oxidation sequenced to afford alcohol **3.53**. This alcohol can then be protected by another protecting group such as the MOM group or the TBDPS group. Addition of the furan into the ketone can be followed by a reductive excision to ablate the alcohol leaving furan **3.56**. You can then obtain the reverse ester **3.59** through the three-step sequence developed towards the synthesis of the reverse ester analogues. Oxidative cleavage of the furan to the acid **3.57** can be followed with a Steglich⁷ esterification to afford the ester **3.58**. The ester can then be epimerized to afford the reverse ester scaffold **3.59**. From here, you can selectively remove the TBS group and perform an esterification with the acid chloride derived from coumaric acid. At this point, a MOM deprotection allows for the installation of the covalent modifiers at C10 and a final deprotection of the PMB group on the reverse ester affords the tool compound. These tool compounds would then be sent to John Beutler for further biological mechanism of action studies to help elucidate the biological pathway leading to the potent and selective activity of these englerin analogues.¹

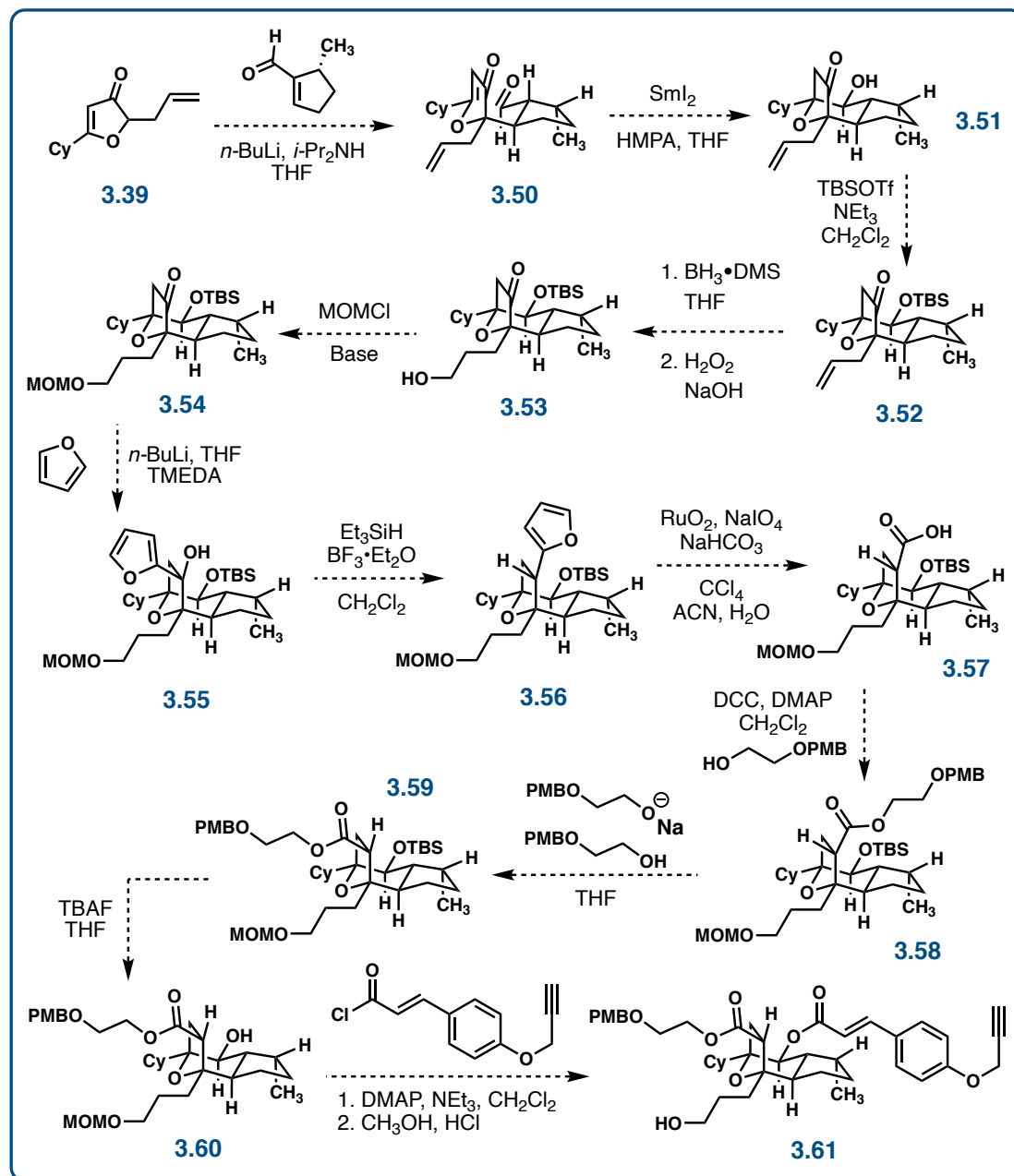


Figure 3.16 Synthetic route towards the proteomic tool compounds using allylic furanone **3.39**

Experimental Procedures

General Information: *These experimental procedures have been published previously in its current or a substantially similar form and I have obtained permission to republish it.*¹ All electrochemical reactions were performed in either an H-type divided cell separated by a sintered glass frit or a single compartment glassfalcon tube with electrodes separated by a glass microscope slide (Fisherbrand®, plain, precleaned, 2.5 cm x 7.5 cm x 0.1 cm). All non-electrochemical reactions were performed in single-neck oven- or flame-dried round bottom flasks fitted with rubber septa under a positive pressure of argon, unless otherwise noted. Air- and moisture-sensitive liquids were transferred via syringe or stainless-steel cannula. Organic solutions were concentrated by rotary evaporation at or below 35°C at 10 Torr (diaphragm vacuum pump) unless otherwise noted. Compounds were isolated using flash column chromatography² with silica gel (60-Å pore size, 40–63µm, standard grade, Silicycle). Analytical thin-layer chromatography (TLC) was performed using glass plates pre-coated with silica gel (0.25 mm, 60-Å pore size, 5–20 µm, Silicycle)

¹ (a) Wu, Z.; Suppo, J. S.; Tumova, S.; Strobe, J.; Bravo, F.; Moy, M.; Weinstein, E. S.; Peer, C. J.; Figg, W. D.; Chain, W. J.; Echavarren, A. M.; Beech, D. J.; Beutler, J. A., *ACS Med. Chem. Lett.* 2020, 11, 1711-1716. (b) Reed, H.; Paul, T. R.; Chain, W. J., *J. Org. Chem.* 2018, 83, 11359-11368. (c) Bush, T. S.; Yap, G. P. A.; Chain, W. J., *Org. Lett.* 2018, 20, 5406-5409. (d) Lewis, R. S.; Garza, C. J.; Dang, A. T.; Pedro, T. K.; Chain, W. J., *Org. Lett.* 2015, 17, 2278-2281. (e) Li, Z.; Nakashige, M.; Chain, W. J., *J. Am. Chem. Soc.* 2011, 133, 6553-6556.

² Still, W. C.; Kahn, M.; Mitra, A. *J. Org. Chem.* 1978, 43, 2923–2925.

impregnated with a fluorescent indicator (254 nm). TLC plates were visualized by exposure to ultraviolet light (UV), then were stained by submersion in aqueous ceric ammonium molybdate solution (CAM), acidic ethanolic p-anisaldehyde solution (anisaldehyde), or aqueous methanolic iron(III) chloride (FeCl₃), followed by brief heating on a hot plate (215°C, 10–15 s).

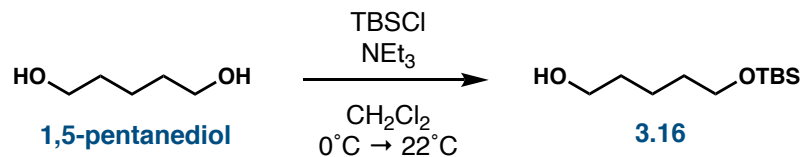
Materials: Commercial reagents and solvents were used as received with the following exceptions. Triethylamine, dichloromethane, diethyl ether, tetrahydrofuran, and 1,2-dimethoxyethane were purified by the method of Pangborn, et. al.³ Tetrabutylammonium hexafluorophosphate was recrystallized from ethanol (23 g /300 mL) at 65°C. Reticulated vitreous carbon (RVC) foam (carbon – vitreous – 3000C – foam; thickness: 10 mm; bulk density: 0.05 g/cm³; porosity: 96.5%; pores/cm: 40) was obtained from Goodfellow USA and cut to appropriate size for reaction scale. After 150 h of use, RVC electrodes were discarded and freshly cut electrodes were used.

Instrumentation: Proton (¹H), carbon (¹³C), fluorine (¹⁹F), and silicon (²⁹Si) nuclear magnetic resonance (NMR) spectra were recorded on Bruker AV400 CryoPlatform QNP or Bruker AVIII600 SMART NMR spectrometers at 23°C. Proton chemical shifts are expressed in parts per million (ppm, δ scale) downfield from tetramethylsilane and are referenced to residual protium in the NMR solvent (CHCl₃: δ 7.26, CD₃COCD₂H: δ 2.05). Carbon chemical shifts are expressed in parts per million

³ Pangborn, A. B.; Giardello, M. A.; Grubbs, R. H.; Rosen, R. K.; Timmers, F. J. *Organometallics* 1996, 15, 1518–1520.

(ppm, d scale) downfield from tetramethylsilane and are referenced to the carbon resonance of the NMR solvent (CDCl_3 : δ 77.16, $\text{CD}_3\text{COCD}_2\text{H}$: δ 29.84). Data are represented as follows: chemical shift, multiplicity (s = singlet, d = doublet, t = triplet, q = quartet, m = multiplet, br = broad, app = apparent), integration, and coupling constant (J) in Hertz (Hz). Accurate mass measurements were obtained using an Agilent 1100 quaternary LC system coupled to an Agilent 6210 LC/MSD-TOF fitted with an ESI or an APCI source, or Thermo Q-Exactive Orbitrap using electrospray ionization (ESI) or a Waters GCT Premier spectrometer using chemical ionization (CI).

Synthesis of TBS-protected 1,5-pentanediol 3.16



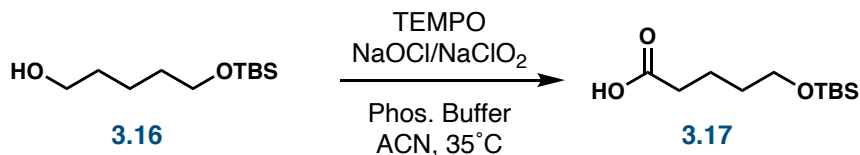
A solution of *tert*-butyldimethylchlorosilane (10.1 g, 66.7 mmol, 1 equiv) in dichloromethane (100 mL) was added dropwise via addition funnel to a stirred solution of pentane-1,5-diol (10.5 mL, 100.0 mmol, 1.50 equiv) and triethylamine (13.9 mL, 100 mmol, 1.50 equiv) in dichloromethane at 0°C. The solution was warmed to 22°C and stirred at that temperature for 16 h. The resultant solution was diluted with water (100 mL) and the aqueous layer was extracted with ethyl acetate (3 × 30 mL). The combined organic layers were washed with water (60 mL) and brine (60 mL) before being dried over anhydrous sodium sulfate. The dried solution was concentrated, then was purified using flash column chromatography (silica gel, starting with 5% ethyl acetate–hexanes, grading to 10% ethyl acetate–hexanes) to afford a clear, colorless oil (11.0 g, 50.3 mmol, 75%).

¹H NMR (600 MHz, CDCl₃) δ: 3.60 (t, *J* = 6.5 Hz, 2H), 3.57 (t, *J* = 6.5 Hz, 2H), 1.51 – 1.62 (m, 4H), 1.33 – 1.40 (m, 2H), 0.85 (s, 9H), 0.00 (s, 6H).

¹³C NMR (151 MHz, CDCl₃) δ: 63.1, 63.0, 32.5, 26.0, 22.0, 18.4, -5.3.

TLC: 50% ethyl acetate–hexanes, $R_f = 0.71$,
(KMnO_4).

Synthesis of Carboxylic Acid 3.17



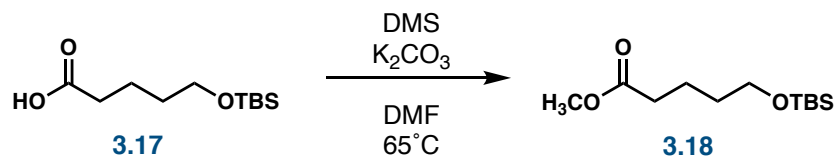
A solution of aqueous sodium hypochlorite (0.28%, 21 mL, 0.82 mmol, 0.020 equiv) and a solution of aqueous sodium chlorite (2.0 M, 42 mL, 82 mmol, 2.0 equiv) were added simultaneously dropwise via addition funnel to a stirred solution of alcohol **3.16** (9.0 g, 41 mmol, 1.0 equiv), TEMPO (450 mg, 2.9 mmol, 0.070 equiv), and phosphate buffer (0.02 M, 160 mL, pH 6.7) in acetonitrile (200 mL) over a 2-hour period at 35°C. The solution was stirred for 4 h, whereupon it was cooled to 22°C, water (100 mL) was added, and the pH of the solution is adjusted to 8 using potassium hydroxide. The solution was cooled to 0°C, whereupon the remaining oxidant was quenched using aqueous sodium sulfite (6.1%, 200 mL). The resultant solution was warmed to 22°C and was stirred for 30 min at that temperature. Diethyl ether (150 mL) was added, and the resultant biphasic solution was adjusted to pH 3-4 using aqueous 2 M HCl. The aqueous layer is discarded, and the organic layer was washed with water (2 x 80 mL) and brine (80 mL). The solution was dried over anhydrous sodium sulfate, and the dried solution was concentrated to afford a clear, colorless oil (7.90 g, 34.0 mmol, 83%).

¹H NMR (600 MHz, CDCl₃) δ: 3.63 (t, *J* = 6.3 Hz, 2H), 2.38 (t, *J* = 7.5 Hz, 2H), 1.70 (quint, *J* = 7.5 Hz, 2H), 1.57 (m, 2H), 0.89 (s, 9H), 0.04 (s, 6H).

^{13}C NMR (151 MHz, CDCl_3) δ : 179.9, 62.8, 33.9, 32.1, 26.1, 21.4, 18.5, -5.2.

TLC: 20% ethyl acetate–hexanes, $R_f = 0.10$,
(KMnO_4).

Synthesis of Ester 3.18



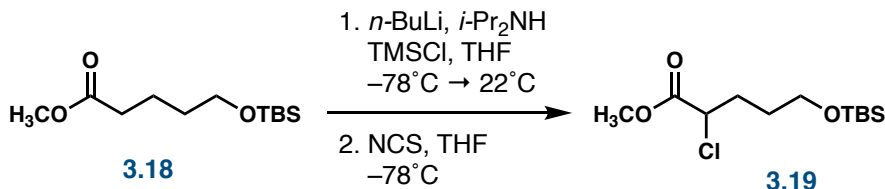
Dimethyl sulfate (2.77 mL, 29.2 mmol, 1.05 equiv) was added dropwise to a stirred solution of carboxylic acid **3.17** (6.46 g, 27.8 mmol, 1 equiv) and potassium carbonate (4.23 g, 30.6 mmol, 1.10 equiv) in dimethylformamide (60 mL) at 65°C. The resultant solution was stirred for 90 min, whereupon the solution was cooled to 0°C and water (40 mL) was added. The aqueous layer was extracted with dichloromethane (3 x 20 mL). The combined organic layers were washed with water (50 mL) and brine (50 mL) before being dried over anhydrous sodium sulfate. The dried solution was concentrated, then was adhered to silica and purified using flash column chromatography (silica gel, 2% ethyl acetate–hexanes) to afford a clear, yellow oil (5.48 g, 22.2 mmol, 80 %).

¹H NMR (600 MHz, CDCl₃) δ: 3.66 (s, 3H), 3.61 (t, *J* = 6.3 Hz, 2H), 2.33 (t, *J* = 7.5 Hz, 2H), 1.70 – 1.65 (m, 2H), 1.50 – 1.56 (m, 2H), 0.88 (s, 9H), 0.04 (s, 6H).

¹³C NMR (151 MHz, CDCl₃) δ: 74.3, 62.8, 51.6, 33.9, 32.3, 26.1, 21.6, 18.5, -5.2.

TLC: 10% ethyl acetate–hexanes, *R_f* = 0.57, (KMnO₄).

Synthesis of α -Chloroester **3.19**



A solution of *n*-butyllithium (2.56 M, 3.91 mL, 10.0 mmol, 1.50 equiv) was added to a stirred solution of *N,N*-diisopropylamine (1.41 mL, 10.0 mmol, 1.50 equiv) in THF (20 mL) at -78°C . The resultant solution was warmed briefly to 0°C , then was cooled to -78°C whereupon chlorotrimethylsilane (1.27 mL, 10.0 mmol, 1.50 equiv) was added followed by a dropwise addition of a solution of ester **3.18** (1.65 g, 6.70 mmol, 1 equiv) in THF (7 mL). The resultant solution was stirred at 22°C for 16 h, whereupon the solution was concentrated carefully to afford the crude silyl enol ether. The clear, yellow oil is taken up in pentane, filtered over celite, and concentrated. A solution of *N*-chlorosuccinimide (1.33 g, 10.0 mmol, 1.50 equiv) in THF (50 mL) is added dropwise to a stirred solution of the crude silyl enol ether in THF (50 mL) at -78°C . The solution is stirred for 16 h, whereupon the excess *N*-chlorosuccinimide is quenched using saturated aqueous sodium thiosulfate solution (20 mL). The organic layer is dried over anhydrous sodium sulfate and concentrated. The crude chloroester **3.19** is taken up in hexanes, filtered, and concentrated. Purification by flash column chromatography (silica gel, 2% diethyl ether–hexanes) afforded a clear, yellow oil (1.27 g, 4.54 mmol, 67%).

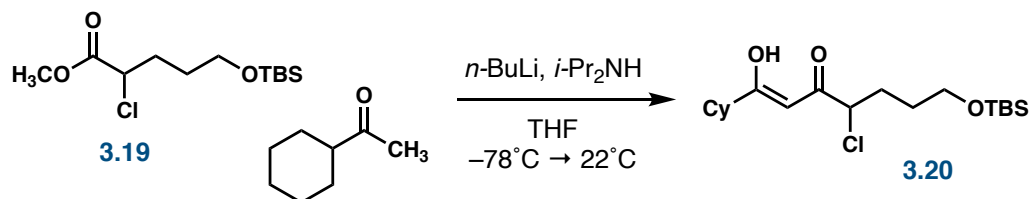
^1H NMR (600 MHz, CDCl_3) δ : 4.35 (dd, $J = 8.1, 5.9$ Hz, 1H), 3.78 (s, 3H),
3.64 (t, $J = 6.3$ Hz, 2H), 2.16 – 2.09 (m, 1H),

2.02 – 1.94 (m, 1H), 1.73 – 1.57 (m, 2H), 0.88
(s, 9H), 0.04 (s, 6H).

^{13}C NMR (151 MHz, CDCl_3) δ : 170.4, 62.2, 57.3, 53.0, 31.9, 29.2, 26.0, 18.4, -
5.2.

TLC: 10% ethyl acetate–hexanes, R_f = 0.29,
(KMnO_4).

Synthesis of Chlorodiketone 3.20



A solution of *n*-butyllithium (2.64 M, 1.70 mL, 4.49 mmol, 1.5 equiv) was added to a stirred solution of *N,N*-diisopropylamine (0.68 mL, 4.8 mmol, 1.6 equiv) in THF (30 mL) at -78°C . The resultant solution was warmed briefly to 0°C , then was cooled to -78°C , whereupon a solution of cyclohexyl methyl ketone (0.58 mL, 4.2 mmol, 1.4 equiv) in THF (2 mL) was added dropwise. The resultant solution was stirred at -78°C for 30 min, whereupon a solution of chloroester **3.19** (0.84 g, 3.0 mmol, 1 equiv) in THF (6 mL) was added. The resultant solution was warmed to 22°C and stirred at that temperature for 8 h. The resultant clear, yellow solution was cooled to 0°C and was quenched with saturated aqueous ammonium chloride solution (10 mL). The layers were separated, and the aqueous layer was extracted with dichloromethane (3 x 7 mL). The combined organic layers were dried over anhydrous sodium sulfate and the dried solution was concentrated. Purification of the residue by flash column chromatography (1% diethyl ether–hexanes), afforded **3.20** as a clear, colorless oil (0.628 g, 1.68 mmol, 59%).

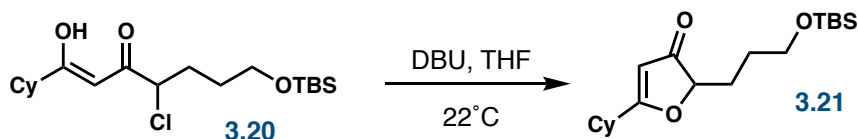
^1H NMR (600 MHz, CDCl_3) δ : 15.21 (s, 1H), 5.79 (s, 1H), 4.27 (dd, $J_1 = 8.3$, $J_2 = 5.6$ Hz, 1H), 3.68 – 3.60 (m, 2H), 2.22 (tt, $J_1 = 11.7$, $J_2 = 3.4$ Hz, 1H), 2.15 – 2.05 (m,

1H), 1.99 – 1.92 (m, 1H), 1.90 – 1.84 (m, 2H),
1.84 – 1.77 (m, 2H), 1.75 – 1.66 (m, 2H), 1.66
– 1.58 (m, 1H), 1.43 – 1.17 (m, 6H), 0.89 (s,
9H), 0.05 (s, 6H).

¹³C NMR (151 MHz, CDCl₃) δ: 197.4, 191.9, 95.6, 62.4, 61.7, 46.4, 32.1, 29.7,
29.5, 26.1, 25.9, 25.9, 25.6, 18.4, -5.2.

TLC: 5% ethyl acetate–hexanes, R_f = 0.59, (UV,
CAM).

Synthesis of Furanone 3.21



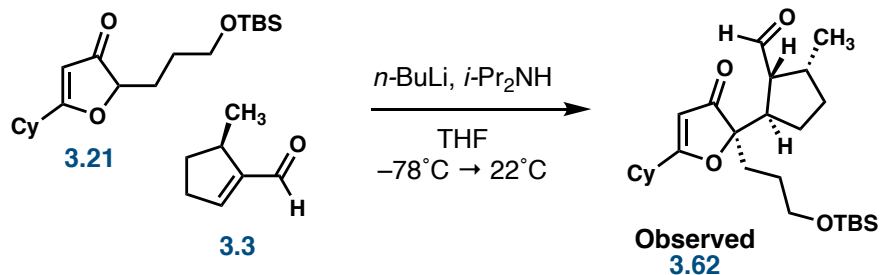
1,8-Diazabicyclo[5.4.0]undec-7-ene (1.51 mL, 10.1 mmol, 1.40 equiv) was added dropwise to a stirred solution of chlorodiketone **3.20** (2.71 g, 7.23 mmol, 1 equiv) in THF (25 mL) at 22°C. A pale, yellow precipitate formed immediately. The resultant suspension was stirred at 22°C for 12 h, whereupon the suspension was partitioned between water (10 mL) and ethyl acetate (10 mL). The layers were separated, and the aqueous phase was extracted with ethyl acetate (3 x 10 mL). The combined organic layers were dried over anhydrous sodium sulfate and the dried solution was concentrated. Purification of the residue using flash column chromatography (silica gel, starting with 5% ethyl acetate–hexanes, grading to 20% ethyl acetate–hexanes) afforded a pale, yellow oil (1.95 g, 5.78 mmol, 80%).

¹H NMR (600 MHz, CDCl₃) δ: 5.37 (s, 1H), 4.43 (dd, $J_1 = 7.7$, $J_2 = 4.3$ Hz, 1H), 3.66 – 3.60 (m, 2H), 2.48 – 2.40 (m, 1H), 1.99 – 1.93 (m, 3H), 1.84 – 1.76 (m, 2H), 1.75 – 1.67 (m, 2H), 1.66 – 1.60 (m, 2H), 1.44 – 1.29 (m, 4H), 1.30 – 1.23 (m, 1H), 0.88 (s, 9H), 0.03 (s, 6H).

^{13}C NMR (151 MHz, CDCl_3) δ : 205.2, 197.8, 101.7, 85.8, 62.8, 39.8, 30.0,
29.9, 28.0, 27.9, 26.1, 25.9, 25.7, 25.7, -5.2.

TLC: 5% ethyl acetate–hexanes, $R_f = 0.07$, (UV,
CAM).

Synthesis of Michael Adduct 3.62



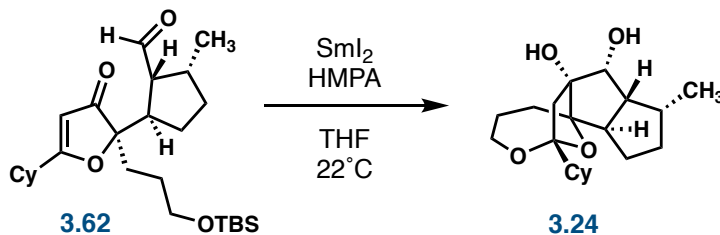
A solution of *n*-butyllithium (2.62 M, 1.87 mL, 4.90 mmol, 1.28 equiv) was added to a stirred solution of *N,N*-diisopropylamine (0.748 mL, 5.30 mmol, 1.28 equiv) in THF (50 mL) at -78°C . The resultant solution was warmed briefly to 0°C , then was cooled to -78°C , whereupon a solution of the 3-furanone **3.21** (1.29 g, 3.81 mmol, 1 equiv) in THF (5 mL) was added dropwise. The resultant solution was stirred at -78°C for 30 min, whereupon a solution of aldehyde **3.3** (485 mg, 4.40 mmol, 1.16 equiv) in THF (5 mL) was added. The reaction mixture was stirred at -78°C for 30 min, then was warmed to 22°C and stirred at that temperature for 1 h. The reaction mixture was then cooled to 0°C , whereupon the remaining enolate was carefully quenched with saturated aqueous ammonium chloride solution (20 mL). The layers were separated, and the aqueous layer was extracted with dichloromethane (3 x 40 mL). The combined organic layers were dried over anhydrous sodium sulfate and the dried solution was concentrated. Purification of the residue by flash column chromatography (silica gel, starting with 1% ethyl acetate–hexanes, grading to 5% ethyl acetate–hexanes) afforded a mixture of diastereomers (d.r. = 3.6:1 major : Σ others) as a clear, yellow oil (0.563 g, 1.25 mmol, 33%).

^1H NMR (600 MHz, CDCl_3) δ : 9.63 (d, $J = 3.3$ Hz, 1H), 5.37 (s, 1H), 3.57 – 3.48 (m, 2H), 2.94 (q, $J = 8.8$ Hz, 1H), 2.71 (ddd, $J = 9.8, 6.8, 3.3$ Hz, 1H), 2.48 – 2.40 (m, 1H), 2.36 – 2.28 (m, 1H), 2.00 – 1.92 (m, 4H), 1.87 – 1.68 (m, 5H), 1.62 – 1.53 (m, 1H), 1.46 – 1.22 (m, 7H), 1.20 (t, $J = 7.0$ Hz, 1H), 1.01 (d, $J = 7.2$ Hz, 3H), 0.86 (s, 9H), 0.01 (s, 6H).

^{13}C NMR (151 MHz, CDCl_3) δ : 206.3, 204.6, 197.5, 103.4, 93.4, 63.0, 54.2, 44.1, 40.0, 39.2, 34.6, 31.6, 30.2, 30.0, 26.8, 26.2, 26.1, 25.9, 25.8, 25.8, 16.1, -5.1.

TLC: 10% ethyl acetate–hexanes, $R_f = 0.19$, (UV, CAM).

Synthesis of Pinacol Product 3.24



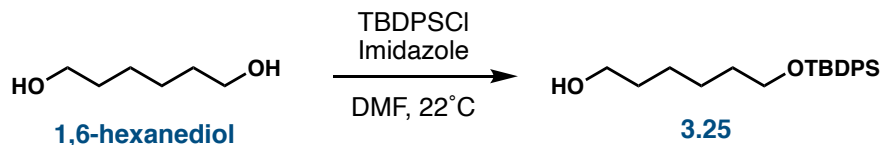
A freshly prepared solution of samarium (II) iodide in THF (0.10 M, 8.5 mL, 0.85 mmol, 4.0 equiv) was added dropwise via cannula over 1 h to a stirred solution of the mixture of diastereomers resulting from the Michael addition (97.5 mg, 0.217 mmol, 1 equiv) and hexamethylphosphoramide (0.700 mL, 4.02 mmol, 18.5 equiv) in THF (10 mL) at 22°C . The resultant solution was stirred for 3 h, whereupon the reaction mixture was cooled to 0°C and excess SmI_2 was quenched using aqueous 1 M HCl (10 mL). The aqueous layer is extracted with dichloromethane (3 x 20 mL). The combined organic layers were washed with saturated aqueous sodium bicarbonate solution (40 mL), dried over anhydrous sodium sulfate, and concentrated. Purification of the residue by flash column chromatography (silica gel, starting with 5% ethyl acetate–hexanes, grading to 30% ethyl acetate–hexanes) afforded diol **3.24** as a white crystal (170 mg, 0.506 mmol, 60%).

^1H NMR (600 MHz, CDCl_3) δ : 3.87 (t, $J = 12.0$, 1H), 3.78 (s, 1H), 3.65 (dt, $J_1 = 12.1$, $J_2 = 3.5$ Hz, 1H), 3.15 (s, 1H), 2.43 – 2.22 (m, 3H), 2.16 (m, 1H), 2.05 – 1.95 (m, 1H), 1.93 – 1.84 (m, 2H), 1.84 – 1.78 (m, 1H), 1.78 – 1.71 (m, 4H), 1.71 – 1.68 (m, 1H), 1.68

– 1.59 (m, 2H), 1.59 – 1.46 (m, 2H), 1.46 –
1.38 (m, 1H), 1.38 – 1.28 (m, 1H), 1.19 (m,
1H), 1.12 (tt, $J_1 = 12.8$, $J_2 = 3.2$ Hz, 1H), 1.04
(d, $J = 7.3$ Hz, 3H), 1.01 – 0.92 (m, 2H).

^{13}C NMR (151 MHz, CDCl_3) δ : 110.2, 94.2, 91.6, 75.7, 61.7, 51.1, 50.3, 49.8,
45.4, 37.7, 32.5, 29.2, 28.7, 28.2, 27.9, 26.6,
26.5, 26.4, 20.5, 19.6.

Synthesis of TBS-protected 1,6-hexanediol 3.25



Imidazole (749 mg, 11.0 mmol, 2.20 equiv) and *tert*-butyldiphenylchlorosilane (1.42 mL g, 5.50 mmol, 1.10 equiv) were added to a stirred solution of hexane-1,6-diol (591 mg, 5.00 mmol, 1 equiv) in DMF (50 mL). The solution was stirred for 3 h, whereupon water (20 mL) was added. The resultant solution was extracted with ethyl acetate (3 × 50 mL). The combined organic layers were dried over anhydrous sodium sulfate. The dried solution was concentrated, then was purified using flash column chromatography (silica gel, starting with 5% ethyl acetate–hexanes, grading to 16% ethyl acetate–hexanes) to afford a clear, colorless oil (1.16 g, 3.26 mmol, 65%).

$^1\text{H NMR}$ (600 MHz, CD_2Cl_2) δ : 7.73 – 7.66 (m, 4H), 7.46 – 7.37 (m, 6H), 3.70 (t, $J = 6.5$ Hz, 2H), 3.59 (t, $J = 6.6$ Hz, 2H), 1.61 (p, $J = 6.7$ Hz, 2H), 1.54 (p, $J = 6.7$ Hz, 2H), 1.47 – 1.31 (m, 4H), 1.07 (s, 9H).

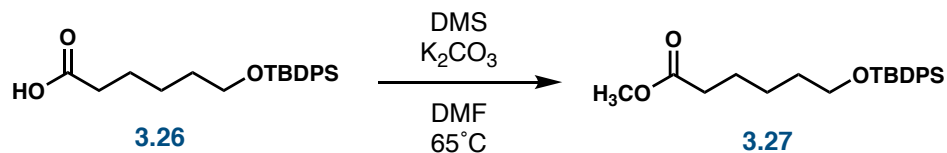
$^{13}\text{C NMR}$ (151 MHz, CD_2Cl_2) δ : 136.0, 134.7, 129.9, 128.0, 64.4, 63.1, 33.3, 33.0, 27.1, 26.1, 26.0, 19.5.

TLC: 10% ethyl acetate–hexanes, $R_f = 0.24$, (UV, KMnO_4).

Hz, 2H), 1.67 – 1.54 (m, 4H), 1.46 – 1.38 (m, 2H), 1.05 (s, 9H).

^{13}C NMR (151 MHz, CDCl_3) δ : 180.0, 135.7, 134.2, 129.7, 127.7, 63.8, 34.2, 32.3, 27.0, 25.5, 24.6, 19.3.

Synthesis of Ester 3.27



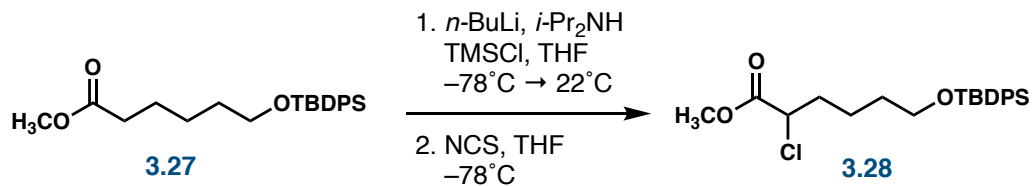
Dimethyl sulfate (1.94 mL, 20.5 mmol, 1.30 equiv) was added dropwise to a stirred solution of carboxylic acid **3.26** (5.84 g, 15.8 mmol, 1 equiv) and potassium carbonate (2.40 g, 17.4 mmol, 1.10 equiv) in DMF (40 mL) at 65°C. The resultant solution was stirred for 90 min, whereupon the solution was cooled to 0°C and water (30 mL) was added. The aqueous layer was extracted with dichloromethane (3 x 20 mL). The combined organic layers were washed with water (30 mL) and brine (30 mL) before being dried over anhydrous sodium sulfate. The dried solution was concentrated, then was adhered to silica and purified using flash column chromatography (silica gel, starting with 5% ethyl acetate–hexanes, grading to 10% ethyl acetate–hexanes) to afford a clear, yellow oil (5.18 g, 13.5 mmol, 85 %).

¹H NMR (400 MHz, CDCl₃) δ: 7.72 – 7.64 (m, 4H), 7.48 – 7.34 (m, 6H), 3.71 – 3.62 (m, 5H), 2.30 (t, *J* = 7.6 Hz, 2H), 1.69 – 1.50 (m, 4H), 1.47 – 1.34 (m, 2H), 1.07 (s, 9H).

¹³C NMR (101 MHz, CDCl₃) δ: 174.3, 135.7, 134.2, 129.7, 127.7, 63.8, 51.6, 34.2, 32.3, 27.0, 25.5, 24.9, 19.3.

TLC: 20% ethyl acetate–hexanes, $R_f = 0.50$, (UV,
KMnO₄).

Synthesis of Chlorodiketone 3.28



A solution of *n*-butyllithium (2.50 M, 6.00 mL, 15.0 mmol, 1.50 equiv) was added to a stirred solution of *N,N*-diisopropylamine (2.12 mL, 15.0 mmol, 1.50 equiv) in THF (30 mL) at -78°C . The resultant solution was warmed briefly to 0°C , then was cooled to -78°C whereupon chlorotrimethylsilane (1.90 mL, 15.0 mmol, 1.50 equiv) was added followed by a dropwise addition of a solution of ester **3.27** (3.85 g, 10.0 mmol, 1 equiv) in THF (10 mL). The resultant solution was stirred at 22°C for 3 h, whereupon the solution was concentrated carefully to afford the crude silyl enol ether. The clear, yellow oil is taken up in pentane, filtered over celite, and concentrated. A solution of *N*-chlorosuccinimide (1.99 g, 15.0 mmol, 1.50 equiv) in THF (75 mL) is added dropwise to a stirred solution of the crude silyl enol ether in THF (75 mL) at -78°C . The solution is stirred for 16 h, whereupon the excess *N*-chlorosuccinimide is quenched using saturated aqueous sodium thiosulfate solution (30 mL). The organic layer is dried over anhydrous sodium sulfate and concentrated. The crude chloroester **3.28** is taken up in hexanes, filtered, and concentrated. Purification by flash column chromatography (silica gel, starting with 1% diethyl ether–hexanes, grading to 3% diethyl ether–hexanes) afforded a clear, yellow oil (2.66 g, 6.30 mmol, 76%).

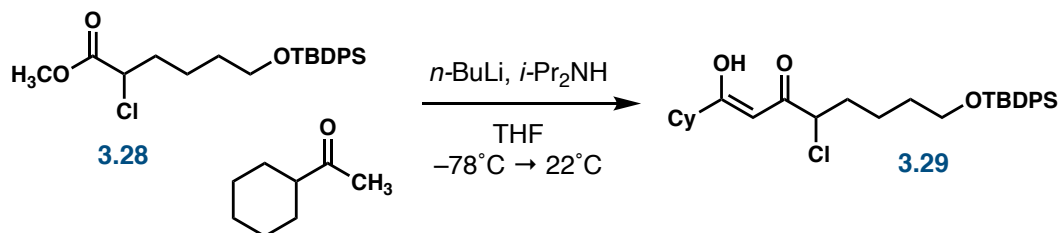
^1H NMR (600 MHz, CDCl_3) δ : 7.67 (d, $J = 7.4$ Hz, 4H), 7.46 – 7.37 (m, 5H), 4.31 – 4.25 (m, 1H), 3.79 (s, 3H), 3.69 (t, $J =$

5.6 Hz, 2H), 2.08 – 1.90 (m, 2H), 1.65 – 1.56
(m, 3H), 1.56 – 1.47 (m, 1H), 1.07 (s, 9H).

^{13}C NMR (151 MHz, CDCl_3) δ : 170.3, 135.7, 134.1, 129.7, 129.7, 129.7, 127.8,
127.8, 63.5, 57.3, 52.9, 34.8, 31.8, 27.0, 22.6,
19.4.

TLC: 10% ethyl acetate–hexanes, R_f = 0.50, (UV,
 KMnO_4).

Synthesis of Chlorodiketone 3.29



A solution of *n*-butyllithium (2.50 M, 6.96 mL, 17.4 mmol, 1.50 equiv) was added to a stirred solution of *N,N*-diisopropylamine (2.63 mL, 18.6 mmol, 1.60 equiv) in THF (120 mL) at -78°C . The resultant solution was warmed briefly to 0°C , then was cooled to -78°C , whereupon a solution of cyclohexyl methyl ketone (2.23 mL, 16.2 mmol, 1.40 equiv) in THF (8 mL) was added dropwise. The resultant solution was stirred at -78°C for 30 min, whereupon a solution of chloroester **3.28** (4.88 g, 11.6 mmol, 1 equiv) in THF (24 mL) was added. The resultant solution was warmed to 22°C and stirred at that temperature for 8 h. The resultant cloudy, orange solution was cooled to 0°C and the excess base was quenched with saturated aqueous ammonium chloride solution (40 mL). The layers were separated, and the aqueous layer was extracted with dichloromethane (3 x 30 mL). The combined organic layers were dried over anhydrous sodium sulfate and the dried solution was concentrated. Purification of the residue by flash column chromatography (1% diethyl ether–hexanes), afforded **3.29** as a clear, yellowish orange oil (4.74 g, 9.24 mmol, 59%).

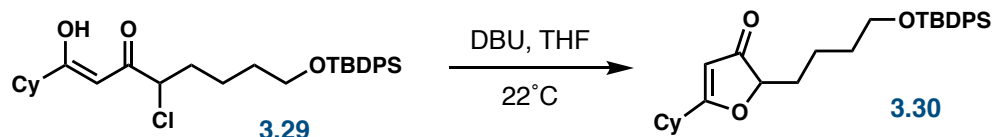
^1H NMR (600 MHz, CDCl_3) δ : 15.24 (s, 1H), 7.72 – 7.62 (m, 4H), 7.47 – 7.33 (m, 6H), 5.79 (s, 1H), 4.19 (dd, $J_1 = 8.3$, $J_2 = 5.6$ Hz, 1H), 3.66 (t, $J = 5.8$ Hz, 2H), 2.22 (tt,

$J_1 = 11.6, J_2 = 3.4$ Hz, 1H), 2.04 – 1.94 (m, 1H), 1.94 – 1.76 (m, 5H), 1.73 – 1.67 (m, 1H), 1.66 – 1.53 (m, 1H), 1.52 – 1.45 (m, 1H), 1.45 – 1.29 (m, 3H), 1.29 – 1.26 (m, 2H), 1.26 – 1.17 (m, 2H), 1.04 (s, 9H).

^{13}C NMR (151 MHz, CDCl_3) δ : 197.4, 192.0, 135.7, 134.0, 129.7, 127.8, 95.6, 63.5, 61.8, 46.4, 35.1, 31.9, 29.7, 27.0, 25.9, 25.8, 22.8, 19.3.

TLC: 5% ethyl acetate–hexanes, $R_f = 0.54$, (UV, *p*-anisaldehyde).

Synthesis of Furanone 3.30



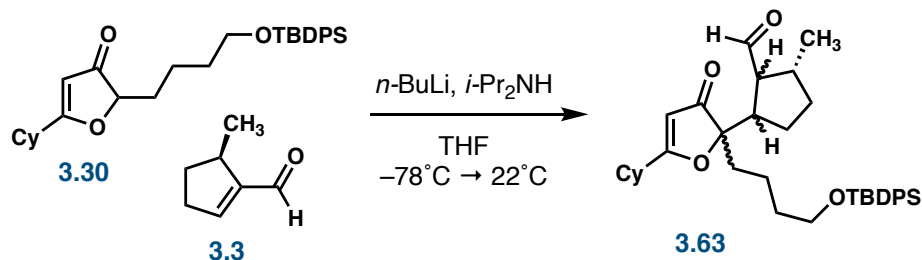
1,8-Diazabicyclo[5.4.0]undec-7-ene (0.31 mL, 2.1 mmol, 1.40 equiv.) was added dropwise to a stirred solution of chlorodiketone **3.29** (0.76 g, 1.5 mmol, 1 equiv.) in THF (5 mL) at 22°C. A pale, yellow precipitate formed immediately. The resultant suspension was stirred at 22°C for 12 h, whereupon the suspension was partitioned between water (3 mL) and ethyl acetate (5 mL). The layers were separated, and the aqueous phase was extracted with ethyl acetate (3 x 5 mL). The combined organic layers were dried over anhydrous sodium sulfate and the dried solution was concentrated. Purification of the residue using flash column chromatography (silica gel, starting with 5% ethyl acetate–hexanes, grading to 20% ethyl acetate–hexanes) afforded a clear, yellow oil (0.73 g, 1.5 mmol, quantitative).

^1H NMR (600 MHz, CDCl_3) δ : 7.68 – 7.63 (m, 4H), 7.46 – 7.36 (m, 6H), 5.38 (d, $J = 2.7$ Hz, 1H), 4.40 (dd, $J_1 = 7.6$, $J_2 = 4.1$ Hz, 1H), 3.70 – 3.62 (m, 2H), 2.47 – 2.38 (m, 1H), 2.00 – 1.94 (m, 2H), 1.94 – 1.89 (m, 1H), 1.89 – 1.74 (m, 2H), 1.74 – 1.69 (m, 1H), 1.69 – 1.63 (m, 1H), 1.63 – 1.46 (m, 4H), 1.41 – 1.29 (m, 4H), 1.29 – 1.19 (m, 2H), 1.05 (s, 9H).

^{13}C NMR (151 MHz, CDCl_3) δ : 205.3, 197.8, 135.7, 134.1, 129.7, 127.7, 101.7, 85.9, 63.6, 39.8, 32.3, 31.1, 30.0, 29.9, 27.0, 25.9, 25.7, 25.7, 21.0, 19.4.

TLC: 5% ethyl acetate–hexanes, $R_f = 0.08$, (UV, CAM).

Synthesis of Michael Adducts 3.63



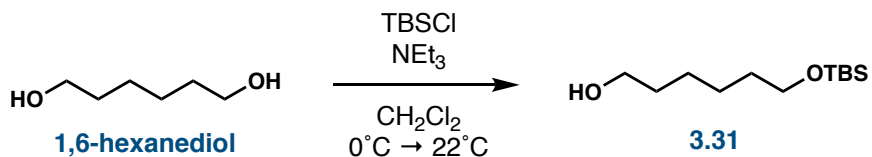
A solution of *n*-butyllithium (2.60 M, 1.20 mL, 3.12 mmol, 1.30 equiv) was added to a stirred solution of *N,N*-diisopropylamine (0.470 mL, 3.36 mmol, 1.40 equiv) in THF (35 mL) at -78°C . The resultant solution was warmed briefly to 0°C , then was cooled to -78°C , whereupon a solution of the 3-furanone **3.30** (1.14 g, 2.40 mmol, 1 equiv) in THF (2 mL) was added dropwise. The resultant solution was stirred at -78°C for 30 min, whereupon a solution of aldehyde **3.3** (306 mg, 2.78 mmol, 1.16 equiv) in THF (2 mL) was added. The reaction mixture was stirred at -78°C for 30 min, then was warmed to 22°C and stirred at that temperature for 1 h. The reaction mixture was then cooled to 0°C , whereupon the remaining enolate was carefully quenched with saturated aqueous ammonium chloride solution (5 mL). The layers were separated, and the aqueous layer was extracted with dichloromethane (3 x 15 mL). The combined organic layers were dried over anhydrous sodium sulfate and the dried solution was concentrated. Purification of the residue by flash column chromatography (silica gel, starting with 10% diethyl ether–hexanes, grading to 20% diethyl ether–hexanes) afforded a mixture of diastereomers (d.r. = 1.2:1 major : Σ others) as a clear, yellow oil (0.587 g, 1.00 mmol, 42%).

^1H NMR (600 MHz, CDCl_3) δ : 9.63 (d, $J = 3.3$ Hz, 1H), 7.68 – 7.59 (m, 3H), 7.43 – 7.32 (m, 5H), 5.38 (s, 1H), 3.65 – 3.50 (m, 1H), 2.92 (q, $J = 8.8$ Hz, 1H), 2.75 – 2.60 (m, 1H), 2.47 – 2.25 (m, 1H), 1.97 – 1.89 (m, 2H), 1.89 – 1.67 (m, 4H), 1.64 – 1.08 (m, 5H), 1.01 (s, 9H).

^{13}C NMR (151 MHz, CDCl_3) δ : 206.3, 204.6, 202.7, 197.5, 135.7, 134.1, 134.0, 129.7, 127.7, 103.3, 93.7, 63.6, 59.7, 54.0, 46.3, 44.1, 39.9, 39.1, 36.8, 34.9, 34.9, 34.5, 33.8, 32.7, 30.2, 30.1, 29.9, 26.9, 26.7, 26.1, 25.8, 25.8, 25.7, 25.7, 19.3, 19.3, 19.2, 18.9, 16.0.

TLC: 20% ethyl acetate–hexanes, $R_f = 0.39$, (UV, CAM).

Synthesis of TBS-protected 1,6-hexanediol 3.31



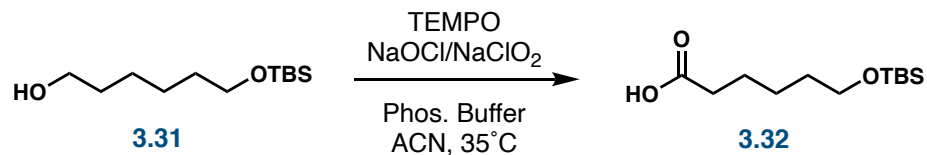
A solution of *tert*-butyldimethylchlorosilane (10.1 g, 66.7 mmol, 1 equiv) in dichloromethane (100 mL) was added dropwise via addition funnel to a stirred solution of hexane-1,6-diol (11.8 g, 100.0 mmol, 1.50 equiv) and triethylamine (13.9 mL, 100 mmol, 1.50 equiv.) in dichloromethane at 0°C. The solution was warmed to 22°C and stirred at that temperature for 16 h. The resultant solution was diluted with water (100 mL) and the aqueous layer was extracted with ethyl acetate (3 × 30 mL). The combined organic layers were washed with water (60 mL) and brine (60 mL) before being dried over anhydrous sodium sulfate. The dried solution was concentrated, then was purified using flash column chromatography (silica gel, starting with 5% ethyl acetate–hexanes, grading to 20% ethyl acetate–hexanes) to afford a clear, colorless oil (9.74 g, 41.9 mmol, 63%).

¹H NMR (400 MHz, CDCl₃) δ: 3.61 (dt, $J_1 = 12.9$, $J_2 = 6.5$ Hz, 4H), 1.60 – 1.45 (m, 4H), 1.36 (t, $J = 6.4$ Hz, 4H), 0.88 (s, 9H), 0.04 (s, 6H).

¹³C NMR (101 MHz, CDCl₃) δ: 63.3, 63.1, 32.9, 32.9, 26.1, 25.8, 25.7, 18.5, -5.1.

TLC: 20% ethyl acetate–hexanes, $R_f = 0.32$,
(KMnO₄, CAM).

Synthesis of Carboxylic Acid 3.32



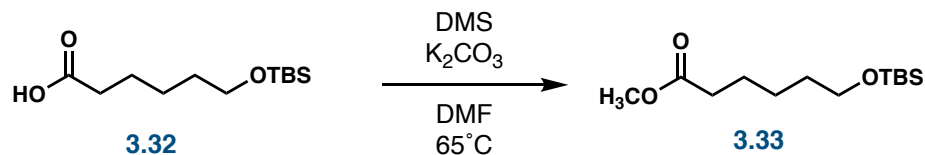
A solution of aqueous sodium hypochlorite (0.28%, 11 mL, 0.43 mmol, 0.020 equiv) and a solution of aqueous sodium chlorite (2.0 M, 22 mL, 44 mmol, 2.0 equiv) were added simultaneously dropwise via addition funnel to a stirred solution of alcohol **3.31** (5.1 g, 22 mmol, 1 equiv), TEMPO (240 mg, 1.5 mmol, 0.070 equiv), and phosphate buffer (0.02 M, 80 mL, pH 6.7) in acetonitrile (100 mL) over a 2-hour period at 35°C. The solution was stirred for 4 h, whereupon it was cooled to 22°C, water (100 mL) was added, and the pH of the solution was adjusted to 8 using potassium hydroxide. The solution was cooled to 0°C, whereupon the remaining oxidant was quenched using aqueous sodium sulfite (6.1%, 100 mL). The resultant solution was warmed to 22°C and was stirred for 30 min at that temperature. Diethyl ether (75 mL) was added, and the resultant biphasic solution was adjusted to pH 3-4 using aqueous 2 M HCl. The aqueous layer was discarded, and the organic layer was washed with water (2 x 40 mL) and brine (40 mL). The solution was dried over anhydrous sodium sulfate, and the dried solution was concentrated to afford a clear, colorless oil (4.42 g, 17.9 mmol, 82%).

¹H NMR (600 MHz, CDCl₃) δ: 3.61 (t, *J* = 6.5 Hz, 2H), 2.36 (td, *J*₁ = 7.6, *J*₂ = 1.7 Hz, 2H), 1.65 (p, *J* = 6.6 Hz, 2H), 1.53 (p,

$J = 6.6$ Hz, 2H), 1.43 – 1.35 (m, 2H), 0.89 (s
9H), 0.04 (s, 6H).

^{13}C NMR (151 MHz, CDCl_3) δ : 180.1, 63.1, 34.2, 32.6, 26.1, 25.5, 24.6, 18.5, -
5.2.

Synthesis of Ester 3.33



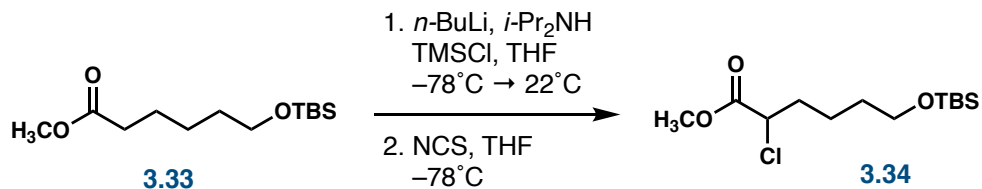
Dimethyl sulfate (3.4 mL, 36 mmol, 2.0 equiv) was added dropwise to a stirred solution of carboxylic acid **3.32** (4.42 g, 17.9 mmol, 1 equiv) and potassium carbonate (7.4 g, 54 mmol, 1.1 equiv) in DMF (50 mL) at 65°C. The resultant solution was stirred for 23 h, whereupon the solution was cooled to 0°C and water (90 mL) was added. The aqueous layer was extracted with dichloromethane (3 x 60 mL). The combined organic layers were washed with water (90 mL) and brine (90 mL) before being dried over anhydrous sodium sulfate. The dried solution was concentrated, then was adhered to silica and purified using flash column chromatography (silica gel, starting with 5% ethyl acetate–hexanes, grading to 10% ethyl acetate–hexanes) to afford a clear, yellow oil (4.06 g, 15.6 mmol, 87 %).

¹H NMR (600 MHz, CDCl₃) δ: 3.66 (s, 3H), 3.60 (t, *J* = 6.5 Hz, 2H), 2.31 (t, *J* = 7.6 Hz, 2H), 1.64 (p, *J* = 7.6 Hz, 2H), 1.59 – 1.49 (m, 2H), 1.40 – 1.32 (m, 2H), 0.89 (s, 9H), 0.04 (s, 6H).

¹³C NMR (151 MHz, CDCl₃) δ: 174.3, 63.1, 51.6, 34.3, 32.6, 26.1, 25.6, 24.9, 18.5, -5.2.

TLC: 20% ethyl acetate–hexanes, $R_f = 0.79$,
(KMnO_4).

Synthesis of α -chloroester 3.34



A solution of *n*-butyllithium (2.50 M, 6.88 mL, 17.2 mmol, 1.10 equiv) was added to a stirred solution of *N,N*-diisopropylamine (2.43 mL, 17.2 mmol, 1.10 equiv) in THF (35 mL) at -78°C . The resultant solution was warmed briefly to 0°C , then was cooled to -78°C whereupon chlorotrimethylsilane (2.18 mL, 17.2 mmol, 1.10 equiv) was added followed by a dropwise addition of a solution of ester **3.33** (4.06 g, 15.6 mmol, 1 equiv) in THF (10 mL). The resultant solution was stirred at 22°C for 3 h, whereupon the solution was concentrated carefully to afford the crude silyl enol ether. The clear, yellow oil is taken up in pentane, filtered over celite, and concentrated. A solution of *N*-chlorosuccinimide (2.30 g, 17.2 mmol, 1.10 equiv) in THF (80 mL) is added dropwise to a stirred solution of the crude silyl enol ether in THF (80 mL) at -78°C . The solution is stirred for 16 h, whereupon the excess *N*-chlorosuccinimide is quenched using saturated aqueous sodium thiosulfate solution (30 mL). The organic layer is dried over anhydrous sodium sulfate and concentrated. The crude chloroester **3.34** is taken up in hexanes, filtered, and concentrated. Purification by flash column chromatography (silica gel, starting with 1% diethyl ether–hexanes, grading to 3% diethyl ether–hexanes) afforded a clear, yellow oil (4.32 g, 14.6 mmol, 94%).

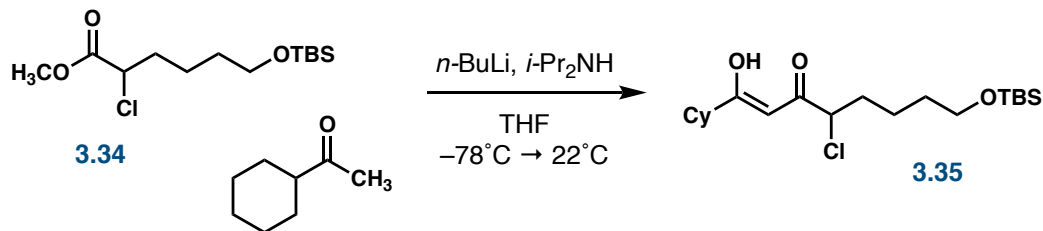
^1H NMR (600 MHz, CDCl_3) δ : 4.28 (dd, $J_1 = 8.1$, $J_2 = 6.0$ Hz, 1H), 3.78 (s, 3H), 3.61 (t, $J = 6.0$ Hz, 2H), 2.11 – 1.87 (m,

2H), 1.56 – 1.38 (m, 4H), 0.88 (s, 9H), 0.04 (s, 6H).

^{13}C NMR (151 MHz, CDCl_3) δ : 170.4, 62.8, 57.3, 53.0, 34.9, 32.1, 26.1, 22.6, 18.5, -5.2.

TLC: 5% ethyl acetate–hexanes, $R_f = 0.50$, (UV, KMnO_4).

Synthesis of Chlorodiketone 3.35



A solution of *n*-butyllithium (2.50 M, 2.3 mL, 5.9 mmol, 1.5 equiv) was added to a stirred solution of *N,N*-diisopropylamine (0.88 mL, 6.2 mmol, 1.6 equiv) in THF (50 mL) at -78°C . The resultant solution was warmed briefly to 0°C , then was cooled to -78°C , whereupon a solution of cyclohexyl methyl ketone (0.76 mL, 5.5 mmol, 1.4 equiv) in THF (8 mL) was added dropwise. The resultant solution was stirred at -78°C for 30 min, whereupon a solution of chloroester **3.34** (1.2 g, 4.0 mmol, 1 equiv) in THF (5 mL) was added. The resultant solution was warmed to 22°C and stirred at that temperature for 8 h. The resultant cloudy, orange solution was cooled to 0°C and the excess base was quenched with saturated aqueous ammonium chloride solution (20 mL). The layers were separated, and the aqueous layer was extracted with dichloromethane (3 x 30 mL). The combined organic layers were dried over anhydrous sodium sulfate and the dried solution was concentrated. Purification of the residue by flash column chromatography (silica gel, starting with 1% diethyl ether–hexanes, grading to 3% diethyl ether–hexanes), afforded **3.35** as a clear, yellow oil (1.12 g, 2.88 mmol, 72%).

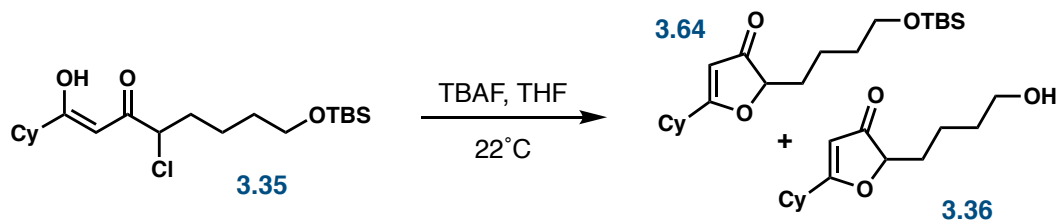
^1H NMR (600 MHz, CDCl_3) δ : 15.22 (s, 1H), 5.80 (s, 1H), 4.21 (dd, $J = 8.3, 5.6$ Hz, 1H), 3.64 – 3.56 (m, 3H), 2.37 – 2.28

(m, 1H), 2.23 (tt, $J_1 = 11.6$, $J_2 = 5.7$ Hz, 1H),
2.12 (s, 1H), 2.05 – 1.98 (m, 1H), 1.95 – 1.75
(m, 7H), 1.73 – 1.64 (m, 2H), 1.60 – 1.50 (m,
4H), 1.50 – 1.43 (m, 1H), 1.43 – 1.36 (m, 2H),
1.36 – 1.24 (m, 1H), 1.24 – 1.16 (m, 1H), 0.89
(s, 9H), 0.04 (s, 6H).

^{13}C NMR (151 MHz, CDCl_3) δ : 197.3, 191.8, 95.5, 62.7, 61.6, 46.3, 35.1, 32.1,
29.5, 28.5, 25.9, 25.8, 25.7, 25.7, 22.7, 18.3, -
5.3.

TLC: 5% ethyl acetate–hexanes, $R_f = 0.64$, (UV,
CAM).

Synthesis of Furnaones 3.36 and 3.64



Tetrabutylammonium fluoride (3.5 mL, 3.5 mmol, 2.5 equiv.) was added to a stirred solution of chlorodiketone **3.35** (0.76 g, 1.5 mmol, 1 equiv.) in THF (15 mL) at 22°C. The resultant yellow solution was stirred at 22°C for 1 h, whereupon water (5 mL) was added. The mixture was extracted with dichloromethane (3 x 15 mL) and the combined organic layers were washed with saturated aqueous ammonium chloride solution. The combined organic layers were dried over anhydrous sodium sulfate and the dried solution was concentrated. Purification of the residue using flash column chromatography (silica gel, starting with 5% ethyl acetate–hexanes, grading to 100% ethyl acetate–hexanes) afforded **3.64** as a clear, yellow oil (197 mg, 0.56 mmol, 40%) and **3.36** as a clear, yellow oil (104 mg, 0.44 mmol, 31%).

Furanone 3.64:

^1H NMR (600 MHz, CDCl_3) δ : 5.37 (s, 1H), 4.40 (dd, $J = 7.7, 4.1$ Hz, 1H), 3.65 – 3.55 (m, 2H), 2.47 – 2.37 (m, 1H), 2.01 – 1.89 (m, 3H), 1.89 – 1.76 (m, 2H), 1.76 – 1.63 (m, 2H), 1.60 – 1.50 (m, 2H), 1.50 – 1.42 (m, 2H), 1.42 – 1.30 (m, 4H), 1.30 – 1.22 (m, 1H), 0.88 (s, 10H), 0.03 (s, 6H).

^{13}C NMR (151 MHz, CDCl_3) δ : 205.3, 197.9, 101.7, 86.0, 62.9, 39.9, 32.6, 31.2, 30.1, 29.9, 26.1, 25.9, 25.7, 25.7, 21.1, 18.5, -5.2.

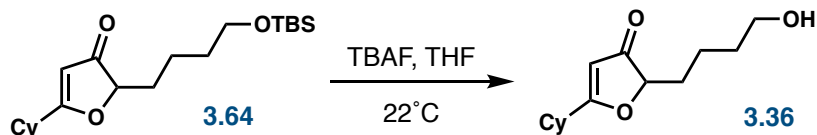
TLC: 5% ethyl acetate–hexanes, $R_f = 0.08$, (UV, CAM).

Furanone 3.36:

^1H NMR (600 MHz, CDCl_3) δ : 5.35 (s, 1H), 4.38 (dd, $J_1 = 7.7$, $J_2 = 4.2$ Hz, 1H), 3.60 (t, $J = 6.5$ Hz, 2H), 2.41 (tt, $J_1 = 11.1$, $J_2 = 3.6$ Hz, 1H), 1.98 – 1.85 (m, 4H), 1.82 – 1.73 (m, 2H), 1.72 – 1.61 (m, 2H), 1.61 – 1.51 (m, 2H), 1.51 – 1.42 (m, 2H), 1.42 – 1.26 (m, 5H), 1.26 – 1.17 (m, 1H).

^{13}C NMR (151 MHz, CDCl_3) δ : 205.4, 198.1, 101.6, 85.8, 62.4, 39.8, 32.3, 31.0, 29.9, 29.8, 25.8, 25.59, 25.58, 20.9.

Synthesis of Alcohol 36

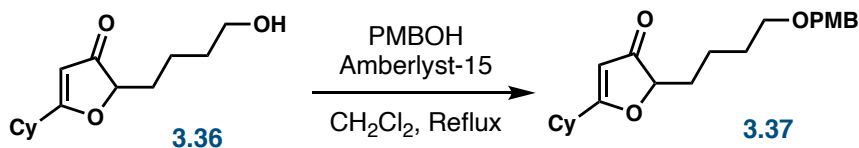


Tetrabutylammonium fluoride (2.5 mL, 2.5 mmol, 2.5 equiv.) was added to a stirred solution of furanone **3.64** (350 mg, 1.0 mmol, 1 equiv.) in THF (10 mL) at 22°C. The resultant bright yellow solution was stirred at 22°C for 2.5 h, whereupon water (5 mL) was added. The mixture was extracted with dichloromethane (3 x 15 mL) and the combined organic layers were washed with saturated aqueous ammonium chloride solution. The combined organic layers were dried over anhydrous sodium sulfate and the dried solution was concentrated. Purification of the residue using flash column chromatography (silica gel, starting with 20% ethyl acetate–hexanes, grading to 100% ethyl acetate–hexanes) afforded **3.36** as a clear, yellow oil (113 mg, 0.475 mmol, 47%).

$^1\text{H NMR}$ (600 MHz, CDCl_3) δ : 5.35 (s, 1H), 4.38 (dd, $J_1 = 7.7$, $J_2 = 4.2$ Hz, 1H), 3.60 (t, $J = 6.5$ Hz, 2H), 2.41 (tt, $J_1 = 11.1$, $J_2 = 3.6$ Hz, 1H), 1.98 – 1.85 (m, 4H), 1.82 – 1.73 (m, 2H), 1.72 – 1.61 (m, 2H), 1.61 – 1.51 (m, 2H), 1.51 – 1.42 (m, 2H), 1.42 – 1.26 (m, 5H), 1.26 – 1.17 (m, 1H).

^{13}C NMR (151 MHz, CDCl_3) δ : 205.4, 198.1, 101.6, 85.8, 62.4, 39.8, 32.3,
31.0, 29.9, 29.8, 25.8, 25.59, 25.58, 20.9.

Synthesis of PMB ether 3.37



A heterogeneous mixture of alcohol **3.36** (220 mg, 0.91 mmol, 1 equiv), anisyl alcohol (0.22 mL, 1.8 mmol, 2.0 equiv), and Amberlyst-15 ion exchange resin (20 mg, 10% by weight) in dichloromethane (10 mL) was heated at reflux for 48 h. The mixture was cooled to 22°C, whereupon the solution was diluted with dichloromethane (10 mL) and water (10 mL). The aqueous layer was extracted with dichloromethane (3 x 10 mL) and the combined organic layers were washed with brine (15 mL). The resultant solution was dried over anhydrous sodium sulfate, concentrated, and adhered to silica for purification using flash column chromatography (silica gel, starting with 10% ethyl acetate–hexanes, grading to 22% ethyl acetate–hexanes) to afford **3.37** as a clear, yellow oil (157 mg, 0.439 mmol, 48%).

¹³C NMR (101 MHz, CDCl₃) δ: 205.4, 198.1, 159.3, 133.2, 129.4, 128.8, 114.1, 113.9, 72.7, 69.8, 65.2, 55.4, 39.8, 31.1, 30.0, 29.9, 29.5, 25.8, 25.7, 21.5.

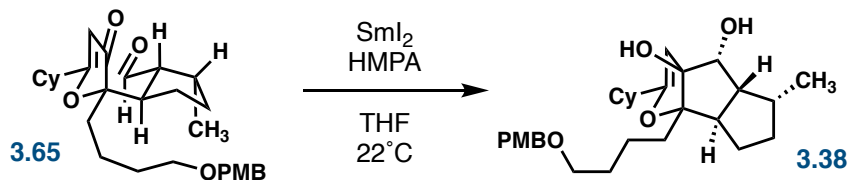
TLC: 40% ethyl acetate–hexanes, R_f = 0.57, (UV, CAM).

^1H NMR (600 MHz, CDCl_3) δ : 9.63 (d, $J = 3.3$ Hz, 1H), 7.24 – 7.19 (m, 3H), 6.91 – 6.88 (m, 1H), 6.88 – 6.83 (m, 3H), 5.38 (d, $J = 7.6$ Hz, 1H), 4.38 (s, 3H), 3.80 (d, $J = 4.8$ Hz, 6H), 3.40 – 3.30 (m, 3H), 3.00 – 2.86 (m, 1H), 2.75 – 2.62 (m, 1H), 2.48 – 2.25 (m, 3H), 2.04 (s, 3H), 1.99 – 1.90 (m, 4H), 1.85 – 1.68 (m, 9H), 1.55 – 1.46 (m, 2H), 1.45 – 1.27 (m, 5H), 1.16 – 1.07 (m, 1H), 1.00 (d, $J = 12.0$ Hz, 3H).

^{13}C NMR (151 MHz, CDCl_3) δ : 206.3, 204.6, 202.7, 197.5, 159.2, 130.8, 129.9, 129.3, 128.8, 114.1, 113.8, 113.8, 103.5, 103.3, 93.6, 72.7, 72.6, 69.7, 65.2, 60.6, 59.7, 55.4, 55.4, 55.4, 54.0, 46.1, 44.0, 39.9, 39.0, 36.8, 34.8, 34.8, 34.5, 33.8, 30.1, 30.1, 29.9, 29.8, 26.7, 26.0, 25.8, 25.71, 25.65, 21.2, 19.5, 19.4, 18.9, 16.0, 14.3.

TLC: 10% ethyl acetate–hexanes, $R_f = 0.11$, (UV, CAM).

Synthesis of Diol 3.38



A freshly prepared solution of samarium (II) iodide in THF (0.10 M, 8.5 mL, 0.85 mmol, 4.0 equiv) was added dropwise via cannula over 1 h to a stirred solution of **3.65** (100 mg, 0.213 mmol, 1 equiv) and hexamethylphosphoramide (0.69 mL, 3.9 mmol, 19 equiv) in THF (10 mL) at 22°C. The resultant solution was stirred for 4 h, whereupon the reaction mixture was cooled to 0°C and excess SmI₂ was quenched using aqueous 1 M HCl (5 mL). The aqueous layer is extracted with dichloromethane (3 x 20 mL). The combined organic layers were washed with saturated aqueous sodium bicarbonate solution (30 mL), dried over anhydrous sodium sulfate, and concentrated. Purification of the residue by flash column chromatography (silica gel, starting with 5% ethyl acetate–hexanes, grading to 30% ethyl acetate–hexanes) afforded diol **3.38** as a yellow oil (16 mg, 0.034 mmol, 16%).

¹H NMR (600 MHz, CDCl₃) δ: 7.26 (d, *J* = 7.1 Hz, 2H), 6.87 (d, *J* = 8.7 Hz, 2H), 4.43 (s, 2H), 4.34 (s, 1H), 3.80 (s, 4H), 3.45 (td, *J*₁ = 5.2, *J*₂ = 2.7 Hz, 2H), 2.46 (ddd, *J*₁ = 14.8, *J*₂ = 10.8, *J*₃ = 6.6 Hz, 1H), 2.35 – 2.29 (m, 1H), 2.28 – 2.19 (m, 1H), 2.18 – 2.08 (m, 1H), 2.07 – 2.00 (m, 1H), 1.88 – 1.82 (m,

2H), 1.79 (ddd, $J_1 = 14.8$, $J_2 = 7.5$, $J_3 = 3.0$ Hz, 1H), 1.76 – 1.69 (m, 1H), 1.68 – 1.57 (m, 4H), 1.56 – 1.48 (m, 2H), 1.48 – 1.36 (m, 2H), 1.31 – 1.12 (m, 5H), 1.02 (d, $J = 7.2$ Hz, 3H).

^{13}C NMR (151 MHz, CDCl_3) δ : 169.1, 159.2, 131.0, 129.4, 113.9, 97.6, 96.3, 91.7, 75.1, 72.6, 70.2, 55.4, 51.1, 50.9, 37.8, 37.6, 34.8, 30.9, 30.4, 30.4, 28.9, 26.3, 26.0, 26.0, 22.0, 20.9, 19.3.

REFERENCES

1. (a) Liu, Y.; Patricelli, M. P.; Cravatt, B. F. *Proceedings of the National Academy of Sciences* **1999**, *96*, 14694-14699. (b) Bogyo, M.; Baruch, A.; Jeffery, D. A.; Greenbaum, D.; Borodovsky, A.; Ovaas, H.; Kessler, B. *Curr Protoc Protein Sci* **2004**, *Chapter 21*, 21 17 21-21 17 35. (c) Bantscheff, M.; Drewes, G. *Bioorg. Med. Chem.* **2012**, *20*, 1973-1978. (d) Browne, C. M.; Jiang, B.; Ficarro, S. B.; Doctor, Z. M.; Johnson, J. L.; Card, J. D.; Sivakumaren, S. C.; Alexander, W. M.; Yaron, T. M.; Murphy, C. J.; et al. *J. Am. Chem. Soc.* **2019**, *141*, 191-203. (e) Crews, C. M.; Collins, J. L.; Lane, W. S.; Snapper, M. L.; Schreiber, S. L. *J. Biol. Chem.* **1994**, *269*, 15411-15414. (f) Moellering, R. E.; Cravatt, B. F. *Chem Biol* **2012**, *19*, 11-22. (g) Knockaert, M.; Gray, N.; Damiens, E.; Chang, Y. T.; Grellier, P.; Grant, K.; Fergusson, D.; Mottram, J.; Soete, M.; Dubremetz, J. F.; et al. *Chemistry & Biology* **2000**, *7*, 411-422. (h) Kidd, D.; Liu, Y.; Cravatt, B. F. *Biochemistry* **2001**, *40*, 4005-4015. (i) Harding, M. W.; Galat, A.; Uehling, D. E.; Schreiber, S. L. *Nature* **1989**, *341*, 758-760. (j) Cuatrecasas, P.; Wilchek, M.; Anfinsen, C. B. *Proceedings of the National Academy of Sciences* **1968**, *61*, 636-643. (k) Chen, X.; Wang, Y.; Ma, N.; Tian, J.; Shao, Y.; Zhu, B.; Wong, Y. K.; Liang, Z.; Zou, C.; Wang, J. *Signal Transduction and Targeted Therapy* **2020**, *5*.
2. (a) Wu, Z.; Zhao, S.; Fash, D. M.; Li, Z.; Chain, W. J.; Beutler, J. A. *J. Nat. Prod.* **2017**, *80*, 771-781. (b) Radtke, L.; Willot, M.; Sun, H.; Ziegler, S.; Sauerland, S.; Strohmam, C.; Fröhlich, R.; Habenberger, P.; Waldmann, H.; Christmann, M. *Angew. Chem. Int. Ed.* **2011**, *50*, 3998-4002.
3. Zhao, M.; Li, J.; Mano, E.; Song, Z.; Tschaen, D. M.; Grabowski, E. J. J.; Reider, P. J. *The Journal of Organic Chemistry* **1999**, *64*, 2564-2566.
4. (a) Khademi, Z.; Heravi, M. M. *Tetrahedron* **2022**, *103*. (b) Claisen, R. L.; Lowman, O. *Ber.* **1887**, *20*, 651-654.
5. (a) Michael, A. *J. Prakt. Chem.* **1883**, *35*, 349. (b) Hagiwara, H. *Natural Product Communications* **2021**, *16*.
6. (a) Wittig, G.; Fritze, P. *Angewandte Chemie International Edition in English* **2003**, *5*, 846-846. (b) Heravi, M. M.; Zadsirjan, V.; Hamidi, H.; Daraie, M.; Momeni, T. Recent applications of the Wittig reaction in alkaloid synthesis.

Elsevier, 2020; pp 201-334(c) Schlosser, M.; Christmann, K. F. *Angewandte Chemie International Edition in English* **2003**, 5, 126-126.

7. (a) Neises, B.; Steglich, W. *Angewandte Chemie International Edition in English* **1978**, 17, 522-524. (b) Jordan, A.; Whymark, K. D.; Sydenham, J.; Sneddon, H. F. *Green Chemistry* **2021**, 23, 6405-6413.

Chapter 4

SYNTHESIS OF AN ACYLDEPSIPEPTIDE FLUORESCENT MECHANISTIC PROBE

4.1 Introduction to Clp

Antibiotic development is a hotly pursued field of science that is urgently expanding due to the nature of bacterial evolution. Bacterial pathogens can become increasingly more resistant to routine and front-line antibiotics enhancing the need to develop novel antibiotics with new mechanisms of action. One series of targets of increasing interest recently are the proteolytic complexes formed between ClpP and the AAA+ partners.¹ AAA+ is an acronym for “ATPases associated with diverse cellular activities” and are necessary for the recognition of substrates and regulation of the proteolytic activity of ClpP. ClpP is a tetradecameric serine peptidase that is only active when associated with AAA+ unfoldases such as ClpX, ClpC, and ClpA.²

In their active form, these proteases selectively degrade misfolded proteins and native protein targets involved in regulating stress responses and virulence-factor production.³ This process begins with two heptameric Clp rings stacking “face to face” forming a barrel-shaped heterotetradecameric channel that acts as a proteolytic chamber. This chamber is large enough to accommodate hundreds of amino acids and consists of 14 active sites where serine peptidases may bind. At the ends of the chamber are narrow passageways that are nearly inaccessible without the assistance of AAA+ partners. The AAA+ promote the entry of proteins through these openings after binding, unfolding, and translocating these substrates into the proteolytic chamber.

These conformational changes allowing this process to occur are driven by ATP hydrolysis after association of the heterotetrameric channel with AAA+ partners.^{2a, d, 3i, 4} Without the association of this channel with AAA+ partners, only small peptides with the ability to diffuse into the channel through pores can be degraded by this protease.⁵

4.1.1 Clp in *Mycobacterium tuberculosis*

These enzymes are essential for virulence in some pathogenic bacteria such as *Mycobacterium tuberculosis* (*Mtb*) highlighting them as appealing targets for antibiotic development.⁶ One feature unique to *Mtb* is that it has two co-transcribed genes, *clpP1* and *clpP2*. Each of the respective cognate gene products *Mtb* ClpP1 and ClpP2 form heptameric rings that are inactive by themselves but active upon heterotetradecamer formation. The assembly of this ClpP1P2 is stabilized by its interaction with ClpX or ClpC1, the active translocation of proteins into the degradation chamber, or the binding of N-blocked peptide agonists that are able to mimic the substrate interactions within the active site.⁷

4.1.2 Acyldepsipeptides (ADEPs) – Introduction and bioactivity

One such class of “agonists” with the ability to mimic these substrate binding interactions is the acyldepsipeptide antibiotics (figure 4.1). The ADEPs feature a potent antibacterial activity against Gram-positive bacterial pathogens, and one cellular target of this class of antibiotics is the ClpP peptidase.^{2a, 6a, c, 8}

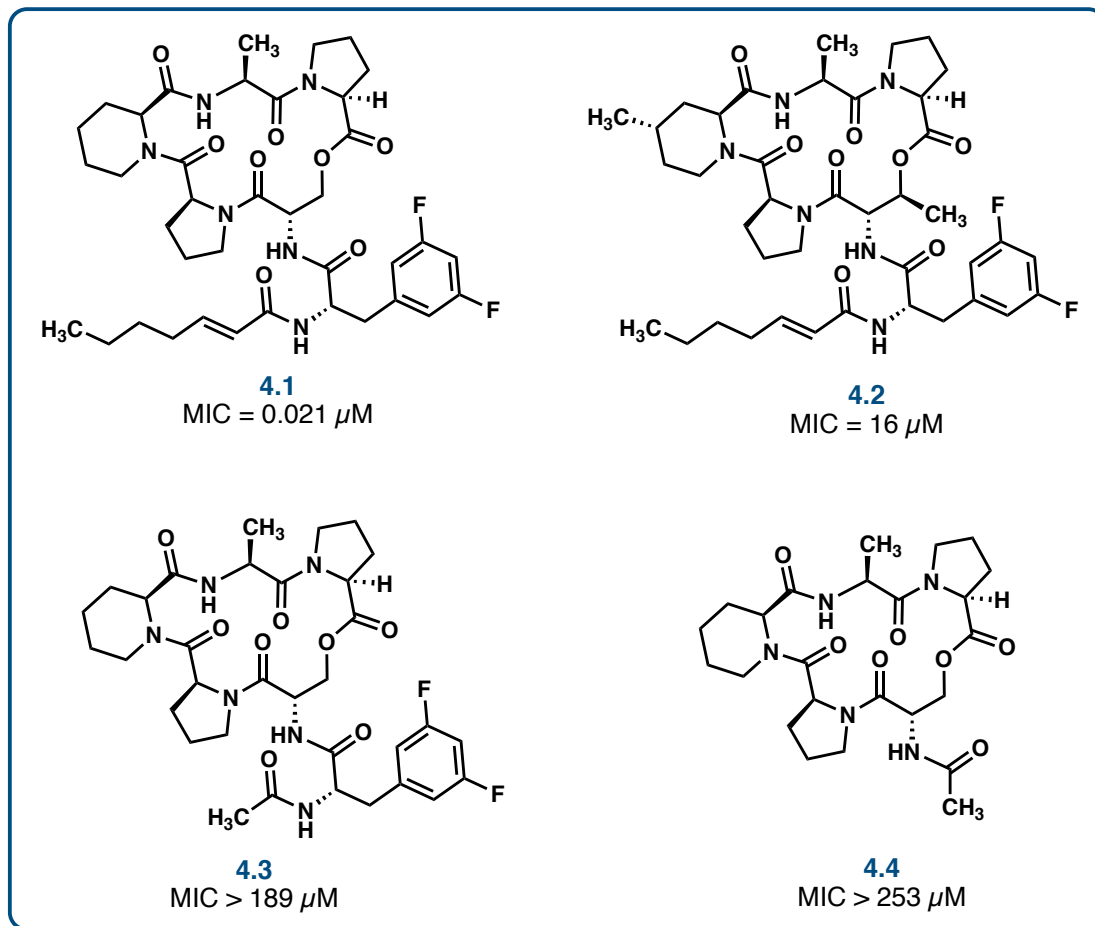


Figure 4.1 Examples of acyldepsipeptide antibiotics

Within *Mtb*, the ADEPs competitively bind to an active site on the heterotetradecamer causing an inhibition of the Clp protease activity. They are able to bind within the same hydrophobic pockets as the AAA+ partners and typically bind by mimicking the LGF loops present in the AAA+ partners.^{6b, c, 7e, 9} The binding of these ADEPs within these active sites leads to a widening of the axial pores at the ends of the channels allowing for the acceptance of a wider variety of proteins into the channel. It can now indiscriminately accept and degrade larger peptides and

unstructured proteins lacking the proper degrons eventually leading to an inhibition of cell division and ultimately cell and bacterial death.^{8a, b, 10}

4.1.3 ADEP Fragments and Analogues

In order to develop a structure-activity relationship of these ADEPs, a variety of analogues were synthesized and biologically evaluated (figure 4.1). Through these studies, it was determined that the *N*-acyl phenylalanine portion of the structure is imperative for its activity, which can be seen by the synthesis of analogues **4.3** and **4.4**. It was suggested that this is the portion of the molecule that mimics the LGF loop allowing for the favorable interactions and binding with Clp proteases.^{5, 11}

With this realization, people began exploring truncated analogues featuring this portion of the molecule, known as ADEP fragments (figure 4.2). It was found that many of these simplified analogues featuring the *N*-acyl phenylalanine portion, retained some of the antibacterial activity against *Mtb*. These fragments offer the benefit of a quicker and more facile synthesis of analogues along with a faster exploration of structural differences. Upon an investigation into the mechanism of action of these ADEP fragments within *Mtb*, it is apparent that they interact differently than the full cyclic ADEPs do.⁵

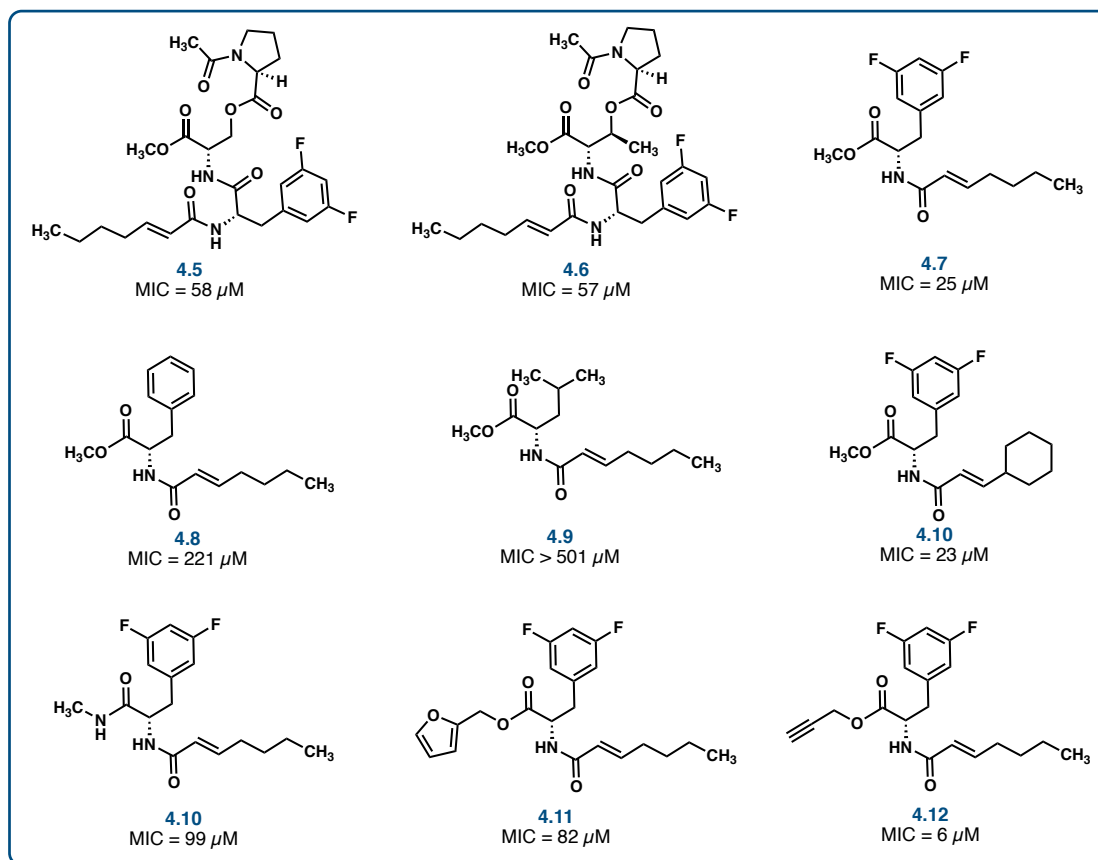


Figure 4.2 Selected acyldepsipeptide fragments and their minimum inhibitory concentrations

It is suggested that they bind to a distinct site on the ClpP1P2 and stabilize the ClpXP1P2 complex. Through this stabilization, they are able to enhance the rate of ATP-dependent degradation of protein substrates by ClpXP1P2. This mechanism is still unclear and is in need of further investigation. There were three suggested mechanisms of action resulting from this stabilization that could lead to the antibacterial activity observed. The first is that an activation of the ClpXP1P2 leads to the degradation of proteins essential for viability of the cell disrupting the regulatory

processes. One example provided is the degradation of a protein that accumulates at a specific point within the cell cycle, that when not present at a high enough concentration, leads to cell cycle arrest.⁵

The second possible mechanism of action resulting from the stabilization of ClpXP1P2 is the disruption of the interaction between ClpC1 and ClpP1P2. This disruption could lead to the inhibition of essential proteolytic processes that are typically carried out by ClpP1P2. Without these processes, the death of the cell and bacteria follow. The final theory is that the stabilization of binding between ClpX and ClpP1P2 sequester the tetradecamer away from ClpC1, which may be a necessary interaction in order to perform essential proteolytic duties. Another suggestion is that it may indeed act in the same manner as the ADEPs and that the exact mechanism of action may change based on a number of parameters such as binding affinity or intracellular concentration.⁵

In order to truly understand these interactions, further investigation into the mechanisms of action must take place. As mentioned previously, one possibility in the execution of this exploration is through the use of tool compounds.

4.2 ADEP Fragment Tool Compound Exploration

In a collaboration with Profs. Joseph M. Fox and Karl Schmitz, we worked to develop an acyldepsipeptide fragment fluorescent mechanistic probe compound. We evaluated possible ADEP fragment fluorescent probe targets and the effects that various changes in the structure may impart on the physiological properties of the compound, and we settled on the fluorescent probe **4.13** (figure 4.3). This is a variation of the ADEP fragment **4.5**¹¹ but features an ethylene diamine linker connecting the TAMRA fluorophore to a serine found within the peptide chain.

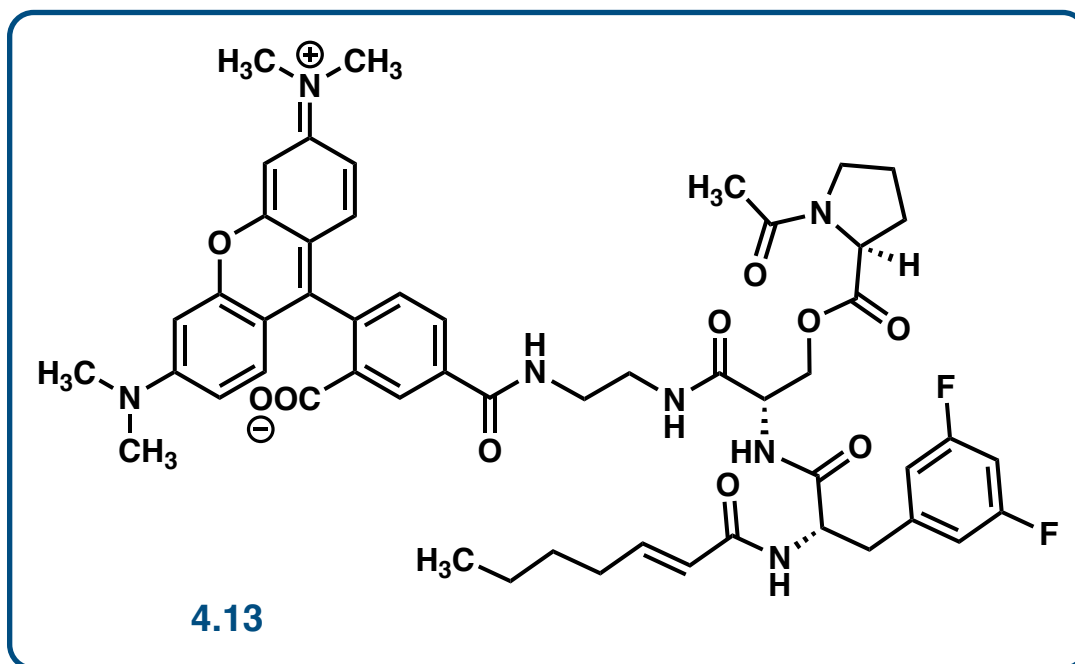


Figure 4.3 Acyldepsipeptide fragment fluorescent probe compound

4.2.1 Prior Synthesis of the ADEPs and their Fragments

The ADEP fragment of the mechanistic probe compound is based on a known material (**4.5** in figure 4.4) previously synthesized by Jason Sello et al. in 2014.¹¹ The synthesis of this ADEP fragment began with *Z*-*L*-serine methyl ester **4.14**. A Stelgich¹² esterification coupling *N*-Boc-*L*-proline to the free alcohol of the serine ester affords diester **4.15** in a 97% yield. Replacing the Boc protecting group with the acetyl group present in the final fragment was accomplished through a Boc deprotection under the action of TFA followed by treatment of the resultant free amine with acetic anhydride under basic conditions. This replacement afforded the amide **4.16** in 85% over the two steps. Hydrogenolysis of the Cbz protecting group reveals the primary amine that then participates in an amide coupling with *N*-Boc-difluorophenylalanine using HATU and *i*-Pr₂NEt. Removal of the Boc group by

treatment with TFA allowed for the final amide coupling of (*E*)-2-heptenoic acid with HATU and *i*-Pr₂NEt to afford the final product **4.5** in 72% yield over the final four steps. This route is simple and high-yielding, so my plan was to follow this route as much as possible in the synthesis of the fluorescent probe.

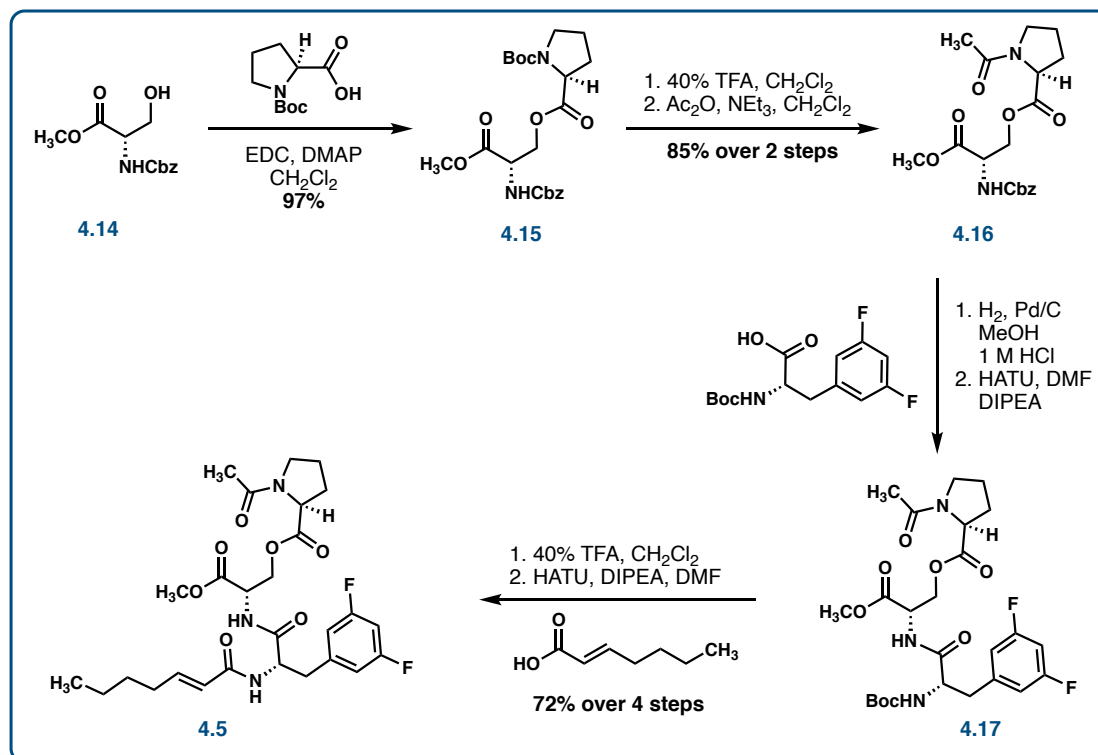


Figure 4.4 Previous synthesis of the acyldepsipeptide fragment **4.5** by Jason Sello et al.

4.2.2 Synthesis of ADEP Fluorescent Probe Compound

There will have to be some modifications made to this route though in order to install the ethylene diamine linker that can be deprotected at the end to participate in an amide coupling with the fluorophore. The struggle we faced was finding a

protecting group that lacked redundant functionality, could withstand the conditions exposed to throughout the synthesis, and that could be selectively removed at the end of the synthesis without interfering with any other portion of the molecule.

After sifting through possible options of protecting groups and determining our best protecting group strategy, we determined that the 2-(trimethylsilyl)ethoxycarbonyl (Teoc) protecting group was most suitable for this route. We anticipated the possibility of a struggle during the deprotection of the Boc groups due to the slight acid sensitivity of the Teoc group. As Louis A. Carpio in 1978 worded it, "...this sensitivity toward acids makes it impossible to use this group in conjunction with *t*-BOC..."¹³ Nevertheless, we found a couple potential ways to selectively remove the Boc group in the presence of a Teoc group, so we decided to go for it anyway. We also were able to purchase the acetyl-protected proline, allowing for the avoidance of one of the Boc deprotection steps.

The synthesis of this fluorescent probe is initiated with the preparation of the Teoc-protected ethylene diamine linker. After screening a variety of polar solvents, we found that the reaction between ethylene diamine and Teoc succinimide proceeds relatively smoothly in DMF, but there were immediately issues during the isolation and purification processes. Due to the high polarity of the monoprotected product, extraction from the aqueous layer proved to be difficult, but was overcome with the addition of a small amount of triethylamine into the biphasic mixture of ethyl acetate, DMF, and water during the extraction. The addition of the triethylamine was used to coax the transfer of the product into the organic layer. Once separated, the purification of the compound was accomplished by pushing the mixture through a short plug of silica gel with the highly polar solvent system of ethyl acetate, isopropanol, and water.

Once the optimal extraction, isolation, and purification conditions were determined the overall reaction afforded the linker at a 64% yield.

The amide coupling of the linker to *Z*-*L*-serine was accomplished using the coupling agent HATU along with *i*-Pr₂NEt in DMF to affording amide **4.18** in a 96% yield as shown in figure 4.5. From here, the free alcohol of the serine can participate in an ester coupling with *N*-acetyl-*L*-proline under Steglich¹² conditions using EDC as a coupling agent to afford peptide **4.19** in an 84% yield. Hydrogenolysis of the Cbz group using H₂ and Pd/C afforded the free amine in quantitative yield. Upon our first attempt to couple the resultant free amine to *N*-Boc-difluorophenylalanine using HATU and *i*-Pr₂NEt, we obtained the desired product in the low yield of 41%. Switching from HATU and *i*-Pr₂NEt to EDC and DMAP increased the yield to 80% affording the peptide **4.22**.

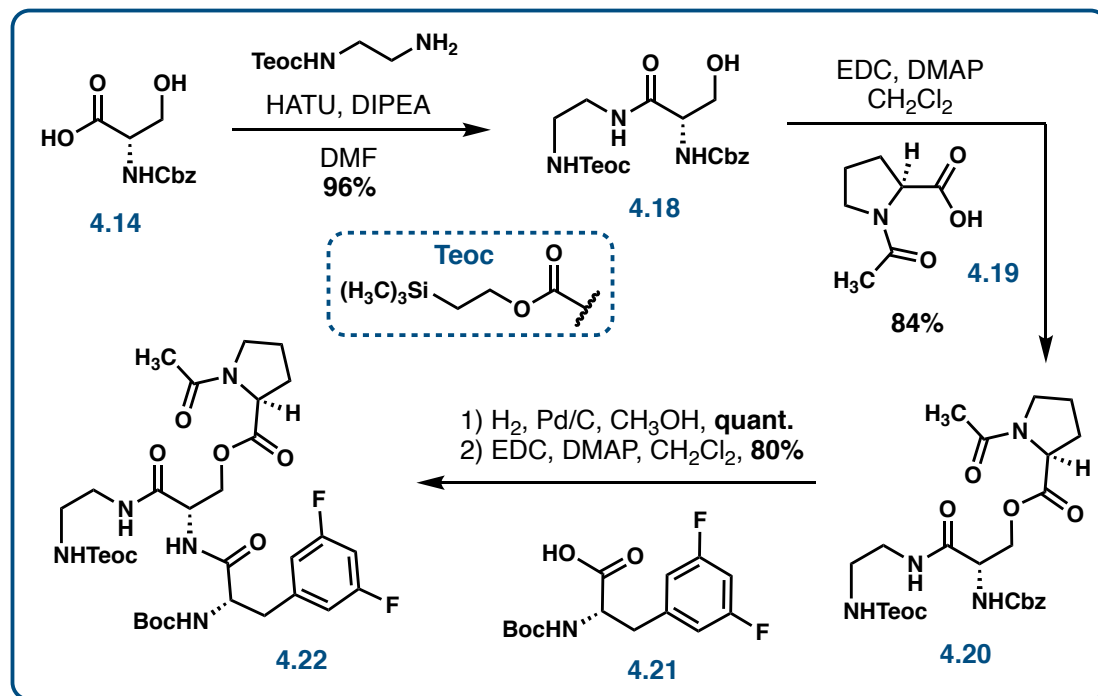


Figure 4.5 Synthesis of peptide **4.22** towards the synthesis of the probe compound **4.13**

The next step in the sequence is the selective deprotection of the Boc group in the presence of the Teoc group. One way around this selective deprotection is by coupling on a difluorophenylalanine with a different protecting group on it. The issue is that the Boc-protected difluorophenylalanine is expensive and that purchasing this compound with a different protecting group, such as Cbz, is even more expensive. We attempted to switch the protecting group on the difluorophenylalanine with a Cbz through a series of steps involving the methylation of the acid to the ester, removal of the Boc group, and protection of the free amine with a Cbz group, but we found that this route was low yielding and inefficient. We decided to dig into the various

conditions that we felt may afford the selective deprotection of the Boc group in the presence of the Teoc group.

To screen these conditions, we chose to not to test them against the precious material **4.22**, but to instead use a mixture of peptide **4.18** and boc-difluorophenylalanine **4.21**. The first set of conditions that we tried were freshly distilled TMSOTf and 2,6-lutidine in dichloromethane at 0°C, but it did not appear that either substrate underwent any deprotection.¹⁴ Another set of conditions that was employed was refluxing the mixture of starting materials in acetonitrile with ceric ammonium nitrate as an oxidative cleavage of the Boc group, but again we did not see any fruitful amount of deprotection of either product.¹⁵

The final method of selective deprotection that we explored was through the use of freshly distilled SiCl₄ and phenol in dichloromethane.¹⁶ The proposed mechanism involves the in-situ generation of HCl as shown in figure 4.6. Upon a first attempt at the usage of this method on a scout reaction of the same two substrates **4.18** and **4.21**, it appeared that the Boc group was cleaved quickly and that as time passed, the reagents began to remove the Teoc group. This showed promise in its application to the actual system. After carefully monitoring the rate of the reaction relative to the removal of the Boc and Teoc groups, we found that the reaction was nearly complete after 2 minutes, at which point, the Teoc group would begin to come off. When applied to the real system **4.22** (figure 4.7), the reaction appeared to be complete after 1 minute and the removal of the Teoc group began after 3 minutes. This was a brief window, but with careful timing, the selective deprotection was possible.

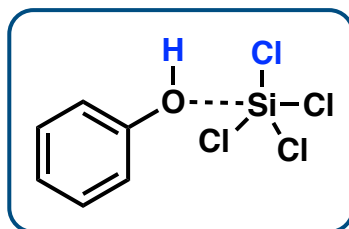


Figure 4.6 Proposed mechanism of the generation of HCl towards the deprotection of the Boc group

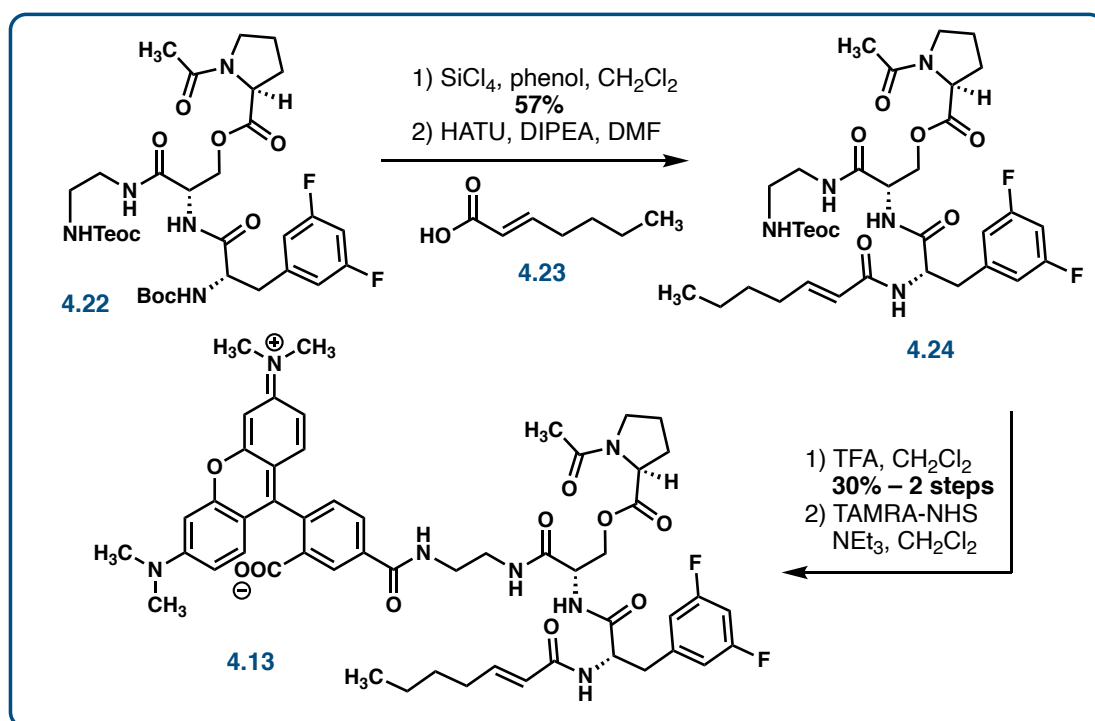


Figure 4.7 Final steps in the synthesis of fluorescent probe compound **4.13**

When brought to a larger scale with the goal of isolation and purification of the product, we obtained yields between 3% and 7%, although the reaction appeared to be roughly the same as the scout reactions when monitoring by TLC. After an

investigation into the reasoning behind this apparent drop in yield we determined that we were losing the material during the quench. We were quenching the reaction with a slow dropwise addition of saturated aqueous sodium bicarbonate at 0°C. Although the solution of bicarbonate is basic, the reaction of water with the SiCl₄ was quick to generate HCl. This HCl may have been in a concentration too high to be fully quenched by the NaHCO₃ before reacting with the remaining Teoc protected amine to afford the doubly deprotected product. To combat this occurrence, once the solution was at 0°C but immediately before the addition of the aqueous NaHCO₃, I shot in 80 equivalents of triethylamine to sequester any HCl formed during the process. This modification to the procedure brought the yield from 7% to 57%, which was high enough to proceed to the following steps.

The next step is the coupling of the heptanoic acid to the resultant free amine, which was accomplished using HATU and *i*-Pr₂NEt. Removal of the Teoc protecting group from peptide **4.24** using TBAF afforded the unprotected ethylene diamine linker in 30% over the two steps. A final coupling of the TAMRA fluorophore using the TAMRA-NHS ester afforded the final ADEP fragment fluorescent probe compound **4.13**, which was handed off to the Schmitz lab for their biological mechanism of action investigations of ADEP fragments against *Mtb*.

Experimental Procedures

General Information: *These experimental procedures have been published previously in its current or a substantially similar form and I have obtained permission to republish it.*¹ All electrochemical reactions were performed in either an H-type divided cell separated by a sintered glass frit or a single compartment glassfalcon tube with electrodes separated by a glass microscope slide (Fisherbrand®, plain, precleaned, 2.5 cm x 7.5 cm x 0.1 cm). All non-electrochemical reactions were performed in single-neck oven- or flame-dried round bottom flasks fitted with rubber septa under a positive pressure of argon, unless otherwise noted. Air- and moisture-sensitive liquids were transferred via syringe or stainless-steel cannula. Organic solutions were concentrated by rotary evaporation at or below 35°C at 10 Torr (diaphragm vacuum pump) unless otherwise noted. Compounds were isolated using flash column chromatography² with silica gel (60-Å pore size, 40–63µm, standard grade, Silicycle). Analytical thin-layer chromatography (TLC) was performed using glass plates pre-coated with silica gel (0.25 mm, 60-Å pore size, 5–20 µm, Silicycle)

¹ (a) Wu, Z.; Suppo, J. S.; Tumova, S.; Strobe, J.; Bravo, F.; Moy, M.; Weinstein, E. S.; Peer, C. J.; Figg, W. D.; Chain, W. J.; Echavarren, A. M.; Beech, D. J.; Beutler, J. A., *ACS Med. Chem. Lett.* 2020, 11, 1711-1716. (b) Reed, H.; Paul, T. R.; Chain, W. J., *J. Org. Chem.* 2018, 83, 11359-11368. (c) Bush, T. S.; Yap, G. P. A.; Chain, W. J., *Org. Lett.* 2018, 20, 5406-5409. (d) Lewis, R. S.; Garza, C. J.; Dang, A. T.; Pedro, T. K.; Chain, W. J., *Org. Lett.* 2015, 17, 2278-2281. (e) Li, Z.; Nakashige, M.; Chain, W. J., *J. Am. Chem. Soc.* 2011, 133, 6553-6556.

² Still, W. C.; Kahn, M.; Mitra, A. *J. Org. Chem.* 1978, 43, 2923–2925.

impregnated with a fluorescent indicator (254 nm). TLC plates were visualized by exposure to ultraviolet light (UV), then were stained by submersion in aqueous ceric ammonium molybdate solution (CAM), acidic ethanolic p-anisaldehyde solution (anisaldehyde), or aqueous methanolic iron(III) chloride (FeCl₃), followed by brief heating on a hot plate (215°C, 10–15 s).

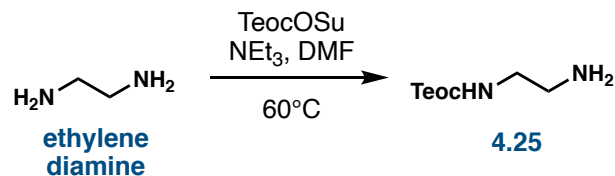
Materials: Commercial reagents and solvents were used as received with the following exceptions. Triethylamine, dichloromethane, diethyl ether, tetrahydrofuran, and 1,2-dimethoxyethane were purified by the method of Pangborn, et. al.³ Tetrabutylammonium hexafluorophosphate was recrystallized from ethanol (23 g /300 mL) at 65°C. Reticulated vitreous carbon (RVC) foam (carbon – vitreous – 3000C – foam; thickness: 10 mm; bulk density: 0.05 g/cm³; porosity: 96.5%; pores/cm: 40) was obtained from Goodfellow USA and cut to appropriate size for reaction scale. After 150 h of use, RVC electrodes were discarded and freshly cut electrodes were used.

Instrumentation: Proton (¹H), carbon (¹³C), fluorine (¹⁹F), and silicon (²⁹Si) nuclear magnetic resonance (NMR) spectra were recorded on Bruker AV400 CryoPlatform QNP or Bruker AVIII600 SMART NMR spectrometers at 23°C. Proton chemical shifts are expressed in parts per million (ppm, δ scale) downfield from tetramethylsilane and are referenced to residual protium in the NMR solvent (CHCl₃: δ 7.26, CD₃COCD₂H: δ 2.05). Carbon chemical shifts are expressed in parts per million

³ Pangborn, A. B.; Giardello, M. A.; Grubbs, R. H.; Rosen, R. K.; Timmers, F. J. *Organometallics* 1996, 15, 1518–1520.

(ppm, d scale) downfield from tetramethylsilane and are referenced to the carbon resonance of the NMR solvent (CDCl_3 : δ 77.16, $\text{CD}_3\text{COCD}_2\text{H}$: δ 29.84). Data are represented as follows: chemical shift, multiplicity (s = singlet, d = doublet, t = triplet, q = quartet, m = multiplet, br = broad, app = apparent), integration, and coupling constant (J) in Hertz (Hz). Accurate mass measurements were obtained using an Agilent 1100 quaternary LC system coupled to an Agilent 6210 LC/MSD-TOF fitted with an ESI or an APCI source, or Thermo Q-Exactive Orbitrap using electrospray ionization (ESI) or a Waters GCT Premier spectrometer using chemical ionization (CI).

Synthesis of Teoc-protected Ethylene Diamine 4.25



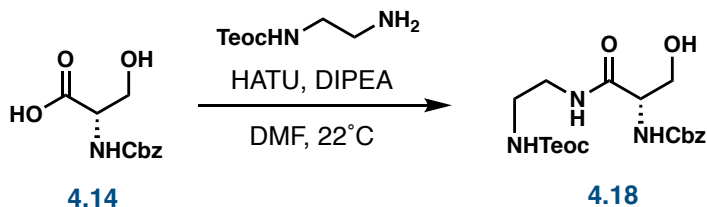
Triethylamine (1.7 mL, 12.0 mmol, 5.2 equiv) followed by *N*-[2-(Trimethylsilyl)ethoxycarbonyloxy]succinimide (600 mg, 2.3 mmol, 1 equiv) was added to a stirred solution of ethylene diamine (0.60 mL, 9.0 mmol, 3.9 equiv) in DMF (25 mL) at 22°C. The solution was stirred for 80 min at that temperature, then water (10 mL) was added. The aqueous layer was extracted with ethyl acetate (3 x 40 mL). The combined organic layers were dried over anhydrous sodium sulfate, and the dried solution was concentrated. Purification of the residue by filtering through a short plug of silica gel (starting with 4:4:1 isopropanol : ethyl acetate : water, grading to 4:4:3 isopropanol : ethyl acetate : water) afforded the monoprotected diamine **4.25** (300 mg, 1.47 mmol, 64%) as a clear, yellow oil.

^1H NMR (400 MHz, CDCl_3) δ : 4.12 (t, $J = 8.6$ Hz, 2H), 3.39 (s, 2H), 3.08 (t, $J = 5.5$ Hz, 2H), 0.97 (t, $J = 8.7$ Hz, 2H), 0.03 (s, 9H).

^{13}C NMR (101 MHz, CDCl_3) δ : 157.8, 63.5, 42.4, 29.8, 17.9, -1.4.

TLC: 20% MeOH–dichloromethane, $R_f = 0.08$
(KMnO₄).

Synthesis of Amide 4.18



HATU (99 mg, 0.26 mmol, 1.1 equiv) and Hunig's base (0.10 mL, 0.52 mmol, 2.2 equiv) were added to a stirred solution of *Z*-*L*-serine (57 mg, 0.24 mmol, 1.0 equiv) in DMF (2.0 mL) at 0°C. The resultant solution was stirred at that temperature for 10 min, then was warmed briefly to 22°C. The solution was recooled to 0°C, whereupon a solution of the Teoc-protected diamine (48 mg, 0.24 mmol, 1.0 mmol) in DMF (0.5 mL) was added. The resultant solution was allowed to warm to 22°C and was stirred at that temperature for 6 h. The solution was diluted with ethyl acetate (10 mL) and washed with water (5 mL), saturated aqueous sodium bicarbonate solution (5 mL), and brine (5 mL). The organic layer was dried over anhydrous sodium sulfate and concentrated. Purification of the residue by flash column chromatography (silica gel, starting with 0% methanol–dichloromethane, grading to 8% methanol–dichloromethane) afforded the amide **4.18** (98 mg, 0.23 mmol, 96%) as a clear, yellow solid.

¹H NMR (400 MHz, CDCl₃) δ: 7.34 (d, *J* = 5.5 Hz, 5H), 7.02 (s, 1H), 6.01 – 5.94 (m, 1H), 5.23 (s, 1H), 5.11 (d, *J* = 3.6 Hz, 2H), 4.21 (s, 1H), 4.11 (t, *J* = 8.5 Hz, 2H), 4.02 (d, *J* = 11.2 Hz, 1H), 3.66 (dd, *J* = 11.6, 5.4

Hz, 1H), 3.39 – 3.27 (m, 3H), 2.87 (s, 2H),
0.94 (t, $J = 8.0$ Hz, 2H), 0.01 (s, 9H).

^{13}C NMR (101 MHz, CDCl_3) δ : 171.4, 157.8, 156.5, 136.0, 128.60, 128.58,
128.34, 128.27, 128.1, 67.3, 63.5, 62.8, 56.0,
40.5, 40.4, 17.7, -1.5.

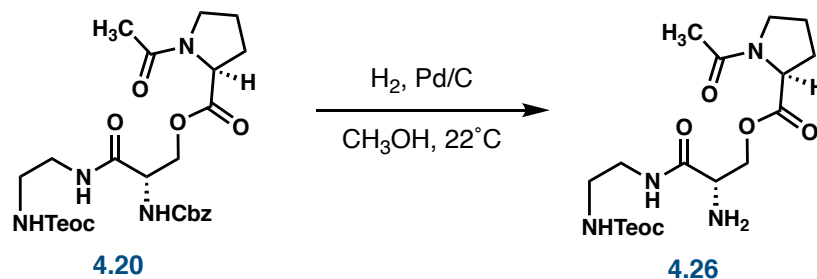
TLC: 10% MeOH–dichloromethane, $R_f = 0.50$
(Ninhydrin, KMnO_4 , UV).

5.8 Hz, 1H), 3.30 (q, $J = 6.0$ Hz, 2H), 2.25 –
1.89 (m, 8H), 1.32 – 1.15 (m, 1H), 0.97 – 0.88
(t, $J = 6.9$ Hz, 1H), 0.01 (s, 9H).

^{13}C NMR (101 MHz, CDCl_3) δ : 171.9, 171.3, 170.5, 169.4, 157.1, 155.7, 136.4,
128.6, 128.2, 67.1, 63.9, 62.9, 60.5, 59.1, 52.7,
48.3, 40.7, 40.1, 29.4, 25.2, 22.4, 21.2, 17.9,
14.3, -1.4.

TLC: 10% MeOH–dichloromethane, $R_f = 0.66$
(Ninhydrin, KMnO_4 , UV).

Synthesis of Free Amine 4.26



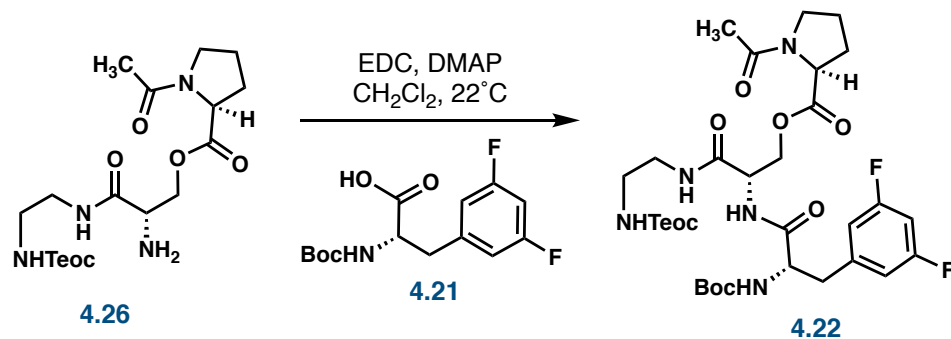
Pd/C (15 mg, 0.014 mmol, 3 mol%) was added to a stirred solution of the protected amine **4.20** (255 mg, 0.45 mmol, 1 equiv) in methanol (25 mL). The reaction flask was sealed with a septum, the headspace was removed under vacuum, and the flask was charged with hydrogen gas. The stirred suspension was then sparged with H_2 for 20 min at 22°C , then was stirred for 90 min. The solution was filtered over celite with methanol and concentrated to give the amine **4.26** (196 mg, 0.45 mmol, quantitative) as a clear, brownish–yellow oil.

^1H NMR (400 MHz, CDCl_3) δ : 7.99 (s, 1H), 7.34 (s, 1H), 5.82 (s, 1H), 4.58 (dd, $J_1 = 11.5$, $J_2 = 4.8$ Hz, 1H), 4.45 (dd, $J_1 = 8.5$, $J_2 = 4.6$ Hz, 1H), 4.40 – 4.30 (m, 1H), 4.18 – 4.07 (m, 4H), 3.92 (s, 1H), 3.70 – 3.60 (m, 1H), 3.58 – 2.48 (m, 1H), 3.44 – 3.38 (m, 1H), 3.38 – 3.30 (m, 1H), 2.22 (s, 1H), 2.19 – 2.12 (m, 2H), 2.11 (s, 2H), 2.04 (s, 4H), 1.26 (t, $J = 7.2$ Hz, 2H), 1.00 – 0.91 (m, 2H), 0.02 (s, 9H).

^{13}C NMR (101 MHz, CDCl_3) δ : 172.5, 171.9, 171.3, 171.0, 157.8, 63.2, 63.0, 62.5, 61.3, 60.6, 59.2, 54.7, 53.6, 48.8, 48.2, 41.0, 40.6, 39.7, 29.6, 29.5, 25.23, 25.16, 22.8, 22.4, 21.2, 17.9, 14.3, -1.3.

TLC: 10% MeOH–dichloromethane, $R_f = 0.32$
(Ninhydrin, UV).

Synthesis of Amide 4.22



4-dimethylaminopyridine (1 mg, 0.006 mmol, 0.1 equiv) and EDC (23 mg, 0.12 mmol, 2.0 equiv) were added to a stirred solution of Boc-difluorophenylalanine (20 mg, 0.065 mmol, 1.1 equiv) and amine **4.26** (25 mg, 0.059 mmol, 1 equiv) in dichloromethane (1 mL). The solution was stirred at 22°C for 26 h, whereupon water (2 mL) was added. The aqueous layer was extracted with ethyl acetate (3 x 10 mL) and the combined organic extracts were washed with saturated aqueous sodium bicarbonate solution (10 mL) and brine (10 mL). The organic solution was dried over anhydrous sodium sulfate and concentrated. Purification of the residue by flash column chromatography (silica gel, starting with 1% methanol–dichloromethane, grading to 10% methanol–dichloromethane) afforded the ester **4.22** (34 mg, 0.047 mmol, 80%) as a clear, yellow oil.

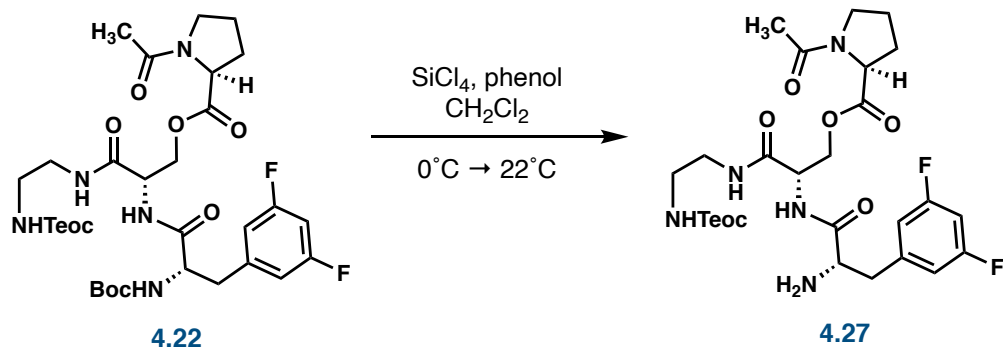
¹H NMR (600 MHz, CDCl₃) δ: 7.32 (d, *J* = 7.8 Hz, 1H), 7.17 (s, 1H), 6.73 – 6.64 (m, 3H), 5.79 (s, 1H), 5.27 (d, *J* = 8.2 Hz, 1H), 4.68 – 4.59 (m, 2H), 4.47 (s, 2H), 4.15 – 4.08 (m, 2H), 3.66 (p, *J* = 5.6 Hz, 1H), 3.57 –

3.47 (m, 1H), 3.32 (s, 3H), 3.17 – 3.10 (m, 1H), 2.98 – 2.91 (m, 1H), 2.25 – 2.09 (m, 4H), 2.09 – 1.96 (m, 1H), 1.38 (d, J = 9.8 Hz, 9H), 1.28 – 1.22 (m, 1H), 0.98 – 0.92 (m, 2H), 0.01 (s, 9H).

^{13}C NMR (151 MHz, CDCl_3) δ : 171.9, 171.8, 168.6, 164.0, 163.9, 162.4, 162.3, 157.6, 155.4, 112.4, 112.2, 102.8, 80.5, 64.4, 63.2, 60.9, 54.5, 53.0, 48.7, 40.9, 40.4, 37.7, 29.8, 28.9, 28.4, 25.1, 22.8, 22.4, 17.9, -1.4.

TLC: 10% MeOH–dichloromethane, $R_f = 0.30$
(Ninhydrin, UV).

Synthesis of Free Amine 4.27

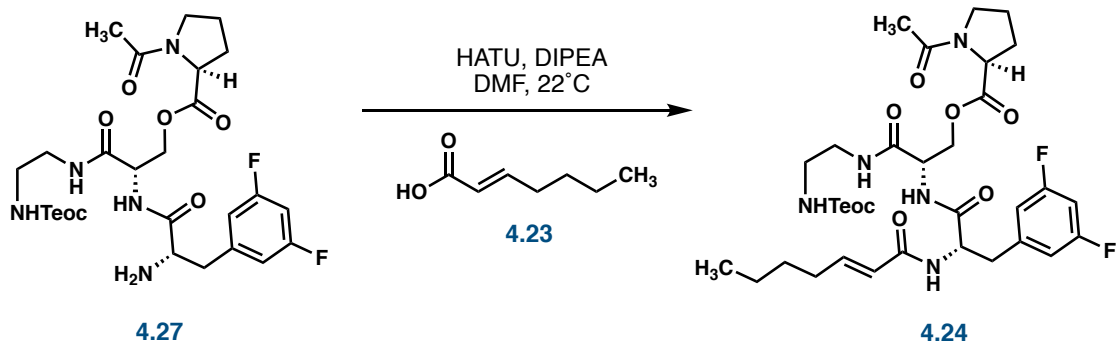


A solution of Boc-protected amine **4.22** (50 mg, 0.070 mmol, 1 equiv) in dichloromethane (1 mL) was added to a stirred solution of silicon tetrachloride (0.16 mL, 1.4 mmol, 20 equiv) and phenol (400 mg, 4.2 mmol, 60 equiv) in dichloromethane (2 mL) at 22°C . The resultant solution was stirred at that temperature for 1 min, whereupon the reaction mixture was cooled to 0°C and diluted with dichloromethane (3 mL). Triethylamine (0.78 mL, 5.6 mmol, 80 equiv) was quickly added to the vigorously stirred solution at 0°C , then the excess silicon tetrachloride was quenched by the dropwise addition of saturated aqueous sodium bicarbonate solution (2 mL). The resultant biphasic solution was separated and the aqueous layer was extracted with ethyl acetate (3 x 5 mL). The combined organic layers were washed with brine (7 mL), then they were dried over anhydrous sodium sulfate and concentrated for purification using flash column chromatography (silica gel, starting with 2% methanol–dichloromethane, grading to 8% methanol–dichloromethane) to afford free amine **4.27** (24.3 mg, 0.396 mmol, 57%) as a clear, yellow oil.

^1H NMR (400 MHz, CDCl_3) δ : 6.90 – 6.61 (m, 4H), 4.76 – 4.54 (m, 1H), 4.54 – 4.29 (m, 1H), 4.17 – 4.07 (m, 2H), 4.07 – 4.89 (m, 1H), 3.89 – 3.70 (m, 1H), 3.70 – 3.54 (m, 1H), 3.54 – 3.44 (m, 1H), 3.44 – 3.37 (m, 1H), 3.37 – 3.25 (m, 2H), 2.25 – 1.92 (m, 8H), 1.25 (d, $J = 2.8$ Hz, 4H), 1.16 (d, $J = 6.2$ Hz, 2H), 1.03 – 0.80 (m, 3H), 0.02 (s, 9H).

TLC: 10% MeOH–dichloromethane, $R_f = 0.33$
(Ninhydrin, UV).

Synthesis of Peptide 4.24



HATU (8.4 mg, 0.022 mmol, 1.1 equiv) and Hunig's base (8.0 μ L, 0.044 mmol, 2.2 equiv) were added to a stirred solution of peptide **4.27** (12 mg, 0.020 mmol, 1 equiv) and (*E*)-heptenoic acid (3.0 μ L, 0.022 mmol, 1.1 equiv) in DMF (0.1 mL) at 22 °C. The resultant solution was stirred at that temperature for 135 min, whereupon the solution was diluted with ethyl acetate (5 mL) and washed with water (1 mL), saturated aqueous sodium bicarbonate solution (1 mL), and brine (1 mL). The organic layer was dried over anhydrous sodium sulfate and concentrated. Purification of the residue by flash column chromatography (silica gel, starting with 2% methanol–dichloromethane, grading to 8% methanol–dichloromethane) afforded the amide **4.24** as a clear, yellow oil.

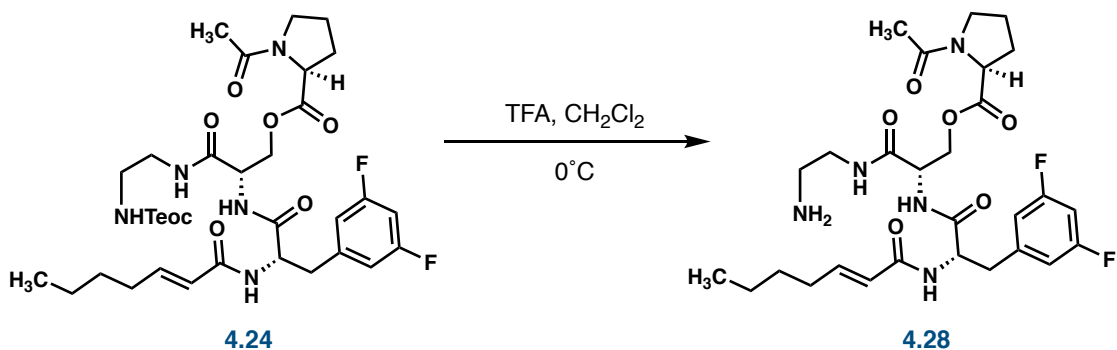
^1H NMR (400 MHz, CDCl_3) δ : 7.65 – 7.56 (m, 1H), 6.79 – 6.66 (m, 3H), 6.10 (d, $J = 25.1$ Hz, 1H), 5.62 – 5.50 (m, 1H), 5.39 – 5.22 (m, 1H), 4.88 – 4.81 (m, 1H), 4.81 (d, $J = 11.1$ Hz, 1H), 4.564 – 4.57 (m, 1H), 4.47 – 4.31 (m, 1H), 4.31 – 4.20 (m, 1H), 4.17 – 4.03

(m, 2H), 3.83 – 3.61 (m, 1H), 3.55 – 3.21 (m, 4H), 3.21 – 3.11 (m, 1H), 3.00 – 2.69 (m, 1H), 2.22 (d, $J = 2.7$ Hz, 2H), 2.09 – 2.02 (m, 1H), 2.02 – 1.94 (m, 2H), 1.70 – 1.63 (m, 1H), 1.25 (d, $J = 2.5$ Hz, 39H), 0.93 – 0.86 (m, 6H), 0.06 – -0.05 (m, 9H).

^{13}C NMR (101 MHz, CDCl_3) δ : 169.8, 158.8, 157.2, 143.8, 139.9, 138.4, 131.1, 128.9, 121.0, 112.1, 111.4, 102.8, 100.2, 99.0, 68.3, 63.0, 61.6, 54.4, 52.1, 48.8, 40.0, 38.7, 36.2, 34.6, 32.1, 29.9, 29.5, 29.1, 24.9, 23.9, 23.2, 22.8, 22.3, 20.4, 18.0, 14.3, 13.8, -1.4.

TLC: 10% MeOH–dichloromethane, $R_f = 0.50$
(Ninhydrin, KMnO_4 , UV).

Synthesis of Free Amine 4.28



Trifluoroacetic acid (1.5 mL) was added to a stirred solution of Teoc-protected amine **4.24** in dichloromethane (3.5 mL) at 0 °C. The solution was stirred at that temperature for 80 min, whereupon the solution was warmed to 22 °C and the TFA was blown off with a stream of nitrogen. The crude yellow oil was purified using UPLC (Phenomenex 00G-4252-N0, Luna 5 μ C18(2) 100A, 250 x 10.00 mm 5 micron, Ret. Time = 6.670 min, Flow Rate = 5 mL/min, 60% ACN-H₂O) to afford the free amine **4.28** (19.4 mg, 0.0335 mmol, 30% over 2 steps) as a clear, colorless oil.

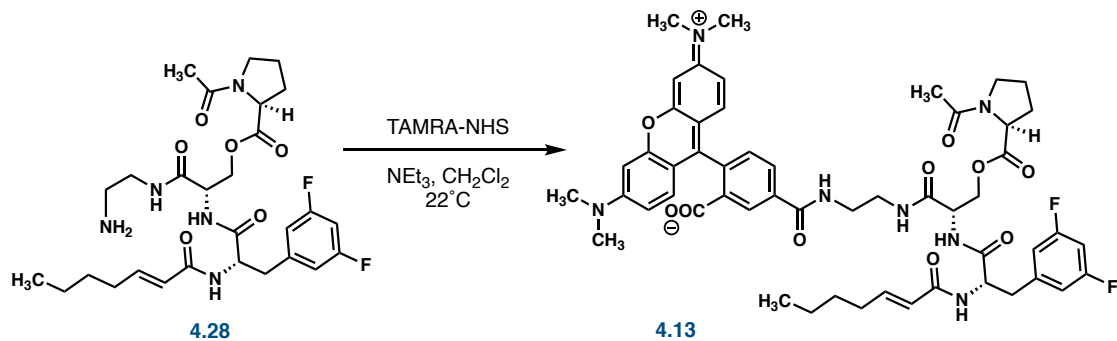
¹H NMR (400 MHz, CDCl₃) δ : 7.71 – 7.29 (m, 3H), 6.88 – 6.61 (m, 4H), 5.83 (d, J = 15.4 Hz, 1H), 5.57 – 5.31 (m, 2H), 4.69 – 4.51 (m, 3H), 4.51 – 4.35 (m, 2H), 4.27 – 4.20 (m, 2H), 3.95 (s, 3H), 3.68 – 3.59 (m, 1H), 3.56 – 3.47 (m, 2H), 3.45 – 3.28 (m, 1H), 3.19 – 3.02 (m, 4H), 3.01 – 2.84 (m, 2H), 2.85 (s, 1H), 2.19 – 2.08 (m, 2H), 2.05 (s, 3H), 2.04 – 1.89 (m,

4H), 1.89 (p, $J = 2.5$ Hz, 3H), 1.42 – 1.21 (m, 4H), 0.90 – 0.80 (m, 5H).

^{13}C NMR (101 MHz, CDCl_3) δ : 173.3, 173.2, 171.5, 171.0, 170.5, 167.4, 164.4, 164.3, 162.0, 161.8, 147.3, 140.2, 139.8, 139.7, 137.4, 136.9, 136.0, 122.4, 121.4, 121.3, 120.5, 112.3, 112.1, 103.2, 102.9, 102.8, 102.7, 77.4, 63.9, 61.3, 53.7, 52.6, 48.8, 40.3, 39.8, 37.4, 36.4, 34.6, 31.9, 30.2, 29.8, 29.7, 29.3, 24.9, 22.5, 22.4, 22.3, 22.3, 13.8, 13.7, 13.7.

TLC: 10% MeOH–dichloromethane, $R_f = 0.50$
(Ninhydrin, KMnO_4 , UV).

Synthesis of Fluorescent Mechanistic Probe 4.13



Triethylamine (1.7 μ L, 0.012 mmol, 2.2 equiv) and TAMRA-NHS (2.9 mg, 0.0055 mmol, 1 equiv) were added to a stirred solution of peptide **4.28** (3.5 mg, 0.0060 mmol, 1.1 equiv) in dichloromethane (1 mL) at 22°C. The solution was stirred at that temperature covered in foil for 80 min, whereupon the solution was concentrated and the crude pink oil was purified using UPLC (Phenomenex 00G–4252–N0; Luna 5 μ C18(2) 100A, 250 x 10.00 mm 5 micron; Ret. Time = 25.000 min; Flow Rate = 5 mL/min; starting at 30% ACN–H₂O, grading to 50% ACN–H₂O) to afford the fluorescent probe **4.13** as a bright pink oil.

HRMS:

Calcd. for C₅₃H₆₀F₂N₇O₁₀ [M+H]⁺: 992.4370.

Found: 992.4357.

REFERENCES

1. (a) Brotz-Oesterhelt, H.; Sass, P. *Int J Med Microbiol* **2014**, *304*, 23-30. (b) Culp, E.; Wright, G. D. *The Journal of Antibiotics* **2017**, *70*, 366-377. (c) Raju, R. M.; Goldberg, A. L.; Rubin, E. J. *Nature Reviews Drug Discovery* **2012**, *11*, 777-789.
2. (a) Alexopoulos, J. A.; Guarne, A.; Ortega, J. *J Struct Biol* **2012**, *179*, 202-210. (b) Joshi, S. A.; Hersch, G. L.; Baker, T. A.; Sauer, R. T. *Nature Structural & Molecular Biology* **2004**, *11*, 404-411. (c) Lee, M. E.; Baker, T. A.; Sauer, R. T. *J. Mol. Biol.* **2010**, *399*, 707-718. (d) Yu, A. Y. H.; Houry, W. A. *FEBS Lett.* **2007**, *581*, 3749-3757.
3. (a) Frees, D.; Gerth, U.; Ingmer, H. *Int J Med Microbiol* **2014**, *304*, 142-149. (b) Frees, D.; Qazi, S. N. A.; Hill, P. J.; Ingmer, H. *Mol. Microbiol.* **2003**, *48*, 1565-1578. (c) Frees, D.; Sorensen, K.; Ingmer, H. *Infect Immun* **2005**, *73*, 8100-8108. (d) Gottesman, S. *Annu. Rev. Cell Dev. Biol.* **2003**, *19*, 565-587. (e) Gottesman, S.; Wickner, S.; Maurizi, M. R. *Genes Dev* **1997**, *11*, 815-823. (f) Kwon, H. Y.; Kim, S. W.; Choi, M. H.; Ogunniyi, A. D.; Paton, J. C.; Park, S. H.; Pyo, S. N.; Rhee, D. K. *Infect Immun* **2003**, *71*, 3757-3765. (g) Kwon, H. Y.; Ogunniyi, A. D.; Choi, M. H.; Pyo, S. N.; Rhee, D. K.; Paton, J. C. *Infect Immun* **2004**, *72*, 5646-5653. (h) Robertson, G. T.; Ng, W. L.; Foley, J.; Gilmour, R.; Winkler, M. E. *J. Bacteriol.* **2002**, *184*, 3508-3520. (i) Sauer, R. T.; Baker, T. A. *Annu. Rev. Biochem* **2011**, *80*, 587-612.
4. (a) Baker, T. A.; Sauer, R. T. *Trends Biochem. Sci* **2006**, *31*, 647-653. (b) Singh, S. K.; Grimaud, R.; Hoskins, J. R.; Wickner, S.; Maurizi, M. R. *Proceedings of the National Academy of Sciences* **2000**, *97*, 8898-8903. (c) Szyk, A.; Maurizi, M. R. *J Struct Biol* **2006**, *156*, 165-174. (d) Wang, J.; Hartling, J. A.; Flanagan, J. M. *Cell* **1997**, *91*, 447-456. (e) Wang, J.; Hartling, J. A.; Flanagan, J. M. *J Struct Biol* **1998**, *124*, 151-163.
5. Schmitz, K. R.; Handy, E. L.; Compton, C. L.; Gupta, S.; Bishai, W. R.; Sauer, R. T.; Sello, J. K. *ACS Chemical Biology* **2023**, *18*, 724-733.
6. (a) Kirstein, J.; Hoffmann, A.; Lilie, H.; Schmidt, R.; Rübsamen-Waigmann, H.; Brötz-Oesterhelt, H.; Mogk, A.; Turgay, K. *EMBO Molecular Medicine* **2009**, *1*, 37-49. (b) Lee, B.-G.; Park, E. Y.; Lee, K.-E.; Jeon, H.; Sung, K. H.; Paulsen, H.; Rübsamen-Schaeff, H.; Brötz-Oesterhelt, H.; Song, H. K. *Nature*

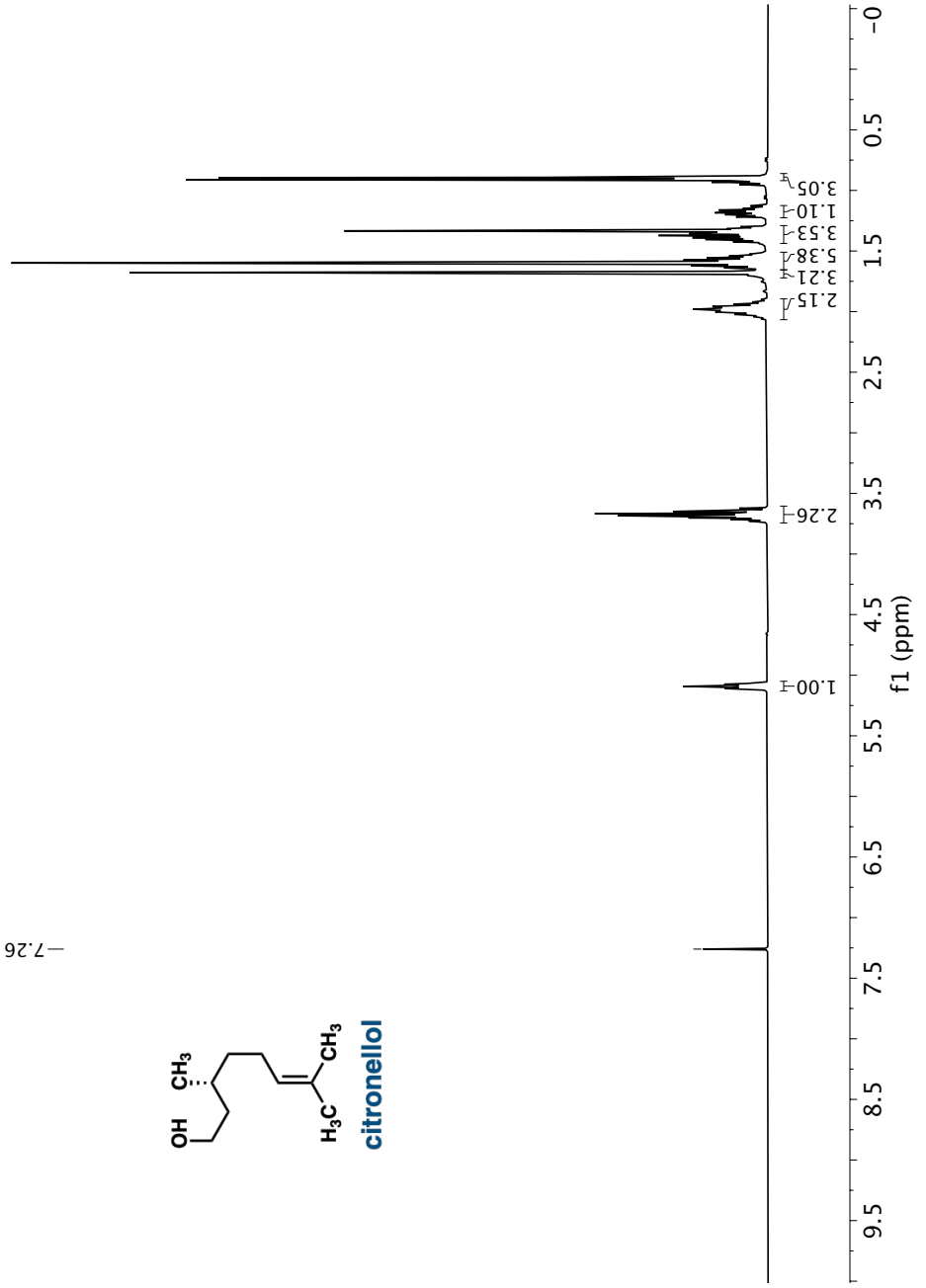
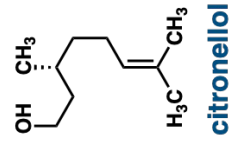
- Structural & Molecular Biology* **2010**, *17*, 471-478. (c) Li, D. H.; Chung, Y. S.; Gloyd, M.; Joseph, E.; Ghirlando, R.; Wright, G. D.; Cheng, Y. Q.; Maurizi, M. R.; Guarne, A.; Ortega, J. *Chem Biol* **2010**, *17*, 959-969.
7. (a) Akopian, T.; Kandrор, O.; Raju, R. M.; Unnikrishnan, M.; Rubin, E. J.; Goldberg, A. L. *The EMBO Journal* **2012**, *31*, 1529-1541. (b) Leodolter, J.; Warweg, J.; Weber-Ban, E. *PLOS ONE* **2015**, *10*, e0125345. (c) Personne, Y.; Brown, A. C.; Schuessler, D. L.; Parish, T. *PLoS ONE* **2013**, *8*, e60228. (d) Raju, R. M.; Unnikrishnan, M.; Rubin, D. H. F.; Krishnamoorthy, V.; Kandrор, O.; Akopian, T. N.; Goldberg, A. L.; Rubin, E. J. *PLoS Pathogens* **2012**, *8*, e1002511. (e) Schmitz, K. R.; Carney, D. W.; Sello, J. K.; Sauer, R. T. *Proceedings of the National Academy of Sciences* **2014**, *111*, E4587-E4595. (f) Schmitz, K. R.; Sauer, R. T. *Mol. Microbiol.* **2014**, *93*, 617-628.
 8. (a) Brötz-Oesterhelt, H.; Beyer, D.; Kroll, H.-P.; Endermann, R.; Ladel, C.; Schroeder, W.; Hinzen, B.; Raddatz, S.; Paulsen, H.; Henninger, K.; et al. *Nature Medicine* **2005**, *11*, 1082-1087. (b) Conlon, B. P.; Nakayasu, E. S.; Fleck, L. E.; Lafleur, M. D.; Isabella, V. M.; Coleman, K.; Leonard, S. N.; Smith, R. D.; Adkins, J. N.; Lewis, K. *Nature* **2013**, *503*, 365-370. (c) Hinzen, B.; Raddatz, S.; Paulsen, H.; Lampe, T.; Schumacher, A.; Häbich, D.; Hellwig, V.; Benet-Buchholz, J.; Endermann, R.; Labischinski, H.; et al. *ChemMedChem* **2006**, *1*, 689-693. (d) Ollinger, J.; O'Malley, T.; Kesicki, E. A.; Odingo, J.; Parish, T. *J. Bacteriol.* **2012**, *194*, 663-668. (e) Osada, H.; Yano, T.; Koshino, H.; Isono, K. *The Journal of Antibiotics* **1991**, *44*, 1463-1466. (f) Socha, A. M.; Tan, N. Y.; LaPlante, K. L.; Sello, J. K. *Bioorg. Med. Chem.* **2010**, *18*, 7193-7202.
 9. Kim, Y.-I.; Levchenko, I.; Fraczkowska, K.; Woodruff, R. V.; Sauer, R. T.; Baker, T. A. *Nature Structural Biology* **2001**, *8*, 230-233.
 10. (a) Leung, E.; Datti, A.; Cossette, M.; Goodreid, J.; McCaw, S. E.; Mah, M.; Nakhamchik, A.; Ogata, K.; El Bakkouri, M.; Cheng, Y. Q.; et al. *Chem Biol* **2011**, *18*, 1167-1178. (b) Sass, P.; Josten, M.; Famulla, K.; Schiffer, G.; Sahl, H.-G.; Hamoen, L.; Brötz-Oesterhelt, H. *Proceedings of the National Academy of Sciences* **2011**, *108*, 17474-17479. (c) Gersch, M.; Famulla, K.; Dahmen, M.; Göbl, C.; Malik, I.; Richter, K.; Korotkov, V. S.; Sass, P.; Rübsamen-Schaeff, H.; Madl, T.; et al. *Nature Communications* **2015**, *6*, 6320. (d) Goodreid, J. D.; Janetzko, J.; Santa Maria, J. P.; Wong, K. S.; Leung, E.; Eger, B. T.; Bryson, S.; Pai, E. F.; Gray-Owen, S. D.; Walker, S.; et al. *J. Med. Chem.* **2016**, *59*, 624-646. (e) Lavey, N. P.; Coker, J. A.; Ruben, E. A.; Duerfeldt, A. S. *J. Nat. Prod.* **2016**, *79*, 1193-1197.
 11. Carney, D. W.; Compton, C. L.; Schmitz, K. R.; Stevens, J. P.; Sauer, R. T.; Sello, J. K. *ChemBioChem* **2014**, *15*, 2216-2220.

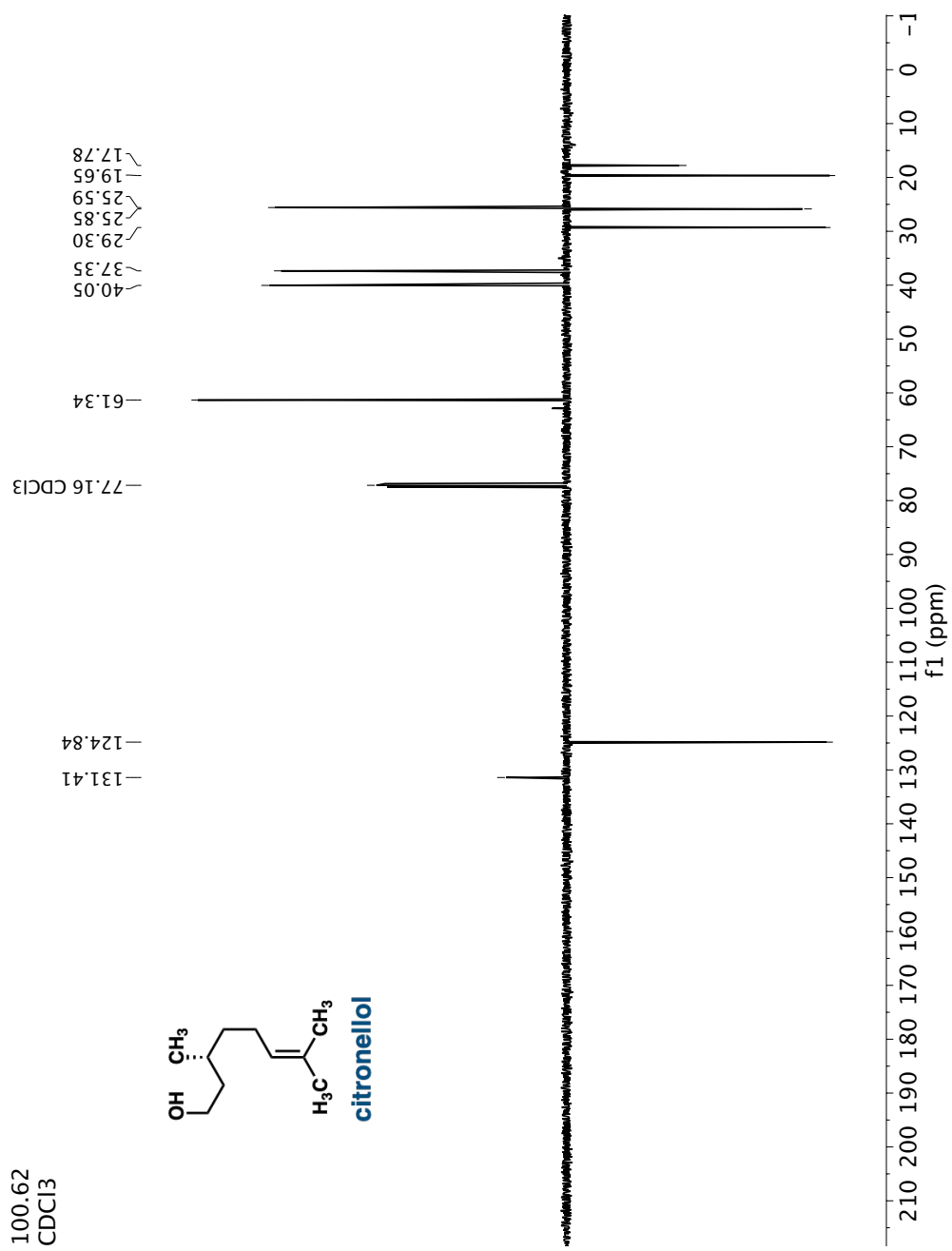
12. (a) Neises, B.; Steglich, W. *Angewandte Chemie International Edition in English* **1978**, *17*, 522-524. (b) Jordan, A.; Whymark, K. D.; Sydenham, J.; Sneddon, H. F. *Green Chemistry* **2021**, *23*, 6405-6413.
13. Carpino, L. A.; Tsao, J. H.; Ringsdorf, H.; Fell, E.; Hettrich, G. *J. Chem. Soc., Chem. Commun.* **1978**, 358-359.
14. Zhang, A. J.; Russell, D. H.; zhu, J.; Burgess, K. *Tetrahedron Lett.* **1998**, *39*, 7439-7442.
15. Jih Ru, H.; Jain, M. L.; Shwu-Chen, T.; Hakimelahi, G. H. *Tetrahedron Lett.* **1996**, *37*, 2035-2038.
16. (a) Sivanandaiah, K. M.; Suresh Babu, V. V.; Gangadhar, B. P. *Tetrahedron Lett.* **1996**, *37*, 5989-5990. (b) Kaiser, E.; Tam, J. P.; Kubiak, T. M.; Merrifield, R. B. *Tetrahedron Lett.* **1988**, *29*, 303-306.

Appendix A
CATALOG OF SPECTRA

400.13
CDCl₃

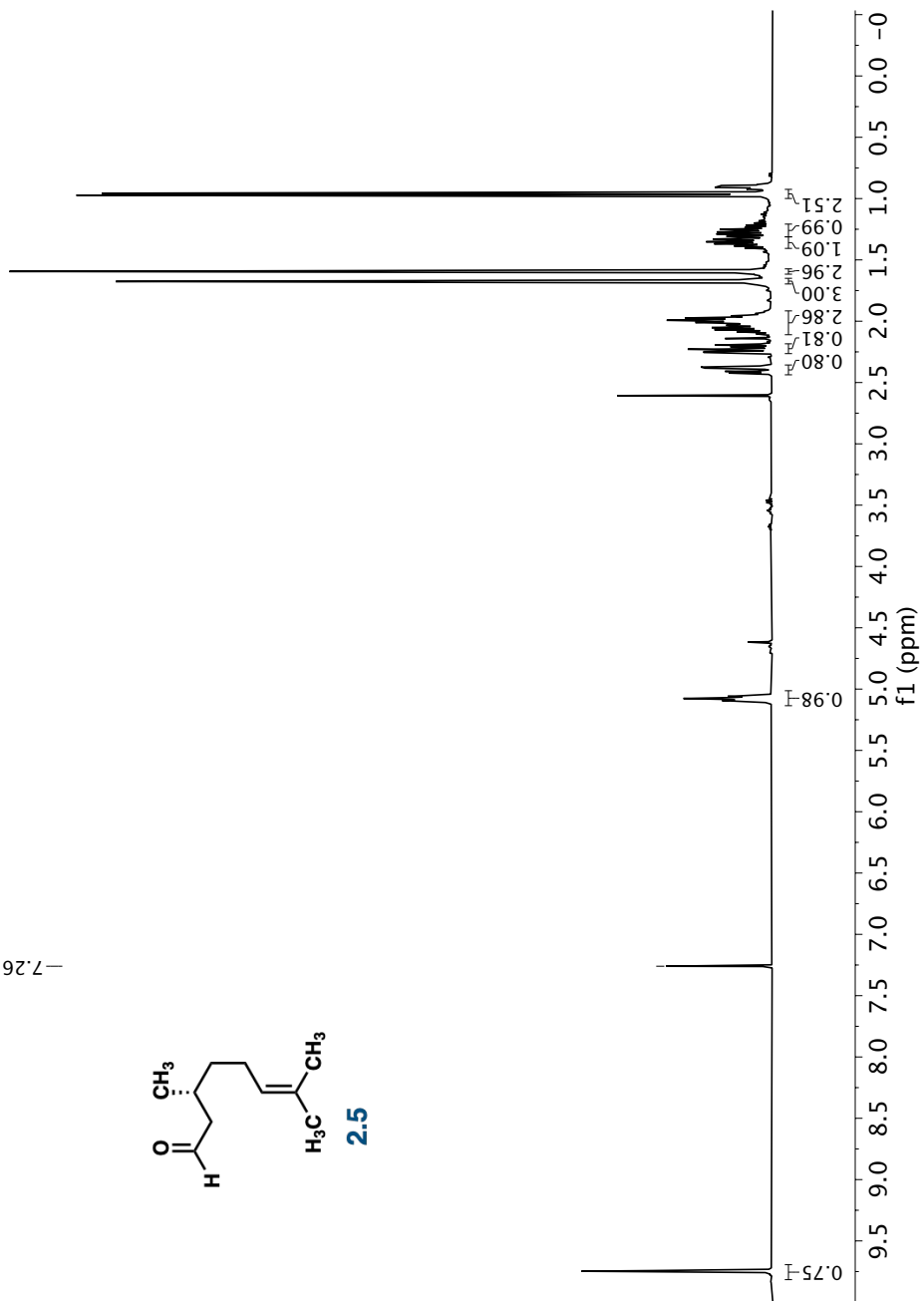
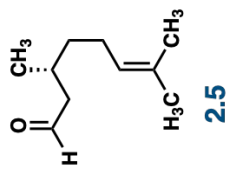
-7.26 CDCl₃

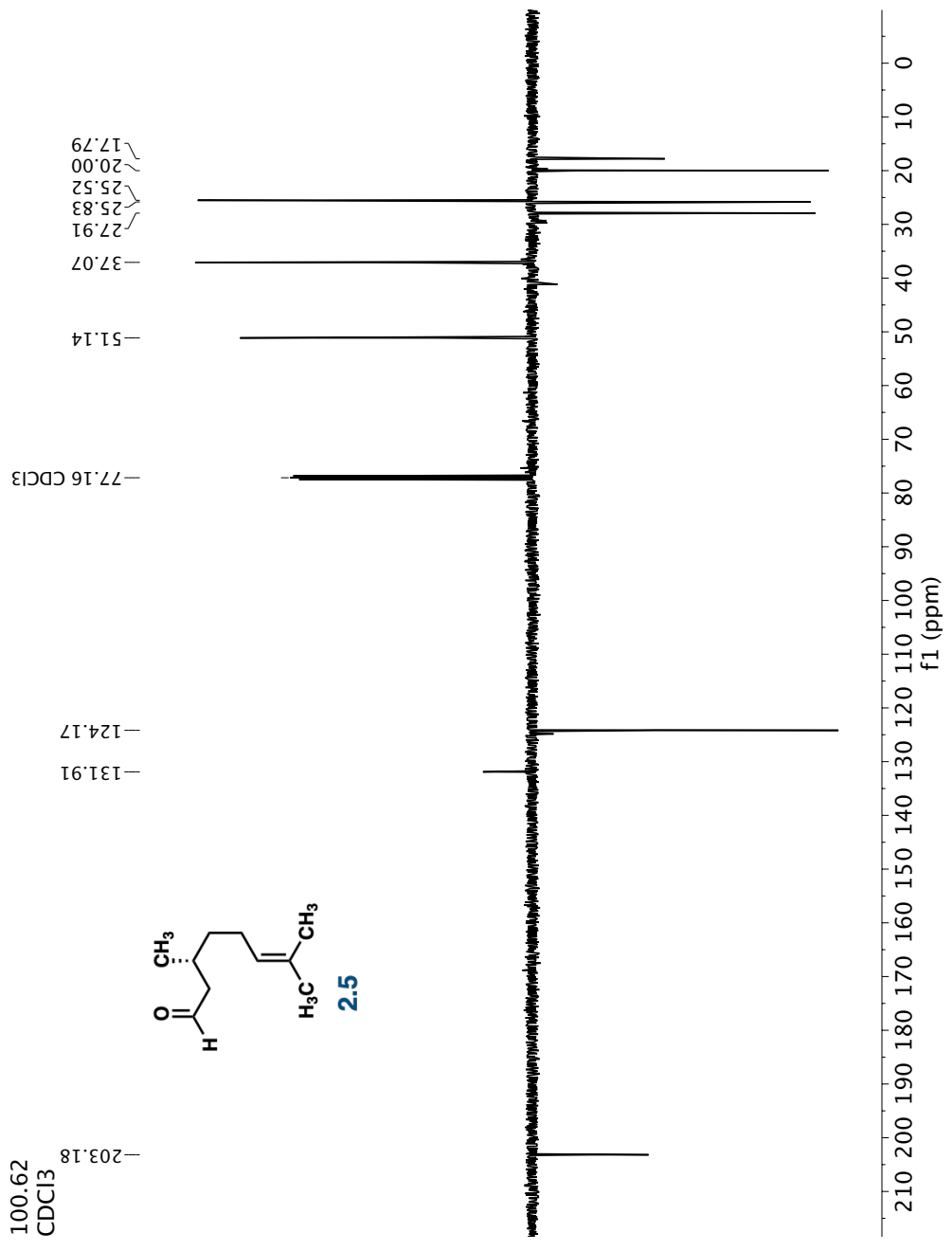




400.13
CDCl₃

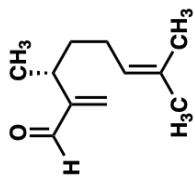
-7.26 CDCl₃



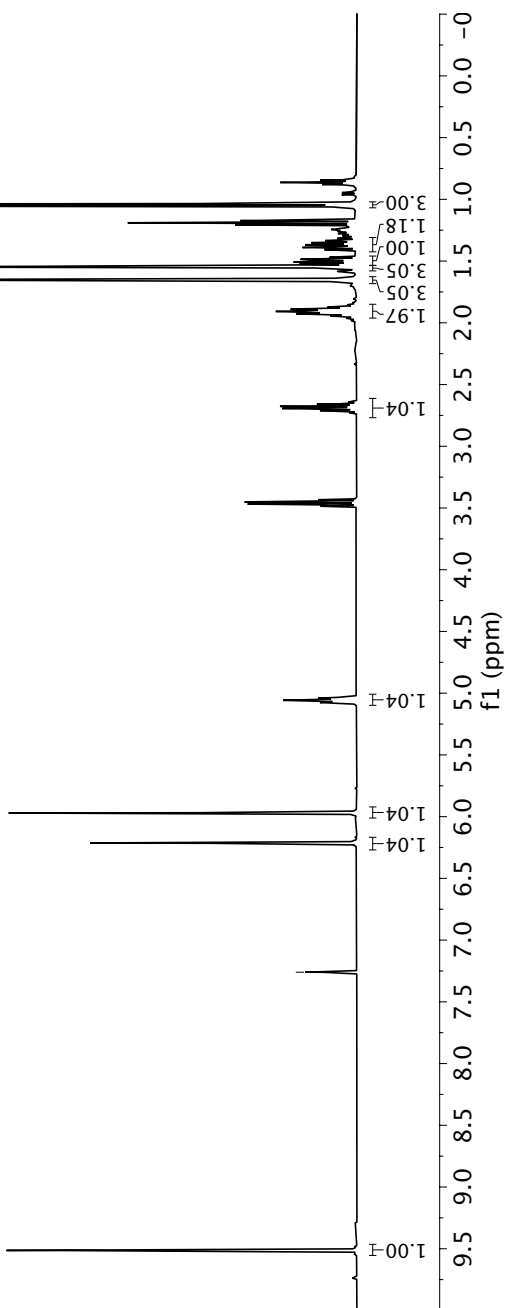


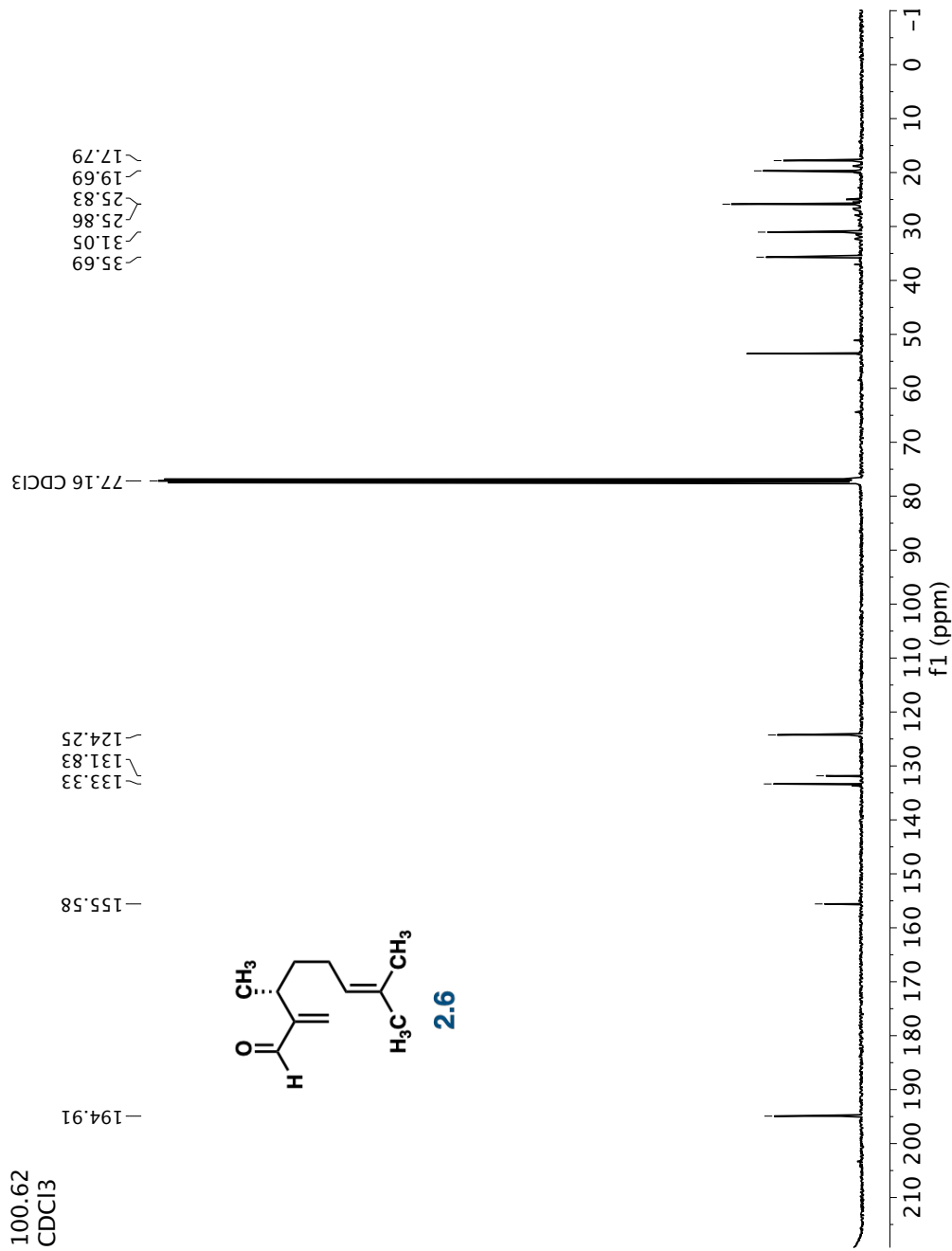
400.13
CDCl₃

-7.26 CDCl₃



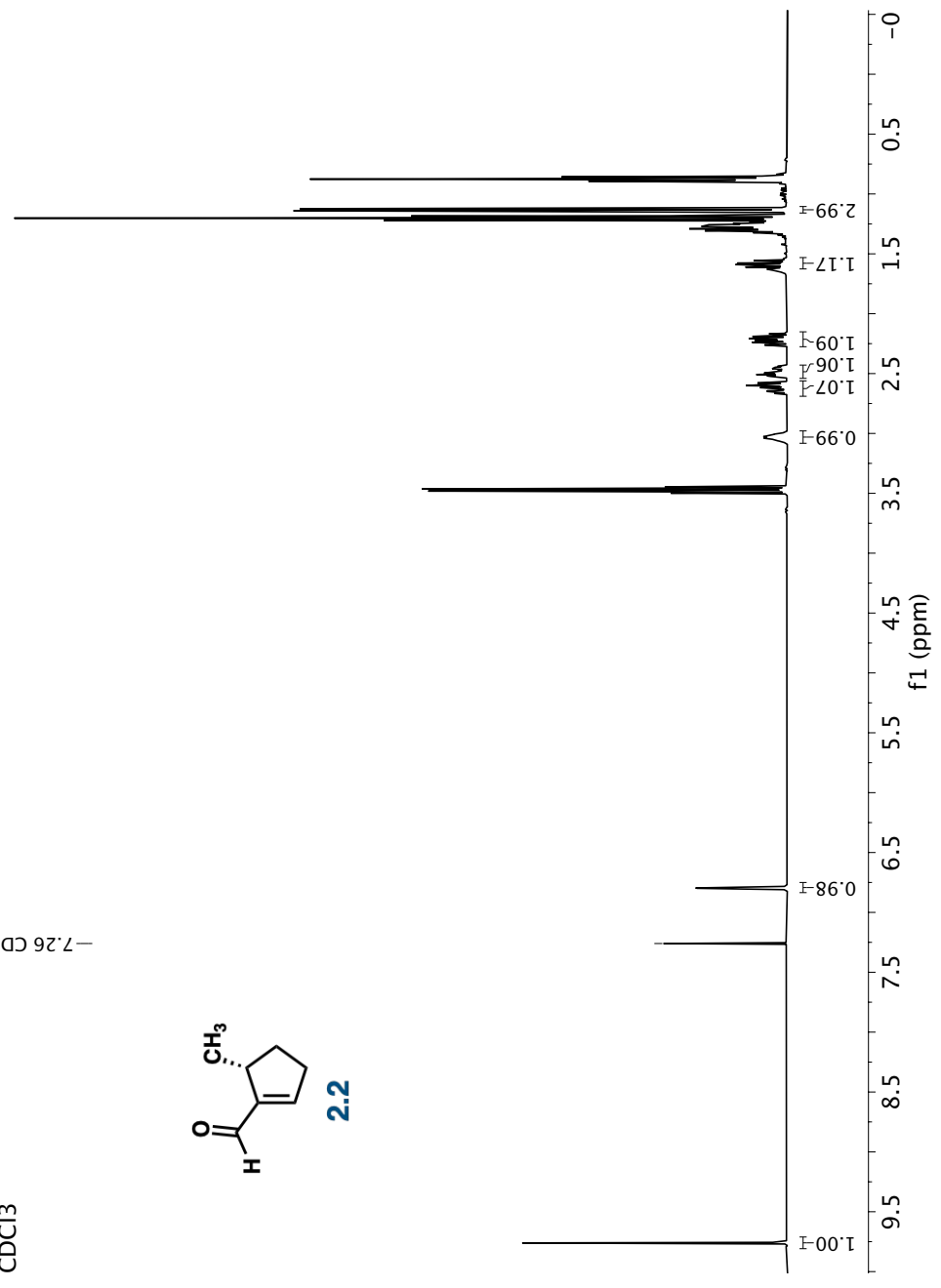
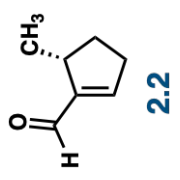
2.6

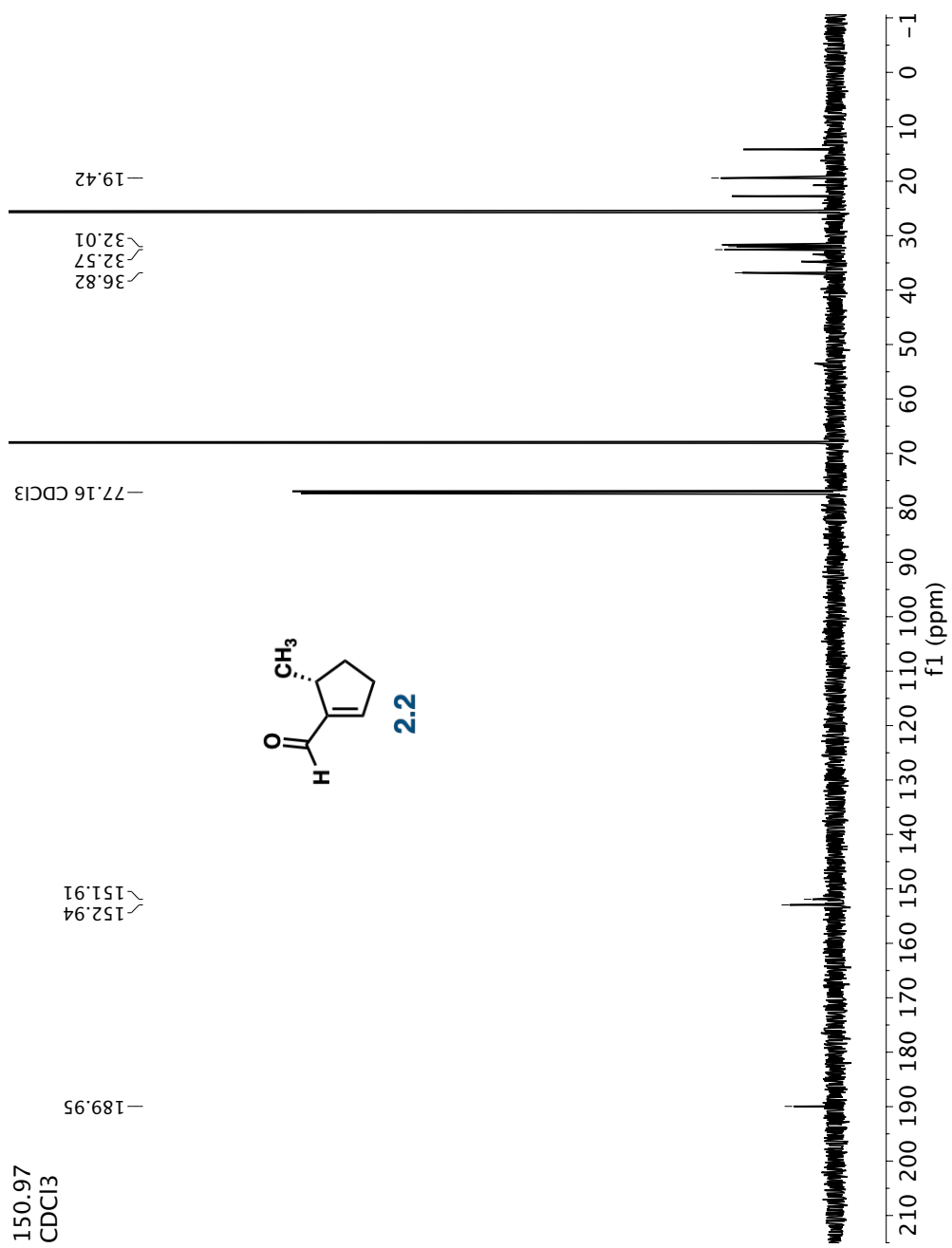




400.13
CDCl₃

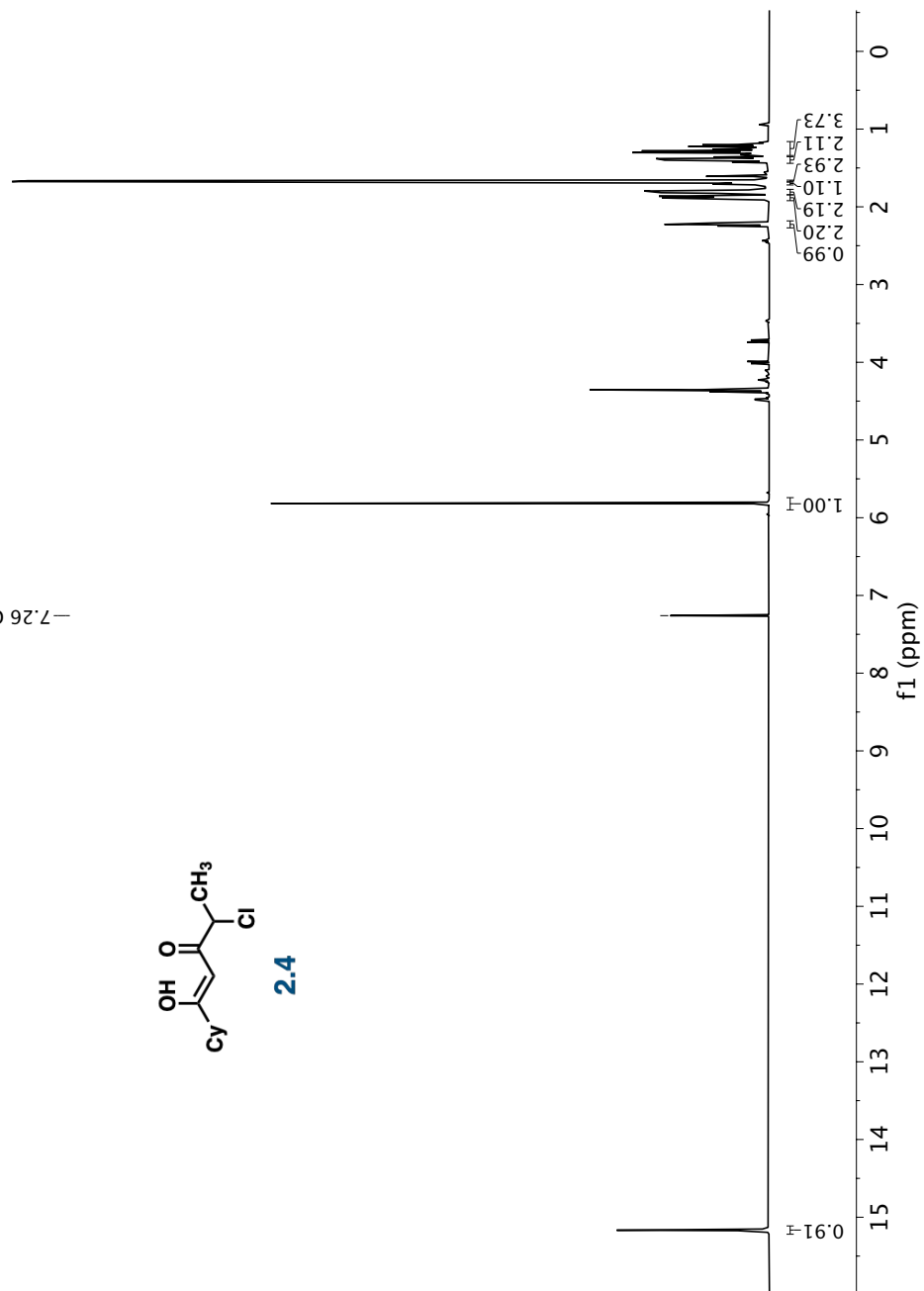
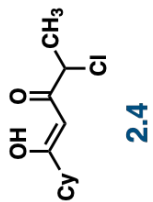
-7.26 CDCl₃

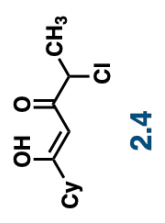
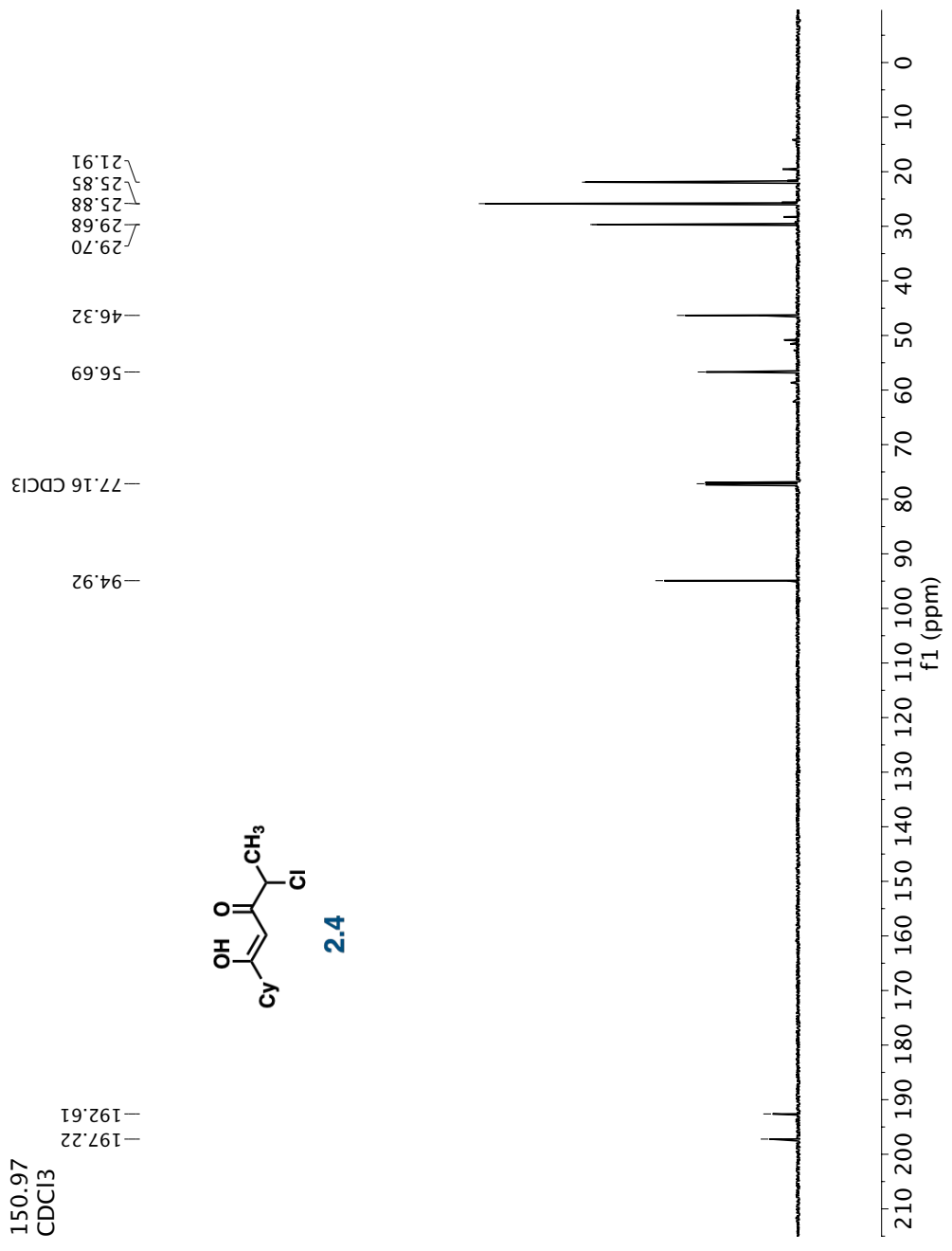




600.32
CDCl₃

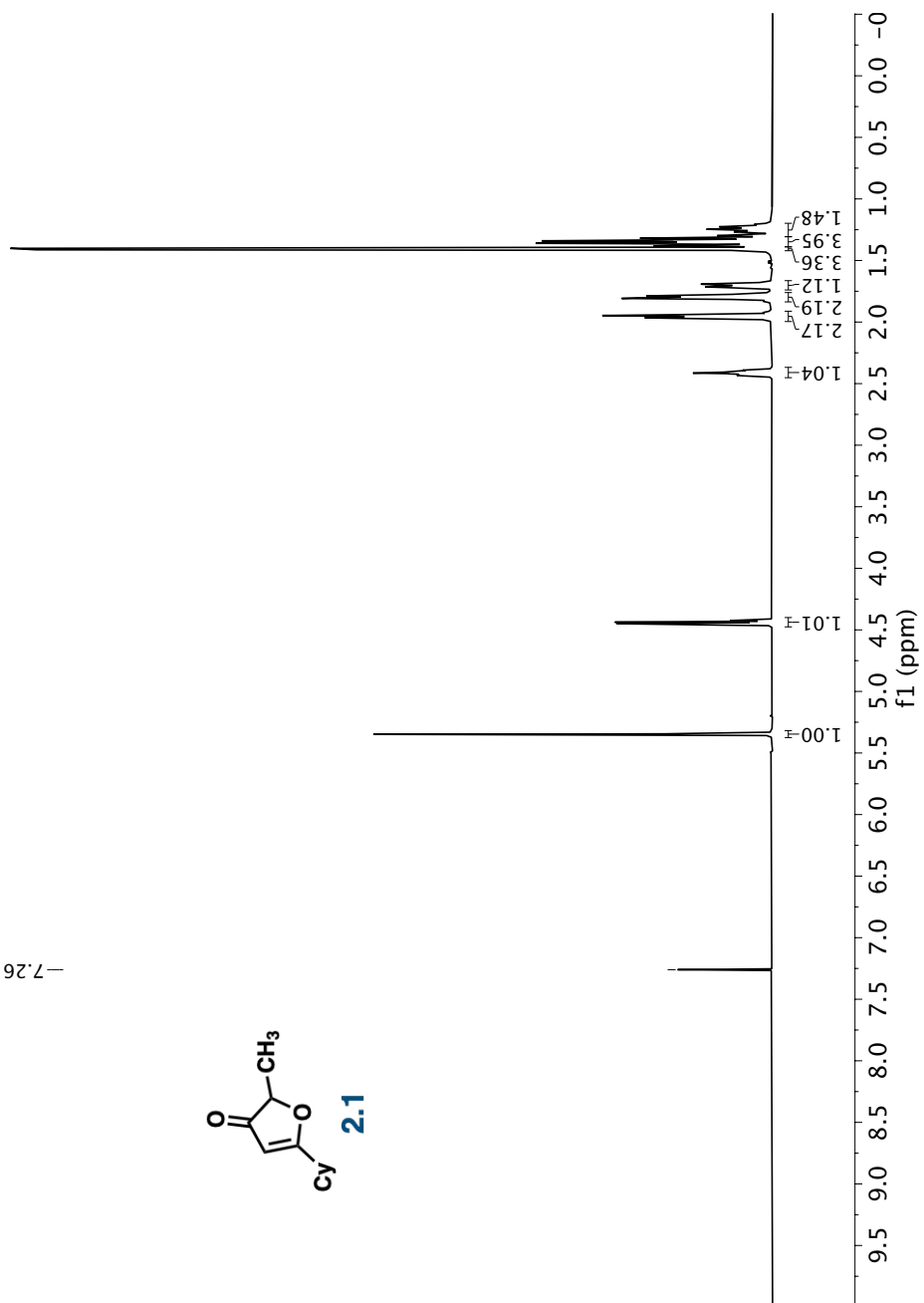
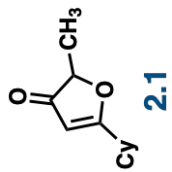
-7.26 CDCl₃

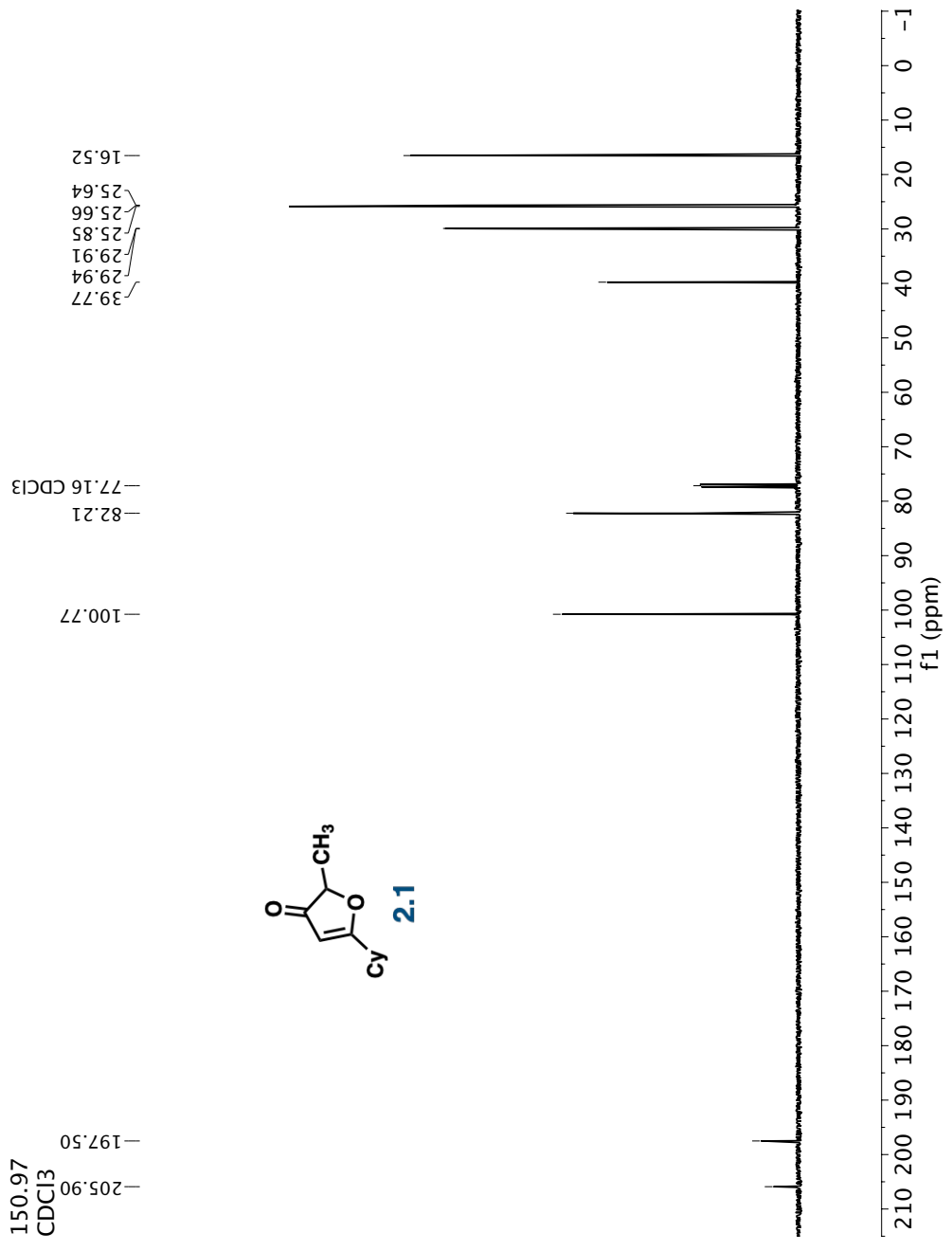




600.32
CDCl₃

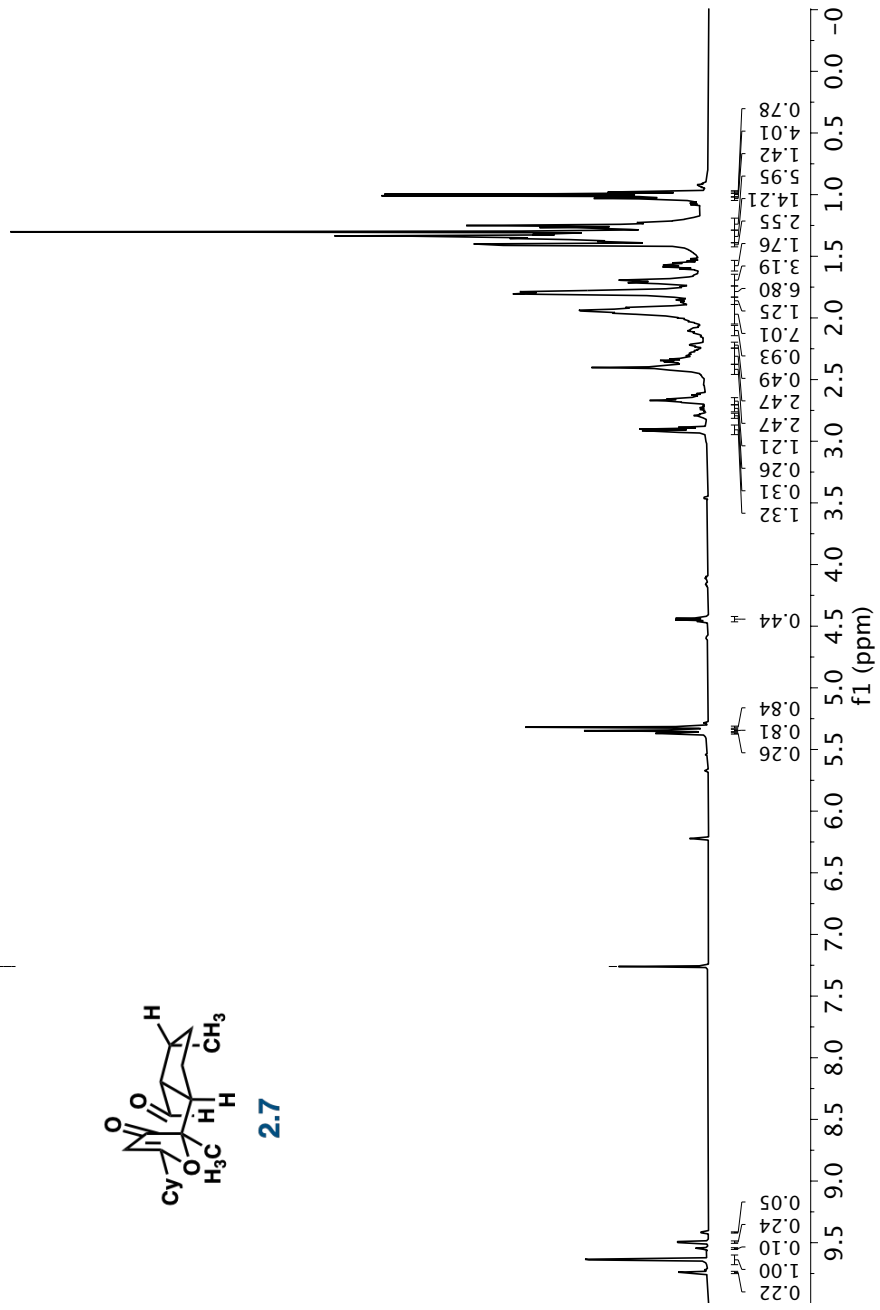
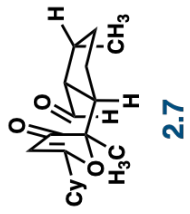
-7.26 CDCl₃

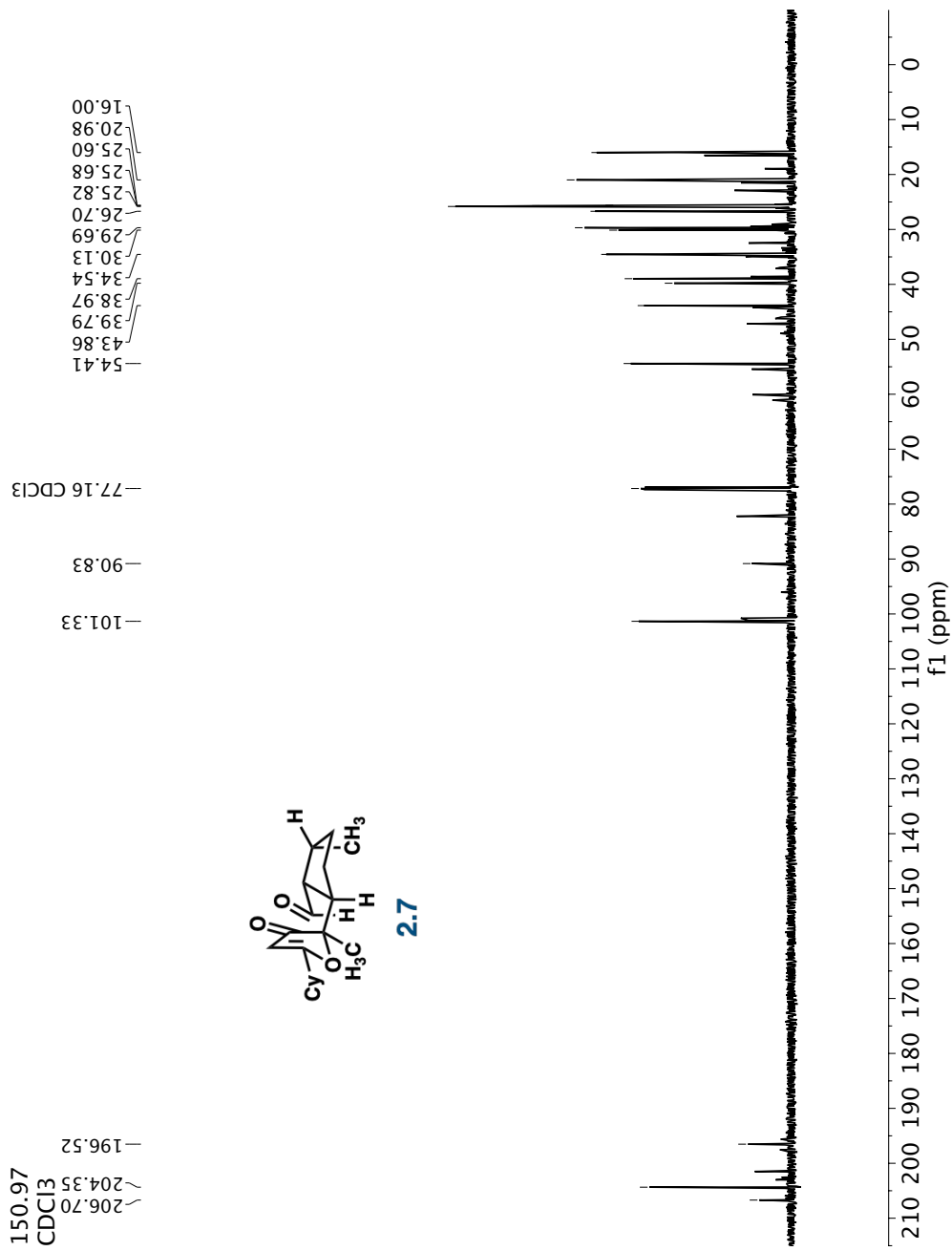




600.32
CDCl₃

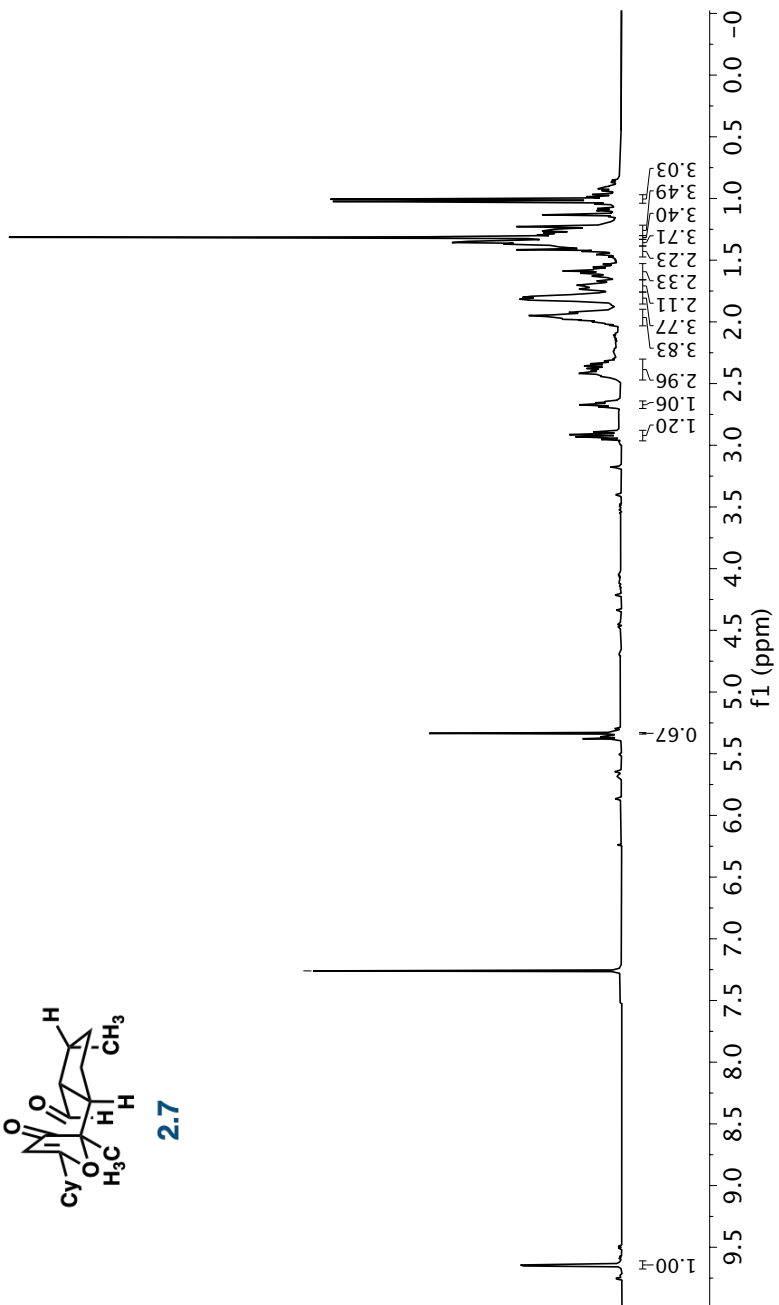
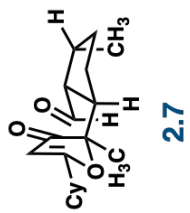
-7.26 CDCl₃

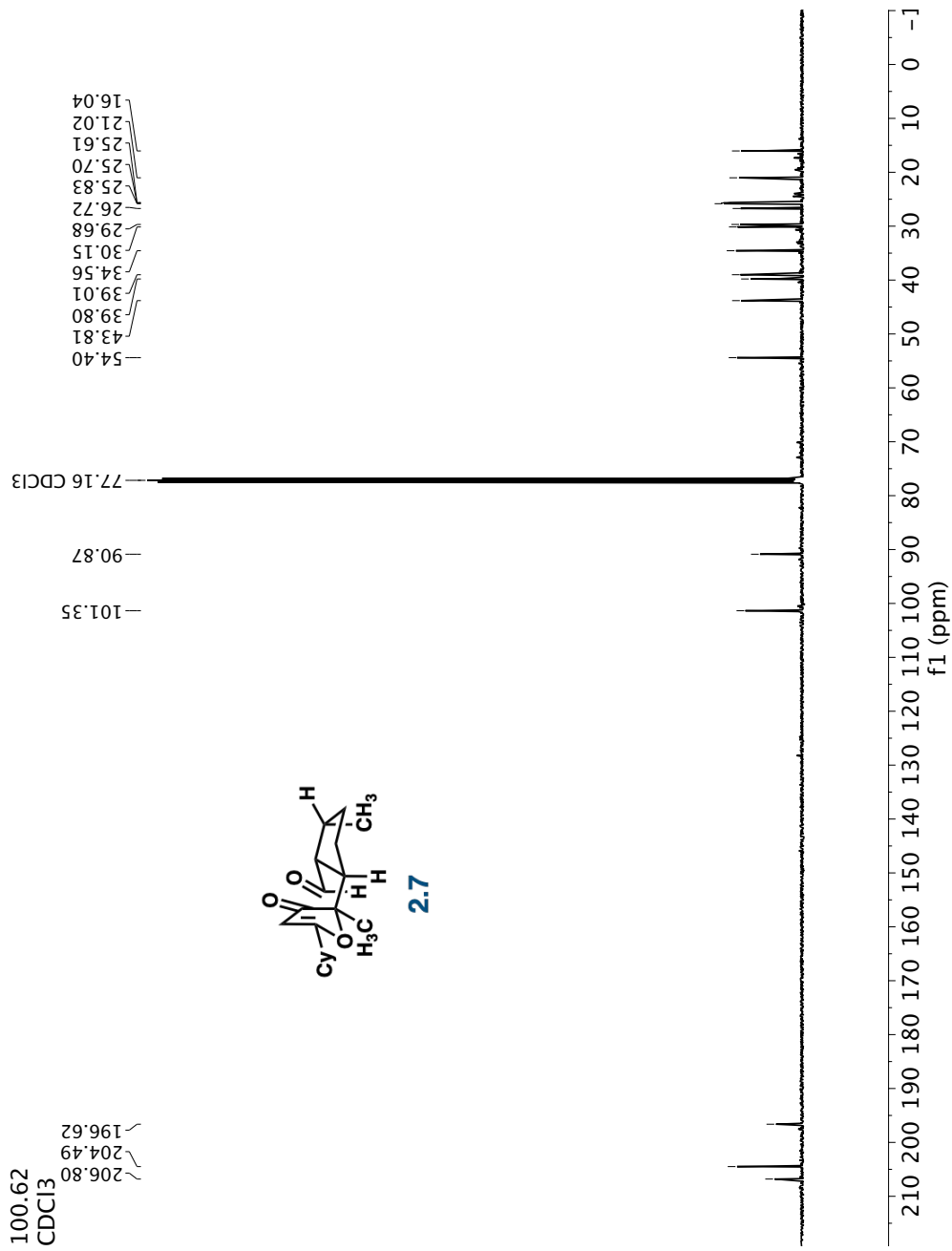




400.13
CDCl₃

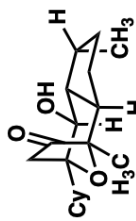
-7.26 CDCl₃



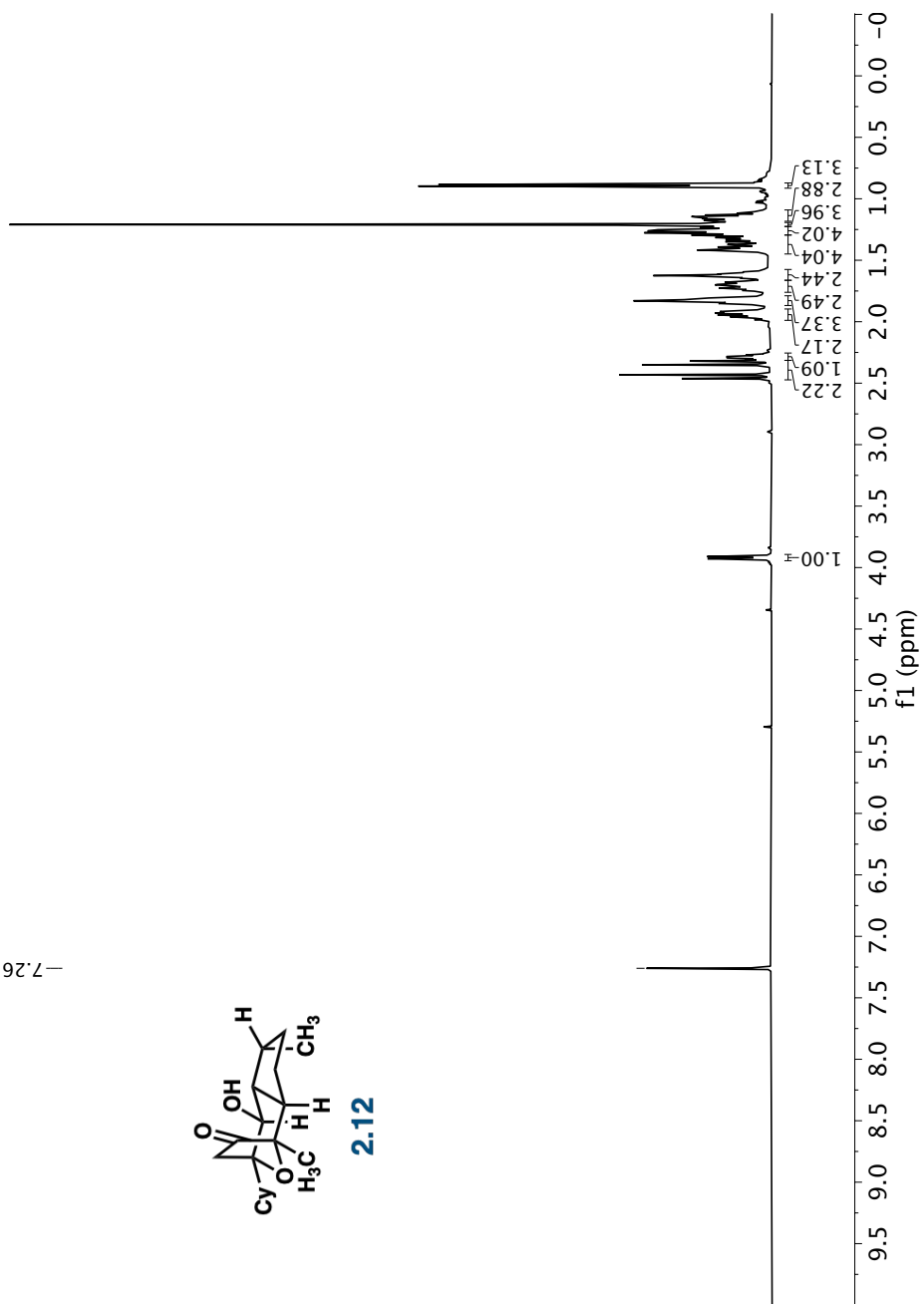


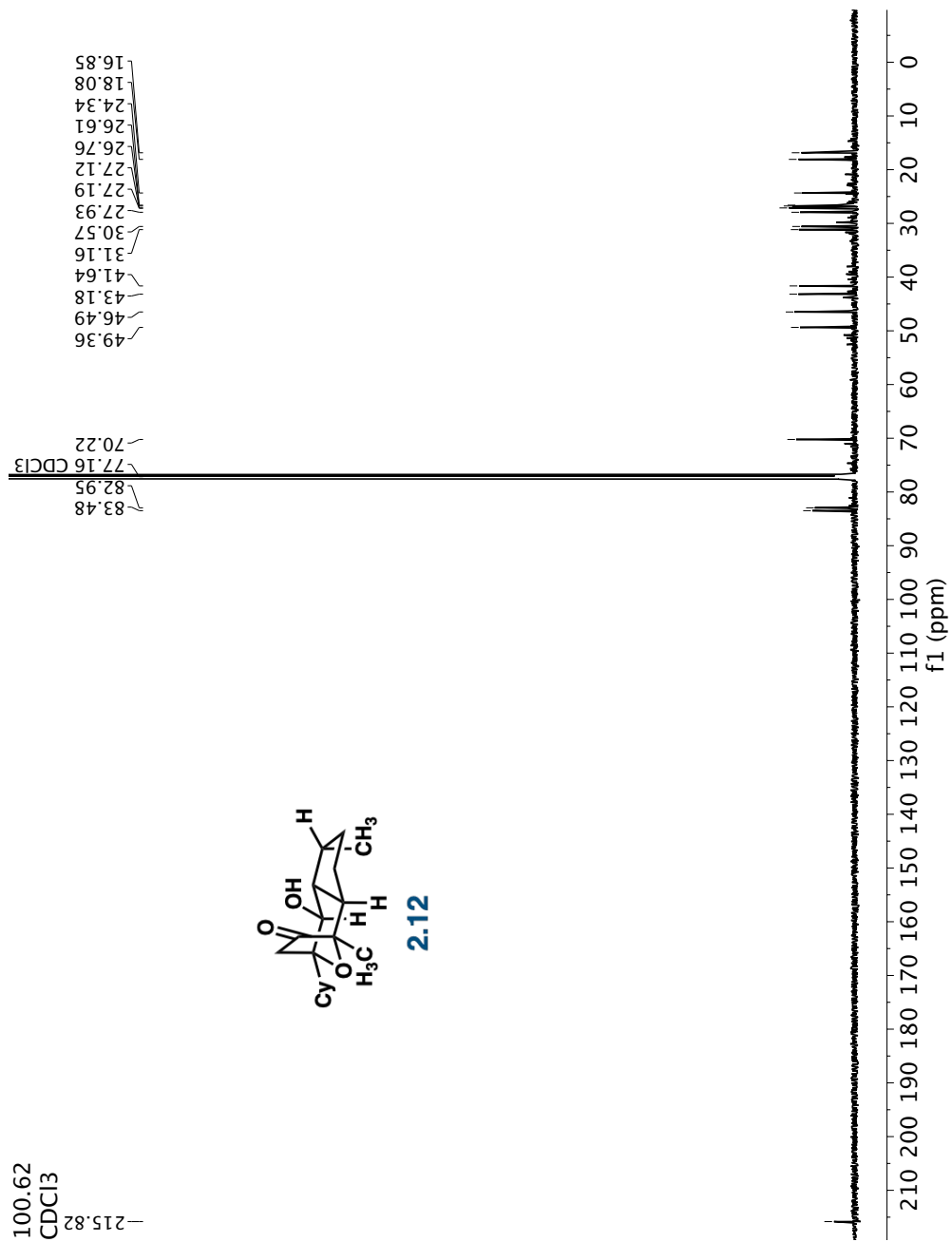
600.32
CDCl₃

-7.26 CDCl₃



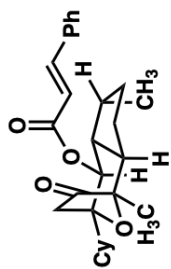
2.12



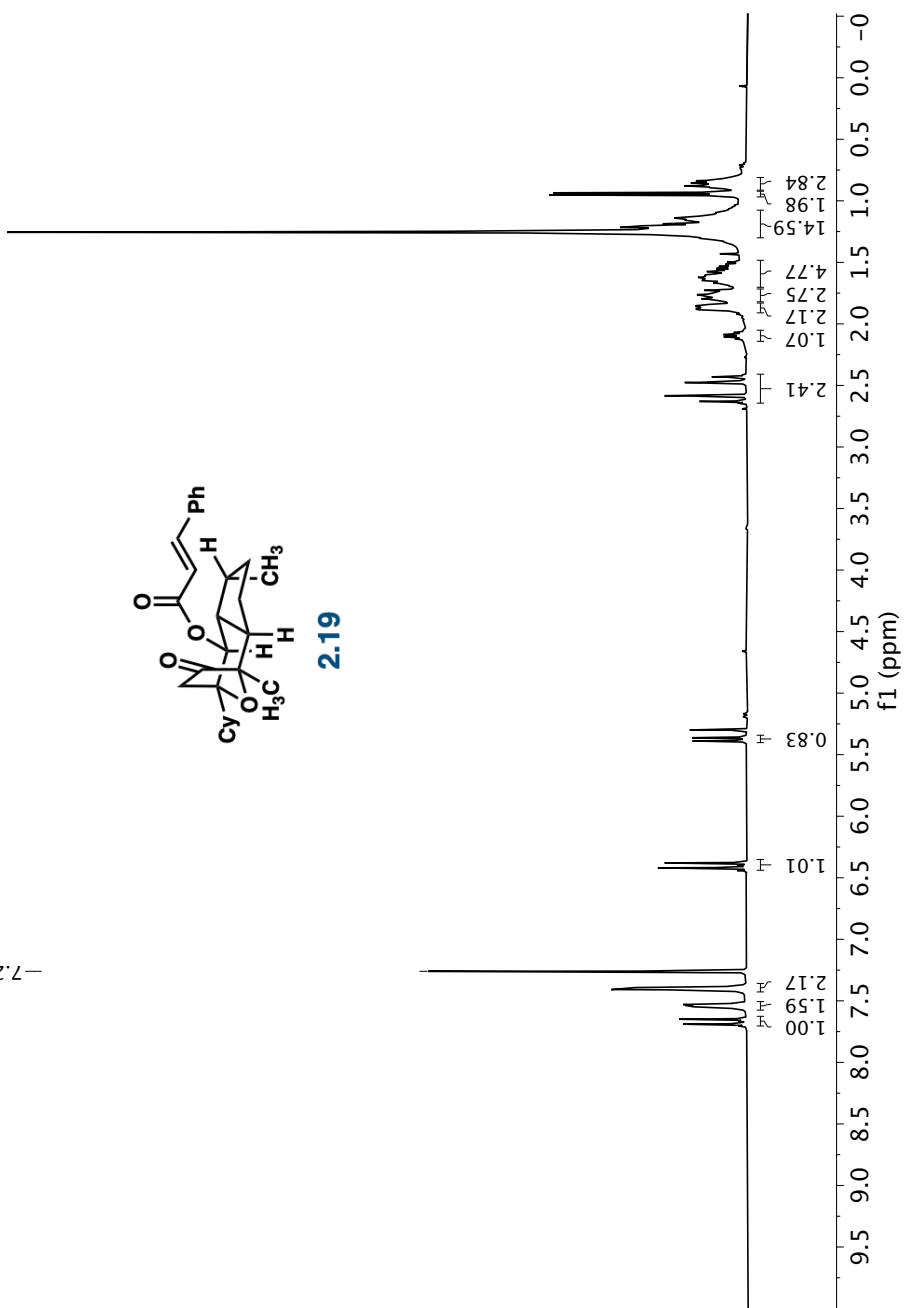


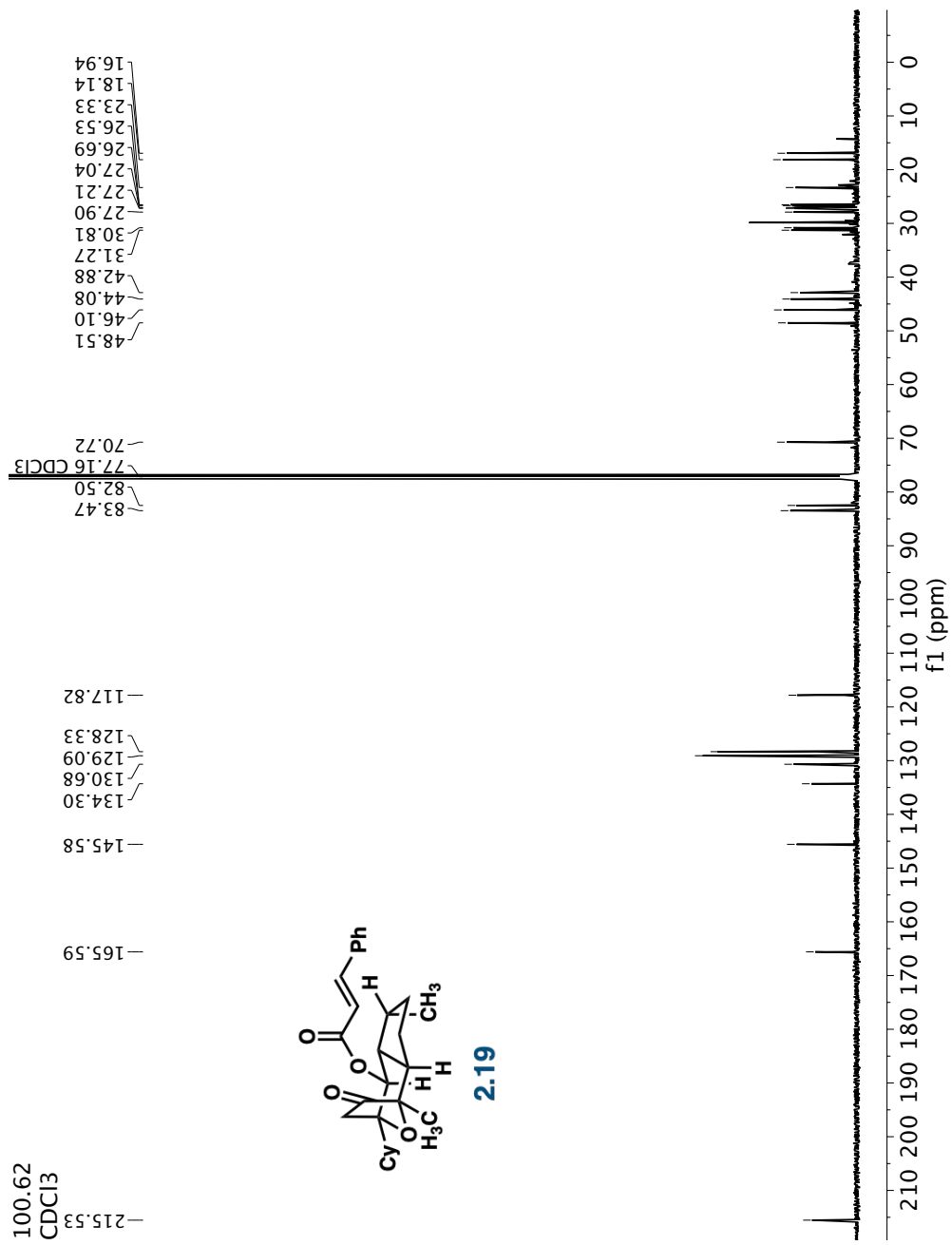
400.13
CDCl₃

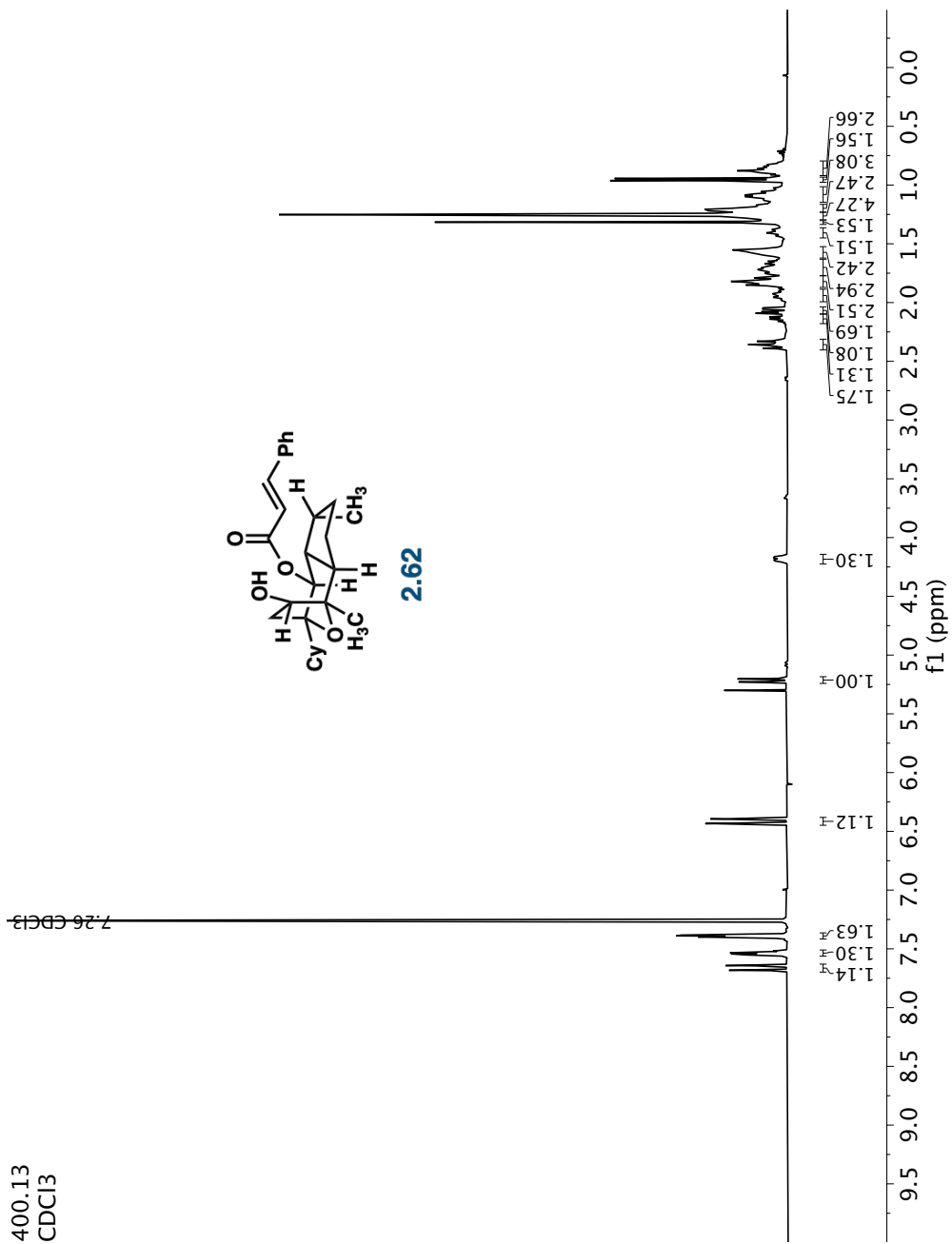
-7.26 CDCl₃

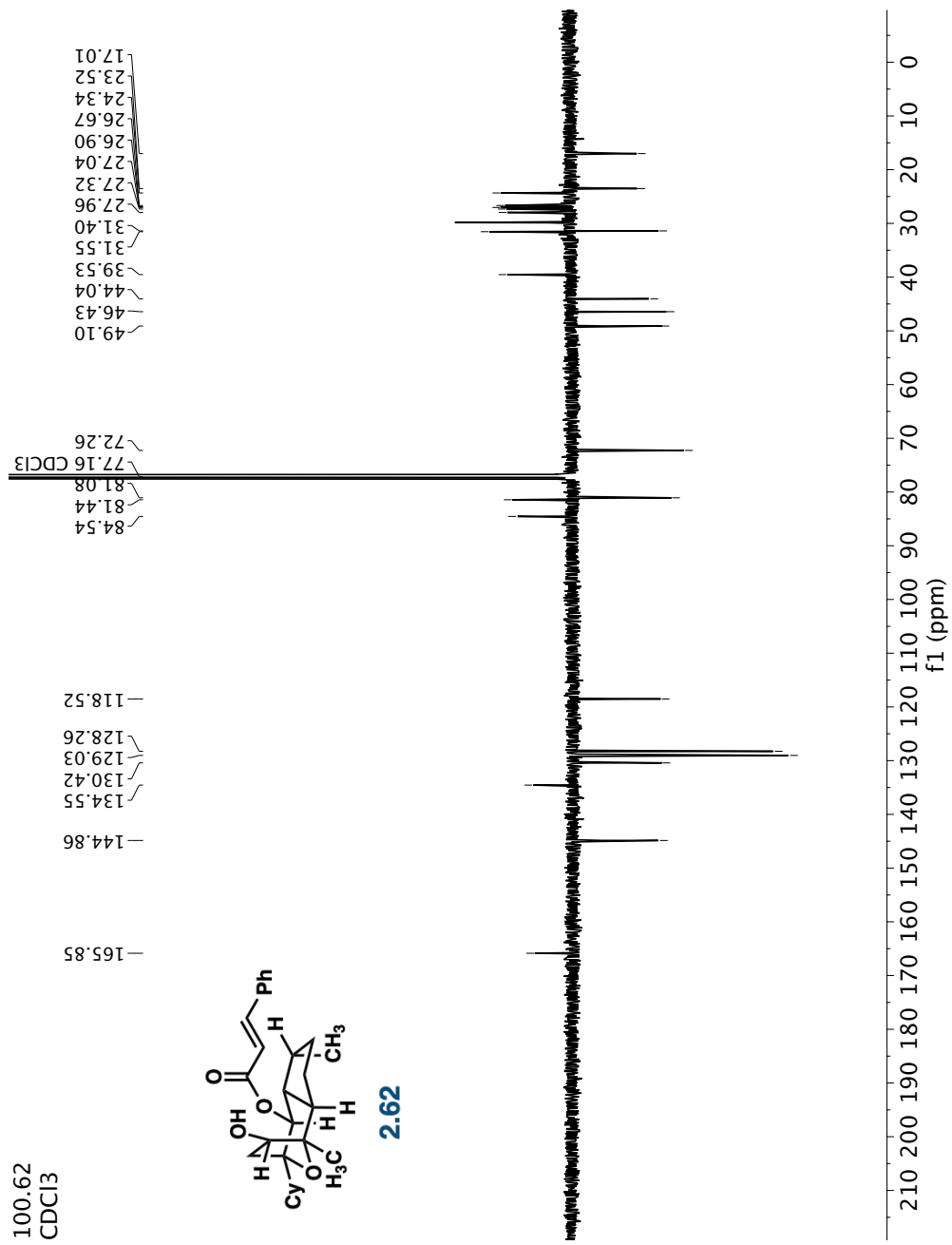


2.19



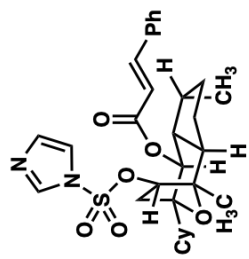




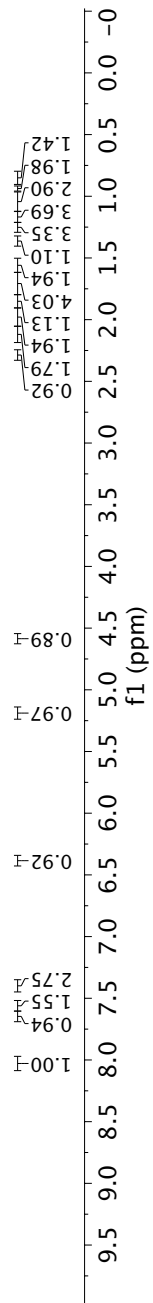


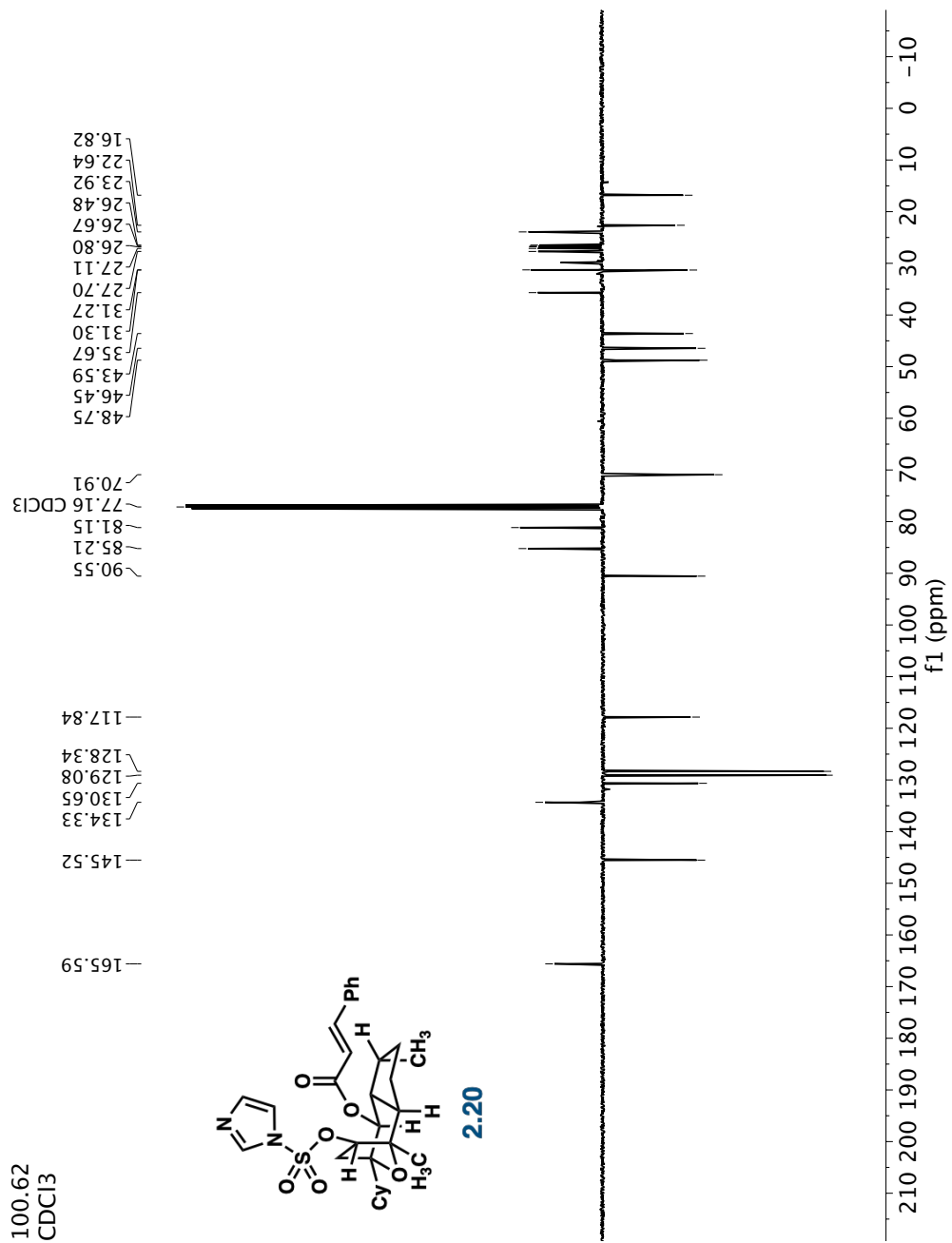
400.13
CDCl₃

-7.26 CDCl₃



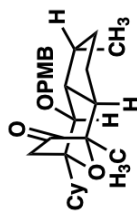
2.20



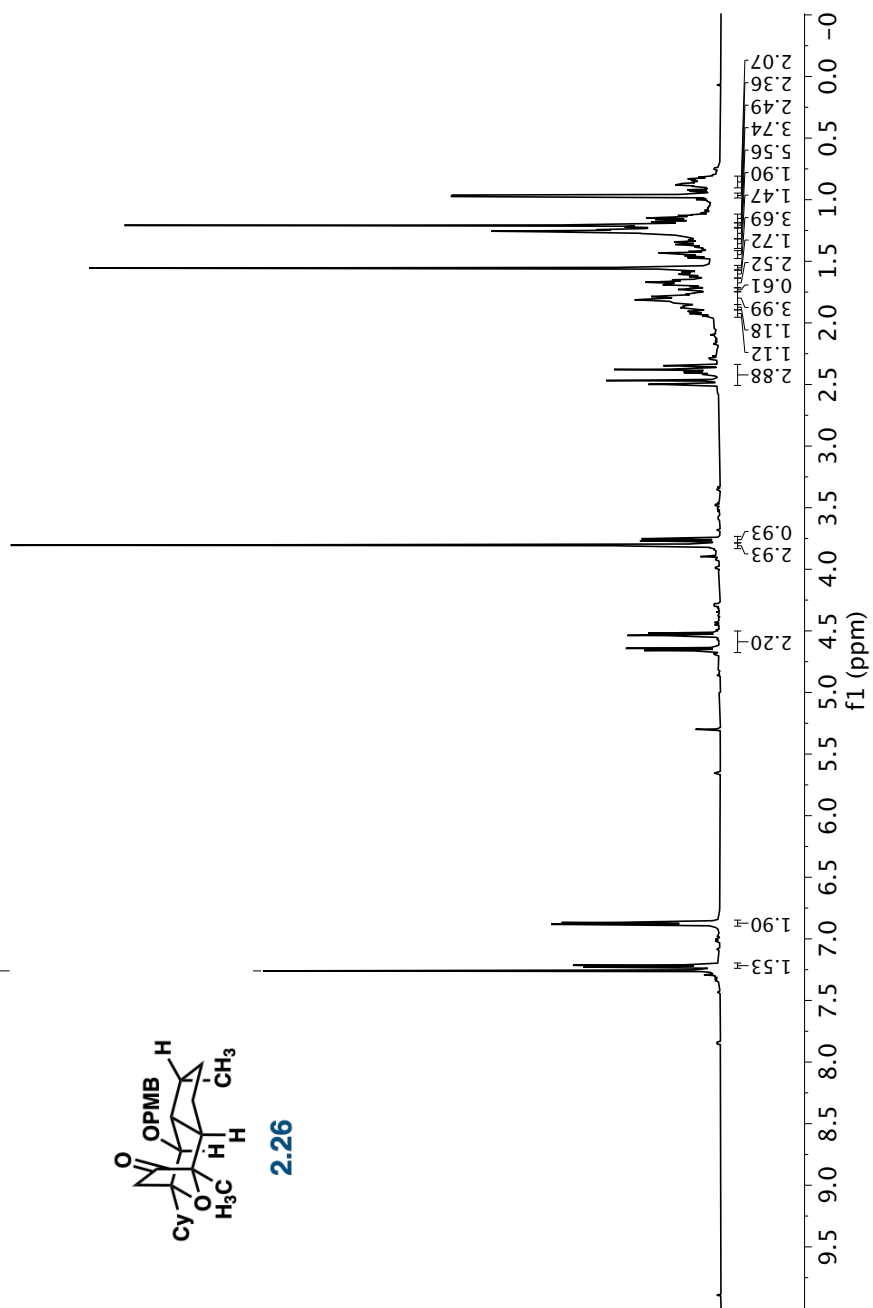


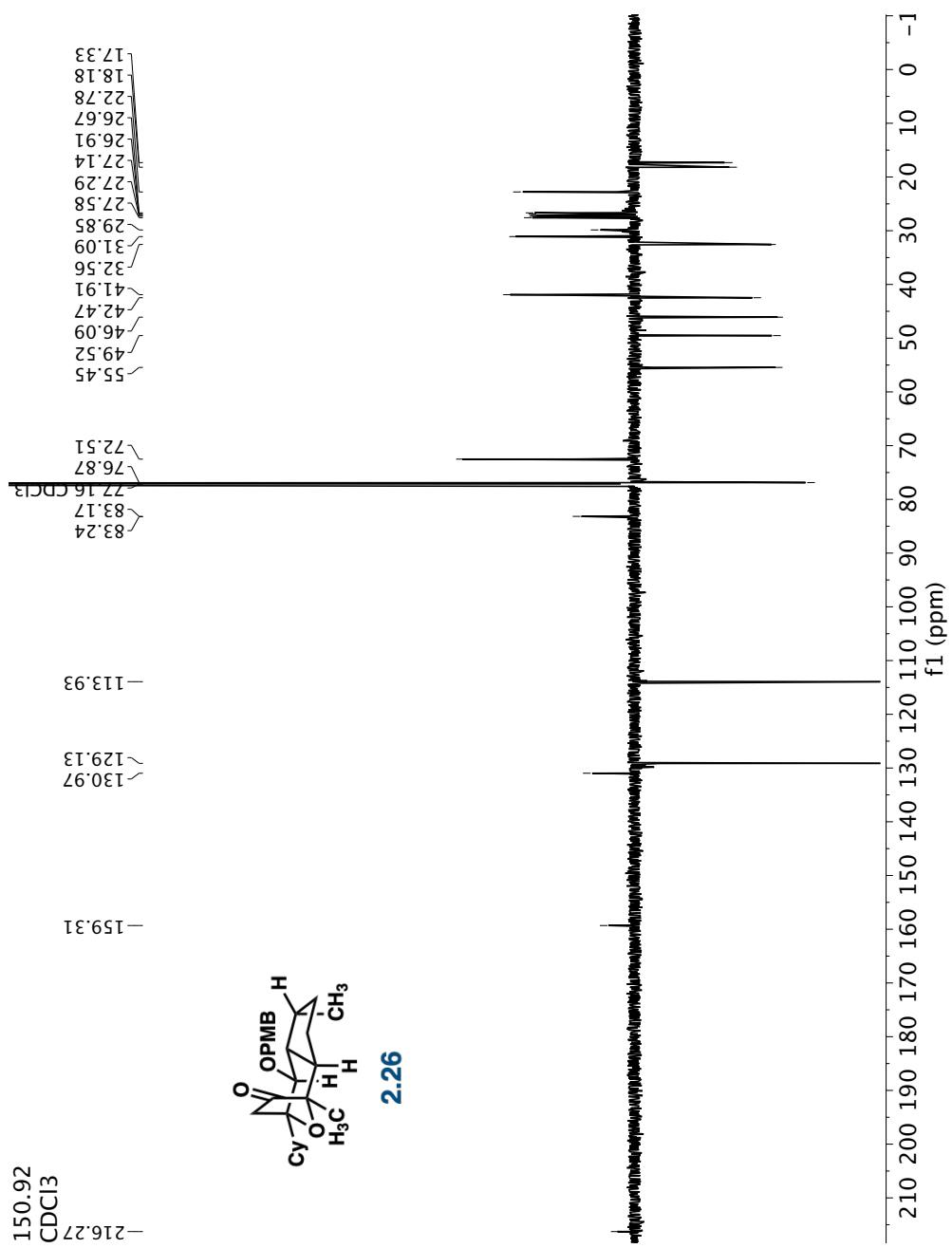
600.13
CDCl₃

-7.26 CDCl₃



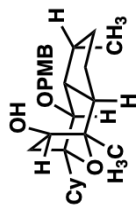
2.26



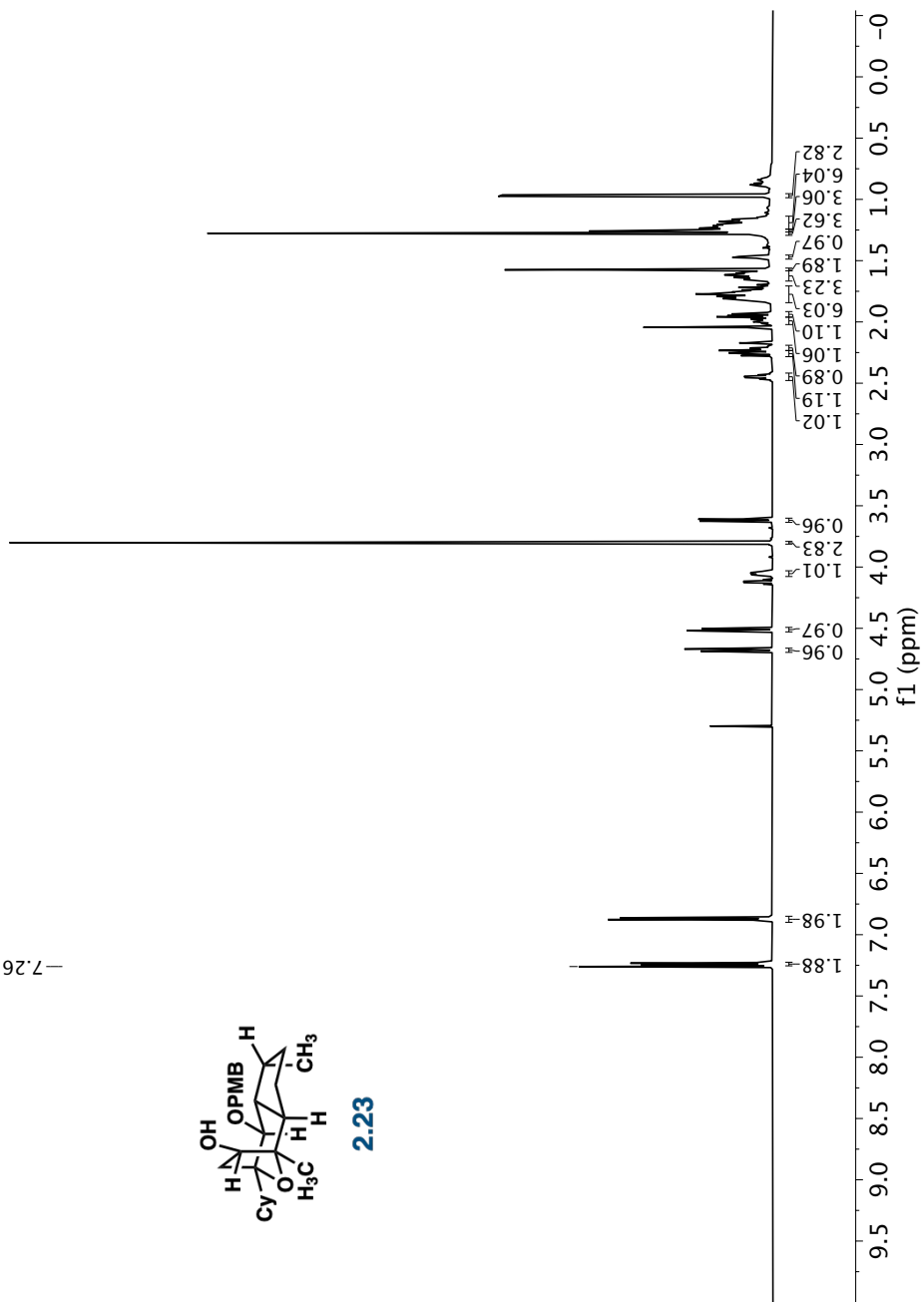


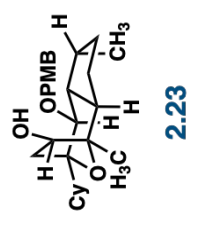
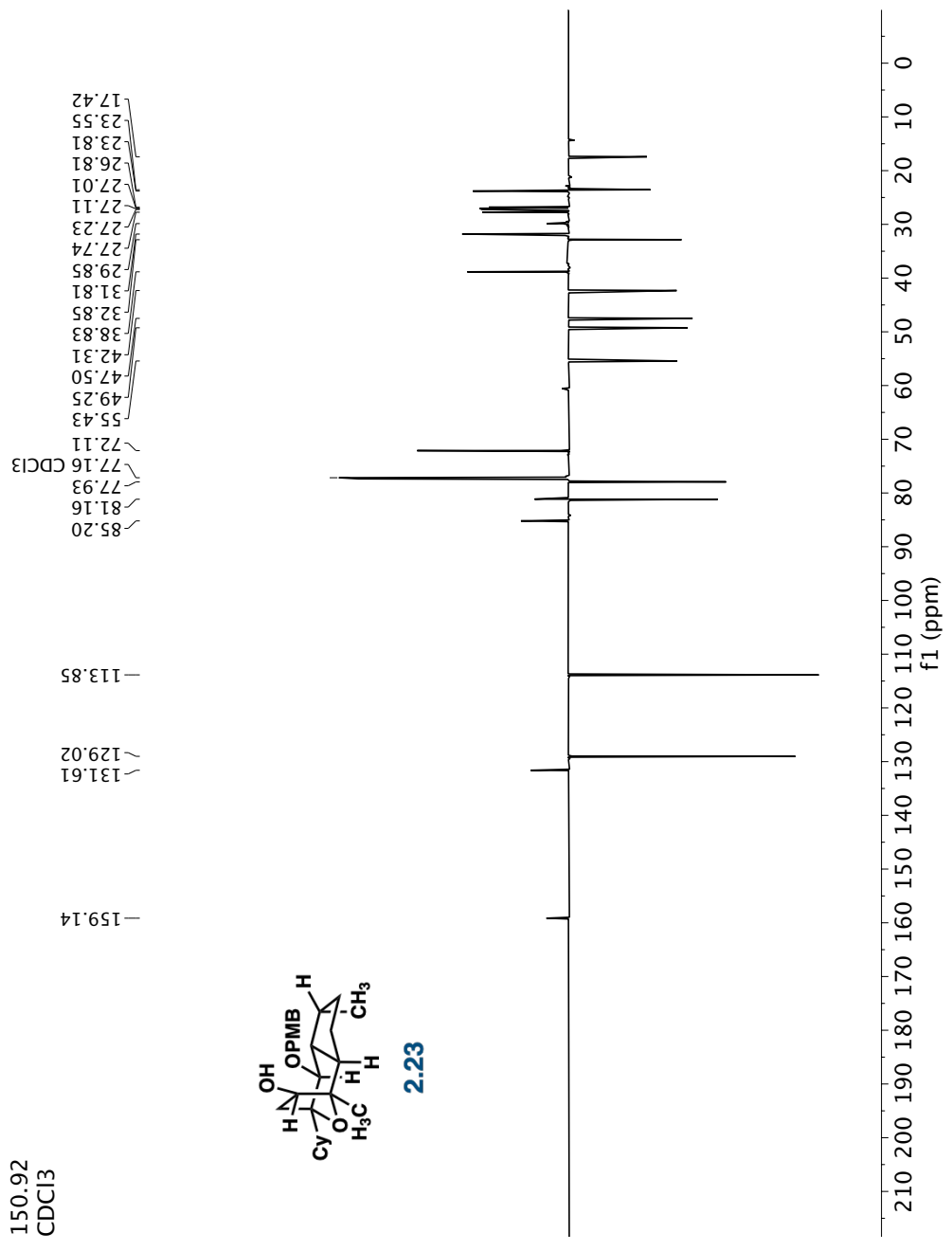
600.13
CDCl₃

-7.26 CDCl₃



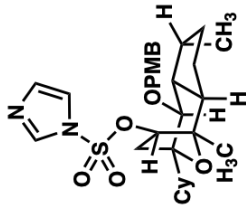
2.23



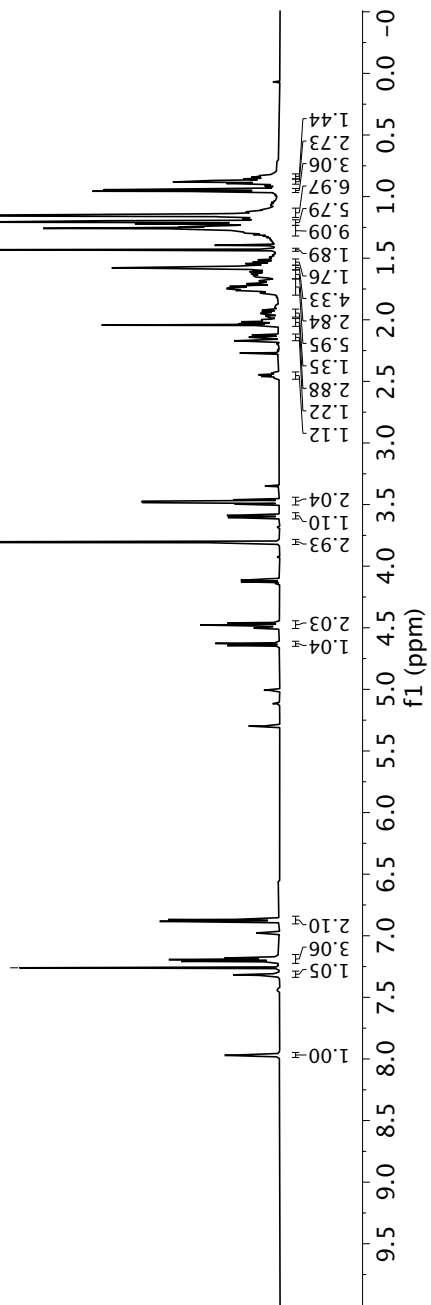


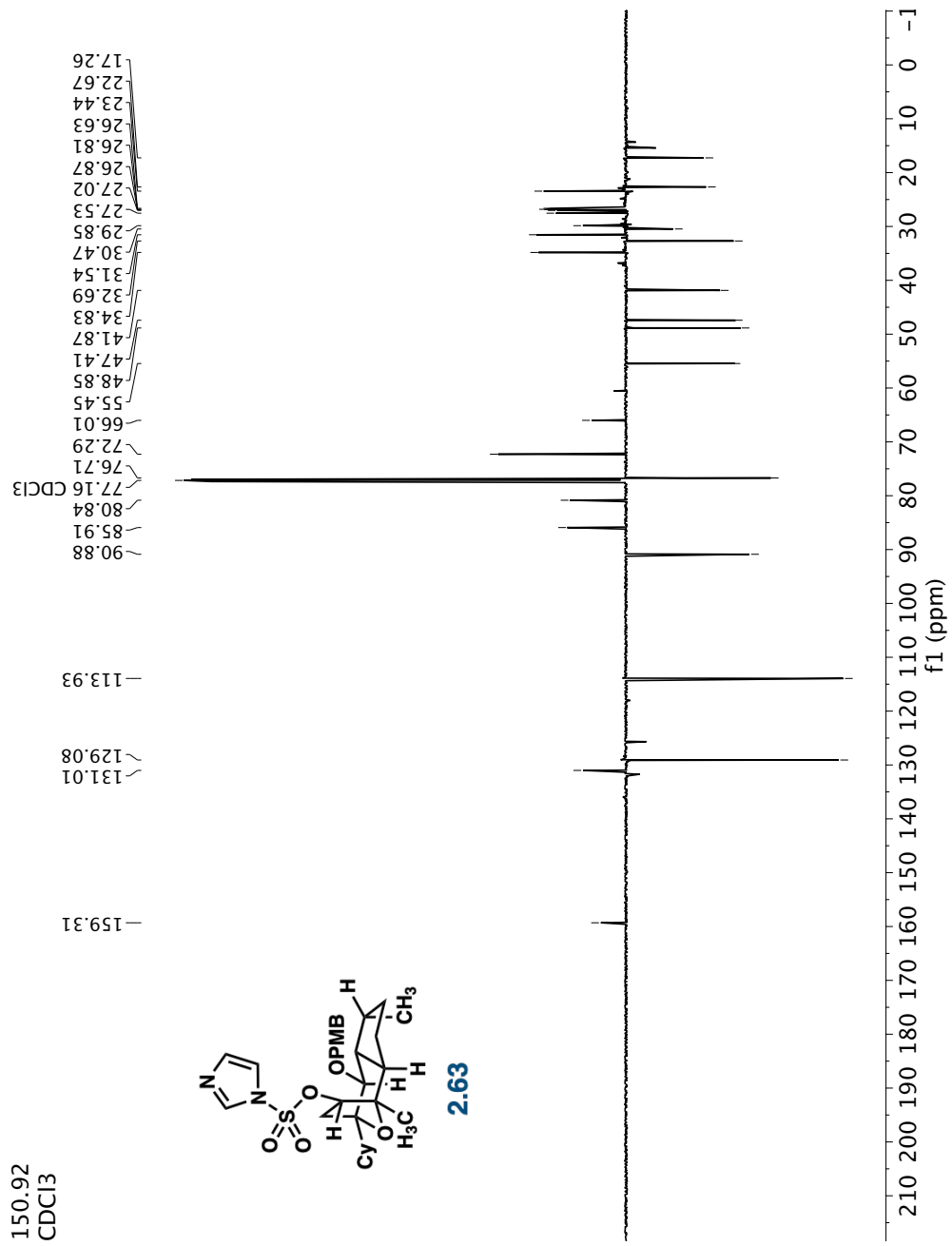
600.13
CDCl₃

-7.26 CDCl₃



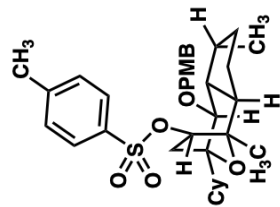
2.63



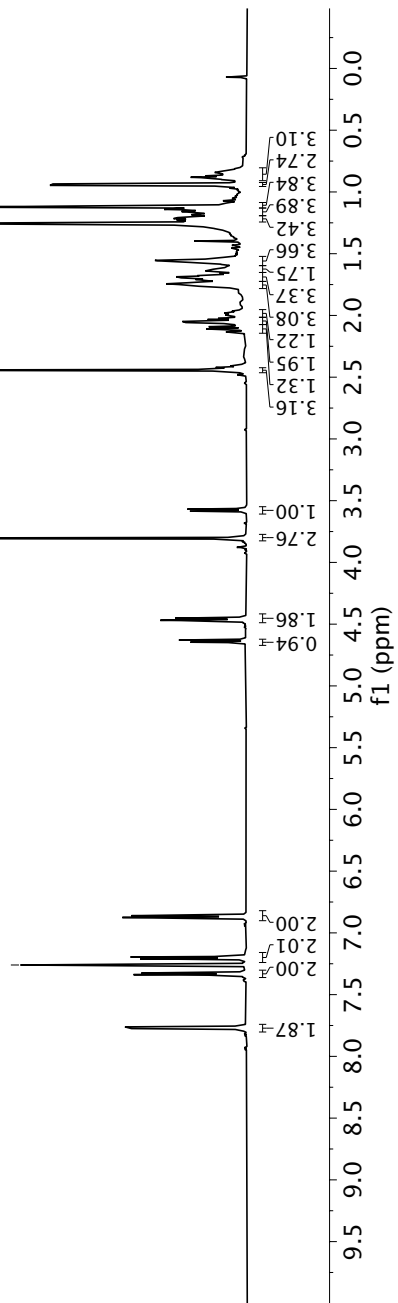


600.13
CDCl3

-7.26 CDCl3



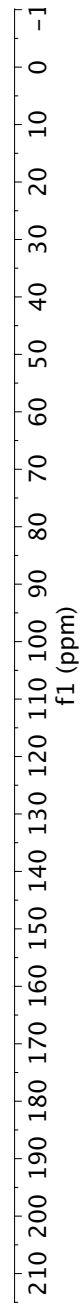
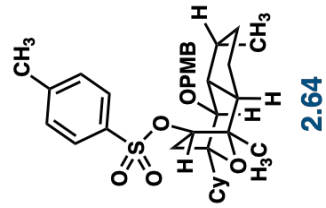
2.64



150.97
CDCl₃

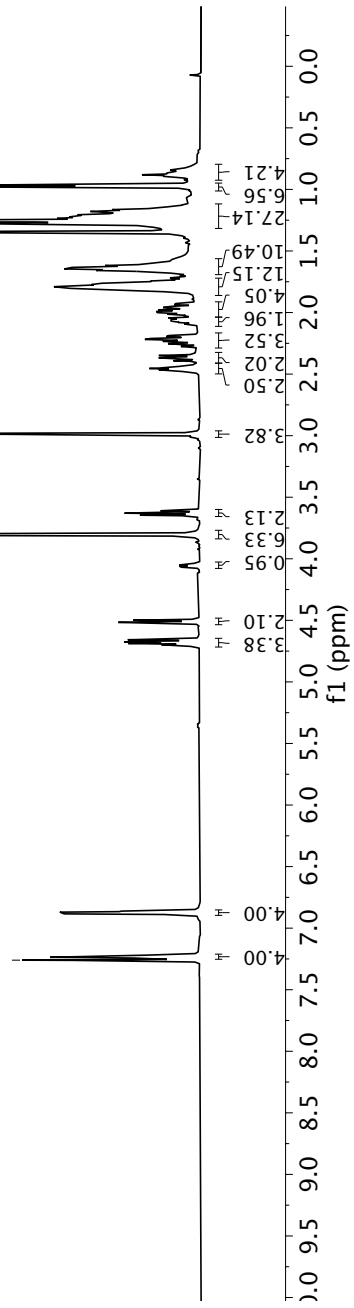
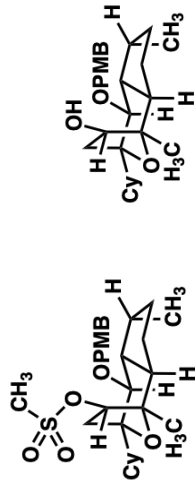
17.30
21.83
22.77
23.41
26.70
26.86
26.97
27.11
27.60
29.85
31.66
32.79
35.74
42.05
47.21
49.06
55.44
72.15
77.16
77.23
80.89
85.67
86.53

113.88
127.98
129.04
130.00
131.30
144.95



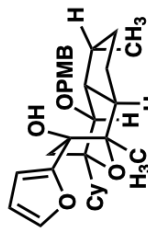
600.13
CDCl3

- 7.26 CDCl3

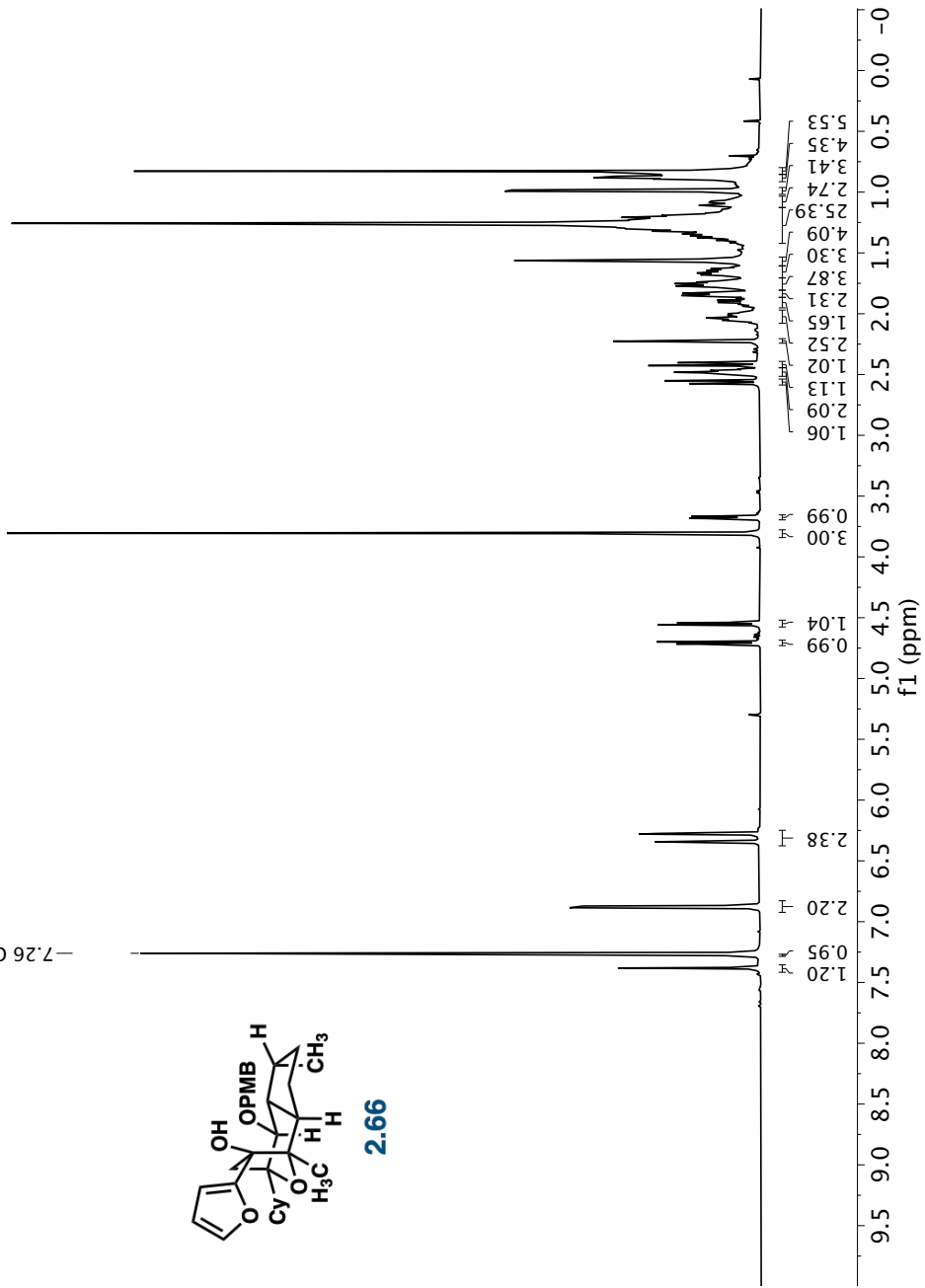


600.13
CDCl₃

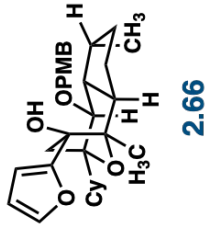
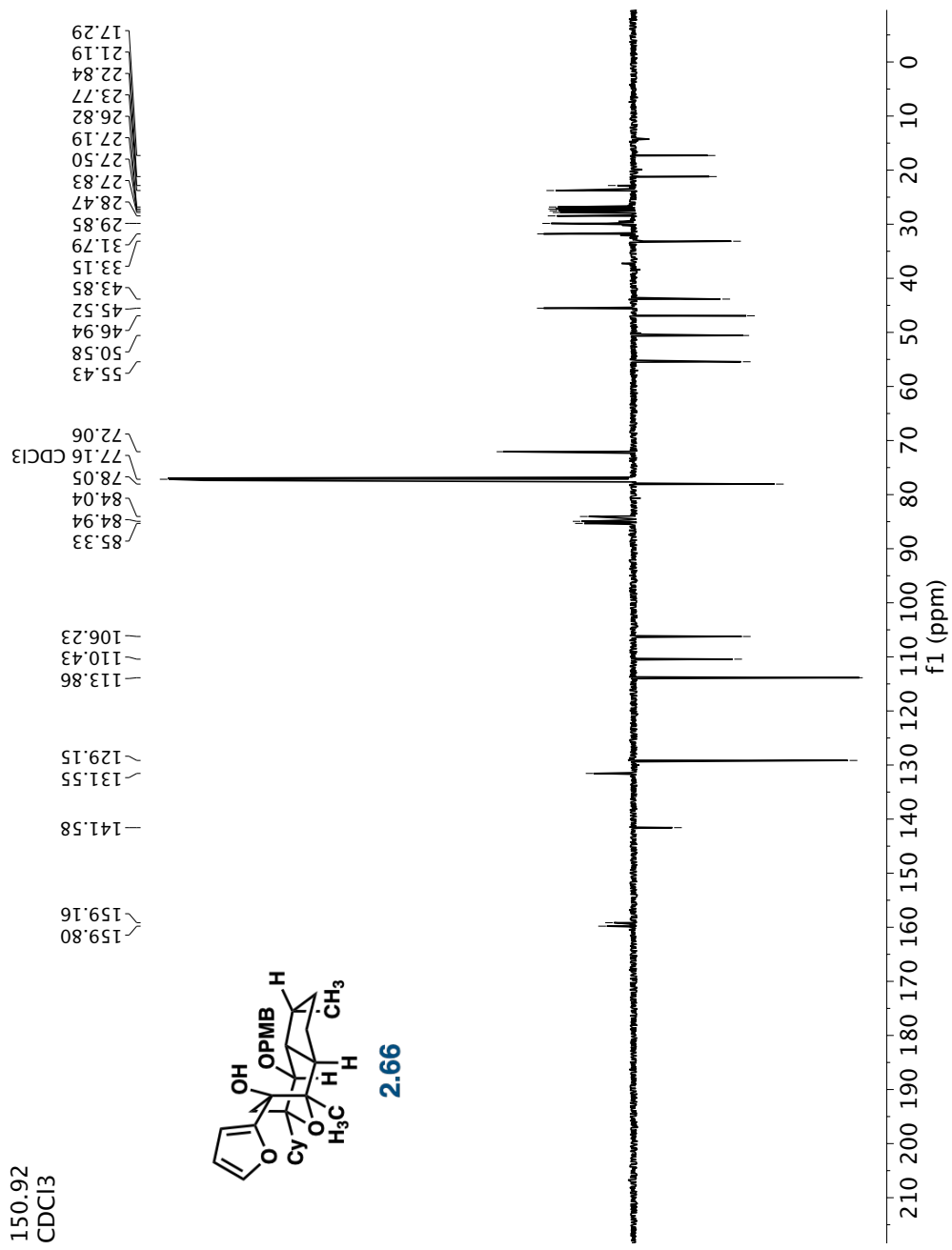
-7.26 CDCl₃

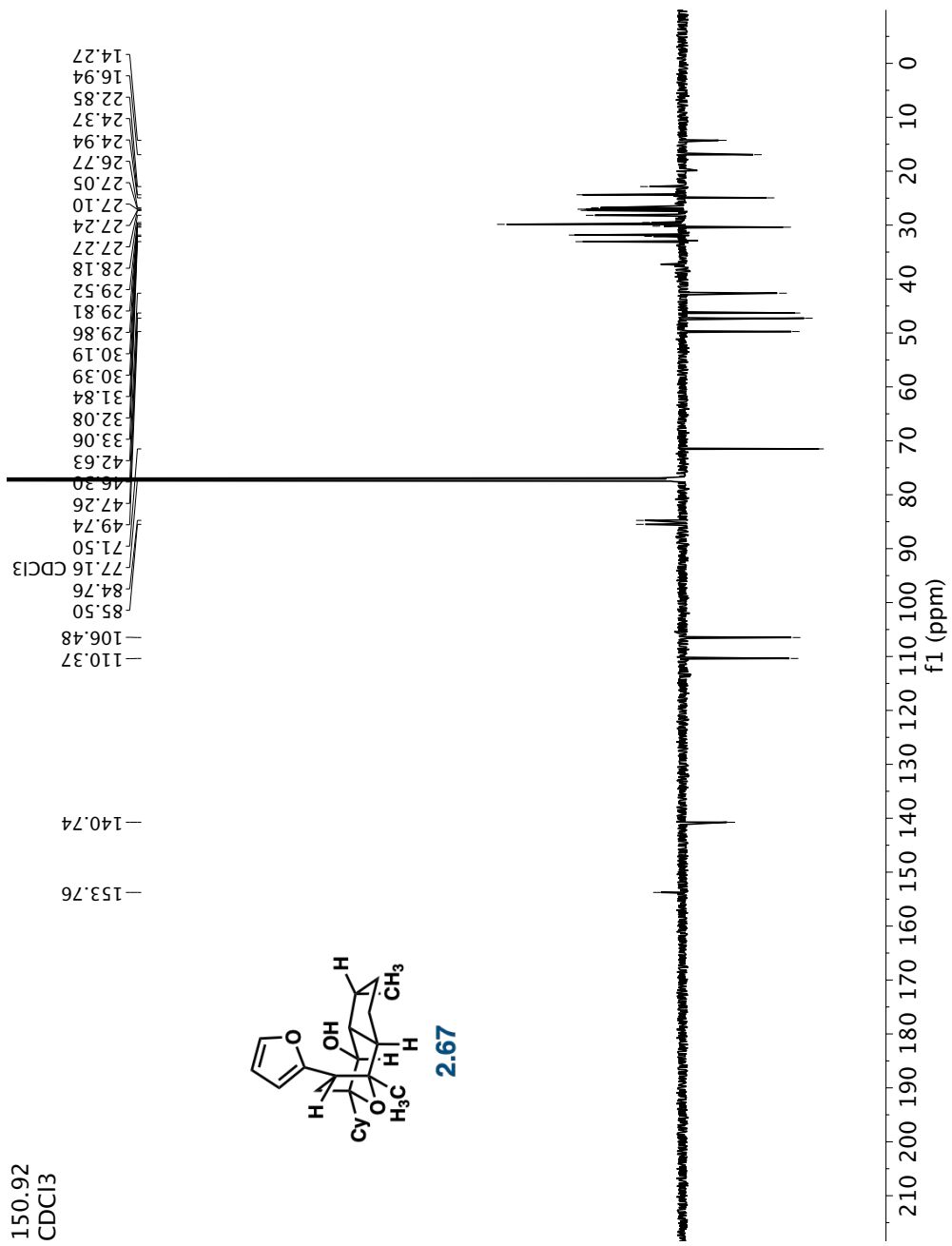


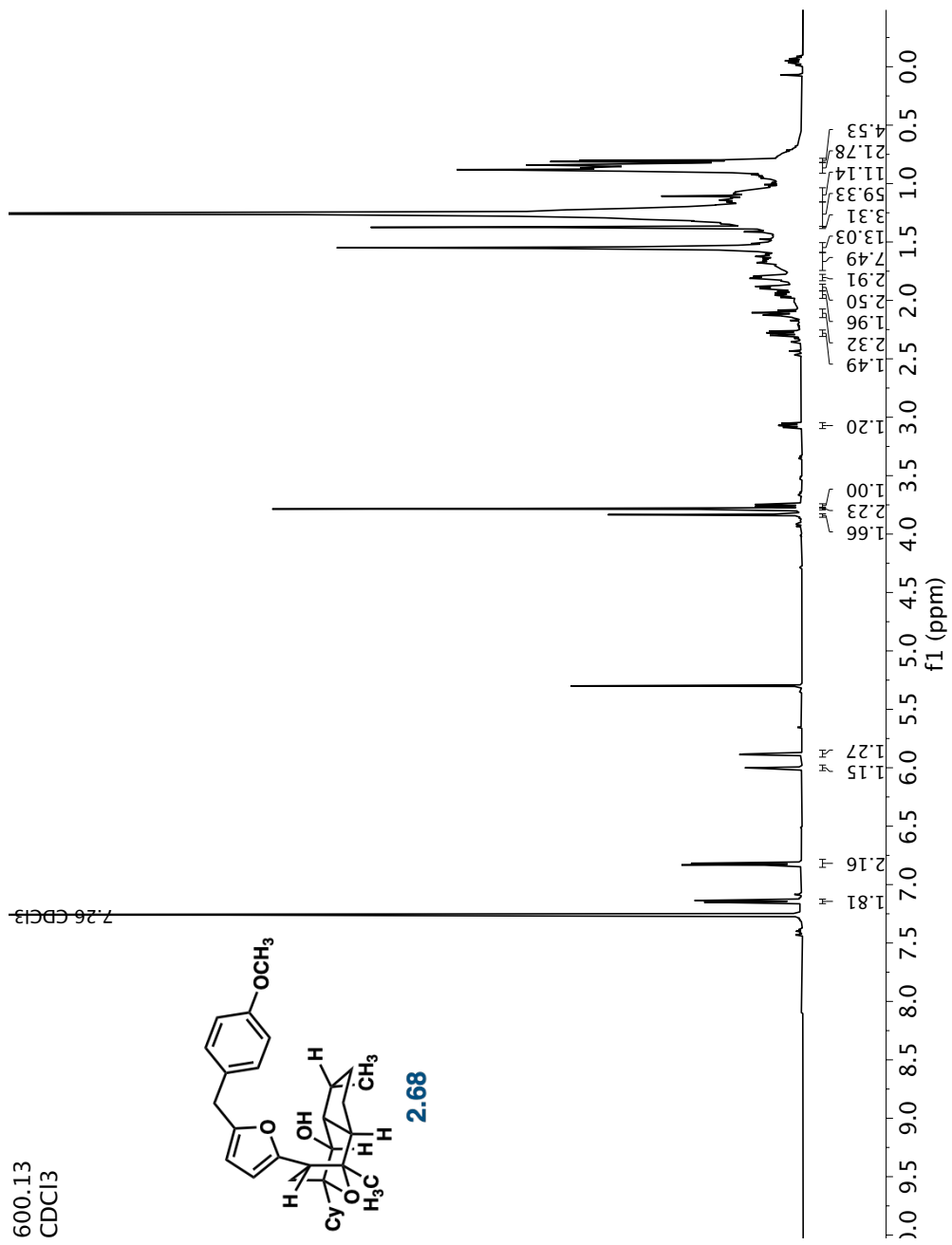
2.66

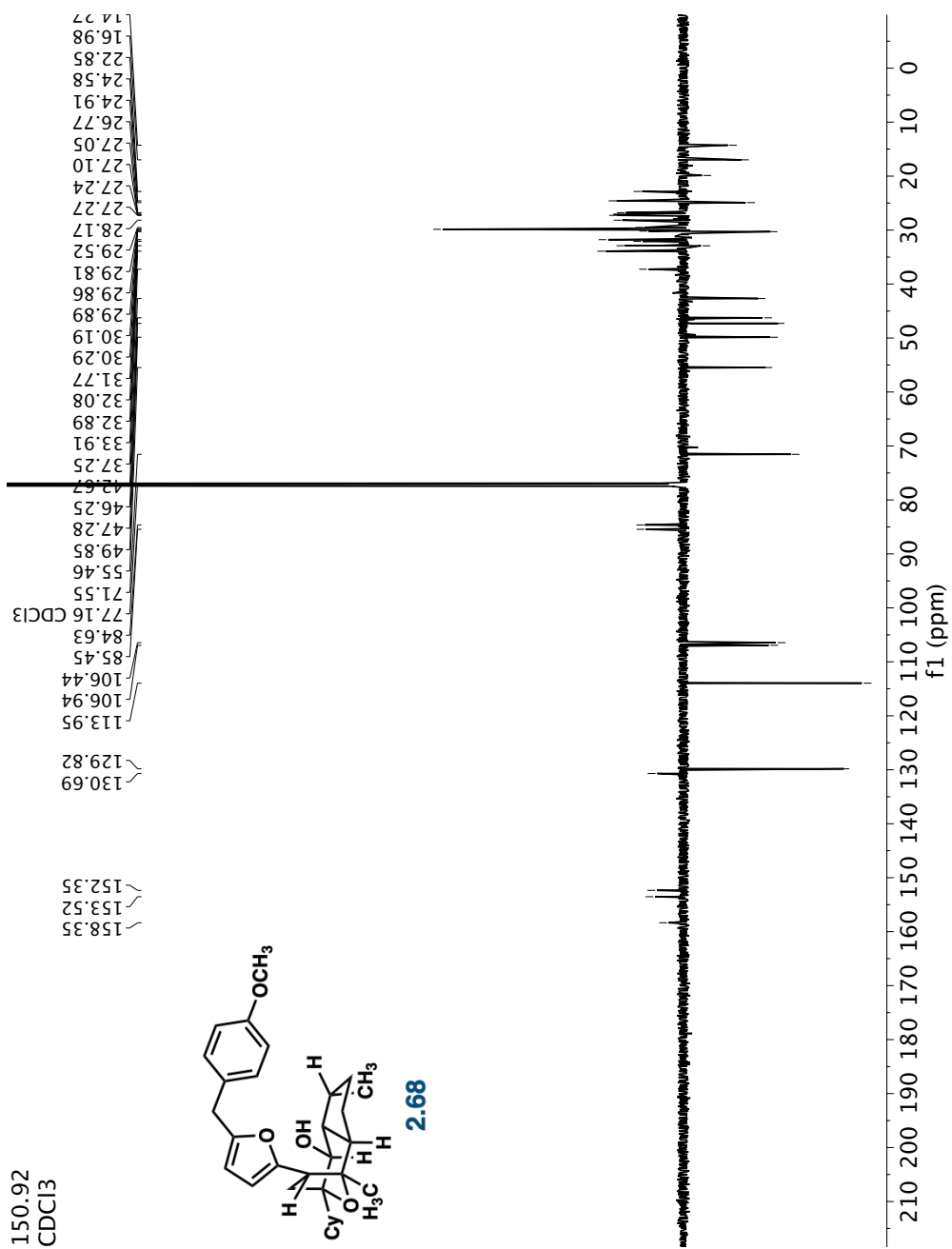


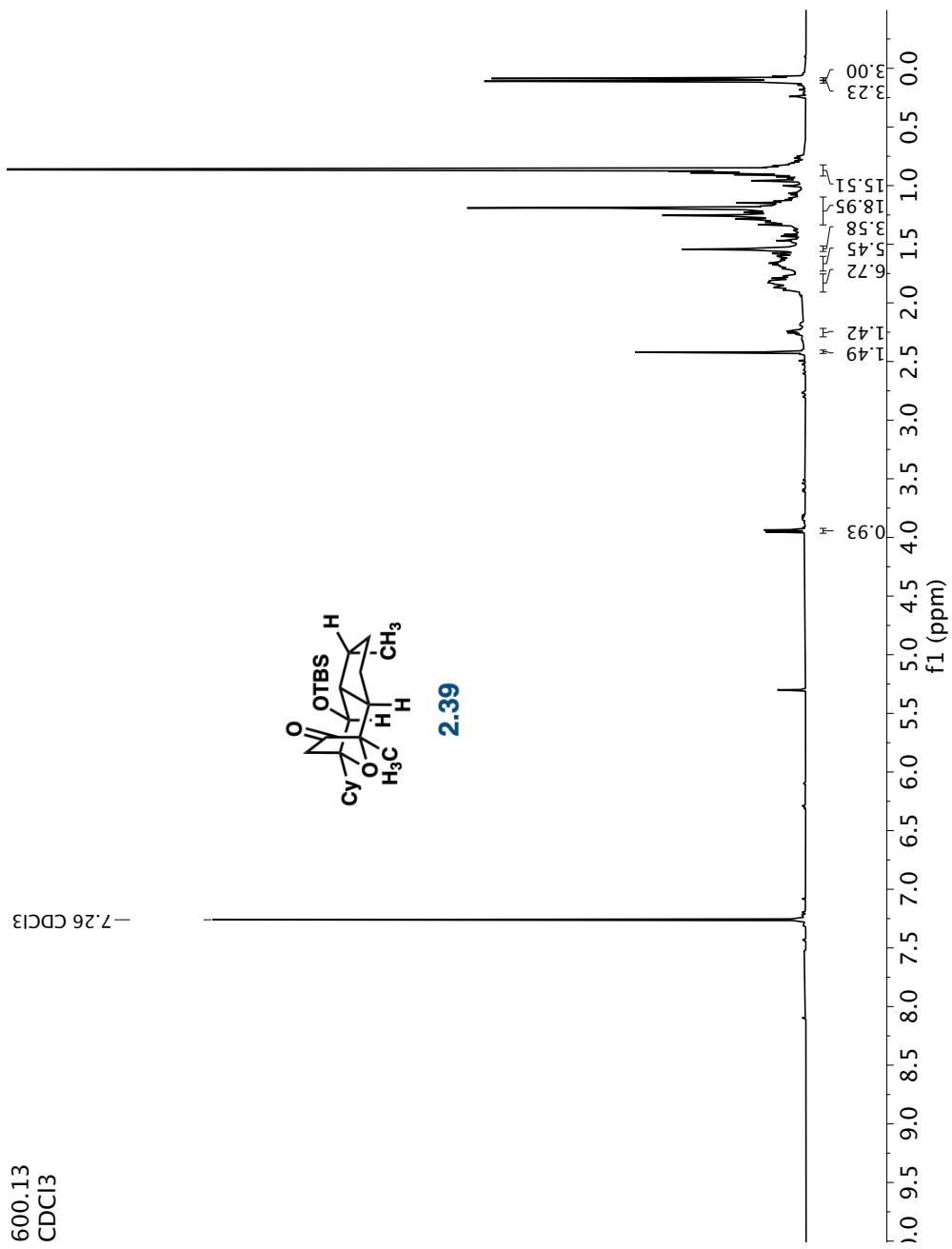
150.92
CDCl₃

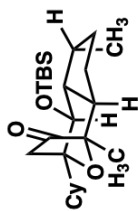
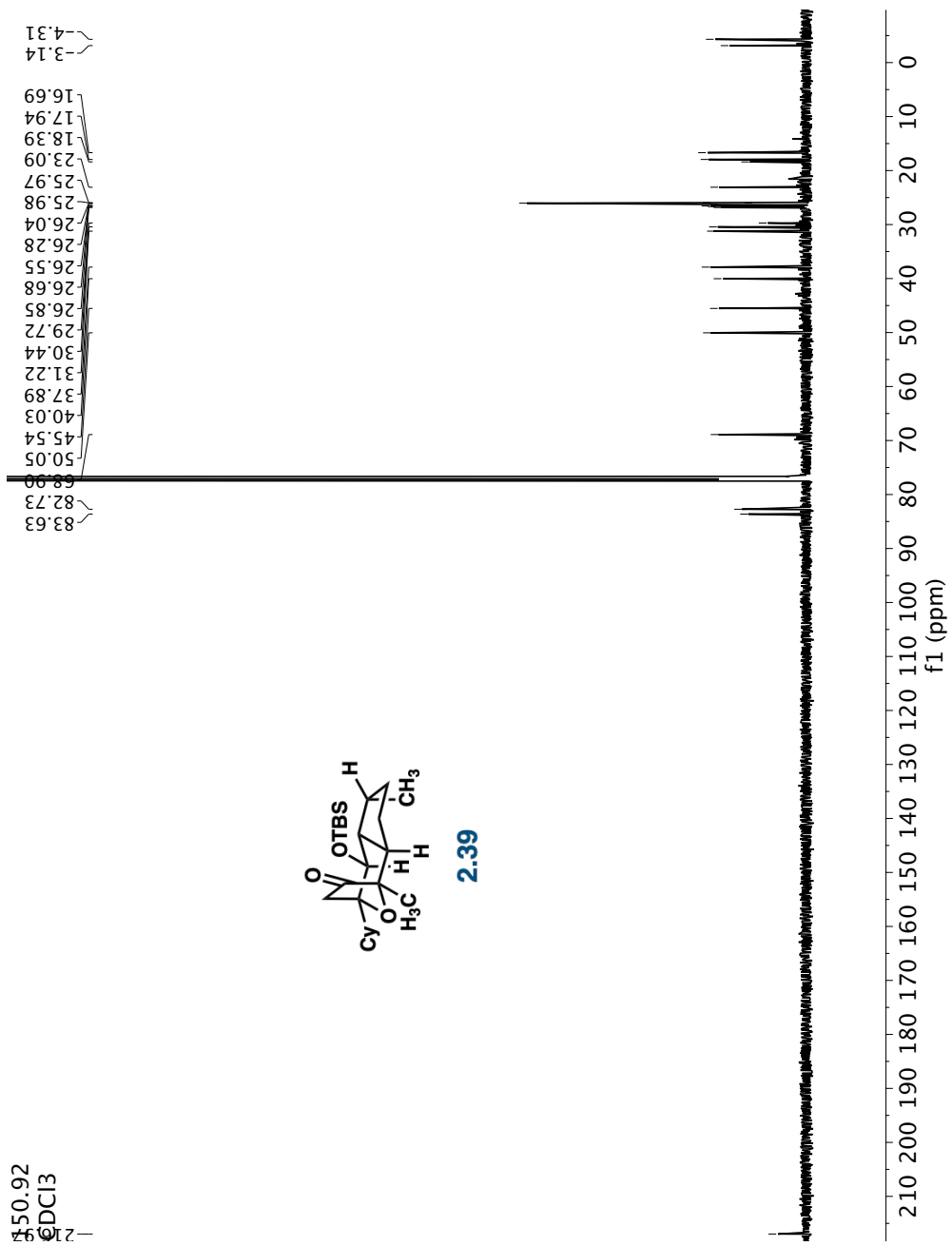








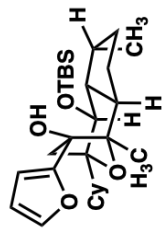




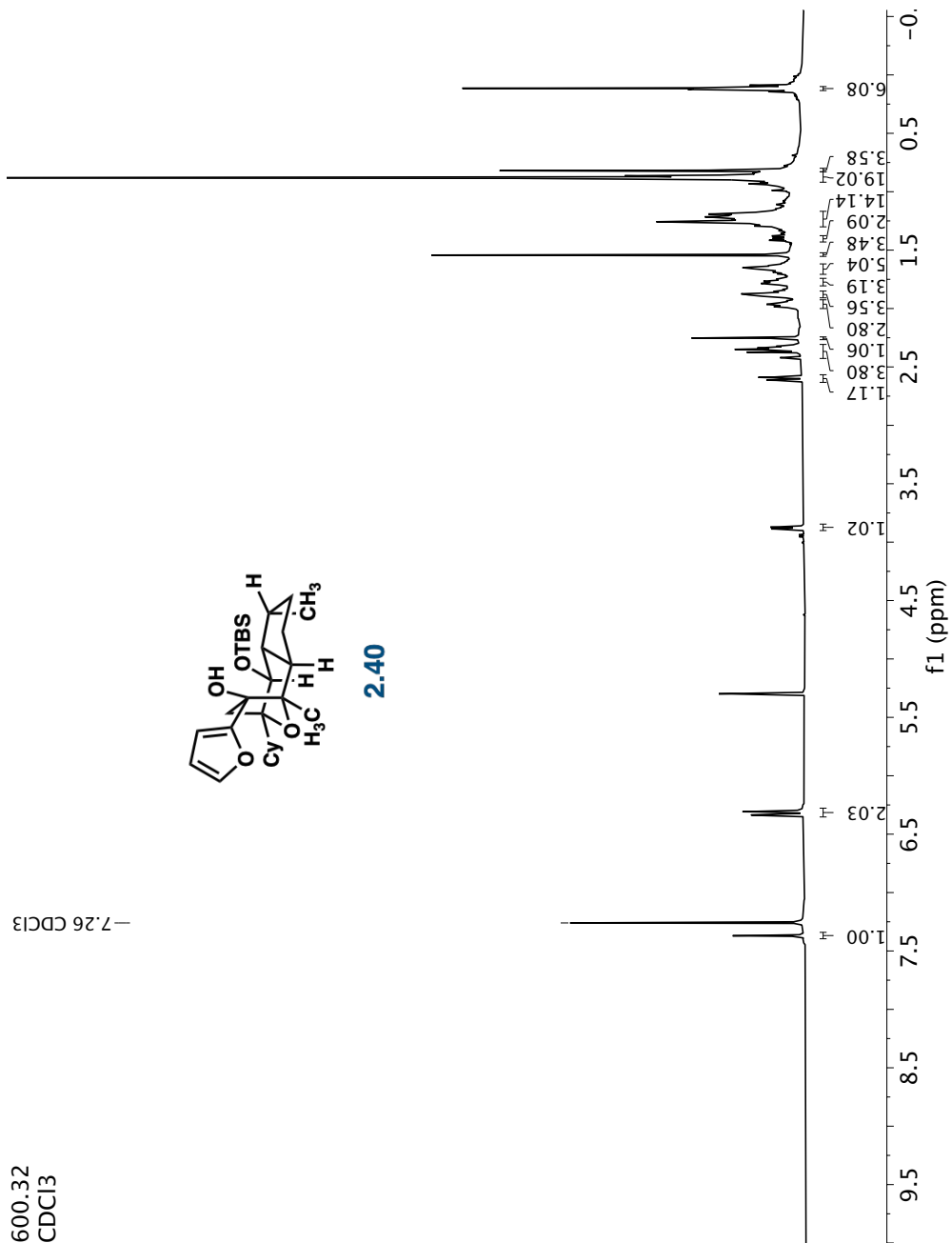
2.39

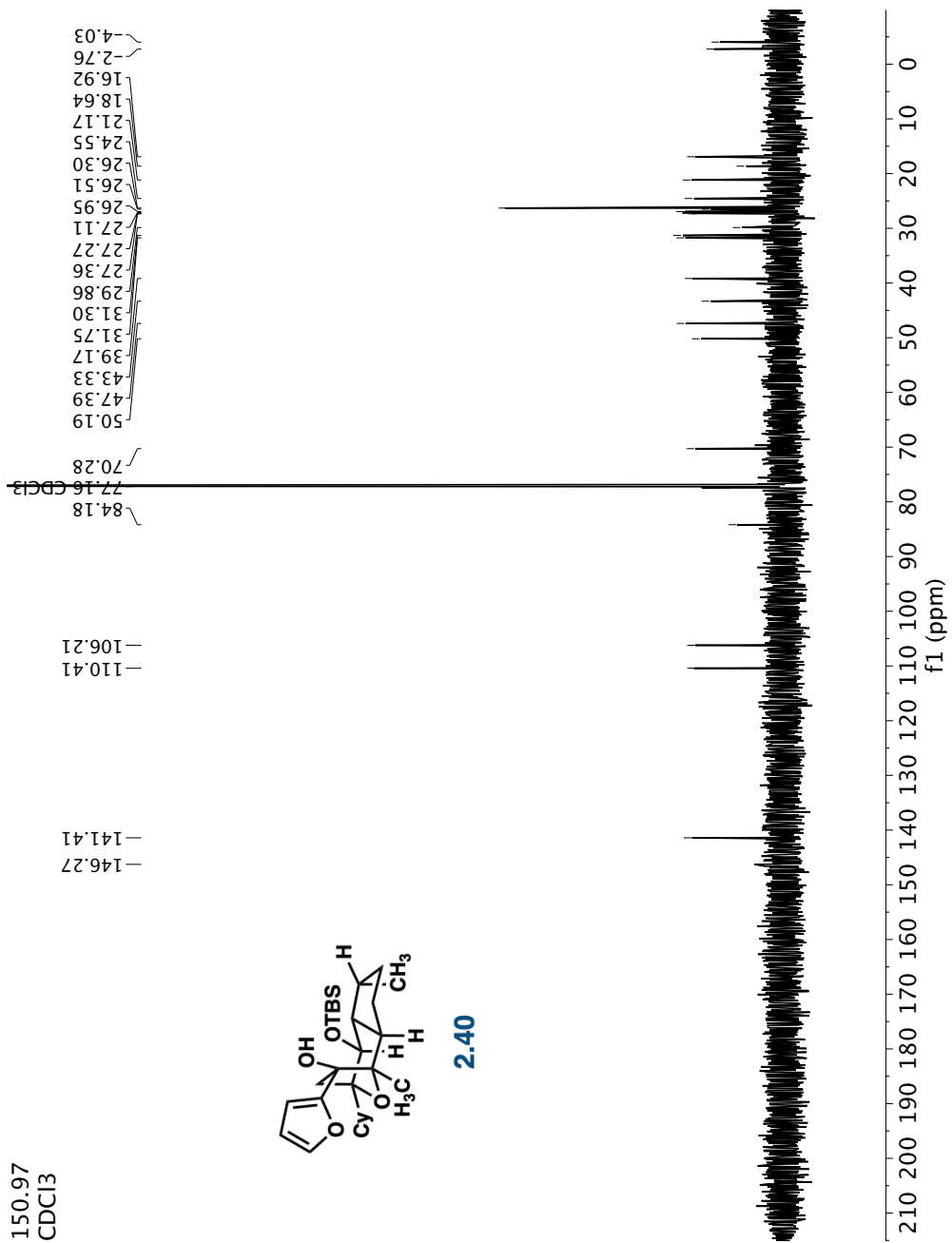
600.32
CDCl₃

-7.26 CDCl₃



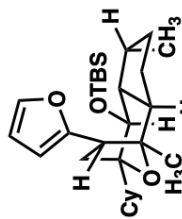
2.40



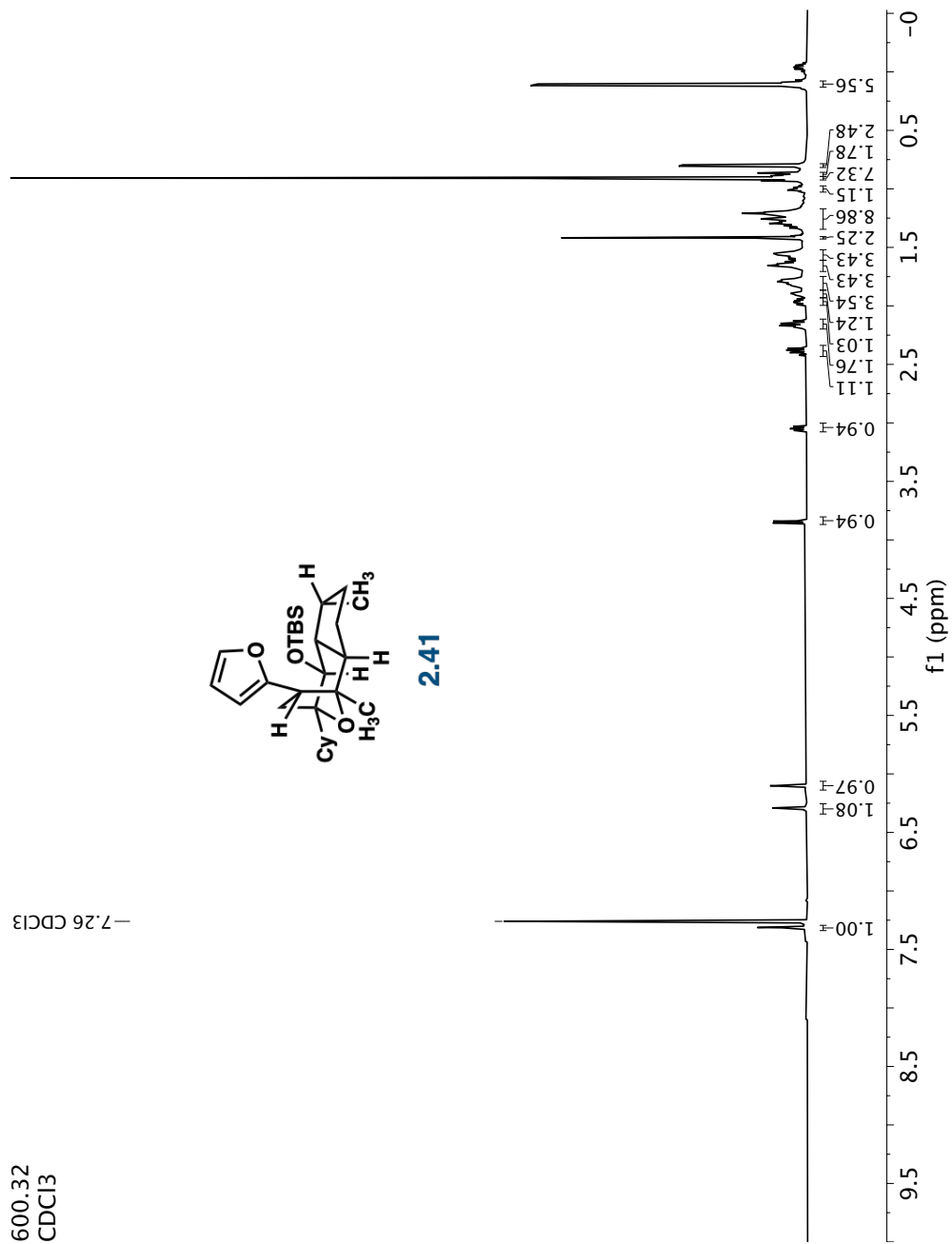


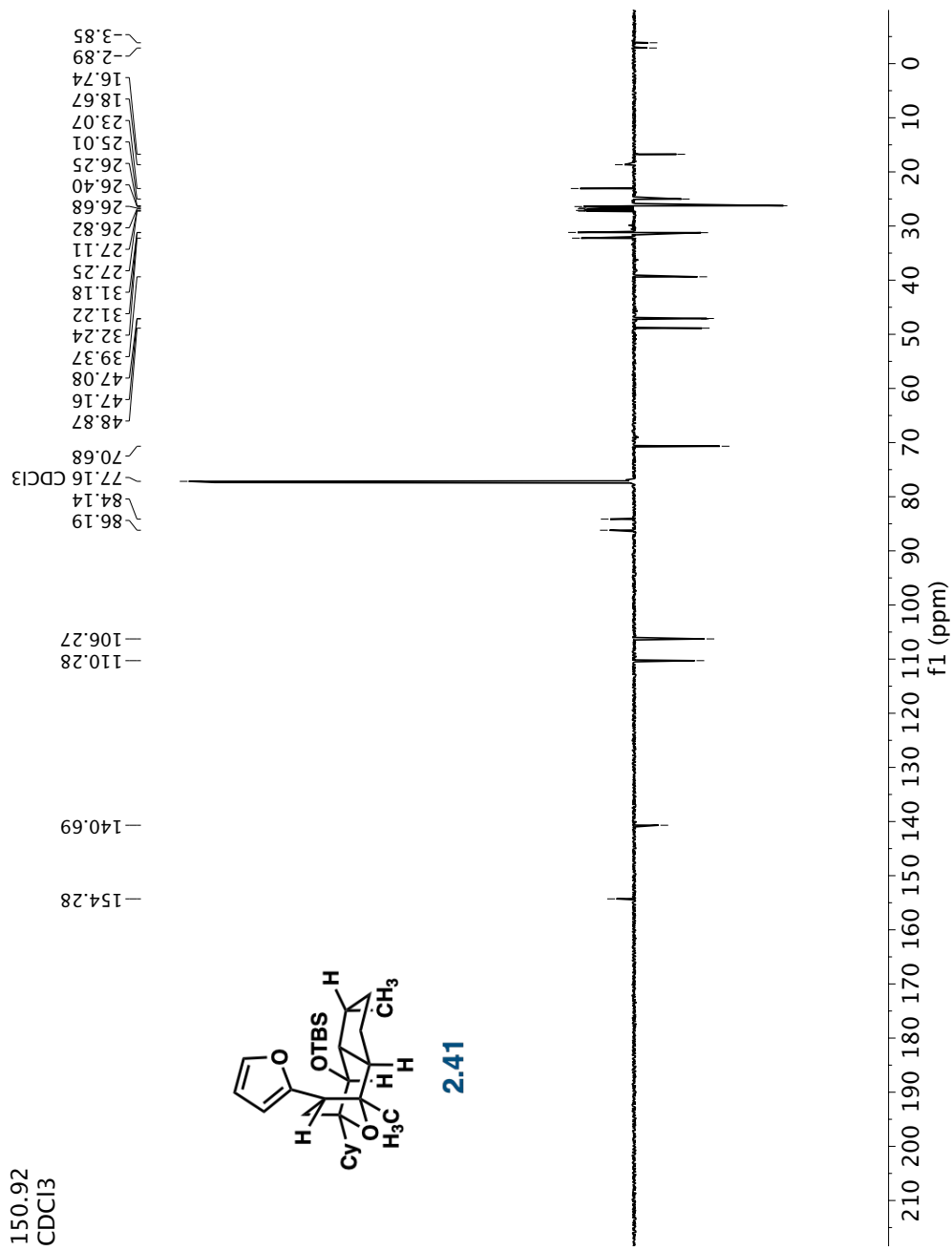
600.32
CDCl3

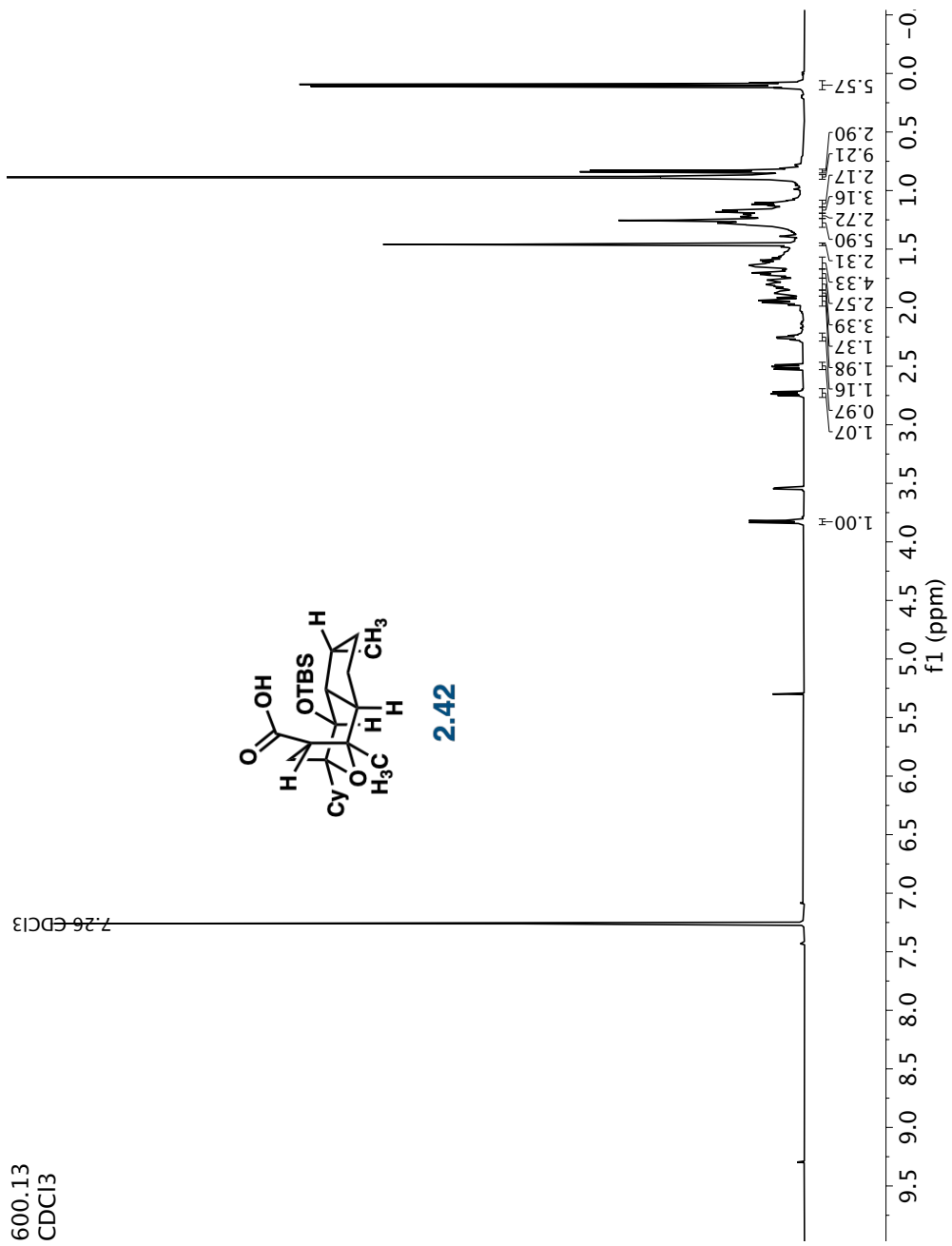
-7.26 CDCl3



2.41





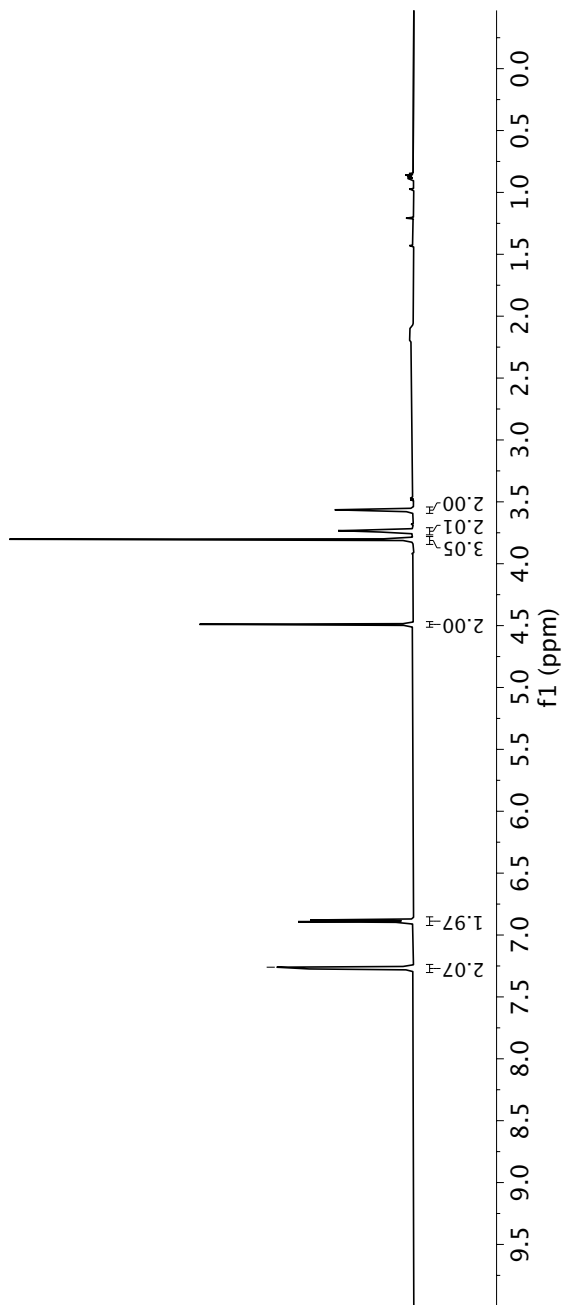


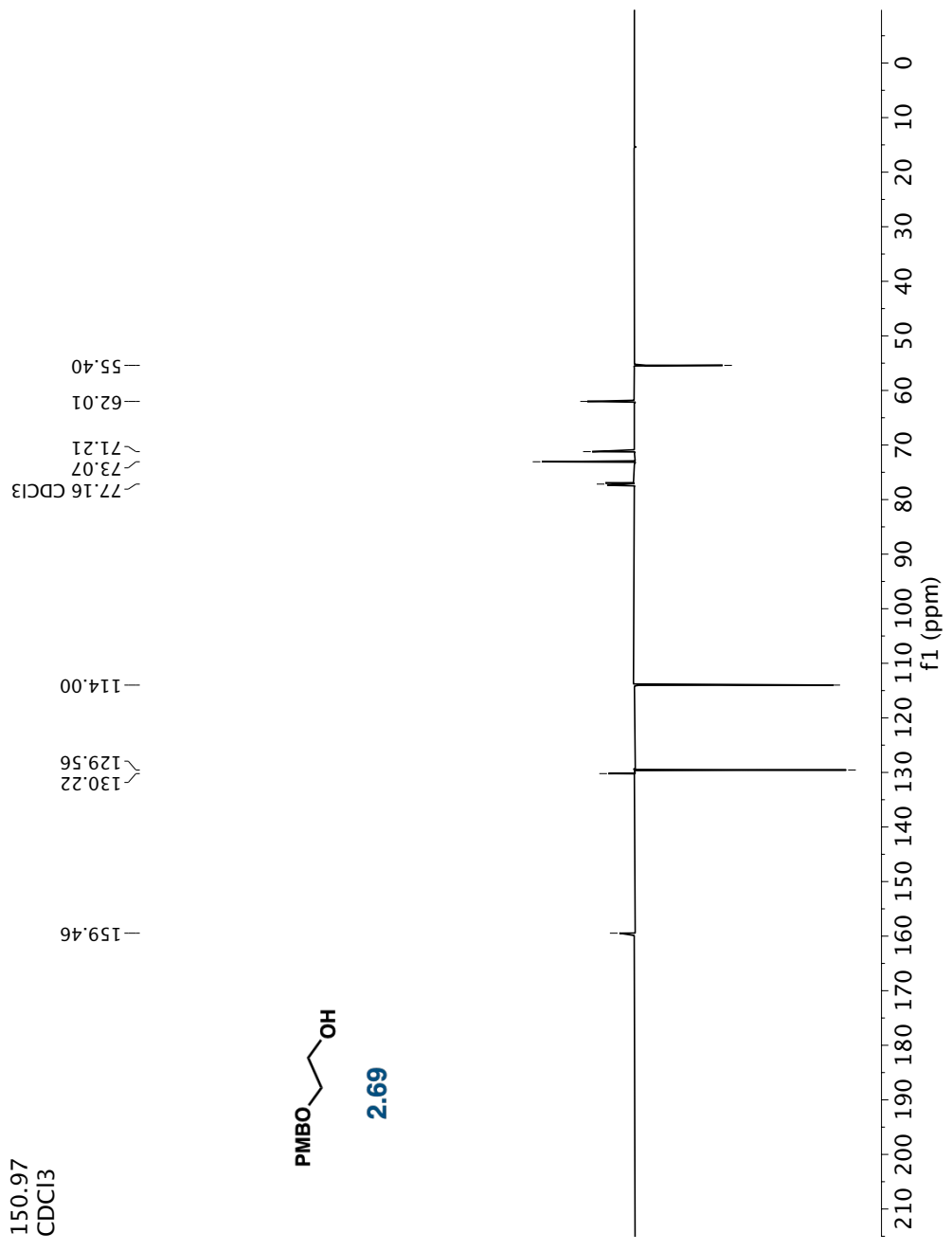
600.32
CDCl₃

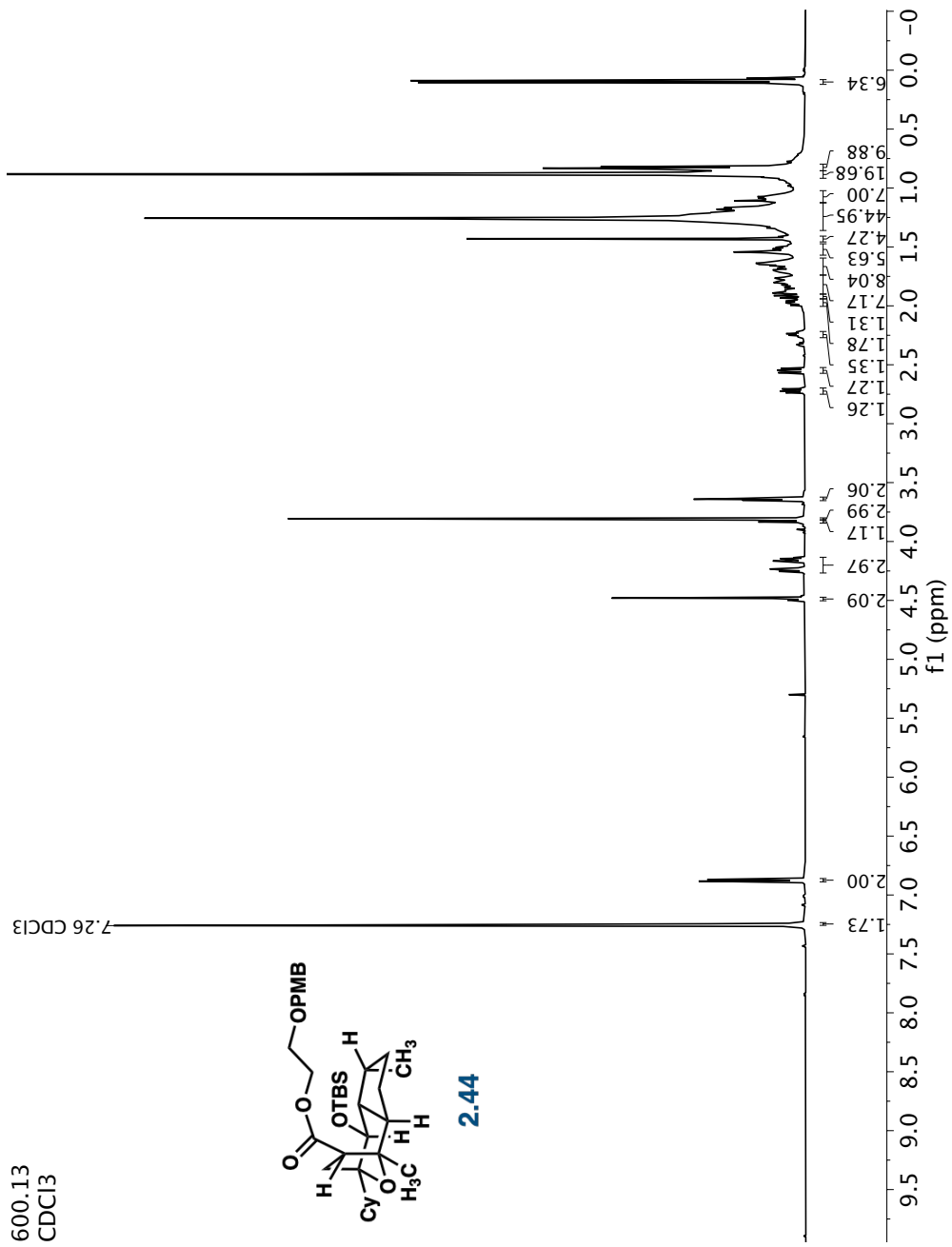
-7.26 CDCl₃

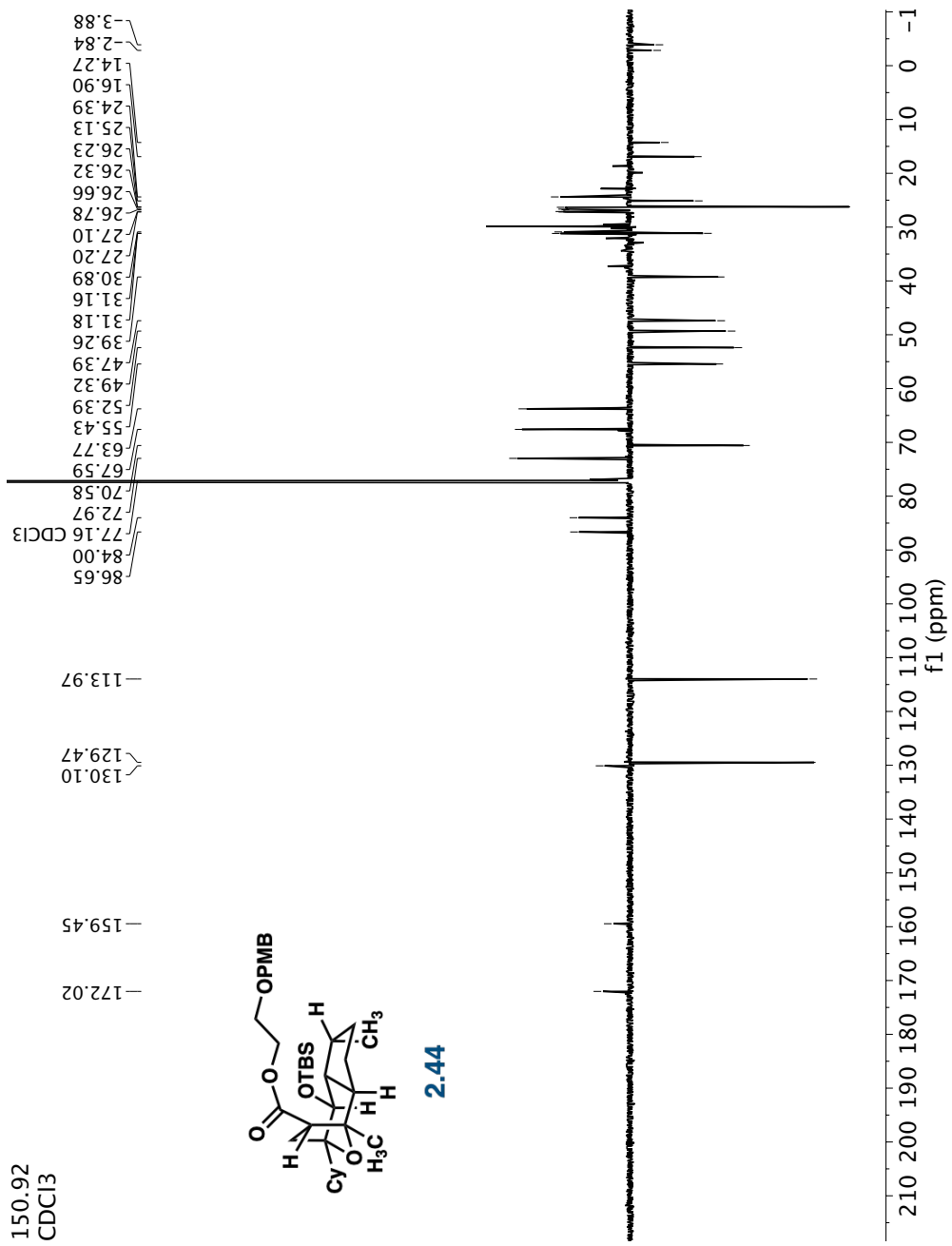


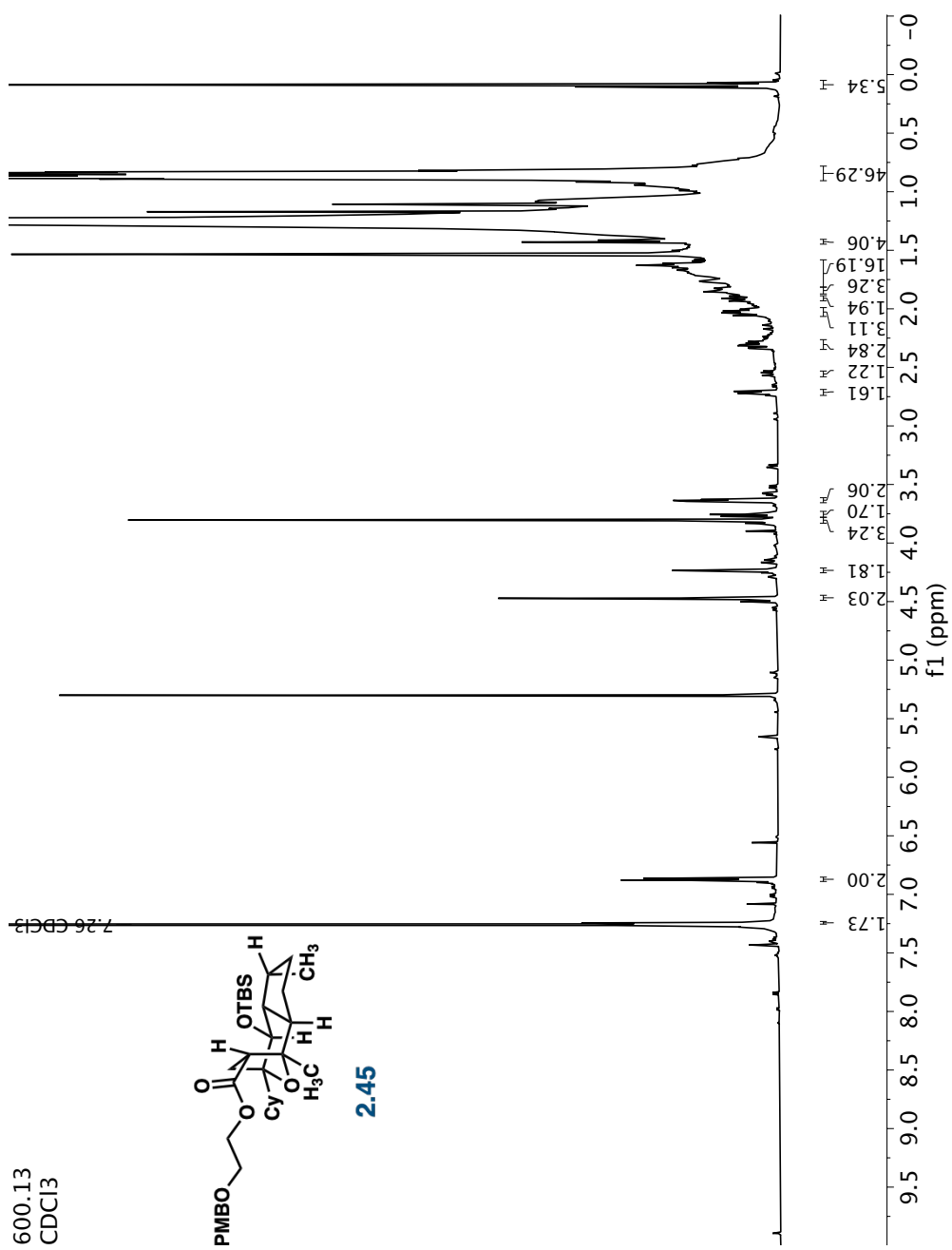
2.69

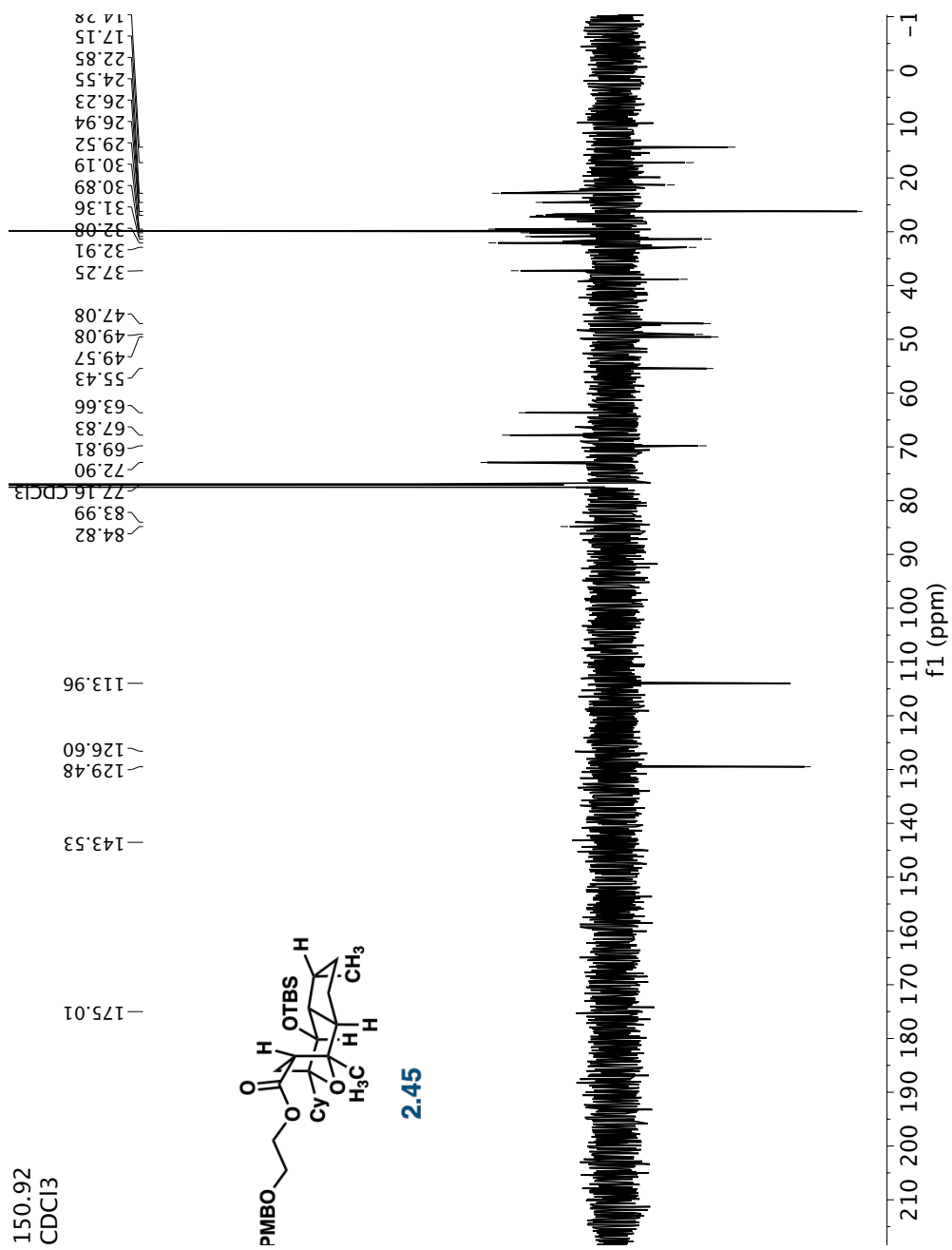




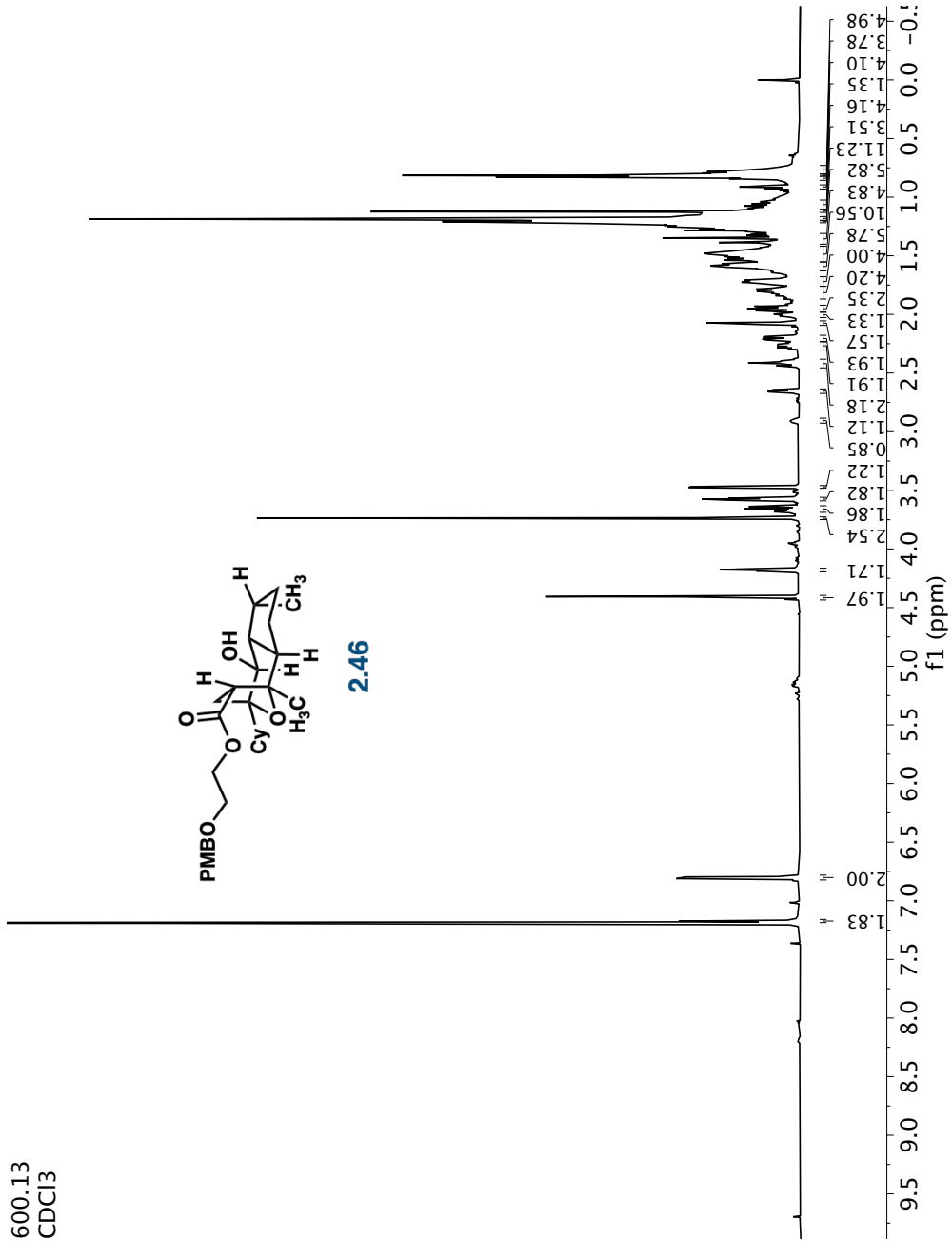


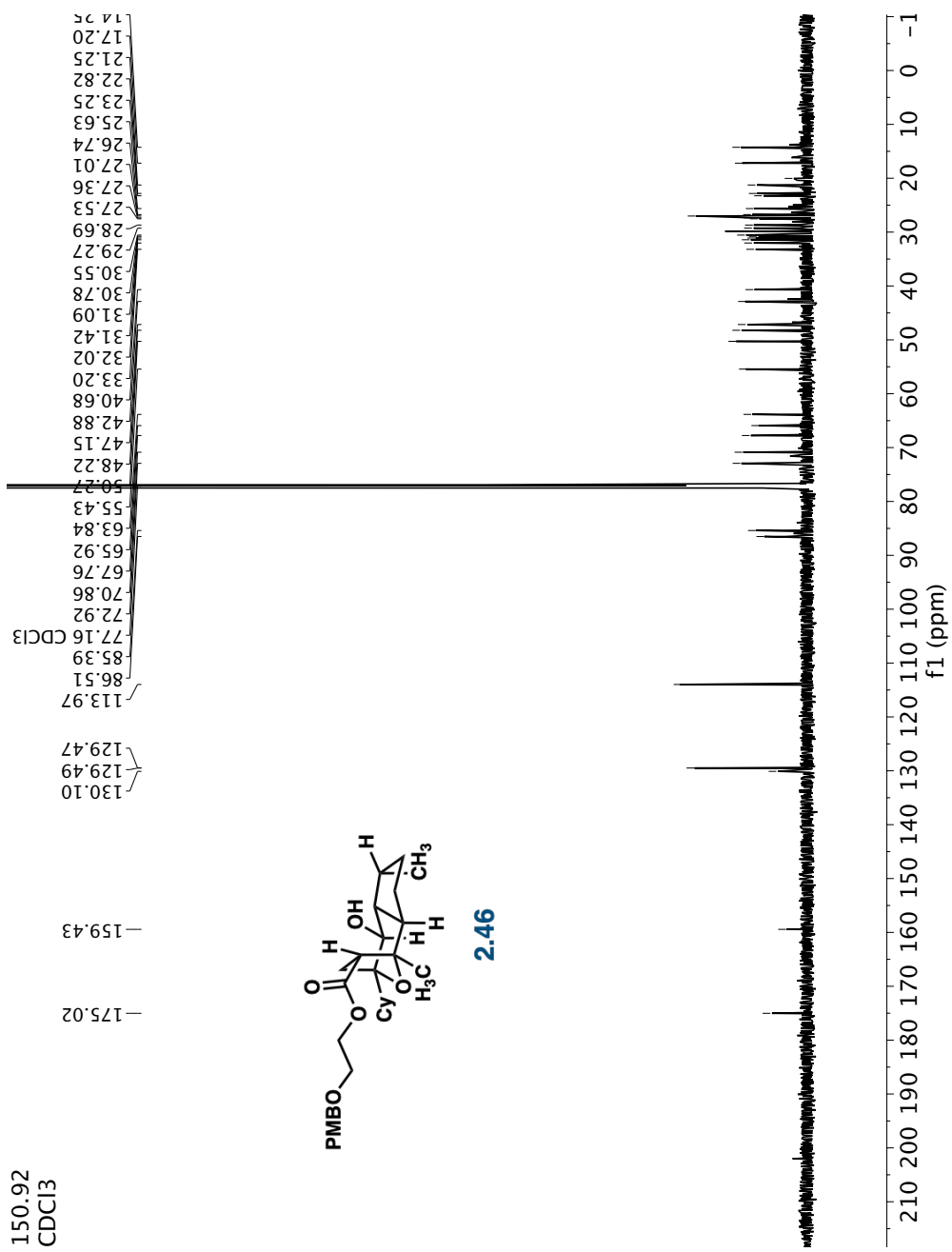


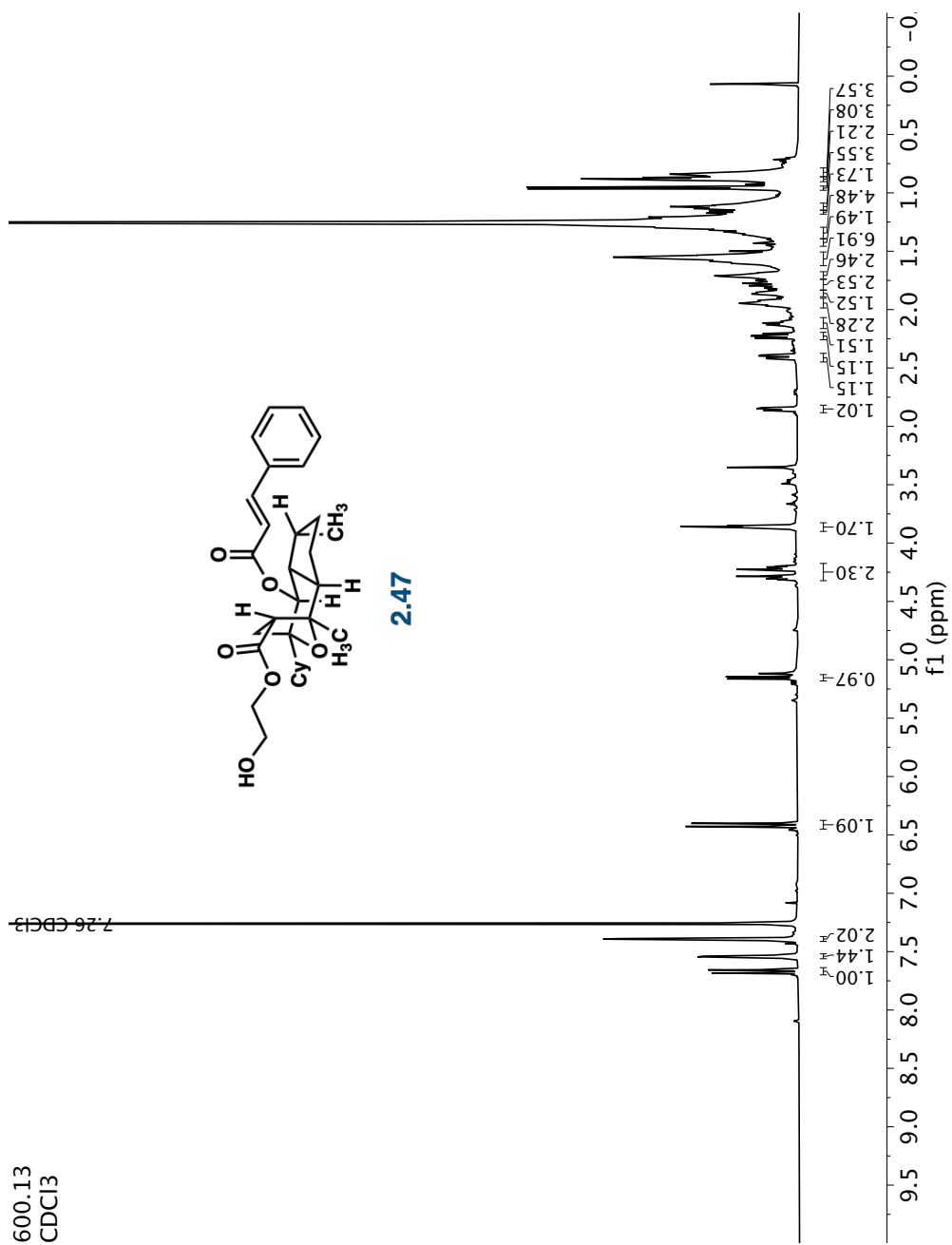


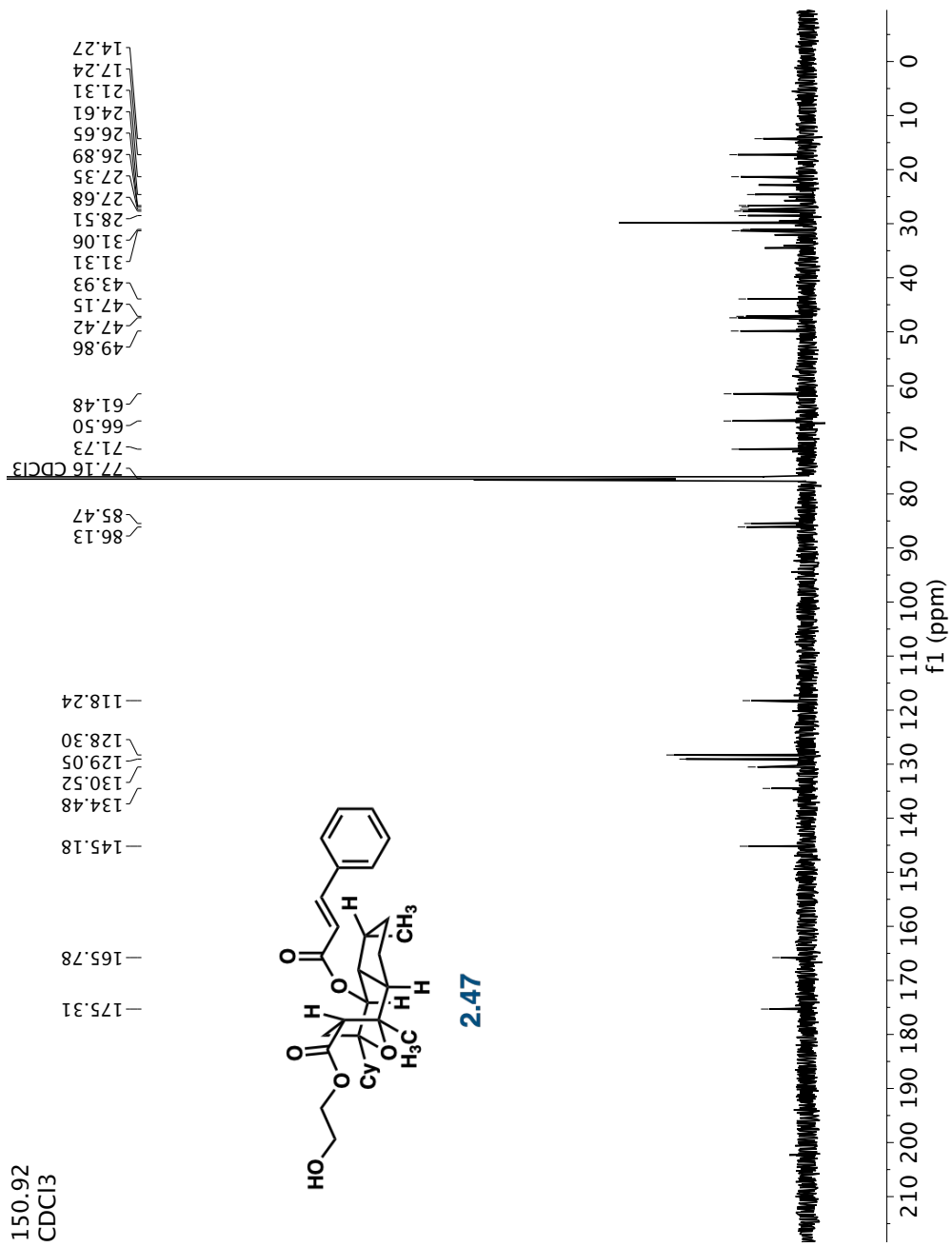


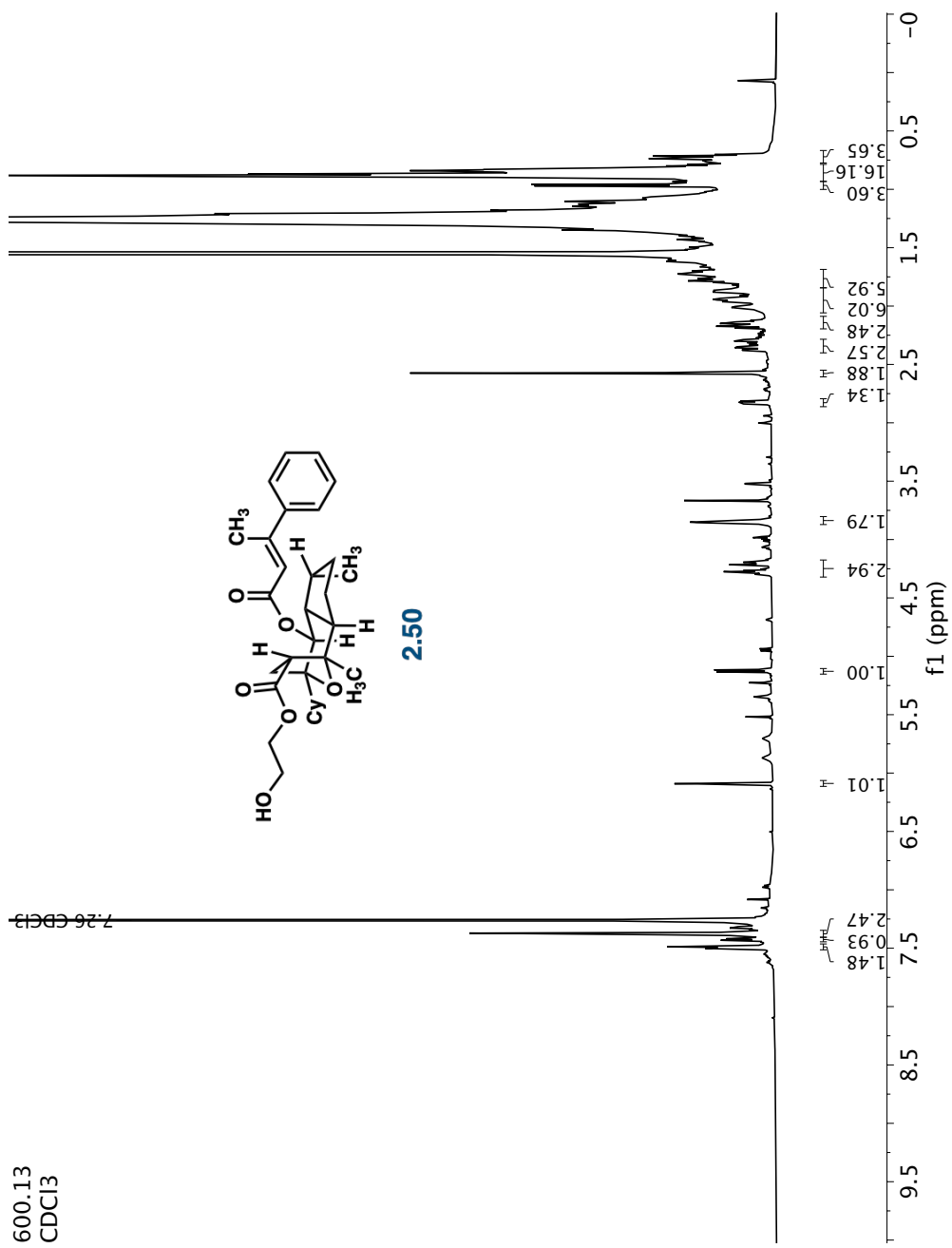
600.13
CDCl3

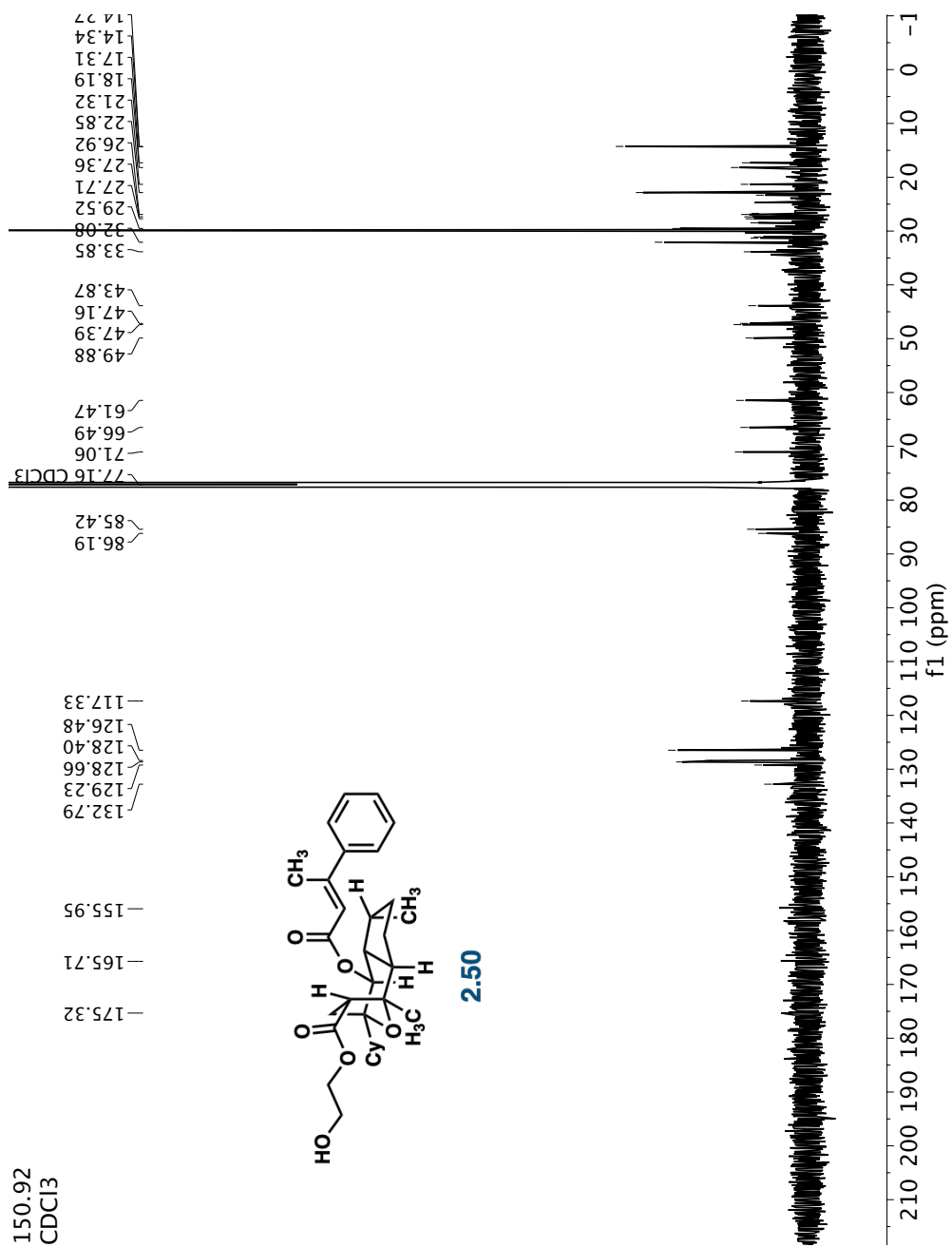


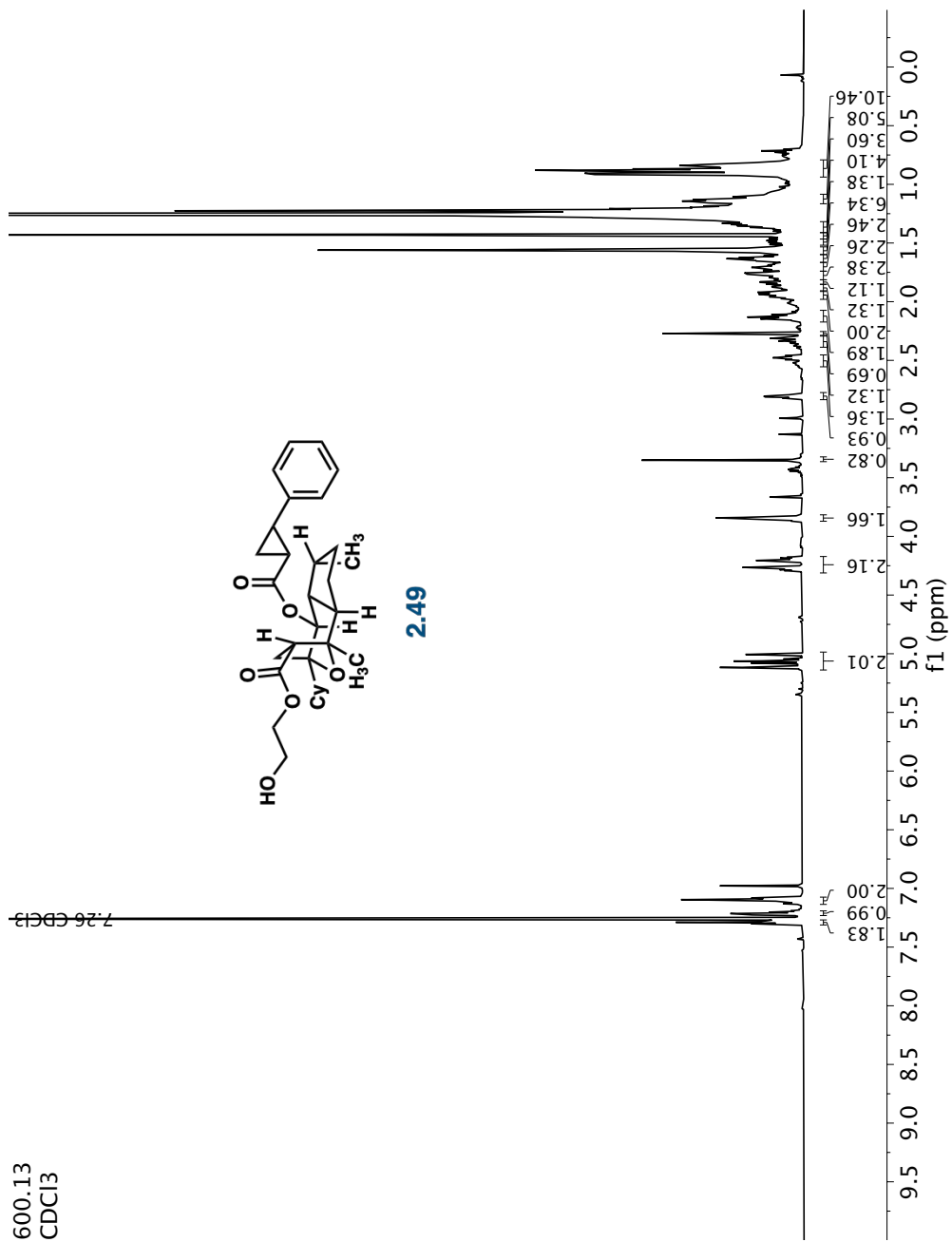


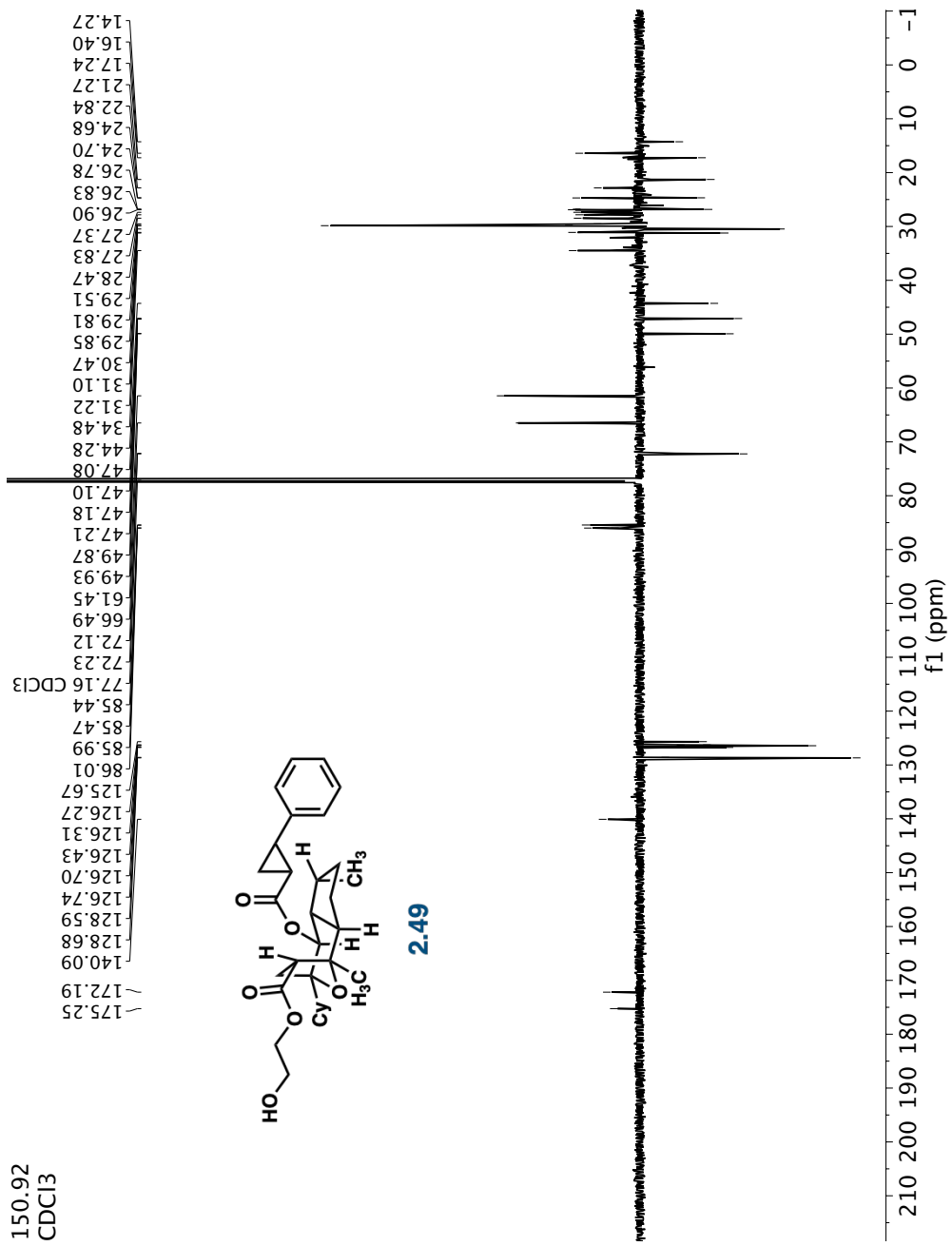


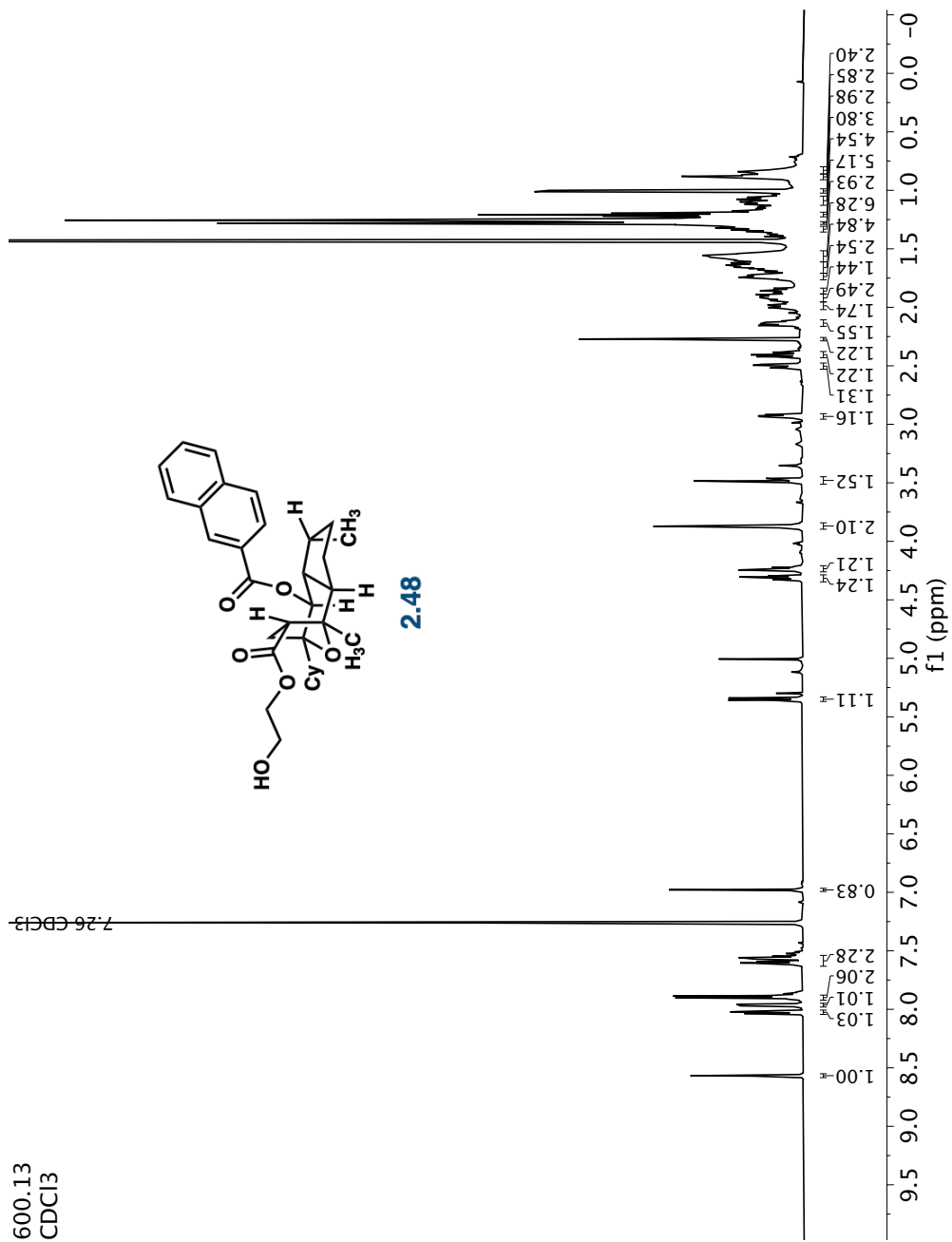


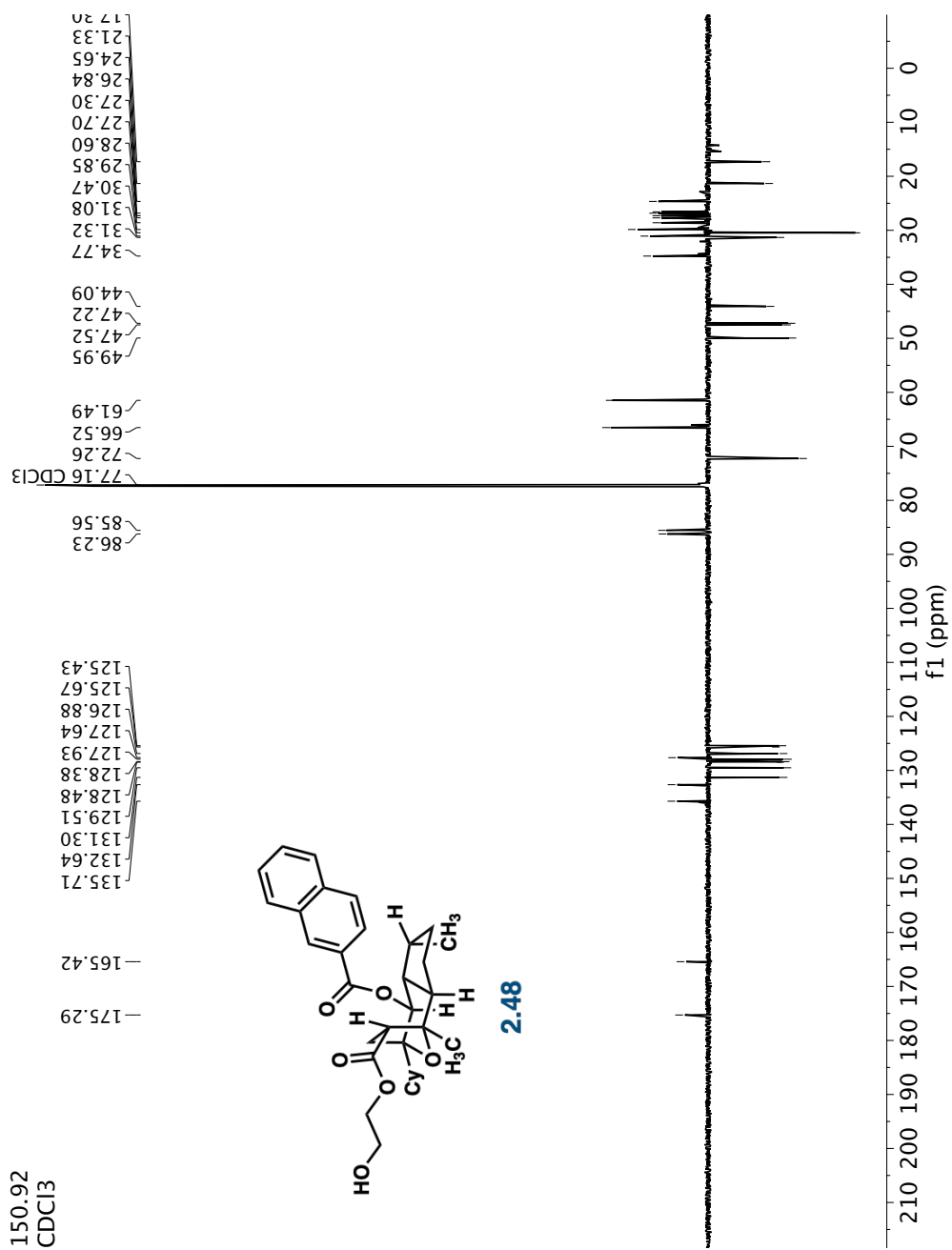


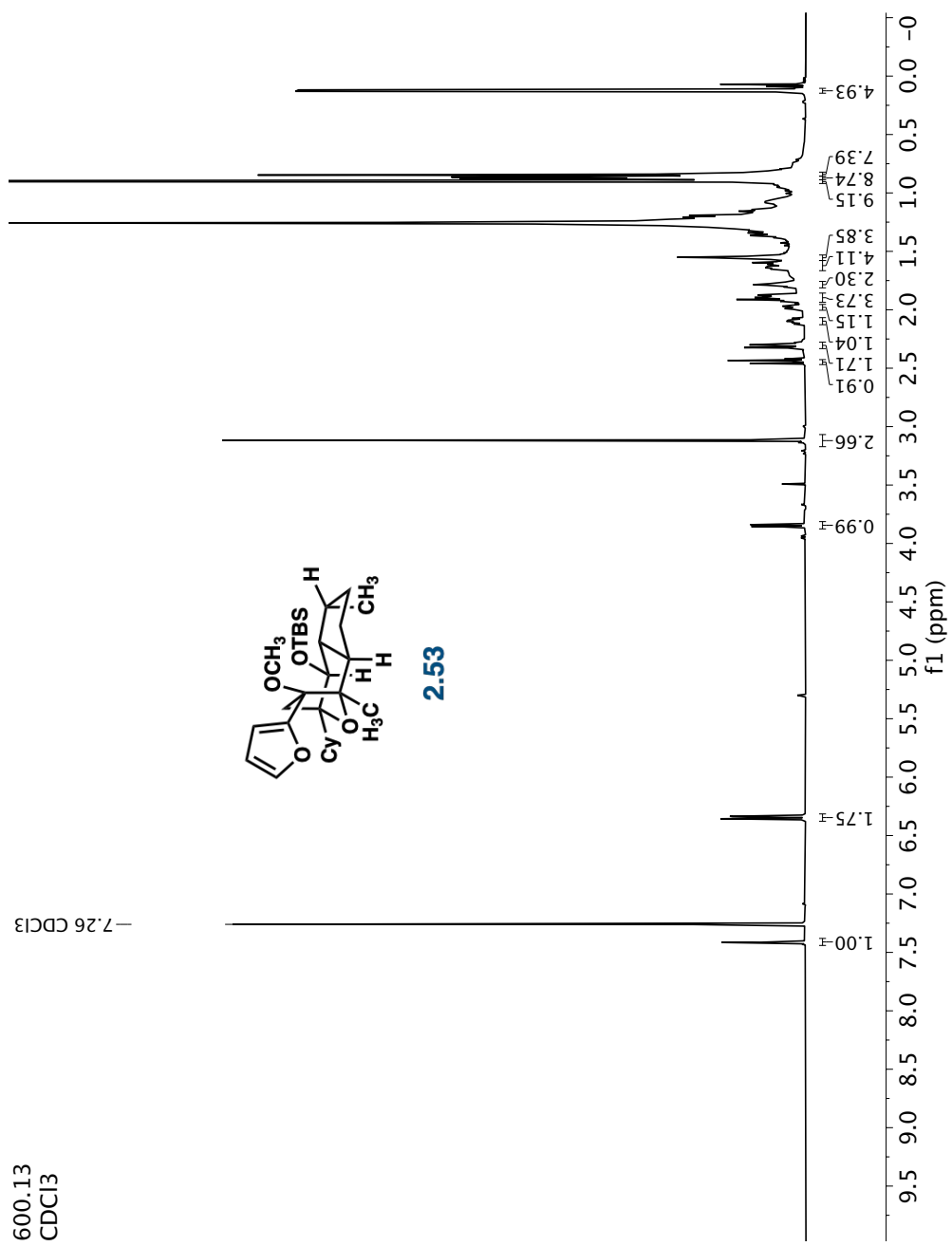


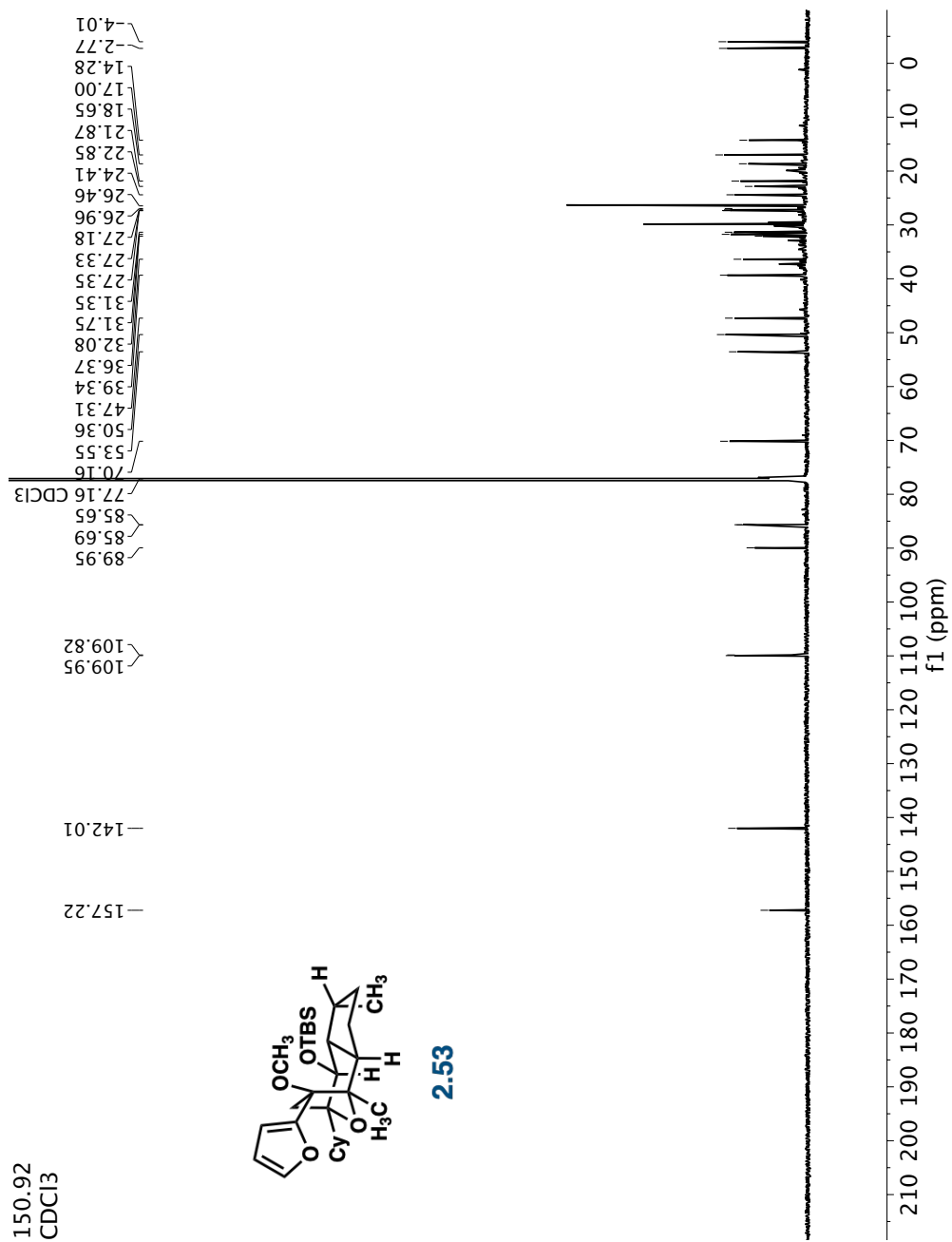




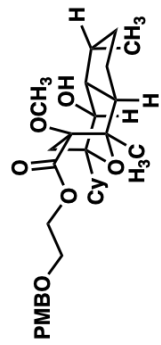




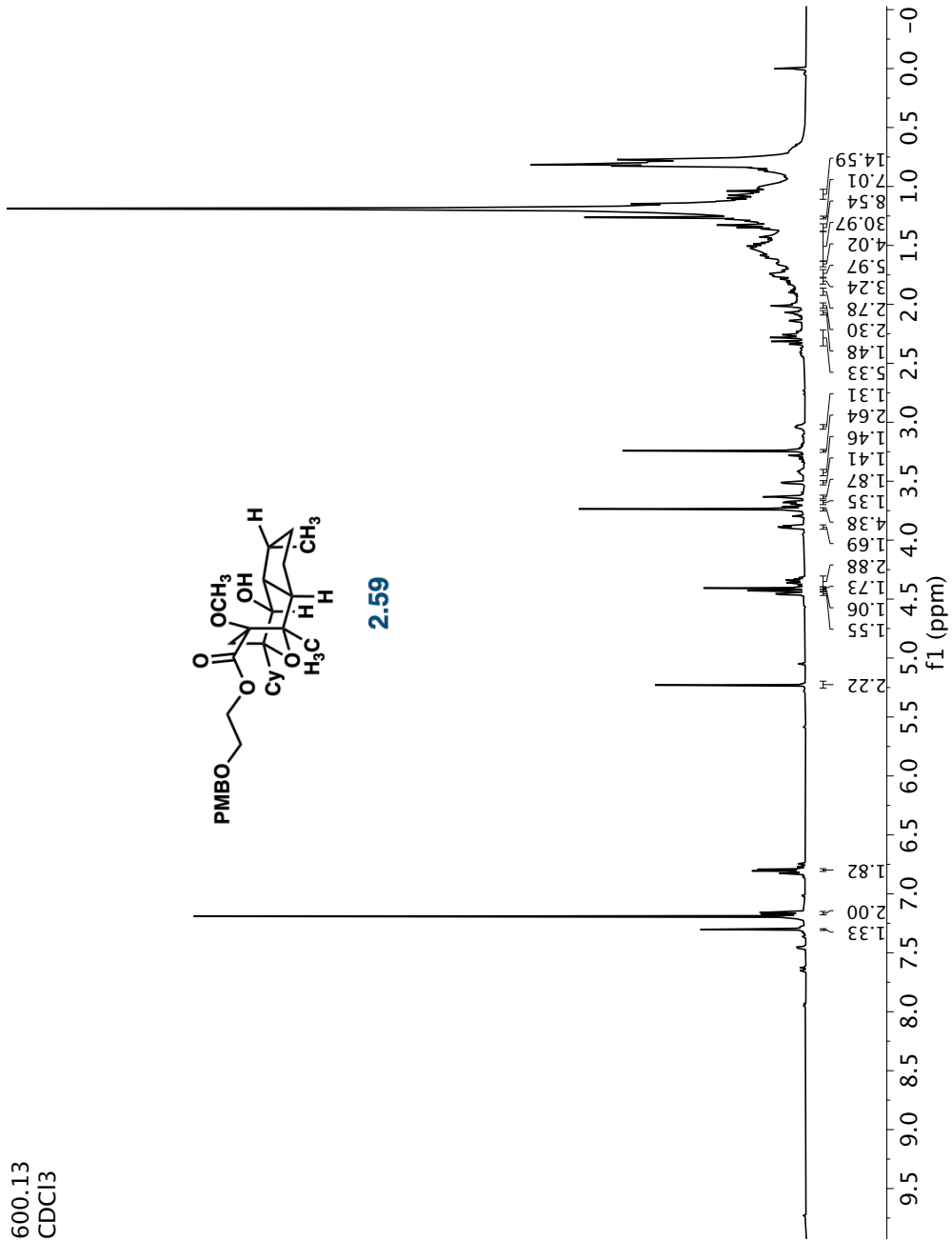


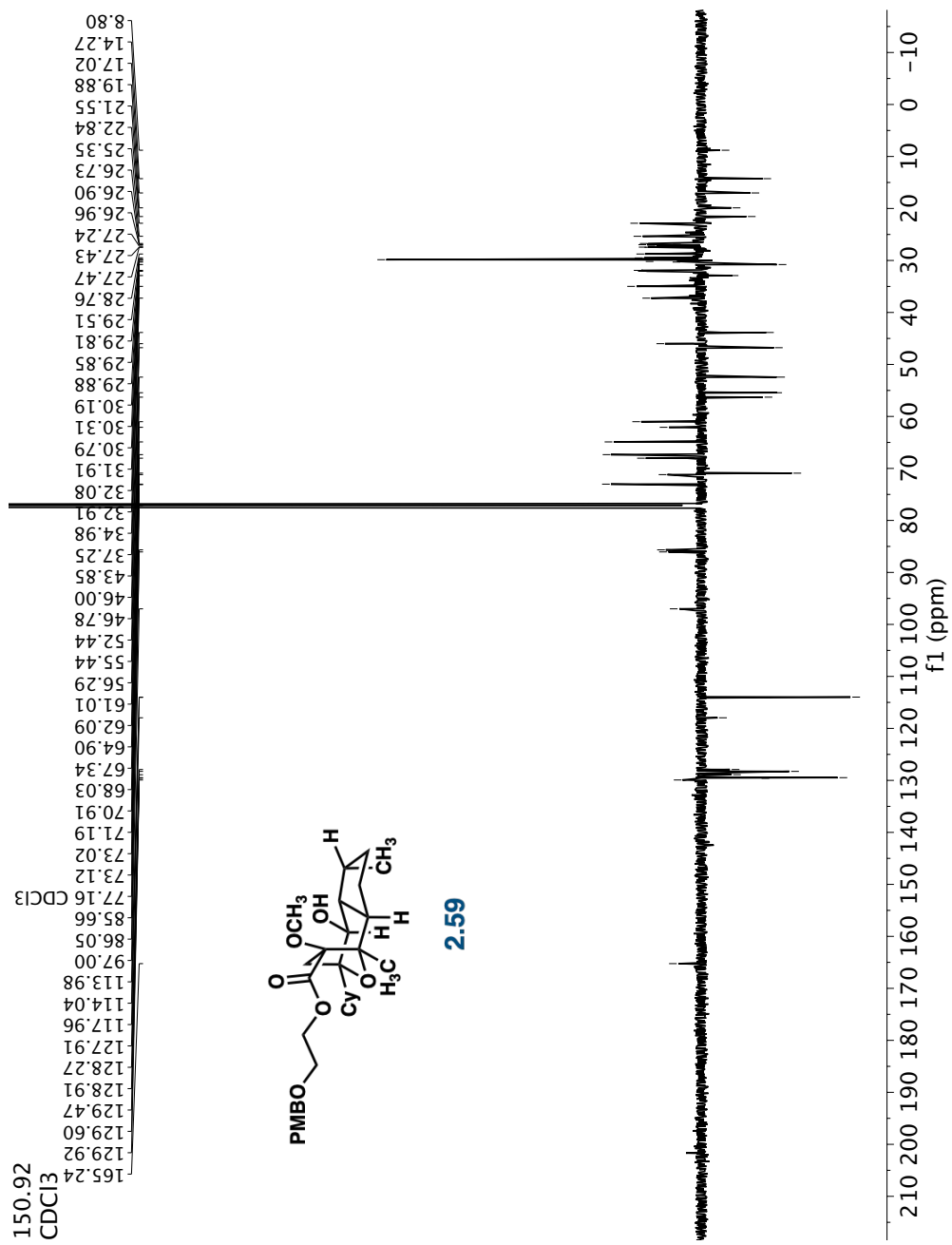


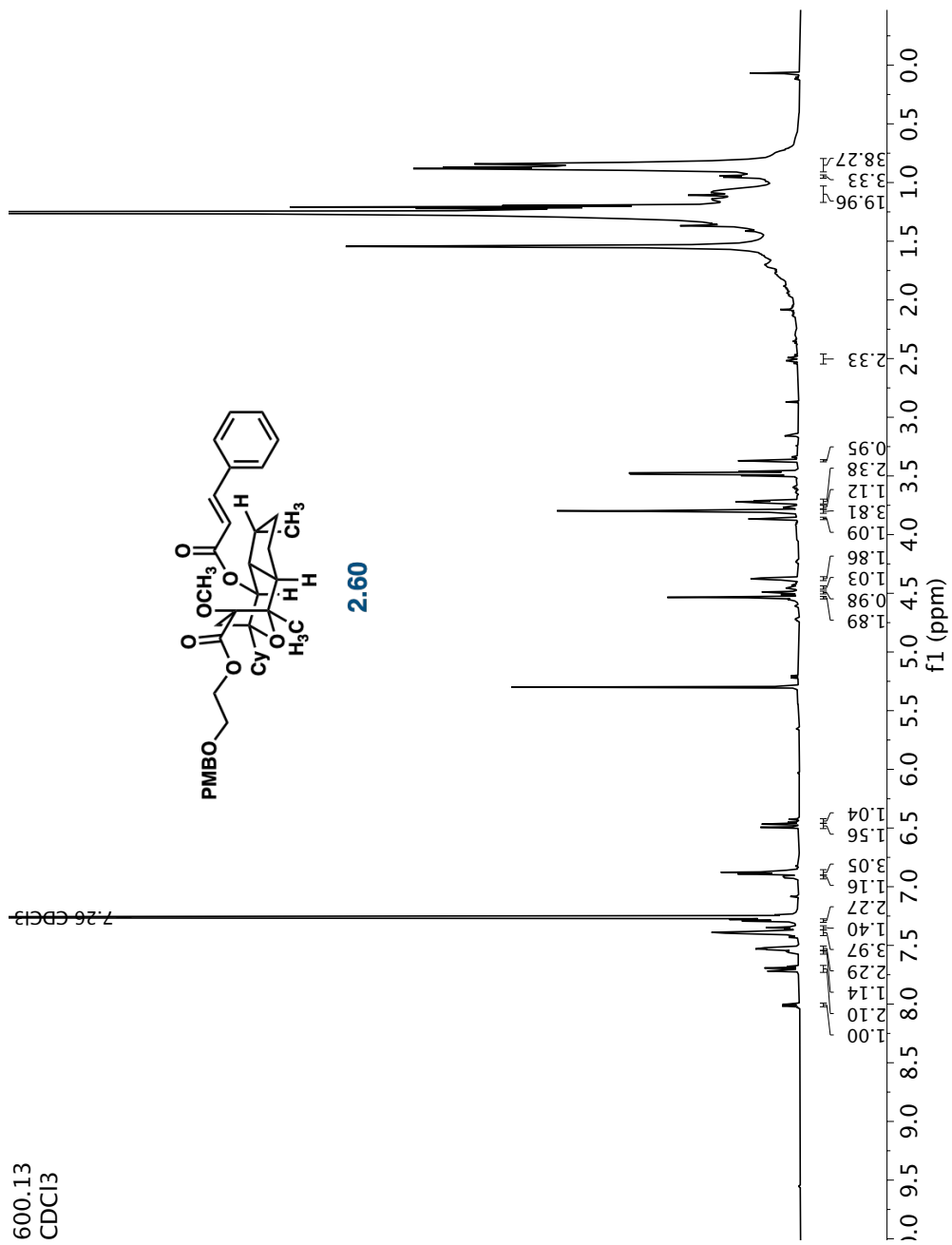
600.13
CDCl₃

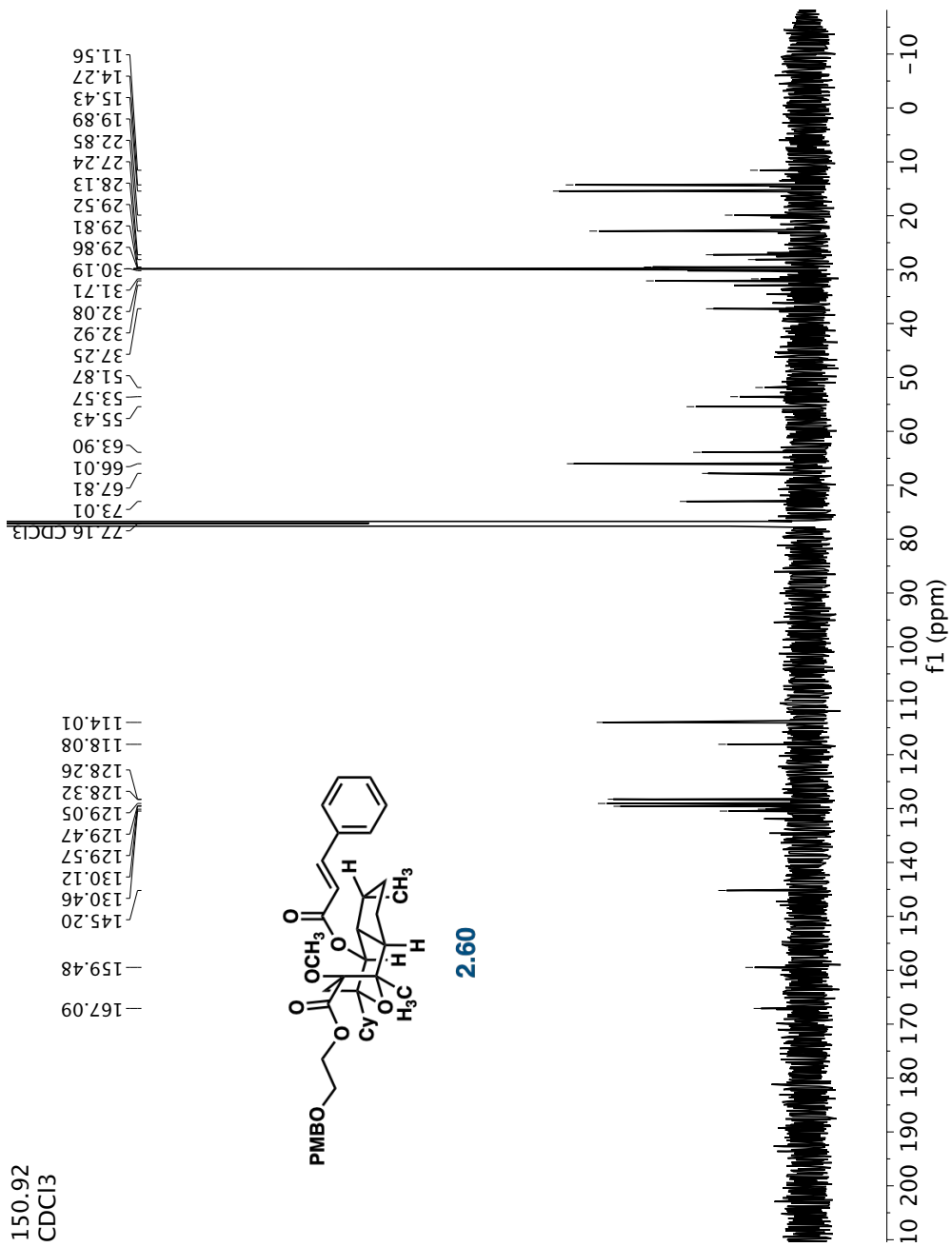


2.59

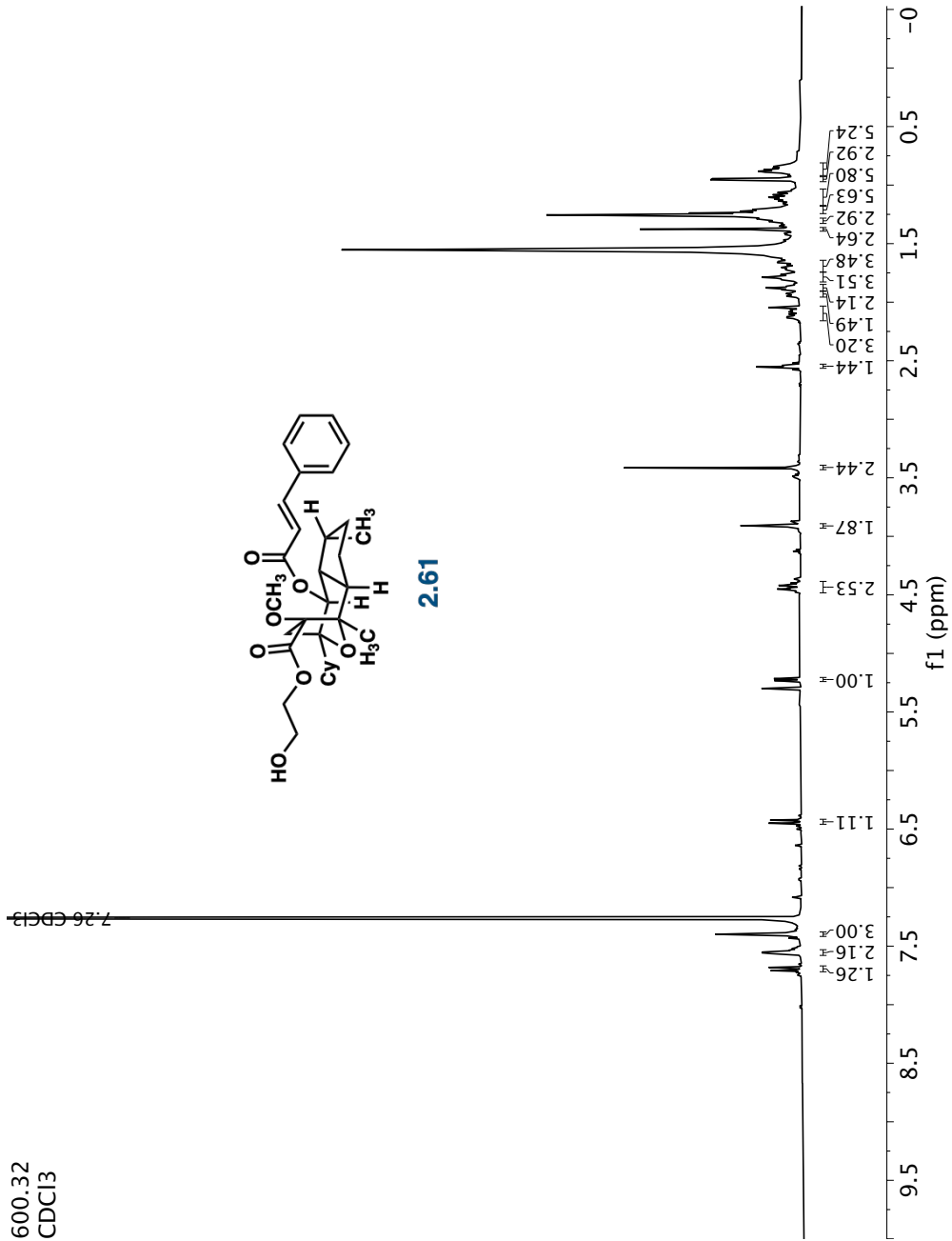


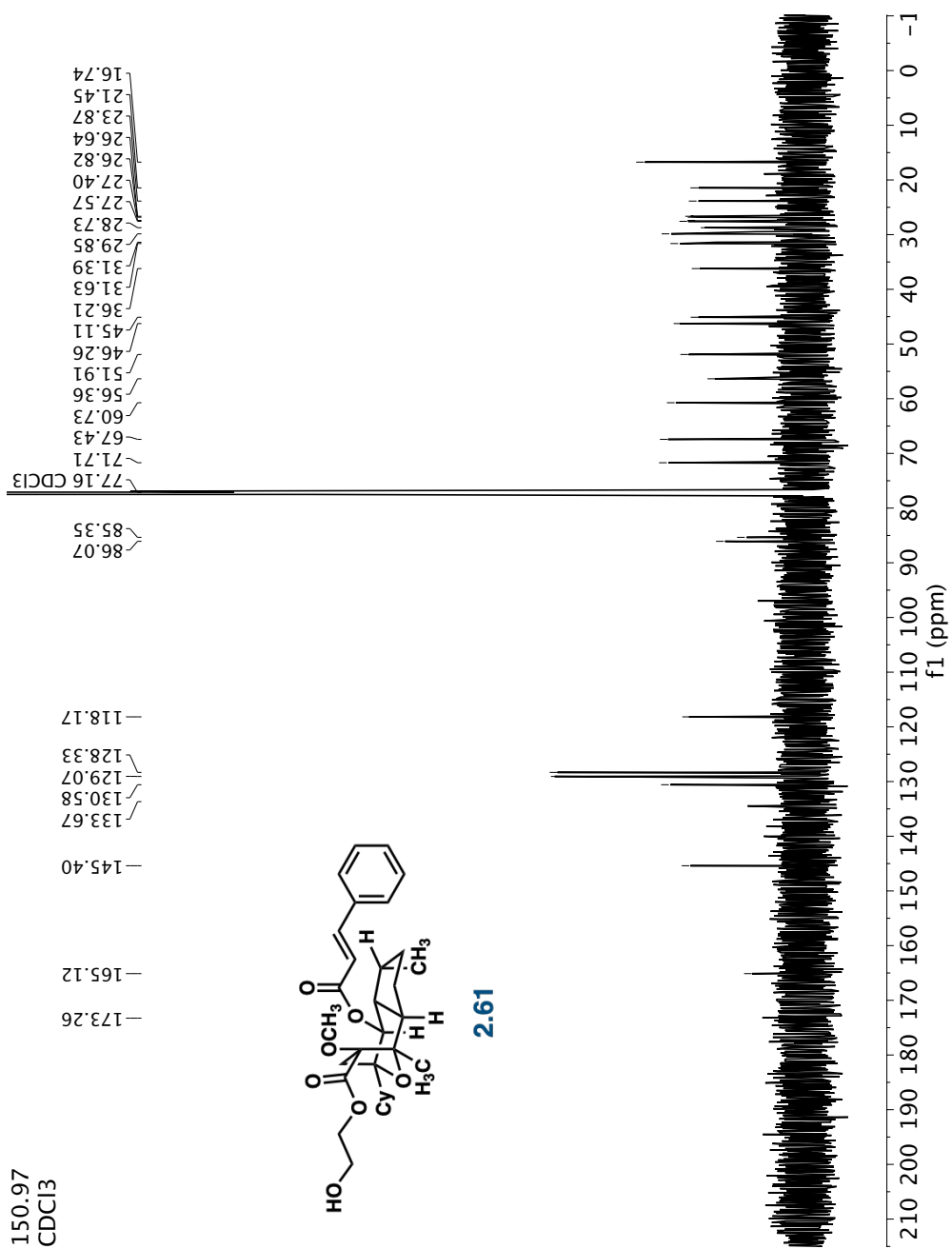






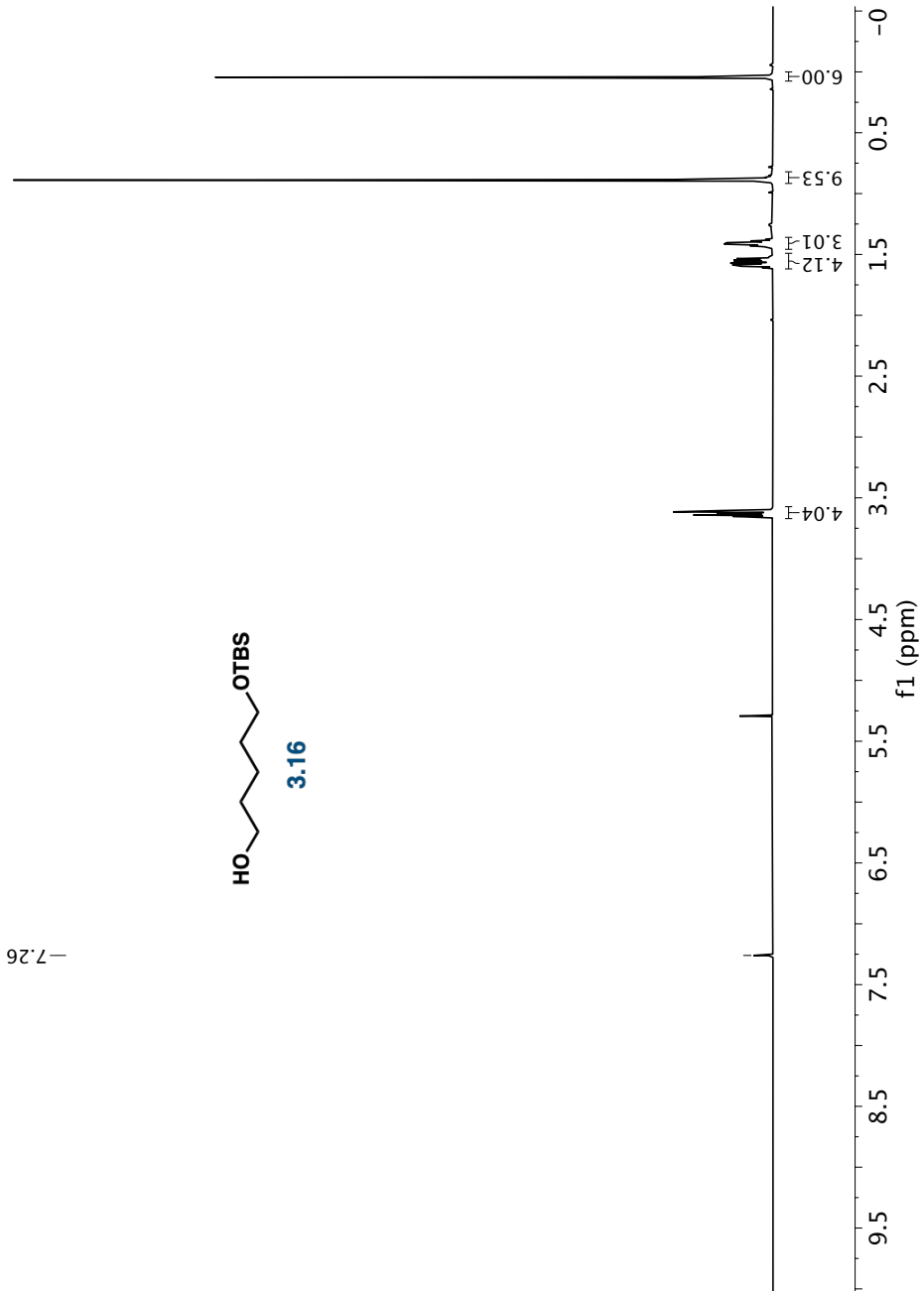
600.32
CDCl₃



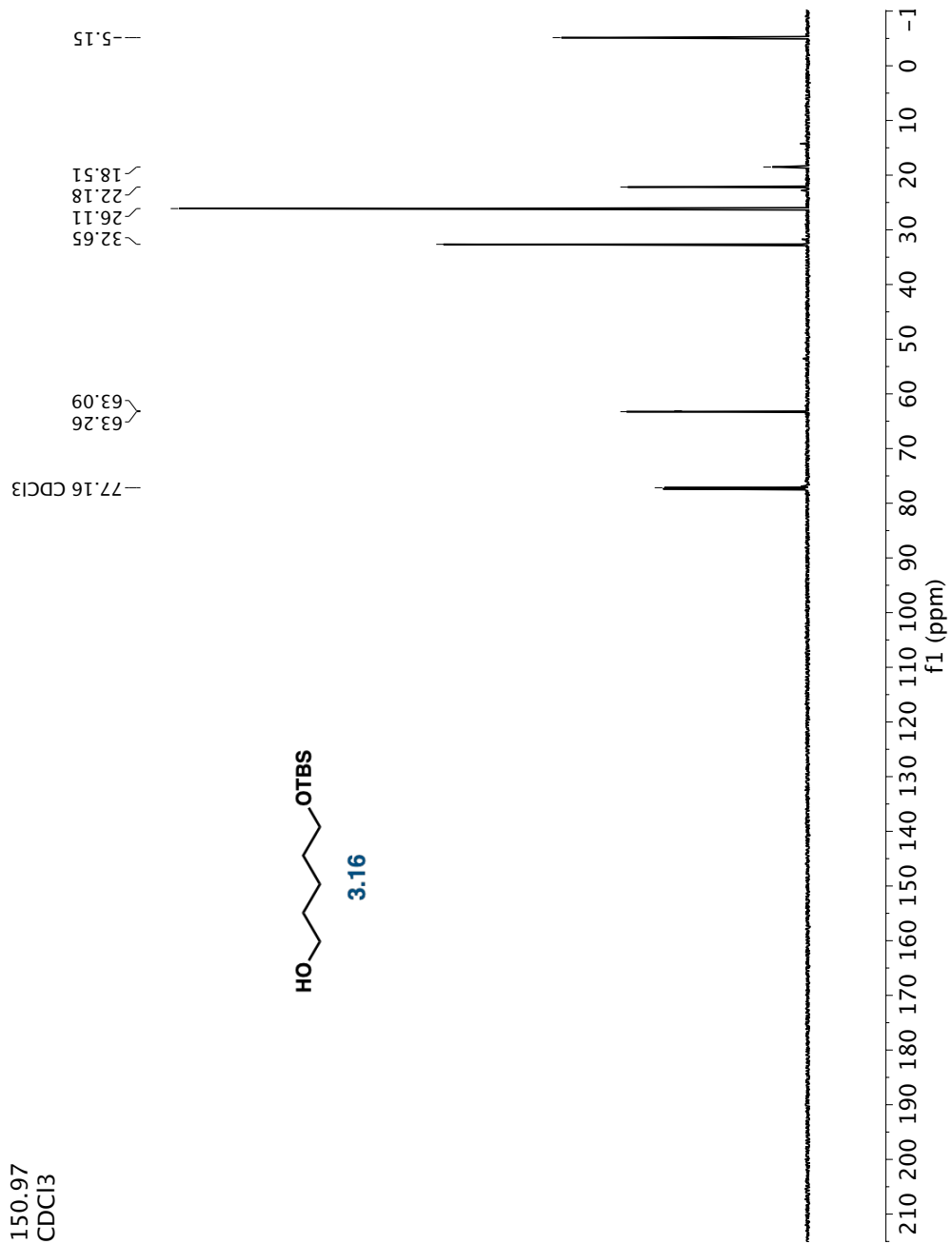


600.32
CDCl₃

-7.26 CDCl₃

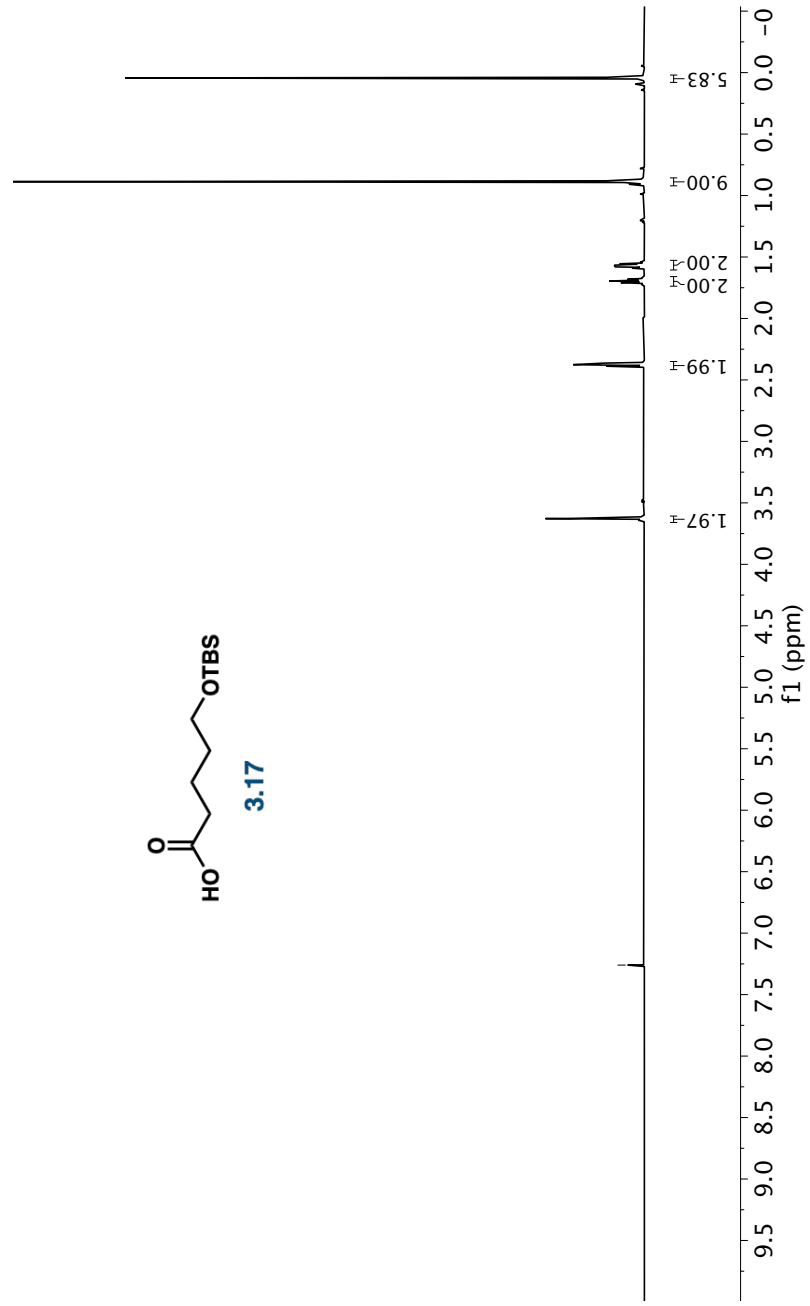


150.97
CDCl₃



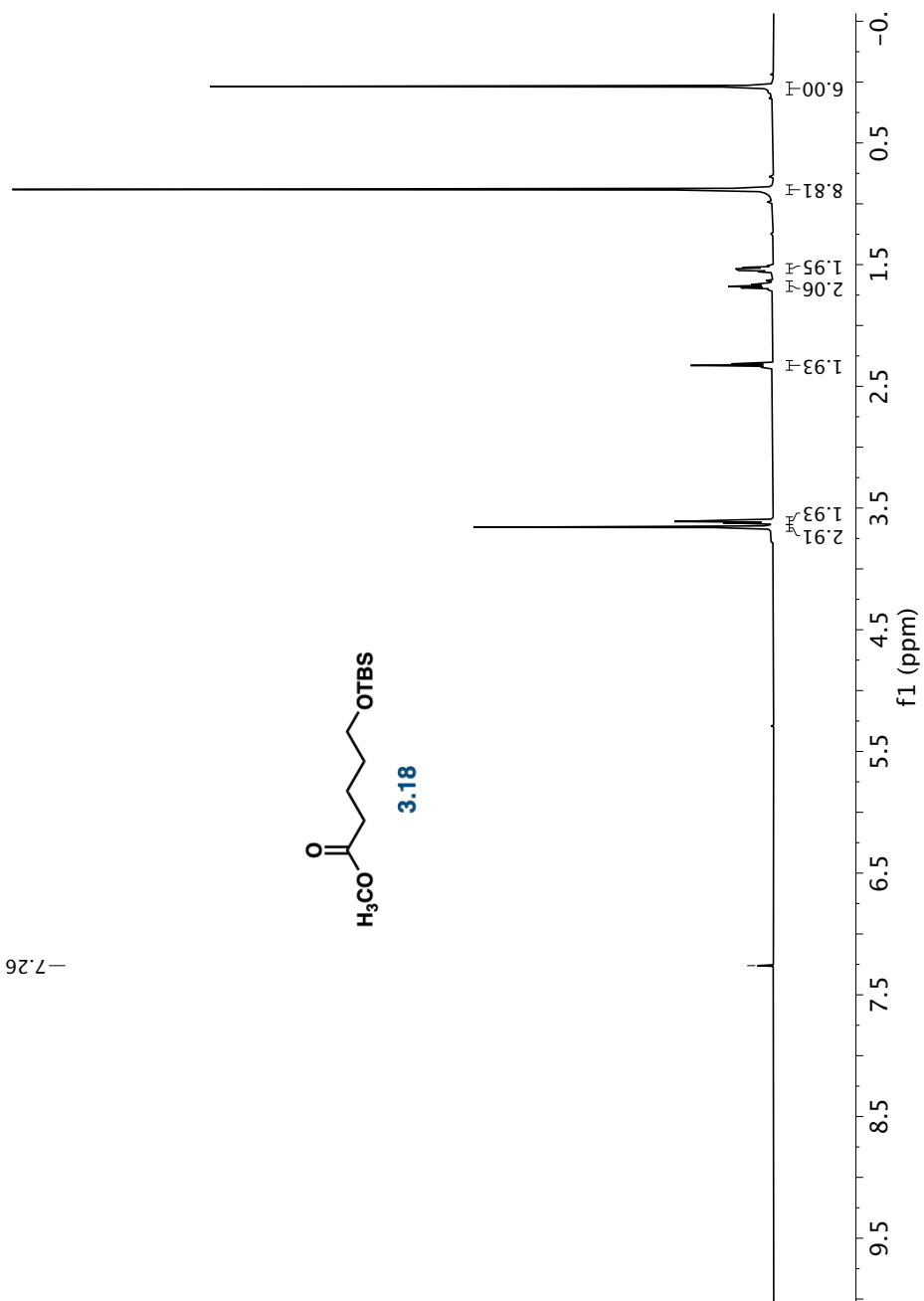
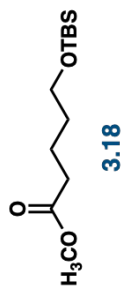
600.32
CDCl₃

-7.26 CDCl₃



600.32
CDCl₃

-7.26 CDCl₃



150.97
CDCl₃

174.25

77.16 CDCl₃

62.79

51.57

33.96

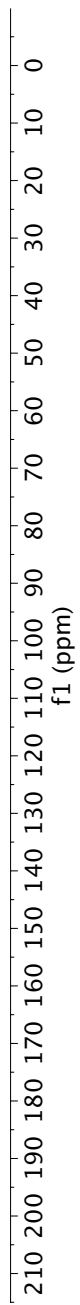
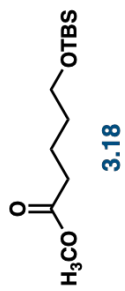
32.32

26.08

21.60

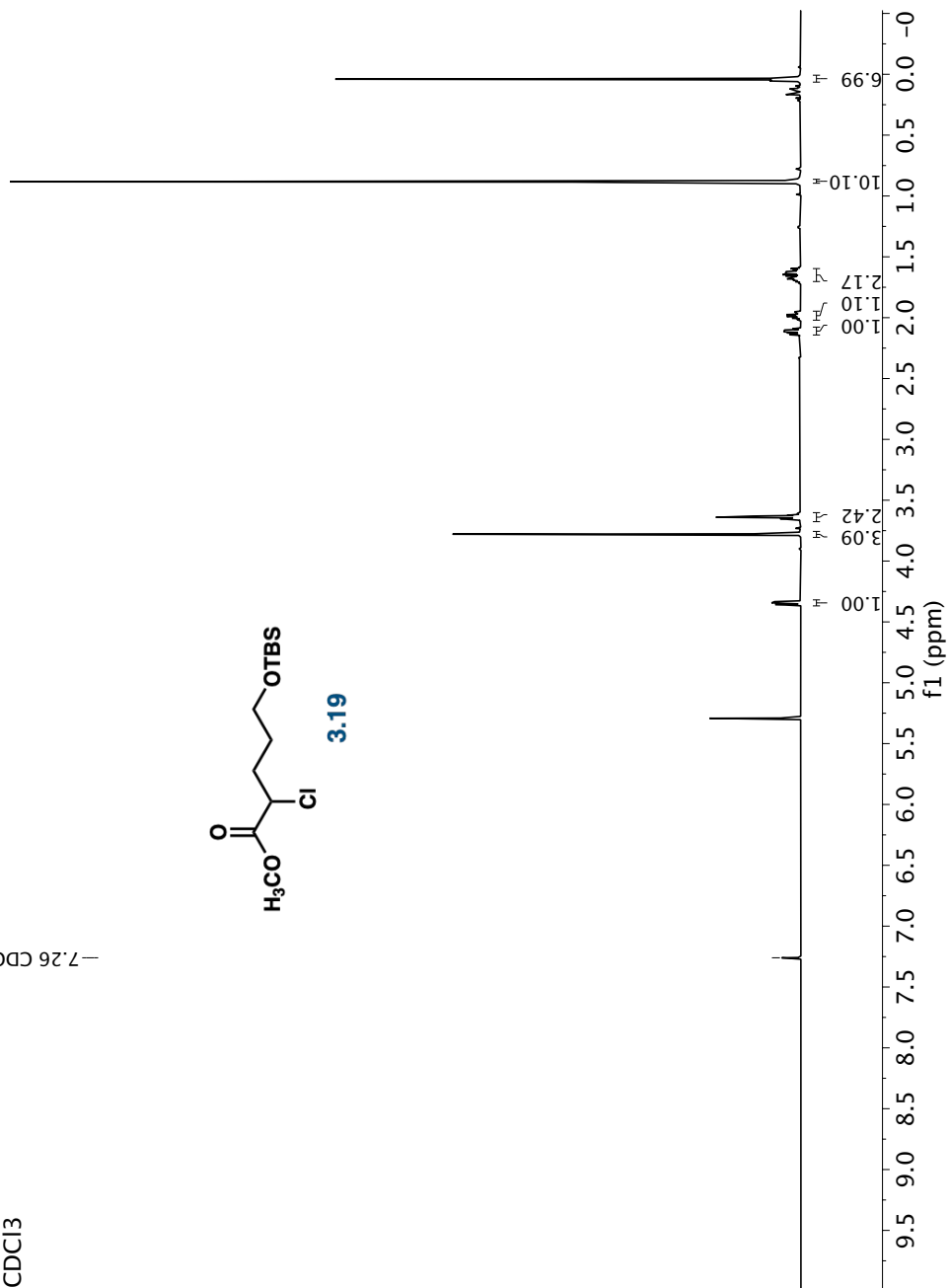
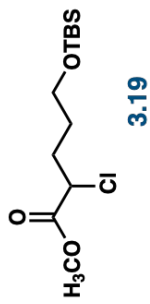
18.46

5.19



600.32
CDCl3

-7.26 CDCl3



150.97
CDCl₃

-170.37

-77.16 CDCl₃

-62.22

-57.27

-52.98

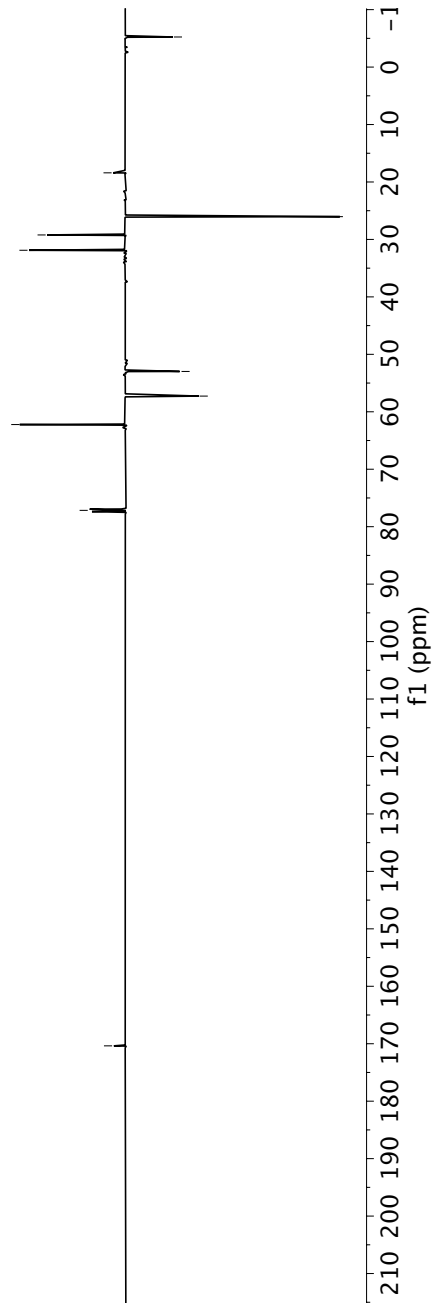
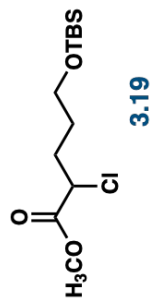
-31.89

-29.22

-26.03

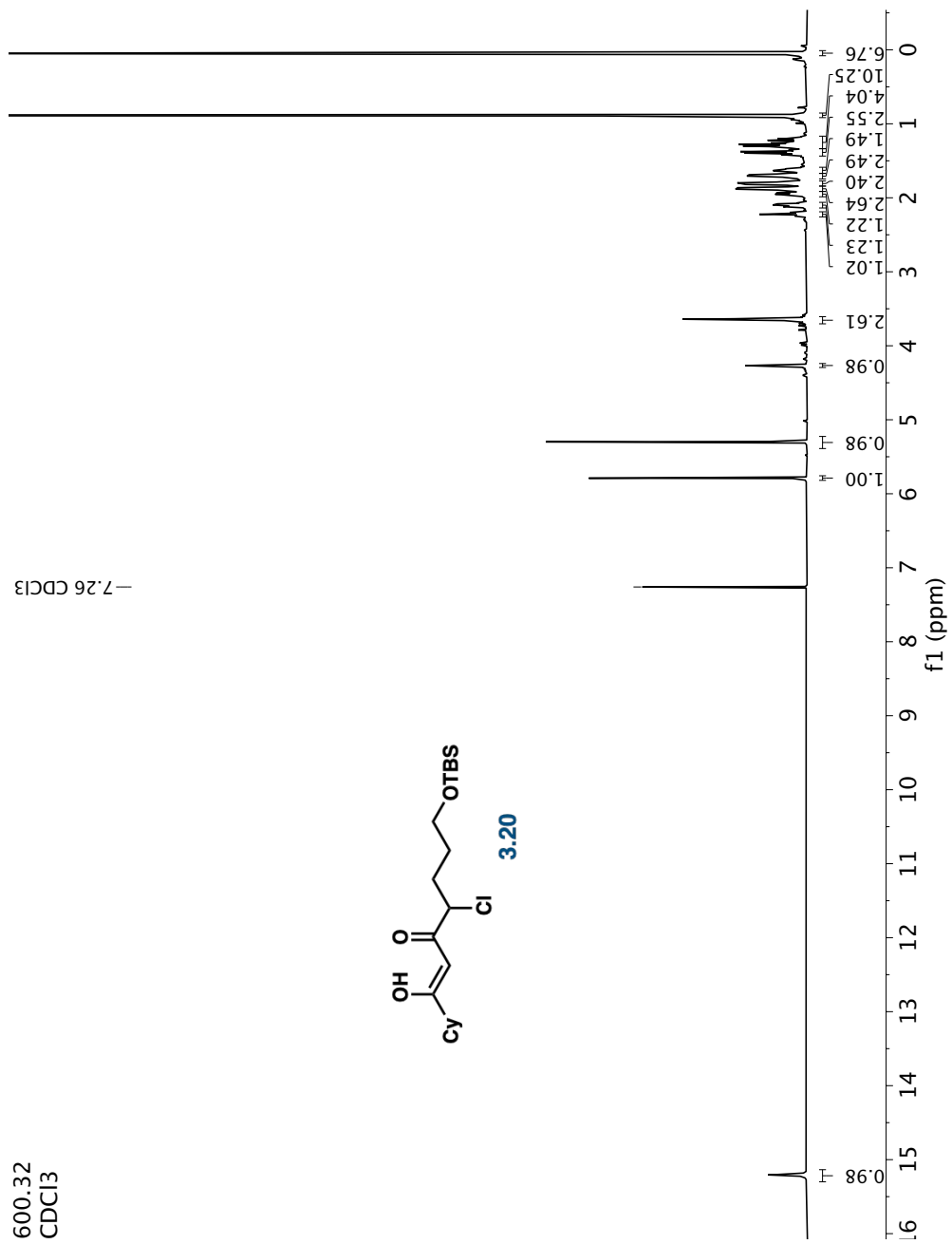
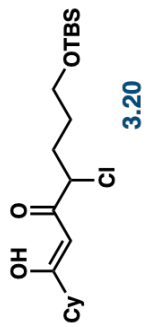
-18.41

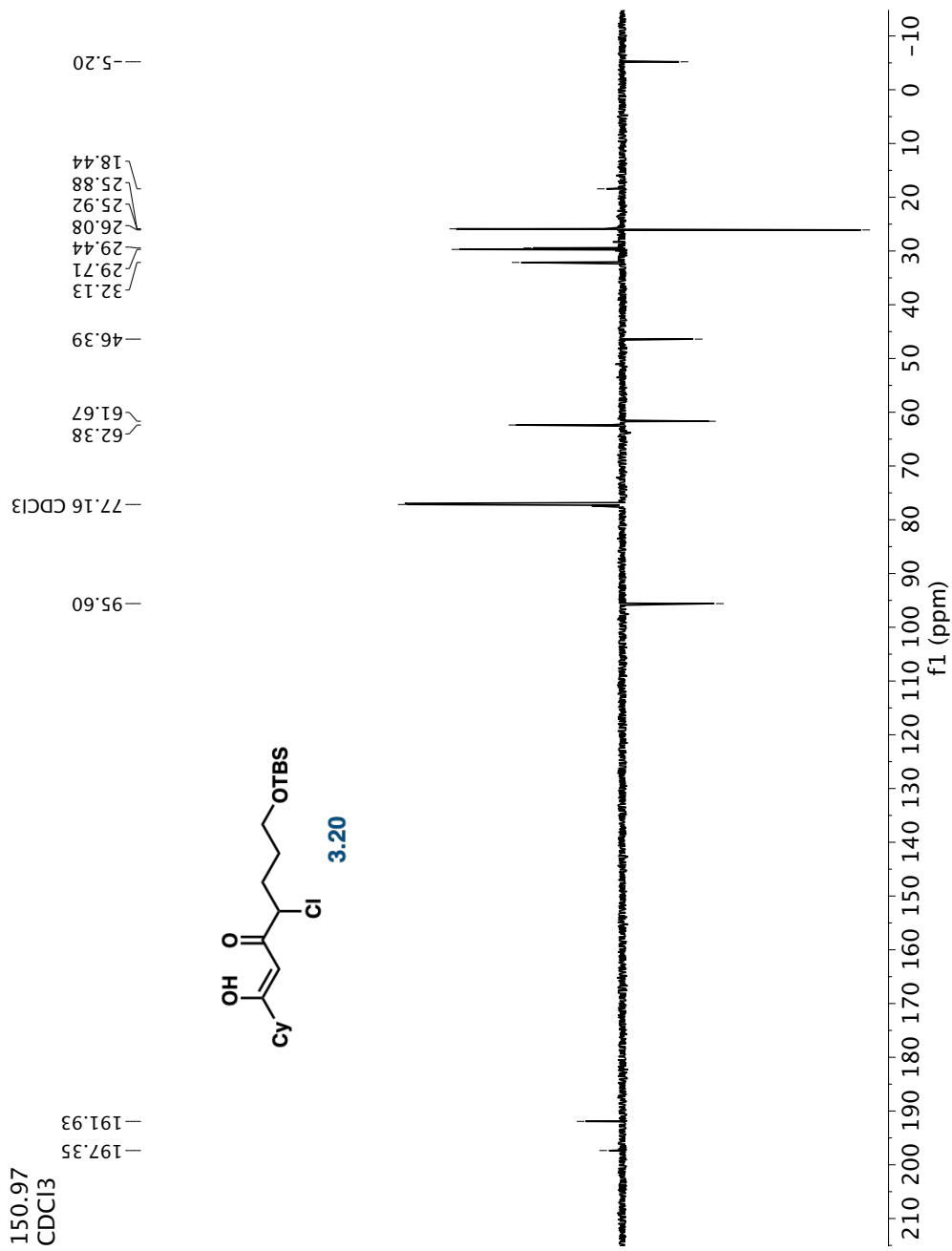
-5.24

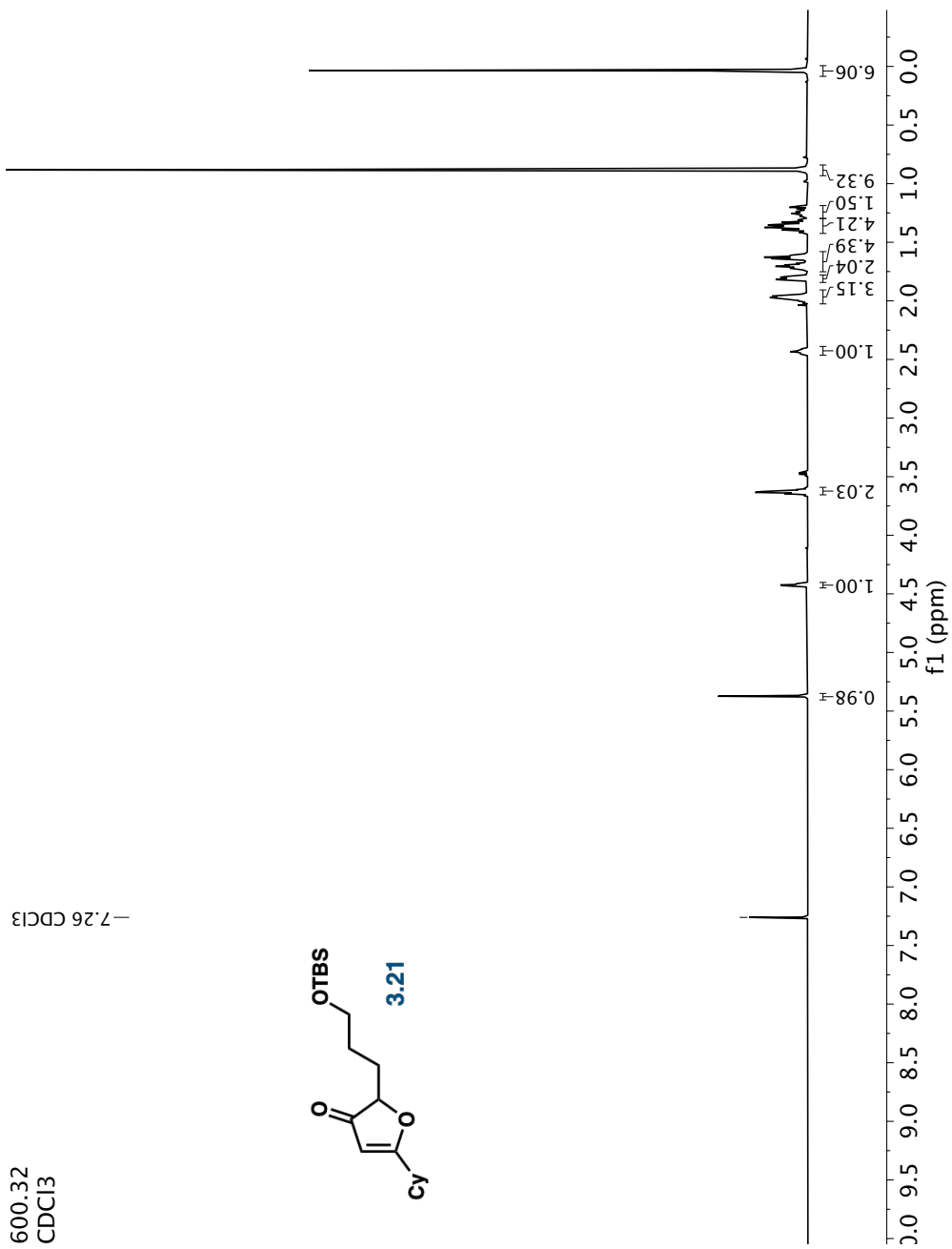


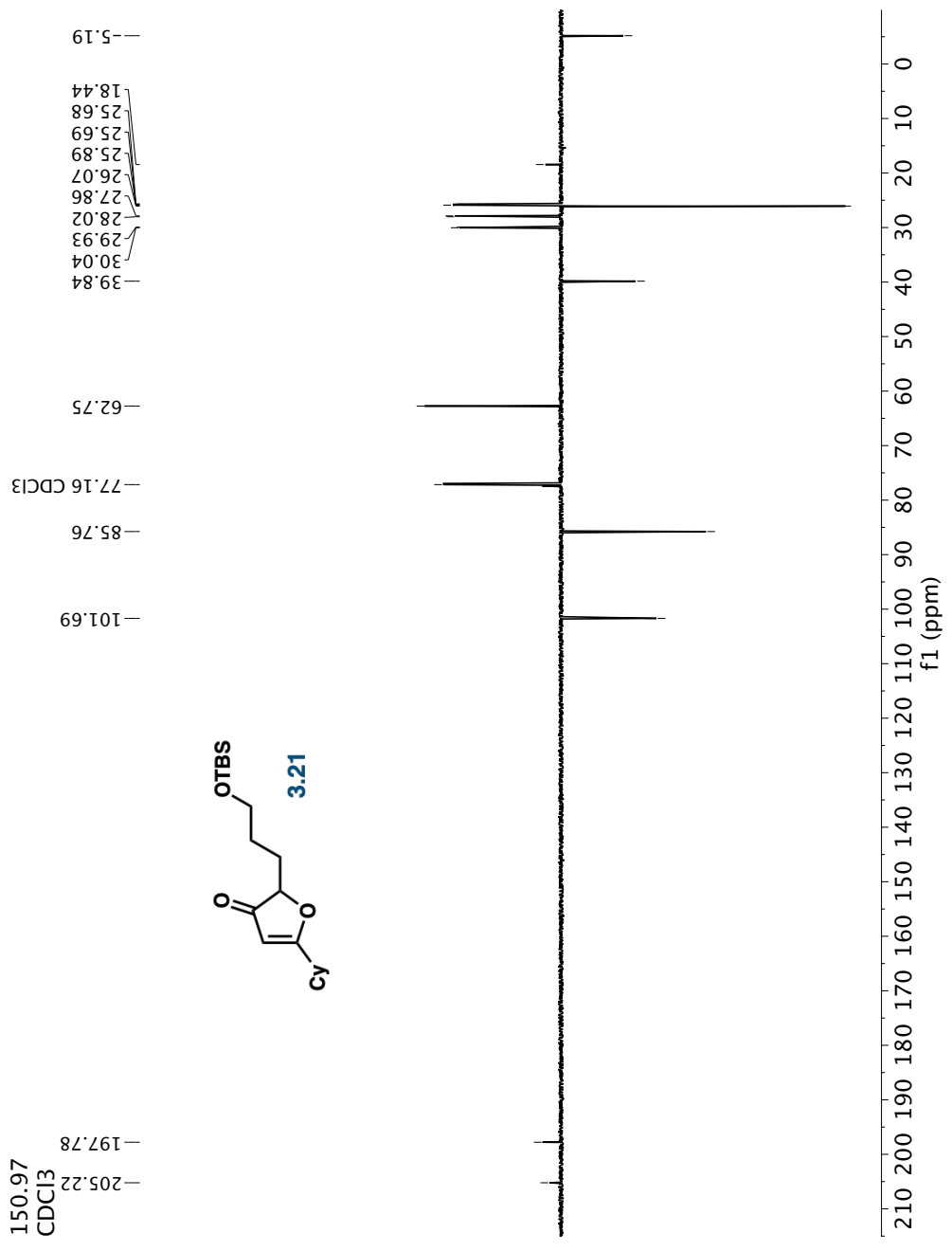
600.32
CDCl₃

-7.26 CDCl₃



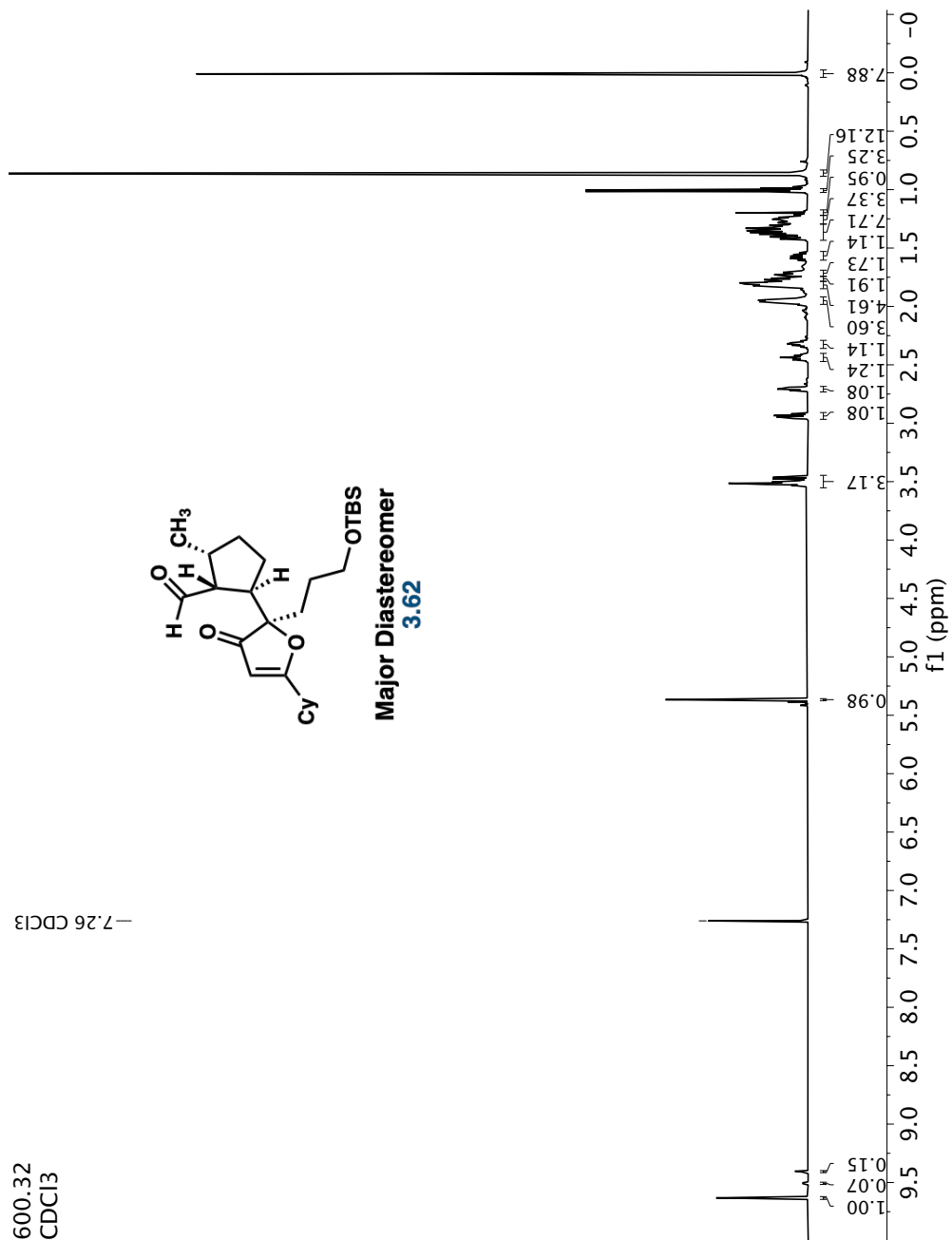
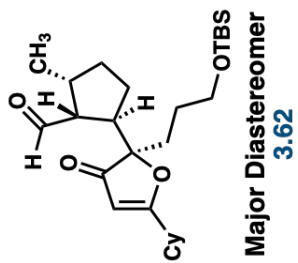


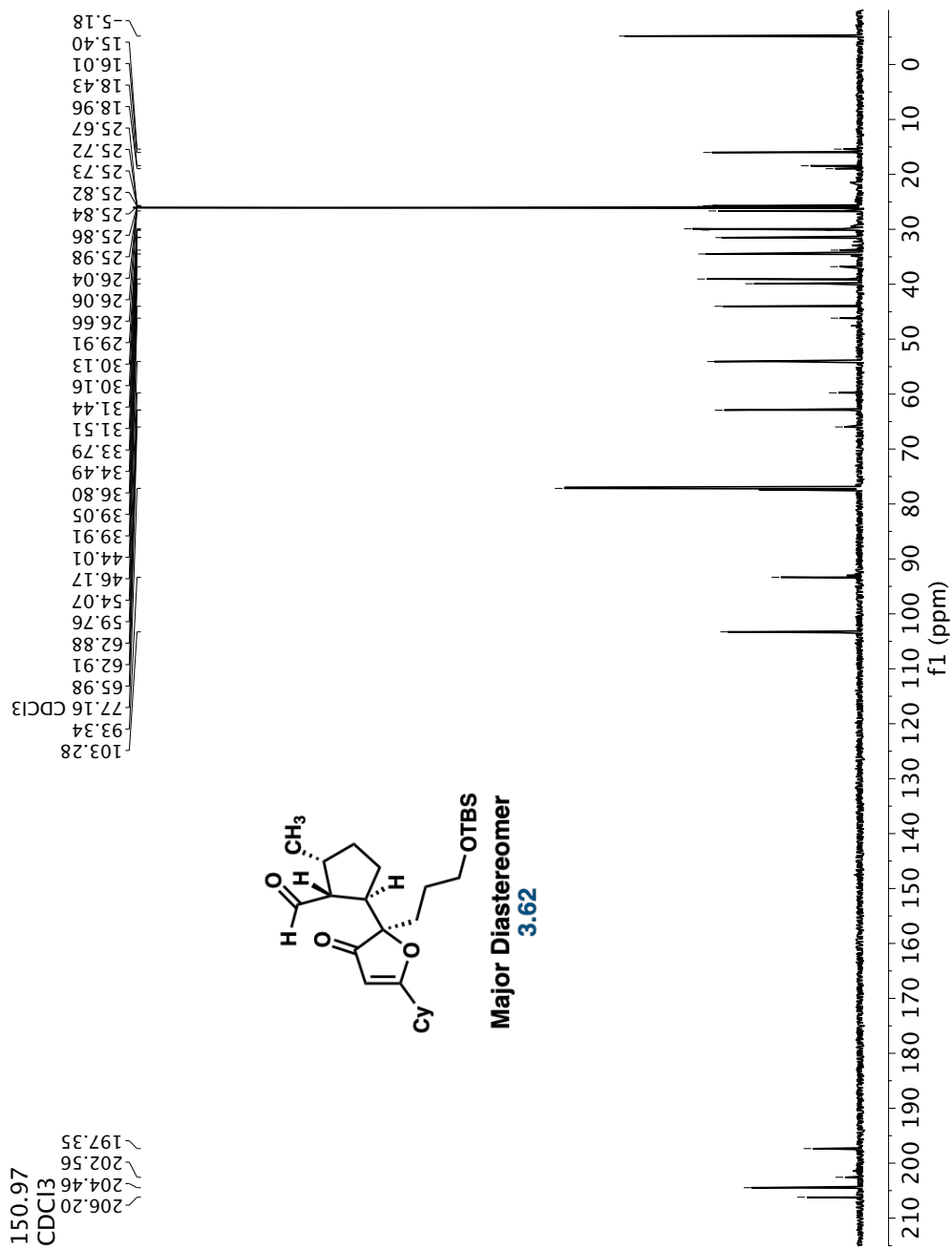




600.32
CDCl₃

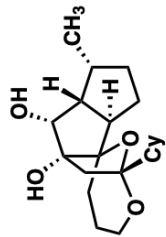
-7.26 CDCl₃



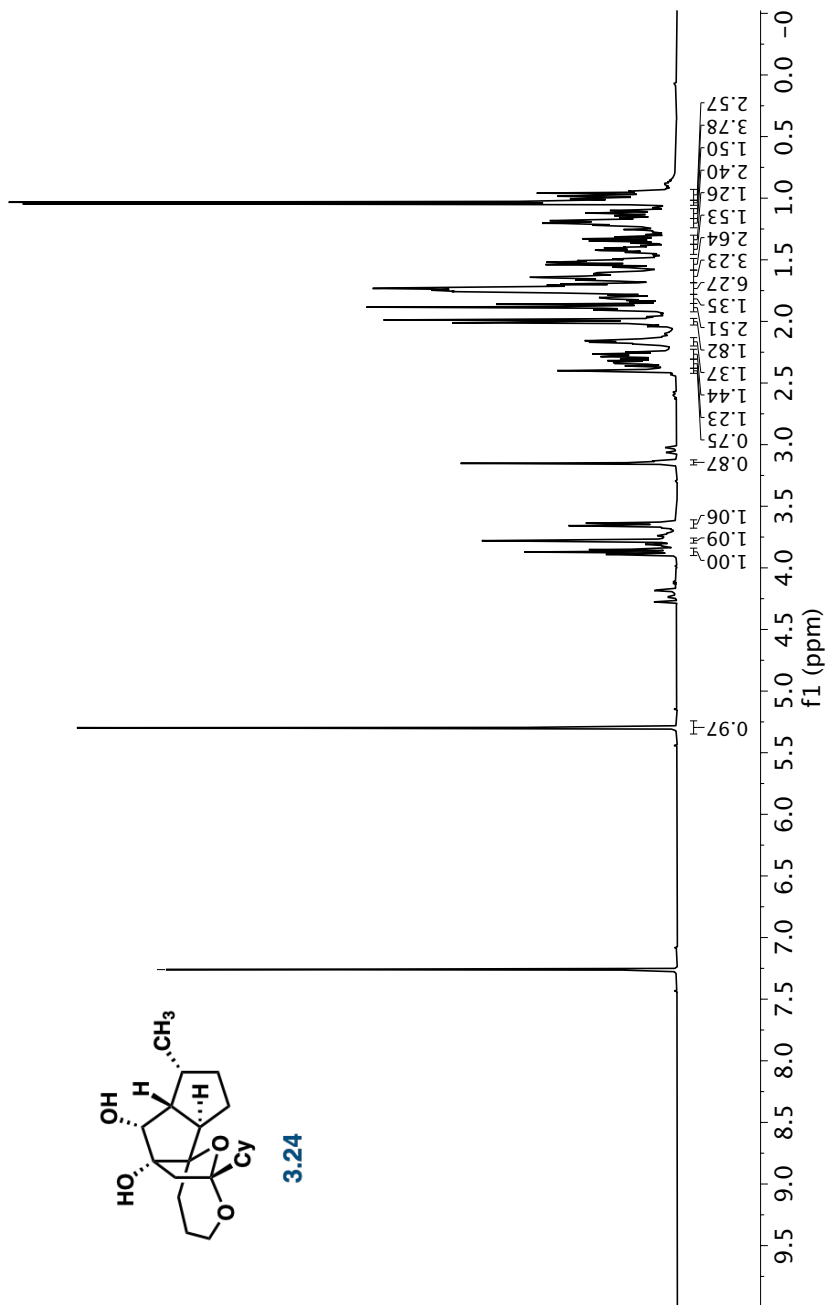


600.32
CDCl₃

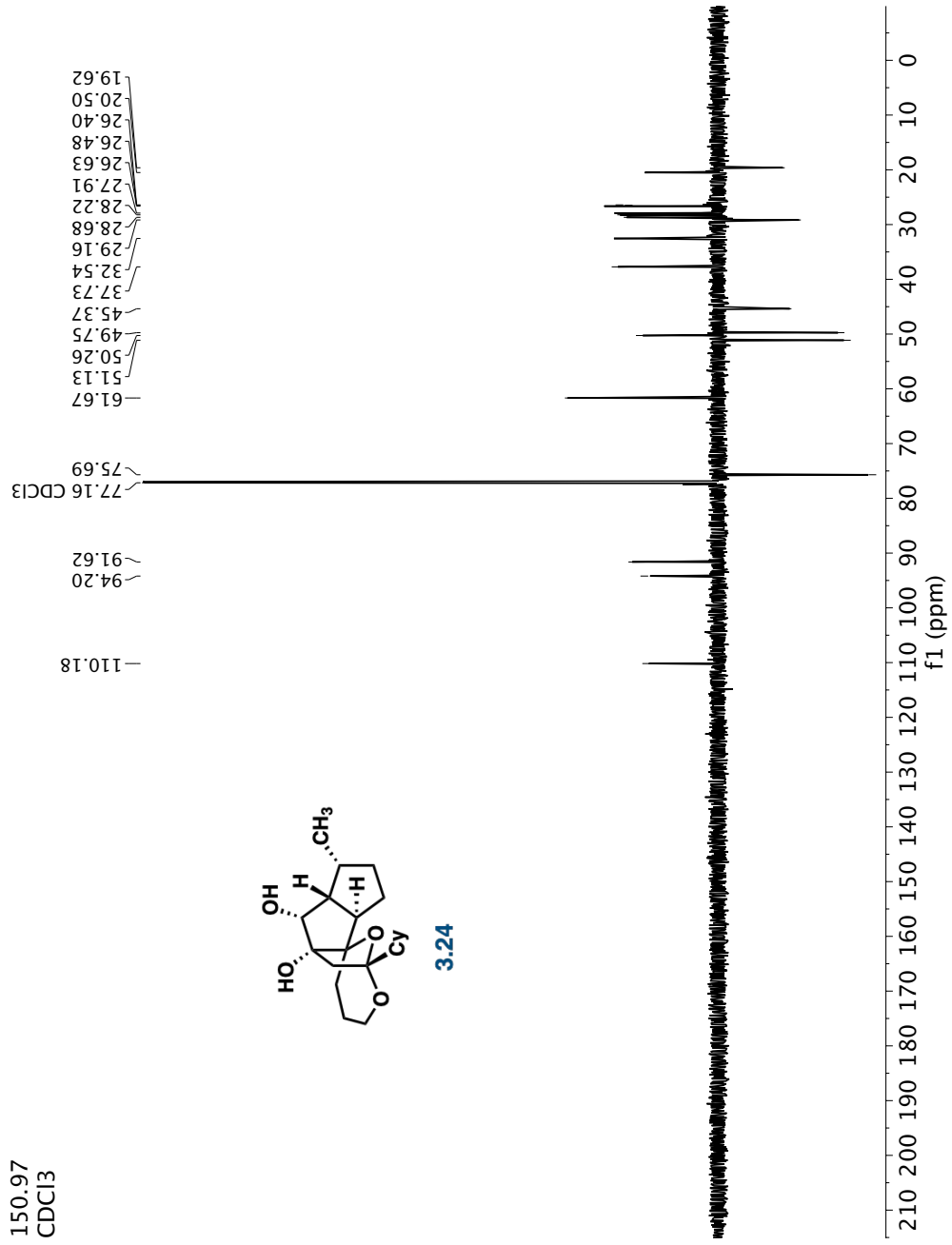
-7.26 CDCl₃



3.24

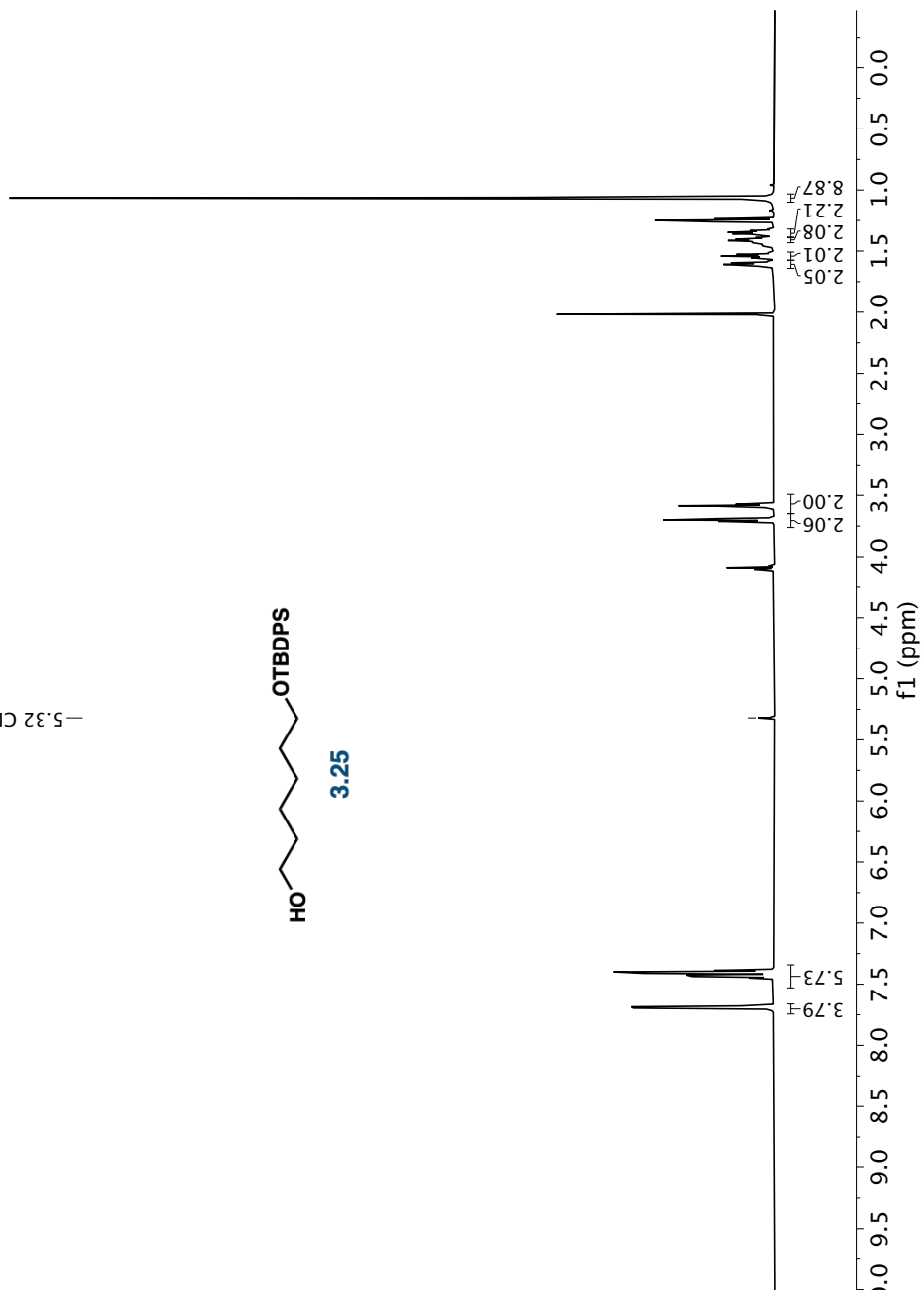


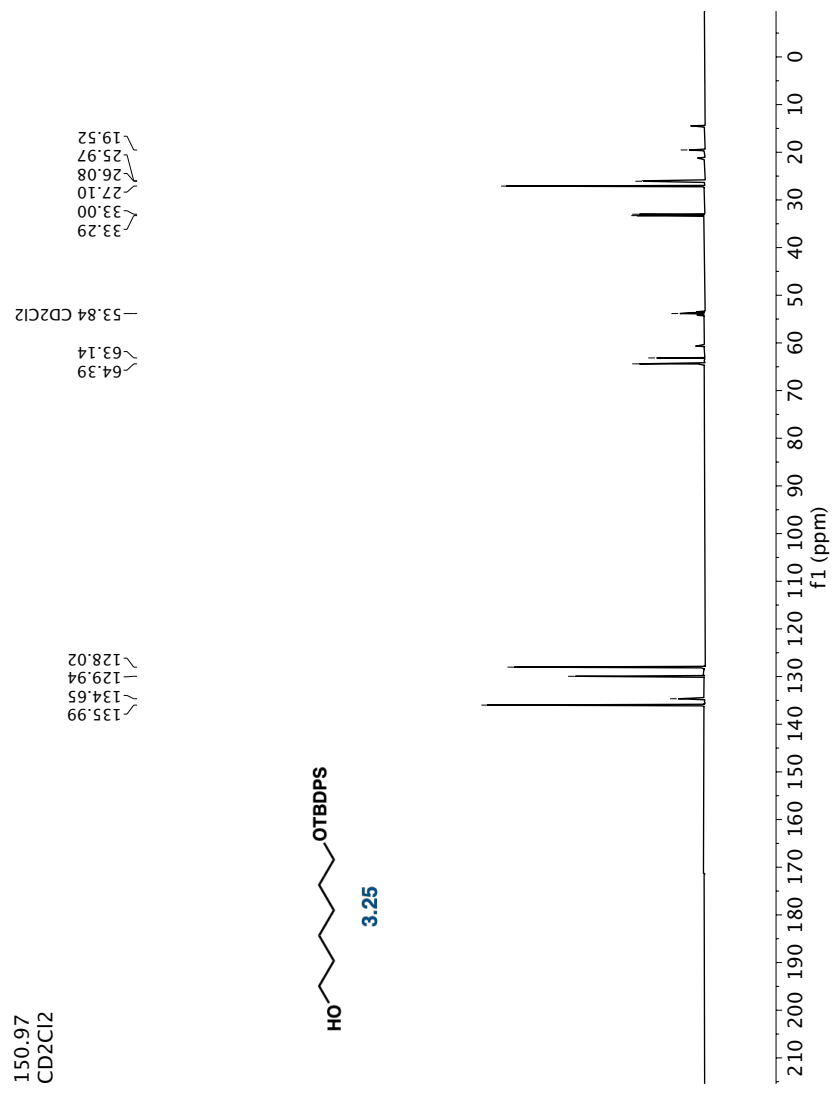
150.97
CDCl₃

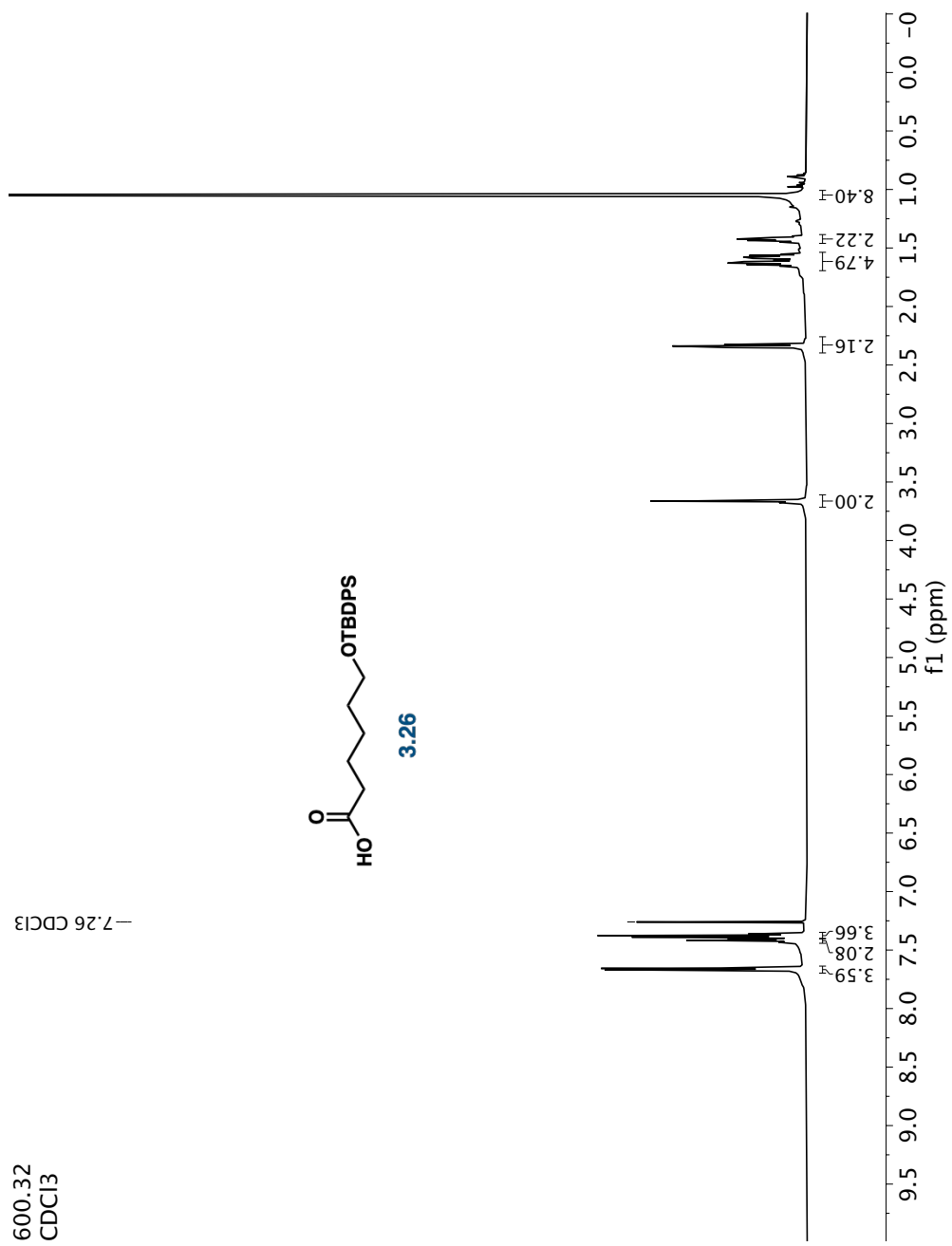


600.32
CD2Cl2

-5.32 CD2Cl2

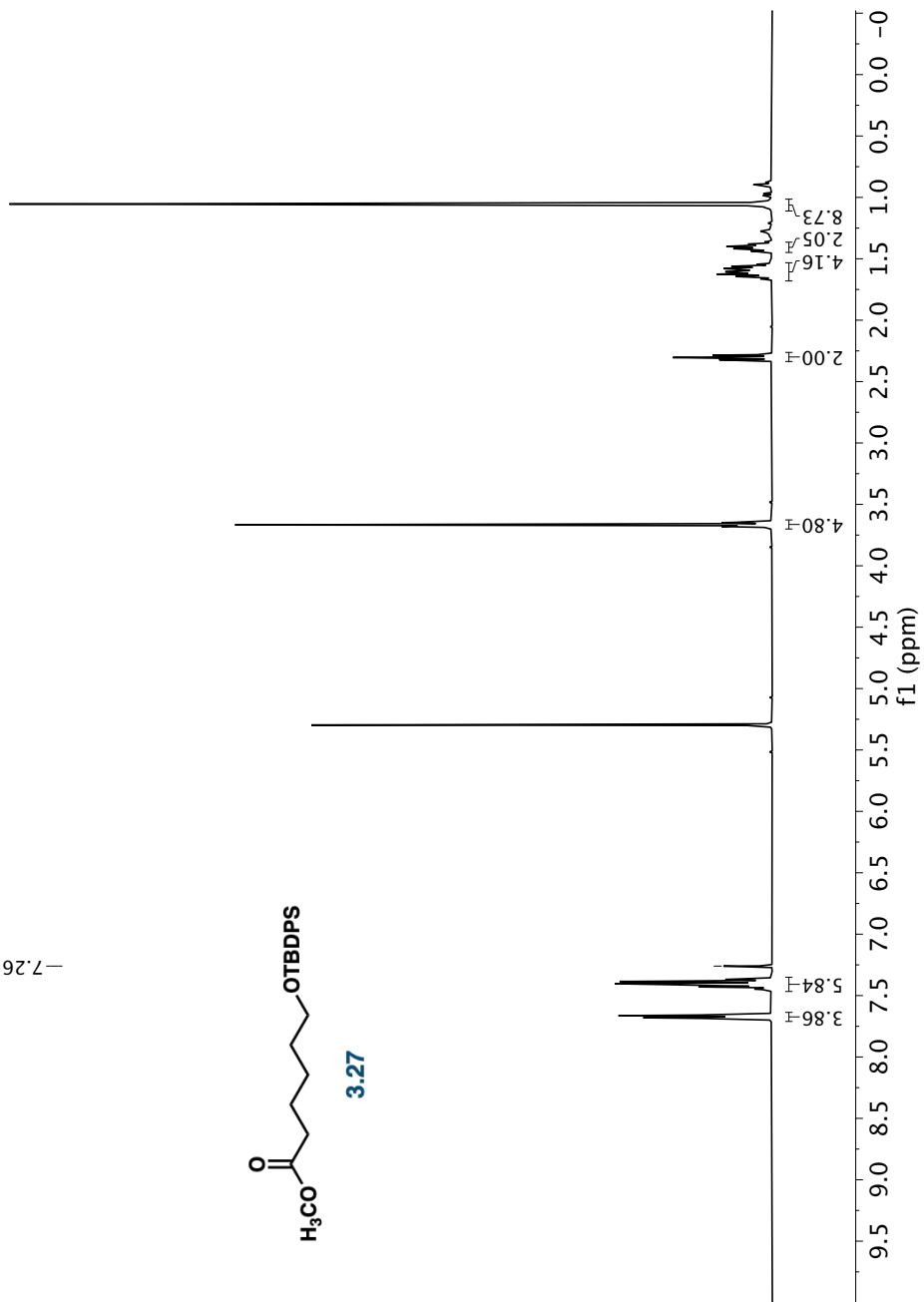


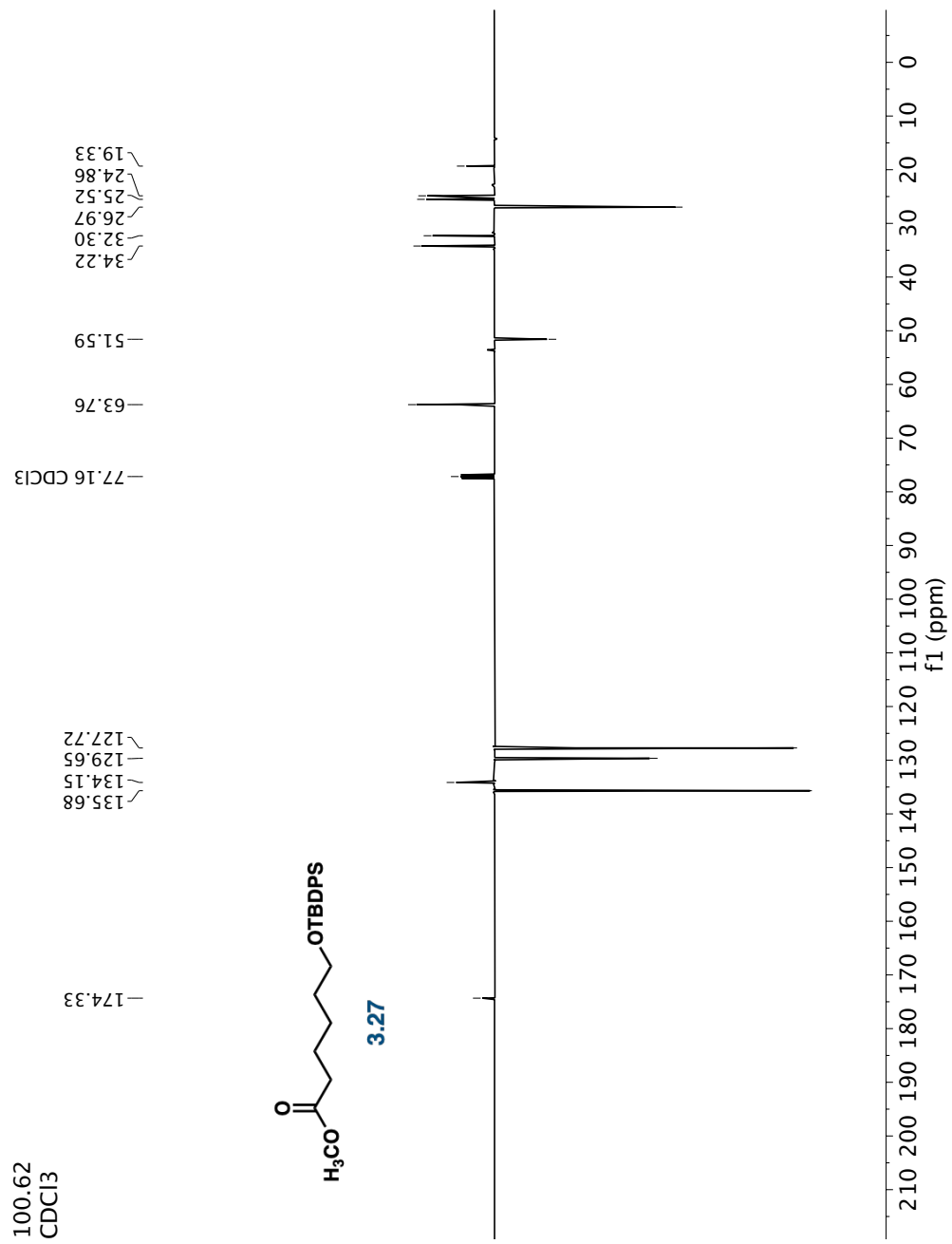




400.13
CDCl₃

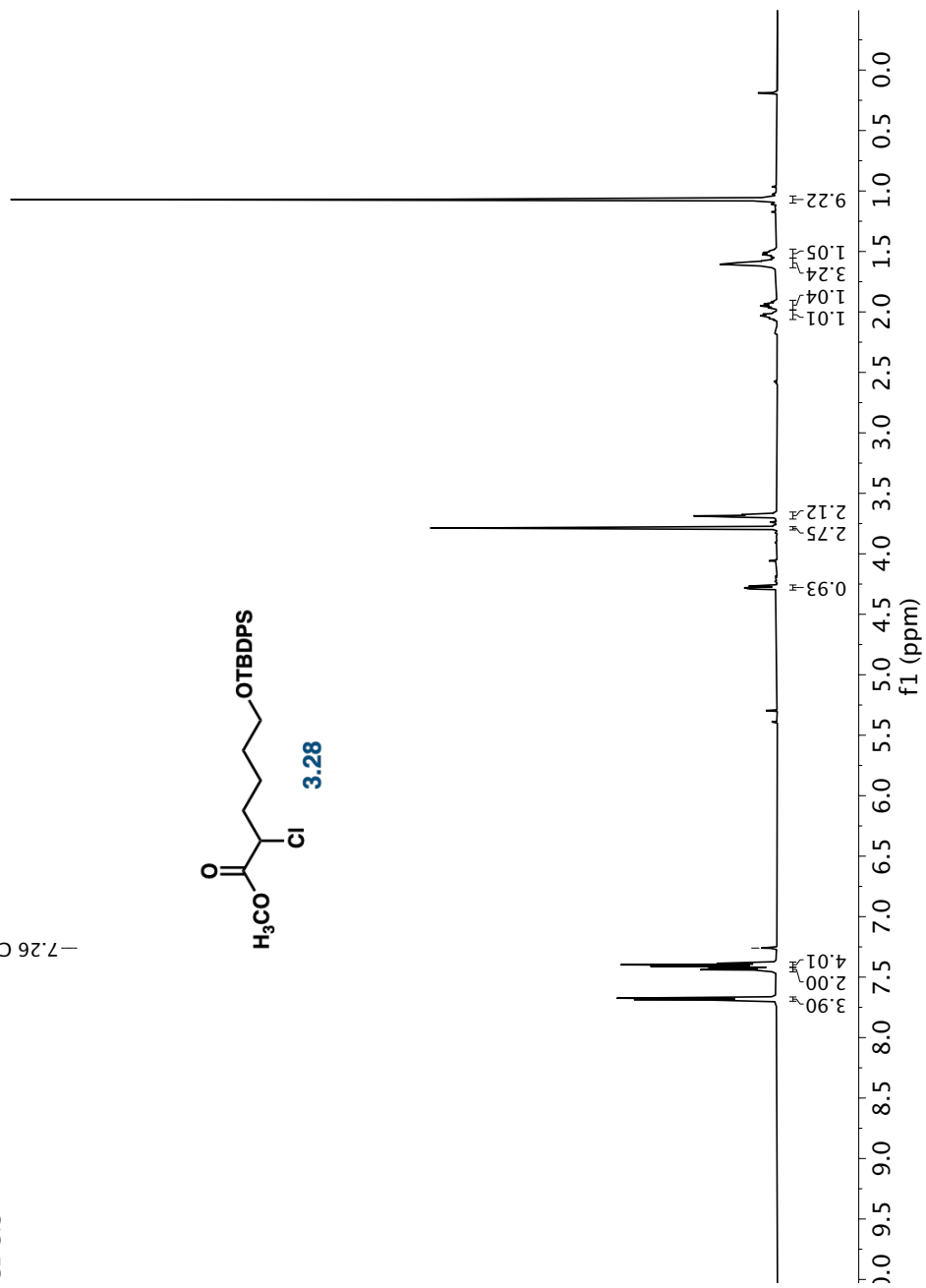
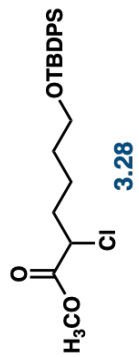
-7.26 CDCl₃





600.32
CDCl₃

-7.26 CDCl₃



150.97
CDCl₃

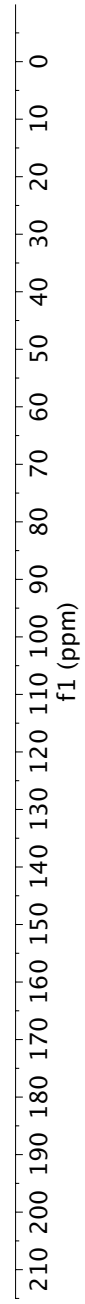
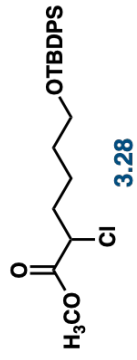
170.33

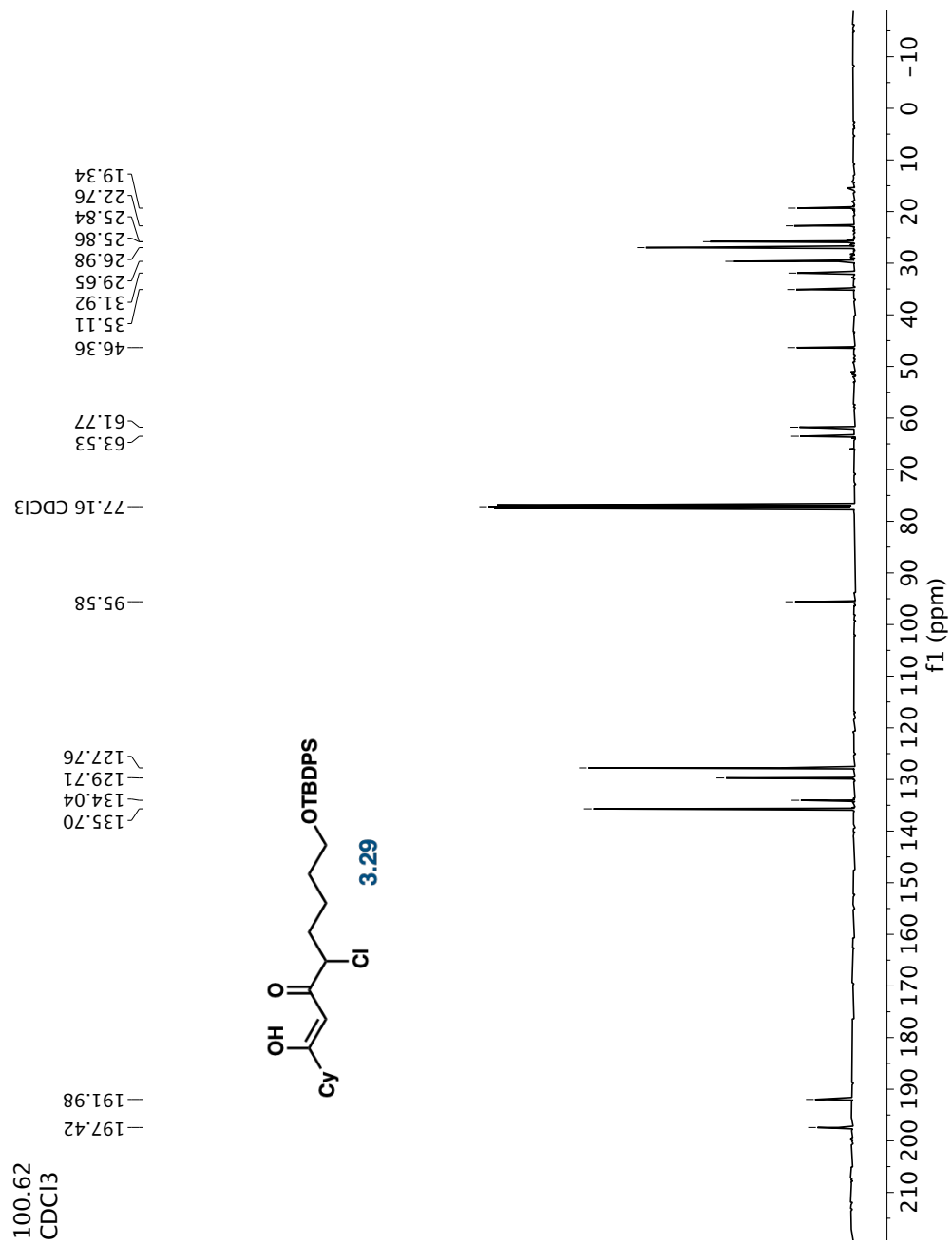
135.70
134.10
129.72
129.70
129.66
127.77
127.75

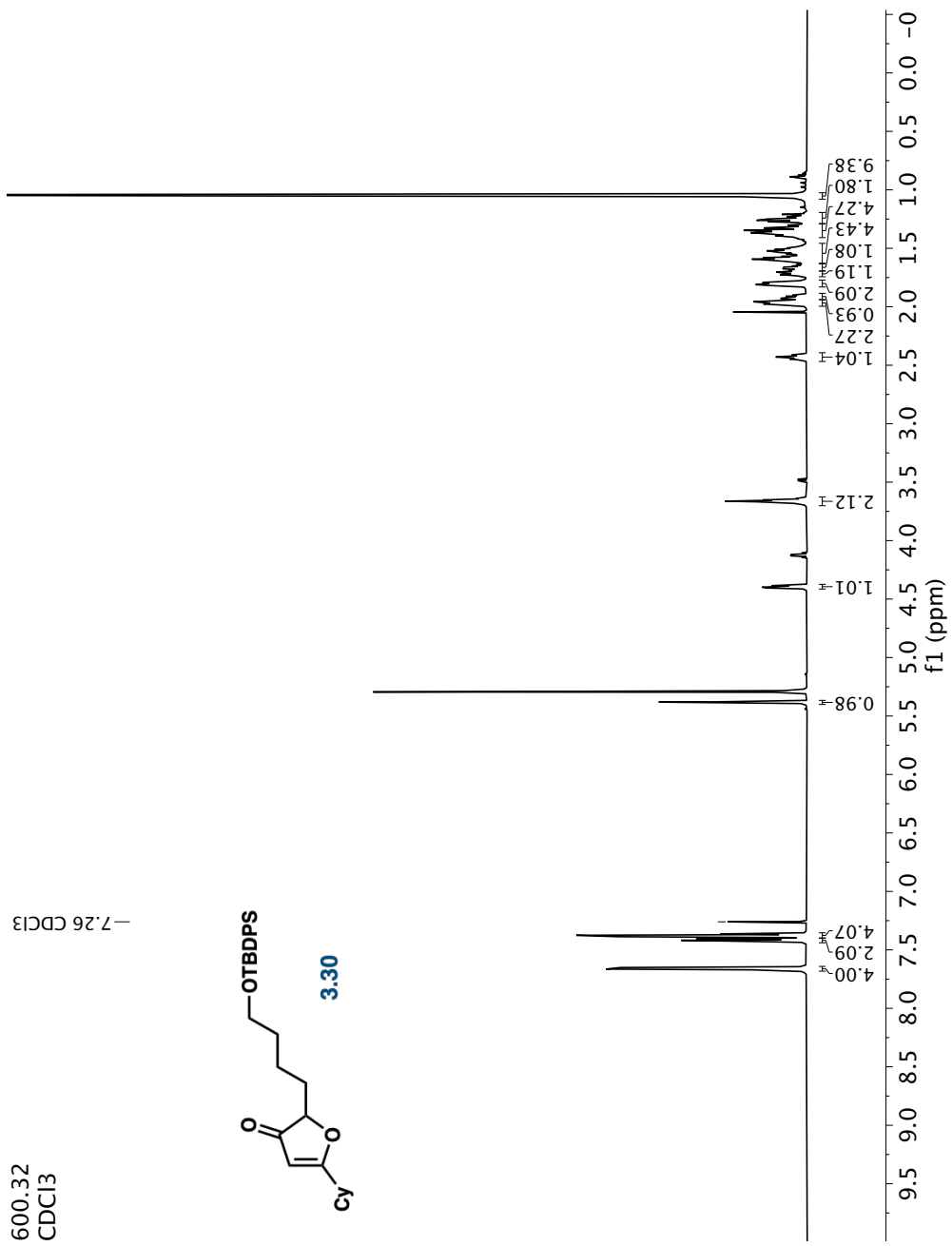
77.16 CDCl₃

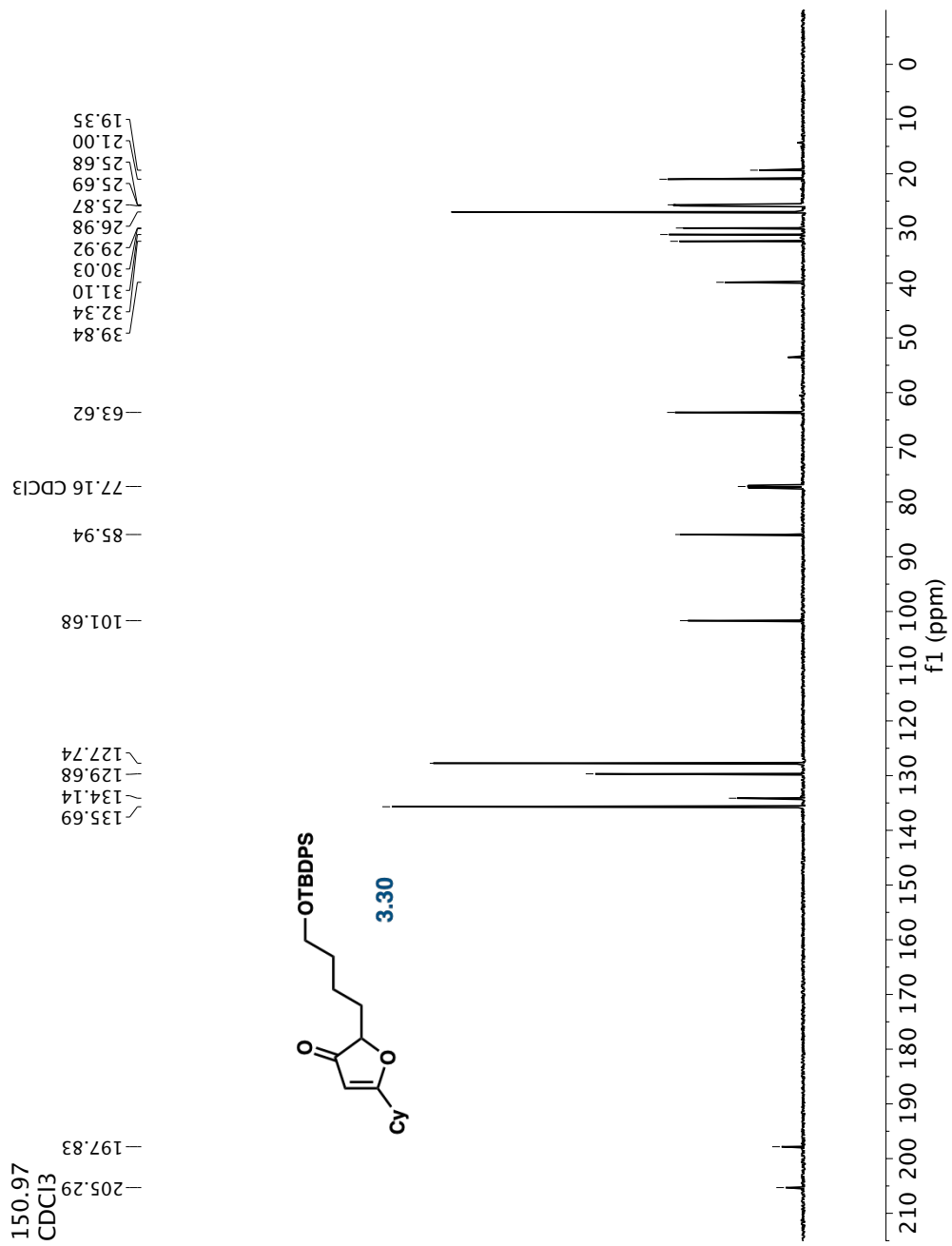
63.51
57.31
52.92

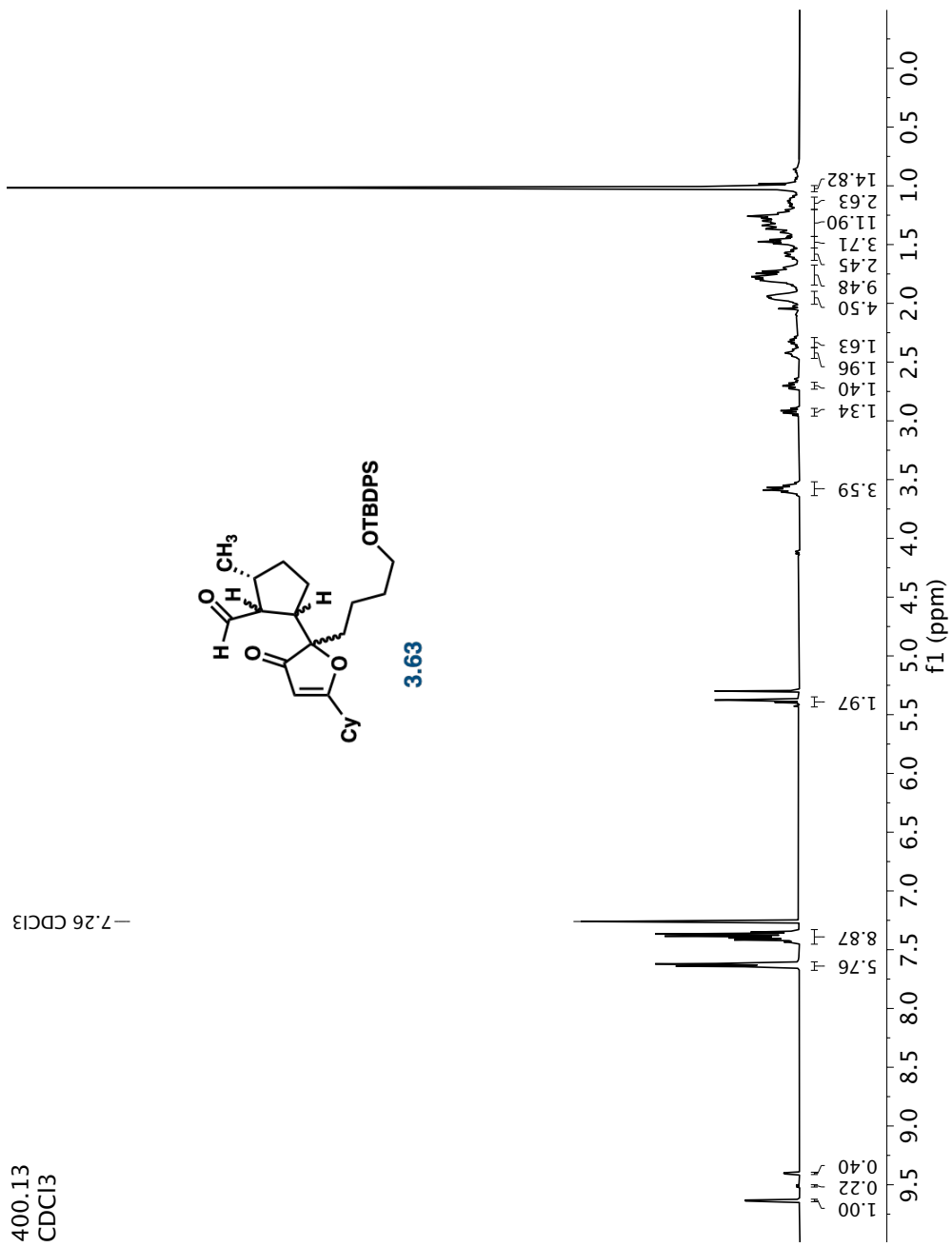
34.83
31.84
27.02
22.62
19.35

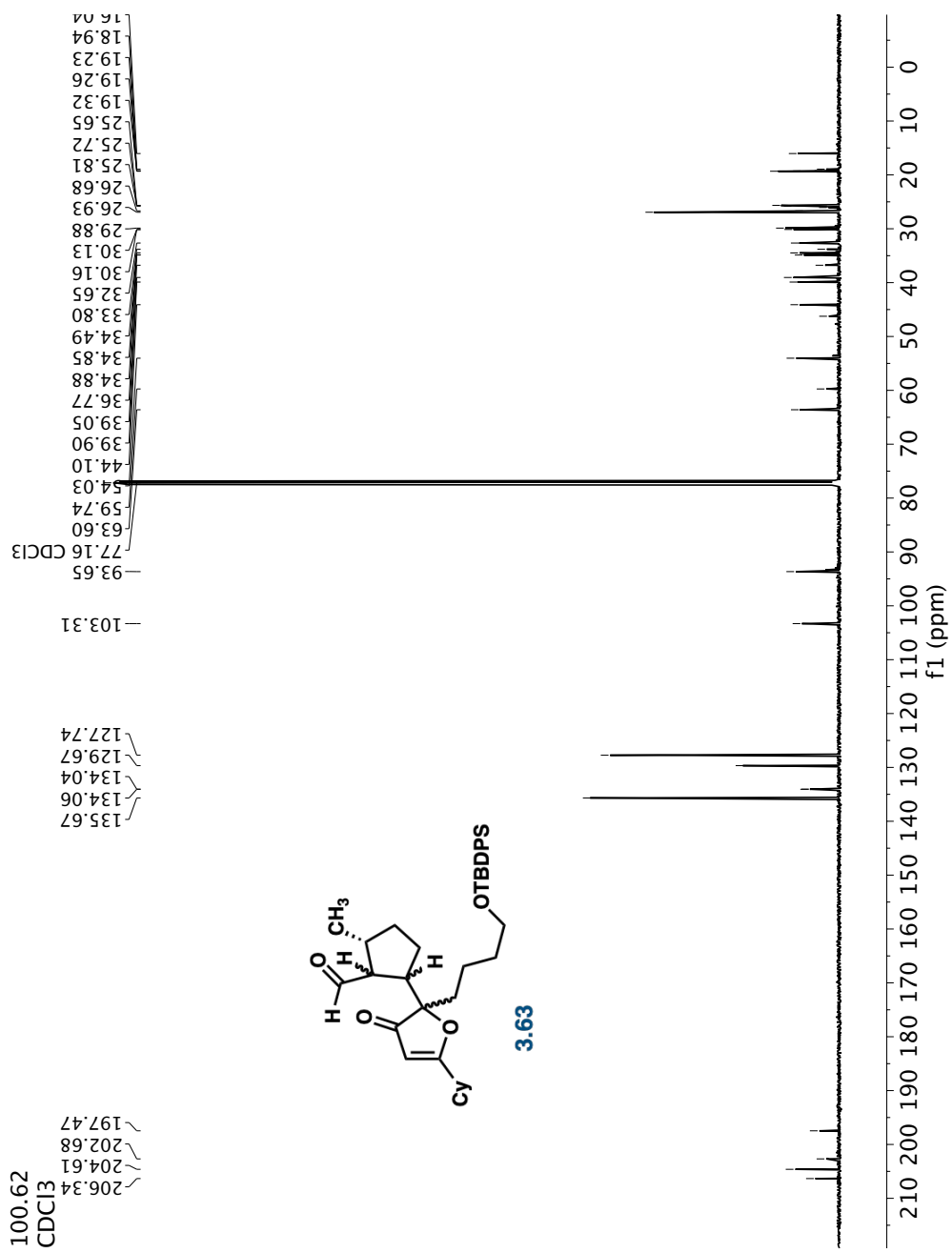










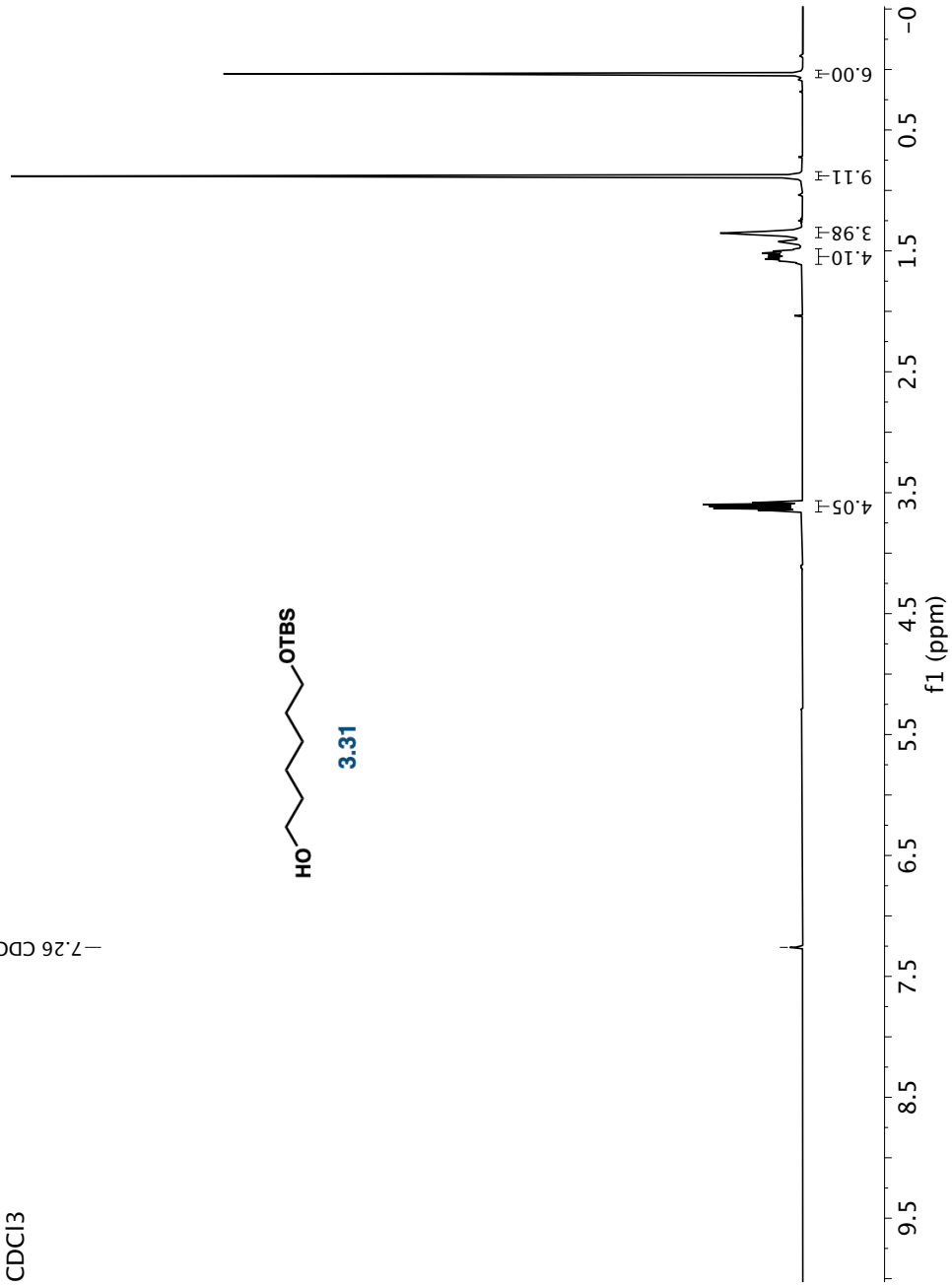


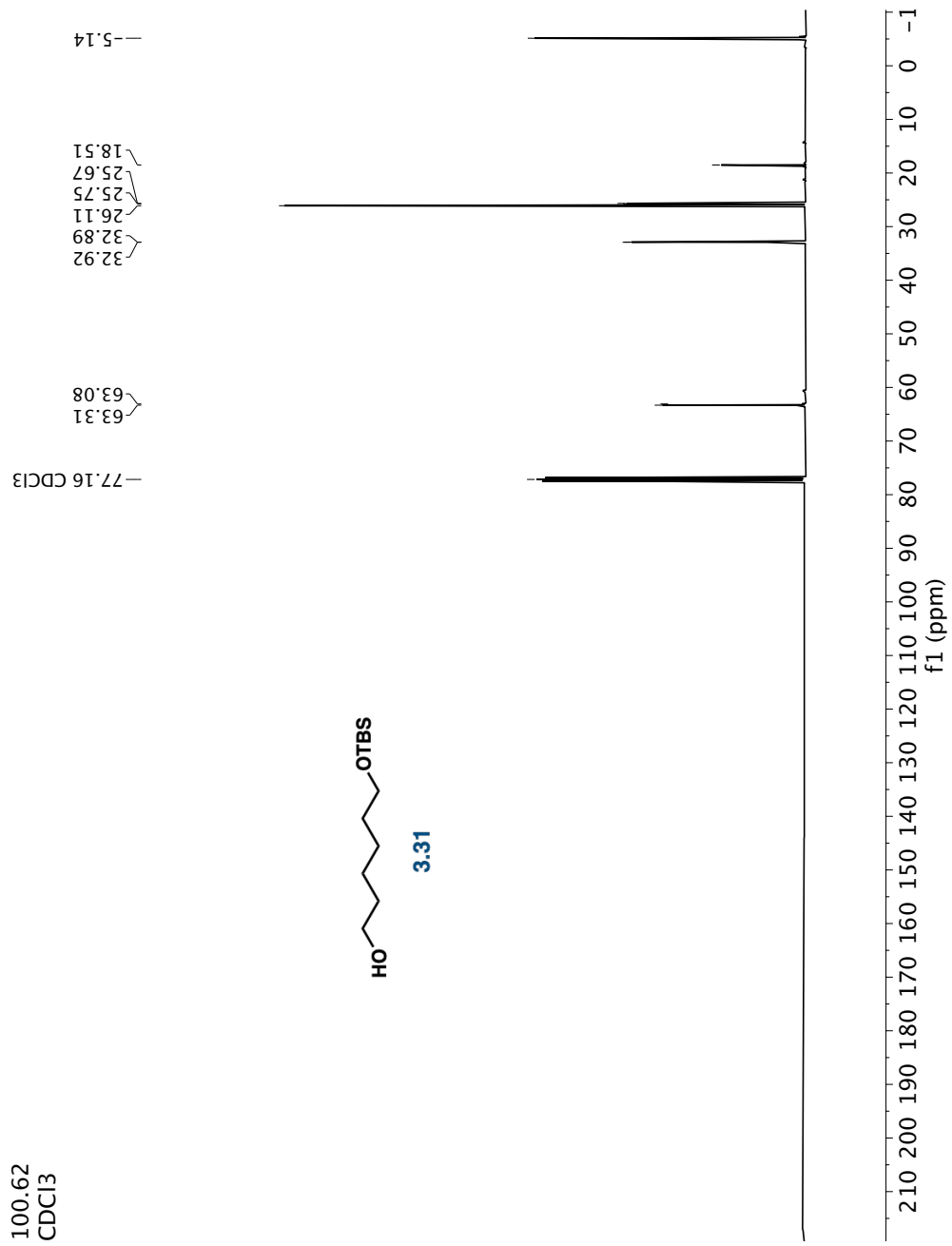
400.13
CDCl₃

-7.26 CDCl₃



3.31



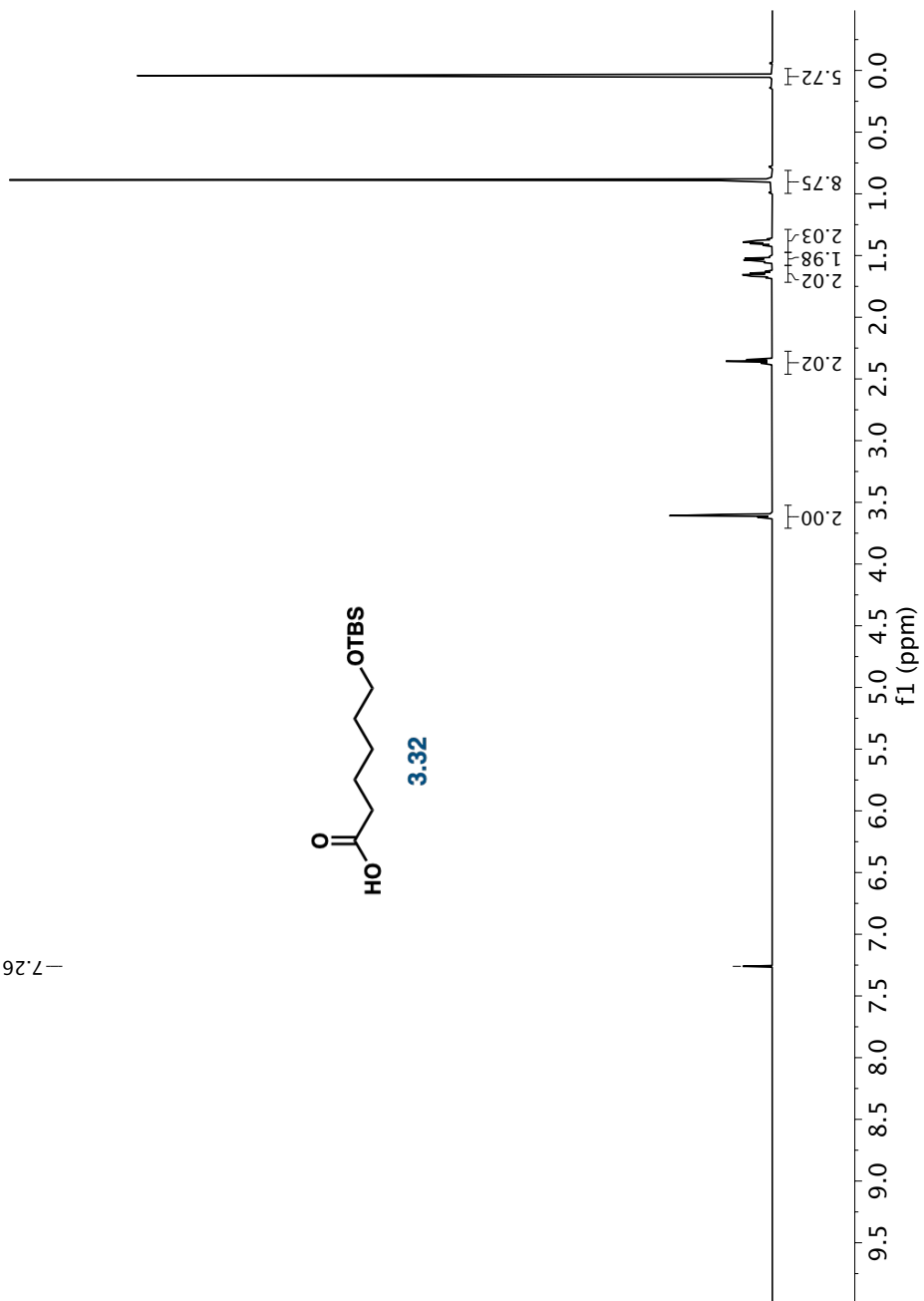


600.13
CDCl₃

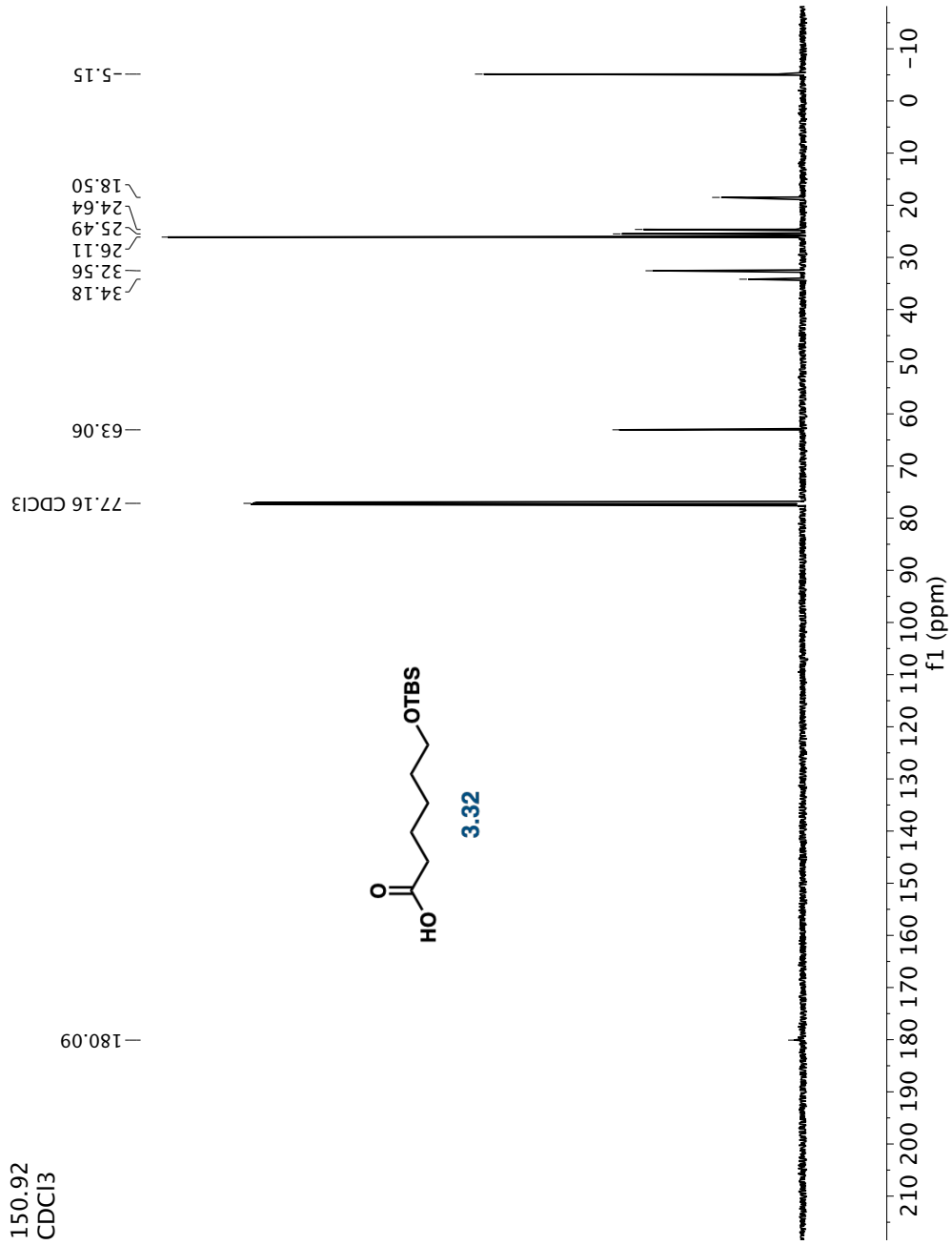
-7.26 CDCl₃



3.32

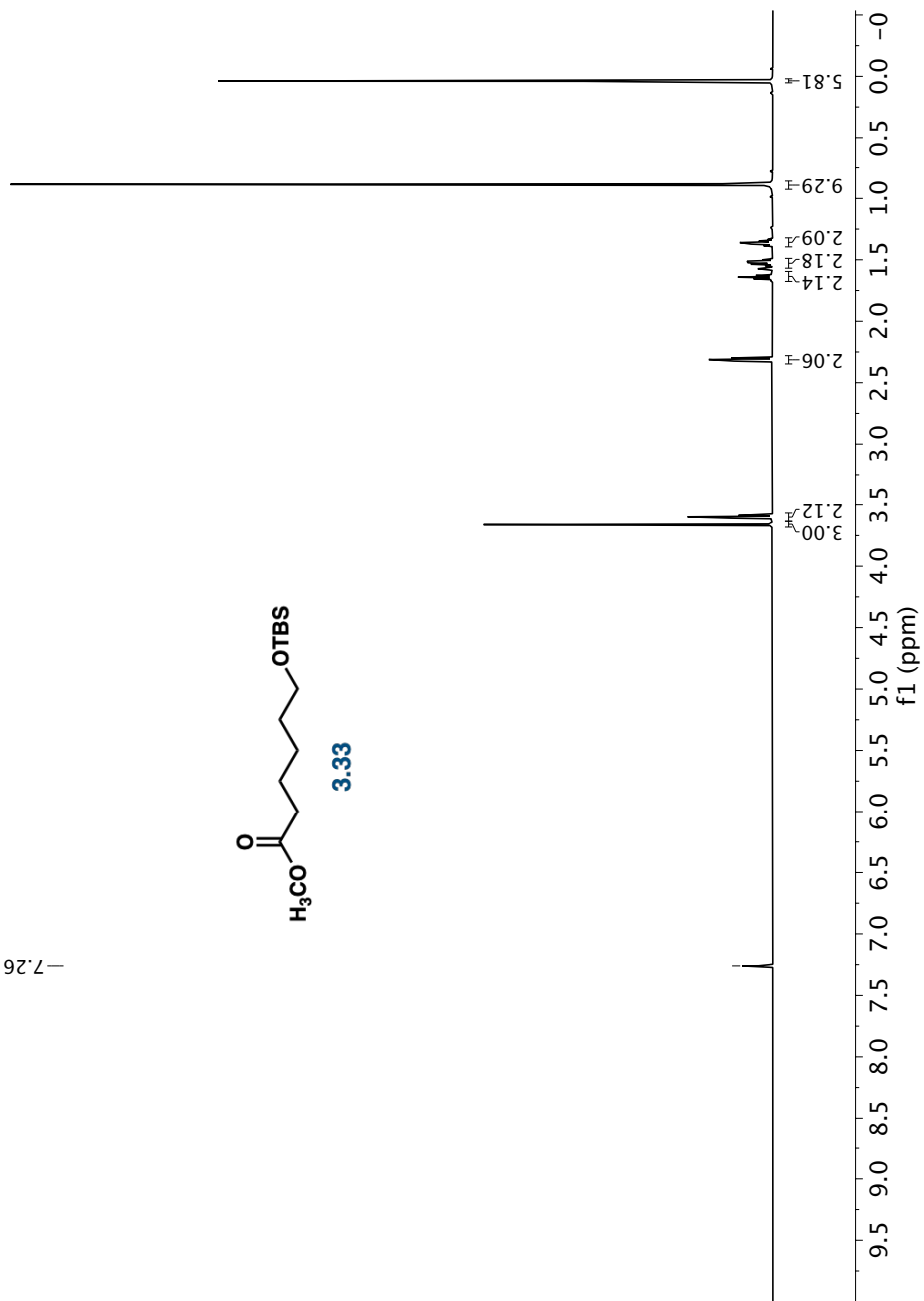


150.92
CDCl₃



600.32
CDCl₃

-7.26 CDCl₃



150.97
CDCl₃

174.34

77.16 CDCl₃

63.10

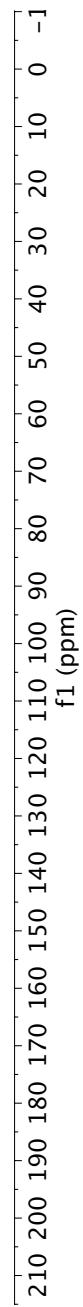
51.58

34.26
32.61
26.11
25.59
24.94
18.49

-5.15

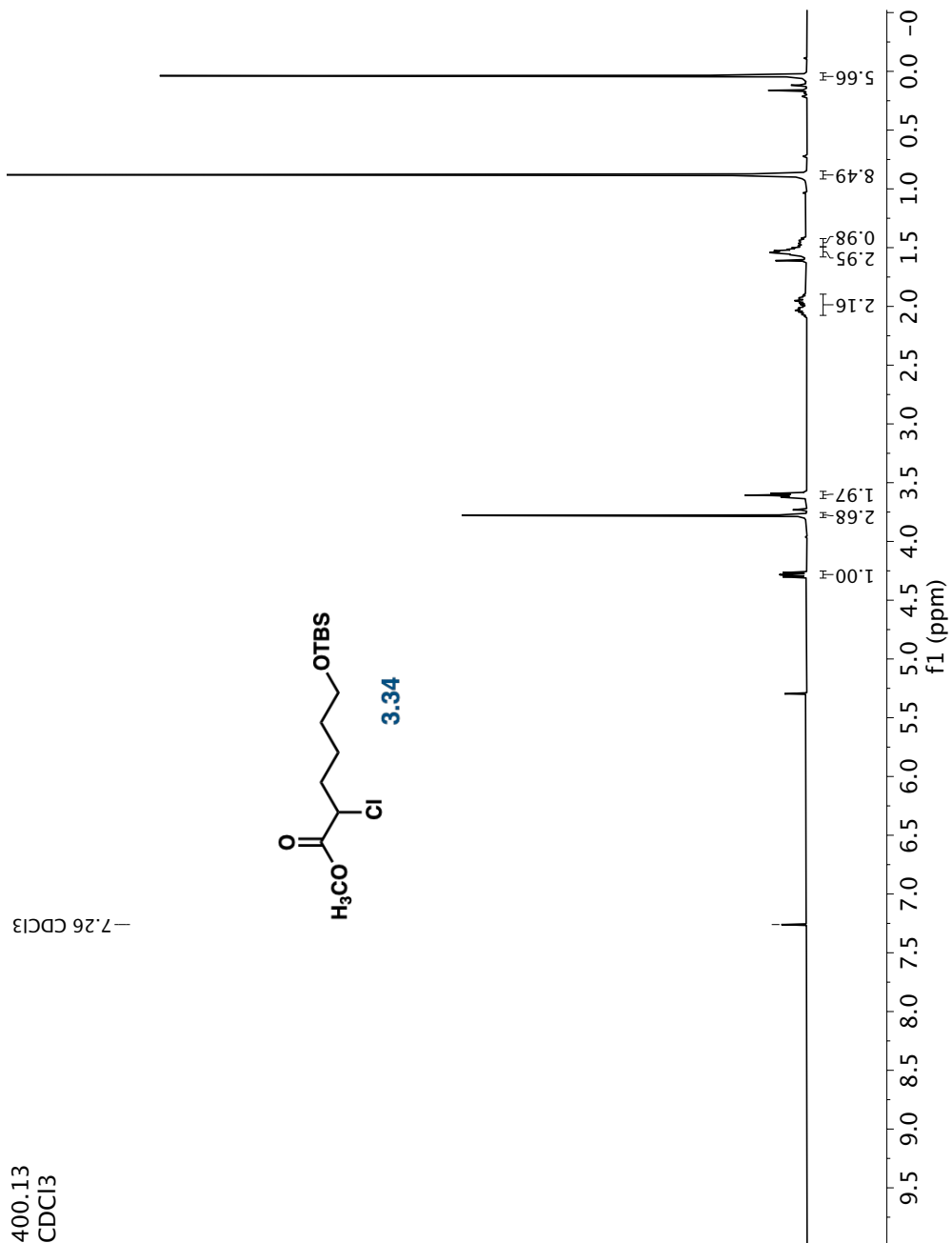
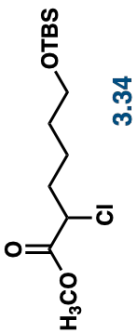


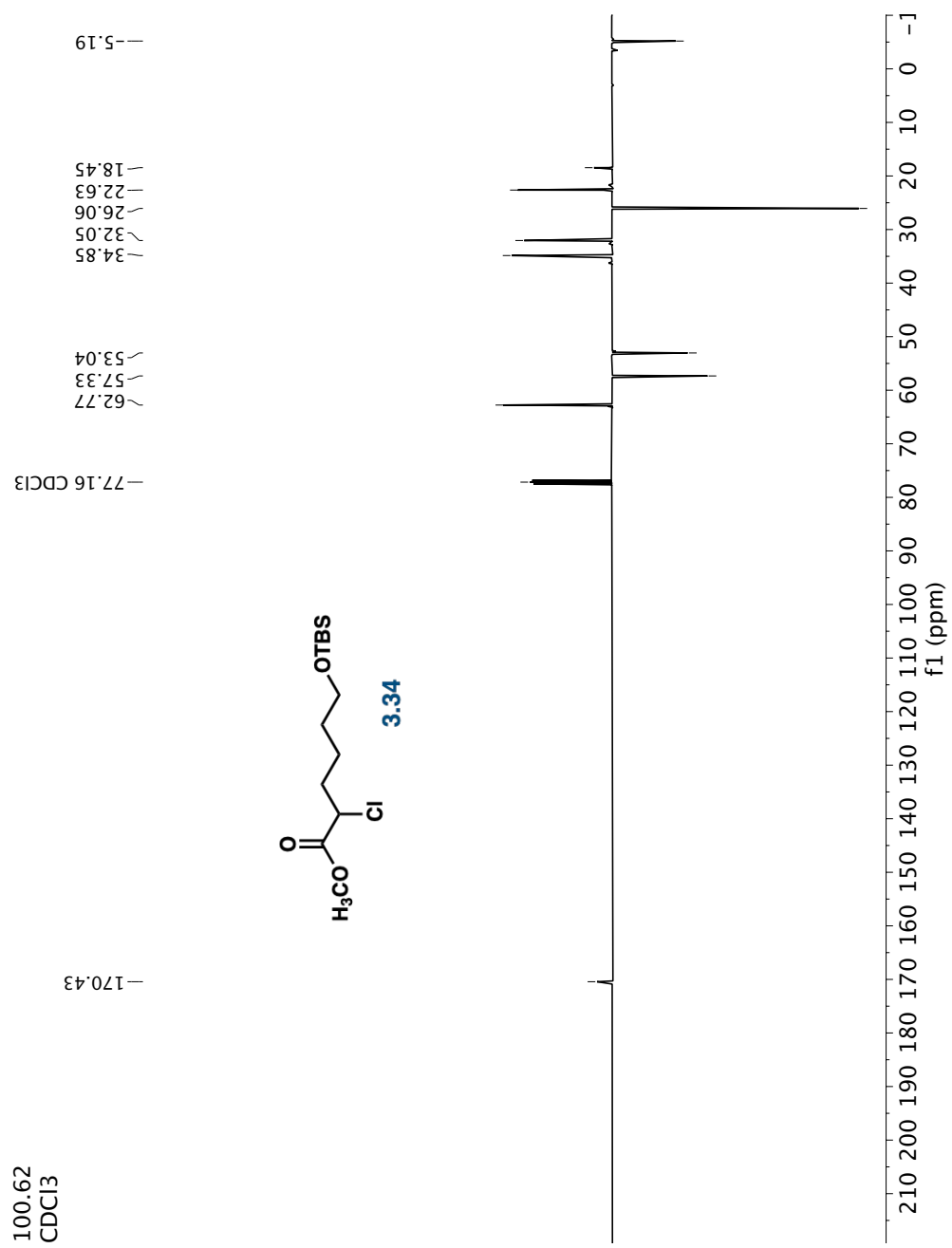
3.33



400.13
CDCl3

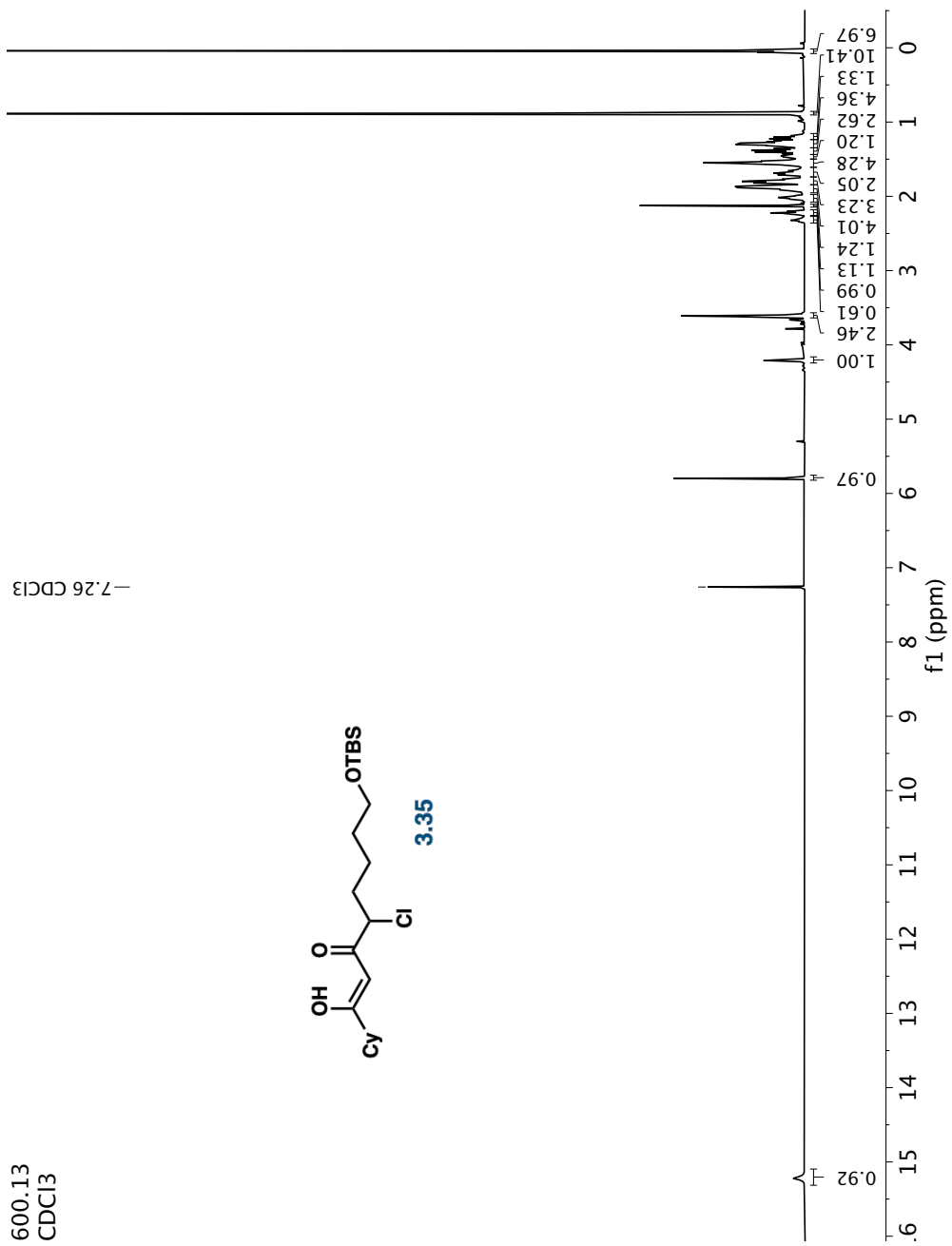
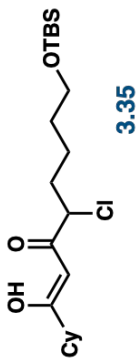
-7.26 CDCl3

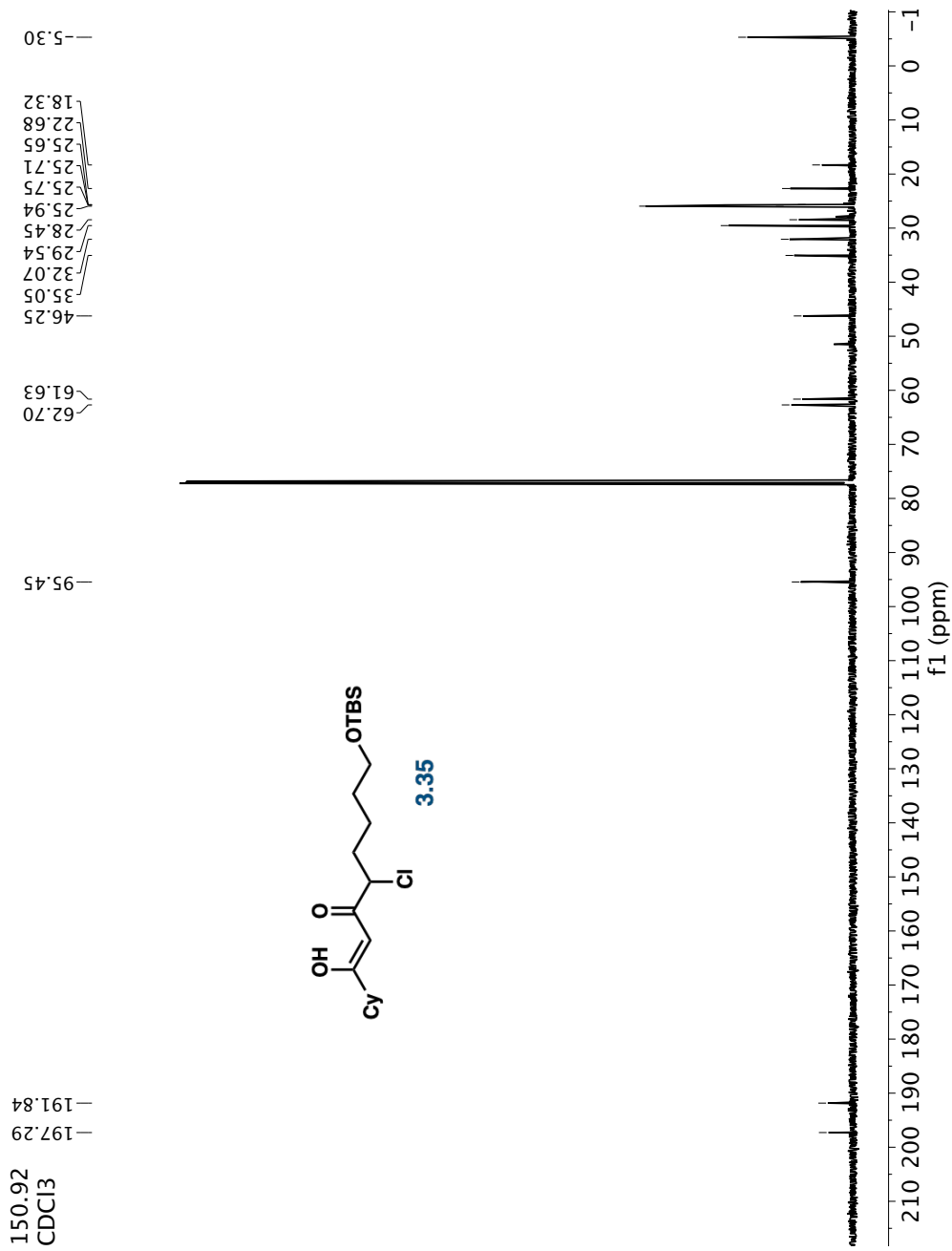


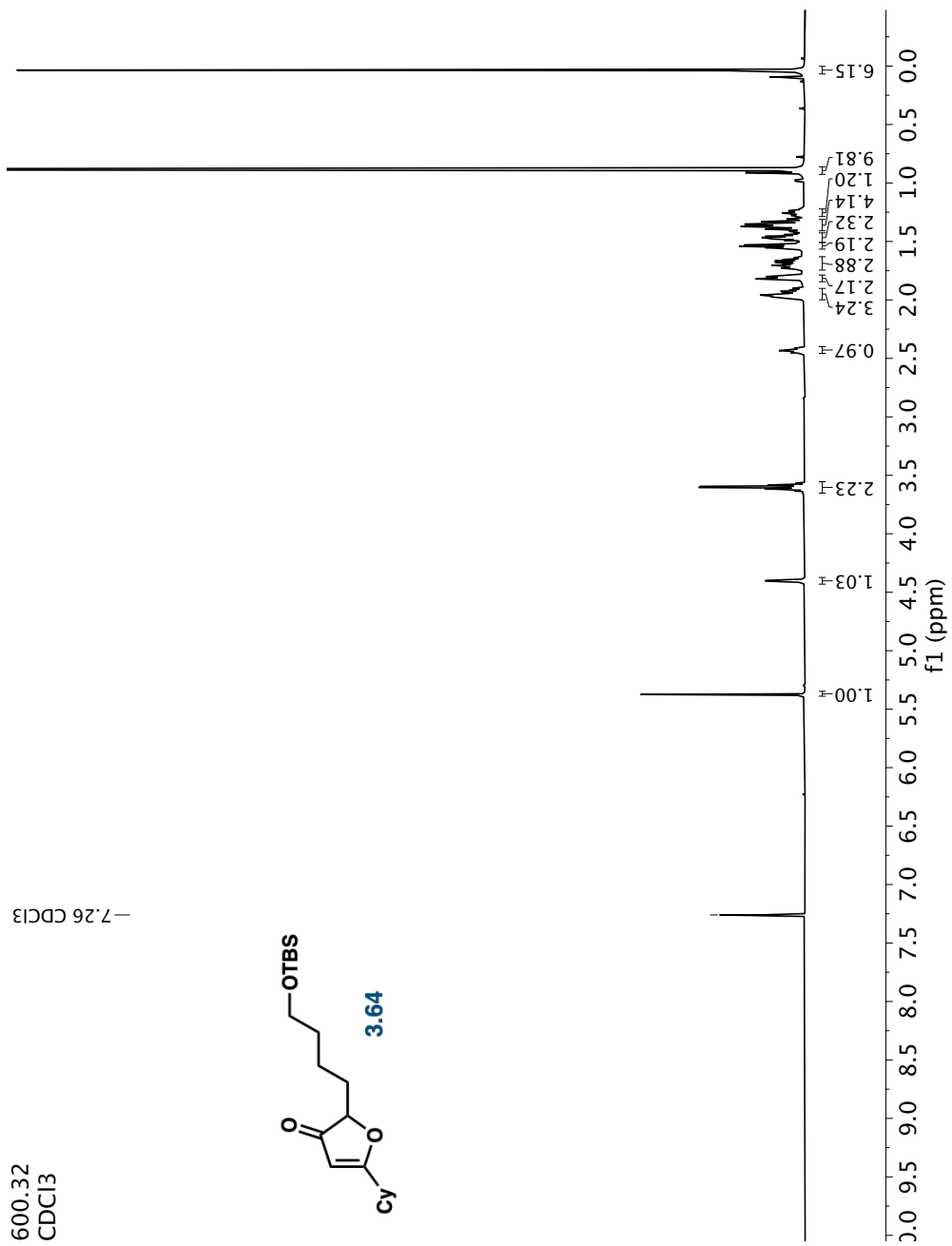


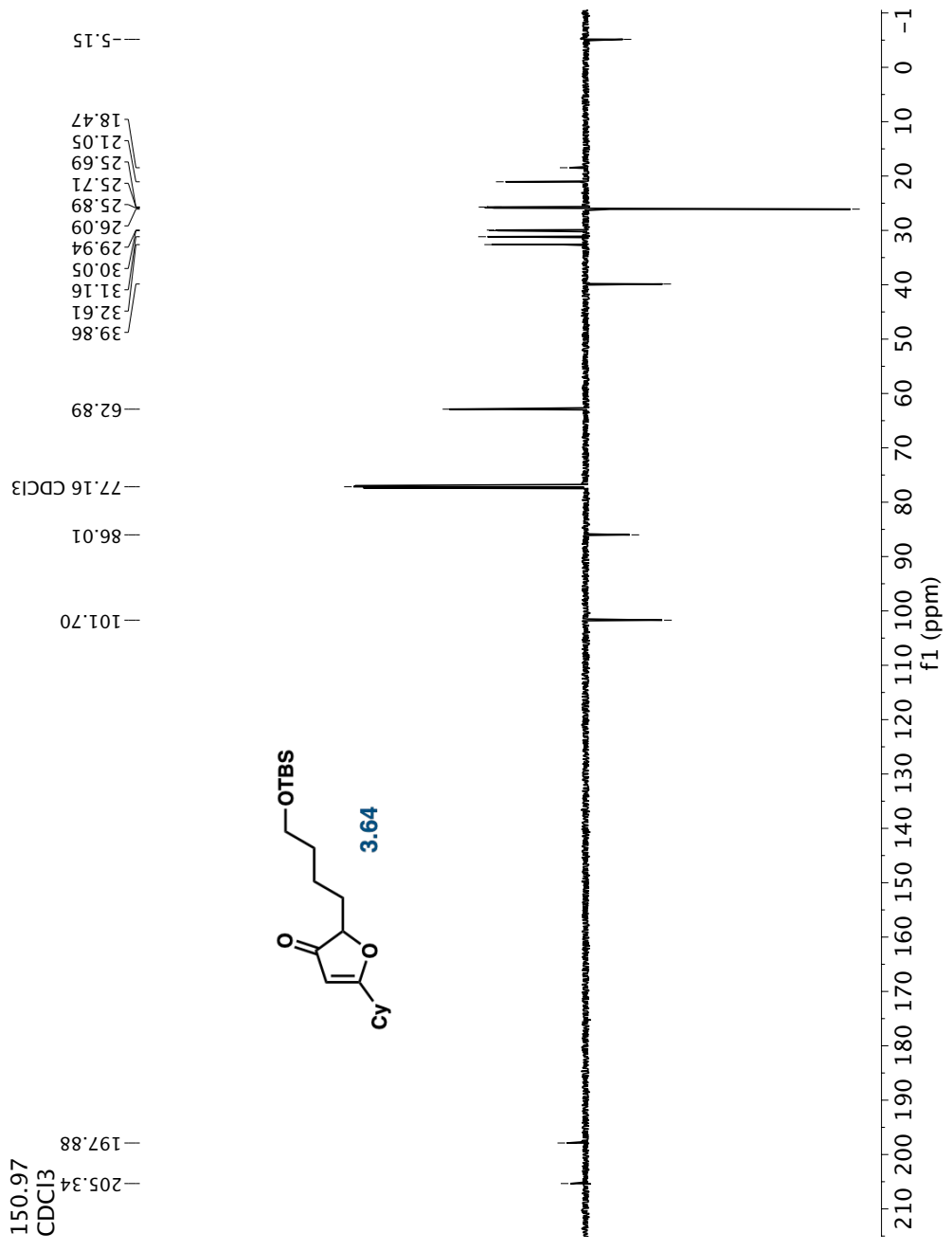
600.13
CDCl3

-7.26 CDCl3



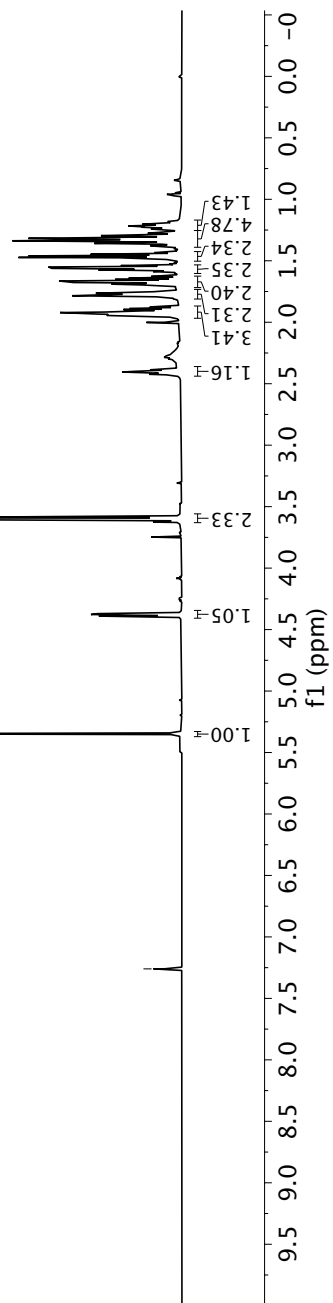
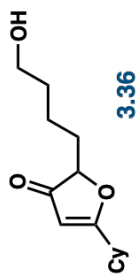


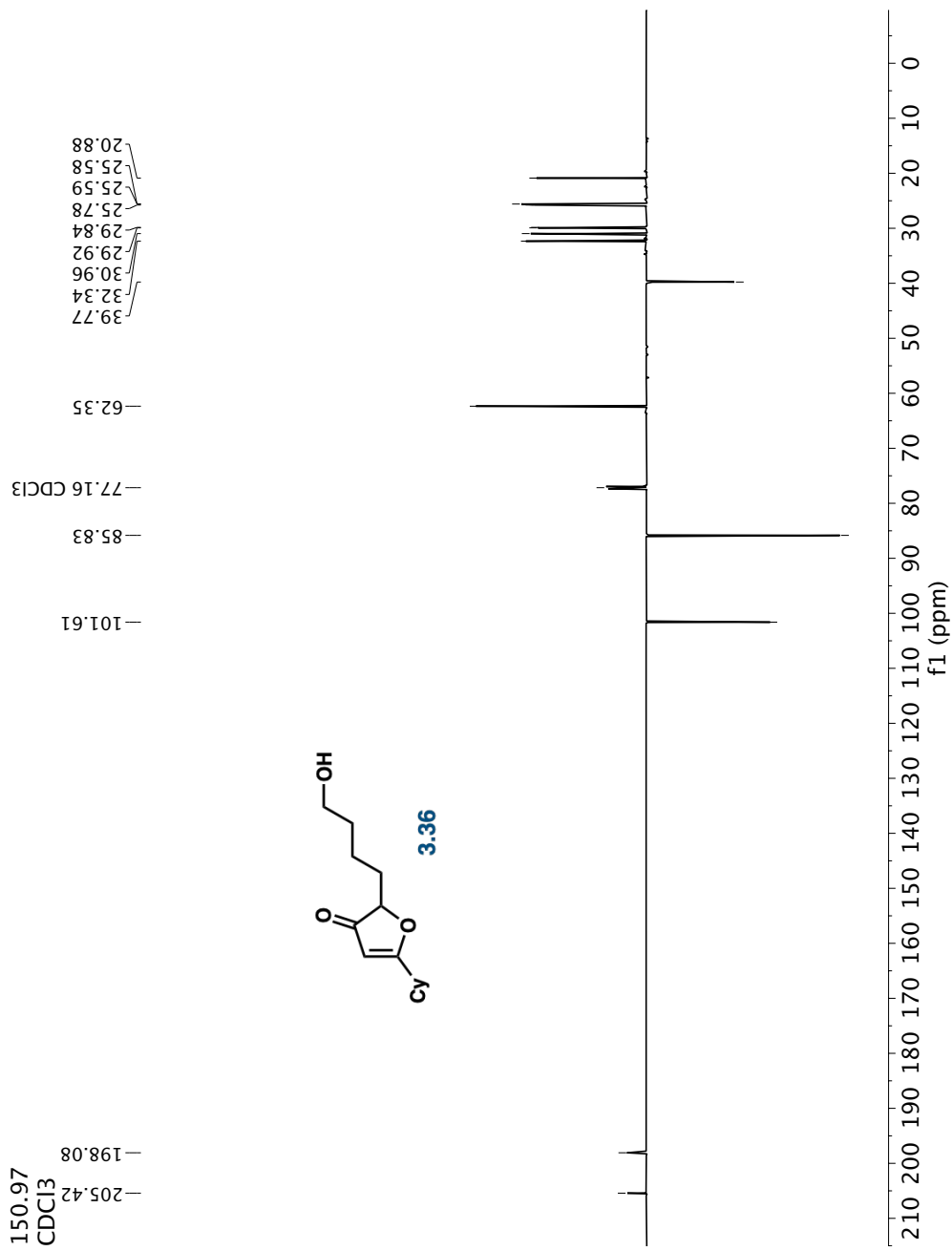




600.32
CDCl₃

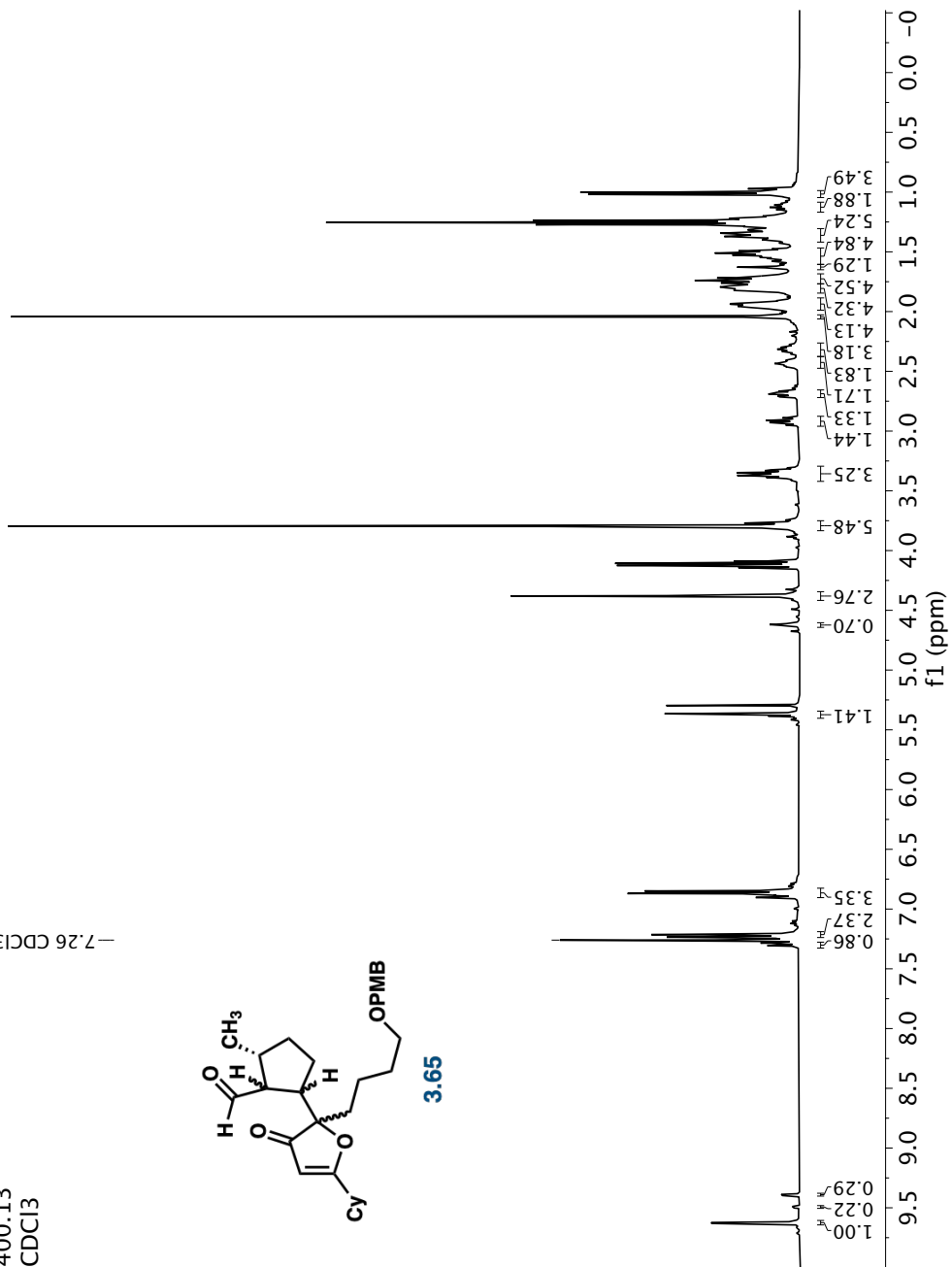
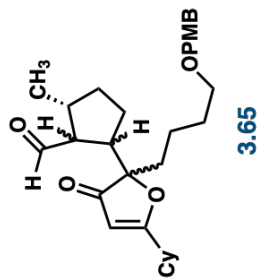
-7.26 CDCl₃

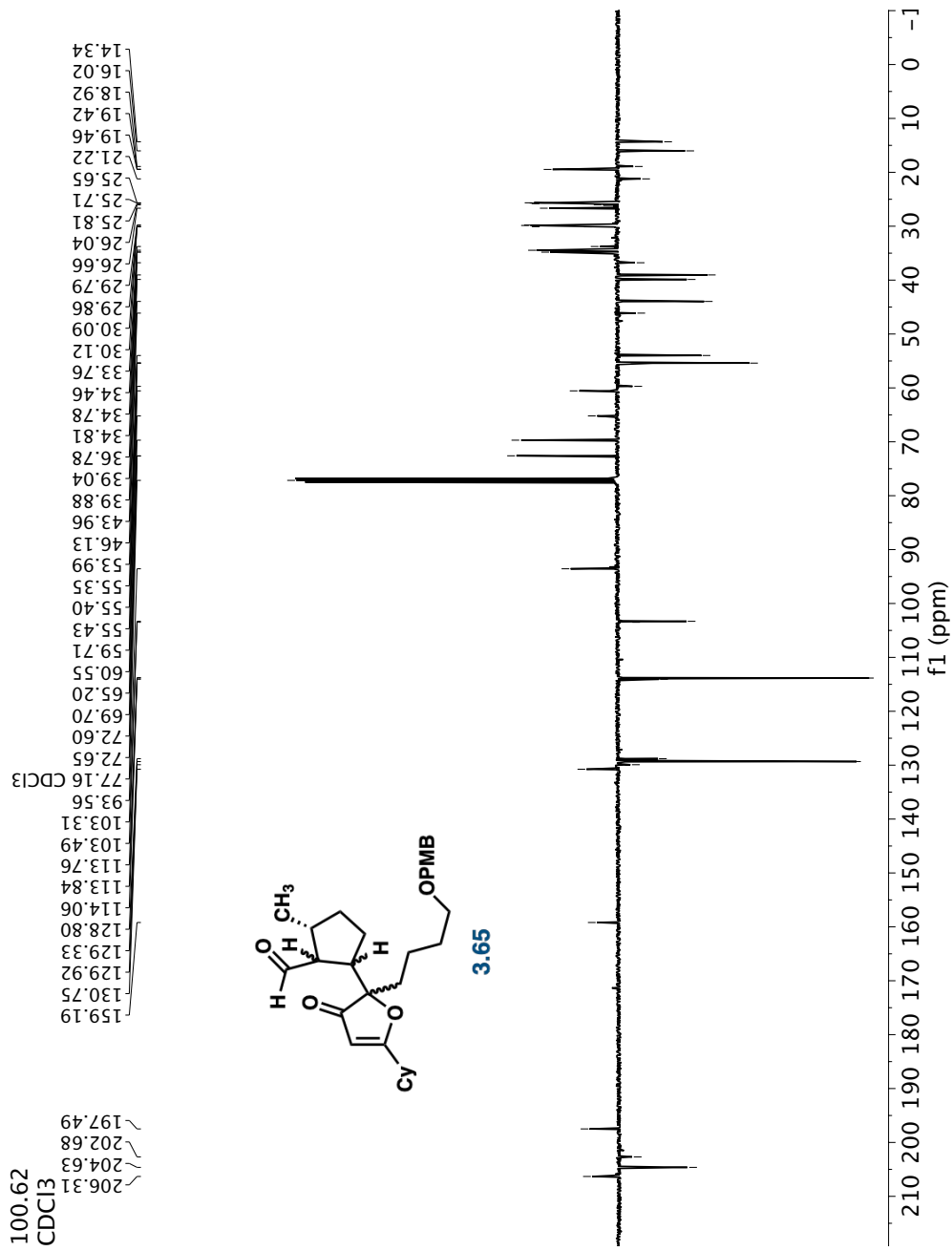




400.13
CDCl₃

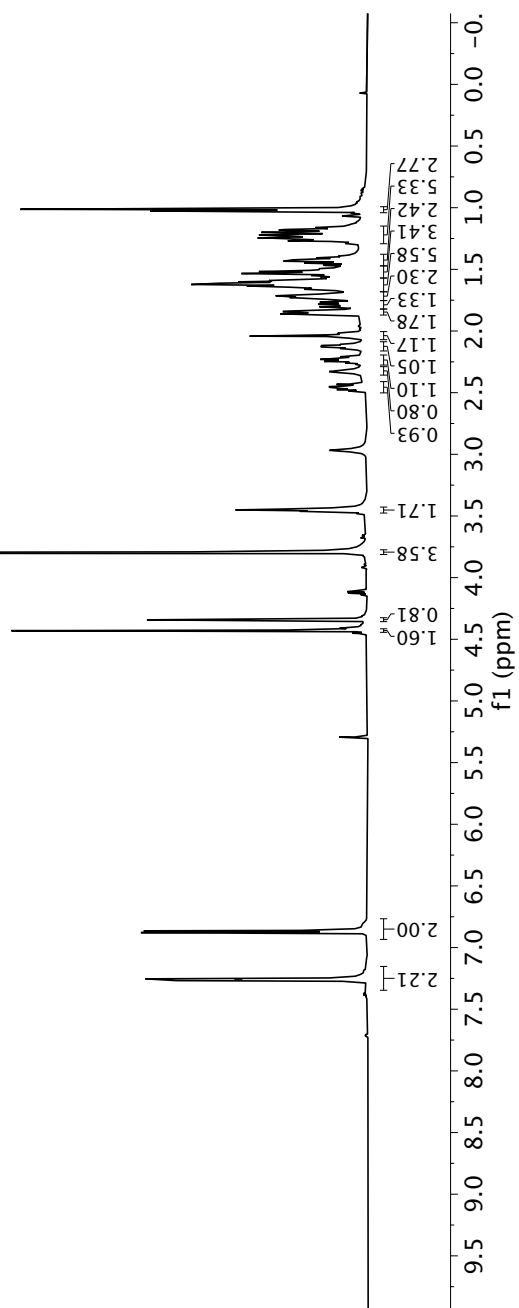
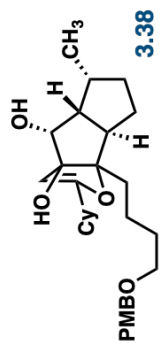
-7.26 CDCl₃





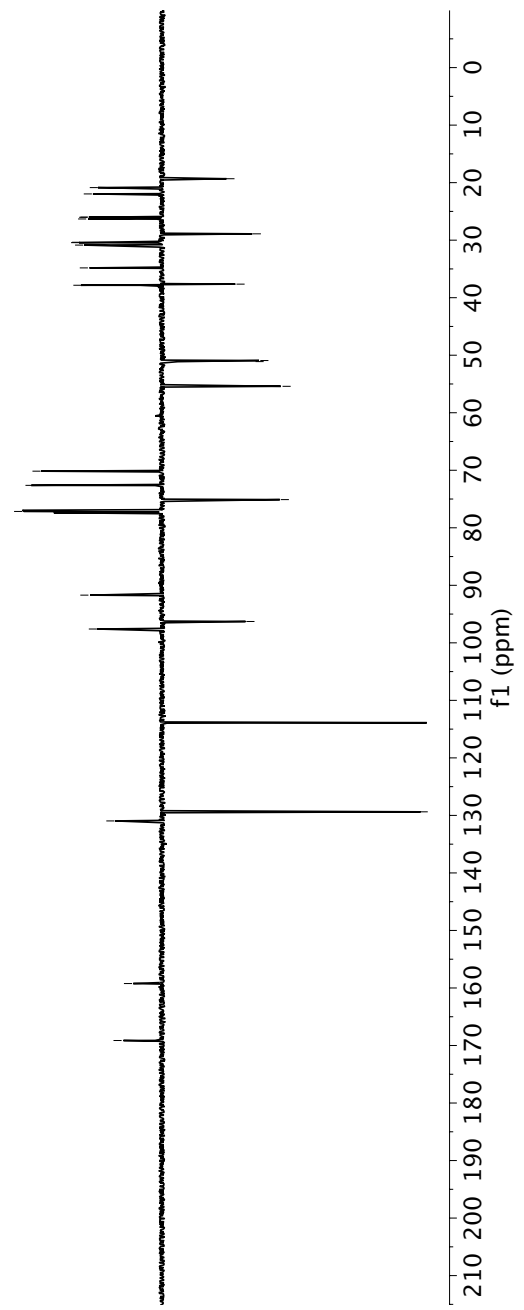
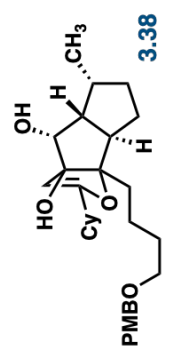
600.32
CDCl₃

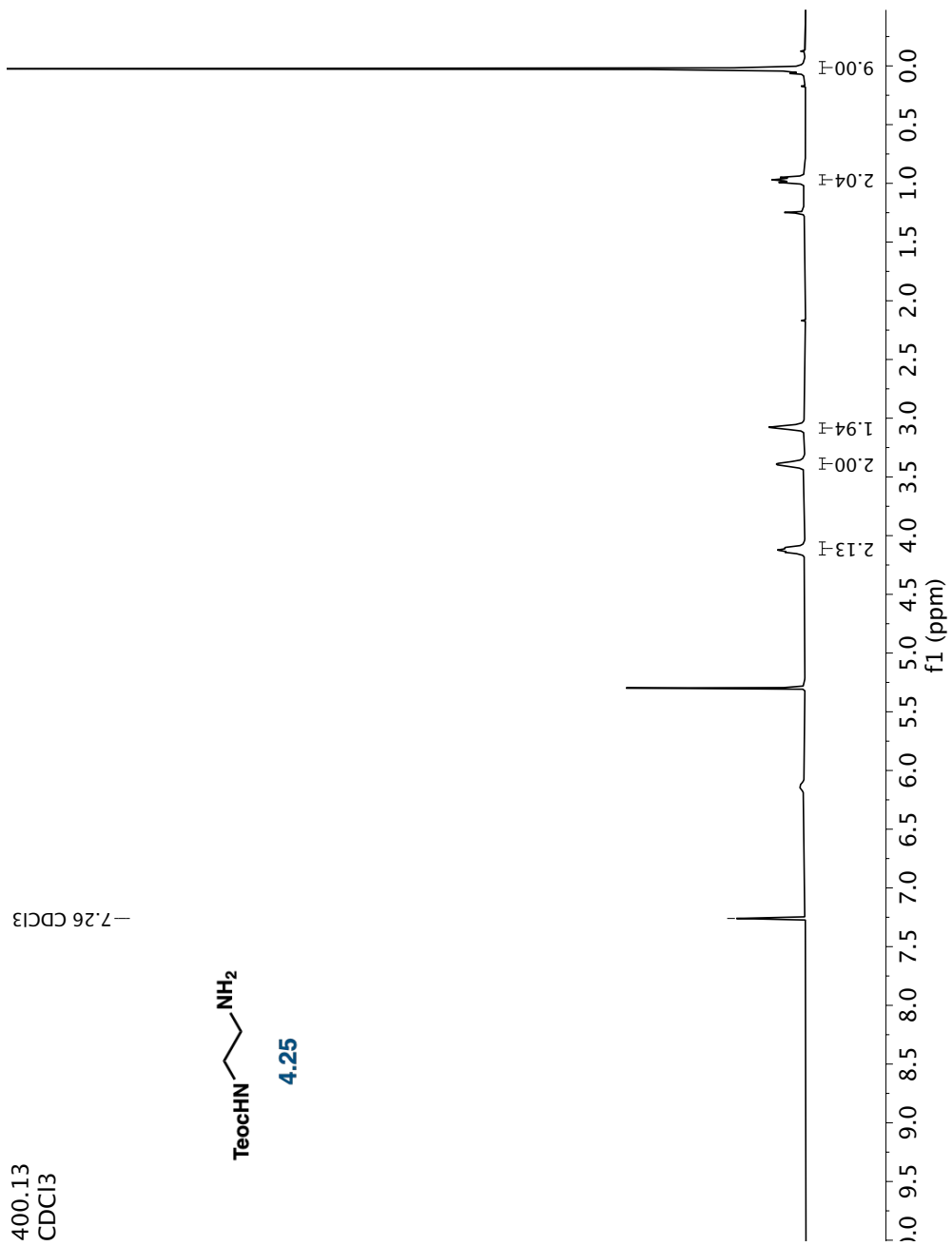
-7.26 CDCl₃



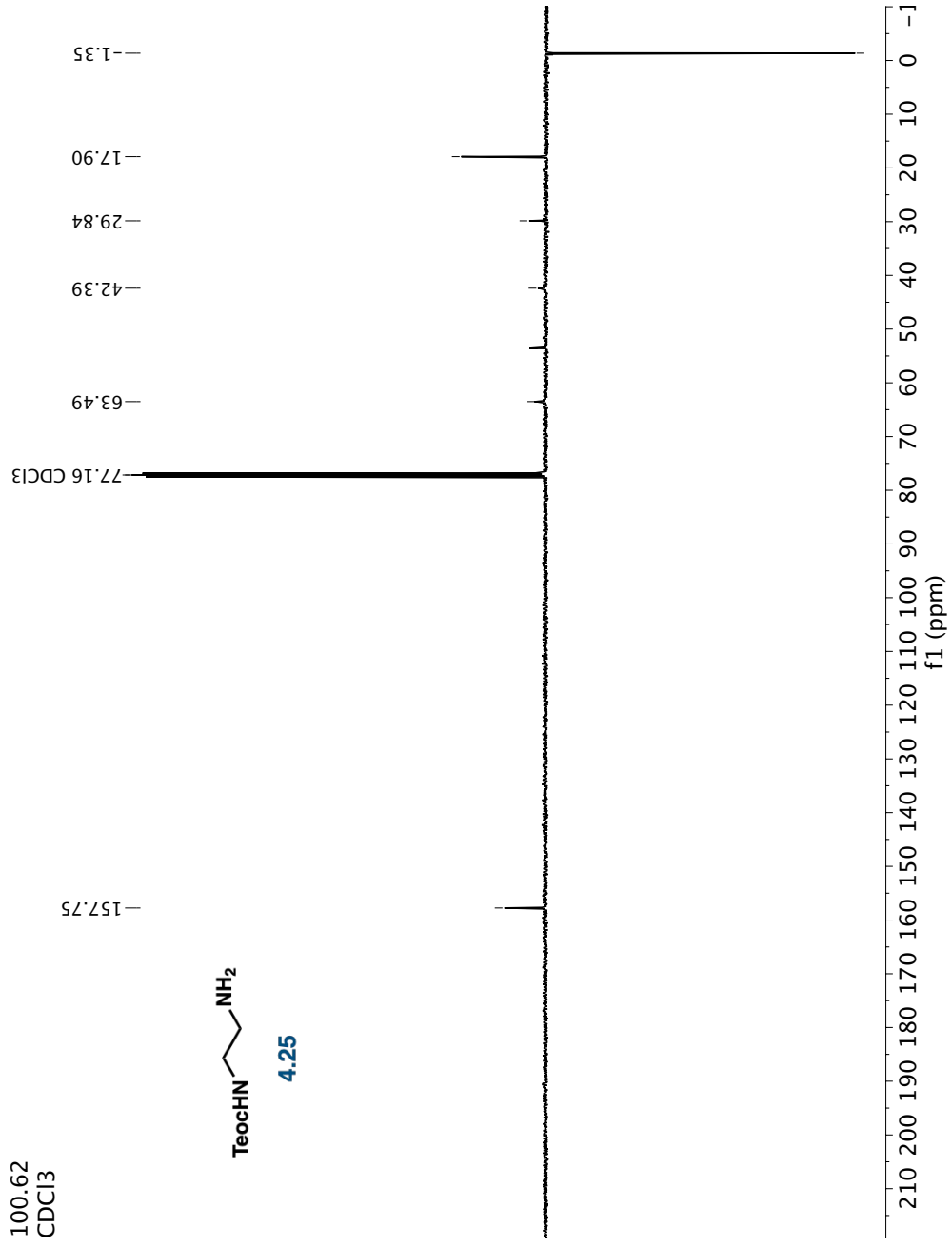
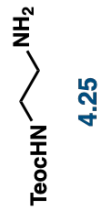
150.97
CDCl₃

77.16 CDCl₃
75.10
72.62
70.16
55.41
51.11
50.92
37.84
37.64
34.82
30.85
30.43
30.37
28.90
26.31
26.02
25.99
21.96
20.86
19.32



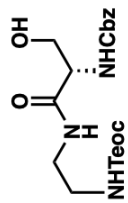


100.62
CDCl₃

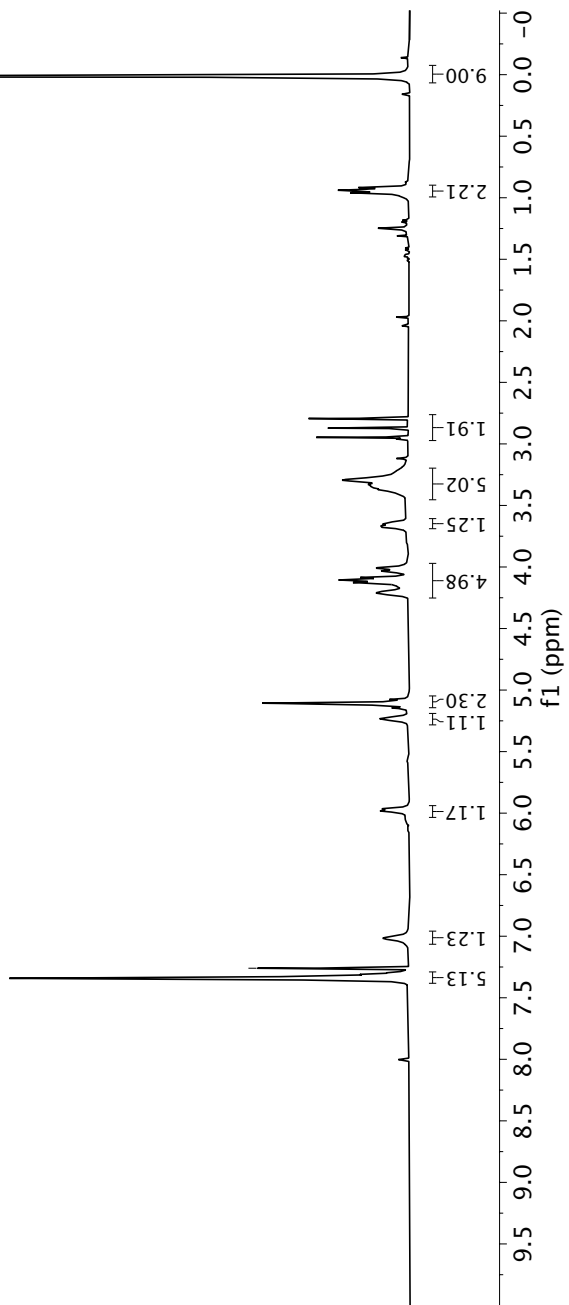


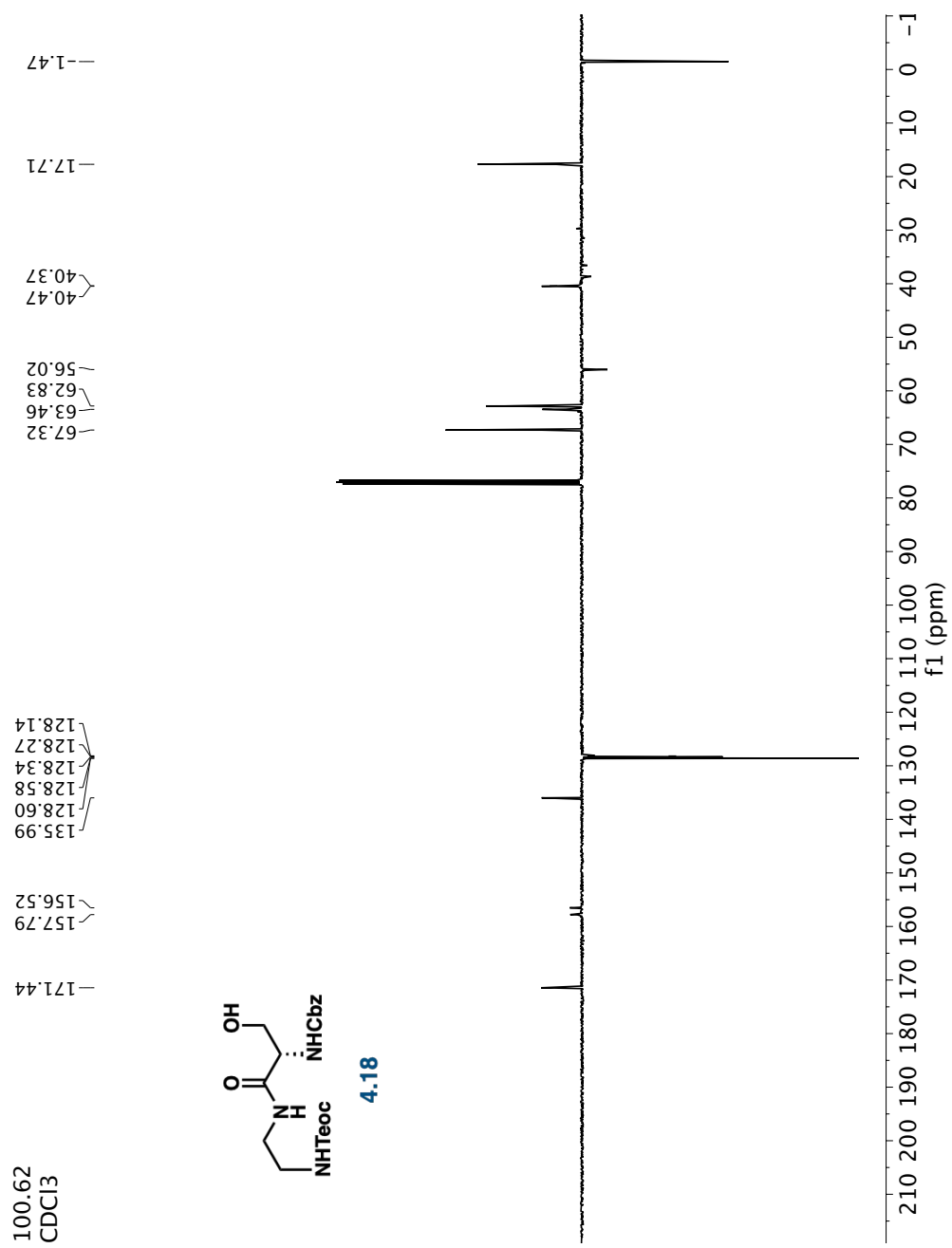
400.13
CDCl₃

-7.26 CDCl₃



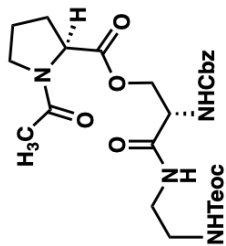
4.18



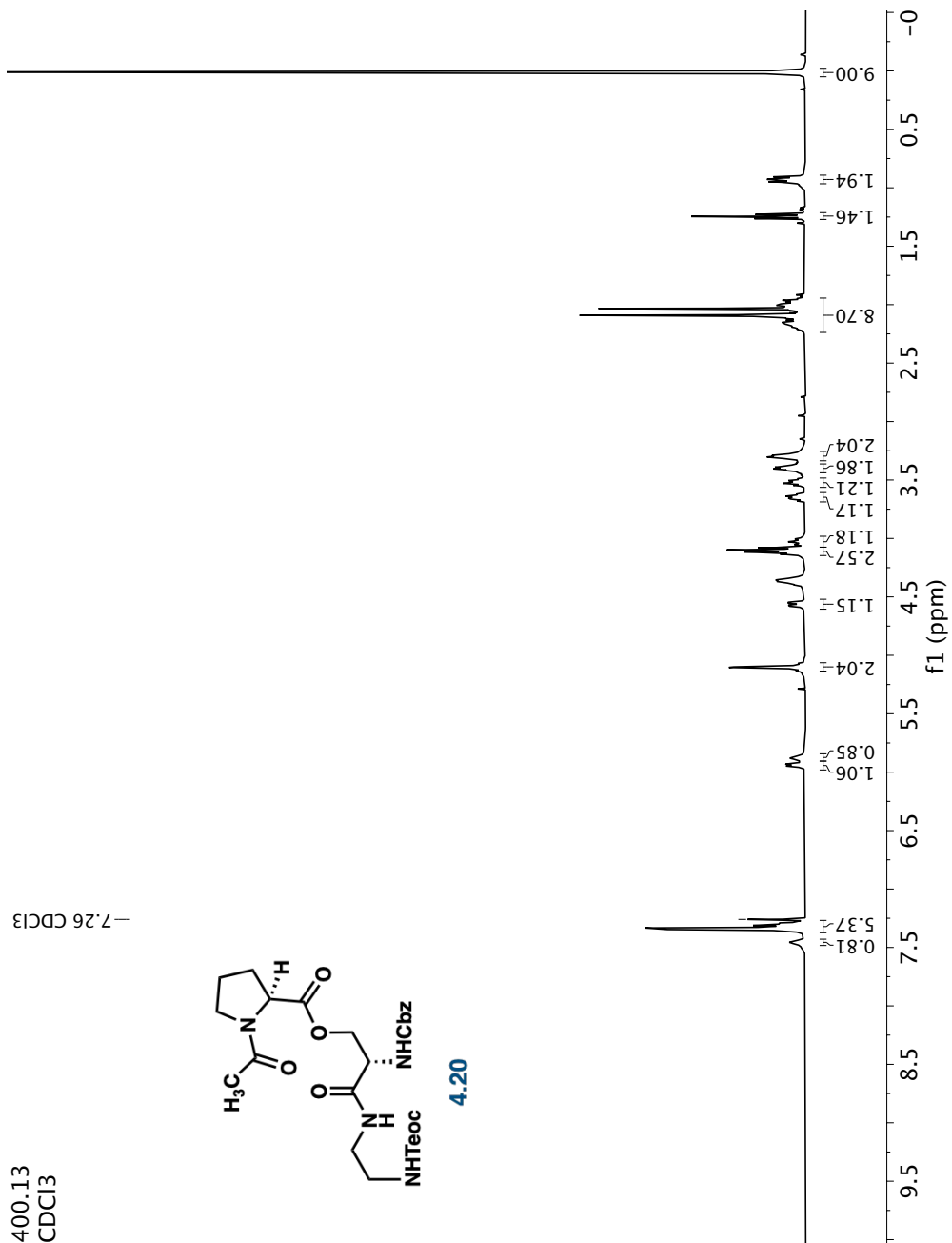


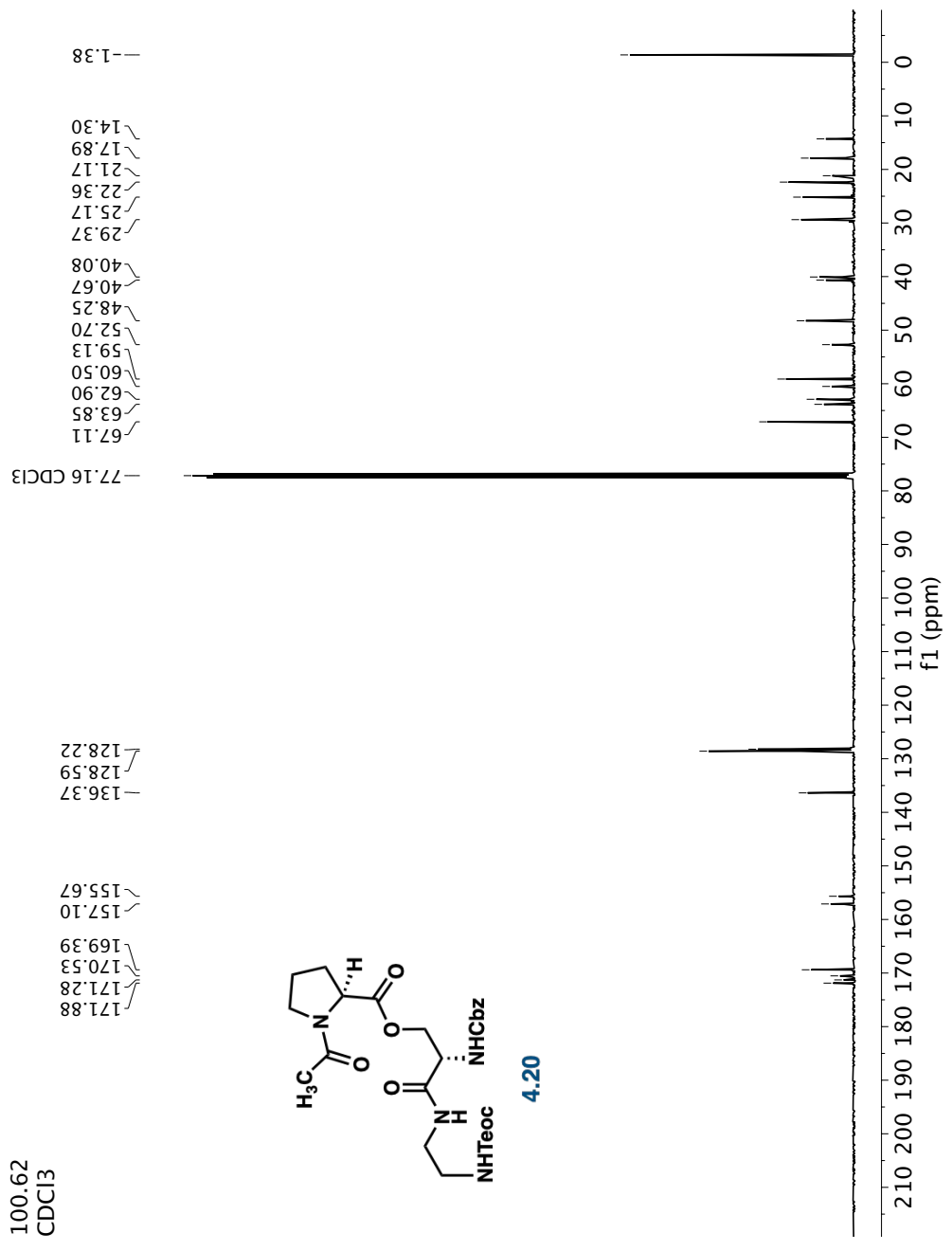
400.13
CDCl₃

-7.26 CDCl₃



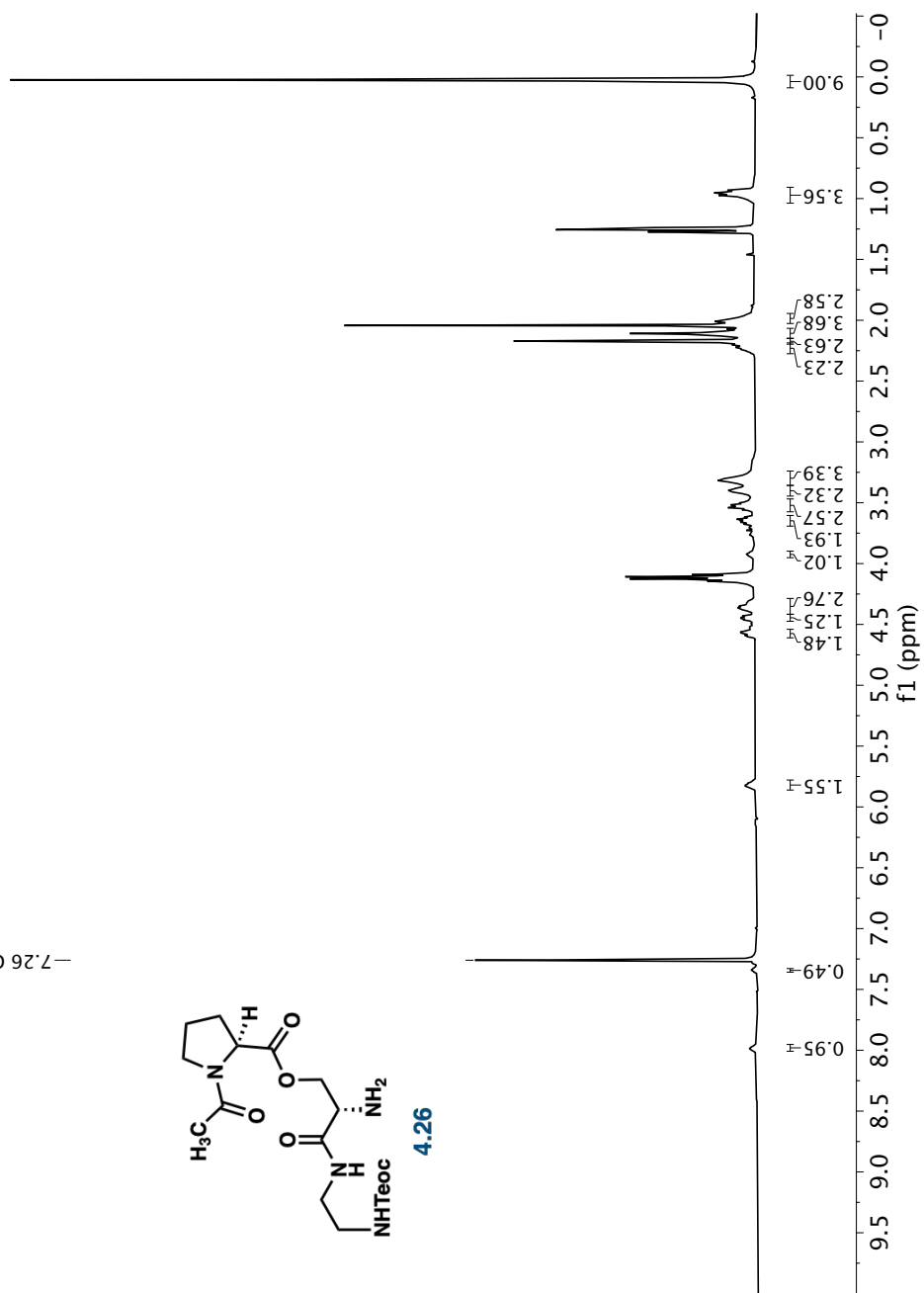
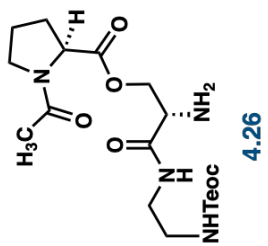
4.20

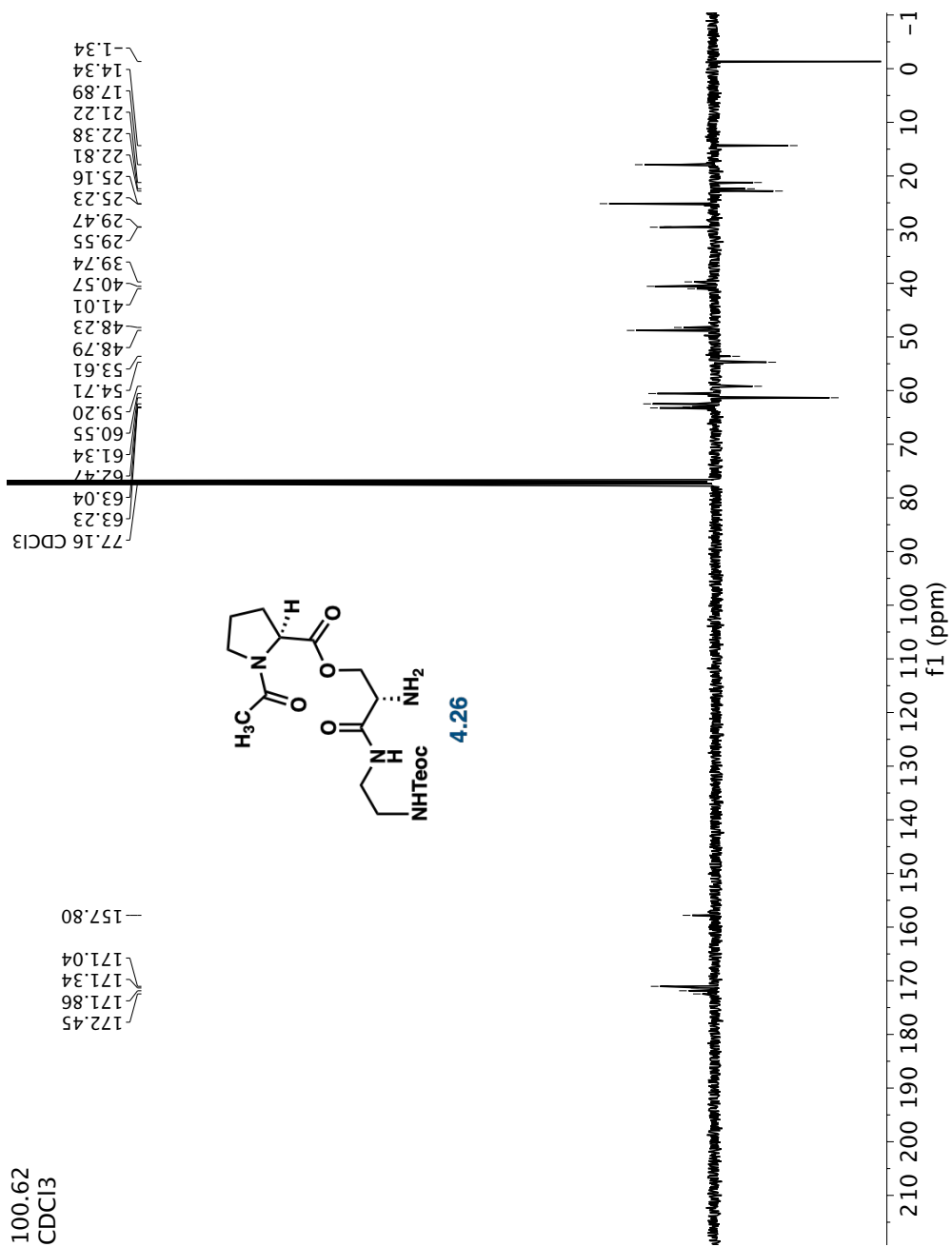




400.13
CDCl₃

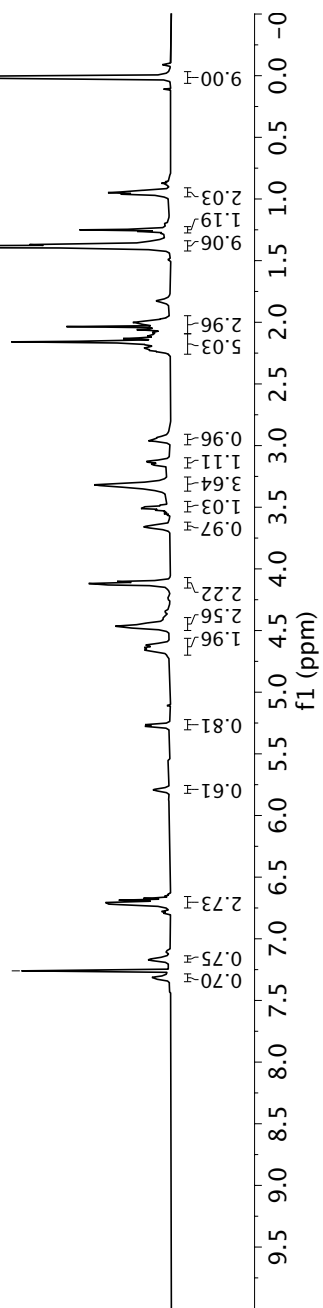
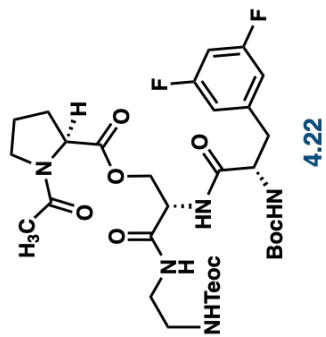
-7.26 CDCl₃



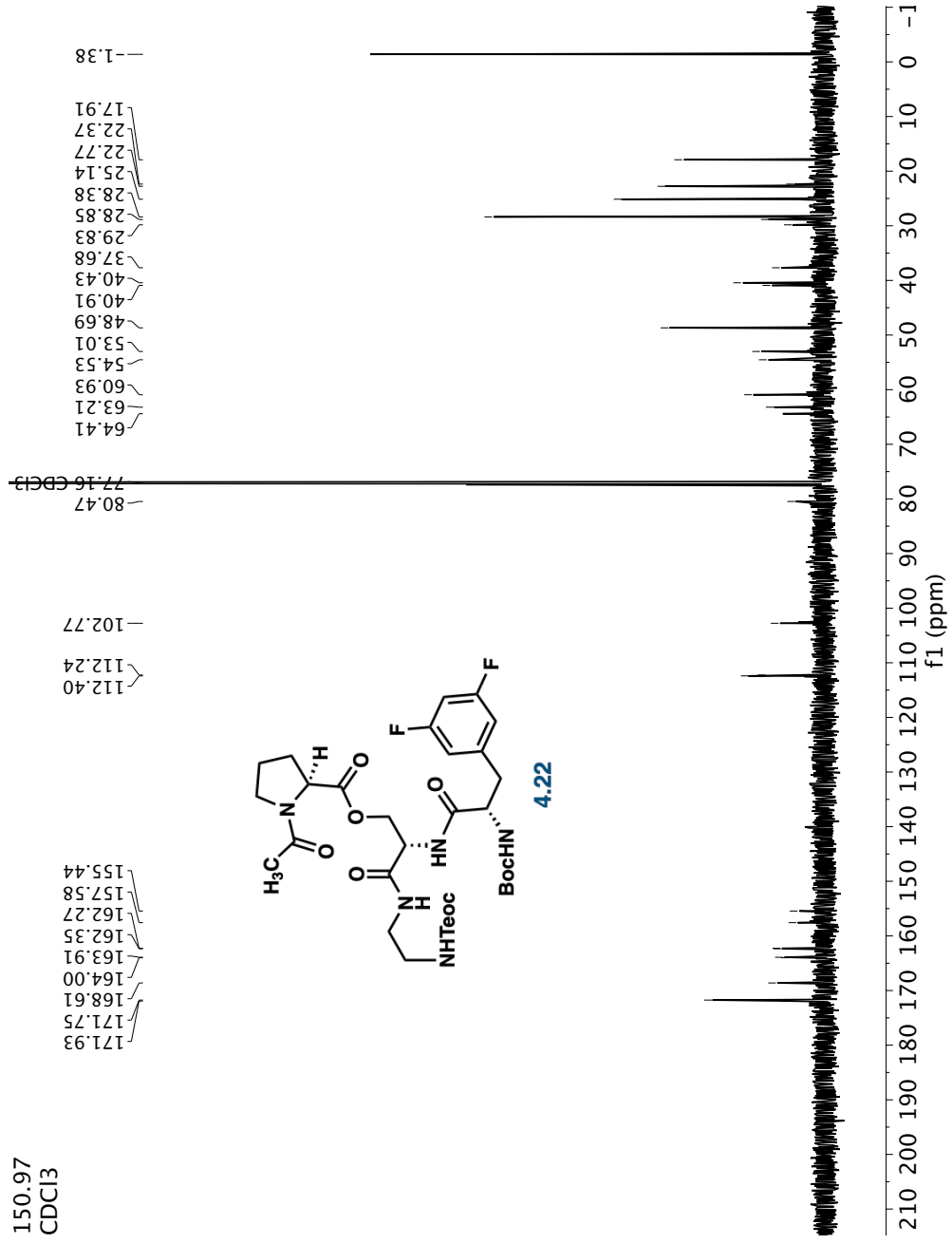


600.32
CDCl₃

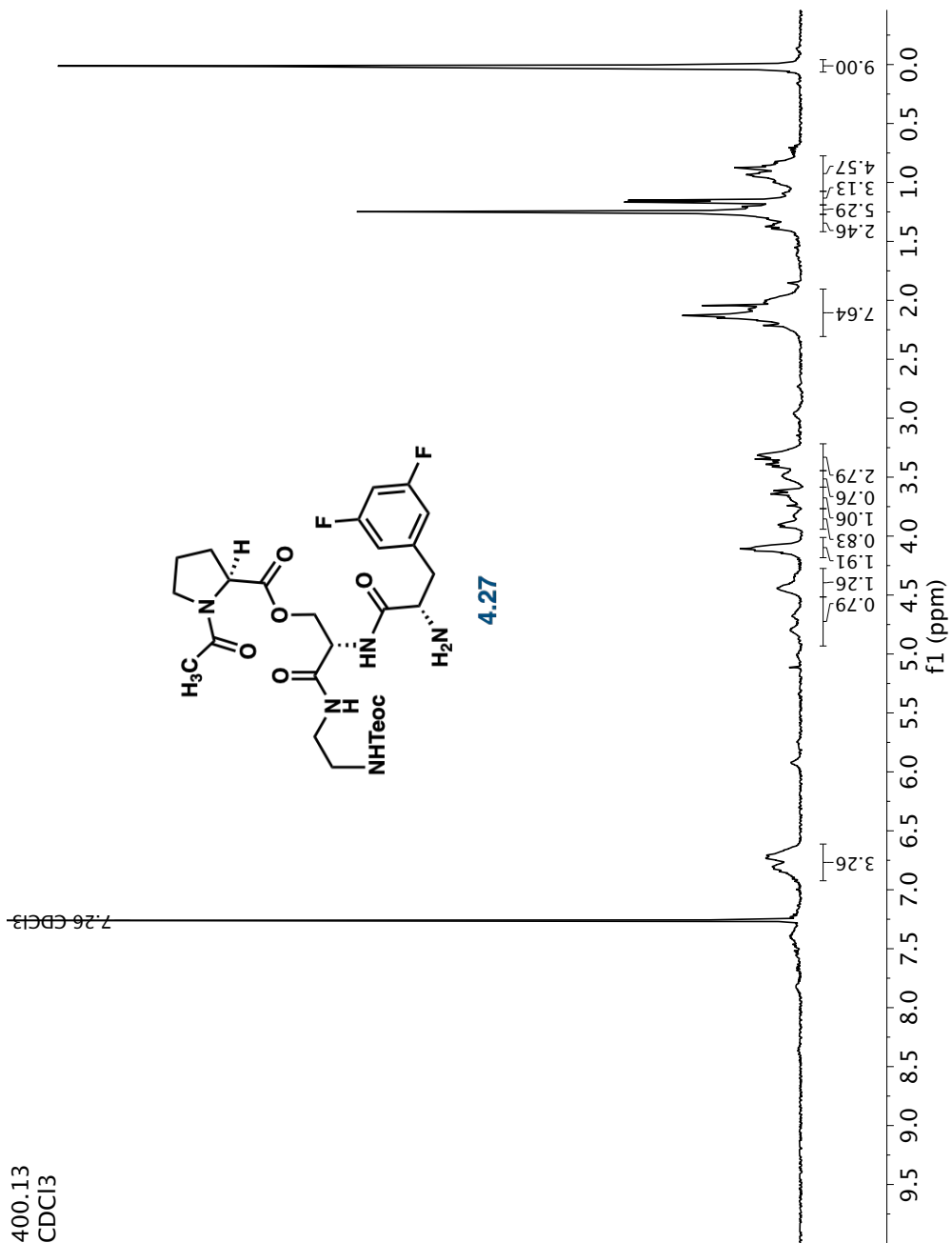
-7.26 CDCl₃

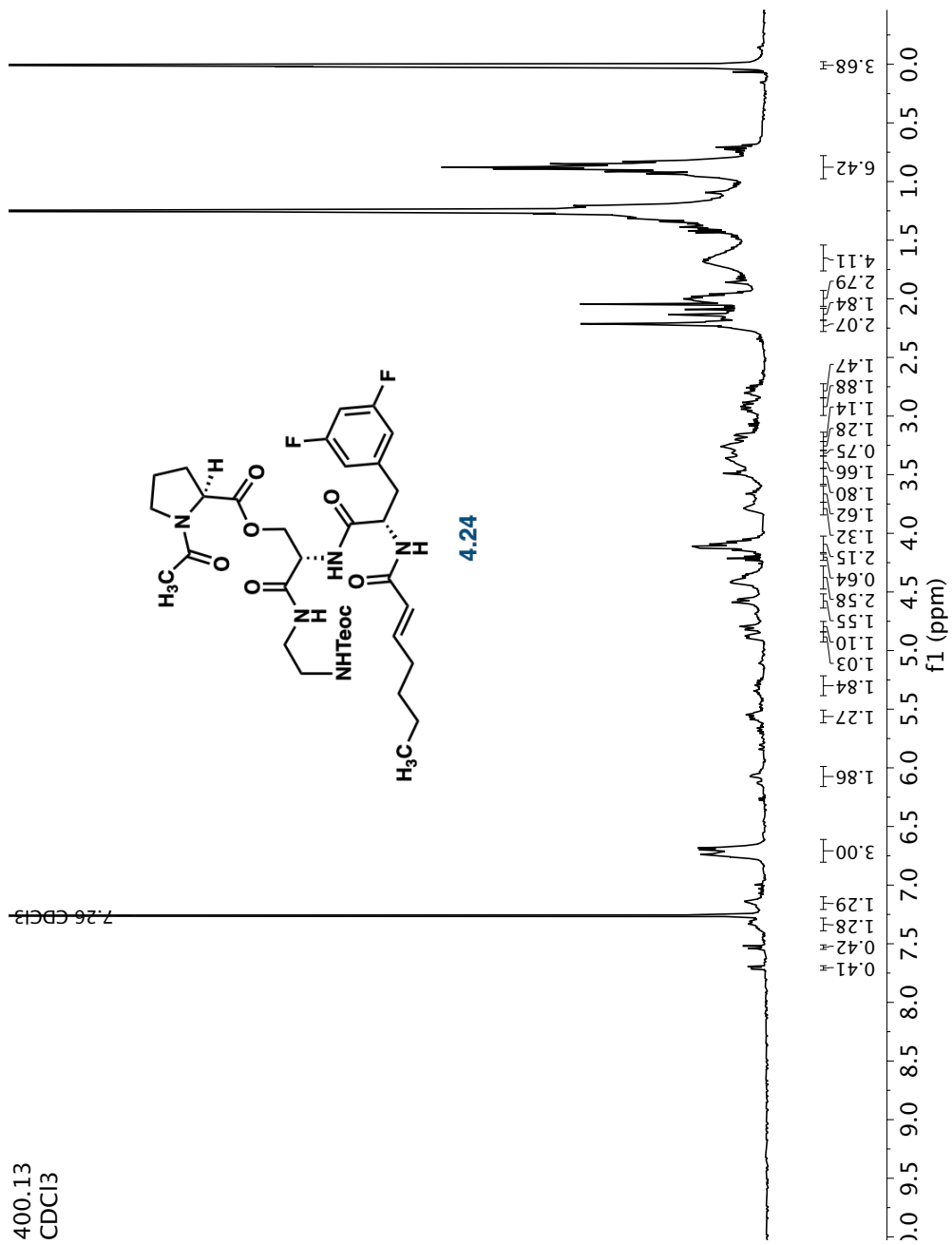


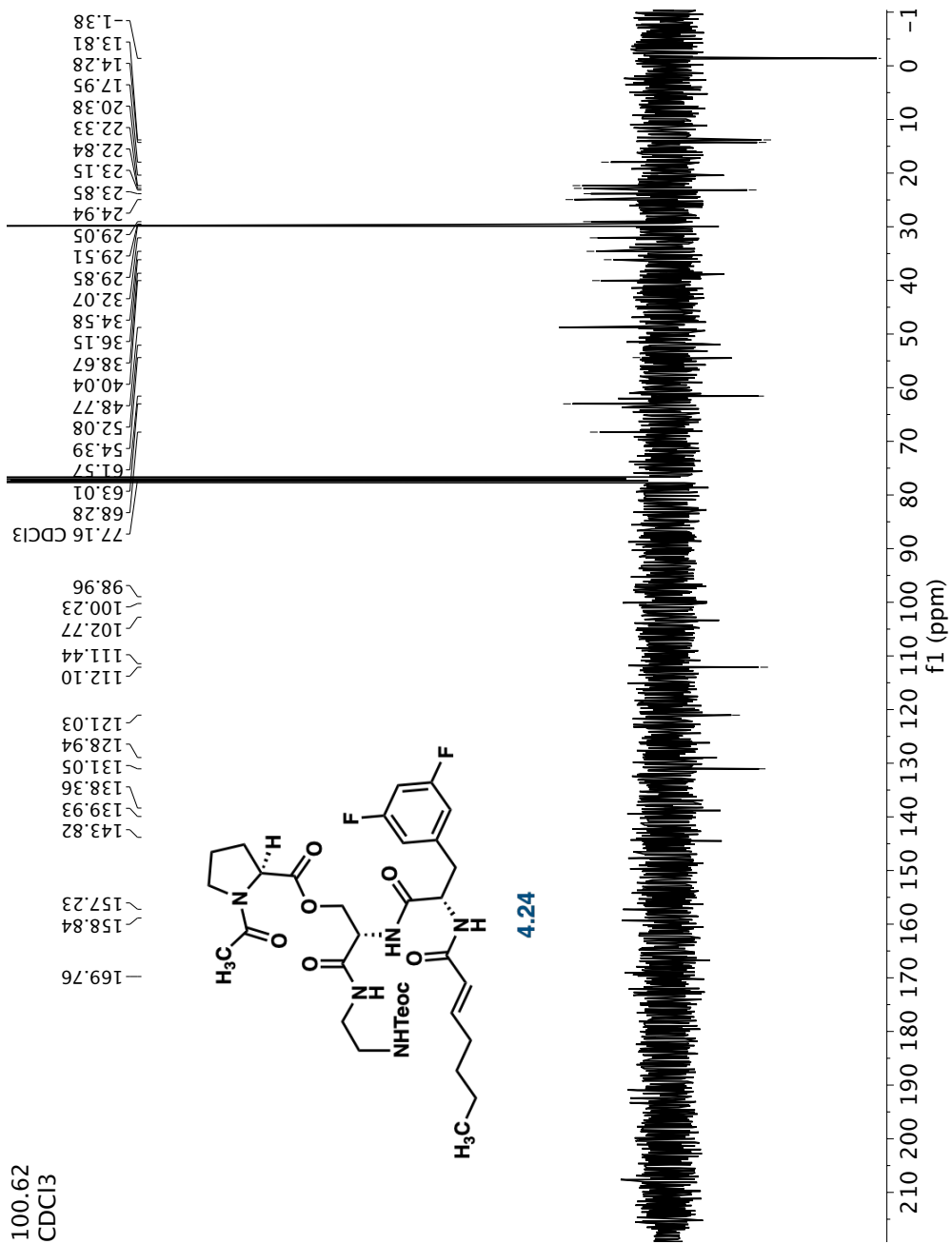
150.97
CDCl₃



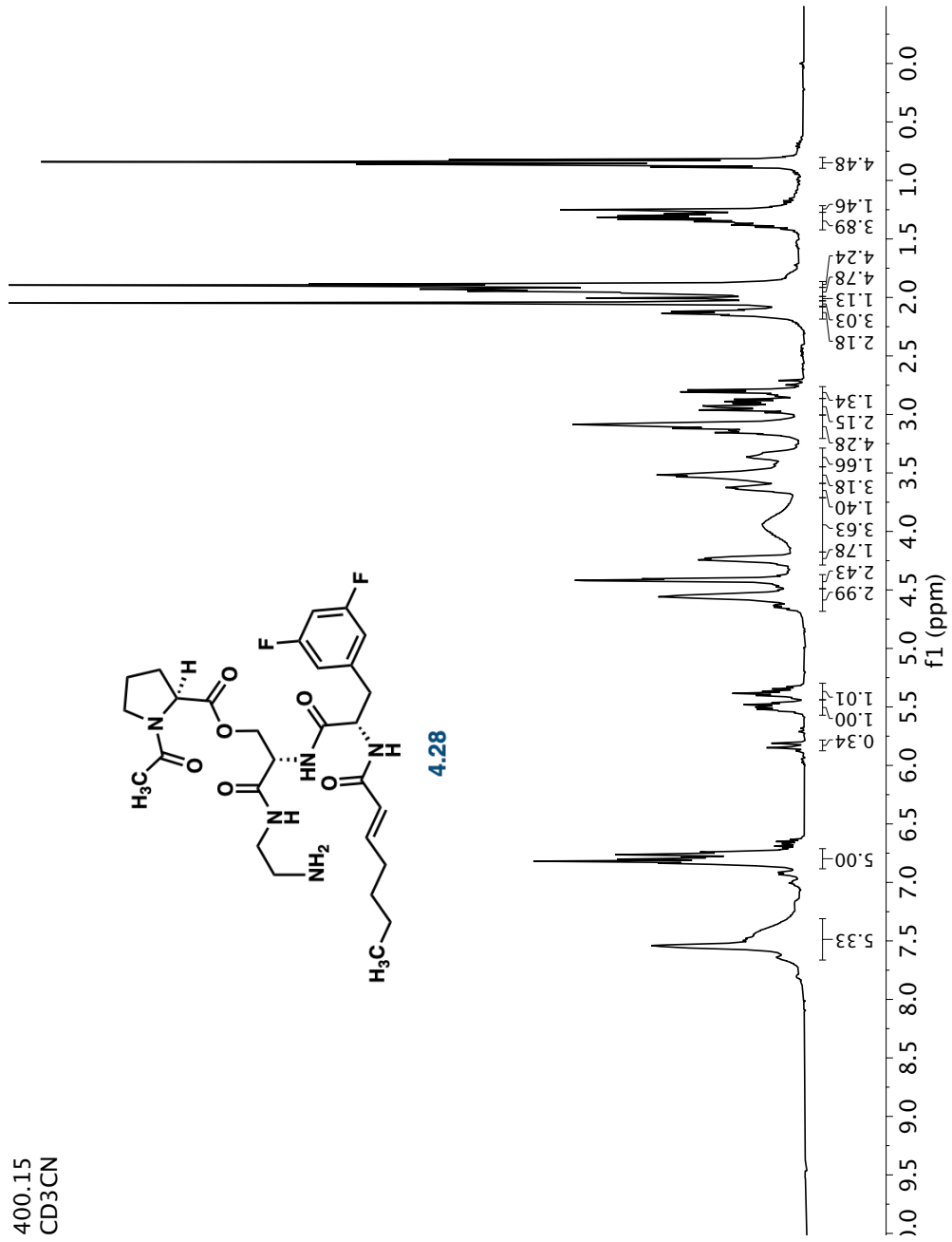
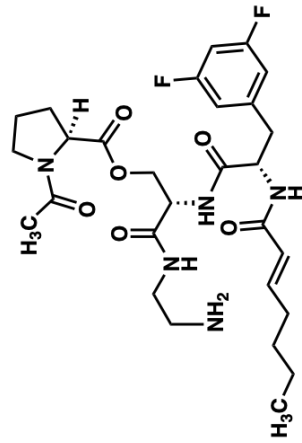
400.13
CDCl₃

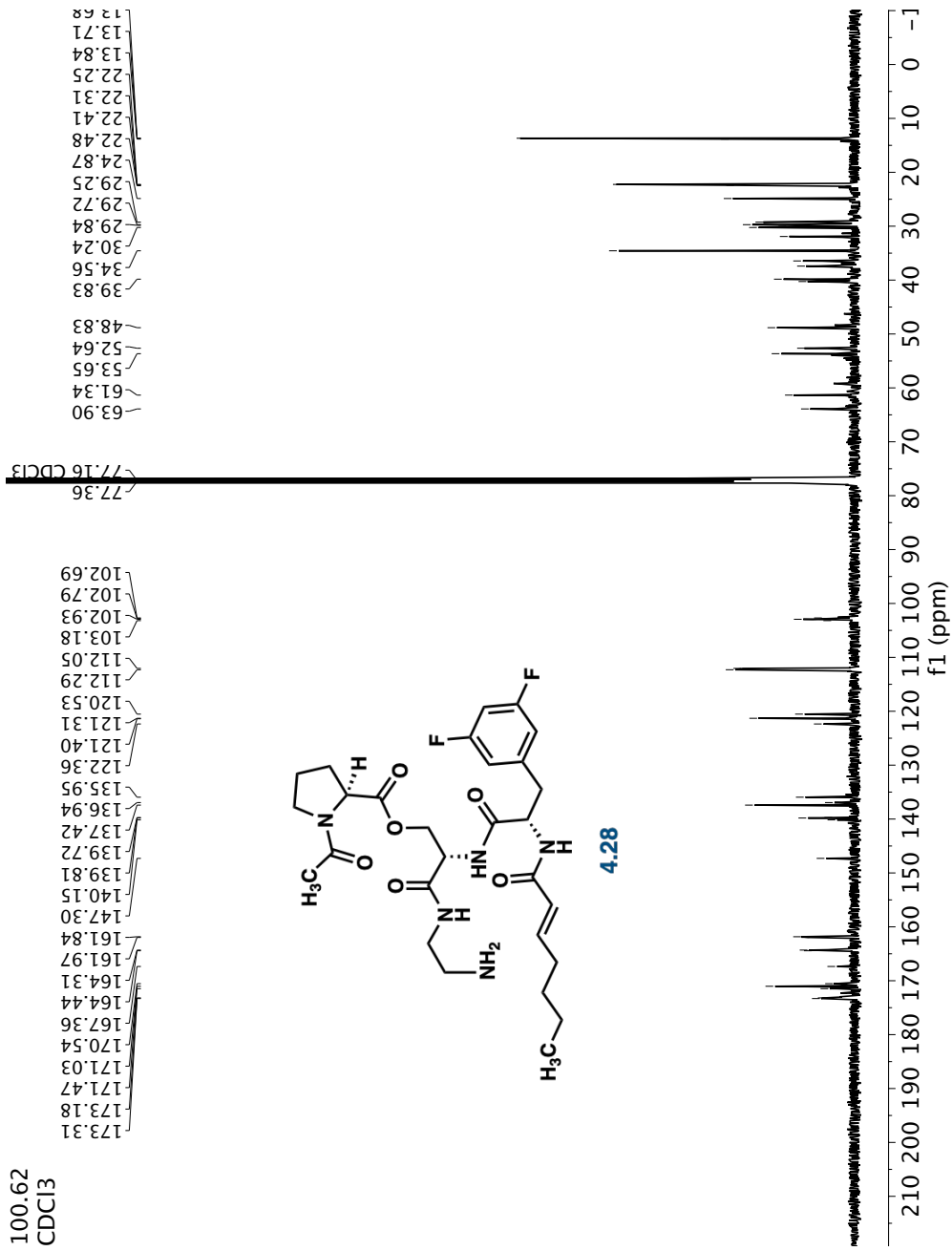






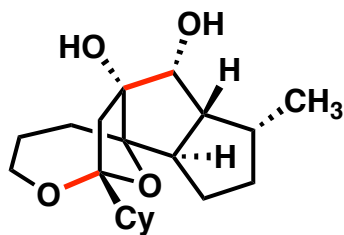
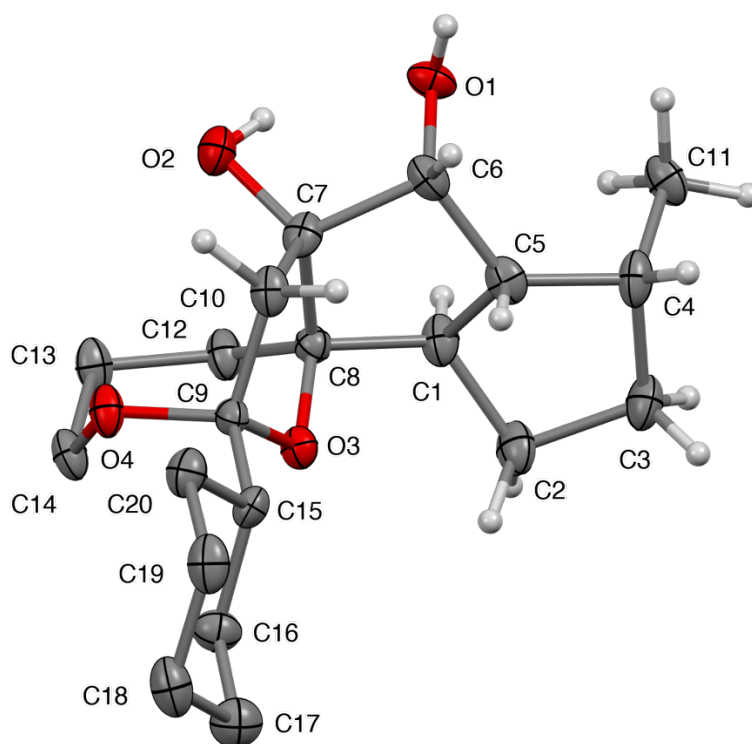
400.15
CD3CN





Appendix B

CRYSTAL STRUCTURE DATA FOR PINACOL PRODUCT 3.24



3.24

Crystallographic Experimental Data for 3.24

X-ray structural analysis for **3.24**: Crystals were grown by slow evaporation of saturated solutions in diethyl ether and mounted using viscous oil onto a plastic mesh and cooled to the data collection temperature. Data were collected on Bruker D8 Venture Photon III diffractometer with Cu- K α radiation ($\lambda = 1.54178 \text{ \AA}$) focused with Goebel mirrors. Unit cell parameters were obtained from 48 data frames, $0.5^\circ \omega$, from different sections of the Ewald sphere.

The unit-cell dimensions, equivalent reflections and systematic absences in the diffraction data are uniquely consistent with $P2_12_12_1/n$. The Flack parameter refined to zero indicating the true hand of the data has been determined. The data were treated with multi-scan absorption corrections.¹ Structures were solved using intrinsic phasing methods² and refined with full-matrix, least-squares procedures on F^2 .³

Non-hydrogen atoms were refined with anisotropic displacement parameters.

Hydrogen atoms were located from the difference map and allowed to refine freely isotropic atomic displacement factors. Atomic scattering factors are contained in the SHELXTL program library.²

¹ Apex3 [Computer Software]; Bruker AXS Inc.: Madison, WI, USA, 2015.

² Sheldrick, G.M. *Acta Cryst.* **2015**, *A71*, 3–8.

³ Sheldrick, G.M. *Acta Cryst.* 2015, *C71*, 3–8.

Crystal data and structure refinement details for 3.24

Identification code	chai052
Empirical formula	C ₂₀ H ₃₂ O ₄
Formula weight	336.45
Temperature/K	100
Crystal system	orthorhombic
Space group	P2 ₁ 2 ₁ 2 ₁
a/Å	10.1226(6)
b/Å	10.6976(6)
c/Å	16.7624(10)
α/°	90
β/°	90
γ/°	90
Volume/Å ³	1815.16(18)
Z	4
ρ _{calc} /cm ³	1.231
μ/mm ⁻¹	0.669
F(000)	736.0
Crystal size/mm ³	0.467 × 0.462 × 0.236

Radiation	CuK α ($\lambda = 1.54178$)
2 Θ range for data collection/ $^{\circ}$	9.808 to 150.628
Index ranges	$-12 \leq h \leq 12$, $-12 \leq k \leq 13$, $-20 \leq l \leq 20$
Reflections collected	12977
Independent reflections	3717 [$R_{\text{int}} = 0.0292$, $R_{\text{sigma}} = 0.0326$]
Data/restraints/parameters	3717/0/345
Goodness-of-fit on F^2	1.061
Final R indexes [$I \geq 2\sigma(I)$]	$R_1 = 0.0300$, $wR_2 = 0.0792$
Final R indexes [all data]	$R_1 = 0.0301$, $wR_2 = 0.0793$
Largest diff. peak/hole / $e \text{ \AA}^{-3}$	0.27/-0.15
Flack parameter	-0.03(3)